Investigations into the chemical analysis and bioactivity of plant proanthocyanidins to support sustainable livestock farming

A dissertation submitted to the University of Reading for the degree of Doctor of Philosophy

School of Agriculture, Policy and Development

CHRISTOS FRYGANAS

Supervisor: Prof Irene Mueller-Harvey

August 2016

Declaration

"I confirm that this is my own work and the use of all material from other sources has been properly cited and fully acknowledged".

Christos Fryganas

August 2016

Acknowledgements

I would like to thank my supervisor, Prof Irene Mueller-Harvey, for her support and guidance during the course of my studies. I am grateful to her for introducing me to tannin chemistry. Her passion for the field is definitely inspiring. Prof Juha-Pekka Salminen made important contributions to my studies by hosting my secondment in his group. In addition, the discussions and exchange of ideas during the meetings of the chemistry workpackage proved very helpful. I would like to acknowledge his full support and constant availability. My gratitude also goes to Dr Herve Hoste for hosting me in his laboratory and for fully supporting me during my parasitology studies. Special thanks go to Dr Radek Kowalczyk for his assistance and commitment during my NMR studies.

This work would never have been possible without the wide range of tanniniferous plants. Therefore, I am grateful to Pick Your Own farm in Goring-on-Thames, Mrs Alison Prudence, Mr Peter Davy and the "LegumePlus" collaborators who kindly provided so many plant samples.

I will always be thankful to the "LegumePlus" fellows, supervisors and partners for sharing ideas and samples, for having fruitful discussions and for all the productive collaborations during these 4 years. I especially enjoyed their interesting workshops, which had such a positive impact on my research.

I would like to thank Dr Wayne Zeller, Dr John Grabber and Dr Martha Vestling for collaboration and advice on chemical analysis. I am grateful to Dr Andrew Williams and his group for making excellent use of my samples to explore new areas of tannin bioactivity. I would also like to thank Mr Carsten Malisch for sharing laboratory tasks and goals during our common secondment in Turku. The thriving collaborations with Dr Nguyen Huyen and Dr Wilbert Pellikaan are also very much appreciated. It has been a great honour and pleasure to work with Dr Marica Engström and Dr Jessica Quijada. Our joint efforts led to high quality publications whilst our discussions helped me with every aspect of my PhD life in and out of the laboratories. My office mate Ms Honorata Ropiak, is very much acknowledged for her help, the constant support and advice during our long journey. Special thanks are due to Dr Olivier Desrues for our common research work, the discussions on parasites, chemistry and statistics and all the memorable entertainment sessions.

I am grateful to the members of the Natural Chemistry Research Group for treating me as an equal group member during my secondment. Dr Maarit Karonen, Dr Jeff Ahern, Ms Marianne Oraviita, Mr Jorma Kim and Ms Anne Koivuniemi assisted me in the laboratory and helped me with the analysis. Support and advice from Dr Blasius Azuhnwi and Ms Marine Rayberine during my parasitology studies in Toulouse are indeed very much appreciated.

I would also like to thank my colleagues at University of Reading, Mr Chris Drake, Dr Prabhat Sakya, Dr Aina Ramsay, Dr Chaweewan Klongsiriwet, Mr Mohammed Dakheel, Ms Sarah Jing Guo, Mr Ron Brown and Prof Ian Givens for their constant support and advice.

I would like to express my deep gratitude to Dr Panos Sakkas and Dr Denis Fragkakis. Their continuous and unconditional support, together with their ability to cushion my frustrations and setbacks, allowed me to reach my goals. I would also like to recognise the long list of friends who stood by me at all important crossroads of my life.

Finally, I would like to thank my mother and my father. Without their patience, their never-ending support and belief in me I would never have been able to dedicate my achievements to them. This thesis is also dedicated to my colleague, Mrs Parwin Majid, who is very much missed.

Abstract

Proanthocyanidins (PA) in some forage legumes have been linked to contradictory effects in animal health and nutrition. Ruminants fed with PA-containing plants do not suffer from bloat and can also reduce gastrointestinal parasite infections, improve protein use efficiency and reduce greenhouse gas emissions. Plants have a wide range of PA contents and compositions. Therefore, screening tools are required to determine the optimal contents and types to exploit PA bioactivities on farms.

This research initially focused on the identification and isolation of PAs with contrasting characteristics from various plant species. These samples were then used to develop novel methods such as UPLC-ESI-MS/MS and ^{13}C HSQC NMR for extractable PAs and ^{13}C CPMAS NMR for PAs within plants, and to probe structure-activity relationships.

These PAs were also subjected to complementary analytical methods, which demonstrated that depolymerisation techniques can provide quantitative information on PA contents and compositions and mass spectrometric techniques on molecular distributions. These analyses revealed an enormous range of molecular profiles. This diversity, however, led to good but not excellent correlations between the degradation methods. It also affected mass spectrometric and liquid-state NMR responses. In particular, there were some discrepancies between thiolysis-HPLC and UPLC-ESI-MS/MS results of sainfoin PA extracts. For solid-state NMR, the PAs from model plants proved too homogeneous for the analysis of the highly complex PAs in sainfoin plants. Nevertheless, this method could rank accessions on the basis of PA composition and discriminated between plant organs via signature spectra. Therefore, final decisions on which of these methods to use will depend on the research objectives and sample numbers.

Finally, anti-parasitic assays discovered that the *in vitro* exsheathement inhibition of the abomasal parasite, *Haemonchus contortus* was dependent on the average molecular size of purified PA mixtures. In addition, collaborative studies showed that prodelphinidins or PA size also affected some anti-parasitic and ruminal fermentation results.

Contents

Chapter 5. Linking contrasting proanthocyanidin structures to *in vitro* anthelmintic activity of *Haemonchus contortus* **181**

List of Tables

Chapter 3:

Chapter 4

Chapter 5

List of Figures

Chapter 3

Chapter 5

Chapter 6

List of Abbreviations

2-D: Two-dimensional

AH: Anthelmintic

BM: Benzyl mercaptan

CHCA: α-cyano- 4-hydroxycinnamic acid

COSY: Correlation spectroscopy

COTS: Cotwold seeds ltd

CP: Cross-polarisation

CV1: Cone voltage 1

DAD: Diode array detector

DMACA: 4-dimethylaminocinnamaldehyde

DHAP: 2,6-dihydroxyacetophenone

DHB: 2,5-dihydroxybenzoic acid

EC_{50}: Effective concentration that causes 50% inhibition

EHA: Egg hatching assay

EIC: Extracted ion chromatogram

ENVT: École nationale vétérinaire de Toulouse

ESI: Electrospray ionisation

GIN: Gastrointestinal nematode

HETCOR: Heteronuclear correlation

HILIC: Hydrophilic interaction liquid chromatography

HMB: 2-hydroxy-5-methoxybenzoic acid

HMBC: Heteronuclear multiple bond correlation

HMQC: Heteronuclear multiple quantum correlation

HPLC: High performance liquid chromatography

HRF: Heterocyclic ring fission

HSQC: Heteronuclear single quantum coherence

HT: Hydrolysable tannin

INRA: Institut national de la recherche agronomique

IR: Infrared

LC: Liquid chromatography

LDA: Larval development assay

LEIA: Larval exsheathment inhibition assay

LoA: Limits of agreement

LMIA: Larval migration inhibition assay

MALDI: Matrix - assisted laser desorption ionisation

MAS: Magic angle spinning

mDP: mean degree of polymerisation

MW: Molecular weight

MRM: Multiple reaction monitoring

MS: Mass spectrometry

MS/MS: Tandem mass spectrometry

NIAB: National institute of agricultural botany

NMR: Nuclear magnetic resonance

NP: Normal-phase

PA: Proanthocyanidin

PBS: Phosphate buffered saline

PC: Procyanidin

PD: Prodelphinidin

PEG: Polyethylene glycol

PF: Profisetinidin

PG: Proguibourtinidin

PP: Propelargonidin

PR: Prorobinetinidin

PVPP: Polyvinylpolypyrrolidone

PYO: Pick-your-own

QM: Quinone methide

RDA: Retro - Diels - Alder

RP: Reverse-phase

SA: Sinapinic Acid

s-DHB: super-DHB (10% methoxy - hydroxybenzoic acid: 90% 2,5 - dihydroxybenzoic acid)

TFA: Trifluoroacetic acid

THAP: 2,4,6-trihydroxyacetophenone

TOF: Time-of-flight

t-IAA: *trans*-3-indole acrylic acid

UPLC: Ultra performance liquid chromatography

URE: University of Reading

UTU: University of Turku

UV: Ultraviolet

WP: Workpackage

Chapter 1. Introduction

Proanthocyanidins (PAs) or condensed tannins are polyphenolic compounds which are usually located at the cell walls and in the vacuoles of numerous plant species [1]. The wide distribution of PAs in the plant kingdom has been linked with plant defensive mechanisms [2, 3] and nutritional properties [4-8]. The use of some PA-containing forages has been associated with several beneficial effects in animal production and, therefore, this has attracted considerable scientific and commercial interest [5, 9-11].

Dietary PAs can benefit livestock as they improve animal health and welfare and they can also reduce the environmental footprint compared to conventional farming practices. Importantly, the ingestion of forages with PAs never causes bloat [12, 13] and can lower parasitic nematode infections in the gastrointestinal tract [14-16]. PA-containing feeds can additionally increase live weight gain, wool production, ruminant fertility, the yields and nutritional quality factors of animal products such as milk and meat [6, 9]. The presence of PAs in feeds can also be beneficial for the environment because PAs have some potential for decreasing methane and nitrous oxide emissions [17-20]. Furthermore, the use of PA-containing plants for controlling parasites can reduce the release of veterinary drugs into the environment [21]. However, it is important to note that some dietary PAs can also have anti-nutritional effects and it is, therefore, important to establish which PAs have what effects in terms of structure-activity relationships across all aspects of livestock nutrition and health [8, 12, 20].

It is thought that the ability of PAs to chelate minerals and to interact with proteins, alkaloids and other biomolecules influences their bioactivity, but the actual mechanisms are still poorly understood [2, 4, 5]. However, plant PAs vary greatly in their structures and usually occur in complex polymeric mixtures. This diversity poses difficulties for measuring PA contents, profiling of PA compositions and understanding their structure-activity relationships [2, 5, 6, 22, 23]. These problems are augmented by a lack of quantitation standards, the wide-spread use of non-specific analytical methods in bioassay studies and the lack of techniques for determining PA contents and compositions directly in plant tissues. Thus, the analysis of PAs in plants and extracts by several different methods is still needed in order to generate complementary information on PA compositions and contents. Such data are required to identify the structural features that influence bioactivity.

- Quantification and characterization of tannins remains one of the great analytical challenges in natural products chemistry.

Meagan D. Mercurio and Paul A. Smith, 2008

1.1. Plant tannins

Tannins belong to a large group of polyphenolic secondary metabolites that are produced by plants. Due to their structural features plant tannins are separated into the subgroups of PAs and hydrolysable tannins (HTs). Some sea flora species, such as brown algae, can contain phlorotannins, which are another tannin subgroup [24, 25]. The studies described in this thesis have entirely focused on PAs and, therefore, the other subgroups are not reviewed here.

1.2. Classification of proanthocyanidin structures

Flavan-3-ol monomers can be linked through C4-C8 and sometimes also via C4-C6 interflavanyl bonds to form B-type PA oligomers and polymers [3, 22, 26] (Figure 1.1A). The location of subunits within the polymeric structure is used to define terminal and extension units (Figure 1.1A). Monomeric subunits can also be linked with an additional ether bond (C2-*O*-C7 or C2-*O*-C5) to an adjacent subunit to form an A-type linkage (Figure 1.1B) [3, 22]. The term proanthocyanidin stems from the characteristic depolymerisation and oxidation during heat treatment in an acidic environment, which releases coloured anthocyanidins [22, 27].

Apart from the type and the position of interflavanyl bonds, several other factors also contribute to the complexity of naturally occurring PA mixtures. These factors are the degree of polymerisation (i.e. size of the polymer chain) (Figure 1.1A), the hydroxylation patterns of the A and B rings and the chiral centres at positions C2 and C3 of the C ring (Figure 1. 2) [3, 4, 22]. Plants tend to synthesise a range of PAs with various molecular weights (MWs) and this increases further their complexity [3, 22].
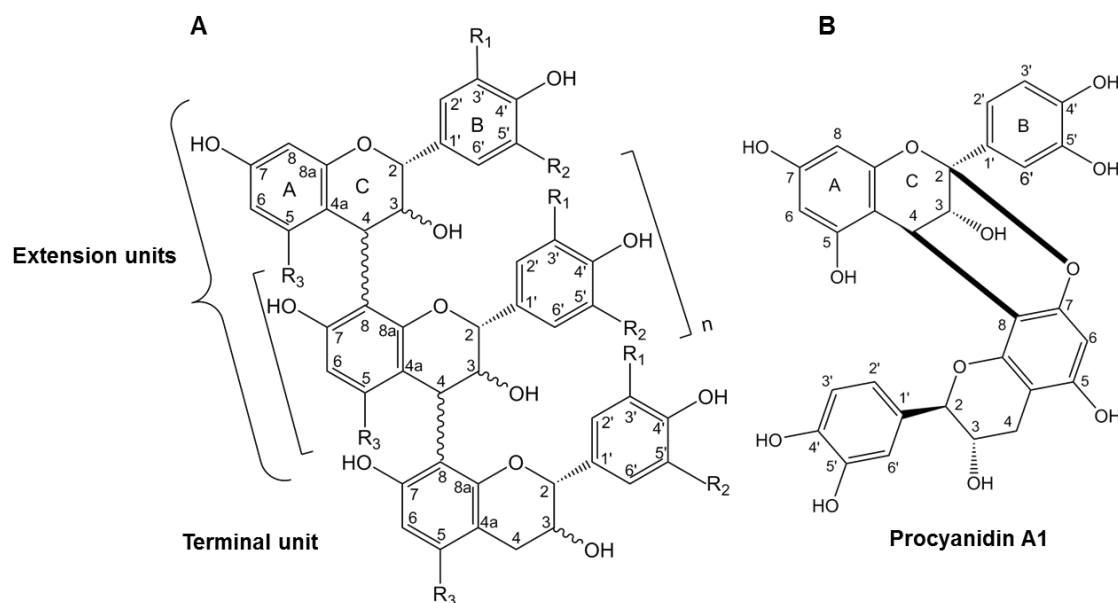
Figure 1.1: A. Example of proanthocyanidin structures with B-type C4-C8 linkages. R1, R2 and R3 are typically either H or OH. **B.** Example of an A-type proanthocyanidin dimer.

Flavan-3-ol subunits are distinguished by the hydroxylation patterns of their A and B rings and they are divided further according to the stereochemistry of the C3 chiral centre in the C ring (Figure 1.2). Normally, the chirality of C2 is of the *R* configuration whereas the chirality centre C3 can be either of *R* or of *S* configuration. In the case of 2*R*:3*R* (*cis*-configuration), the compounds acquire the prefix epi- in contrast to 2*R*:3*S* (*trans*-configuration) [22].

In addition to these PA classes (Figure 1.2), less common structures such as proluteolinidins and proapigeninidins have been identified as well [28].

R$_1$	R$_2$	R$_3$	Proanthocyanidin	Subunit
OH	H	OH	Procyanidin (PC)	(epi)catechin
OH	OH	OH	Prodelphinidin (PD)	(epi)gallocatechin
H	H	OH	Propelargonidin (PP)	(epi)afzelechin
OH	H	H	Profisetinidin (PF)	(epi)fisetinidol
H	H	H	Proguibourtinidin (PG)	(epi)guibourtinidol
OH	OH	H	Prorobinetinidin (PR)	(epi)robinetinidol

Figure 1.2: Classification of proanthocyanidins

Here, only the procyanidins (PCs) and prodelphinidins (PDs) are discussed as according to current evidence, they are the most widespread PAs in forage legumes, which are of particular interest in ruminant nutrition.

In addition, acyl or glycosyl substitution can lead to greater structural complexity of PAs [4, 22, 29]. Gallic acid (GA) is the substituent reported the most at the hydroxyl of the position C3 but also *O*-gallates can be formed at the positions C5, C7 or C3′ [3, 22, 29]. Carbohydrate units can also be linked to the basic PA structure, but glycosylation is not often reported [28, 30, 31].

1.3 Effects of dietary proanthocyanidins in ruminant production, animal health, and environmental sustainability

Forages that contain PAs have been linked to a number of beneficial and detrimental effects on animals and the environment [5, 6, 9, 10]. It has been suggested that some of the observed contradictory effects stem from variations in PA structures and concentrations [5, 6, 32]. Such variations occur between species and within accessions of forage legumes such as sainfoin (*Onobrychis viciifolia*) [31, 33-35], birdsfoot trefoil (*Lotus corniculatus*) [36, 37], big trefoil (*Lotus pedunculatus*) [37, 38], sericea lespedeza (*Lespedeza cuneata*) [39], sulla (*Hedysarum coronarium*) [40], erect canary clover (*Dorycnium rectum*) [41], sickle bush (*Dichrostachys cinerea*) [42] and white clover (*Trifolium repens*) [43-45].

1.3.1 Ruminant production

Effects of proanthocyanidins on voluntarily feed intake

The presence of large numbers of hydroxyl and benzene groups in PAs leads to the formation of complexes with proteins and, interestingly, some of these interactions can be highly specific [46]. This protein binding and precipitating capacity, which is termed as astringency [6], can negatively affect the voluntary feed intake of PA-containing feeds [8, 20]. In addition, PAs can slow down the digestion rate of fibres and proteins, which can cause a high rumen fill and lower voluntary intake [6, 20].

However, investigations into the intake rates of PA-containing feeds have generated contradictory results. For instance, the PA-containing sainfoin gave as high or higher voluntary feed intakes as white clover or lucerne (*Medicago sativa*), which have little or no amounts of PAs, respectively [47, 48]. A comparison of sainfoin, birdsfoot trefoil and chicory (*Cichorium intybus*) showed that much more sainfoin was eaten, despite having the highest PA content [49]. In contrast, deactivation of PAs with polyethylene glycol (PEG) in a lentisk (*Pistacia lentiscus*) diet increased feed intake and improved digestibility in goats [50]. Such increases in feed intake have often found after PEG addition to PA feeds and suggest that a low digestion rate may be the major factor limiting intake [6]. Forages with high PA contents (e.g. sericea lespedeza) are often linked with low voluntary feed intake, thus those with moderate concentrations are often preferred [1, 5, 10, 12, 51]. However, the link between PA concentrations in forages and voluntary feed intake is not clear-cut as many other parameters may also influence this relationship. For instance, PD-based PAs found in the extract of a calliandra (*Calliandra calothyrsus*) accession, were correlated with higher intakes compared to accessions with PC-rich PAs [10]. However, PD-based PAs of big trefoil had the opposite effect [1, 6]. Moreover, studies with fresh and processed sainfoin have demonstrated no impact on feed intake, despite the large variation of assayable PA contents in these samples and a prevalence of PDs [47]. Higher intake rates were also observed in cows that were provided with PA-rich supplements (e.g. peanut skins and tamarind seed husks) in feeds [5].

Taken together, these findings suggest that the contradictory results could stem from differences in PA concentrations or structures and varying responses from different animals [11]. It is important to note that feeding trials should provide information not only on total fibre, lignin and protein contents, as these are well known to affect feed intake [5], but also on the PA contents and structures of the diets [6, 11].

Effects of proanthocyanidins on protein digestibility and ruminal fermentation

The benefits generated by PAs in terms of animal nutrition appear primarily to stem from their interactions with proteins. During mastication dietary PAs can

complex with proline-rich proteins of the saliva or with feed proteins, which leads to less soluble protein and changes the fermentation patterns in the rumen [6]. McMahon et al. reviewed several studies, which stated that in contrast to browsing ruminants, grazing ruminants tend to lack the salivary proteins that can strongly bind PAs [12]. Therefore, protein digestion seems to be a function of PA and protein concentrations and PA affinity to proteins [6, 10, 52].

The PA-protein complexes are relatively stable under rumen conditions with pH values of 6 - 7 and this decreases ruminal protein degradation. Given the changing pH patterns in the digestive tract, the PA-protein complexes dissociate when they enter the abomasum (pH<3.5) and the small intestine (pH>7); it is thought that dissociation from PAs renders the protein more available for acid and enzymic degradation [6, 8, 10, 53]. This transfer of PA-protected proteins across the rumen has been called "rumen escape protein" (Figure 1.3) and some authors have postulated that certain plant PAs can thus improve protein utilisation [5, 8]. For example, feeding of birdsfoot trefoil and sulla to ruminants increased the dietary uptake of amino acids in the small intestine in contrast to big trefoil and sainfoin. It was suggested that these variations were due to different PA structures [9]. However, the reasons are not obvious, as birdsfoot trefoil PAs mostly consist mostly of PCs, whereas the three other forages have mostly PDs [5, 6, 12].
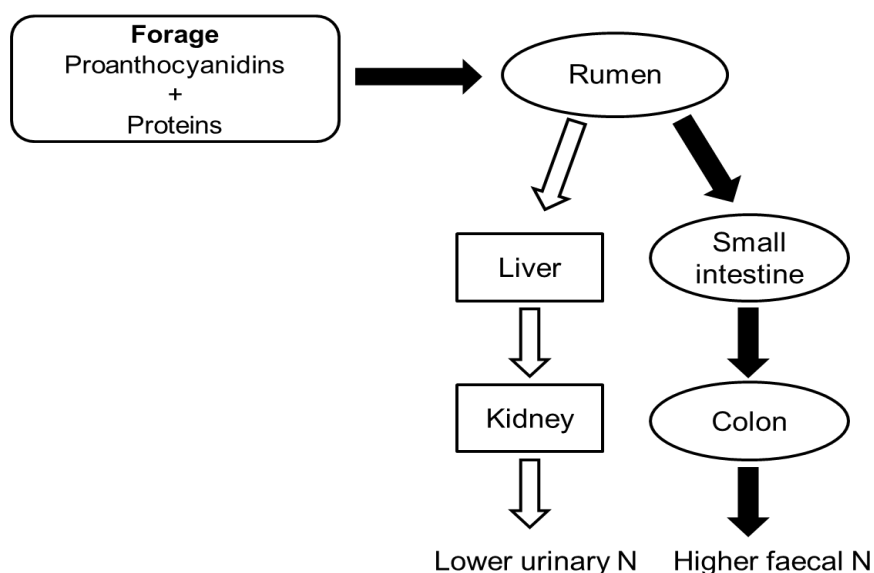
Figure 1.3: Schematic representation of the "rumen escape protein" process, adapted from I. Mueller-Harvey, 2006 [5]. N: nitrogen.

The affinity of PAs to dietary proteins is considered to play a major role in protein digestion [5, 9, 10]. Several structural features of both PAs and proteins impact on the extent of their interaction [10, 12, 19]. As an example, McNaab et al. reported that PDs from big trefoil extracts were bound more strongly to Rubisco than the PCs from birdsfoot trefoil extracts [54]. There are several possible reasons for how the PAs may reduce protein degradation in the rumen: i) PA-coated proteins may be more difficult to colonise by rumen microflora than free proteins, ii) PAs may inhibit proteases and iii) PAs may reduce the growth of proteolytic bacteria or have other as yet unknown effects on the rumen microflora [5, 9, 12, 55]. Moreover, lower digestibility can either derive directly from the interaction of PAs with the digestive enzymes or indirectly from PA binding to dietary components (i.e. proteins, carbohydrates, etc.) which are the enzyme substrates [6, 8, 17, 56].

The effect of PAs on rumen microflora activity has also been studied as a possible mechanism to explain the "rumen escape protein" which leads to more dietary protein reaching the small intestine [5, 10, 17, 18]. It was found that the populations and the growth of several species of rumen proteolytic bacteria (e.g. *Clostridium proteoclasticum*, *Eubacterium sp.*, *Streptococcus bovis* and *Butyrivibrio fibrisolvens*) were decreased *in vitro* and *in vivo* when birdsfoot trefoil replaced a PA-free diet in sheep [10]. *In vitro* tests showed that sainfoin PAs decreased the growth and the proteolytic activity of *S. bovis* and *B. fibrisolvens* [57]. A diverse set of PAs from various forage legumes also inhibited the *in vitro* cellulolytic activity of *Fibrobacter succinogenes* [58]. Three erect canary clover fractions with low, medium and high MW PAs decreased significantly ($p<0.001$) the *in vitro* growth of the rumen bacteria *Clostridium aminophilum*, *B. fibrisolvens*, *C. proteoclasticum*, *Ruminococcus albus* and *Peptostreptococcus anaerobius* [41]. However, different concentrations, mDP values of PAs and incubation times resulted in diverse individual responses for all bacteria species. The authors observed that lower MW PAs inhibited more effectively the growth of *C. aminophilum*, *B. fibrisolvens and C. proteoclasticum* where *R. albus* and *P. anaerobius* were affected only by the PA concentration. They also suggested that mDP was more important for growth inhibition of bacteria than PD:PC ratios, due to the high PD proportions within total PAs in all PA fractions.

It can be concluded that the mechanisms of PAs for enhancing protein utilisation in ruminants are likely to depend on a balance of several factors and if this balance is not optimal, deleterious effects may result instead [5, 6]. If dietary protein is bound too tightly, much of it may be lost in the faeces and formation of complexes between PAs and other feed constituents may impede the digestion of fibre, starch, etc. [5, 6, 10]. It is also possible that PAs may impact negatively on digestive enzymes or the rumen microflora [5, 6, 10]. Therefore, PAs are a "double edge sword" according to Waghorn et al. and interdisciplinary research is needed to elucidate the reasons for some of the contradictory observations [6].

Effects of proanthocyanidins on livestock production, milk, cheese and meat quality

The reductions of voluntary feed intake and digestibility of several tanniniferous feeds can have an adverse impact on live weight gains, wool production and quality of the end-products such as milk and meat [1, 59, 60]. In contrast, a few PA types appear to be able to improve ruminant production [20] and the nutritional quality of milk, cheese and meat from ruminants [5, 9, 10, 61].

A few forage PAs have generated higher milk yields and protein contents and have lowered the fat contents compared to lucerne and other conventional feeds [5]. Examples are as follows: birdsfoot trefoil increased the milk production of sheep [10] and also milk, lactose and protein production of lactating ewes, but fat content was decreased during mid and late lactation periods [1, 10]. However, sainfoin hay fed to dairy goats had no effect on milk production and composition [62]. A detailed comparison of milk composition was conducted with cows fed sainfoin, two different accessions of birdsfoot trefoil and lucerne as a PA free diet [61]. Whilst the sainfoin diet lowered the milk urea content, there was no change with the one birdsfoot accession (Pollom) and a slight increase was observed with the other birdsfoot trefoil accession (Bull) and lucerne. Milk analysis also showed an increase of the 18:3n-3 fatty acids on the sainfoin diet. In contrast, feeding sulla at the flowering stage to sheep did not alter milk protein production but increased fat content [63]. These interesting findings suggest that PAs could perhaps also be used to produce human foods of higher nutritive value.

Some differences in the fatty acid profiles of cheese from cows fed sainfoin, birdsfoot trefoil and lucerne were also identified [61].The sainfoin diet increased the 18:3n-3 proportion in cheese lipids compared to the birdsfoot trefoil diet. Sainfoin also caused an increase of 20:5n-3 and 22:5n-3 after the control period of the trial. These results may indicate that some PA-forages can have noticeable effects not only in milk but in cheese production as well.

Dietary PAs may also affect meat quality in terms of fatty acid composition, colour, tenderness and aroma that can influence consumer perception and demand [60, 64]. A study from Priolo et al. studied the effects of carob (*Ceratonia silique*) pulp on lamb meat [65]. It was found that carcass yield and total fat were lower compared to two control diets that consisted either of maize or a carob diet which had its PAs 'neutralised' by PEG. However, the sensory panel preferred the meat from the PEG and maize treatments. Carob feeding also resulted in lower voluntary feed intake, lamb performance, and digestibility of dry matter and fibre, which suggested that the PAs in carob produce no beneficial effects on lamb nutrition and meat composition [65]. However, the concentrations of saturated fatty acids and linolenic acid in lamb meat were higher in the control group compared to the sulla and sulla-PEG diets whereas linoleic acid concentration was higher in the sulla-fed group [64]. In addition, feeding sulla had some effects on compounds that cause off-flavours in meat as higher skatole and unaltered indole concentrations were recorded.

These findings demonstrated that diets with different types of PAs can have very different effects on meat composition and fatty acid profiles. Therefore, plant PAs offer new opportunities for improving the quality of animal products and meeting consumer needs.

1.3.2 Ruminant Health

Grazing animals are exposed to pathogens that threaten animal health and cause economic losses in the livestock farming. PA-containing forages are of interest as some have shown potential for preventing or mitigating some health risks and also bloat incidents. Therefore, such forages are being investigated to harness their medicinal properties [6, 10-13, 21, 66, 67].

Anti-bloating effects of proanthocyanidins

Bloat occurs when a stable protein foam forms in the rumen, which traps fermentation gases and disrupts the normal eructation mechanisms for releasing these gases from the rumen [11, 19, 68]. As a consequence, the trapped gasses expand the rumen and exert pressure on other vital organs [12]. The detrimental effects can lead to a reduction of voluntary feed intake in mild cases (frothy bloat), but if the rumen expands too far can negatively affect vital functions of the lungs, the intestinal tract or the heart and leads to a rapid and painful death (free-gas bloat) [12, 13, 19].

It is thought that the production of frothy foam occurs when: i) some protein-rich forages are rapidly fermented, which increases gas production and the numbers of rumen bacteria, ii) soluble plant components are released that contribute to the stabilisation of the foam and trapping of ruminal gasses and iii) some bacteria produce dextran slime that increases the viscosity of ruminal fluid [12, 13].

If detected in time, bloating can be treated by rapid administration of oils or detergents, which disperse the foam, but the risk of possible residues delays slaughtering and increases consumer concern for safe foods [19]. However, the presence of PAs whether in forages or as additives completely mitigates bloat and has been proposed as an alternative to treatment with synthetic chemicals [12, 13, 19]. Although the actual mechanisms of how PAs prevent bloat are not clear, it is believed that PAs are possibly involved in the destabilisation of foam, the inhibition of slime-producing bacteria and the reduction of proteolysis rates ([10, 12, 32].

The inclusion of sainfoin herbage, hay and pellets in a lucerne based diet significantly reduced bloat incidents in steers over a 3-year period and was linked to lower soluble protein in the rumen fluid [55]. Similar effects were observed in cattle with dock (*Rumex obtusifolius*) [48]. A study that evaluated the *in vitro* and *in vivo* anti-bloating activity of quebracho PAs that were used to supplement a wheat diet for steers showed that these PAs reduced bloat scores, rumen fluid protein content, biofilm production, gas production and microbial activities [68]. These results suggested that PAs can contribute to several mechanisms that are important for bloat prevention. However, there is still a lack of information on what PA content is needed to prevent bloat. Further research is needed to establish PA

concentration thresholds and the effect the different PAs have on these thresholds. Finally, it is important to focus the research on those PA types to have positive rather than negative on animal nutrition or health.

Anti-parasitic effects of proanthocyanidins

Gastrointestinal parasites are a worldwide threat to the health and well-being of grazing livestock [14, 16]. Several nematode species can infect the different compartments of the gastrointestinal tract and lead to lower appetite, diarrhoea and anaemia, which can be lethal (Table 1.1) [14]. In addition, these infections can compromise animal performance and result in significant economic losses [14, 69].

Table 1.1: Important gastrointestinal nematodes of sheep, goats and cattle, their site of infection in the host and the main consequences of the infection, adapted from S. Athanasiadou and I. Kyriazakis, 2004 [14].

	Site of infection	Nematodes	Main effect on the host
Sheep, goats	Abomasum	*Haemonchus contortus*	Anaemia, possibly death
		Teladorsagia circumcincta	Reduced food intake
	Small intestine	*Nematodirus battus*	Dehydration
		Trichostrongylus colubriformis	Reduced nutrient utilisation
		Trichostrongylus vitrinus	Reduced nutrient utilisation
Cattle	Abomasum	*Haemonchus placei*	Anaemia
		Ostertagia ostertagi	Reduced food intake
	Small intestine	*Cooperia oncophora*	Reduced nutrient utilisation
		Cooperia punctata	Reduced nutrient utilisation

The mitigation of parasitic infections in farmed animals has relied on the wide-spread use of synthetic drugs [14, 16, 70]. However, their application over the long-term has rendered several helminth species resistant to benzimidazoles, imidothiazoles and macrocyclic lactones, which are the three major classes of drugs used for chemoprophylaxis and treatment [71]. In addition, there is now also cross-resistance of nematode species to several synthetic drugs due to an

extensive use of anthelmintic (AH) drug combinations, which was used to treat a wide range of nematode species [16, 71]. These practices are costly and can put the animal's health at risk. Consumers are also concerned about drug residues in animal products and about environmental contamination [14, 16, 71]. Therefore, alternative farming practices are required to deal with parasites [14, 66]. Parasites need to be considered as an integral part of the landscape and have co-evolved with grazing animals. Several scientists now believe, therefore, that parasites should be managed rather than eliminated [72]. PA-containing plants can act as nutraceuticals that provide nutrients and pharmaceuticals [66]. In addition, some authors have argued that low levels of parasites can stimulate the animal's own immune system and thus avoid the need for frequent AH drug applications [66].

The uptake of plant bioactive compounds during grazing is considered as one of the most effective and sustainable solutions for protecting animals from parasites [14-16]. Forage PAs can interfere with all stages of the parasitic life cycle (Figure 1.4) not only in small ruminants but also in cattle and pigs [39, 66, 73-83].
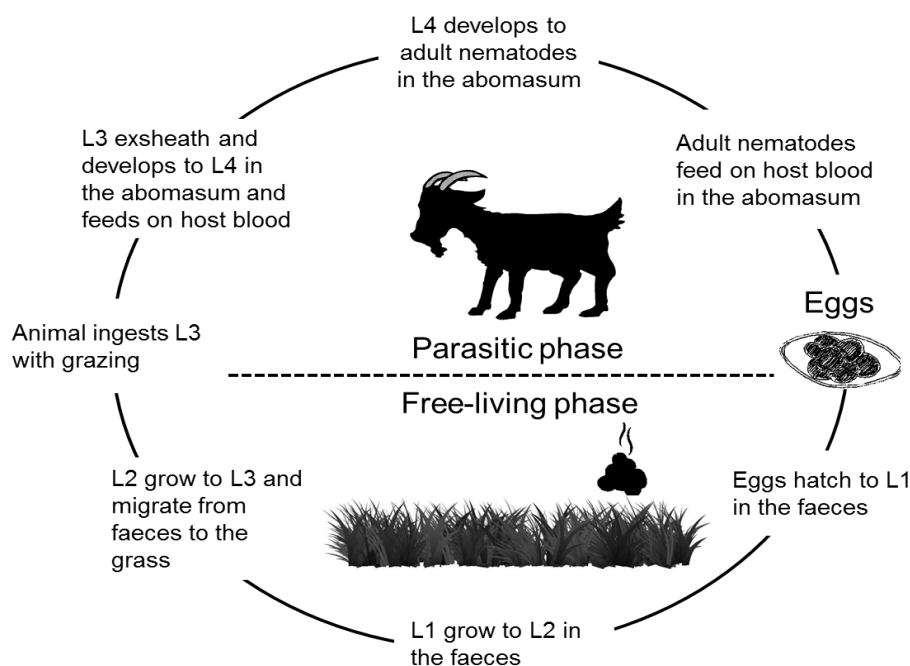
Figure 1.4: The life-cycle of Haemonchous contortus, adapted from Hoste et al., 2012 [21].

Evidence is emerging that PAs can reduce i) the number of L3 infective larvae in the digestive tract, ii) the quantity of eggs in faeces by lowering nematode numbers or by interfering with the reproduction process and iii) can also inhibit the development of eggs to L1 larvae [66]. On that basis, *in vitro* assays have been developed to screen plant extracts for AH activity and to evaluate the ability of isolated compounds to interfere with key stages of the nematode life cycle (Table 1.2) [16, 21, 66].

Table 1.2: *In vitro* bioassays used in plant extract screening for anthelmintic activity, adapted from Hoste et al., 2012 [21].

Bioassay	Target stage	Process inhibited
Egg Hatch Assay	Eggs	Hatching to L1 stage larvae
Larval Migration Inhibition	L3	Motion of L3 stage larvae
Larval Feeding Inhibition	L1	Feeding of L1 stage larvae
Larval Exsheathment	L3	Exsheathment of L3 stage larvae
Larval development	Eggs → L1	Development to L1 larvae
Adult motility	L5/adults	Motility of adult nematodes

The evaluations of PAs against several important parasites with *in vitro* bioassays have generated an enormous amount of data [66]. Screening studies have shown the AH efficacy of PA extracts from a variety of plants against *Haemonchus contortus* [79, 84-88], *Trichostrongylus colubriformis* [79, 84, 88, 89], *Trichostrongylus vitrines* [88] *Dictyocaulus viviparus* [90], *Teladorsagia circumcincta* [84, 91], *Cooperia curticei* [92]. However, chemical characterisation of PAs in the above and many other studies has been missing and the findings were instead compared to samples where PAs had been deactivated with PEG or polyvinyl polypyrrolidone (PVPP) as it is generally assumed that differences before and after PEG/PVPP treatment can largely be attributed to PAs. However, the efficacy of PAs varied between the different bioassays and nematodes species. Given the variable contents and compositions of forage PAs, chemical characterisation is essential in order to be able to link PA structural characteristics with AH activities.

In vitro studies by Mollan et al. showed that flavan-3-ols that give rise to PDs were particularly potent against the eggs and L1 larvae of *T. colubriformis* in the egg hatching assay (EHA), the larval development assay (LDA) and the larval migration inhibition assay (LMIA) [89]. In the same study extracts from legumes with higher PD/PC ratios also proved more effective compared to those with lower PD/PC ratios. Similarly, the flavan-3-ol monomers that make up PDs inhibited more effectively the exsheathment of L3 from *H. contortus* and *T. colubriformis* than the flavan-3-ols that make up PCs [80]. Interestingly, high molar percentages of PD subunits in a large number of purified PA samples inhibited *H. contortus* but not *T. colubriformis* exsheathment [77]. This suggests different modes of actions against parasites that reside in different sites of the digestive tract (Table 1.1) [77]. The cattle nematodes *Ostertagia ostertagi* and *Cooperia oncophora* were also highly susceptible to PAs with high PD/PC ratios [75, 76]. In accordance with the above findings epigallocatechin and gallocatechin were also more potent than epicatechin and catechin against the swine parasite, *Ascaris suum* [74]. The swine nematode, *Oesophagostomum dentatum*, was also susceptible to several PA extracts expanding the group of parasites that can be inhibited by PAs [73].

PA samples with longer average polymer sizes significantly enhanced the AH activity against *O. ostertagi* and *C. oncophora* [75, 76] and *H. contortus* from ruminants [77] and *A. suum* [74] and *O. dentatum* [73] from pigs. It appears that the stereochemistry of the flavan-3-ol C-ring had a negligible effect on AH activity [80, 89]. However, the galloylation of flavan-3-ol monomers has been linked to enhanced AH efficacy compared to their non-galloylated counterparts when tested against *T. colubriformis* [80, 89] and *H. contortus* [80]. Moreover, recent studies have also provided some evidence that PAs can act synergistically or antagonistically with other naturally occurring compounds against parasites [87, 93].

In vivo investigations have validated some of these *in vitro* results and demonstrated that PA-containing forages can potentially be used to manage parasitic infections without compromising animal welfare or production. Such results have been obtained with sainfoin [62, 79], sulla [94], chicory [95], birdsfoot trefoil [95] and sericea lespedeza [96-99].

Various authors have hypothesised that PAs affect the parasites via two possible mechanisms [21]. The first mode of action implies that PAs interact

directly with the parasite and disrupt several of its important biological functions [16, 88] due to interactions between dietary PAs and nematode proteins [21, 88]. Such interactions could explain the cuticle lesions, other structural damages and the aggregates around the orifices that have been observed by scanning electron microscopy and transmission electron microscopy [16, 73, 74, 76]. The second mechanism assumes an indirect involvement of PAs in the AH effects [21]. It is thought that forage PAs improve the supply of rumen-escape protein to the small intestine, which can boost innate immunity of the host [16, 88]. In addition, parasite death through nutrient deprivation after complexation with PAs has also been proposed [88].

To sum up, considerable progress has been made in establishing which types of PAs can best protect animals from gastrointestinal parasites, however, more work is needed to fully understand the mechanisms. In addition, there is a need to link PA contents and structures to the different life-cycle stages of each nematode species.

1.3.3 Environmental effects

Effects of proanthocyanidins on methane emissions from ruminants

Many studies on global warming have focused on the emissions of CO_2 and CH_4 gases from human activities [18, 100]. However, compared to CO_2, CH_4 is a much more potent greenhouse gas [18] and ruminant animals contribute a large share to the annual total CH_4 production [18]. Such CH_4 losses also translate into substantial energy losses for the animals and consequently impact on the sustainability of farming [18].

Animal feeds are decomposed via fermentation in the rumen in an anaerobic environment in which, the microflora generate H_2 and CO_2. Methanogenic archaea then form CH_4 using H_2 and CO_2 as substrates [18]. Therefore, approaches to suppress CH_4 formation are based on inhibiting methanogenic microorganisms and/or interfering with metabolic processes that increase the H_2 and CO_2 concentrations in the rumen [10, 101].

There is some evidence that bioactive compounds in forages can mitigate methanogenesis from ruminants [11, 17, 18]. Several *in vitro* and some *in vivo*

studies have focused on using dietary PAs to reduce CH_4 production. Hatew et al. evaluated the *in vitro* efficacy of several sainfoin accessions for reducing CH_4 formation [55, 102]. Accessions with high molar percentages of PDs in PAs could be linked to lower CH_4 production, but the impact of PA content was less clear. Bhatta et al. achieved a CH_4 reduction *in vitro* with commercial mixtures of PAs and HTs [103] and *in vitro* methanogenesis was also decreased 25–51% with quebracho PAs in some studies [68]. When sainfoin was incubated in an artificial rumen, CH_4 formation declined as the sainfoin dose increased compared to alfalfa incubations [55]. Big trefoil was found more effective than PA-free lucerne in CH_4 mitigation *in vitro* [101]. In grazing experiments, willow fodder blocks reduced CH_4 emissions by 20% in young sheep compared to a control diet but there was no effect in the 2nd period of the experiment [104]. Moreover, supplementation of forages with black wattle (*Acacia mearnsii*) reduced CH_4 by 13% on average in sheep [105] and a dose response effect was observed in cows [106]. Other *in vivo* studies showed that birdsfoot trefoil reduced the CH_4 emissions in wether sheep but there was not any difference in the CH_4 output of cows compared to the control diet [107]. Interestingly, a reduction of CH_4 emissions in cows was achieved with *Lotus* silage [107] and sulla [108].

There is some evidence that PAs can act selectively against methanogens in the rumen. However, it is important to establish structure-activity relations as there were some apparent inconsistencies. For example, big trefoil fractions with oligomeric PAs did not inhibit two *Methanobrevibacter ruminantium* strains in contrast to a polymeric PA fraction [101]. In addition, there were strain effects, which could have been due to direct action against the methanogens or low amounts of available H_2 for CH_4. Moreover, the concentration of mixtures containing different amounts of HTs and PAs was also an important factor for the reduction of methanogenic populations [103]. In addition, PA effects on protozoal growth and on key enzymes have been proposed as possible mechanisms by few studies but this will require further investigations [17, 18].

Effects of proanthocyanidins on nitrogenous emissions

Apart from CH_4 reductions, forage PAs have also shown potential for reducing environmental N_2O emissions from ruminant production systems [5, 6,

19]. As discussed in Section 1.3.1 ruminants often make inefficient use of dietary protein [5]. This usually leads to increased nitrogen levels in the urine [5, 20]. Urinary nitrogen from urea is readily transformed in the soil to N_2O which is a potent greenhouse gas.

There is some evidence that PA-containing forages can lower urinary nitrogen and thus N_2O emissions from volatilisation [6, 19, 20]. Studies with legume forages such as *Acacia angustissima*, calliandra, leucaena (*Leucaena leucocephala*) [109], sainfoin [110-112] and birdsfoot trefoil [112, 113] have shown efficacy in nitrogen shift from urine to faeces. The replacement of ryegrass with red clover and lucerne showed an effect only with supplements of *Acacia mearnsii* and highlighted the role of PAs as red clover and lucerne are PA-free legumes [105].

To summarise, more *in vivo* studies are required to establish the mechanistic links between PA structures and concentrations on protein digestion, nitrogen flow in the gastrointestinal tract and greenhouse gas emissions [5].

1.4 Chemical analysis of proanthocyanidins

1.4.1 Conventional methods

The vanillin assay

The vanillin assay is simple, inexpensive and specific for flavan-3-ols, PAs and dihydrochalcones [22, 114]. The principle of this assay is based on a condensation reaction of a vanillin carbocation with PAs at positions C6 or C8 of the A-ring under strong acidic conditions (Figure 1.5) [22, 23].

The resulting coloured adduct is measured at 500 nm. However, measurements at this wavelength can be affected by the chlorophyll and anthocyanidins [22]. In addition, several other factors can influence the results such as the type of solvent, the nature and the concentration of the acidic catalyst, the reaction time, the water content and the vanillin concentration [22, 23, 114, 115]. The major problems for PA quantitation emerge from the selection of standards and the fact that the reaction yield is affected by PA subunit composition

and the choice of acidic catalyst [23, 115]. However, it can be used for a rapid, initial screening of large numbers of samples for flavan-3-ol and PAs [22].
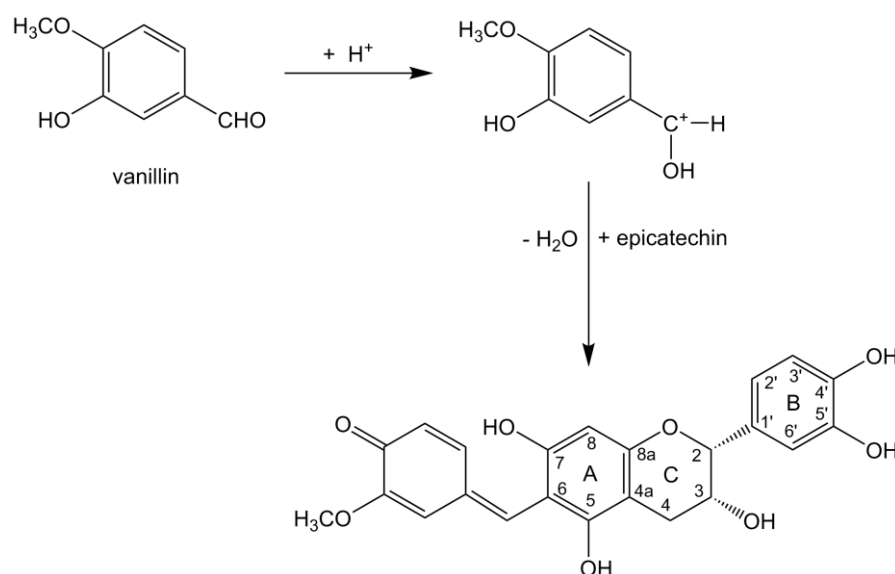
Figure 1.5: Condensation of epicatechin with vanillin, adapted from W. Hummer and P. Schreier, 2008 [22].

The 4-dimethylaminocinnamaldehyde assay

In contrast to the vanillin assay, the 4-dimethylaminocinnamaldehyde (DMACA) reagent reacts only with the terminal units and the coloured product is measured at 640 nm (Figure 1.6) [22]. It is more tolerant to anthocyanin interferences and easier to perform since the reaction occurs at room temperature [22]. However, other aromatic compounds with a 5,7-hydroxylation pattern can also form blue adducts, such as dihydrochalcones [22, 116], and this can limit the specificity of the assay for PAs in some plants.

Despite these shortcomings several studies have used the DMACA assay for PA analysis [117-119]. Histochemical staining of PAs in white clover and birdsfoot trefoil tissues allowed their localisation and identified distinctly different accumulation patterns [120]. Moreover, post-column derivatisation with DMACA has been employed with high performance liquid chromatography (HPLC) analysis of PAs and enabled the determination of flavan-3-ols, PA dimers and trimers in 56 food products [121] and sainfoin [122].
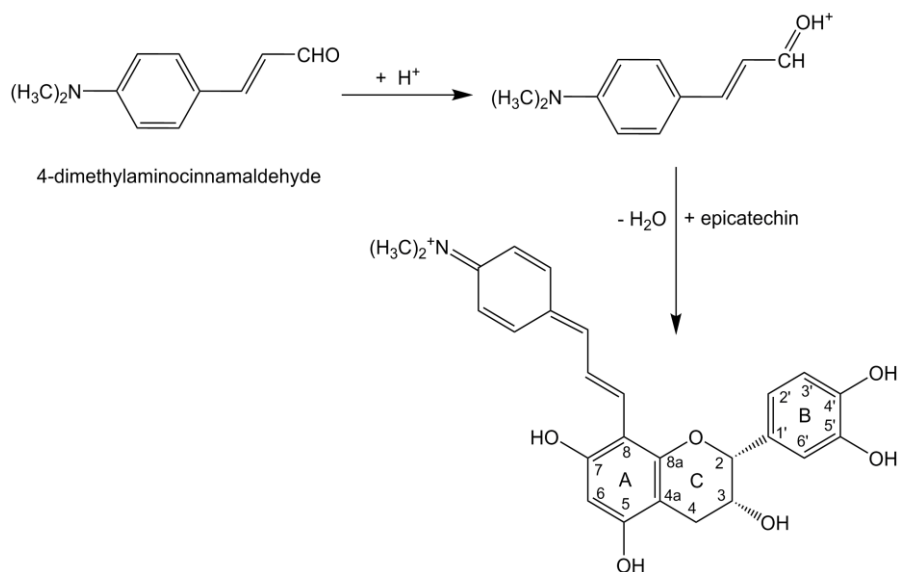
Figure 1.6: Condensation of epicatechin with 4-dimethylaminocinnamahaldehyde, adapted from W. Hummer and P. Schreier, 2008 [22].

The HCl-butanol assay

The HCl-butanol reagent depolymerises PAs under acidic conditions and in the presence of ferric ions (i.e. iron). The extension subunits form carbocations that are readily oxidised to coloured anthocyanidins, whereas the terminal units do not react (Figure 1.7) [22]. The coloured products of the reaction are measured at ca 550 nm [123-125].
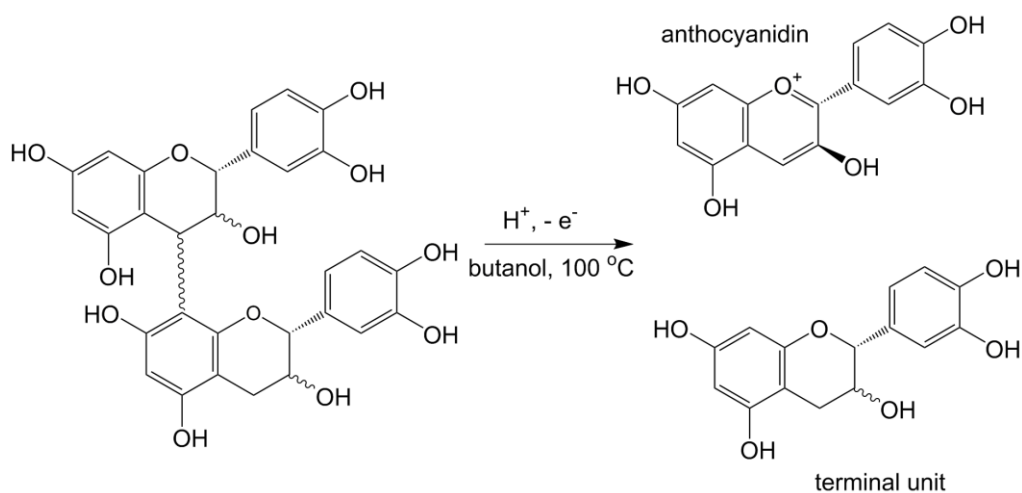
Figure 1.7: Degradation of a procyanidin dimer using the HCl-butanol reagent, adapted from Schofield et al., 2008 [23].

The method has been widely used for the analysis of extractable and bound PAs [22, 23, 124-126]. However, the PA analysis with the HCl-butanol assay also suffers from several limitations [22, 23]. Colour formation is influenced by the hydroxylation pattern, the type of interflavanyl bond of the PAs and the possible side-reactions [22, 23, 125]. Therefore, the use of standards isolated from the study plants has been suggested [22, 23]. In addition, reviews of this assay concluded that colour yields depended on the reaction conditions [22, 23]. For example, the water content, presence of iron (Fe III), the organic solvents, the temperature and heating times can affect the reproducibility of the assay [125, 127, 128]. However, contradictory effects have been reported by a number of studies [23, 125-128]. Finally, studies have also reported that the HCl-butanol reagent does not always interact quantitatively with PAs [23, 128]. As a result, inclusion of acetone as a co-solvent was tested and revealed complete degradation of PAs in *Lotus spp.* by the HCl-butanol assay [128].

To sum up, these colorimetric methods can be used to confirm the presence of PAs in samples and provide semi-quantitative information on total PA contents. However, more work needs to be done on response factors to convert colour yields into PA contents. Currently the modified HCl-butanol-acetone assay [128] is the best assay for determining PA contents, but it requires PA standards that have been analysed for PA contents by other methods such as thiolysis. This area is still evolving as naturally occurring PAs are characterised by an enormous structural complexity and therefore, in depth qualitative and quantitative information is required for understanding their bioactivities.

1.4.2. Derivatisation methods

Benzyl mercaptan and phloroglucinol degradation

Proanthocyanidins can be depolymerised under mild acidic conditions in the presence of an excess of a nucleophile. The extension units are released as reactive carbocations after cleavage and they are attached to the nucleophile whilst the terminal units are released as free flavan-3-ols [37, 129-133]. The nucleophile reagents that are most often used for PA degradation are benzyl mercaptan (BM), alternatively known as toluene-α-thiol, and phloroglucinol,

therefore these reactions are termed thiolysis (Figure 1.8) and phloroglucinolysis [23, 130, 132, 133].
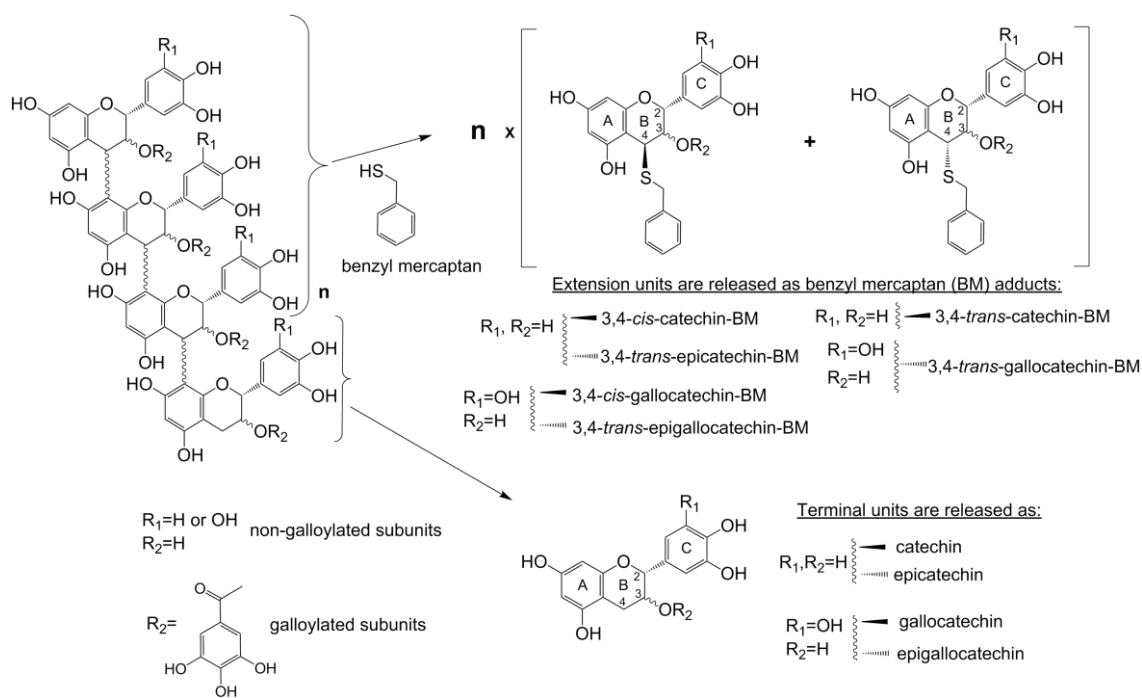
Figure 1.8: Thiolysis of proanthocyanidins, adapted from Gea et al., 2011 [131]. Catechin and gallocatechin extension units are derivatized to the 3,4-*cis* and 3,4-*trans* BM adducts, whereas epicatechin and epigallocatechin are derivatized to the 3,4-*trans* BM adduct

Both reactions do not alter the absolute configuration in the positions C2 and C3 of the C ring [132]. The products from PA cleavage are subsequently analysed by high performance liquid chromatography (HPLC) [130, 132, 133]. The main advantages of these reactions are that they provide qualitative and quantitative information in terms of PA content, flavan-3-ol composition, mean degree of polymerisation (mDP), PC/PD and *cis/trans* ratios, once the response factors of all degradation products are known [37, 130-132, 134]. Another advantage is that PA quantification and structural information is possible after direct application of the nucleophile reagents to the plant matrices. Thus, PA contents and compositions from sainfoin [131, 135], extracted bark residues [136, 137], pellets of sericea lespedeza [39], apple [138, 139], coffee pulp [140] and plums [141] have been determined after *in situ* depolymerisation. However, the acidic degradation with

nucleophiles is limited to PCs, PDs and PPs as PFs, PGs and A-type PAs are not as readily cleaved to their subunits [23, 134, 142].

Several studies have reported differences in the performance of BM and phloroglucinol for PA depolymerisation. The reaction with BM resulted in higher total yields of the products compared to phloroglucinol degradation of PAs that have been extracted from pine barks [132]. Moreover, Kennedy et al. showed that the concentration of phloroglucinol affected the mDP values and the subunit composition [143]. W. Hummer and P. Schreier suggested that the heterogeneity of interflavanyl bonds could affect the depolymerisation efficiency [22]. For these reasons BM is preferred as the nucleophile despite its unpleasant odour [23].

To sum up, experimental parameters such as temperature [131, 132], reaction time [130-132, 143, 144], water content [132, 143] and reagent concentrations [132] may lead to incomplete or side reactions, degradation and epimerisation of the products. Therefore, the reaction parameters should be carefully optimised to exploit this simple, sensitive and inexpensive thiolysis method for PA characterisation.

1.4.3. Chromatographic methods

Reverse-phase high performance liquid chromatography

The use of reverse-phase (RP)-HPLC methods for the separation and detection of PAs is very common [22, 145, 146] and instruments equipped with ultra-violet (UV), diode array detectors (DADs) or fluorescence detectors allow their detection via characteristic spectra [22, 145]. The UV spectra from PAs present two absorption maxima at 220 nm and 280 nm [22, 147]. However, these maxima are not affected by the MW and thus they cannot distinguish between monomeric flavan-3-ols and PA oligomers or polymers [147].

The stationary phase in RP columns is less polar than the mobile phase and therefore a binary solvent system (e.g. water/methanol) elutes the compounds on a decreasing polarity basis [145]. Therefore, compounds with more hydroxyl groups elute earlier than those with less hydroxyl groups [121]. Moreover, a flavan-3-ol with 2*R*:3*S* stereochemistry in the C-ring will elute earlier than its

2*R*:3*R* stereoisomer. Hence, the different flavan-3-ols elute in the following order [133]:

gallocatechin < epigallocatechin < catechin < epicatechin

The retention of PAs is also affected by the type of interflavanyl bonds. If oligomeric PAs contain C4-C6 and/or A-type interflavanyl bonds, they are retained more strongly on the column than PAs with C4-C8 linkages [121]. Moreover, galloylation of monomeric flavan-3-ols delays the elution from the column as well [121, 147]. Given the great complexity of PAs in plant samples, their complete separation with RP columns is impossible. Hence, only small oligomers are detected as distinct peaks and they do not elute according to their MWs [22]. Larger oligomers and polymers tend to elute as a non-resolved hump and there are peak overlaps with other plant compounds [148-150]. Therefore, pre-column (e.g. thiolysis) or post-column (e.g. DMACA) derivatisation and coupling with mass spectrometry techniques are used to tackle the incomplete separation of PAs by RP-HPLC [22, 145, 146].

Normal-phase high performance liquid chromatography

The elution in normal-phase (NP)-HPLC is quite different to RP-HPLC. PAs can be eluted according to MW, which means that a partial separation can be achieved even with compounds of the same degree of polymerisation [22, 145]. It is thus possible to separate PAs up to decamers but polymeric PAs cluster as a late eluting, unresolved peak [151-156].

The NP-HPLC methods are suitable for the separation and analysis of homopolymeric PA oligomers. However, peak resolution deteriorates if PAs are substituted PAs (e.g. galloylated) or heteropolymers [145, 157]. Another drawback of this technique is the nature of the mobile phases. Chlorinated solvents pose a hazard to the environment and care is required for their disposal [116, 145]. In addition, when NP-HPLC is used for preparative work, the eluent might cause problems with subsequent assays. Chlorinated solvents may also lead to strong adsorption of PAs on columns as these eluents are poorly miscible with water [158]. Despite some useful applications of NP-HPLC in food analysis [154, 159,

160], the disadvantages of these harmful solvents cannot be overlooked. Therefore, new stationary phases have been designed for more user-friendly solvents that can function in the NP-HPLC mode [161].

Hydrophilic interaction chromatography

Hydrophilic interaction chromatography (HILIC) is a relatively new technique for PA separation. The HILIC columns contain diols, amides or zwitterionic packing materials that have different selectivity than RP-HPLC but retain the separation mode of NP-HPLC and can utilise the safer RP-HPLC solvents [158, 161]. According to Yanagida et al. the polarity of PA molecules increases with MW and this decreases their solubility in organic solvents, hence HILIC columns operating with aqueous solvents have different retention mechanisms and are more suitable for PA separation [162]. Thus, diol-phase columns enabled the separations of PAs from cocoa seeds [161], from apples [162, 163], and from birch bark up to 14-mers [158]. A recent study used a HILIC column with different packing material for the separation of PAs from sea buckthorn berries [164].

It has been suggested that hetero-polymeric PAs, that consist for instance of both PC and PD subunits, do not elute from HILIC columns according to their MWs [158]. Substituents (e.g. galloyl groups) and the numerous isomers that can exist in large PA compounds will also complicate these separations [164].

Novel approaches for proanthocyanidin separation

Given that different PA classes co-exist in the form of complex polymeric mixtures in plants, researchers continue to investigate new approaches for PA separation. The enormous structural diversity of PAs in a sample, therefore, requires combinatorial separation and detection methods to collect multidimensional information [165]. Kalili et al. developed an off-line two-dimensional (2D) liquid chromatography (LC) method that was used for apple and cocoa PAs [163]. This aimed to acquire firstly information on PA size by HILIC separation and secondly on PA isomers via their hydrophobicity by RP-HPLC. An online combination of HILIC and RP-HPLC separations was then used for the analysis of tea polyphenols and grape PAs [166, 167]. Although the complete

separation of all compounds was not possible, the method reduced peak overlap and simplified data interpretation by plotting extracted ion contours in two dimensions and by accurate mass determinations. Other researchers have also proposed the consecutive use of columns with different chromatographic modes [168, 169]. This online coupling has shown poor peak resolution compared to off-line or stop-flow concepts; however, 2D chromatography seems to have potential for future optimisation of PA profiling [170, 171].

1.4.4. Mass spectrometric methods

Liquid chromatography - mass spectrometry

Recent advances in mass spectrometry (MS) have provided advanced analytical tools for investigating PA compositions. These MS methods enable the selective and highly sensitive identification and quantification of PAs from crude extracts [145, 172, 173].

The mass spectrometers are equipped with interfaces that ionise the molecules. The positively or negatively charged molecules are transferred into the gas phase and their separation is based on their different mass-to-charge (*m/z*) ratios [174]. This process is highly dependent on the ion source and the analyser. Although several ion sources have been used for the ionisation of PAs, electrospray ionisation (ESI) is the most widely used [175]. The charged droplets formed by ESI are evaporated, and ions of a particular polarity are directed by the applied current into the mass spectrometer [176]. The ESI is fast, sensitive and can be used either in direct infusion experiments or in conjunction with HPLC and ultra-performance liquid chromatography (UPLC) [172, 174, 177]. This ionisation interface is also compatible with several different analysers such as quadrupoles, time-of-flight (TOF), ion-trap and Fourier transform ion cyclotron resonance [174, 178]. ESI is a mild ionisation technique, which mostly generates molecular ion peaks and only few fragments [151, 179]. It also leads to the formation of multiply charged ions (Table 1.3), which facilitate PA analysis since the resulting *m/z* values can be assigned to polymers of quite large molecular sizes [148, 156, 158, 160, 179].

Table 1.3: Characteristic *m/z* values of ions corresponding to procyanidin polymers that were obtained with ESI-mass spectrometry operating in a deprotonating mode; adapted from Hammerstone et al., 1999 [156]. DP: degree of polymerisation

DP	Molecular ion	Multiply charged ions	
	$[M-H]^-$	$[M-2H]^{2-}$	$[M-3H]^{3-}$
1	289	-	-
2	577	-	-
3	865	-	-
4	1153	576	-
5	1441	720	-
6	1729	864	-
7	2017	1008	672
8	2305	1152	768
9	2593	1296	864
10	2881	1440	960

The isotopic pattern of these peaks is derived from the natural isotopic distribution of ^{13}C [148, 174]. However, some researchers cautioned that if large hetero-polymeric PAs are present the multiply charged ions complicate peak interpretations due to overlap and therefore ESI may not be suited to such samples [160, 174, 180]. Some reports have also stated that ESI, when operated in a deprotonating mode, tended to decompose multiply charged polymers and cleaved them further. Therefore, a cascade of reactions can take place and singly charged fragments belonging to a larger polymer can be detected [160, 180].

Despite these shortcomings, the ESI has made important contributions to PA analysis. Depending on the type of analyser and the careful selection of experimental parameters ESI can via specific fragmentation patterns provide information on PA polymers [148, 151, 177, 180], the type and the sequence of consisting subunits within oligomers [160, 181, 182], the type of interflavanyl bonds [142, 160, 182-184] and the presence of substituents [142, 166, 174, 185, 186]. Figure 1.9 briefly presents the 3 most documented ESI fragmentation patterns of PAs. However, ESI-MS cannot elucidate the absolute configuration of chiral centres and the site of interflavanyl bonds [160, 177].
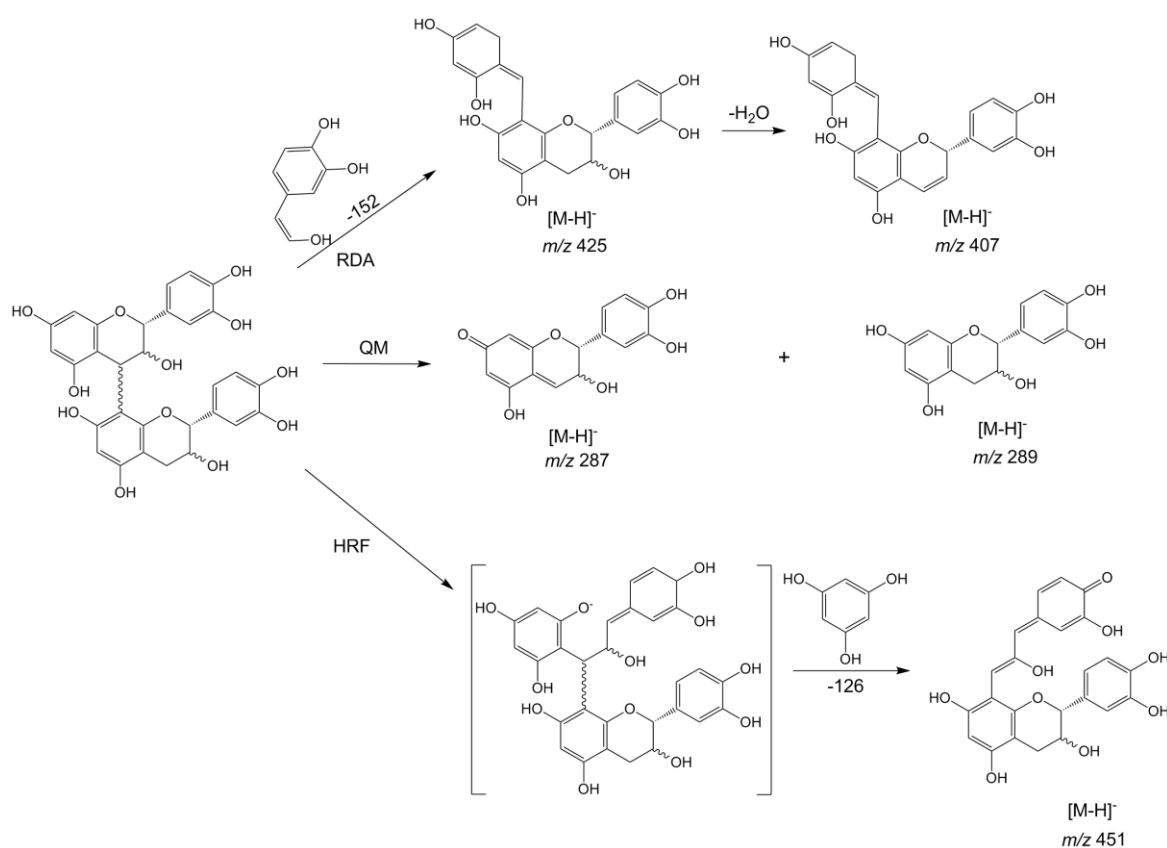
Figure 1.9: Fragmentation pathway of a procyanidin dimer in negative ion mode by ESI-MS, adapted from Gu et al. 2003 [160] and D. Callemien and S. Collin, 2008 [187]. The fragmentation mechanisms are: retro-Diels-Alder fragmentation (RDA), quinone methide cleavage (QM) and heterocyclic ring fission (HRF).

Matrix-assisted laser desorption/ionisation

The matrix-assisted laser desorption/ionisation (MALDI) is an MS technique, which requires the mixing of the analyte with a liquid or solid matrix, usually an aromatic organic acid. A small aliquot of the mixture is spotted on a MALDI target. Evaporation of the solvent leads to crystallisation. The sample spot is then irradiated with a laser beam. Thus the matrix is vaporised and the analyte is desorbed into the gas phase and ionised [174, 188]. The majority of MALDI instruments operate with a UV nitrogen laser but infrared laser systems are also used [188]. This ionisation technique is most often coupled with TOF analysers, which separate the ions of different *m/z* values according to the time they need to reach the detector [188, 189]. The lighter ions will be then detected first followed by the heavier ones.

MALDI-TOF MS is a soft ionisation technique that produces generally only a singly charged molecular ion for each PA compound, therefore this technique is ideally suited for the analysis of complex PAs [188, 190]. In addition, the relative simple and cheap TOF analysers can provide high mass resolution, which allows the interpretation of isotopic peak patterns [188, 190, 191].

Although, MALDI MS has been used for many different types of PAs, the actual mechanism behind this process has not been yet fully elucidated [188]. The matrix selection is particularly critical for data acquisition as there is no theoretical model that can link analyte and matrix structures to optimal MALDI-TOF MS performance. Thus, several different matrices have been used successfully for PAs from various plant sources. Matrix studies have concluded that *trans*-3-indole acrylic acid (*t*-IAA), 2,5-hydroxyl-benzoic acid (DHB) and a DHB mixture with 2-hydroxy-5-methoxybenzoic acid (HMB)(s-DHB, DHB:HMB, 9:1 w/w) are more suitable for PA analysis than α-cyano-4-hydroxycinnamic acid (CHCA), sinapinic acid (SA), dithranol, 2,6-dihydroxyacetophenone (DHAP) and 2,4,6-trihydroxyacetophenone (THAP) [31, 188, 192, 193]. If ionisation is problematic then the sample-matrix mixture can be fortified with a cationising agent, such as organic or inorganic salts; this can minimise the noise and decrease the signals from other salts in the sample [188]. The use of NaCl, NaI, LiBr and caesium trifluoro-acetate is well documented for PA analysis [28, 31, 188, 190, 194-197].

Peak assignments are based on a comparison with the predicted *m/z* PA values. The following formula is used for estimating *m/z* values of hetero-polymeric PAs and also covers the possible presence of galloyl residues. Calculation of the molecular weight also needs to include the cation:

$$m/z \,(\text{PA}) = (m/z\, 288.08)n + (m/z)(2 \times 1.0078) + (m/z\, 16)\alpha + (m/z\, 152)b + (m/z)\, s$$

where (m/z) 288.08 corresponds to the molecular weight of one extender catechin or epicatechin unit (MW = 288.08 amu), n denotes the degree of polymerisation (DP), 2×1.0078 stands for one H in each of the top and bottom units, α accounts for the number of the gallocatechin or epigallocatechin units ($\Delta m = 16\, \text{amu}$), b represents the number of galloyl residues ($\Delta m = 152\, \text{amu}$), and s is the molecular weight of the cation used for the ionisation (Na$^+$, Li$^+$ or Cs$^+$). If a glycosyl group is

present another term needs to be added: $(m/z\,162)g$, where g represents the number of the glycosyl groups ($\Delta m = 162\,\mathrm{amu}$) [31, 196].

Despite the advantages of MALDI-TOF MS for detecting individual PA molecules, several issues remain. Weak co-crystallisation of the sample with the matrix can result in spot-to-spot variation of the MS signal and sample spots can be damaged by the laser [31, 192]. Spotting of the same sample on different targets can also produce different spectra [188, 198]. A serious issue in PA analysis by MALDI MS is the correct assignment of peaks that differ by $\Delta m = 16\,\mathrm{amu}$. PAs readily form adducts with sodium and potassium ions i.e. [M+Na]$^+$ and [M+K]$^+$. The atomic mass difference between K$^+$ and Na$^+$ is $\Delta m = 16\,\mathrm{amu}$ but this mass difference also corresponds to an additional oxygen atom in the polymer. Since, many PA molecules also differ from each other by just one oxygen atom, this complicates the assignments [190]. Therefore, several authors suggested that mass spectra should be compared after using more than one cationising agents such as Li$^+$ or Cs$^+$ [31, 188, 191, 197].

The mass spectra also depend on whether they have been collected in the linear or reflectron mode [188]. Linear mode enables the detection of larger PAs, whereas peak resolution and signal-to-noise ratio is better in the reflectron mode. An important drawback of this technique is the fact that detection of large PA polymers is problematic due to suppression of ionisation, lower desorption efficiency and adduct cluster formation due to in-source fragmentation. These problems, combined with the lack of standards prevent quantification of PAs by MALDI-TOF MS [188, 190]. In addition, there can be problems with the interpretation of the spectra with complex isotopic patterns. Peaks can be also misinterpreted because a difference of 2 amu be due to either the co-existence of A-type and B-type PA molecules or extensive fragmentation within the instrument [31, 190]. However, methods for the deconvolution of A-type and B-type PAs have now been developed and can partly address this issue [31, 191, 198].

1.4.5. Nuclear magnetic resonance methods

Solution-state nuclear magnetic resonance

Nuclear magnetic resonance (NMR) is a useful tool for the structural elucidation of complex PAs [22]. This technique is based on the overall spin change of ^{1}H and ^{13}C nuclei when a magnetic field is applied. The magnetic field and the molecular structure define the resonance frequency, whilst the environment of a particular nucleus causes a characteristic shift of the resonance line within the chemical structure. Therefore, NMR unlike MS can provide information on the absolute configuration at the C2 and C3 positions of the C-ring (*cis/trans*), the type of interflavanyl linkage (A- or B-type) and their location (C4-C6 or C4-C8), the flavan-3-ol subunit composition and the average number of monomeric subunits [26, 199-202]. However, the rotation around the interflavanyl bonds is sterically hindered and this causes peak broadening [200, 203]. Initially, this problem was tackled with derivatising PAs into peracetates or methyl ether acetates [200, 202] or collecting spectra at high (100 °C) [203], low (e.g. -20 °C and -40 °C) [204] or various temperatures from -60 °C to 50 °C [205]. These approaches sharpened the peaks although the high temperatures can decompose PAs.

The ^{1}H NMR spectra provide information on protons in the C-ring with signals between δ 2.6-5.5 ppm, and the A- and B-rings with signals between δ 6.0-7.8 ppm. Information on the stereochemistry of the C-ring can also be acquired since the signals of the 2,3 *cis, trans* isomers do not overlap [204, 206]. The chemical shifts of C4-C6 and C4-C8 interflavanyl bonds were identified at δ 4.58 ppm and δ 4.91-4.97 ppm respectively [26]. In general, the interpretation of ^{1}H NMR spectra is complicated due to band broadening and peak overlap, especially at ambient temperatures [200, 204].

In contrast to ^{1}H NMR spectra, the collection of ^{13}C NMR spectra is often more informative for PA structural elucidation. Substitution patterns of the A- and B-rings, stereochemistry and substitution of the C-ring and often the position of the interflavanyl bonds, can be identified from the chemical shifts [43, 199, 200, 204, 207]. The signals from the C-ring can be found between δ 25-85 ppm, whereas the signals from the A-and B-ring resonances are located between δ 96-160 ppm. The

configuration of the C3 can also be identified, since the 2,3 *trans* structure causes a shift near *δ* 84 ppm whereas the 2,3 *cis* causes a shift near *δ* 77 ppm. It has been demonstrated that the PC/PD ratio can be obtained from the integrated signals that correspond to the hydroxyl groups of the B-ring [41, 199, 208, 209]. In addition, the resonance caused by C3 can be used to distinguish between extension (*δ* 72-73) and terminal units (*δ* 67-68). Therefore, the degree of polymerisation can also be estimated, but this becomes more difficult if A-type bonds are present [199, 205, 209].

Two-dimensional nuclear magnetic resonance

The developments of 2D NMR techniques have added substantial new information to our understanding of the structural complexity of PAs. Moreover, small sample quantities can be used without the need for derivatisation [200]. Several NMR experiments have been performed using correlation spectroscopy (COSY), heteronuclear shift correlation (HETCOR), heteronuclear multiple quantum correlation (HMQC), heteronuclear multiple bond correlation (HMBC) and heteronuclear single quantum coherence (HSQC) experiments [36, 200-202, 204-206, 210, 211]. The COSY experiments measure the 2D correlation of *J*-couplings between neighbouring protons in a bond. The HETCOR, HMQC and HMBC techniques are based on hetero-nuclei correlations between carbon and hydrogen. From these techniques, HETCOR informs about the presence of directly linked carbons and protons. In contrast, HMQC and HMBC experiments are based on indirect detection of a carbon-proton bond, through proton signalling. HMQC provides information on direct carbon-proton coupling, but HMBC measures longer range couplings over 2 to 3 bonds. A combination of these techniques can clearly discriminate between the isomers and unambiguously assign peaks [200, 204, 206, 212]. A recently developed HSQC method allowed quantification of PC/PD and *cis*/*trans* ratios within PA mixtures and is an alternative to thiolysis-HPLC analysis [211]. A novel approach was recently published based on phosphitylation to label model PAs and HTs followed by subsequent analysis of the ^{31}P-NMR spectra that could distinguish several types of reactive hydroxyl groups [213, 214]. Finally, HSQC analysis of PAs is also possible by dissolving plant tissues in

solvent mixtures that form gels and generates a sufficiently sensitive signal response without the need for first extracting PAs [128].

Solid-state nuclear magnetic resonance

In contrast to solution-state NMR experiments, in the solid-state experiments many interactions between the spin and its surroundings are anisotropic. For example, the magnitude of the interaction is a function of the orientation of the (molecular) fragment containing the spin relative to the direction of the magnetic field B_0. The majority of cases requires the consideration of anisotropic interactions such as the dipole-dipole interaction, the chemical shift anisotropy and the electrical quadrupole interactions for spins with I>1/2 [215].

Since solid-state NMR requires a minimum of sample preparation and can generate PA fingerprint spectra, this technique has found many applications. For instance, qualitative assessments of PA concentrations in pine needles were used as a marker for their decomposition [216]. Solid-state NMR analysis of *Acacia mangium* showed that these PAs were linked mainly via C4-C6 rather than C4-C8 bonds between the subunits [189]. Solid-state ^{13}C NMR spectroscopy on extracted residues has also shown that PA concentrations were underestimated by the HCl-butanol assay that was used in the study [124]. A cross-polarisation (CP) mass angle spinning (MAS) ^{13}C NMR analysis of several nut species provided information on PA content and composition [217]. The same technique was also used to evaluate the PA differences of vegetable tanned leather and other tanning processes [218] and to compare the PA contents and extraction efficiencies in several *Acacia* species [219].

To summarise, sections 1.3 and 1.4 presented the potential of PA-containing forages for improving animal nutrition and health and described what is currently known about the mechanisms that may be responsible for their bioactivities. In addition, this chapter provided an overview of the analytical challenges that remain when PA contents and compositions are determined. One particular PA-containing forage, sainfoin, was examined in detail in an interdisciplinary research project "Healthy Hay" that was funded by the European Union (MRTN-CT-2006-035805). "Healthy Hay" produced new knowledge on the phylogeny and agronomy of sainfoin, on the complexity of sainfoin PAs and their

contributions to nutrition, health and welfare of ruminant livestock. It also laid the foundation for another interdisciplinary research project, the "LegumePlus" project, which is described below.

1.5. The "LegumePlus" project

The studies presented in this thesis were conducted as part of a four year EU Marie Curie Initial Training Network entitled 'Optimising plant polyphenols in legumes for ruminant nutrition plus health plus environmental sustainability ("LegumePlus" project, PITN-GA-2011-289377). This project investigated the efficacy of plant PAs to: i) improve protein use efficiency, ii) reduce methane gas production and biohydrogenation, iii) improve milk and meat products, iv) inhibit parasite nematodes and v) to integrate and generate knowledge to improve selected European legumes. These objectives required interdisciplinary expertise and, therefore, 14 research teams from European scientific institutions formed a consortium to work on 7 workpackages (WPs) (Figure 1.10).
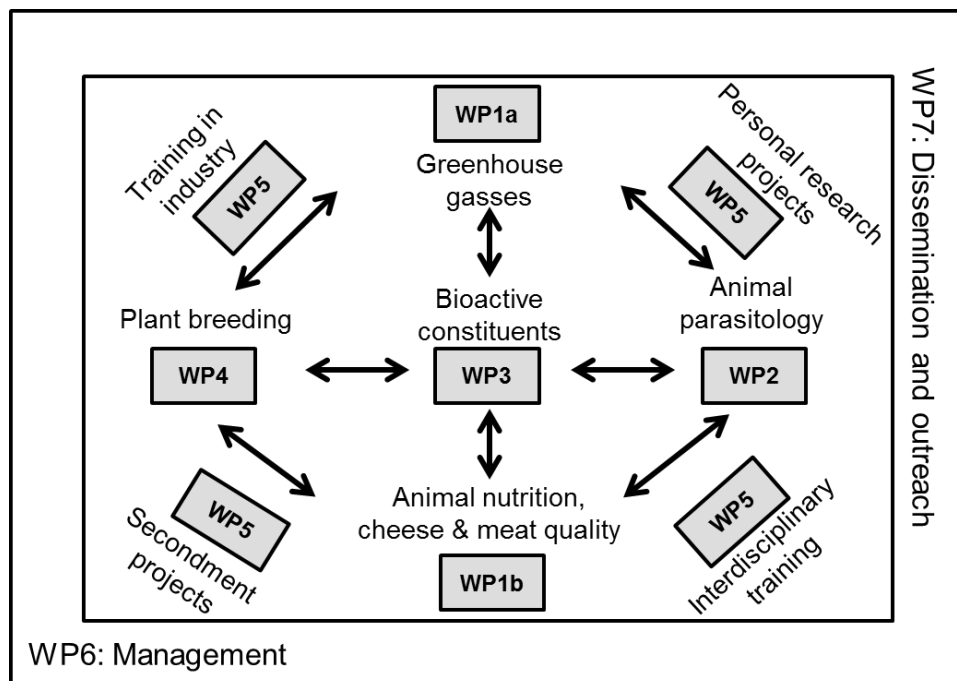
Figure 1.10: Schematic representation of "LegumePlus" project organisation.

WP1 studied the effects of bioactive legumes on nutrient use, environmental losses and ruminant product quality. WP2 investigated the mode of action of bioactive legumes and model PAs against parasitic gastro-intestinal nematodes. WP3 focused on chemical identification of bioactive plant compounds. WP4 worked on the agronomy and the development of molecular markers for a new sainfoin breeding programme and also included an integration of knowledge in order to improve sainfoin and birdsfoot trefoil. WP5 dealt with network wide training activities and WP6 was dedicated to ITN management. Finally, the dissemination and outreach activities fell under the WP7.

The "LegumePlus" network consisted of the following partners from 6 European countries:

- University of Reading (Reading, UK)
- National Institute of Agricultural Botany (Cambridge, UK)
- Institute of Biological, Environmental and Rural Sciences (Aberystwyth, UK)
- Institute for Livestock Sciences (Posieux, Switzerland)
- Institute for Sustainability Sciences (Zurich, Switzerland)
- University of Copenhagen (Copenhagen, Denmark)
- IHAP/INRA (Toulouse, France)
- DAPL/INRA (Theix, France)
- Wageningen University and Research Centrum (Wageningen, The Netherlands)
- University of Turku (Turku, Finland)
- Delley Samen und Pflanzen AG (Delley, Switzerland)
- Cotswold Seeds Ltd (Moreton in Marsh, UK)
- AECS QuikPrep Ltd (UK)
- NIR Consult (UK)
- Think write (Bristol, UK)

The research described in this thesis contributed to WP1, WP2, WP3, WP7 and included also collaborations with Dr Marica Engström (who held an individual PhD fellowship), Dr Andrew Williams (who held a fellowship from the Danish Council for Independent Research), Dr John Grabber and Dr Wayne Zeller (USDA, Madison, Wisconsin). The present studies focused on:

- Identification of contrasting PAs from different plant sources and subsequent characterisation of extracts and purified fractions by thiolysis-HPLC (WP3).

- Characterisation of model PAs with a suite of complementary techniques (WP3).

- Comparison of thiolysis-HPLC and UPLC-ESI-MS/MS methods for the chemical analysis of PAs in sainfoin extracts (WP3).

- Creation of several series of purified PAs with narrow ranges of structural features and evaluation of their *in vitro* anti-parasitic properties for establishing structure-activity relationships (WP2, WP3).

- Development of a ^{13}C CPMAS NMR method for the *in situ* analysis of sainfoin plants (WP1, WP3).

- Extracts and purified fractions of contrasting PAs were supplied to "LegumePlus" partners to enable studies on nutrient use and environmental losses (Wageningen University, WP1), the mode of action of bioactive PAs against parasitic nematodes (IHAP/INRA, University of Copenhagen and other collaborations, WP2) and chemical method developments (University of Turku and other collaborations, WP3).

- Results were presented at conferences and in peer reviewed publications (WP7).

1.6. Research aims and thesis organisation

The first part of this thesis describes the identification of PAs from different plant sources in order to obtain PAs with contrasting characteristics. This covered the chemical analysis of extracts and purified fractions with complementary methods. These model PAs were used to support the development of quantification methods and to determine their bioactivities. Furthermore, methods that can provide structural information at a molecular level of PAs, in samples and in plants, can shed light on molecular distribution profiles and can be used to probe structure-activity relationships. The plan was that this could help to select forages with desired bioactivities rapidly and support the breeding of new plant

varieties with optimised bioactivities. Thus, the studies of this thesis had the following specific objectives:

- To extract and isolate PAs with contrasting structural features regarding flavan-3-ol subunit contents and cover a range of average molecular sizes.
- To analyse a subset of these contrasting PAs with several complementary techniques and evaluate the results and methods.
- To perform rapid screening for PAs in sainfoin samples using two analytical methods and compare the quality of the data.
- To evaluate whether RP-HPLC separation can be used to create PA series with narrow average sizes.
- To link contrasting PA structures to their *in vitro* anti-parasitic activity of *Haemonchus contortus*.
- To develop a solid-state NMR for the rapid screening of sainfoin accessions.
- To provide project partners and other collaborators with extracts and fractions of contrasting PAs for chemical and biological measurements.

The thesis is organised as follows:

Chapter 2 describes the screening of plants and seeds for contrasting PAs.

Chapter 3 provides information on the characterisation of purified PA samples with complementary techniques and discusses the pros and cons of the methods.

Chapter 4 compares an established method (thiolysis-HPLC) and a novel (UPLC-ESI-MS/MS) for the analysis of sainfoin extracts.

Chapter 5 describes the creation of model PAs using semi-preparative HPLC and their subsequent assessment for *in vitro* anti-parasitic activity.

Chapter 6 presents the development of a ^{13}C CPMAS NMR experiment for the laboratory based selection of sainfoin accessions according to PA content and composition.

Chapter 7 provides a summary of the studies and information on the collaborations between the author, "LegumePlus" colleagues and other partners.

Appendix A contains supporting information on the analysis of model PA samples. The author of this thesis contributed with PA samples and their analysis to several publications (Appendices B-J).

References

1. Barry TN, McNabb WC: **The implications of condensed tannins on the nutritive value of temperate forages fed to ruminants**. *The British Journal of Nutrition* 1999, 81(4):263-272.

2. Salminen JP, Karonen M, Sinkkonen J: **Chemical ecology of tannins: Recent developments in tannin chemistry reveal new structures and structure-activity patterns**. *Chemistry* 2011, 17(10):2806-2816.

3. Dixon RA, Xie DY, Sharma SB: **Proanthocyanidins - a final frontier in flavonoid research?** *The New Phytologist* 2005, 165(1):9-28.

4. Santos-Buelga C, Scalbert A: **Proanthocyanidins and tannin-like compounds - nature, occurrence, dietary intake and effects on nutrition and health.** *Journal of the Science of Food and Agriculture* 2000, 80(7):1094-1117.

5. Mueller-Harvey I: **Unravelling the conundrum of tannins in animal nutrition and health.** *Journal of the Science of Food and Agriculture* 2006, 86(13):2010-2037.

6. Waghorn G: **Beneficial and detrimental effects of dietary condensed tannins for sustainable sheep and goat production - Progress and challenges.** *Animal Feed Science and Technology* 2008, 147(1-3):116-139.

7. Aron PM, Kennedy JA: **Flavan-3-ols: Nature, occurrence and biological activity.** *Molecular Nutrition & Food Research* 2008, 52(1):79-104.

8. Reed JD: **Nutritional toxicology of tannins and related polyphenols in forage legumes.** *Journal of Animal Science* 1995, 73(5):1516-1528.

9. Min BR, Barry TN, Attwood GT, McNabb WC: **The effect of condensed tannins on the nutrition and health of ruminants fed fresh temperate forages: A review.** *Animal Feed Science and Technology* 2003, 106(1-4):3-19.

10. Piluzza G, Sulas L, Bullitta S: **Tannins in forage plants and their role in animal husbandry and environmental sustainability: A review.** *Grass and Forage Science* 2014, 69(1):32-48.

11. Rochfort S, Parker AJ, Dunshea FR: **Plant bioactives for ruminant health and productivity.** *Phytochemistry* 2008, 69(2):299-322.

12. McMahon LR, McAllister TA, Berg BP, Majak W, Acharya SN, Popp JD, Coulman BE, Wang Y, Cheng KJ: **A review of the effects of forage condensed tannins on ruminal fermentation and bloat in grazing cattle.** *Canadian Journal of Plant Science* 2000, 80(3):469-485.

13. Wang YX, Majak W, McAllister TA: **Frothy bloat in ruminants: Cause, occurrence, and mitigation strategies.** *Animal Feed Science and Technology* 2012, 172(1-2):103-114.

14. Athanasiadou S, Kyriazakis I: **Plant secondary metabolites: Antiparasitic effects and their role in ruminant production systems.** *Proceedings of the Nutrition Society* 2004, 63(4):631-639.

15. Githiori JB, Athanasiadou S, Thamsborg SM: **Use of plants in novel approaches for control of gastrointestinal helminths in livestock with emphasis on small ruminants.** *Veterinary Parasitology* 2006, 139(4):308-320.

16. Hoste H, Jackson F, Athanasiadou S, Thamsborg SM, Hoskin SO: **The effects of tannin-rich plants on parasitic nematodes in ruminants.** *Trends in Parasitology* 2006, 22(6):253-261.

17. Patra AK, Saxena J: **A new perspective on the use of plant secondary metabolites to inhibit methanogenesis in the rumen.** *Phytochemistry* 2010, 71(11-12):1198-1222.

18. Bodas R, Prieto N, Garcia-Gonzalez R, Andres S, Giraldez FJ, Lopez S: **Manipulation of rumen fermentation and methane production with plant secondary metabolites.** *Animal Feed Science and Technology* 2012, 176(1-4):78-93.

19. Aerts RJ, Barry TN, McNabb WC: **Polyphenols and agriculture: Beneficial effects of proanthocyanidins in forages.** *Agriculture, Ecosystems & Environment* 1999, 75(1-2):1-12.

20. Makkar HPS: **Effects and fate of tannins in ruminant animals, adaptation to tannins, and strategies to overcome detrimental effects of feeding tannin-rich feeds.** *Small Ruminant Research* 2003, 49(3):241-256.

21. Hoste H, Martinez-Ortiz-De-Montellano C, Manolaraki F, Brunet S, Ojeda-Robertos N, Fourquaux I, Torres-Acosta JF, Sandoval-Castro CA: **Direct and indirect effects of bioactive tannin-rich tropical and temperate legumes against nematode infections.** *Veterinary Parasitology* 2012, 186(1-2):18-27.

22. Hummer W, Schreier P: **Analysis of proanthocyanidins.** *Molecular Nutrition & Food Research* 2008, 52(12):1381-1398.

23. Schofield P, Mbugua DM, Pell AN: **Analysis of condensed tannins: A review.** *Animal Feed Science and Technology* 2001, 91(1-2):21-40.

24. Van Alstyne KL, McCarthy JJ, Hustead CL, Kearns LJ: **Phlorotannin allocation among tissues of northeastern Pacific kelps and rockweeds.** *Journal of Phycology* 1999, 35(3):483-492.

25. Shibata T, Kawaguchi S, Hama Y, Inagaki M, Yamaguchi K, Nakamura T: **Local and chemical distribution of phlorotannins in brown algae.** *Journal of Applied Phycology* 2004, 16(4):291-296.

26. Nonaka GI, Hsu FL, Nishioka I: **Structures of dimeric, trimeric, and tetrameric procyanidins from *Areca Catechu* L.** *Journal of Chemical Society, Chemical Communications* 1981(15):781-783.

27. Porter LJ: **Flavans and proanthocyanidins. In: *The Flavonoids: Advances in Research since 1980.*** Edited by Harborne JB. Boston, MA: Springer US; 1988: 21-62.

28. Krueger CG, Vestling MM, Reed JD: **Matrix-assisted laser desorption/ionization time-of-flight mass spectrometry of heteropolyflavan-3ols and glucosylated heteropolyflavans in sorghum [*Sorghum bicolor* (L.) Moench].** *Journal of Agricultural and Food Chemistry* 2003, 51(3):538-543.

29. Ferreira D, Slade D: **Oligomeric proanthocyanidins: Naturally occurring O-heterocycles.** *Natural Products Reports* 2002, 19(5):517-541.

30. Ojwang LO, Yang L, Dykes L, Awika J: **Proanthocyanidin profile of cowpea (*Vigna unguiculata*) reveals catechin-O-glucoside as the dominant compound.** *Food Chemistry* 2013, 139(1-4):35-43.

31. Stringano E, Cramer R, Hayes W, Smith C, Gibson T, Mueller-Harvey I**: Deciphering the complexity of sainfoin (*Onobrychis viciifolia*) proanthocyanidins by MALDI-TOF mass spectrometry with a judicious choice of isotope patterns and matrixes.** *Analytical Chemistry* 2011, 83(11):4147-4153.

32. Min BR, Attwood GT, McNabb WC, Molan AL, Barry TN: **The effect of condensed tannins from *Lotus corniculatus* on the proteolytic activities and growth of rumen bacteria.** *Animal Feed Science and Technology* 2005, 121(1-2):45-58.

33. Malisch CS, Luscher A, Baert N, Engstrom MT, Studer B, Fryganas C, Suter D, Mueller-Harvey I, Salminen JP: **Large variability of proanthocyanidin content and composition in sainfoin (*Onobrychis viciifolia*).** *Journal of Agricultural and Food Chemistry* 2015, 63(47):10234-10242.

34. Marais JP, Mueller-Harvey I, Brandt EV, Ferreira D: **Polyphenols, condensed tannins, and other natural products in *Onobrychis viciifolia* (sainfoin).** *Journal of Agricultural and Food Chemistry* 2000, 48(8):3440-3447.

35. Theodoridou K, Aufrere J, Andueza D, Le Morvan A, Picard F, Stringano E, Pourrat J, Mueller-Harvey I, Baumont R: **Effect of plant development during first and second growth cycle on chemical composition, condensed tannins and nutritive value of three sainfoin (*Onobrychis viciifolia*) varieties and lucerne.** *Grass and Forage Science* 2011, 66(3):402-414.

36. Foo LY, Newman R, Waghorn G, McNabb WC, Ulyatt MJ: **Proanthocyanidins from *Lotus corniculatus*.** *Phytochemistry* 1996, 41(2):617-624.

37. Meagher LP, Lane G, Sivakumaran S, Tavendale MH, Fraser K: **Characterization of condensed tannins from *Lotus* species by thiolytic degradation and electrospray mass spectrometry.** *Animal Feed Science and Technology* 2004, 117(1-2):151-163.

38. Foo LY, Lu Y, McNabb WC, Waghorn G, Ulyatt MJ: **Proanthocyanidins from *Lotus pedunculatus*.** *Phytochemistry* 1997, 45(8):1689-1696.

39. Kommuru DS, Barker T, Desai S, Burke JM, Ramsay A, Mueller-Harvey I, Miller JE, Mosjidis JA, Kamisetti N, Terrill TH: **Use of pelleted sericea lespedeza (*Lespedeza cuneata*) for natural control of coccidia and gastrointestinal nematodes in weaned goats.** *Veterinary Parasitology* 2014, 204(3-4):191-198.

40. Tibe O, Meagher LP, Fraser K, Harding DR: **Condensed tannins and flavonoids from the forage legume sulla (*Hedysarum coronarium*).** *Journal of Agricultural and Food Chemistry* 2011, 59(17):9402-9409.

41. Sivakumaran S, Molan AL, Meagher LP, Kolb B, Foo LY, Lane GA, Attwood GA, Fraser K, Tavendale M: **Variation in antimicrobial action of proanthocyanidins from *Dorycnium rectum* against rumen bacteria.** *Phytochemistry* 2004, 65(17):2485-2497.

42. Rubanza CDK, Shem MN, Ichinohe T, Fujihara T: **Quantification and characterisation of condensed tannin of selected indigenous browse tree species leaves of north-western Tanzania.** *Journal of Food Agriculture and Environment* 2008, 6(2):145-149.

43. Foo LY, Lu Y, Molan AL, Woodfield DR, McNabb WC: **The phenols and prodelphinidins of white clover flowers.** *Phytochemistry* 2000, 54(5):539-548.

44. Meagher LP, Widdup K, Sivakumaran S, Lucas R, Rumball W: **Floral *Trifolium* proanthocyanidins: Polyphenol formation and compositional diversity.** *Journal of Agricultural and Food Chemistry* 2006, 54(15):5482-5488.

45. Burggraaf V, Waghorn G, Woodward S, Thom E**: Effects of condensed tannins in white clover flowers on their digestion *in vitro*.** *Animal Feed Science and Technology* 2008, 142(1-2):44-58.

46. Hagerman AE, Butler LG: **The specificity of proanthocyanidin-protein interactions.** *The Journal of Biological Chemistry* 1981, 256(9):4494-4497.

47. Wang YX, McAllister TA, Acharya S: **Condensed tannins in sainfoin: Composition, concentration, and effects on nutritive and feeding value of sainfoin forage.** *Crop Science* 2015, 55(1):13-22.

48. Waghorn G, Jones W, Shelton I, McNabb W: **Condensed tannins and the nutritive value of herbage.** In: *Proceedings of the New Zealand Grassland Association* 1990: 171-176.

49. Scharenberg A, Arrigo Y, Gutzwiller A, Soliva CR, Wyss U, Kreuzer M, Dohme F: **Palatability in sheep and *in vitro* nutritional value of dried and ensiled sainfoin (*Onobrychis viciifolia*), birdsfoot trefoil (*Lotus corniculatus*), and chicory (*Cichorium intybus*).** *Archives of Animal Nutrition* 2007, 61(6):481-496.

50. Decandia M, Sitzia M, Cabiddu A, Kababya D, Molle G: **The use of polyethylene glycol to reduce the anti-nutritional effects of tannins in goats fed woody species.** *Small Ruminant Research* 2000, 38(2):157-164.

51. Terrill TH, Windham WR, Hoveland CS, Amos HE: **Forage preservation method Influences on tannin concentration, intake, and digestibility of sericea lespedeza by sheep.** *Agronomy Journal* 1989, 81(3):435-439.

52. Hedqvist H, Mueller-Harvey I, Reed JD, Krueger CG, Murphy M: **Characterisation of tannins and *in vitro* protein digestibility of several *Lotus corniculatus* varieties.** *Animal Feed Science and Technology* 2000, 87(1-2):41-56.

53. Jones WT, Mangan JL: **Complexes of the condensed tannins of sainfoin (*Onobrychis viciifolia* Scop.) with fraction 1 leaf protein and with submaxillary mucoprotein, and their reversal by polyethylene glycol and pH.** *Journal of the Science of Food and Agriculture* 1977, 28(2):126-136.

54. McNabb WC, Peters JS, Foo LY, Waghorn GC, Jackson FS: **Effect of condensed tannins prepared from several forages on the *in vitro* precipitation of ribulose-1,5-bisphosphate carboxylase (Rubisco) protein and its digestion by trypsin (EC 2.4.21.4) and chymotrypsin (EC 2.4.21.1).** *Journal of the Science of Food and Agriculture* 1998, 77(2):201-212.

55. McMahon LR, Majak W, McAllister TA, Hall JW, Jones GA, Popp JD, Cheng KJ: **Effect of sainfoin on *in vitro* digestion of fresh alfalfa and bloat in steers.** *Canadian Journal of Animal Science* 1999, 79(2):203-212.

56. Scalbert A: **Antimicrobial properties of tannins.** *Phytochemistry* 1991, 30(12):3875-3883.

57. Jones GA, McAllister TA, Muir AD, Cheng KJ: **Effects of sainfoin (*Onobrychis viciifolia* Scop.) condensed tannins on growth and proteolysis by four strains of ruminal bacteria.** *Applied and Environmental Microbiology* 1994, 60(4):1374-1378.

58. McAllister TA, Martinez T, Bae HD, Muir AD, Yanke LJ, Jones GA: **Characterization of condensed tannins purified from legume forages: Chromophore production, protein precipitation, and inhibitory effects on cellulose digestion.** *Journal of Chemical Ecology* 2005, 31(9):2049-2068.

59. Kumar R, Singh M: **Tannins - their adverse role in ruminant nutrition.** *Journal of Agricultural and Food Chemistry* 1984, 32(3):447-453.

60. Vasta V, Nudda A, Cannas A, Lanza M, Priolo A: **Alternative feed resources and their effects on the quality of meat and milk from small ruminants.** *Animal Feed Science and Technology* 2008, 147(1-3):223-246.

61. Girard M, Dohme-Meier F, Wechsler D, Goy D, Kreuzer M, Bee G: **Ability of 3 tanniferous forage legumes to modify quality of milk and Gruyere-type cheese.** *Journal of Dairy Science* 2016, 99(1):205-220.

62. Hoste H, Gaillard L, Le Frileux Y: **Consequences of the regular distribution of sainfoin hay on gastrointestinal parasitism with nematodes and milk production in dairy goats.** *Small Ruminant Research* 2005, 59(2-3):265-271.

63. Molle G, Decandia M, Giovanetti V, Cabiddu A, Fois N, Sitzia M: **Responses to condensed tannins of flowering sulla (*Hedysarum coronarium* L.) grazed by dairy sheep Part 1: Effects on feeding behaviour, intake, diet digestibility and performance.** *Livestock Science* 2009, 123(2-3):138-146.

64. Priolo A, Bella M, Lanza M, Galofaro V, Biondi L, Barbagallo D, Salem HB, Pennisi P: **Carcass and meat quality of lambs fed fresh sulla (*Hedysarum coronarium* L.) with or without polyethylene glycol or concentrate.** *Small Ruminant Research* 2005, 59(2-3):281-288.

65. Priolo A, Waghorn GC, Lanza M, Biondi L, Pennisi P: **Polyethylene glycol as a means for reducing the impact of condensed tannins in carob pulp: Effects on lamb growth performance and meat quality.** *Journal of Animal Science* 2000, 78(4):810-816.

66. Hoste H, Torres-Acosta JF, Sandoval-Castro CA, Mueller-Harvey I, Sotiraki S, Louvandini H, Thamsborg SM, Terrill TH: **Tannin containing legumes as a model for nutraceuticals against digestive parasites in livestock.** *Veterinary Parasitology* 2015, 212(1-2):5-17.

67. Athanasiadou S, Kyriazakis I: **Plant secondary metabolites: Antiparasitic effects and their role in ruminant production systems.** *Proceedings of the Nutrition Society* 2007, 63(04):631-639.

68. Min BR, Pinchak WE, Anderson RC, Fulford JD, Puchala R: **Effects of condensed tannins supplementation level on weight gain and *in vitro* and *in vivo* bloat precursors in steers grazing winter wheat.** *Journal of Animal Science* 2006, 84(9):2546-2554.

69. Terrill TH, Miller JE, Burke JM, Mosjidis JA, Kaplan RM: **Experiences with integrated concepts for the control of *Haemonchus contortus* in sheep and goats in the United States.** *Veterinary Parasitology* 2012, 186(1-2):28-37.

70. Hoste H, Torres-Acosta JF: **Non chemical control of helminths in ruminants: Adapting solutions for changing worms in a changing world.** *Veterinary Parasitology* 2011, 180(1-2):144-154.

71. Waller PJ: **Sustainable nematode parasite control strategies for ruminant livestock by grazing management and biological control.** *Animal Feed Science and Technology* 2006, 126(3-4):277-289.

72. Hoste H, Torres-Acosta JFJ, Quijada J, Chan-Perez I, Dakheel MM, Kommuru DS, Mueller-Harvey I, Terrill TH: **Chapter Seven - Interactions between nutrition and infections with *Haemonchus contortus* and related gastrointestinal nematodes in small ruminants.** In: *Advances in Parasitology.* Edited by Robin BG, Georg Von S-H, vol. Volume 93: Academic Press; 2016: 239-351.

73. Williams AR, Ropiak HM, Fryganas C, Desrues O, Mueller-Harvey I, Thamsborg SM: **Assessment of the anthelmintic activity of medicinal plant extracts and purified condensed tannins against free-living and parasitic stages of *Oesophagostomum dentatum*.** *Parasites & Vectors* 2014, 7(1):518.

74. Williams AR, Fryganas C, Ramsay A, Mueller-Harvey I, Thamsborg SM: **Direct anthelmintic effects of condensed tannins from diverse plant sources against *Ascaris suum*.** *PLoS One* 2014, 9(5):e97053.

75. Novobilsky A, Stringano E, Hayot Carbonero C, Smith LM, Enemark HL, Mueller-Harvey I, Thamsborg SM: ***In vitro* effects of extracts and purified tannins of sainfoin (*Onobrychis viciifolia*) against two cattle nematodes.** *Veterinary Parasitology* 2013, 196(3-4):532-537.

76. Desrues O, Fryganas C, Ropiak HM, Mueller-Harvey I, Enemark HL, Thamsborg SM: **Impact of chemical structure of flavanol monomers and condensed tannins on *in vitro* anthelmintic activity against bovine nematodes.** *Parasitology* 2016, 143(4):444-454.

77. Quijada J, Fryganas C, Ropiak HM, Ramsay A, Mueller-Harvey I, Hoste H: **Anthelmintic activities against *Haemonchus contortus* or *Trichostrongylus colubriformis* from small ruminants are influenced by structural features of condensed tannins.** *Journal of Agricultural and Food Chemistry* 2015, 63(28):6346-6354.

78. Bahuaud D, Martinez-Ortiz de Montellano C, Chauveau S, Prevot F, Torres-Acosta F, Fouraste I, Hoste H: **Effects of four tanniferous plant extracts on the *in vitro* exsheathment of third-stage larvae of parasitic nematodes.** *Parasitology* 2006, 132(Pt 4):545-554.

79. Manolaraki F, Sotiraki S, Stefanakis A, Skampardonis V, Volanis M, Hoste H: **Anthelmintic activity of some Mediterranean browse plants against parasitic nematodes.** *Parasitology* 2010, 137(4):685-696.

80. Brunet S, Hoste H: **Monomers of condensed tannins affect the larval exsheathment of parasitic nematodes of ruminants.** *Journal of Agricultural and Food Chemistry* 2006, 54(20):7481-7487.

81. Hounzangbe-Adote MS, Paolini V, Fouraste I, Moutairou K, Hoste H: ***In vitro* effects of four tropical plants on three life-cycle stages of the parasitic nematode, *Haemonchus contortus*.** *Research in Veterianry Science* 2005, 78(2):155-160.

82. Moreno-Gonzalo J, Manolaraki F, Frutos P, Hervas G, Celaya R, Osoro K, Ortega-Mora LM, Hoste H, Ferre I: ***In vitro* effect of heather extracts on *Trichostrongylus colubriformis* eggs, larvae and adults.** *Veterinary Parasitology* 2013, 197(3-4):586-594.

83. Moreno-Gonzalo J, Manolaraki F, Frutos P, Hervas G, Celaya R, Osoro K, Ortega-Mora LM, Hoste H, Ferre I: ***In vitro* effect of heather (*Ericaceae*) extracts on different development stages of *Teladorsagia circumcincta* and *Haemonchus contortus*.** *Veterinary Parasitology* 2013, 197(1-2):235-243.

84. Paolini V, Fouraste I, Hoste H: ***In vitro* effects of three woody plant and sainfoin extracts on 3rd-stage larvae and adult worms of three gastrointestinal nematodes.** *Parasitology* 2004, 129(Pt 1):69-77.

85. Barrau E, Fabre N, Fouraste I, Hoste H: **Effect of bioactive compounds from sainfoin (*Onobrychis viciifolia* Scop.) on the *in vitro* larval migration of *Haemonchus contortus*: Role of tannins and flavonol glycosides.** *Parasitology* 2005, 131(Pt 4):531-538.

86. Alonso-Diaz MA, Torres-Acosta JF, Sandoval-Castro CA, Hoste H: **Comparing the sensitivity of two *in vitro* assays to evaluate the anthelmintic activity of tropical tannin rich plant extracts against *Haemonchus contortus*.** *Veterinary Parasitology* 2011, 181(2-4):360-364.

87. Vargas-Magana JJ, Torres-Acosta JF, Aguilar-Caballero AJ, Sandoval-Castro CA, Hoste H, Chan-Perez JA: **Anthelmintic activity of acetone-water extracts against *Haemonchus contortus* eggs: Interactions between tannins and other plant secondary compounds.** *Veterinary Parasitology* 2014, 206(3-4):322-327.

88. Athanasiadou S, Kyriazakis I, Jackson F, Coop RL: **Direct anthelmintic effects of condensed tannins towards different gastrointestinal nematodes of sheep: *In vitro* and *in vivo* studies.** *Veterinary Parasitology* 2001, 99(3):205-219.

89. Molan AL, Meagher LP, Spencer PA, Sivakumaran S: **Effect of flavan-3-ols on *in vitro* egg hatching, larval development and viability of infective larvae of *Trichostrongylus colubriformis*.** *International Journal for Parasitology* 2003, 33(14):1691-1698.

90. Molan AL, Hoskin SO, Barry TN, McNabb WC: **Effect of condensed tannins extracted from four forages on the viability of the larvae of deer lungworms and gastrointestinal nematodes.** *The Veterinary Record* 2000, 147(2):44-48.

91. Brunet S, Jackson F, Hoste H: **Effects of sainfoin (*Onobrychis viciifolia*) extract and monomers of condensed tannins on the association of abomasal nematode larvae with fundic explants.** *International Journal for Parasitology* 2008, 38(7):783-790.

92. **Heckendorn F, Haring DA, Maurer V, Zinsstag J, Langhans W, Hertzberg H: Effect of sainfoin (*Onobrychis viciifolia*) silage and hay on established populations of *Haemonchus contortus* and *Cooperia curticei* in lambs.** *Veterinary Parasitology* 2006, 142(3-4):293-300.

93. Klongsiriwet C, Quijada J, Williams AR, Mueller-Harvey I, Williamson EM, Hoste H: **Synergistic inhibition of *Haemonchus contortus* exsheathment by flavonoid monomers and condensed tannins.** *International Journal for Parasitology Drugs and Drug Resistance* 2015, 5(3):127-134.

94. Niezen JH, Charleston WA, Robertson HA, Shelton D, Waghorn GC, Green R: **The effect of feeding sulla (*Hedysarum coronarium*) or lucerne (*Medicago sativa*) on lamb parasite burdens and development of immunity to gastrointestinal nematodes.** *Veterinary Parasitology* 2002, 105(3):229-245.

95. Heckendorn F, Haring DA, Maurer V, Senn M, Hertzberg H: **Individual administration of three tanniferous forage plants to lambs artificially infected with *Haemonchus contortus* and *Cooperia curticei*.** *Veterinary Parasitology* 2007, 146(1-2):123-134.

96. Joshi BR, Kommuru DS, Terrill TH, Mosjidis JA, Burke JM, Shakya KP, Miller JE**: Effect of feeding sericea lespedeza leaf meal in goats experimentally infected with *Haemonchus contortus*.** *Veterinary Parasitology* 2011, 178(1-2):192-197.

97. Lange KC, Olcott DD, Miller JE, Mosjidis JA, Terrill TH, Burke JM, Kearney MT: **Effect of sericea lespedeza (*Lespedeza cuneata*) fed as hay, on natural and experimental *Haemonchus contortus* infections in lambs.** *Veterinary Parasitology* 2006, 141(3–4):273-278.

98. Shaik SA, Terrill TH, Miller JE, Kouakou B, Kannan G, Kaplan RM, Burke JM, Mosjidis JA: **Sericea lespedeza hay as a natural deworming agent against gastrointestinal nematode infection in goats.** *Veterinary Parasitology* 2006, 139(1–3):150-157.

99. Terrill TH, Mosjidis JA, Moore DA, Shaik SA, Miller JE, Burke JM, Muir JP, Wolfe R: **Effect of pelleting on efficacy of sericea lespedeza hay as a natural dewormer in goats.** *Veterinary Parasitology* 2007, 146(1–2):117-122.

100. Patra AK, Saxena J: **A new perspective on the use of plant secondary metabolites to inhibit methanogenesis in the rumen.** *Phytochemistry* 2010, 71(11–12):1198-1222.

101. Tavendale MH, Meagher LP, Pacheco D, Walker N, Attwood GT, Sivakumaran S: **Methane production from *in vitro* rumen incubations with *Lotus pedunculatus* and *Medicago sativa*, and effects of extractable condensed tannin fractions on methanogenesis.** *Animal Feed Science and Technology* 2005, 123(0):403-419.

102. Hatew B, Hayot Carbonero C, Stringano E, Sales LF, Smith LMJ, Mueller-Harvey I, Hendriks WH, Pellikaan WF: **Diversity of condensed tannin structures affects rumen *in vitro* methane production in sainfoin (*Onobrychis viciifolia*) accessions.** *Grass and Forage Science* 2015, 70(3):474-490.

103. Bhatta R, Uyeno Y, Tajima K, Takenaka A, Yabumoto Y, Nonaka I, Enishi O, Kurihara M: **Difference in the nature of tannins on *in vitro* ruminal methane and volatile fatty acid**

production and on methanogenic archaea and protozoal populations. *Journal of Dairy Science* 2009, 92(11):5512-5522.

104. Ramírez-Restrepo CA, Barry TN, Marriner A, López-Villalobos N, McWilliam EL, Lassey KR, Clark H: **Effects of grazing willow fodder blocks upon methane production and blood composition in young sheep.** *Animal Feed Science and Technology* 2010, 155(1):33-43.

105. Carulla JE, Kreuzer M, Machmüller A, Hess HD: **Supplementation of *Acacia mearnsii* tannins decreases methanogenesis and urinary nitrogen in forage-fed sheep.** *Australian Journal of Agricultural Research* 2005, 56(9):961-970.

106. Grainger C, Clarke T, Auldist MJ, Beauchemin KA, McGinn SM, Waghorn GC, Eckard RJ: **Potential use of *Acacia mearnsii* condensed tannins to reduce methane emissions and nitrogen excretion from grazing dairy cows.** *Canadian Journal of Animal Science* 2009, 89(2):241-251.

107. **Woodward SI, Waghorn GC, Ulyatt MJ, Lassey KR: Early indications that feeding *Lotus* will reduce methane emissions from ruminants,** vol. 61: New Zealand Society of Animal Production; 2001.

108. **Woodward SI, Waghorn GC, Lassey KR, Laboyrie PG: Does feeding sulla (*Hedysarum coronarium*) reduce methane emissions from dairy cows?,** vol. 62: New Zealand Society of Animal Production; 2002.

109. Hove L, Topps JH, Sibanda S, Ndlovu LR: **Nutrient intake and utilisation by goats fed dried leaves of the shrub legumes *Acacia angustissima*, *Calliandra calothyrsus* and *Leucaena leucocephala* as supplements to native pasture hay.** *Animal Feed Science and Technology* 2001, 91(1–2):95-106.

110. Theodoridou K, Aufrere J, Andueza D, Pourrat J, Le Morvan A, Stringano E, Mueller-Harvey I, Baumont R: **Effects of condensed tannins in fresh sainfoin (*Onobrychis viciifolia*) on *in vivo* and *in situ* digestion in sheep.** *Animal Feed Science and Technology* 2010, 160(1-2):23-38.

111. Theodoridou K, Aufrère J, Niderkorn V, Andueza D, Le Morvan A, Picard F, Baumont R: *In vitro* **study of the effects of condensed tannins in sainfoin on the digestive process in the rumen at two vegetation cycles.** *Animal Feed Science and Technology* 2011, 170(3–4):147-159.

112. Fraser MD, Fychan R, Jones R: **Voluntary intake, digestibility and nitrogen utilization by sheep fed ensiled forage legumes.** *Grass and Forage Science* 2000, 55(3):271-279.

113. Waghorn GC, Ulyatt MJ, John A, Fisher MT: **The effect of condensed tannins on the site of digestion of amino acids and other nutrients in sheep fed on *Lotus corniculatus* L.** *British Journal of Nutrition* 1987, 57(01):115-126.

114. Butler LG, Price ML, Brotherton JE: **Vanillin assay for Proanthocyanidins (condensed Tannins) - modification of the solvent for estimation of the degree of polymerization.** *Journal of Agricultural and Food Chemistry* 1982, 30(6):1087-1089.

115. Sun BS, Ricardo-da-Silva JM, Spranger I: **Critical factors of vanillin assay for catechins and proanthocyanidins.** *Journal of Agricultural and Food Chemistry* 1998, 46(10):4267-4274.

116. Kelm MA, Hammerstone JF, Schmitz HH: **Identification and quantitation of flavanols and proanthocyanidins in foods: How good are the datas?** *Clinical and Developmental Immunology* 2005, 12(1):35-41.

117. Li YG, Tanner G, Larkin P: **The DMACA-HCl protocol and the threshold proanthocyanidin content for bloat safety in forage legumes.** *Journal of the Science of Food and Agriculture* 1996, 70(1):89-101.

118. Glavnik V, Simonovska B, Vovk I: **Densitometric determination of (+)-catechin and (-)-epicatechin by 4-dimethylaminocinnamaldehyde reagent.** *Journal of Chromatography A* 2009, 1216(20):4485-4491.

119. Treutter D: **Chemical-reaction detection of catechins and proanthocyanidins with 4-dimethylaminocinnamaldehyde.** *Journal of Chromatography* 1989, 467(1):185-193.

120. Abeynayake SW, Panter S, Mouradov A, Spangenberg G: **A high-resolution method for the localization of proanthocyanidins in plant tissues.** *Plant Methods* 2011, 7(1):13.

121. de Pascual-Teresa S, Santos-Buelga C, Rivas-Gonzalo JC: **Quantitative analysis of flavan-3-ols in Spanish foodstuffs and beverages.** *Journal of Agricultural and Food Chemistry* 2000, 48(11):5331-5337.

122. Regos I, Treutter D: **Optimization of a high-performance liquid chromatography method for the analysis of complex polyphenol mixtures and application for sainfoin extracts (*Onobrychis viciifolia*).** *Journal of Chromatography A* 2010, 1217(40):6169-6177.

123. Kosinska A, Chavan UD, Amarowicz R: **Separation of low molecular weight rapeseed proteins by RP-HPLC-DAD - a short report.** *Czech Journal of Food Sciences* 2006, 24(1):41-44.

124. Makkar HPS, Gamble G, Becker K**: Limitation of the butanol-hydrochloric acid-iron assay for bound condensed tannins.** *Food Chemistry* 1999, 66(1):129-133.

125. Porter LJ, Hrstich LN, Chan BG: **The conversion of procyanidins and prodelphinidins to cyanidin and delphinidin.** *Phytochemistry* 1985, 25(1):223-230.

126. Terrill TH, Rowan AM, Douglas GB, Barry TN: **Determination of extractable and bound condensed tannin concentrations in forage plants, protein concentrate meals and cereal grains.** *Journal of the Science of Food and Agriculture* 1992, 58(3):321-329.

127. Dalzell SA, Kerven GL: **A rapid method for the measurement of *Leucaena* spp proanthocyanidins by the proanthocyanidin (butanol/HCl) assay.** *Journal of the Science of Food and Agriculture* 1998, 78(3):405-416.

128. Grabber JH, Zeller WE, Mueller-Harvey I: **Acetone enhances the direct analysis of procyanidin- and prodelphinidin-based condensed tannins in *Lotus* species by the butanol-HCl-iron assay.** *Journal of Agricultural and Food Chemistry* 2013, 61(11):2669-2678.

129. Thompson RS, Jacques D, Haslam E, Tanner RJN: **Plant proanthocyanidins. Part I. Introduction; the isolation, structure, and distribution in nature of plant procyanidins.** *Journal of the Chemical Society, Perkin Transactions 1* 1972(0):1387.

130. Guyot S, Marnet N, Laraba D, Sanoner P, Drilleau JF: **Reversed-phase HPLC following thiolysis for quantitative estimation and characterization of the four main classes of phenolic compounds in different tissue zones of a French cider apple variety (*Malus domestica* var. Kermerrien).** *Journal of Agricultural and Food Chemistry* 1998, 46(5):1698-1705.

131. Gea A, Stringano E, Brown RH, Mueller-Harvey I: *In situ* **analysis and structural elucidation of sainfoin (*Onobrychis viciifolia*) tannins for high-throughput germplasm screening.** *Journal of Agricultural and Food chemistry* 2011, 59(2):495-503.

132. Matthews S, Mila I, Scalbert A, Pollet B, Lapierre C, duPenhoat CLMH, Rolando C, Donnelly DMX: **Method for estimation of proanthocyanidins based on their acid**

depolymerization in the presence of nucleophiles. *Journal of Agricultural and Food chemistry* 1997, 45(4):1195-1201.

133. Koupai-Abyazani MR, McCallum J, Bohm BA: **Identification of the constituent flavanoid units in sainfoin proanthocyanidins by reversed-phase high-performance liquid chromatography.** *Journal of Chromatography A* 1992, 594(1-2):117-123.

134. Ropiak HM, Ramsay A, Mueller-Harvey I: **Condensed tannins in extracts from European medicinal plants and herbal products.** *Journal of Pharmaceutical and Biomedical Analysis* 2016, 121:225-231.

135. Stringano E, Hayot Carbonero C, Smith LM, Brown RH, Mueller-Harvey I: **Proanthocyanidin diversity in the EU 'HealthyHay' sainfoin (*Onobrychis viciifolia*) germplasm collection.** *Phytochemistry* 2012, 77:197-208.

136. Matthews S, Mila I, Scalbert A, Donnelly DMX: **Extractable and non-extractable proanthocyanidins in barks.** *Phytochemistry* 1997, 45(2):405-410.

137. Hellstrom JK, Mattila PH: **HPLC determination of extractable and unextractable proanthocyanidins in plant materials.** *Journal of Agricultural and Food Chemistry* 2008, 56(17):7617-7624.

138. Guyot S, Marnet N, Sanoner P, Drilleau J-F: **Direct thiolysis on crude apple materials for high-performance liquid chromatography characterization and quantification of polyphenols in cider apple tissues and juices.** In: *Methods in Enzymology.* Edited by Lester P, vol. Volume 335: Academic Press; 2001: 57-70.

139. Guyot S, Le Bourvellee C, Marnet N, Drilleau JF: **Procyanidins are the most abundant polyphenols in dessert apples at maturity.** *Lebensmittel-Wissenschaft & Technologie* 2002, 35(3):289-291.

140. Ramirez-Coronel MA, Marnet N, Kolli VS, Roussos S, Guyot S, Augur C: **Characterization and estimation of proanthocyanidins and other phenolics in coffee pulp (*Coffea arabica*) by thiolysis-high-performance liquid chromatography.** *Journal of Agricultural and Food Chemistry* 2004, 52(5):1344-1349.

141. Nunes C, Guyot S, Marnet N, Barros AS, Saraiva JA, Renard CM, Coimbra MA: **Characterization of plum procyanidins by thiolytic depolymerization.** *Journal of Agricultural and Food Chemistry* 2008, 56(13):5188-5196.

142. Gu L, Kelm MA, Hammerstone JF, Beecher G, Holden J, Haytowitz D, Prior RL: **Screening of foods containing proanthocyanidins and their structural characterization using LC-MS/MS and thiolytic degradation.** *Journal of Agricultural and Food Chemistry* 2003, 51(25):7513-7521.

143. Kennedy JA, Jones GP: **Analysis of proanthocyanidin cleavage products following acid-catalysis in the presence of excess phloroglucinol.** *Journal of Agricultural and Food Chemistry* 2001, 49(4):1740-1746.

144. Ramsay A, Drake C, Grosse Brinkhaus A, Girard M, Copani G, Dohme-Meier F, Bee G, Niderkorn V, Mueller-Harvey I: **Sodium hydroxide enhances extractability and analysis of proanthocyanidins in ensiled sainfoin (*Onobrychis viciifolia*).** *Journal of Agricultural and Food Chemistry* 2015, 63(43):9471-9479.

145. Valls J, Millan S, Marti MP, Borras E, Arola L: **Advanced separation methods of food anthocyanins, isoflavones and flavanols.** *Journal of Chromatography A* 2009, 1216(43):7143-7172.

146. Naczk M, Shahidi F: **Phenolics in cereals, fruits and vegetables: Occurrence, extraction and analysis.** *Journal of Pharmaceutical and Biomedical Analysis* 2006, 41(5):1523-1542.

147. Bartolome B, Hernandez T, Bengoechea ML, Quesada C, GomezCordoves C, Estrella I: **Determination of some structural features of procyanidins and related compounds by photodiode-array detection.** *Journal of Chromatography A* 1996, 723(1):19-26.

148. Guyot S, Doco T, Souquet JM, Moutounet M, Drilleau JF: **Characterization of highly polymerized procyanidins in cider apple (*Malus sylvestris* var Kermerrien) skin and pulp.** *Phytochemistry* 1997, 44(2):351-357.

149. Karonen M, Leikas A, Loponen J, Sinkkonen J, Ossipov V, Pihlaja K: **Reversed-phase HPLC-ESI/MS analysis of birch leaf proanthocyanidins after their acidic degradation in the presence of nucleophiles.** *Phytochemical analysis : PCA* 2007, 18(5):378-386.

150. Jerez M, Pinelo M, Sineiro J, Nunez MJ: **Influence of extraction conditions on phenolic yields from pine bark: Assessment of procyanidins polymerization degree by thiolysis.** *Food Chemistry* 2006, 94(3):406-414.

151. Karonen M, Loponen J, Ossipov V, Pihlaja K: **Analysis of procyanidins in pine bark with reversed-phase and normal-phase high-performance liquid chromatography-electrospray ionization mass spectrometry.** *Analytica Chimica Acta* 2004, 522(1):105-112.

152. Gu L, Kelm M, Hammerstone JF, Beecher G, Cunningham D, Vannozzi S, Prior RL: **Fractionation of polymeric procyanidins from lowbush blueberry and quantification of procyanidins in selected foods with an optimized normal-phase HPLC-MS fluorescent detection method.** *Journal of Agricultural and Food Chemistry* 2002, 50(17):4852-4860.

153. Shoji T, Masumoto S, Moriichi N, Kanda T, Ohtake Y: **Apple (*Malus pumila*) procyanidins fractionated according to the degree of polymerization using normal-phase chromatography and characterized by HPLC-ESI/MS and MALDI-TOF/MS.** *Journal of Chromatography A* 2006, 1102(1-2):206-213.

154. Prior RL, Lazarus SA, Cao GH, Muccitelli H, Hammerstone JF: **Identification of procyanidins and anthocyanins in blueberries and cranberries (*Vaccinium* spp.) using high-performance liquid chromatography/mass spectrometry.** *Journal of Agricultural and Food Chemistry* 2001, 49(3):1270-1276.

155. Wu X, Gu L, Prior RL, McKay S: **Characterization of anthocyanins and proanthocyanidins in some cultivars of *Ribes, Aronia,* and *Sambucus* and their antioxidant capacity.** *Journal of Agricultural and Food Chemistry* 2004, 52(26):7846-7856.

156. Hammerstone JF, Lazarus SA, Mitchell AE, Rucker R, Schmitz HH: **Identification of procyanidins in cocoa (*Theobroma cacao*) and chocolate using high-performance liquid chromatography mass spectrometry.** *Journal of Agricultural and Food Chemistry* 1999, 47(2):490-496.

157. Stringano E: **Analysis of sainfoin (*Onobrychis viciifolia*) proanthocyanidins by complementary and newly developed techniques.** *PhD thesis* - University of Reading; 2011.

158. Karonen M, Liimatainen J, Sinkkonen J: **Birch inner bark procyanidins can be resolved with enhanced sensitivity by hydrophilic interaction HPLC-MS.** *Journal of Separation Science* 2011, 34(22):3158-3165.

159. Prior RL, Gu L: **Occurrence and biological significance of proanthocyanidins in the American diet.** *Phytochemistry* 2005, 66(18):2264-2280.

160. Gu L, Kelm MA, Hammerstone JF, Zhang Z, Beecher G, Holden J, Haytowitz D, Prior RL: **Liquid chromatographic/electrospray ionization mass spectrometric studies of proanthocyanidins in foods.** *Journal of Mass Spectrometry : JMS* 2003, 38(12):1272-1280.

161. Kelm MA, Johnson JC, Robbins RJ, Hammerstone JF, Schmitz HH: **High-performance liquid chromatography separation and purification of cacao (*Theobroma cacao* L.) procyanidins according to degree of polymerization using a diol stationary phase.** *Journal of Agricultural and Food Chemistry* 2006, 54(5):1571-1576.

162. Yanagida A, Murao H, Ohnishi-Kameyama M, Yamakawa Y, Shoji A, Tagashira M, Kanda T, Shindo H, Shibusawa Y: **Retention behavior of oligomeric proanthocyanidins in hydrophilic interaction chromatography.** *Journal of Chromatography A* 2007, 1143(1-2):153-161.

163. Kalili KM, de Villiers A: Off-line comprehensive 2-dimensional hydrophilic interaction x reversed phase liquid chromatography analysis of procyanidins. *Journal of Chromatography A* 2009, 1216(35):6274-6284.

164. Kallio H, Yang W, Liu P, Yang B: **Proanthocyanidins in wild sea buckthorn (*Hippophae rhamnoides*) berries analyzed by reversed-phase, normal-phase, and hydrophilic interaction liquid chromatography with UV and MS detection.** *Journal of Agricultural and Food Chemistry* 2014, 62(31):7721-7729.

165. Montero L, Herrero M, Prodanov M, Ibanez E, Cifuentes A: **Characterization of grape seed procyanidins by comprehensive two-dimensional hydrophilic interaction x reversed phase liquid chromatography coupled to diode array detection and tandem mass spectrometry.** *Analytical and Bioanalytical Chemistry* 2013, 405(13):4627-4638.

166. Kalili KM, Vestner J, Stander MA, de Villiers A: **Toward unraveling grape tannin composition: application of online hydrophilic interaction chromatography x reversed-phase liquid chromatography-time-of-flight mass spectrometry for grape seed analysis.** *Analytical Chemistry* 2013, 85(19):9107-9115.

167. Beelders T, Kalili KM, Joubert E, de Beer D, de Villiers A: **Comprehensive two-dimensional liquid chromatographic analysis of rooibos (*Aspalathus linearis*) phenolics.** *Journal of Separation Science* 2012, 35(14):1808-1820.

168. Cacciola F, Jandera P, Blahova E, Mondello L: **Development of different comprehensive two dimensional systems for the separation of phenolic antioxidants.** *Journal of Separation Science* 2006, 29(16):2500-2513.

169. Dugo P, Cacciola F, Herrero M, Donato P, Mondello L: **Use of partially porous column as second dimension in comprehensive two-dimensional system for analysis of polyphenolic antioxidants.** *Journal of Separation Science* 2008, 31(19):3297-3308.

170. Kalili KM, de Villiers A: **Systematic optimisation and evaluation of on-line, off-line and stop-flow comprehensive hydrophilic interaction chromatography × reversed phase liquid chromatographic analysis of procyanidins, Part I: Theoretical considerations.** *Journal of Chromatography A* 2013, 1289:58-68.

171. **Kalili KM, de Villiers A: Systematic optimisation and evaluation of on-line, off-line and stop-flow comprehensive hydrophilic interaction chromatography × reversed phase liquid chromatographic analysis of procyanidins. Part II: Application to cocoa procyanidins.** *Journal of Chromatography A* 2013, 1289:69-79.

172. Motilva MJ, Serra A, Macia A: **Analysis of food polyphenols by ultra high-performance liquid chromatography coupled to mass spectrometry: An overview.** *Journal of Chromatography A* 2013, 1292(0):66-82.

173. Flamini R: **Recent applications of mass spectrometry in the study of grape and wine polyphenols.** *ISRN Spectroscopy* 2013, 2013:1-45.

174. Fulcrand H, Mane C, Preys S, Mazerolles G, Bouchut C, Mazauric JP, Souquet JM, Meudec E, Li Y, Cole RB, Cheynier V: **Direct mass spectrometry approaches to characterize polyphenol composition of complex samples.** *Phytochemistry* 2008, 69(18):3131-3138.

175. Holcapek M, Jirasko R, Lisa M: **Recent developments in liquid chromatography-mass spectrometry and related techniques.** *Journal of Chromatography A* 2012, 1259(0):3-15.

176. Kebarle P, Tang L: **From ions in solution to ions in the gas-phase - the mechanism of electrospray mass-spectrometry.** *Analytical Chemistry* 1993, 65(22):A972-A986.

177. Mari A, Eletto D, Pizza C, Montoro P, Piacente S: **Integrated mass spectrometry approach to profile proanthocyanidins occurring in food supplements: analysis of *Potentilla erecta* L. rhizomes.** *Food Chemistry* 2013, 141(4):4171-4178.

178. Prasain JK, Wang CC, Barnes S: **Mass spectrometric methods for the determination of flavonoids in biological samples.** *Free Radical Biology & Medicine* 2004, 37(9):1324-1350.

179. Friedrich W, Eberhardt A, Galensa R: **Investigation of proanthocyanidins by HPLC with electrospray ionization mass spectrometry.** *European Food Research and Technology* 2000, 211(1):56-64.

180. Mouls L, Mazauric JP, Sommerer N, Fulcrand H, Mazerolles G: **Comprehensive study of condensed tannins by ESI mass spectrometry: Average degree of polymerisation and polymer distribution determination from mass spectra.** *Analytical and Bioanalytical Chemistry* 2011, 400(2):613-623.

181. Li HJ, Deinzer ML: **Tandem mass spectrometry for sequencing proanthocyanidins.** *Analytical Chemistry* 2007, 79(4):1739-1748.

182. Sarnoski PJ, Johnson JV, Reed KA, Tanko JM, O'Keefe SF: **Separation and characterisation of proanthocyanidins in Virginia type peanut skins by LC-MSn.** *Food Chemistry* 2012, 131(3):927-939.

183. Roux EL, Doco T, Sarni-Manchado P, Lozano Y, Cheynier V: **A-type proanthocyanidins from pericarp of *Litchi chinensis.*** *Phytochemistry* 1998, 48(7):1251-1258.

184. Tarascou I, Mazauric JP, Meudec E, Souquet JM, Cunningham D, Nojeim S, Cheynier V, Fulcrand H: **Characterisation of genuine and derived cranberry proanthocyanidins by LC-ESI-MS.** *Food Chemistry* 2011, 128(3):802-810.

185. Tourino S, Fuguet E, Jauregui O, Saura-Calixto F, Cascante M, Torres JL: **High-resolution liquid chromatography/electrospray ionization time-of-flight mass spectrometry combined with liquid chromatography/electrospray ionization tandem mass spectrometry to identify polyphenols from grape antioxidant dietary fiber.** *Rapid Communications in Mass Spectrometry : RCM* 2008, 22(22):3489-3500.

186. Fraser K, Harrison SJ, Lane GA, Otter DE, Hemar Y, Quek SY, Rasmussen S: **HPLC-MS/MS profiling of proanthocyanidins in teas: A comparative study.** *Journal of Food Composition and Analysis* 2012, 26(1-2):43-51.

187. Callemien D, Guyot S, Collin S: **Use of thiolysis hyphenated to RP-HPLC-ESI(-)-MS/MS for the analysis of flavanoids in fresh lager beers.** *Food Chemistry* 2008, 110(4):1012-1018.

188. Monagas M, Quintanilla-Lopez JE, Gomez-Cordoves C, Bartolome B, Lebron-Aguilar R: **MALDI-TOF MS analysis of plant proanthocyanidins.** *Journal of Pharmaceutical and Biomedical Analysis* 2010, 51(2):358-372.

189. Hoong YB, Pizzi A, Md. Tahir P, Pasch H: **Characterization of *Acacia mangium* polyflavonoid tannins by MALDI-TOF mass spectrometry and CP-MAS 13C NMR**. *European Polymer Journal* 2010, 46(6):1268-1277.

190. Reed JD, Krueger CG, Vestling MM: **MALDI-TOF mass spectrometry of oligomeric food polyphenols.** *Phytochemistry* 2005, 66(18):2248-2263.

191. Mateos-Martin ML, Fuguet E, Quero C, Perez-Jimenez J, Torres JL: **New identification of proanthocyanidins in cinnamon (*Cinnamomum zeylanicum* L.) using MALDI-TOF/TOF mass spectrometry.** *Analytical and Bioanalytical Chemistry* 2012, 402(3):1327-1336.

192. Behrens A, Maie N, Knicker H, Kogel-Knabner I: **MALDI-TOF mass spectrometry and PSD fragmentation as means for the analysis of condensed tannins in plant leaves and needles.** *Phytochemistry* 2003, 62(7):1159-1170.

193. Ohnishi-Kameyama M, Yanagida A, Kanda T, Nagata T: **Identification of catechin oligomers from apple (*Malus pumila* cv. Fuji) in matrix-assisted laser desorption/ionization time-of-flight mass spectrometry and fast-atom bombardment mass spectrometry.** *Rapid Communications in Mass Spectrometry : RCM* 1997, 11(1):31-36.

194. Krueger CG, Dopke NC, Treichel PM, Folts J, Reed JD: **Matrix-assisted laser desorption/ionization time-of-flight mass spectrometry of polygalloyl polyflavan-3-ols in grape seed extract.** *Journal of Agricultural and Food Chemistry* 2000, 48(5):1663-1667.

195. Pasch H, Pizzi A, Rode K: **MALDI–TOF mass spectrometry of polyflavonoid tannins.** *Polymer* 2001, 42(18):7531-7539.

196. Vivas N, Nonier MF, de Gaulejac NV, Absalon C, Bertrand A, Mirabel M: **Differentiation of proanthocyanidin tannins from seeds, skins and stems of grapes (*Vitis vinifera*) and heartwood of quebracho (*Schinopsis balansae*) by matrix-assisted laser desorption/ionization time-of-flight mass spectrometry and thioacidolysis/liquid chromatography/electrospray ionization mass spectrometry.** *Analytica Chimica Acta* 2004, 513(1):247-256.

197. Chai WM, Chen CM, Gao YS, Feng HL, Ding YM, Shi Y, Zhou HT, Chen QX: **Structural analysis of proanthocyanidins isolated from fruit stone of Chinese hawthorn with potent antityrosinase and antioxidant activity.** *Journal of Agricultural and Food Chemistry* 2014, 62(1):123-129.

198. Feliciano RP, Krueger CG, Shanmuganayagam D, Vestling MM, Reed JD: **Deconvolution of matrix-assisted laser desorption/ionization time-of-flight mass spectrometry isotope patterns to determine ratios of A-type to B-type interflavan bonds in cranberry proanthocyanidins.** *Food Chemistry* 2012, 135(3):1485-1493.

199. Czochanska Z, Foo LY, Newman RH, Porter LJ: **Polymeric proanthocyanidins - stereochemistry, structural Units, and molecular-weight.** *Journal of the Chemical Society, Perkin Transactions 1* 1980(10):2278-2286.

200. de Bruyne T, Pieters LAC, Dommisse RA, Kolodziej H, Wray V, Domke T, Vlietinck AJ: **Unambiguous assignments for free dimeric proanthocyanidin phenols from 2D NMR.** *Phytochemistry* 1996, 43(1):265-272.

201. Davis AL, Cai Y, Davies AP, Lewis JR: **1H and 13C NMR assignments of some green tea polyphenols.** *Magnetic Resonance in Chemistry* 1996, 34(11):887-890.

202. Balde AM, Pieters LA, Gergely A, Kolodziej H, Claeys M, Vlietinck AJ: **A-Type proanthocyanidins from stem-bark of *Pavetta owariensis*.** *Phytochemistry* 1991, 30(1):337-342.

203. Kolodziej H: **1H NMR spectral studies of procyanidin derivatives: Diagnostic 1H NMR parameters applicable to the structural elucidation of oligomeric procyanidins.** In: *Plant Polyphenols.* Edited by Hemingway R, Laks P, vol. 59: Springer US; 1992: 295-319.

204. Shoji T, Mutsuga M, Nakamura T, Kanda T, Akiyama H, Goda Y: **Isolation and structural elucidation of some procyanidins from apple by low-temperature nuclear magnetic resonance.** *Journal of Agricultural and Food Chemistry* 2003, 51(13):3806-3813.

205. Hellstrom J, Sinkkonen J, Karonen M, Mattila P: **Isolation and structure elucidation of procyanidin oligomers from saskatoon berries (*Amelanchier alnifolia*).** *Journal of Agricultural and Food Chemistry* 2007, 55(1):157-164.

206. Tarascou I, Barathieu K, Simon C, Ducasse MA, Andre Y, Fouquet E, Dufourc EJ, de Freitas V, Laguerre M, Pianet I: **A 3D structural and conformational study of procyanidin dimers in water and hydro-alcoholic media as viewed by NMR and molecular modeling.** *Magnetic Resonance in Chemistry : MRC* 2006, 44(9):868-880.

207. Idowu TO, Ogundaini AO, Salau AO, Obuotor EM, Bezabih M, Abegaz BM: **Doubly linked, A-type proanthocyanidin trimer and other constituents of *Ixora coccinea* leaves and their antioxidant and antibacterial properties.** *Phytochemistry* 2010, 71(17-18):2092-2098.

208. Czochanska Z, Foo LY, Newman RH, Porter LJ, Thomas WA, Jones WT: **Direct proof of a homogeneous polyflavan-3-ol structure for polymeric proanthocyanidins.** *Journal of the Chemical Society, Chemical Communications* 1979(8):375-377.

209. Foo LY, Lu YR, Howell AB, Vorsa N: **The structure of cranberry proanthocyanidins which inhibit adherence of uropathogenic P-fimbriated *Escherichia coli in vitro*.** *Phytochemistry* 2000, 54(2):173-181.

210. Forveffle L: **Multivariate statistical analysis of two-dimensional NMR data to differentiate grapevine cultivars and clones.** *Food Chemistry* 1996, 57(3):441-450.

211. Zeller WE, Ramsay A, Ropiak HM, Fryganas C, Mueller-Harvey I, Brown RH, Drake C, Grabber JH: **1H-13C HSQC NMR spectroscopy for estimating procyanidin/prodelphinidin and cis/trans-flavan-3-ol ratios of condensed tannin samples: Correlation with thiolysis.** *Journal of Agricultural and Food Chemistry* 2015, 63(7):1967-1973.

212. Qaadan F, Nahrstedt A, Schmidt M, Mansoor K: **Polyphenols from *Ginkgo biloba*.** *Scientia Pharmaceutica* 2010, 78(4):897-907.

213. Melone F, Saladino R, Lange H, Crestini C: **Tannin structural elucidation and quantitative 31P NMR analysis. 2. Hydrolyzable tannins and proanthocyanidins.** *Journal of Agricultural and Food Chemistry* 2013, 61(39):9316-9324.

214. Melone F, Saladino R, Lange H, Crestini C: **Tannin structural elucidation and quantitative 31P NMR Analysis. 1. Model Compounds.** *Journal of Agricultural and Food Chemistry* 2013, 61(39):9307-9315.

215. Veeman WS: **Nuclear magnetic resonance, a simple introduction to the principles and applications.** *Geoderma* 1997, 80(3-4):225-242.

216. Parfitt RL, Newman RH: **13C NMR study of pine needle decomposition.** *Plant and Soil* 2000, 219(1/2):273-278.

217. Preston CM, Sayer BG: What's in a nutshell: **An investigation of structure by carbon-13 cross-polarization magic-angle spinning nuclear magnetic resonance spectroscopy.** *Journal of Agricultural and Food Chemistry* 1992, 40(2):206-210.

218. Romer FH, Underwood AP, Senekal ND, Bonnet SL, Duer MJ, Reid DG, van der Westhuizen JH: **Tannin fingerprinting in vegetable tanned leather by solid state NMR spectroscopy and comparison with leathers tanned by other processes.** *Molecules* 2011, 16(2):1240-1252.

219. Reid DG, Bonnet SL, Kemp G, van der Westhuizen JH: **Analysis of commercial proanthocyanidins. Part 4: solid state 13C NMR as a tool for i*n situ* analysis of proanthocyanidin tannins, in heartwood and bark of quebracho and acacia, and related species.** *Phytochemistry* 2013, 94(0):243-248.

Chapter 2. Identification of plant sources containing contrasting proanthocyanidins

Chapter 2 describes the screening of seed and plant matrices for proanthocyanidins (PAs). Initially, the presence of PAs was assessed with the HCl-butanol assay. Subsequently PA content and structural features were determined by thiolytic degradation and HPLC analysis. The aim of this study was to identify readily available sources of PAs with contrasting compositions in order to probe their bioactivities by the author and the LegumePlus partners.

2.1 Introduction

It is important to appreciate that most PAs occur in plants as highly diverse polymeric mixtures of large complexity [1]. The PA concentrations and polymer types are specific to plant species and plant parts [2]. Furthermore, the PA contents and possibly compositions can also be affected by agronomic and climate factors that influence plant metabolic processes and hence PA production [3]. In particular, forage legumes such as sainfoin, *Lotus spp.*, sulla, white clover, and sericea lespedeza have very different PA profiles [4-13], which complicates the measurement of PA contents, profiling their composition and the isolation of individual PA compounds.

Several biological studies with PAs have presented contradictory findings and, therefore, the ability of PAs to add value to ruminant production and the sustainability of production systems has posed challenges [2, 14, 15]. Some *in vivo* and *in vitro* anthelmintic (AH) studies have reported contradictory results that may be linked to PA types, polymer profiles or contents, the target nematode and its niche, the various biological processes of each life-cycle stage and finally the host animal [2, 3, 16, 17]. In addition, a positive AH effect may coincide with an anti-nutritional effect (i.e. decrease in feed intake or protein digestibility) [14, 15]. Similarly, direct and indirect inhibition of rumen methanogenesis could be linked to PA dose, composition and mean degree of polymerisation (mDP) [18, 19]. However, adverse effects on nutrient intake and fermentation processes have been observed and were also dependent on PA chemodiversity [14, 15, 19].

Probing of these PA structure-activity relationships requires accurate quantification and characterisation of PAs that are present in plant tissues or in extracts. Use of different PA types extracted from various plant sources could facilitate the unravelling of their bioactivities. Therefore, purification of model PAs,

which possess small to large mDP values, PC/PD and *cis/trans* ratios within total PAs will be used to test of the following hypotheses:

- There is an optimal mDP value in PA samples that leads to effective parasite control.
- The polymer size of PAs prevails over their PD content in AH activity.
- The gas production (total and methane) are inhibited by PAs of large mDP.
- Purified fractions of contrasting PAs can be used as quantification standards in chemical analyses of complex PAs from a wide range of plant sources.
- A panel of PAs with a wide range of structural characteristics will enable probing of their physicochemical interactions such as chromatography, ionisation and depolymerisation reactions.

Consequently numerous candidates of PA-containing plants were collected and preserved. The initial screening for PAs was performed with a rapid *in situ* HCl-butanol assay. The procedure is simple, fast and PA presence can be easily confirmed through the formation of coloured anthocyanidins. However, quantification can be affected by limitations that are related to the matrix, the reagent or to the reference compound used for quantification [1, 6, 20, 21]. Therefore, this HCl-butanol assay was used only for a qualitative assessment, i.e. presence or absence of PAs. Subsequently, small quantities of PAs were extracted from PA-containing plants. Thiolytic degradation of PAs in these crude extracts was followed by HPLC analysis. This yielded information on flavan-3-ol contents, from which PA content, mDP and PC/PD and *cis/trans* ratios could be determined.

2.2   Materials and methods

2.2.1 Sample collection and treatment

2.2.1.1   Seed samples

Seeds of several plant species were kindly provided by Cotswold Seeds Ltd (COTS, Moreton-in-Marsh, Gloucestershire, UK) and initially stored at -20 °C. Prior to PA screening small quantities of seeds were soaked in acetone/water (1:1 v/v) and crushed with a pestle and mortar. PAs are located in cell walls [2] and vacuoles [22, 23] and crushing can assist the HCl-butanol reagent to interact with PAs during the rapid screening. Post crushing, acetone was evaporated at room temperature. The *in situ* HCl-butanol assay identified several PA sources (Table 2.1). These seed species were then lyophilised and stored at -20 °C. Lyophilised seeds were finely ground using an A-10 S1 Laboratory Grinder (IKA®-Werke GmbH & Co. KG, Staufen, Germany).

2.2.1.2   Plant samples

A large variety of plant species were obtained from the UK, Finland and France, either by the author, colleagues, research partners or associated partners from the LegumePlus consortium and farmers. Fresh samples were air-dried at room temperature or stored at -20 °C and subsequently lyophilised. Prior to PA extraction, samples were ground to pass a 1 mm sieve.

2.2.2 Chemicals and reagents

Hydrochloric acid (36%), formic acid, acetic acid, butan-1-ol, HPLC grade acetone, HPLC grade methanol, HPLC grade dichloromethane, HPLC grade hexane, HPLC grade acetonitrile were purchased from Fisher Scientific (Loughborough, UK). (±) – dihydroquercetin (98%) was from Apin Chemicals (Abingdon, UK). Benzyl mercaptan (BM) was supplied by Sigma-Aldrich (Poole, UK). Deionised water was purified with a Milli-Q system (Millipore, Watford, UK).

2.2.3   Extraction of proanthocyanidins

2.2.3.1   Seed samples

Lyophilised and milled seeds were defatted with hexane in a mass (g) to volume (ml) ratio (1:4.5 w/v). The defatting procedure was performed three times for 30 minutes under sonication [24]. The mixtures were filtered under vacuum and the defatted seed residue left to dry at room temperature for 45 min. Residues were weighed and stored at -20 °C. Defatted seed powder was weighed (1-5 g) into a conical flask. Aqueous acetone (7:3 v/v) was added in a mass to volume ratio (1:10 w/v) and the mixture was stirred for 60 min. Filtration followed and the filtrate was extracted further with dichloromethane (1:5 v/v) to remove lipids. The upper phase was kept and acetone was removed using a rotary evaporator at <37 °C. This yielded the crude PA extract. Extracts were frozen, freeze-dried and finally stored at -20 °C until further analysis.

2.2.3.2   Plant samples

Lyophilised and ground plant tissue (4 g) was weighed into a conical flask and extracted with aqueous acetone (25 ml, 7:3 v/v). The mixture was stirred for 60 min, filtered under vacuum and dichloromethane (12.5 ml) was added to the filtrate to remove lipids and chlorophyll. The mixture was vigorously shaken. The upper phase was collected and the polyphenolic extract concentrated to the water phase under vacuum using a rotatory evaporator at <37 °C. The remaining aqueous solution was centrifuged at 3000 rpm for 6 min. The supernatant with the water soluble polyphenols was transferred to a scintillation vial, lyophilised and stored at -20 °C.

2.2.4   HCl - butanol assay

Dried and finely ground plant or seed tissue (50 mg) was added into 10 ml tubes in triplicate. The HCl-butanol reagent (5 ml, 95:5 v/v) was added to the 10 ml tubes. Two of the replicated samples were placed in a heating block at 100 °C for 60 minutes. The third tube was left at room temperature as a blank as flavan-4-ols and flavan-3,4-diols generate false positives. Red colour in the heated test tubes

and its absence in the blanks confirmed the presence of PAs. The colour generated from the *in situ* reaction of HCl-butanol with hazelnut pericarp was used as positive control for the qualitative evaluation of colour intensity.

2.2.5 Thiolysis

Thiolytic degradation was carried out according to Novobilský et al. [25]. Briefly, 4 mg of crude extract was weighed into 10 ml test tubes and dissolved in 1.5 ml of methanol acidified with 500 µl of 3.3% HCl in methanol (3.3 ml of 36% HCl in 100 ml methanol). Benzyl mercaptan reagent (50 µl) was added and tubes were placed in a stirred water bath (40 °C) for 1 h. The thiolysis reaction was stopped by addition of 1.5 ml of ultra-pure water. Dihydroquercetin was dissolved in methanol at a concentration of 0.047 mg/ml and added (0.5 ml) as an internal standard; test tubes were then mixed and centrifuged prior to HPLC analysis.

2.2.6 HPLC analysis of thiolysis reaction products

The analysis and quantification of reaction products followed the procedures described by Gea et al. [26] and the chromatographic conditions were described in Williams et al. [27]. Samples (20 µl) were injected into an HPLC system connected to an ACE C18 column (3 µm; 250 x 4.6 mm; Hichrom Ltd; Theale; U.K.) fitted with a corresponding ACE guard column and kept at room temperature. The Gilson HPLC system (Anachem Instruments, Luton, U.K.) consisted of a 234 autoinjector, two 306 pumps with 10 SC pump heads, a manometric module 805, a dynamic mixer 811C, and a UVD340U diode array detector (Dionex, Macclesfield, U.K.). Data were acquired with Chromeleon software (version 6.8). The flow rate was 0.75 ml min^{-1} using acetic acid (1%) in water (solvent A) and HPLC-grade acetonitrile (solvent B). The following gradient program was employed: 0-35 min, 36% B; 35-40 min, 36-50% B; 40-45 min, 50-100% B; 45-50 min, 100-0% B; 50-55 min, 0% B. Flavan-3-ol terminal and extension units were identified by their retention times and ultraviolet-visible (UV-vis) spectra between 220 and 595 nm. Peak areas at 280 nm were integrated and quantified using molar response factors relative to dihydroquercetin: 0.30 for terminal units of catechin (C) or epicatechin (EC), 0.06 for terminal units for

gallocatechin (GC) or epigallocatechin (EGC), 0.26 for extension BM adducts of C or EC, and 0.06 for extension BM adducts of GC or EGC [26, 28, 29].

2.2.7 Determination of proanthocyanidin composition

Integration and quantification of peaks provided structural information on the PA content and composition. The average PA size, expressed as mean degree of polymerisation (mDP), was calculated according to Labarbe et al. [30] from the following equation :

$$mDP = \frac{\text{amount of extension and terminal flavan} - 3 - \text{ol units (mol)}}{\text{amount of terminal flavan} - 3 - \text{ol units (mol)}}$$

PC/PD ratios were estimated from the equation presented below:

$$PC/PD = \frac{\text{percentage of catechin} + \text{ epicatechin units (mol)}}{\text{percentage of gallocatechin} + \text{epigallocatechin units (mol)}}$$

Calculation of c*is/trans* flavan-3-ol ratios was based on the following equation:

$$cis/trans = \frac{\text{percentage of epicatechin} + \text{epigallocatechin units (mol)}}{\text{percentage of catechin} + \text{gallocatechin units(mol)}}$$

2.3   Results and discussion

2.3.1   HCl - butanol assay

2.3.1.1   Seed samples

The HCl-butanol assay revealed the presence of PAs in nine out of the thirty tested seed samples. PA-containing seed species are listed in Table 2.1 and seed species without PAs are presented in Table 2.2.

Table 2.1: Summary of seed samples that gave a positive reaction for proanthocyanidins with the HCl-butanol reagent; COTS: Cotswold Seeds Ltd.

Plant material	Lab number	Source/supplier	Part
Pimpinella saxifrage (Burnet forage herb)	LP-13062012-BFH	COTS	Seeds
Rumex acetosa (Common sorrel wildflower)	LP-13062012-CSW	COTS	Seeds
Trifolium hybridum (Dawn alsike clover)	LP-13062012-DAC	COTS	Seeds
Ranunculus acris (Meadow buttercup wildflower)	LP-13062012-MBW	COTS	Seeds
Filipendula ulmaria (Meadowsweet wildflower)	LP-13062012-MW	COTS	Seeds
Silene dioica (Red campion wildflower)	LP-13062012-RCW	COTS	Seeds
Trifolium pratense (Red clover; Milvus var.)	LP-13062012-MRC	COTS	Seeds
Sanguisorba minor (Salad burnet wildfower)	LP-13062012-SBW	COTS	Seeds
Silene latifolia (White campion wildflower)	LP-13062012-WCW	COTS	Seeds

Table 2.2: Summary of seed samples that gave a negative reaction for proanthocyanidins with the HCl-butanol reagent; COTS: Cotswold Seeds Ltd.

Plant material	Lab number	Source/supplier	Part
Trifolium repens (White clover; AberHerald var.)	LP-13062012-WC	COTS	Seeds
Lotus corniculatus (Birdsfoot trefoil; Leo var)	LP-13062012-LBT	COTS	Seeds
Centaurea cyanus (Cornflower annual wildflower)	LP-13062012-CAW	COTS	Seeds
Trifolium incarnatum (Crimson clover; Heusers Ostsaat var.)	LP-13062012-HOCC	COTS	Seeds
Vicia sativa (Early English Vetch)	LP-13062012-EV	COTS	Seeds
Knautia arvensis (Field scabious wildflower)	LP-13062012-FSW	COTS	Seeds
Gallium verum (Lady bedstraw wildflower)	LP-13062012-LBW	COTS	Seeds
Centaura nigra (Lesser knapweed wildflower)	LP-13062012-LKW	COTS	Seeds
Medicago sativa (Lucerne; FEE var.)	LP-13062012-FL	COTS	Seeds
Malva moschata (Musk mallow wildflower)	LP-13062012-MMW	COTS	Seeds
Leucanthemum vulgare (Ox-eye daisy wildflower)	LP-13062012-ODW	COTS	Seeds
Hypericum perforatum) (Perforate St. John's wort wildflower)	LP-13062012-PWW	COTS	Seeds
Trifolium resupinatum (Persian clover; Gorby var.)	LP-13062012-GPC	COTS	Seeds
Lychnis flos-cuculi (Ragged robin wildflower)	LP-13062012-RRW	COTS	Seeds
Plantago lanceolata (Ribgrass forage herb)	LP-13062012-RFH	COTS	Seeds
Prunella vulgaris (Self-heal wildflower)	LP-13062012-SHW	COTS	Seeds
Petroselenium crispum (Sheep's Parsley forage herb)	LP-13062012-SPFH	COTS	Seeds
Melilotus officinalis (Sweet clover commercial)	LP-13062012-SW	COTS	Seeds
Daucus carota (Wild carrot wildflower)	LP-13062012-WCWF	COTS	Seeds
Medicago lupulina (Yellow trefoil; Virgo Pajbjerg var.)	LP-13062012-YT	COTS	Seeds

2.3.1.2   Plant samples

Table 2.3 summarises plant samples, which gave a positive response with the HCl-butanol reagent as described in section 2.2.4.

Table 2.3: Summary of plant samples collected in large quantities and screened for proanthocyanidins with the HCl-butanol reagent; * signifies that presence of proanthocyanidins was already known.

Plant material	Lab number	Source/supplier	Plan part	HCl-butanol
Malus spp. (Apple)	LP-09082012-AL	URE campus, Reading, UK	Leaves	*
	LP-09082012 -AL1	URE campus, Reading, UK	Leaves	*
	LP-28082012 -A-a)	URE campus, Reading, UK	Leaves	*
	LP-28082012 -A-b)	URE campus, Reading, UK	Leaves	*
	LP-28082012 -A-c)	URE campus, Reading, UK	Leaves	*
	LP-17102012-AT	SAPD, URE campus, Reading, UK	Fruits	*
Ribes nigrum (Black currant)	LP-22062008-BC	Hildred PYO-farm, Goring-on-Thames, UK	Leaves	Positive
	LP-13082012 -BC	Hildred PYO-farm, Goring-on-Thames, UK	Leaves	*
	LP-20082012 -BC	Hildred PYO-farm, Goring-on-Thames, UK	Leaves	*
Salix caprea (Goat willow)	LP-26052012-GW	A. Prudence, Goring-on-Thames, UK	White fluff	Positive
	LP-26052012-GW	A. Prudence, Goring-on-Thames, UK	Catkins	Positive
	LP-16072012-W-a	A. Prudence, Goring-on-Thames, UK	Leaves	*
	LP-16072012-W-b	A. Prudence, Goring-on-Thames, UK	Branches	*
Corylus avellana (Hazelnut)	LP-15072012-HS	INRA, Toulouse, France	Pericarp membrane	Positive
Medicago sativa (Lucerne)	HH-1208-L	COTS, Moreton-in- Marsh, UK	Seeds	*
Pinus sylvestris (Scots pine tree)	LP-21082012-P	UTU, Turku, Finland	Bark	*
Ribes rubrum (Red currant)	LP-15072012-RC-a	I. Mueller-Harvey, Reading, UK	Leaves	*
	LP-15072012-RC-b	I. Mueller-Harvey, Reading, UK	Branches	*
	LP-20082012-RC	Hildred PYO-farm, Goring-on-Thames	Leaves	*
	LP-22062008-RC	Hildred PYO-farm, Goring-on-Thames	Leaves	Positive
Onobrychis viciifolia (Sainfoin)	HH-072007-S	Hartley Farm, Gloucestershire, UK	Whole plant	Positive
	LP-24052012-S	Peter Davy, Barrham, Kent, UK	Whole plant	Positive
	LP-0706-2012-S	Peter Davy, Barrham, Kent, UK	Whole plant	Positive
Salix babylonica (Weeping willow)	LP-26052012-WW	Emmer Green, UK	White fluff	Positive
	LP-26052012-WW	Emmer Green, UK	Catkins	Positive
Trifolium repens (White clover)	LP-10052012-WC	URE campus, Reading, UK	Flowers	Positive
	LP-19062012-WC	URE campus, Reading, UK	Flowers	*
	LP-17062012-WC	Great Bookham, UK	Flowers, stems	*
	LP-22062012-WC	NIAB, Cambridge, UK	Flowers	*

2.3.2 Thiolysis and HPLC analysis

2.3.2.1 Seed samples

Tannin contents in the crude extracts of seeds ranged from 31.1 mg/g extract (*Ranunculus acris*) to 210 mg/g extract (*Pimpinella saxifrage*). The average polymer size of PAs exhibited mDP values from 1.41 (*Filipendula ulmaria)* to 17.8 (*Silene latifolia).* The PC/PD ratios covered the range from 36.8 : 63.2 (*Ranunculus acris)* to 100 : 0 (*Rumex acetosa* and *Silene latifolia)* whereas the *cis/trans* ratios ranged from 43.1 : 56.9 (*Filipendula ulmaria)* to 99.1 : 0.9 (*Silene latifolia*) (Table 2.4). PAs in *Sanguisorba minor* and *Pimpinella saxifrage* extracts consisted of both C and EC subunits in contrast to the other PC-dominated species where EC was the main subunit (Table 2.5).

Table 2.4: Proanthocyanidin characterisation of acetone/water (7:3, v/v) seed extracts by thiolytic degradation; Average values of proanthocyanidin (PA) content, mean degree of polymerisation (mDP), procyanidin (PC) percentage within total PAs after two separate thiolysis reactions.

Origin of PA extract	Lab No	PA content (mg/g extract)	mDP	PC %	*cis* %
Ranunculus acris (Meadow buttercup wildflower)	LP-13062012-MBW	31.1	3.50	36.8	52.6
Trifolium pratense (Red clover; Milvus var.)	LP-13062012-MRC	73.4	2.48	58.4	63.0
Filipendula ulmaria (Meadowsweet wildflower)	LP-13062012-MW	78.9	1.41	84.5	43.1
Trifolium hybridum (Dawn alsike clover)	LP-13062012-DAC	113	5.87	97.0	84.6
Silene dioica (Red campion wildflower)	LP-13062012-RCW	115	14.0	83.7	91.6
Rumex acetosa (Common sorrel wildflower	LP-13062012-CSW	172	14.9	100	96.8
Sanguisorba minor (Salad burnet wildfower)	LP-13062012-SBW	193	4.52	97.9	45.5
Silene latifolia (White campion wildflower)	LP-13062012-WCW	206	17.8	100	99.1
Pimpinella saxifrage (Burnet forage herb)	LP-13062012-BFH	210	5.12	100	46.9

In some seed extracts, there was considerable variability in the results between the replicates. It would be appear that unidentified compounds interfered with the quantification of extender units. There were noticeable inconsistencies

with some of the peak intensities between replicates, which suggested that the thiolysis reaction conditions were not optimal for these samples.

Thiolysis-HPLC analysis revealed five PC-dominated PA samples. The extracted PAs from these particular seed species had mDP values of <20. Large standard deviations of PA contents in these extracts cast some doubt on the measured PA concentrations. In addition, PAs in these species consisted almost exclusively of EC, which has a *cis* configuration. This stereochemistry is quite common in PC homo-polymers and these samples, therefore, could not provide the desired PA diversity that was required for the LegumePlus research. Procyanidins dominated by catechin (a *trans*-flavan-3-ol) would have been more desirable PAs.

Table 2.5: Average values of proanthocyanidin (PA) monomer contents (mg/g extract) in acetone/water (7:3 v/v) extracts of seeds after two separate thiolysis reactions; GC: gallocatechin, EGC: epigallocatechin, C: catechin, EC: epicatechin; nd: not detected

Origin of PA extract	GC	EGC	C	EC	GC	EGC	C	EC
	Terminal units				Extender units			
Ranunculus acris (LP-13062012-MBW)	nd	7.48	2.28	2.54	10.3	3.63	0.723	4.177
Trifolium pratense (LP-13062012-MRC)	30.9	7.86	nd	3.91	nd	nd	5.3	25.5
Filipendula ulmaria (LP-13062012-MW)	10.9	2.98	28.2	14.9	nd	nd	6.26	15.7
Trifolium hybridum (LP-13062012-DAC)	3.94	nd	2.84	12.7	nd	nd	11.0	82.7
Silene dioica (LP-13062012-RCW)	nd	nd	1.02	7.17	9.14	10.7	nd	87.3
Rumex acetosa (LP-13062012-CSW)	nd	nd	5.49	5.96	nd	nd	nd	161
Sanguisorba minor (LP-13062012-SBW)	4.26	nd	5.21	33.5	nd	nd	95.6	54.0
Silene latifolia (LP-13062012-WCW)	nd	nd	1.88	9.68	nd	nd	nd	194
Pimpinella saxifrage (LP-13062012-BFH)	nd	nd	4.24	36.8	nd	nd	108	60.9

2.3.2.2 Plant samples

Several parts of the apple fruit are well-known PA sources [31-33] with very high MW PCs [34-37]. In this study, several *Malus spp* leaf extracts were evaluated and showed diverse PA contents and profiles (Table 2.6 and 2.7). Only one sample, LP-09082012-AL1, had a PC/PD ratio of 100 : 0, but the PA content in the extract was rather low (28.9 mg/g extract) and the mDP value of 11.4 was comparable to apple fruits of different varieties [35]. This leaf extract was very hygroscopic after lyophilisation presumably due to the presence of sugars and this made it difficult to weigh subsamples for analysis. This probably accounts for the high standard deviation and would have affected the quantification of the reaction products. It was concluded that due to the poor reproducibility of the leaf extract analysis and the difficult lyophilisation of fruit extracts, other plant materials should be investigated as PC sources.

A number of studies on different *Salix spp.* reported that their PA contents and compositions are dependent on the *Salix* species. *Salix cinerea, Salix caprea, Salix alba* and *Salix fragilis* contained mostly PCs apart from *Salix cinerea* that contained significant amounts of PDs [38-42]. Three different extracts were prepared from *Salix caprea* (goat willow). The extract from the branches yielded 327 mg PAs/g extract (Table 2.6). The catkin and leaf extracts contained 158 and 174 mg PAs/g extract respectively. Interestingly, the percentage of PCs also varied. PAs in the leaf sample consisted almost exclusively of PCs (95.1%) however the branch and the catkin samples contained a noticeable amount of PDs (23.7% and 38.5%, respectively, Table 2.6). In a published study though, the main components in catkins were C and EC, while PDs were not detected [41]. The mDP values were 4.38 for the leaf, 4.17 for the branch and 6.25 for the catkin PAs and the *cis*-flavan-3-ols ranged from 16 to 25%. This indicated that these PAs were mostly composed of catechin, especially in the leaf sample. The *Salix caprea* samples were, therefore, selected for their high catechin content (*trans*-flavan-3-ol).

PAs extracted from the *Salix babylonica* catkins had a low mDP value of 1.80 (Table 2.6) and also a lower percentage of PCs (52.6 %) than the other willow matrices. Moreover, these PAs had a higher percentage of *cis*-flavan-3-ols (35.0%) than the *Salix caprea* PAs.

Table 2.6: Proanthocyanidin characterisation of acetone/water (7:3, v/v) plant extracts by thiolytic degradation; PA: proanthocyanidin, mDP: mean degree of polymerisation, PC: procyanidin; Standard deviation in brackets.

Origin of PA extract	Lab Number	Plant part	PA content (mg/g extract)	mDP	PC %	*cis* %
Malus spp. (Apple)	LP-09082012-AL1*	Leaves	28.9 (0.354)	11.4 (2.05)	100 (0.00)	95.2 (0.707)
	LP-09082012-AL**	Leaves	169 (170)	56.2 (61.1)	24.2 (10.79)	44.6 (11.4)
	LP-28082012-A-a	Leaves	117 (57.3)	40.7 (28.9)	35.5 (12.7)	57.5 (14.9)
	LP-28082012-A-b	Leaves	85.3 (0.78)	37.9 (4.30)	52.3 (0.212)	41.9 (0.141)
Ribes nigrum (Black currant)	LP-22062008-BC	Leaves	146 (7.28)	20.1 (2.58)	7.00 (1.27)	14.8 (0.283)
Ribes rubrum (Red currant)	LP-22062008-RC	Leaves	41.5 (17.04)	2.70 (0.205)	43.4 (0.354)	86.4 (4.45)
	LP-15072012-RC-a	Leaves	158 (9.33)	7.33 (0.021)	6.25 (0.212)	53.4 (0.424)
	LP-20082012-RC	Leaves	196 (6.72)	15.9 (1.94)	7.10 (0.990)	82.2 (3.89)
	LP-15072012-RC-b	Branches	221 (9.55)	7.59 (0.049)	20.8 (0.212)	50.8 (1.13)
Salix caprea (Goat willow)	LP-26052012-GW	Catkins	158 (17.0)	6.25 (0.382)	61.5 (0.283)	24.6 (1.98)
	LP-16072012-W-a**	Leaves	174 (100)	4.38 (0.171)	95.1 (3.08)	16.2 (10.9)
	LP-16072012-W-b**	Branches	327 (20.2)	4.17 (0.438)	76.3 (5.00)	20.7 (15.2)
Salix babylonica (Weeping willow)	LP-26052012-WW	Catkins	170 (14.7)	1.80 (0.064)	52.6 (2.12)	35.0 (0.141)
Trifolium repens (White clover)	LP-22062012-WC**	Flowers	122 (16.5)	8.70 (1.58)	4.05 (2.54)	56.0 (3.00)
	LP-10052012-WC	Flowers	226 (254)	2.73 (1.43)	16.6 (15.8)	66.4 (38.5)
Pinus sylvestris (Scots pine tree)	LP-21082012-P**	Bark	309 (46.2)	6.30 (0.538)	87.1 (7.14)	79.3 (2.55)
Corylus avellana (Hazelnut)	LP-15072012-HS	Pericarp	748 (33.4)	12.5 (0.290)	78.5 (0.354)	51.5 (0.424)

*Acetone/water (7:3, v/v) extracts analysed in 2 replicates (*n=2*)

** Acetone/water (7:3, v/v) extracts analysed in 4 replicates (*n=4*)

Compared to *Salix caprea* branches (327 mg/g extract), bark from *Pinus sylvestris* had a similar PA content (309 mg/g extract) (Table 2.6). In addition, the mDP of 6.30 suggested a prevalence of oligomers with a substantial amount of

PDs (12.9%) (Table 2.6). These results differed from previous studies since amounts of PDs have not been detected in *Pinus spp.* extracts before [43-46].

The extract of *Corylus avellana* pericarp had the highest PA concentration (748 mg/g extract) amongst any of the tested plant extracts (Table 2.6). The mDP value was 12.5, the PC percentage was 78.5%, which agreed with previous investigations on hazelnut pericarp [47, 48] and nut phenolics [32, 37]. The 51.5 : 48.5 ratio showed an almost equal content of *cis-* and *trans-* flavan-3-ols within the PAs.

Three red currant leaf samples and a red currant branch sample were examined for extractable PA content and composition (Table 2.6). A number of studies have reported that PD-rich PAs occur in red currant and black currant fruits [31, 49-53] and leaves [38, 53, 54]. The leaf samples varied in PA content. The red currant leaf sample, which was collected in 2008 (LP-22062008-RC), had very low PA content (41.5 mg/g of extract), an unexpectedly large percentage of PCs (43.4%) and a very low mDP value (2.70). The extract from another leaf sample (LP-20082012-RC), which had been collected in 2012, had more PAs (196 mg/g extract), and an mDP of 15.9. In addition, the PAs in this sample contained only 7.10% of PCs. The extract from the branches had a similar PA content (221 mg/g extract) but a lower mDP of 7.59. The *cis*-flavan-3-ol percentage varied between these red currant matrices: leaf PAs had 82.2% and branch PAs had 50.8% *cis*-flavan-3-ols. Therefore, the LP-20082012-RC sample was used as a source of PD polymers that contained mainly epigallocatechin subunits (Table 2.7).

PAs extracted from black currant leaves had a very similar PC/PD ratio to the red currant leaf sample (i.e. 7.00 : 93.0 vs 6.25 : 93.75) (Table 2.5, LP-20082012-RC) which is consistent with published results on PAs from fruits of the *Ribes spp.* [37, 50, 55]. This black currant leaf extract had an mDP value of 20.1 and PA content of 146 mg/g extract. Moreover, in accordance to the literature an important difference existed in the *cis* percentage values with 82.9% and 14.8% for the red and black currant leaf extracts respectively. The black currant leaves, therefore, represent a rather unusual source of PDs as they contain mostly gallocatechin rather than epigallocatechin in flavan-3-ol extension units.

Table 2.7: Proanthocyanidin monomer contents (mg/g extract) in acetone/water (7:3 v/v) extracts of seeds; PA: proanthocyanidin, GC: gallocatechin, EGC: epigallocatechin, C: catechin, EC: epicatechin; Standard deviation in brackets; nd: not detected

Origin of PA extract	GC	EGC	C	EC	GC	EGC	C	EC
	Terminal units				Extender units			
Malus spp. (LP-09082012-AL1)*	nd	nd	1.39 (0.185)	1.18 (0.671)	nd	nd	nd	26.3 (0.172)
Malus spp. (LP-09082012-AL)**	nd	0.308 (0.615)	0.637 (0.448)	2.32 (0.626)	64.1 (64.3)	55.9 (53.5)	15.0 (17.4)	30.7 (61.3)
Malus spp. (LP-28082012-A-a)	nd	nd	2.34 (0.339)	0.838 (1.18)	41.0 (3.58)	38.1 (48.2)	2.13 (3.02)	32.6 (3.33)
Malus spp. (LP-28082012-A-b)	nd	nd	2.04 (0.073)	0.220 (0.311)	40.7 (0.154)	0.00 (0.00)	6.80 (0.134)	35.5 (0.752)
Ribes nigrum (LP-22062008-BC)	nd	3.33 (0.559)	3.33 (0.280)	0.677 (0.458)	118 (5.51)	14.8 (1.05)	3.48 (0.059)	2.82 (1.52)
Ribes rubrum (LP-22062008-RC)	nd	nd	0.941 (0.145)	14.7 (7.36)	2.42 (0.908)	21.0 (8.60)	1.92 (0.586)	0.444 (0.628)
Ribes rubrum (LP-15072012-RC-a)	13.8 (0.562)	nd	7.71 (0.757)	0.00 (0.00)	50.4 (2.21)	83.5 (5.61)	1.45 (0.064)	0.664 (0.106)
Ribes rubrum (LP-15072012-RC-b)	13.7 (1.06)	3.98 (0.203)	0.884 (0.007)	10.9 (0.185)	83.3 (1.44)	74.4 (5.22)	11.0 (0.323)	23.1 (2.14)
Salix caprea (LP-26052012-GW)	nd	nd	22.7 (1.01)	2.48 (0.180)	47.1 (3.23)	13.6 (3.86)	48.9 (5.53)	22.9 (3.22)
Salix caprea (LP-16072012-W-a)*	0.206 (0.412)	nd	29.4 (33.5)	9.81 (11.4)	8.41 (7.83)	2.06 (2.50)	116 (62.1)	8.20 (6.12)
Salix caprea (LP-16072012-W-b)*	5.23 (2.06)	1.06 (1.23)	39.9 (1.85)	32.9 (38.1)	49.5 (2.60)	22.1 (18.5)	164 (8.29)	12.9 (5.53)
Salix babylonica (LP-26052012-WW)	74.5 (8.47)	nd	12.1 (1.79)	8.50 (1.56)	6.05 (5.06)	nd	18.1 (4.12)	51.1 (3.82)
Trifolium repens (LP-22062012-WC)*	11.4 (1.50)	nd	3.60 (3.47)	0.00 (0.00)	38.2 (6.32)	68.0 (6.12)	1.33 (0.109)	0.284 (0.330)
Trifolium repens (LP-10052012-WC)	107 (151)	nd	nd	16.7 (6.08)	17.4 (20.5)	83.6 (75.0)	nd	0.668 (0.316)
Pinus sylvestris (LP-21082012-P)**	nd	15.5 (5.71)	26.7 (2.45)	6.50 (2.74)	15.6 (18.2)	10.5 (3.54)	22.0 (4.17)	212 (28.6)
Corylus avellana (LP-15072012-HS)	nd	nd	51.5 (1.24)	8.11 (0.008)	77.9 (8.70)	83.2 (1.07)	234 (9.63)	294 (12.7)

*Acetone/water (7:3, v/v) extracts analysed in 2 replicates (*n=2*).

** Acetone/water (7:3, v/v) extracts analysed in 4 replicates (*n=4*).

Finally, *Trifolium repens* flower extracts were also a good source of PDs (Table 2.6) [13]. Thiolysis-HPLC analysis of two different white clover samples confirmed the high PD content in their extracts [9, 13]. Although the sample collected from the National Institute of Agricultural Botany (NIAB) (LP-22062012-WC) had less extractable PAs than the sample collected in Reading (LP-

10052012-WC), it had PAs with higher mDP and PD percentage values (Table 2.6). In addition, the *cis* percentage was found to be 56.0% and thus differed considerably from the *Ribes nigrum* and *Ribes rubrum* PAs. Therefore, the white clover PAs could be used to complement the red and black currant PD samples.

2.4   Conclusions

The initial screening with the HCl-butanol assay enabled the selection of plants with high PA contents. These plants were used to prepare acetone/water extracts for characterising the PAs by thiolytic degradation and RP-HPLC analysis. The released flavan-3-ol subunits allowed calculation of PA content, mDP, PC/PD and *cis/trans*-flavan-3-ol ratios and revealed a wide range of PA compositions.

This is the first reported PA analysis of commercially available seed samples from wild flowers. However, these seed extracts proved to be unsuitable as convenient sources for a diverse set of PAs for several reasons. Firstly, seeds required defatting, which is time-consuming for large scale PA extractions; secondly PA contents and structures of these seeds offered no particular advantages over other plant sources and thirdly standard deviations of the thiolysis results obtained with the extracts were surprisingly large, suggesting that unidentified compounds interfered with PA characterisation. Three of the seed sources with higher PA concentrations in the extracts (172-210 mg/g extract) had pure PCs (*Rumex acetosa*, *Silene latifolia* and *Pimpinella saxifrage*). *R. acetosa* and *S. latifolia* PAs also had high mDP values (15-18) and mostly *cis*-flavan-3-ols (>97%), whereas *P. saxifrage* had a relatively low mDP (5) and more *trans*-flavan-3-ols (53.1%). Given the low to medium PA concentrations, the amount of seeds that would ultimately have been required for generating gram quantities of PA extracts and purified fractions proved to be too expensive. Therefore, other plant sources were used to provide the different types of PCs.

The final set of PAs extracted from a number of different plant samples and parts (branches, leaves, flowers, seed pericarp) resulted in a collection of PAs that covered a wide range of concentrations and compositions. The PA contents ranged of 41.5 to 748 mg/g of extract, the mDP values from 1.80 to 20.1, the PC/PD ratios from 4.05 : 95.1 to 95.1 : 4.9 and the *cis/trans* ratios from 14.8 : 85.2 to 86.4 : 13.6. This set of contrasting PAs was, therefore, used for the

development of novel analytical methods and for biological measurements such as AH and gas production assays by the author and LegumePlus collaborators.

References

1. Hummer W, Schreier P: **Analysis of proanthocyanidins.** *Molecular Nutrition & Food Research* 2008, 52(12):1381-1398.

2. Piluzza G, Sulas L, Bullitta S: **Tannins in forage plants and their role in animal husbandry and environmental sustainability: A review.** *Grass and Forage Science* 2014, 69(1):32-48.

3. Rochfort S, Parker AJ, Dunshea FR: **Plant bioactives for ruminant health and productivity.** *Phytochemistry* 2008, 69(2):299-322.

4. Stringano E, Cramer R, Hayes W, Smith C, Gibson T, Mueller-Harvey I: **Deciphering the complexity of sainfoin (*Onobrychis viciifolia*) proanthocyanidins by MALDI-TOF mass spectrometry with a judicious choice of isotope patterns and matrixes.** *Analytical Chemistry* 2011, 83(11):4147-4153.

5. Stringano E, Hayot Carbonero C, Smith LM, Brown RH, Mueller-Harvey I: **Proanthocyanidin diversity in the EU 'HealthyHay' sainfoin (*Onobrychis viciifolia*) germplasm collection.** *Phytochemistry* 2012, 77:197-208.

6. Grabber JH, Zeller WE, Mueller-Harvey I: **Acetone enhances the direct analysis of procyanidin- and prodelphinidin-based condensed tannins in *Lotus* species by the butanol-HCl-iron assay.** *Journal of Agricultural and Food Chemistry* 2013, 61(11):2669-2678.

7. Marais JP, Mueller-Harvey I, Brandt EV, Ferreira D: **Polyphenols, condensed tannins, and other natural products in *Onobrychis viciifolia* (sainfoin).** *Journal of Agricultural and Food Chemistry* 2000, 48(8):3440-3447.

8. Terrill TH, Windham WR, Evans JJ, Hoveland CS: **Condensed tannin concentraton in sericea lespedeza as influenced by preservation method.** *Crop Science* 1990, 30(1):219.

9. Meagher LP, Widdup K, Sivakumaran S, Lucas R, Rumball W: **Floral *Trifolium* proanthocyanidins: Polyphenol formation and compositional diversity.** *Journal of Agricultural and Food Chemistry* 2006, 54(15):5482-5488.

10. Meagher LP, Lane G, Sivakumaran S, Tavendale MH, Fraser K: **Characterization of condensed tannins from *Lotus* species by thiolytic degradation and electrospray mass spectrometry.** *Animal Feed Science and Technology* 2004, 117(1-2):151-163.

11. Monagas M, Quintanilla-Lopez JE, Gomez-Cordoves C, Bartolome B, Lebron-Aguilar R: **MALDI-TOF MS analysis of plant proanthocyanidins.** *Journal of Pharmaceutical and Biomedical analysis* 2010, 51(2):358-372.

12. Tibe O, Meagher LP, Fraser K, Harding DR: **Condensed tannins and flavonoids from the forage legume sulla (*Hedysarum coronarium*).** *Journal of Agricultural and Food Chemistry* 2011, 59(17):9402-9409.

13. Foo LY, Lu Y, Molan AL, Woodfield DR, McNabb WC: **The phenols and prodelphinidins of white clover flowers.** *Phytochemistry* 2000, 54(5):539-548.

14. Mueller-Harvey I: **Unravelling the conundrum of tannins in animal nutrition and health.** *Journal of the Science of Food and Agriculture* 2006, 86(13):2010-2037.

15. Waghorn G: **Beneficial and detrimental effects of dietary condensed tannins for sustainable sheep and goat production-Progress and challenges.** *Animal Feed Science and Technology* 2008, 147(1-3):116-139.

16. Hoste H, Jackson F, Athanasiadou S, Thamsborg SM, Hoskin SO: **The effects of tannin-rich plants on parasitic nematodes in ruminants.** *Trends in Parasitology* 2006, 22(6):253-261.

17. Hoste H, Martinez-Ortiz-De-Montellano C, Manolaraki F, Brunet S, Ojeda-Robertos N, Fourquaux I, Torres-Acosta JF, Sandoval-Castro CA: **Direct and indirect effects of bioactive tannin-rich tropical and temperate legumes against nematode infections.** *Veterinary Parasitology* 2012, 186(1-2):18-27.

18. Bodas R, Prieto N, Garcia-Gonzalez R, Andres S, Giraldez FJ, Lopez S: **Manipulation of rumen fermentation and methane production with plant secondary metabolites.** *Animal Feed Science and Technology* 2012, 176(1-4):78-93.

19. Patra AK, Saxena J: **A new perspective on the use of plant secondary metabolites to inhibit methanogenesis in the rumen.** *Phytochemistry* 2010, 71(11-12):1198-1222.

20. Schofield P, Mbugua DM, Pell AN: **Analysis of condensed tannins: A review.** *Animal Feed Science and Technology* 2001, 91(1-2):21-40.

21. Makkar HPS, Gamble G, Becker K: **Limitation of the butanol-hydrochloric acid-iron assay for bound condensed tannins.** *Food Chemistry* 1999, 66(1):129-133.

22. McMahon LR, McAllister TA, Berg BP, Majak W, Acharya SN, Popp JD, Coulman BE, Wang Y, Cheng KJ: **A review of the effects of forage condensed tannins on ruminal fermentation and bloat in grazing cattle.** *Canadian Journal of Plant Science* 2000, 80(3):469-485.

23. Marles MA, Ray H, Gruber MY: **New perspectives on proanthocyanidin biochemistry and molecular regulation.** *Phytochemistry* 2003, 64(2):367-383.

24. Hammerstone JF, Lazarus SA, Mitchell AE, Rucker R, Schmitz HH: **Identification of procyanidins in cocoa (*Theobroma cacao*) and chocolate using high-performance liquid chromatography mass spectrometry.** *Journal of Agricultural and Food Chemistry* 1999, 47(2):490-496.

25. Novobilsky A, Mueller-Harvey I, Thamsborg SM: **Condensed tannins act against cattle nematodes.** *Veterinary Parasitology* 2011, 182(2-4):213-220.

26. Gea A, Stringano E, Brown RH, Mueller-Harvey I: ***In situ* analysis and structural elucidation of sainfoin (*Onobrychis viciifolia*) tannins for high-throughput germplasm screening.** *Journal of Agricultural and Food Chemistry* 2011, 59(2):495-503.

27. Williams AR, Fryganas C, Ramsay A, Mueller-Harvey I, Thamsborg SM: **Direct anthelmintic effects of condensed tannins from diverse plant sources against *Ascaris suum*.** *PLoS One* 2014, 9(5):e97053.

28. Sivakumaran S, Molan AL, Meagher LP, Kolb B, Foo LY, Lane GA, Attwood GA, Fraser K, Tavendale M: **Variation in antimicrobial action of proanthocyanidins from *Dorycnium rectum* against rumen bacteria.** *Phytochemistry* 2004, 65(17):2485-2497.

29. Ropiak HM, Ramsay A, Mueller-Harvey I: **Condensed tannins in extracts from European medicinal plants and herbal products.** *Journal of Pharmaceutical and Biomedical analysis* 2016, 121:225-231.

30. Labarbe B, Cheynier V, Brossaud F, Souquet JM, Moutounet M: **Quantitative fractionation of grape proanthocyanidins according to their degree of polymerization.** *Journal of Agricultural and Food Chemistry* 1999, 47(7):2719-2723.

31. de Pascual-Teresa S, Santos-Buelga C, Rivas-Gonzalo JC: **Quantitative analysis of flavan-3-ols in Spanish foodstuffs and beverages.** *Journal of Agricultural and Food Chemistry* 2000, 48(11):5331-5337.

32.   Gu L, Kelm MA, Hammerstone JF, Beecher G, Holden J, Haytowitz D, Gebhardt S, Prior RL: **Concentrations of proanthocyanidins in common foods and estimations of normal consumption.** *Journal of Nutrition* 2004, 134(3):613-617.

33.   Hellstrom JK, Mattila PH: **HPLC determination of extractable and unextractable proanthocyanidins in plant materials.** *Journal of Agricultural and Food Chemistry* 2008, 56(17):7617-7624.

34.   Ohnishi-Kameyama M, Yanagida A, Kanda T, Nagata T: **Identification of catechin oligomers from apple (*Malus pumila* cv. Fuji) in matrix-assisted laser desorption/ionization time-of-flight mass spectrometry and fast-atom bombardment mass spectrometry.** *Rapid Communications in Mass Spectrometry : RCM* 1997, 11(1):31-36.

35.   Guyot S, Doco T, Souquet JM, Moutounet M, Drilleau JF: **Characterization of highly polymerized procyanidins in cider apple (*Malus sylvestris* var Kermerrien) skin and pulp.** *Phytochemistry* 1997, 44(2):351-357.

36.   Guyot S, Marnet N, Drilleau J: **Thiolysis-HPLC characterization of apple procyanidins covering a large range of polymerization states.** *Journal of Agricultural and Food Chemistry* 2001, 49(1):14-20.

37.   Gu L, Kelm MA, Hammerstone JF, Beecher G, Holden J, Haytowitz D, Prior RL: **Screening of foods containing proanthocyanidins and their structural characterization using LC-MS/MS and thiolytic degradation.** *Journal of Agricultural and Food Chemistry* 2003, 51(25):7513-7521.

38.   Bate-Smith EC: **Phytochemistry of proanthocyanidins.** *Phytochemistry* 1975, 14(4):1107-1113.

39.   Behrens A, Maie N, Knicker H, Kogel-Knabner I: **MALDI-TOF mass spectrometry and PSD fragmentation as means for the analysis of condensed tannins in plant leaves and needles.** *Phytochemistry* 2003, 62(7):1159-1170.

40.   Maie N, Behrens A, Knicker H, Kogel-Knabner I: **Changes in the structure and protein binding ability of condensed tannins during decomposition of fresh needles and leaves.** *Soil Biology & Biochemistry* 2003, 35(4):577-589.

41.   Thompson RS, Jacques D, Haslam E, Tanner RJN: **Plant proanthocyanidins. Part I. Introduction; the isolation, structure, and distribution in nature of plant procyanidins.** *Journal of the Chemical Society, Perkin Transactions 1* 1972(0):1387.

42.   Czochanska Z, Foo LY, Newman RH, Porter LJ: **Polymeric Proanthocyanidins - stereochemistry, structural units, and molecular-weight.** *Journal of the Chemical Society, Perkin Transactions 1* 1980(10):2278-2286.

43.   Pan HF, Lundgren LN: **Phenolics from inner bark of *Pinus sylvestris*.** *Phytochemistry* 1996, 42(4):1185-1189.

44.   Matthews S, Mila I, Scalbert A, Donnelly DMX: **Extractable and non-extractable proanthocyanidins in barks.** *Phytochemistry* 1997, 45(2):405-410.

45.   Ku CS, Mun SP: **Characterization of proanthocyanidin in hot water extract isolated from *Pinus radiata* bark.** *Wood Science and Technology* 2007, 41(3):235-247.

46.   Karonen M, Loponen J, Ossipov V, Pihlaja K: **Analysis of procyanidins in pine bark with reversed-phase and normal-phase high-performance liquid chromatography-electrospray ionization mass spectrometry.** *Analytica Chimica Acta* 2004, 522(1):105-112.

47. Del Rio D, Calani L, Dall'Asta M, Brighenti F: **Polyphenolic composition of hazelnut skin.** *Journal of Agricultural and Food Chemistry* 2011, 59(18):9935-9941.

48. Monagas M, Garrido I, Lebron-Aguilar R, Gomez-Cordoves MC, Rybarczyk A, Amarowicz R, Bartolome B: **Comparative flavan-3-ol profile and antioxidant capacity of roasted peanut, hazelnut, and almond skins.** *Journal of Agricultural and Food chemistry* 2009, 57(22):10590-10599.

49. Gavrilova V, Kajdzanoska M, Gjamovski V, Stefova M: **Separation, characterization and quantification of phenolic compounds in blueberries and red and black currants by HPLC-DAD-ESI-MSn.** *Journal of Agricultural and Food Chemistry* 2011, 59(8):4009-4018.

50. Maatta KR, Kamal-Eldin A, Torronen AR: **High-performance liquid chromatography (HPLC) analysis of phenolic compounds in berries with diode array and electrospray ionization mass spectrometric (MS) detection:** *Ribes* **species.** *Journal of Agricultural and Food Chemistry* 2003, 51(23):6736-6744.

51. Feliciano RP, Krueger CG, Shanmuganayagam D, Vestling MM, Reed JD: **Deconvolution of matrix-assisted laser desorption/ionization time-of-flight mass spectrometry isotope patterns to determine ratios of A-type to B-type interflavan bonds in cranberry proanthocyanidins.** *Food Chemistry* 2012, 135(3):1485-1493.

52. Hellstrom JK, Torronen AR, Mattila PH: **Proanthocyanidins in common food products of plant origin.** *Journal of Agricultural and Food Chemistry* 2009, 57(17):7899-7906.

53. Porter LJ: **Flavans and proanthocyanidins. In:** *The Flavonoids: Advances in Research since 1980.* Edited by Harborne JB. Boston, MA: Springer US; 1988: 21-62.

54. Czochanska Z, Foo LY, Newman RH, Porter LJ, Thomas WA, Jones WT: **Direct proof of a homogeneous polyflavan-3-ol structure for polymeric proanthocyanidins.** *Journal of the Chemical Society, Chemical Communications* 1979(8):375-377.

55. Wu X, Gu L, Prior RL, McKay S: **Characterization of anthocyanins and proanthocyanidins in some cultivars of** *Ribes*, *Aronia*, **and** *Sambucus* **and their antioxidant capacity.** *Journal of Agricultural and Food Chemistry* 2004, 52(26):7846-7856.

Chapter 3. Complementary analyses of proanthocyanidin profiles from different plant species

3.1　Introduction

Proanthocyanidins (PAs) (syn. condensed tannins) are polyphenolic compounds that are plant secondary metabolites and they are located in various organs of numerous plant sources. The most common PA compounds comprise of linked (epi)catechin subunits that form procyanidins (PCs) and (epi)gallocatechin subunits that form prodelphinidins (PDs). These flavan-3-ol units, which differ in hydroxylation patterns and stereochemistry are linked via interflavanyl bonds and form highly diverse polymeric mixtures. This diversity increases with the degree of polymerisation and with the number and the type of interflavanyl bonds between adjacent units (-C-C- links give rise to B-type PAs, whereas -C-C- plus -C-*O*-C- links give rise to A-type PAs) [1, 2].

Some PA-containing forages have the potential to benefit animal nutrition and sustainable livestock production [3-5]. More efficient dietary protein utilisation [3], bloat prevention [6], reduction of gastro-intestinal nematodes [7] and lower methane production [8] are some of the positive effects, which are associated with certain PA-containing feeds. However, undesirable effects have also been reported [3, 9]. Therefore, it is hypothesised that the diversity of PAs, in terms of amounts and structures, may impact on their bioactivity [3-7, 10]. Interdisciplinary research is needed to establish which specific PA features generate what beneficial effects.

The interpretation of data from bioactivity measurements requires valid data from PA quantification and characterisation. However, several of the widely used analytical methods for PA analysis have limitations. For instance, the vanillin assay and other colorimetric assays lack specificity for PAs [11]. On the contrary, the 4-dimethylaminocinnamaldehyde assay (DMACA) suffers from low sensitivity as it measures only the response from the terminal PA units [2]. Despite its extended use the HCl-butanol assay is highly dependent on experimental factors [2, 11], and method optimisations are still ongoing [12]. Moreover, given the complexity of PA mixtures, PA analysis poses many challenges as quantification standards are lacking [2].

In order to overcome the analytical problems, the current studies on PA characterisation use combinations of more up-to-date analytical techniques that provide quantitative but also compositional information on PAs [2, 11]. The

analysis of thiolytic degradation products by high performance liquid chromatography (HPLC) is useful for providing quantitative information on PA complexity by cleaving PAs into their flavan-3-ol subunits [13-15]. Recently a ultra-performance liquid chromatography - electrospray ionisation - tandem mass spectrometry (UPLC-ESI-MS/MS) method was developed, which uses multiple reaction monitoring (MRM) as a rapid tool for qualitative and quantitative PA analysis [16]. A semi-quantitative approach is based on ^{1}H-^{13}C heteronuclear single quantum correlation (HSQC) nuclear magnetic resonance (NMR), which appears to have some potential in quantitative PA characterisation [12, 17]. Matrix-assisted laser desorption/ionisation - time of flight (MALDI-TOF) MS has also been extensively reported as a technique for qualitative PA characterisation [18]. Finally, the unique features of hydrophilic interaction chromatography (HILIC) have facilitated the subsequent mass spectrometric detection of procyanidins (PCs) [19, 20]. Therefore, the PA samples were also subjected to HILIC separation and diode array detection prior to qualitative characterisation by ESI-TOF-MS.

Following the same concept of using combinations of techniques, this study used the methods listed above aiming to:

i)   overcome some of the limitations from using one analytical method

ii)   to provide complementary information on PA content and composition from structurally diverse purified PA samples

iii)   compare the data obtained from the different analytical approaches

iv)   evaluate the pros and cons of each of these methods

3.2   Materials and methods

3.2.1 Sample collection and treatment

Samples from a variety of plant species were collected, were preserved, ground and stored as described in Chapter 2 (Table 2.3). Nine plant sources were selected for bulk PA extraction and purification. In particular, model PAs were extracted from leaves and twigs of *Salix caprea* (goat willow), leaves of *Ribes rubrum* (red currant) and *Ribes nigrum* (black currant), catkins of *Salix babylonica*

(weeping willow), flowers of *Trifolium repens* (white clover), pericarp of *Coryllus avellana* (hazelnut), bark of *Pinus sylvestris* (Scots pine tree) and whole plants of *Onobrychis viciifolia* (sainfoin).

3.2.2 Chemicals and reagents

HPLC-grade acetonitrile was purchased from Fisher Scientific (Loughborough, UK) and Sigma-Aldrich (Steinheim, Germany). Formic acid was from VWR (Helsinki, Finland). Water purification was performed with a Millipore Synergy water purification system (Merck KGaA, Darmstadt, Germany) and a Milli-Q system (Millipore, Watford, UK). Hydrochloric acid (36%), acetic acid, HPLC-grade acetone and HPLC-grade methanol were supplied from Fisher Scientific (Loughborough, UK). Benzyl mercaptan and acetone-d_6 (99.9%) were obtained from Sigma-Aldrich (Poole, UK) and (±) – dihydroquercetin (98%) was from Apin Chemicals (Abingdon, UK). Deuterium oxide (D_2O) was from CK Isotopes (Ibstock, UK). Catechin was from Sigma (Sigma Chemical Co., St. Louis, MO, USA) and vanillin from Acros Organics (Geel, Belgium). Sephadex^{TM} LH-20 was purchased from GE Healthcare (Little Chalfont, UK). The compounds 2,5-dihydroxybenzoic acid (DHB), super - DHB (sDHB, 10% methoxy - hydroxybenzoic acid: 90% 2,5 - dihydroxybenzoic acid) and trifluoro acetic acid (TFA) were purchased from Sigma-Aldrich (Poole, UK). Sodium chloride and lithium bromide were from Fluka (Gillingham, UK) and caesium chloride was from Fisher Scientific (Loughborough, UK).

3.2.3 Extraction of proanthocyanidins

Proanthocyanidin extraction followed the procedure described in section 2.2.3.2. Plant powder (50 g) was extracted with acetone/water (7:3 v/v, 500 ml) and 250 ml dichloromethane was used to remove chlorophyll. These crude plant extracts were then lyophilised and stored at -20 °C for further analysis and purification.

3.2.4 Vanillin Assay

Vanillin (0.5 g) was weighed into a 10 ml capped tube and dissolved in 5 ml concentrated HCl. A droplet from an extract or purified fraction was spotted onto a filter paper and a drop of the vanillin solution was added. A red colour indicated the presence of monomeric flavan-3-ols or PAs.

3.2.5 Purification of proanthocyanidins by column chromatography

Prior to PA purification, the crude plant extract was dissolved in distilled water (2 l). The solution was filtered under vacuum and the filtrate poured into a separating funnel attached to the Sephadex^{TM} LH-20 column. The tap was adjusted so that the extract entered the column without disturbing the bed. The column was then washed with distilled water (2 l) to remove impurities such as sugars and monomeric flavonoids while PAs were retained by the resin. After the washing step, PA presence in the eluate was assessed with the vanillin assay. The eluates in the majority of different extracts were flavan-3-ol-free. PAs were retrieved from the column by two acetone/water elution steps. Elution with acetone/water (3:7 v/v) yielded the first purified PA fraction (F1), whereas elution with acetone/water (1:1 v/v) generated the second purified PA fraction (F2). The organic solvent was evaporated with a rotary evaporator and purified fractions (F1 and F2) were lyophilised and stored at -20 °C for further analysis. The chromatographic column was washed with 2 l of acetone/water (8:2 v/v) prior to the next purification.

3.2.6 Thiolysis - HPLC analysis

The thiolysis reaction was performed according to Novobilský et al. [21] and as described in section 2.2.5. Briefly, the PA sample (4 mg) was weighed into 10 ml screw-capped vials, dissolved in methanol (1.5 ml) and acidified with HCl (0.5 ml, 3.3% in methanol, v/v). The addition of benzyl mercaptan (BM) followed (50 µl) and the reaction mixture was stirred at 40 °C for 1 h. The reaction was stopped by adding ultra-pure water (2.5 ml) to the vials at room temperature. Identification and quantification of the thiolysis products was performed by HPLC linked to a diode

array detector. The chromatographic conditions and settings of the instrument were described in section 2.2.6. Determination of PA content and composition was done according to section 2.2.7.

3.2.7 UPLC-ESI-MS/MS analysis

Sample analysis with UPLC-ESI-MS/MS followed the procedures described by Engström et al. [16]. In brief, the analysis was carried out using an ultra-high performance liquid chromatography system (UHPLC, Acquity UPLC®, Waters Corporation, Milford, MA, USA) combined with a triple quadrupole mass spectrometer (Xevo® TQ, Waters Corporation, Milford, MA, USA). The UHPLC system consisted of a sample manager, a binary solvent manager, and a diode array detector (DAD). An Acquity UPLC® BEH Phenyl (2.1×100 mm, 1.7 µm, Waters Corporation, Wexford, Ireland) column was used. The flow rate of the eluent was 0.5 ml/min. The elution profile used two solvents, 0.1 % formic acid/ultrapure water (A) and acetonitrile (B): 0–0.5 min, 99.9% A, 0.1% B; 0.5–5.0 min, 0–30% B in A (linear gradient); 5.0–6.0 min, 30–35% B in A (linear gradient); 6.0–9.5 min, column wash and stabilisation. Negative ionisation mode was used for the MS analysis. The ESI conditions were: capillary voltage 2.4 kV, desolvation temperature 500 °C, source temperature 150 °C, desolvation and cone gas (N_2) 1000 and 100 l/h respectively, and argon as the collision gas. The developed multiple reaction monitoring method required a range of collision energies and cone voltages for the effective generation of precursor and daughter ions from oligomeric and polymeric PAs (Table 3.1). Calibration curves for the determination of procyanidin and prodelphinidin contents were constructed according to Engström et al. [16] using purified PA fractions (F2) from the *S. caprea* leaves and the *T. repens* flowers (Table 3.2).

Table 3.1: Cone voltages and collision energies used in the multiple reaction monitoring method for fragmentation of procyanidin (PC) and prodelphinidin (PD) terminal and extension units.

PA unit	precursor ion m/z	cone voltage 1 / V	cone voltage 2 / V	cone voltage 3 / V	cone voltage 4 / V	cone voltage 5 / V	cone voltage 6 / V	fragment ion m/z	collision energy eV
PC extension	287	30	50	75	85	110	140	125	15
PC terminal	289	30	50	75	85	110	140	145	15
PD extension	303	30	55	80	110	130	150	125	20
PD terminal	305	30	55	80	110	130	150	125	20

The mean degree of polymerisation (mDP) was calculated according to the formula:

$$mDP = \frac{0.37A_{287} + 0.42A_{289} + 2.15A_{303} + 0.68A_{305}}{0.42\,A_{289} + 0.68\,A_{305}}$$

where: A_{287}, A_{289}, A_{303}, and A_{305} represent the sum of peak areas in the MRM chromatograms of procyanidin extension units (*m/z* 287→125), procyanidin terminal units (*m/z* 289→145), prodelphinidin extension units (*m/z* 303→125) and prodelphinidin terminal units (*m/z* 305→125), respectively, that were produced by the five highest cone voltages (Table 3.1). Identification of the PA fragmentation patterns and of the transition states of precursor-daughter ions was based on quinone methide cleavage [16, 22].

3.2.8 HILIC-DAD-ESI-TOF-MS analysis

The purified PA fractions were separated and analysed by HILIC-DAD-ESI-TOF-MS according to Karonen et al. [19]. In brief, stock solutions (10 mg/ml) of the Sephadex™ LH-20 PA fractions were prepared in ultra-pure water. The system consisted of an Agilent HPLC 1200 Series equipped with a diode array detector (Agilent Technologies, Waldbronn, Germany) and a micrOTOF$_Q$ ESI-mass spectrometer (Bruker Daltonics, Bremen, Germany). A Phenomenex Luna HILIC column (4.6 x 250 mm, cross linked diol, 5 µm) with a SecurityGuard was used for the separation of the polymeric compounds at 30 °C. Acetonitrile was used for the

mobile phase A, water and formic acid (99.9:0.1, v/v) were used for the mobile phase B. The elution gradient was: 0-40 min linear, 95% A to 35% A, 40-45 min linear, 35% A to 95% A and 45-75 min 95% A isocratic. The flow rate was 0.8 ml/min and was reduced to 0.27 ml/min by splitting just before the introduction into the ion source. 50 μl was injected for each measurement. Chromatograms were recorded between 190 to 950 nm. The software controlling the HPLC system was a Hystar (version 3.2, Bruker BioSpin, Rheinstetten, Germany) and the software manipulating the mass spectrometer, which was operated in a negative ion mode, was a Bruker Compass micrOTOF control (Bruker Daltonics). The capillary voltage was maintained at +4000 V with the end plate offset at -500 V. The nebuliser gas (N_2) had a pressure of 1.6 bars and the drying gas (N_2) had a flow of 8.0 l/min and temperature of 200 °C. The full scan covered 100 to 3000 *m/z*. Sodium formate (5 mM) was used for the calibration. Sodium formate was injected through a six-port valve at the end of the LC-MS experiment in order to provide high accuracy mass measurements. The high precision calibration (HPC) mode was chosen for the internal mass spectrum calibration. The minimal number of calibration points was seven and standard deviation was below 10 ppm. The data were analysed with Bruker DataAnalysis (version 4.0, Bruker Daltonics) software.

3.2.9 Nuclear magnetic resonance analysis

Purified PAs (15 mg) were transferred to a 1.5 ml Eppendorf tube, dissolved in a deuterium oxide/acetone-d6 mixture (4:1 v/v) and frozen at -80 °C until analysis. Before analysis the solutions were thawed and transferred to standard NMR tubes. The [1]H-[13]C Heteronuclear Single Quantum Coherence (HSQC) NRM spectra were recorded on a Bruker Avance III 500 spectrometer, operating at 11.74T with the proton (^{1}H) and carbon (^{13}C) frequencies of 500.13 MHz and 125.76 MHz respectively. The Bruker BBO probe with the z-gradient was used and all measurements were conducted at a constant temperature of 297 K. The standard Bruker hsqcedetgpsp.3 pulse sequence was applied. The number of scans was 32 per increment, 512 increments in the ^{13}C dimension and the recycle delay was 1.5 s. The total acquisition time per spectrum was 7 h 25 min. The 2D FFT was performed with the 4096 points in both dimensions with qsine filter and

0.3 Hz line broadening. The spectra were referenced to the acetone-d6 in deuterium oxide resonance at 2.20 and 29.90 ppm.

Integrals from characteristic cross peak resonances for H/C-2′/5′ (PC), H/C-6′ (PC) and H/C-2′/6′ (PD) were used for the estimation of PC mg percentage within total PAs (in mg PCs/100 mg PAs) according to the following formula [6, 62]:

$$\%\mathrm{PC} = \mathrm{PC\text{-}6'}/[(\mathrm{PD\text{-}2'6'}/2) + \mathrm{PC\text{-}6'}] \times 100$$

Integrals from the different cross peak resonances for H/C-4 of the terminal methylene units and the linked units to another flavan-3-ol were used for the estimation of the mean degree of polymerisation (mDP) according to the following formula:

$$\mathrm{mDP} = \mathrm{H/C4}/[\mathrm{H/C4\alpha} + (\mathrm{H/C4\beta}/2)]$$

where H/C4 represents the integral of the cross peak resonance for the H/C-4 of the linked methylene units and $\mathrm{H/C4\alpha \,\&\, \beta}$ the integrals of the cross peak resonances for the H/C-4 of the terminal (non-linked) methylene unit.

Integrals of the cross peak resonances for the H/C-4 *cis*- and *trans*-flavan-3-ols that were centred around ^{1}H/^{13}C chemical shifts of 4.5-4.8/36.0 and 4.4−4.65/37.5 ppm respectively, were used to estimate *cis/trans* ratios according to the following equation [17]:

$$\% \, cis = \frac{cis - \mathrm{flavan} - 3 - \mathrm{ols}}{[cis - \mathrm{flavan} - 3 - \mathrm{ols} + trans - \mathrm{flavan} - 3 - \mathrm{ols}]} \times 100$$

3.2.10 Matrix assisted laser desorption ionisation TOF MS analysis

Samples at University of Reading were prepared according to the following procedures. The DHB matrix stock solution was prepared by dissolving 5 mg in 1 ml acetonitrile/water (1:1 v/v) containing 0.1% TFA. The stock solution of s-DHB was prepared by dissolving 20 mg in acetonitrile/water (7:3 v/v) containing 0.1%

TFA. The dried PA fractions were dissolved in acetonitrile/methanol (1:2 v/v) in final concentrations of 4 mg/ml. The solutions with the cationising agents were prepared by dissolving NaCl, LiBr and CsCl in ultra-pure water at a concentration of 0.2 M. In a new 1.5 ml tube the purified PA fraction, the solid matrix and the cationising agent were mixed in a volumetric ratio of 1:1:0.5 respectively, using 10 or 20 μl of the PA sample. The solution was gently mixed using a pipette. A small aliquot of the solution (0.5 μl) was deposited on an AnchorChip steel target at an angle of 45° to avoid the "coffee ring" effect that results in heterogeneous sample distribution [23]. The deposited spots were left to dry at room temperature.

The MALDI-TOF MS analysis, at the University of Reading, was performed on an Ultraflex TOF/TOF mass spectrometer (Bruker Daltonics, Bremen, Germany) equipped with delayed extraction and a nitrogen laser (337 nm). In the positive reflectron mode an accelerating voltage of 25.0 kV and a reflectron voltage of 26.3 kV were used. For all the spectra the data from 500 shots were accumulated. Frequency of the irradiation energy was set at 50 Hz. The calibration of the instrument employed the use of Peptide Calibration Standard II purchased from Bruker Daltonics.

Sample preparation and MALDI-TOF MS analysis, at the University of Madison (Mass Spectrometry Facility, Chemistry Instrument Center, Madison, USA) were performed as described by Feliciano et al. [23].

The peak assignments were compared to the predicted *m/z* values of PAs. The following formula was adapted from Stingano et al. [24] for estimating *m/z* values of heterogeneous PAs:

$$m/z \,(\mathrm{PA}) = (m/z\ 288.08)n + (m/z)(2 \times 1.0078) + (m/z\ 16)a + (m/z\ 152)b + (m/z)\,s$$

where (m/z) 288.08 corresponds to the molecular weight (MW) of one extender (epi)catechin unit (MW = 288.08 amu), n denotes the degree of polymerisation (DP), 2×1.0078 stands for one H in each of the top and bottom units, a accounts for the number of the (epi)gallocatechin units ($\Delta m = 16\,\mathrm{amu}$), b represents the number of possible galloyl residues ($\Delta m = 152\,\mathrm{amu}$), and s is the molecular weight of the cation used for the ionisation (Na⁺, Li⁺ or Cs⁺). If glycosyl groups are present another term needs to be added: $(m/z\ 162)g$, where g represents the number of

the glycosyl groups $(\Delta m = 162\,\mathrm{amu})$. FlexControl and FlexAnalysis (Bruker Daltonik GmbH, Bremen, Germany, version 3.0) were used for data acquisition and data processing, respectively. The software mMass (version 5.5.0) was used for spectra analysis and for the recording of absolute intensities (ai).

3.3 Results and discussion

3.3.1 Comparison of methods for analysis of total proanthocyanidin, procyanidin and prodelphinidin contents

Quantitative techniques

Thiolysis assumes that the cleavage of the inteflavanyl bonds is complete [23]. The reaction products were separated by reversed-phase chromatography and identified from the retention times and UV spectra of commercially available standards. Each peak that corresponded to a terminal or extension flavan-3-ol subunit was integrated and quantified using response factors relative to dihydroquercetin [13]. The sums of the peak intensities provided information on PA content, on PC and PD subunit contents within total PAs and on *cis*- and *trans*-flavan-3-ol contents within total PAs.

In contrast to the thiolysis-HPLC method, PAs were fragmented due to ionisation after chromatographic separation in UPLC-ESI-MS/MS analysis [16]. Several MRM experiments selectively recorded the responses for PC and PD terminal and extension units. The peak areas were summed and quantitative information was obtained from calibration curves that were constructed using the above PC- and PD-rich purified PA fractions [16].

The PA contents determined by thiolysis-HPLC and UPLC-ESI-MS/MS analysis are presented in Table 3.2. The contents of samples 3F2 and 5F2-9F2, determined by the two methods, were comparable as the quantification error could explain the deviations. However, noticeable discrepancies were found in samples 1F2, 2F2 and 4F2 where the contents determined by the thiolysis-HPLC method were lower than those determined by UPLC-ESI-MS/MS method.

Table 3.2: Characterisation of proanthocyanidin fractions, eluted from Sephadex[TM] LH-20 (acetone/water, 1:1 v/v, F2) by thiolysis-HPLC, UPLC-ESI-MS/MS and ^{1}H-^{13}C HSQC NMR methods; PA content (mg/g extract), mDP values, PC and *cis* contents (mg/100 mg PAs); Standard deviation in brackets (*n=2*); nd: not detected; nt: not tested

PA origin	Extract type	Thiolysis				UPLC-ESI-MS/MS			^{1}H-^{13}C HSQC NMR	
		PA mg/g fraction	mDP	PC (mg/100 mg PAs)	*cis* (mg/100 mg PAs)	PA mg/g fraction	mDP	PC (mg/100 mg PAs)	mDP	PC (mg/100 mg PAs)
Salix caprea (Goat willow; leaves)	1F2	838 (35.5)	5.28 (0.163)	95.0 (1.17)	4.32 (0.370)	1154	6.35	97.4	5.56	100
Coryllus avellana (Hazelnut; pericarp)	2F2	675 (12.9)	9.15 (0.106)	78.2 (1.62)	47.7 (0.707)	852	9.75	82.1	8.97	80.1
Salix caprea (Goat willow; twigs)	3F2	932 (214)	5.27 (0.078)	77.8 (1.43)	62.8 (0.772)	1044	6.57	84.5	5.30	84.1
Pinus sylvestris (Scots pine tree; bark)	4F2	800 (48.4)	6.59 (0.382)	88.2 (3.54)	78.0 (3.67)	1234	5.60	96.6	6.40	100
Onobrychis viciifolia (Sainfoin; plant)	5F2	1136 (81.6)	8.70 (0.014)	34.0 (0.068)	79.1 (0.495)	1009	9.12	41.2	nt	nt
Salix babylonica (Weeping willow; catkins)	6F2	974 (44.6)	8.01 (0.622)	65.8 (3.52)	57.6 (2.44)	970	8.93	71.0	6.82	73.9
Ribes rubrum (Red currant; leaves)	7F2	682 (21.4)	9.95 (0.156)	9.20 (0.080)	64.5 (1.88)	717	11.2	11.0	nd	0.00
Ribes nigrum (Black currant; leaves)	8F2	1227 (34.1)	6.52 (0.255)	5.27 (0.169)	6.93 (0.263)	1172	8.32	5.26	5.70	0.00
Trifolium repens (White clover; flowers)	9F2	1115 (47.9)	8.62 (0.00)	1.19 (0.004)	58.9 (1.25)	1156	9.35	1.69	8.76	0.00

The high PA content values in the limited number of fractions did not provide good result correlation between the two methods. However, it has been reported that correlation is improved with increased sample populations that cover a wide range of PA contents [16]. Despite the limited number of fractions in this study the total PC and PD contents (in mg/g fraction) by the two methods showed excellent correlations of R^2 = 0.93 and 0.98, respectively (Figure 3.1).
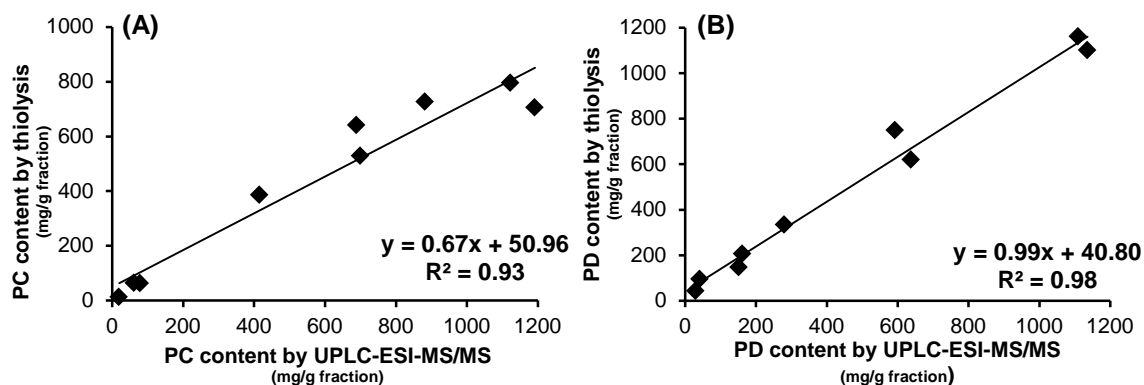
Figure 3.1: Correlations between procyanidin (A) and prodelphinidin content (B) in mg/g fraction, determined by thiolysis and UPLC-ESI-MS/MS; PC: procyanidin, PD: prodelphinidin

These quantitative differences in PA contents by the two methods may have been caused by several factors which could explain why some of the results were different. During thiolysis incomplete polymer degradation [13, 14, 25] and the presence of impurities or side reactions, including epimerisation, may affect reaction yields and have been often suspected to affect quantitation [22, 26-28]. However, in this study the baseline was flat in all chromatograms (Figure 3.2-3.10), therefore, complete PA depolymerisation can be assumed as incomplete reactions tend to result in an elevated baseline [25, 27]. In addition, a preliminary study (data not presented) evaluated the stability of purified PAs and found that storage conditions (-20 and -80 °C, over a 3-year period) had no effect on polymer degradation yields as also reported by Guyot et al. [29]. It is more likely that quantification was affected by difficulties during peak assignments and integrations in the poorly resolved area of BM-adducts [25]. Terminal units especially tend to be present in very low amounts and this poses problems for peak integrations (Figures 3.2-3.10). In addition, a recent review on the response factors used in this study showed that were close but not identical to molar response factors relative to dihydroquercetin that were used by other studies [30]. Hence, these analytical implications may have contributed to the unusual cases where the PA content had values >1000 mg of fraction (samples 5F2, 8F2 and 9F2, Table 3.2). The difference of PA contents between the two methods was more noticeable for 3 of the 5 PC-rich samples (Table 3.2). This observation agreed with the results from Engström et al. where PC quantitation was less accurate compared to PD

quantitation [16] and was also evident in the correlation of PC and PD contents (mg/g of extract) (Figure 3.1). Another possibility is that the standards chosen for the MS/MS calibrations were not fully representative for all PA types in the analysed samples and this could have contributed to quantitation errors. The calibration curves used for UPLC-ESI-MS/MS analysis were based on a set of purified PAs that had been analysed by thiolysis and this could thus have affected the PA content determinations, especially in PC-rich samples [16]. The latter may have been also associated with the samples that presented a PA content >1000 mg of fraction but further investigations will be required on this subject.
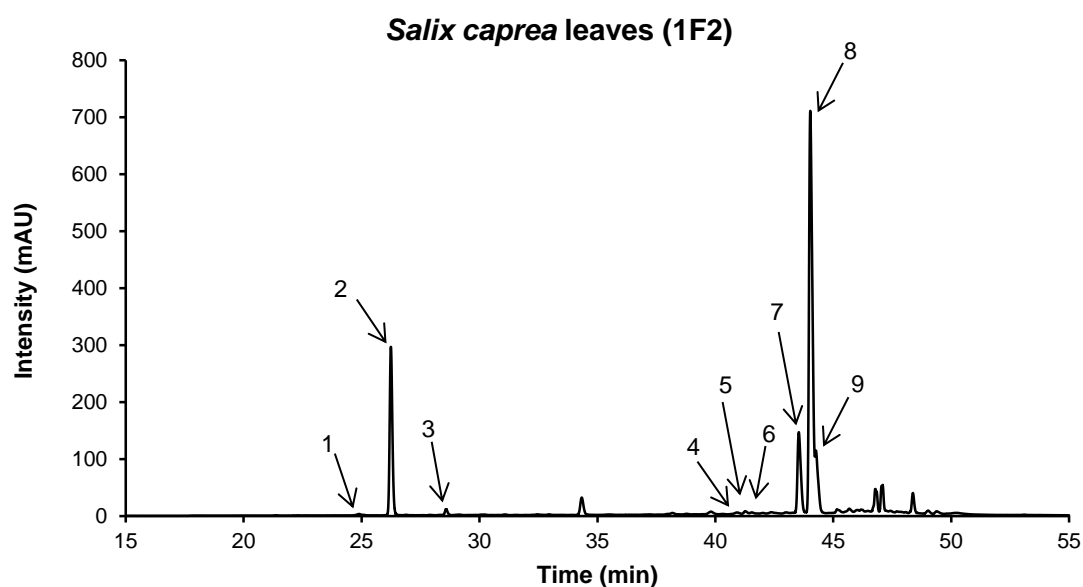
Figure 3.2: Chromatogram of thiolysis reaction products from *S. caprea* leaf proanthocyanidins. Peak assignments: 1, epigallocatechin; 2, catechin; 3, epicatechin; 4, gallocatechin-BM (*trans)*; 5, gallocatechin-BM (*cis)*; 6 epicatechin-BM *,* 7, catechin-BM (*trans*); 8, catechin-BM (*cis*); 9, epicatechin-BM; BM: benzyl mercaptan
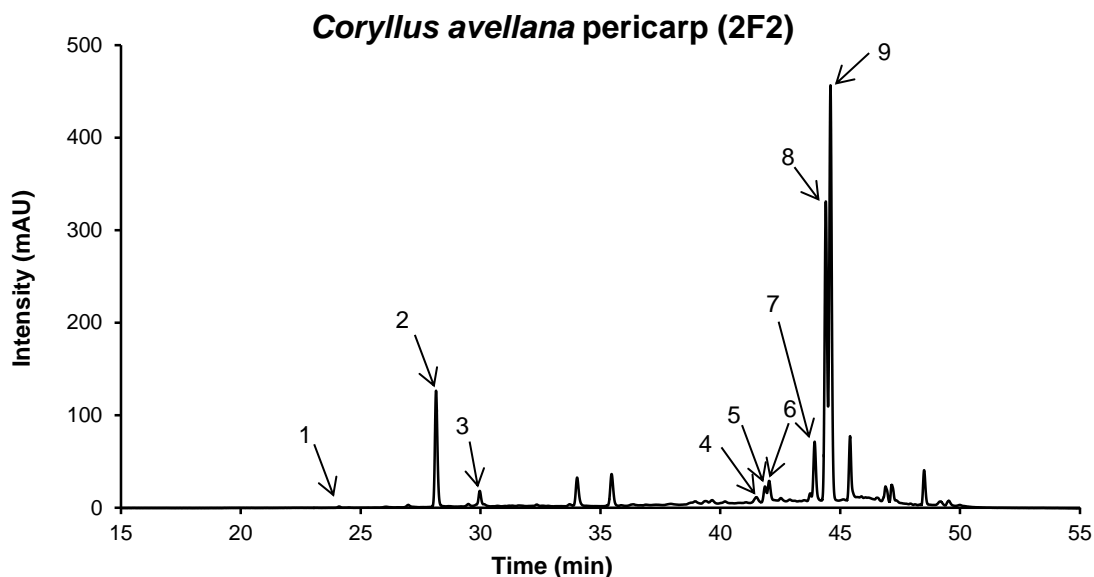
Figure 3.3: Chromatogram of thiolysis reaction products from C. avellana pericarp proanthocyanidins. Peak assignments: 1, epigallocatechin; 2, catechin; 3, epicatechin; 4, gallocatechin-BM (*trans*); 5, gallocatechin-BM (cis); 6, epigallocatechin-BM; 7, catechin-BM (*trans*); 8, catechin-BM (*cis*); 9, epicatechin-BM; BM: benzyl mercaptan
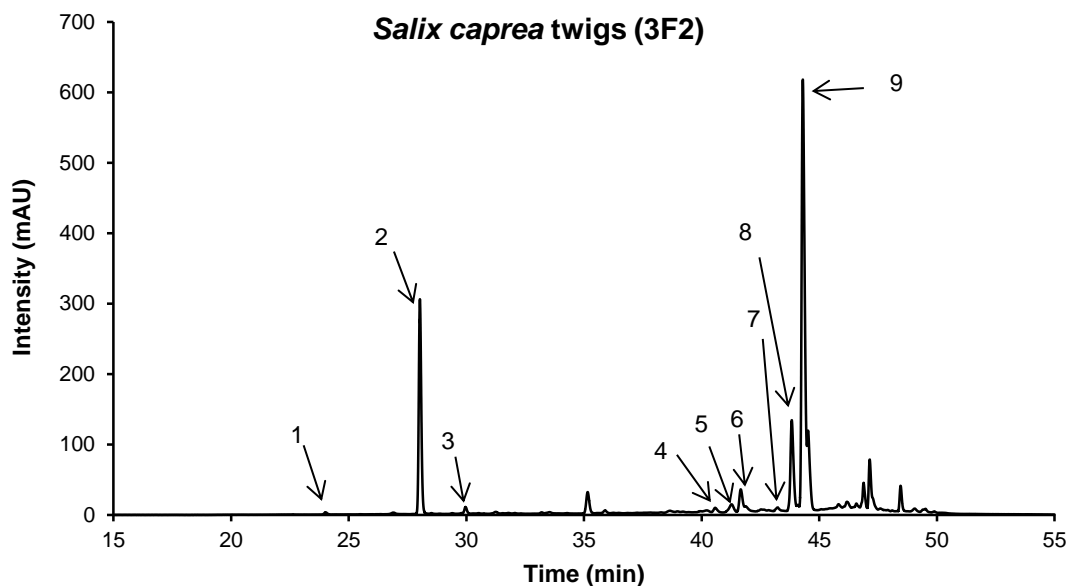
Figure 3.4: Chromatogram of thiolysis reaction products from a *S. caprea* twig proanthocyanidins. Peak assignments: 1, epigallocatechin; 2, catechin; 3, epicatechin; 4, gallocatechin-BM (*trans)*; 5, gallocatechin-BM (*cis)*; 6, epigallocatechin-BM*,* 7; catechin-BM (*trans*); 8, catechin-BM (*cis*); 9, epicatechin-BM; BM: benzyl mercaptan
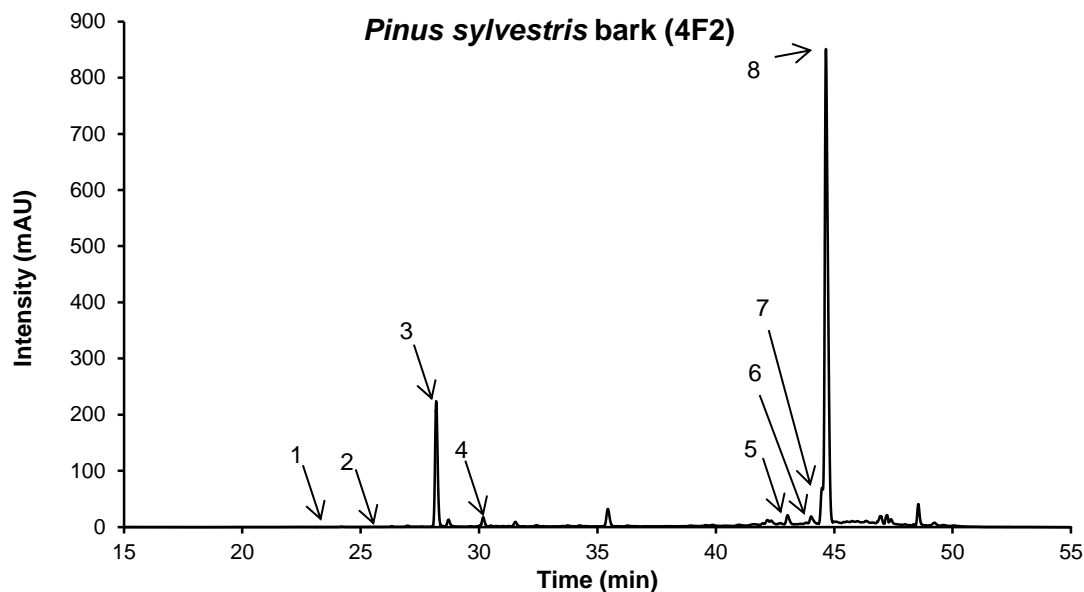
Figure 3.5: Chromatogram of thiolysis reaction products of *Pinus sylvestris*, bark proanthocyanidins. Peak assignments: 1, gallocatechin; 2, epigallocatechin; 3, catechin; 4, epicatechin; 5, epigallocatechin-BM, 6, catechin-BM (*trans*); 7, catechin-BM (*cis*); 8, epicatechin-BM; BM: benzyl mercaptan
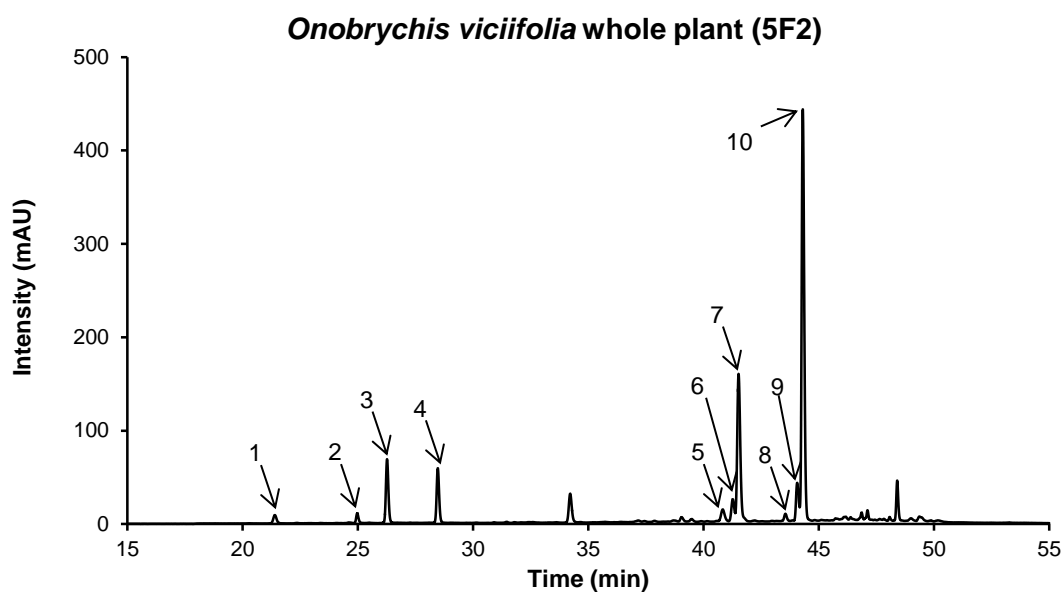
Figure 3.6: Chromatogram of thiolysis reaction products of *O. viciifolia*, whole plant proanthocyanidins. Peak assignments: 1, gallocatechin; 2, epigallocatechin; 3, catechin; 4, epicatechin; 5, gallocatechin-BM (*trans*); 6, gallocatechin-BM (*cis*); 7, epigallocatechin-BM, 8, catechin-BM (*trans*); 9, catechin-BM (*cis*); 10, epicatechin-BM; BM: benzyl mercaptan
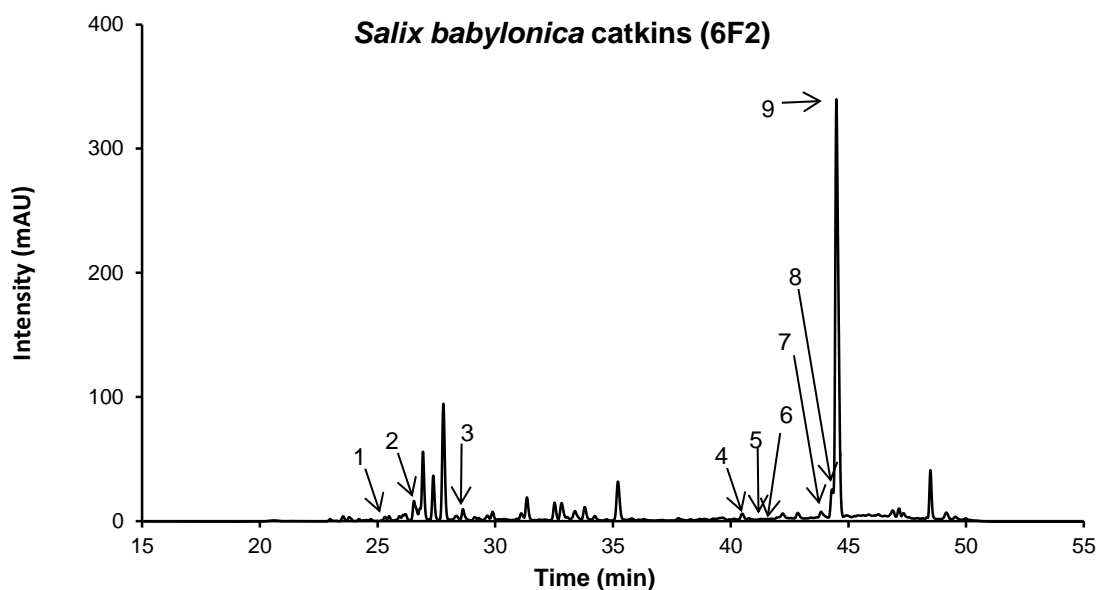
Figure 3.7: Chromatogram of thiolysis reaction products of *S. babylonica*, catkin proanthocyanidins. Peak assignments: 1, epigallocatechin; 2, catechin; 3, epicatechin; 4, gallocatechin-BM (*trans*); 5, gallocatechin-BM (*cis*); 6, epigallocatechin-BM, 7, catechin-BM (*trans*); 8, catechin-BM (*cis*); 10, epicatechin-BM; BM: benzyl mercaptan
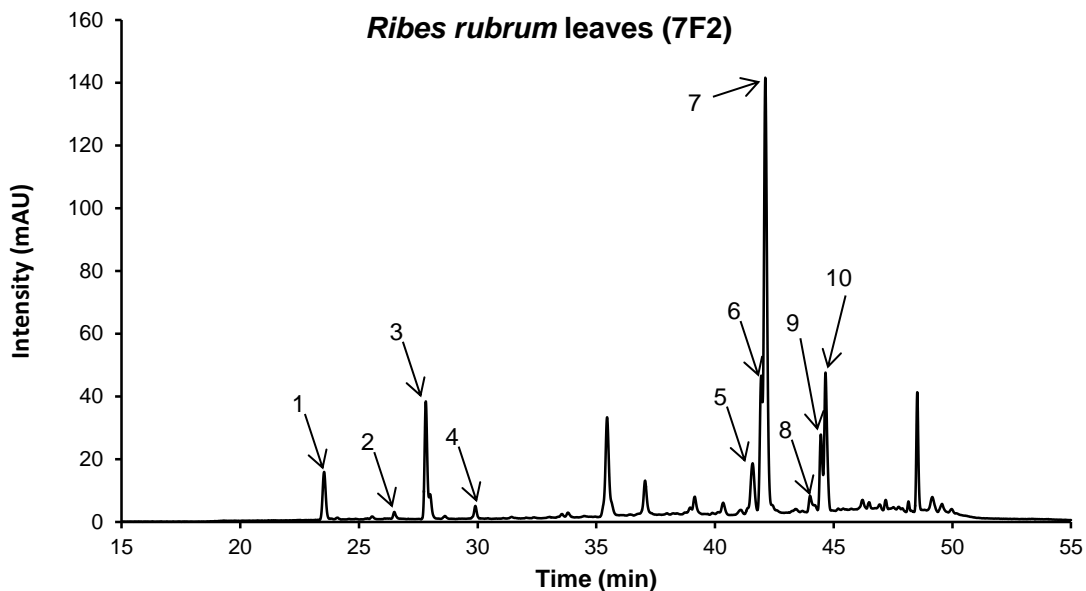
Figure 3.8: Chromatogram of thiolysis reaction products from *R. rubrum*, leaf proathocyanidins. Peak assignments: 1, gallocatechin; 2, epigallocatechin; 3, catechin; 4, epicatechin; 5, gallocatechin-BM (*trans*); 6, gallocatechin-BM (*cis*); 7, epigallocatechin-BM, 8, catechin-BM (*trans*); 9, catechin-BM (*cis*); 10, epicatechin-BM; BM: benzyl mercaptan
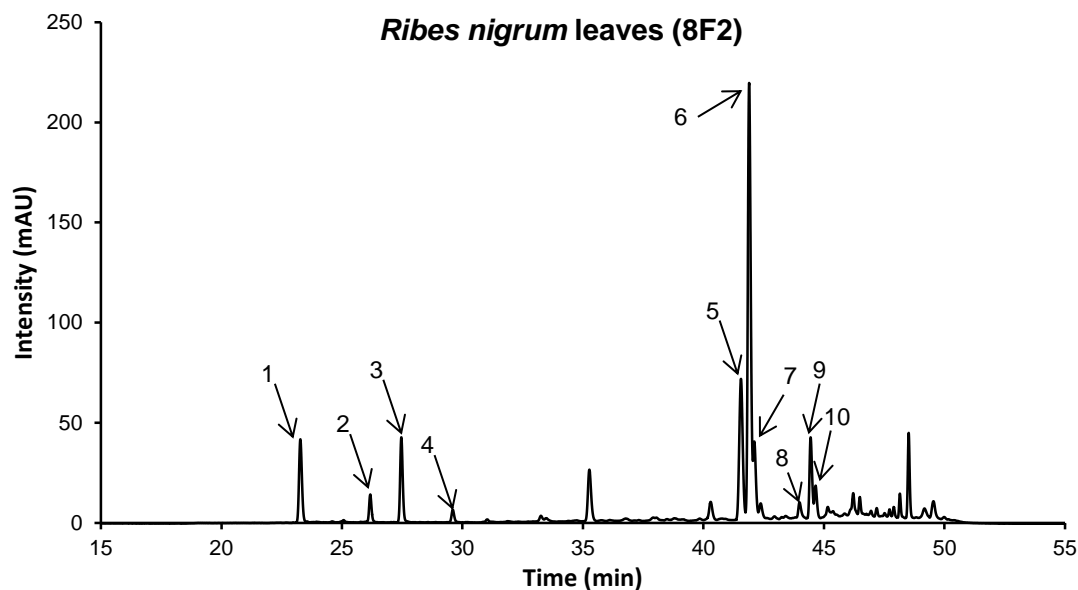
Figure 3.9: Chromatogram of thiolysis reaction products from *R. nigrum*, leaf pranthocyanidins. Peak assignments: 1, gallocatechin; 2, epigallocatechin; 3, catechin; 4, epicatechin; 5, gallocatechin-BM (*trans*); 6, gallocatechin-BM (*cis*); 7, epigallocatechin-BM, 8, catechin-BM (*trans*); 9, catechin-BM (*cis*); 10, epicatechin-BM; BM: benzyl mercaptan
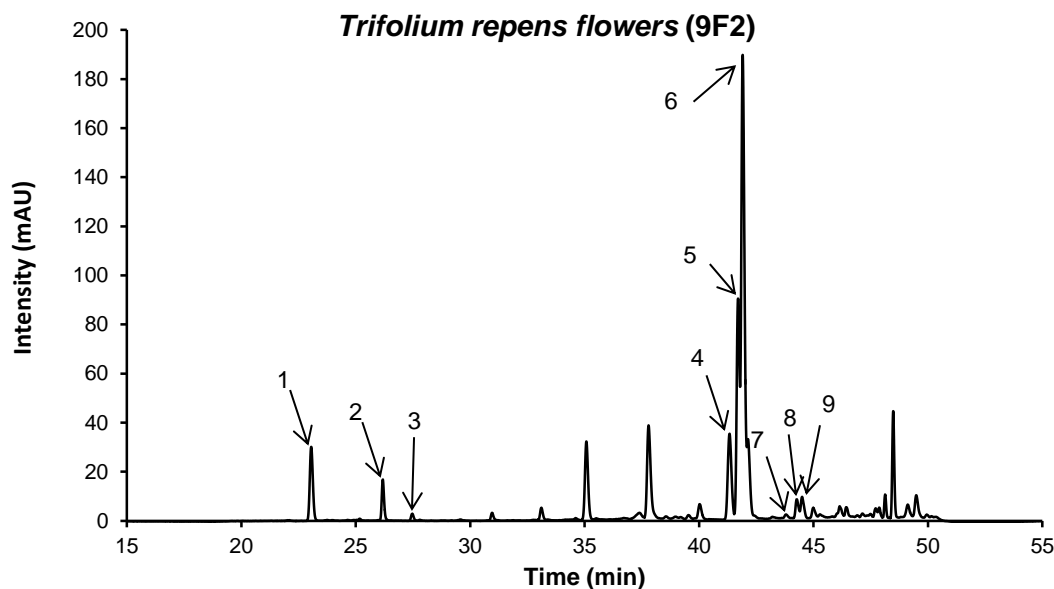
Figure 3.10: Chromatogram of thiolysis reaction products of *T. repens*, flower proanthocyanidins. Peak assignments: 1, gallocatechin; 2, epigallocatechin; 3, catechin; 4, gallocatechin-BM (*trans*); 5, gallocatechin-BM (*cis*); 6, epigallocatechin-BM, 7, catechin-BM (*trans*); 8, catechin-BM (*cis*); 9, epicatechin-BM; BM: benzyl mercaptan

94

Semi-quantitative and qualitative techniques

Although MALDI-TOF MS is a powerful tool for the characterisation of individual compounds in PA mixtures, it cannot yield quantitative information [18, 31-33]. The signal intensities do not correspond to the relative abundance of different PA compounds [18]. Particular problems occur in the detection of large PA polymers. The soft ionisation of this technique produces only singly charged ions and as the MW increases the charge density is reduced [31]. It has been suggested that large PA polymers are most likely decomposed due to collisions in the TOF tube during reflectron mode detection or could have lower velocity impact, whereas linear mode detection suffers from background noise that affects the identification of isotopic patterns [32]. Quantification is also hampered by ion suppression in complex samples [18], saturation of the detector [32] and more importantly the unavailability of commercial PA standards [18, 31]. Recent studies have shown that PA analysis by MALDI-TOF MS can also suffer from adduct formation due to esterification of PAs with matrix molecules during the experiments [34]. The same study also found several other structural transformations from uncontrolled reactions caused by the irradiation and the ionisation processes [34]. Another problem with MALDI-TOF MS analysis is caused by heterogeneous co-crystallisation with the different matrices and the cationising agents which can result in diverse spot topologies. As a result, irradiation of the different matrix-analyte combinations can generate highly variable spectra from the same spot, which complicates PA quantification and characterisation [18, 24].

Similarly to MALDI-TOF MS, PA analysis by HILIC-DAD-ESI-TOF-MS provides only compositional and no quantitative information [19, 35]. These quantification constraints derive from the lack of commercial standards and the failure of the HILIC column to separate compounds with similar MW [35].

The PA responses in NMR spectroscopy differ between unknown and the chosen standard compounds which are used for quantification, therefore NMR spectroscopy does not provide information on PA contents [36, 37].

3.3.2 Comparison of methods for analysing the degrees of PA polymerisation

Quantitative techniques

There are several different approaches that can be used to determine the degree of polymerisation of PAs. Depolymerisation techniques provide information on the mDP, i.e. the average DP of all PA compounds in a mixture. Thiolytic degradation with benzyl mercaptan releases the flavan-3-ol subunits from PA polymers and these subunits are then analysed by HPLC. Another approach uses a post-column polymer fragmentation with a range of cone voltages (Table 3.1) at the electrospray ionisation interface during UPLC-ESI-MS/MS analysis.

There was a good correlation of mDP values obtained by thiolysis and UPLC-ESI-MS/MS analysis (R^2=0.76) (Figure 3.11A), although the range of the chosen PA samples from 5 to 10 was relatively narrow. This means that further tests will be needed to evaluate the robustness of these methods by examining a wider range of PA samples. This may require adjusting the thiolysis conditions, the various electrospray ionisation conditions and/or the empirical formula used for mDP estimation in the UPLC-ESI-MS/MS analysis [16]. If free flavan-3-ols are present, mDP underestimations often occur with the thiolysis-HPLC analysis [13, 16]. The advantage of UPLC-ESI-MS/MS method over thiolysis is that information on free flavan-3-ol presence is readily available without the need for a separate analysis [16] and therefore, they can easily be excluded from mDP determinations.

Semi-quantitative and qualitative techniques

The presence of a multitude of compounds and rotational restrictions around the interflavanyl bonds tend to produce broad and unresolved signals in NMR spectra [25]; nevertheless, some NMR studies have attempted to estimate average MWs of PAs [38-40] by integrating the cross peak contours of the terminal and the linked methylene units (Figures 3.12C - 3.14C). However, the correlation of mDP values between thiolysis and NMR was slightly lower (R^2=0.67) than with UPLC-ESI-MS/MS (Figure 3.11B).
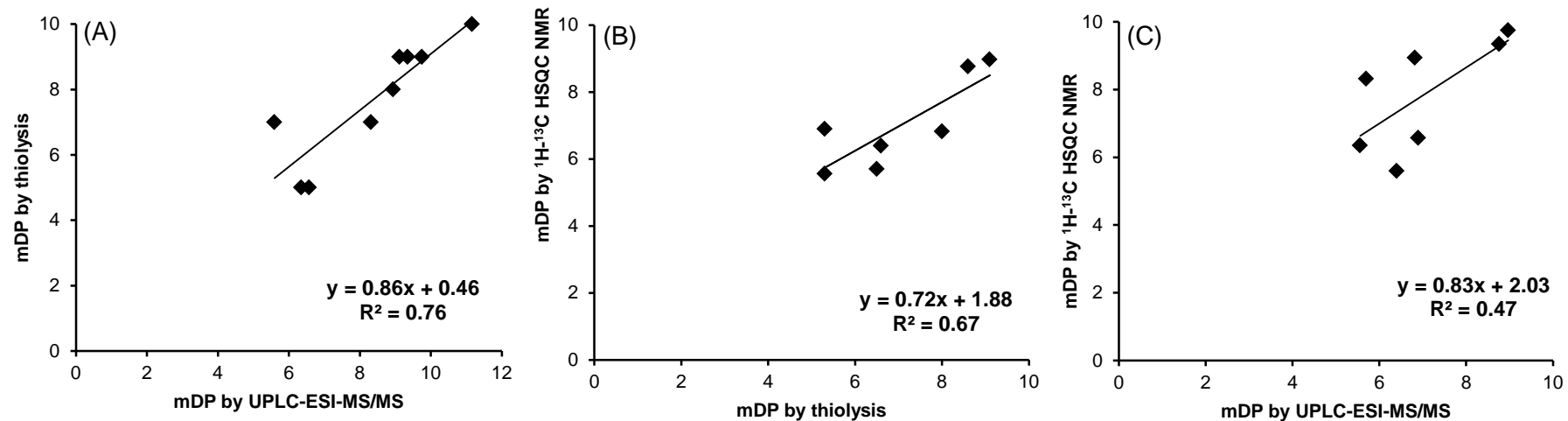
Figure 3.11: Correlation of mean degree of polymerisation (mDP) values between: (A) thiolysis and UPLC-ESI-MS/MS, (B) ^{1}H-^{13}C HSQC NMR and thiolysis and (C) ^{1}H-^{13}C HSQC NMR and UPLC-ESI-MS/MS. Note: The O. viciifolia (5F2) proanthocyanidin sample was not measured and the signal intensity did not allow determination of the mDP value in the R. rubrum leaf (7F2) proanthocyanidin sample with ^{1}H-^{13}C HSQC NMR, therefore, they were excluded from the correlations.
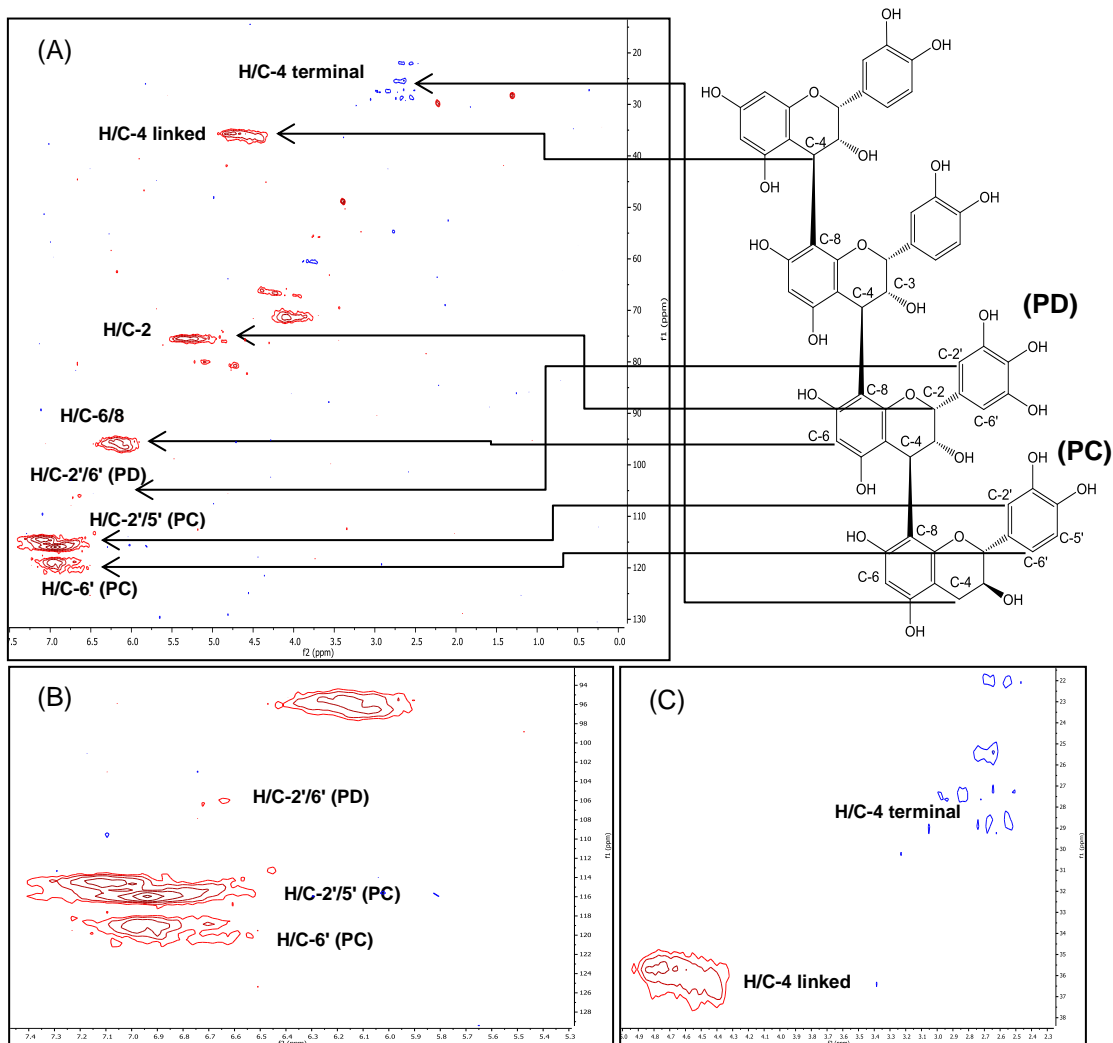
Figure 3.12: (A) Signal assignments for the ^{1}H-^{13}C HSQC NMR spectrum of proanthocyanidins from *P. sylvestris* bark (Table 3.2). (B) B-ring aromatic region cross peak signals including the H/C-2´, 5´ and 6´ signals from procyanidin (PC) flavan-3-ol units. The region where the H/C-2´, 6´ prodelphinidin (PD) signal should appear is vacant. (C) Cross peak signals for H/C-4 linked (extension) and terminal flavan-3-ol units.
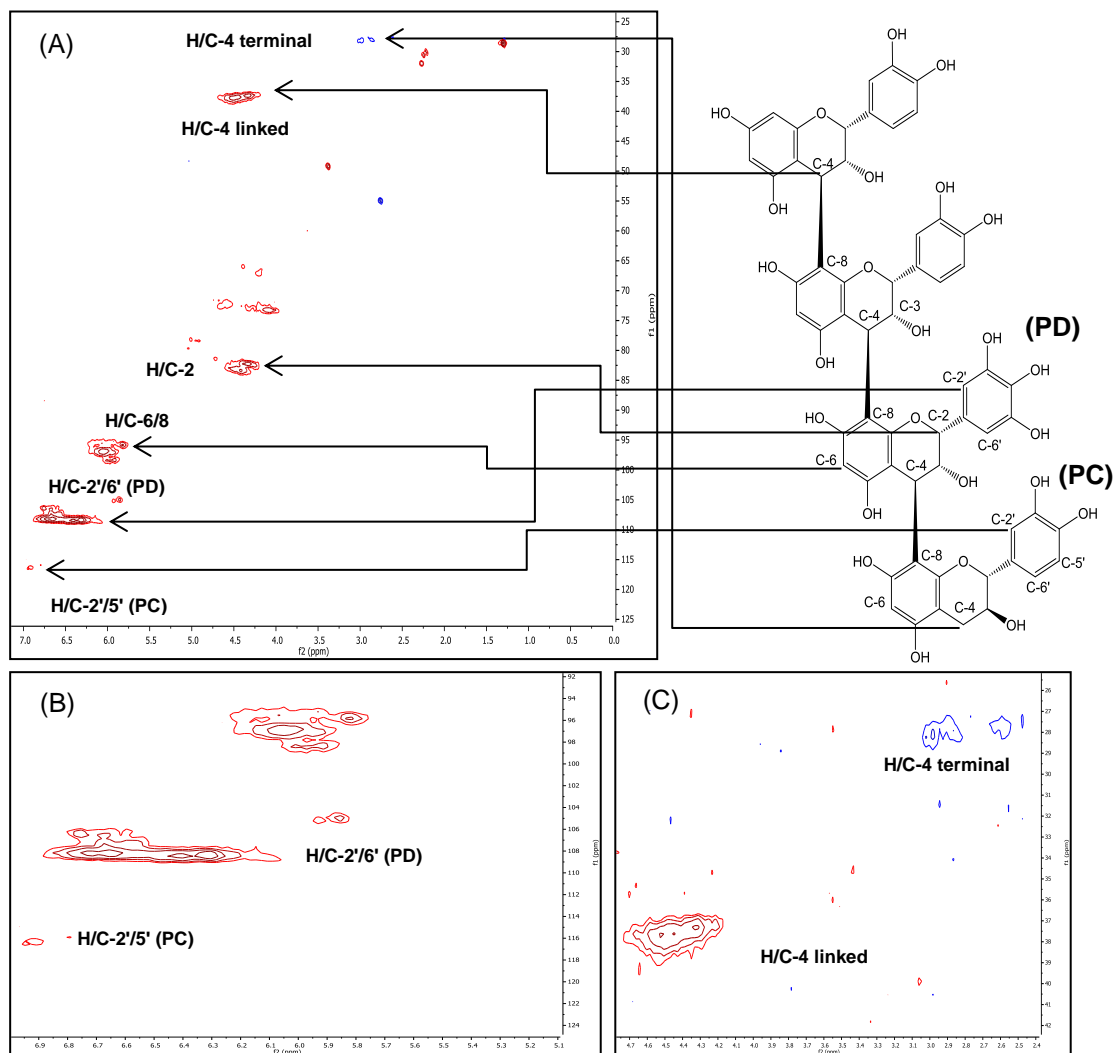
Figure 3.13: (A) Signal assignments for the ^{1}H-^{13}C HSQC NMR spectrum of proanthocyanidins from *R. nigrum* leaves (Table 3.2). (B) B-ring aromatic region cross peak signals including the H/C-2´, 6´ from prodelphinidin (PD) flavan-3-ol units and a weak H/C-2´, 5´ signal from procyanidin (PC) flavan-3-ol units. The region where the H/C-2´, 5´ procyanidin signal should appear is vacant. (C) Cross peak signals for H/C-4 linked (extension) and terminal flavan-3-ol units
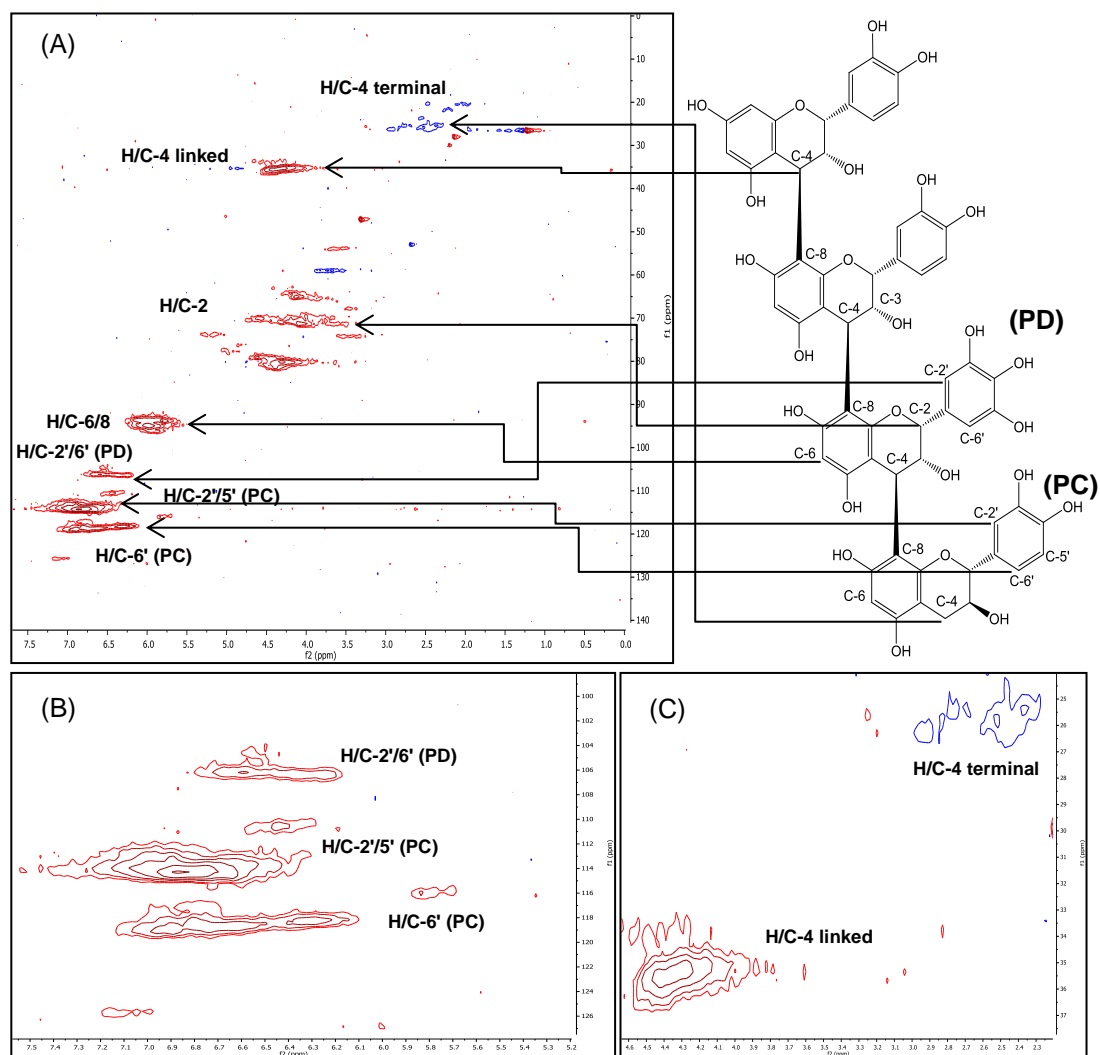
Figure 3.14: (A) Signal assignments for the ^{1}H-^{13}C HSQC NMR spectrum of proanthocyanidins from *S. caprea* twigs (Table 3.2). (B) B-ring cross peak signals including H/C-2´, 6´ prodelphinidin (PD) signal and the H/C-2´, 5´ and 6´ signals from procyanidin (PC) flavan-3-ol units. (C) Cross peak signals for H/C-4 linked (extension) and terminal flavan-3-ol units.

It will be interesting to explore why the correlation between NMR and UPLC-ESI-MS/MS (Figure 3.11C) was so low (R^2=0.47). It should be noted that the *O. viciifolia* PA fraction was not measured by ^1H-^{13}C HSQC NMR and the mDP of *R. rubrum* leaf (7F2) PAs was not determined due to the low response of the terminal methylene units. Therefore, these results were excluded from the mDP correlations (Table 3.2). This decreased the sample population and could account for the weak correlations. Zeller et al. also reported that T1 and T2 relaxation and resonance offset effects result in signals that are not proportional to the corresponding nuclei ratios [17]. The same study stated that the integration of the signal of C4 methylene units of terminal flavan-3-ol units could not be directly correlated with the relative intensities of the nuclei that generate the signal [17]. It seems that PAs with higher mDP values than a threshold of ca 10 were, therefore, more difficult to analyse by NMR than thiolysis or UPCL-ESI-MS/MS (Table 3.2) due to the above sensitivity and integration issues.

In general mDP values provide only a global picture of the complex PA polymers since depolymerisation masks the actual presence of individual oligomers and polymers in the sample and provides no information about the MW distribution [16, 18, 41]. However, this analytical challenge can be partially resolved by mass spectrometric techniques that employ TOF analysers, which can detect individual PA molecules with high resolution over a theoretically unlimited mass range [18, 24, 33, 35, 42].

Collection of spectra in the MALDI-TOF MS reflectron mode yielded information on individual PA molecules and gave a polymer range, which agreed with the mDP values from thiolysis and UPLC-ESI-MS/MS. Complexation of PAs with DHB and Na$^+$ allowed detection of polymers with >10 subunits (Tables 3.3-3.9).

Table 3.3: Predicted and observed monoisotopic *m/z* values from MALDI-TOF MS analysis of the Na^{+} adduct ions of purified B-type *S. caprea* leaf (1F2) proanthocyanidins. C: (epi)catechin flavan-3-ol; G: (epi)gallocatechin flavan-3-ol subunits

chain length		nC	(n-1)C + 1G	(n-2)C + 2G	(n-3)C + 3G	(n-4)C + 4G	(n-5)C + 5G	(n-6)C + 6G
				composition of oligomers and polymers				
2-mer (n=2)	pred	601.13	617.12	633.12				
	obsd							
3-mer (n=3)	pred	899.19	905.19	921.18	937.18			
	obsd							
4-mer (n=4)	pred	1177.26	1193.25	1209.25	1225.24	1241.24		
	obsd							
5-mer (n=5)	pred	1465.31	1481.32	1497.31	1513.31	1529.3	1545.26	
	obsd	1465.10						
6-mer (n=6)	pred	1753.38	1769.38	1785.37	1801.37	1817.36	1833.36	1849.35
	obsd	1753.13						
7-mer (n=7)	pred	2041.44	2057.44	2073.44	2089.43	2105.43	2121.42	2137.42
	obsd	2041.10	2057.03					
8-mer (n=8)	pred	2329.51	2345.51	2361.68	2377.50	2393.49	2409.49	2425.48
	obsd	2329.96						
9-mer (n=9)	pred	2617.57	2633.57	2649.57	2665.56	2681.55	2697.55	2713.54
	obsd	2617.79						
10-mer (n=10)	pred	2905.64	2921.64	2937.63	2953.62	2969.62	2985.61	3001.61
	obsd	2905.45						
11-mer (n=11)	pred	3193.70	3209.70	3225.69	3241.69	3257.68	3273.68	3289.67
	obsd	3193.26						

Table 3.4: Predicted and observed monoisotopic *m/z* values from MALDI-TOF MS analysis of the Na$^+$ adduct ions of purified B-type *C. avellana* pericarp (2F2) proanthocyanidins. C: (epi)catechin flavan-3-ol; G: (epi)gallocatechin flavan-3-ol subunits.

chain length		nC	(n-1)C + 1G	(n-2)C + 2G	(n-3)C + 3G	(n-4)C + 4G	(n-5)C + 5G	(n-6)C + 6G
				composition of oligomers and polymers				
2-mer (n=2)	pred	601.13	617.12	633.12				
	obsd							
3-mer (n=3)	pred	899.19	905.19	921.18	937.18			
	obsd			921.29				
4-mer (n=4)	pred	1177.26	1193.25	1209.25	1225.24	1241.24		
	obsd							
5-mer (n=5)	pred	1465.31	1481.32	1497.31	1513.31	1529.3	1545.26	
	obsd	1465.57						
6-mer (n=6)	pred	1753.38	1769.38	1785.37	1801.37	1817.36	1833.36	1849.35
	obsd	1753.69	1769.70					
7-mer (n=7)	pred	2041.44	2057.44	2073.44	2089.43	2105.43	2121.42	2137.42
	obsd	2041.76	2057.76	2073.73				
8-mer (n=8)	pred	2329.51	2345.51	2361.68	2377.50	2393.49	2409.49	2425.48
	obsd	2329.65	2345.73					
9-mer (n=9)	pred	2617.57	2633.57	2649.57	2665.56	2681.55	2697.55	2713.54
	obsd	2617.60	2633.53					

Table 3.5: Predicted and observed monoisotopic *m/z* values from MALDI-TOF MS analysis of the Na^{+} adduct ions of purified B-type *S. caprea* twig (3F2) proanthocyanidins. C: (epi)catechin flavan-3-ol; G: (epi)gallocatechin flavan-3-ol subunits.

chain length		nC	(n-1)C + 1G	(n-2)C + 2G	(n-3)C + 3G	(n-4)C + 4G	(n-5)C + 5G	(n-6)C + 6G
				composition of oligomers and polymers				
2-mer (n=2)	pred	601.13	617.12	633.12				
	obsd							
3-mer (n=3)	pred	899.19	905.19	921.18	937.18			
	obsd							
4-mer (n=4)	pred	1177.26	1193.25	1209.25	1225.24	1241.24		
	obsd	1177.05	1193.03					
5-mer (n=5)	pred	1465.31	1481.32	1497.31	1513.31	1529.3	1545.26	
	obsd	1465.18	1481.18	1497.16				
6-mer (n=6)	pred	1753.38	1769.38	1785.37	1801.37	1817.36	1833.36	1849.35
	obsd	1753.25	1769.29	1785.23				
7-mer (n=7)	pred	2041.44	2057.44	2073.44	2089.43	2105.43	2121.42	2137.42
	obsd	2041.24	2057.24	2073.16				
8-mer (n=8)	pred	2329.51	2345.51	2361.68	2377.50	2393.49	2409.49	2425.48
	obsd	2329.16	2345.18					
9-mer (n=9)	pred	2617.57	2633.57	2649.57	2665.56	2681.55	2697.55	2713.54
	obsd	2616.92						

Table 3.6: Predicted and observed monoisotopic *m/z* values from MALDI-TOF MS analysis of the Na^{+} adduct ions of purified B-type *P. sylvestris* bark (4F2) proanthocyanidins. C: (epi)catechin flavan-3-ol; G: (epi)gallocatechin flavan-3-ol subunits.

chain length		nC	(n-1)C + 1G	(n-2)C + 2G	(n-3)C + 3G	(n-4)C + 4G	(n-5)C + 5G	(n-6)C + 6G
				composition of oligomers and polymers				
2-mer (n=2)	pred	601.13	617.12	633.12				
	obsd							
3-mer (n=3)	pred	899.19	905.19	921.18	937.18			
	obsd							
4-mer (n=4)	pred	1177.26	1193.25	1209.25	1225.24	1241.24		
	obsd	1176.93						
5-mer (n=5)	pred	1465.31	1481.32	1497.31	1513.31	1529.3	1545.26	
	obsd	1465.04	1481.03					
6-mer (n=6)	pred	1753.38	1769.38	1785.37	1801.37	1817.36	1833.36	1849.35
	obsd	1753.06	1769.03					
7-mer (n=7)	pred	2041.44	2057.44	2073.44	2089.43	2105.43	2121.42	2137.42
	obsd	2041.00	2056.98					
8-mer (n=8)	pred	2329.51	2345.51	2361.68	2377.50	2393.49	2409.49	2425.48
	obsd	2328.86	2345.84					
9-mer (n=9)	pred	2617.57	2633.57	2649.57	2665.56	2681.55	2697.55	2713.54
	obsd	2617.68						
10-mer (n=10)	pred	2905.64	2921.64	2937.63	2953.62	2969.62	2985.61	3001.61
	obsd	2905.40						
11-mer (n=11)	pred	3193.70	3209.70	3225.69	3241.69	3257.68	3273.68	3289.67
	obsd	3193.07						
12-mer (n=12)	pred	3481.77	3497.76	3513.75	3529.75	3545.74	3561.74	3577.73
	obsd	3481.63						

Table 3.7: Predicted and observed monoisotopic *m/z* values from MALDI-TOF MS analysis of the Na$^+$ adduct ions of purified B-type *S. babylonica* catkin (6F2) proanthocyanidins. C: (epi)catechin flavan-3-ol; G: (epi)gallocatechin flavan-3-ol subunits.

chain length		nC	(n-1)C + 1G	(n-2)C + 2G	(n-3)C + 3G	(n-4)C + 4G	(n-5)C + 5G	(n-6)C + 6G
				composition of oligomers and polymers				
2-mer (n=2)	pred	601.13	617.12	633.12				
	obsd							
3-mer (n=3)	pred	899.19	905.19	921.18	937.18			
	obsd				937.12			
4-mer (n=4)	pred	1177.26	1193.25	1209.25	1225.24	1241.24		
	obsd	1177.11	1193.12	1209.11				
5-mer (n=5)	pred	1465.31	1481.32	1497.31	1513.31	1529.30	1545.26	
	obsd	1465.21	1481.21	1497.19	1513.19			
6-mer (n=6)	pred	1753.38	1769.38	1785.37	1801.37	1817.36	1833.36	1849.35
	obsd	1753.23	1769.25	1785.26	1801.25			
7-mer (n=7)	pred	2041.44	2057.44	2073.44	2089.43	2105.43	2121.42	2137.42
	obsd	2041.18	2057.22	2073.26	2089.13	2105.11		
8-mer (n=8)	pred	2329.51	2345.51	2361.68	2377.5	2393.49	2409.49	2425.48
	obsd	2329.07	2345.08	2361.04	2376.99	2393.14		
9-mer (n=9)	pred	2617.57	2633.57	2649.57	2665.56	2681.55	2697.55	2713.54
	obsd	2617.92	2633.79	2649.89	2665.87	2905.60		
10-mer (n=10)	pred	2905.64	2921.64	2937.63	2953.62	2969.62	2985.61	3001.61
	obsd		2921.65	2937.61				

Table 3.8: Predicted and observed monoisotopic *m/z* values from MALDI-TOF MS analysis of the Na^{+} adduct ions of purified B-type *R. rubrum* leaf (7F2) proanthocyanidins. C: (epi)catechin flavan-3-ol; G: (epi)gallocatechin flavan-3-ol subunits.

chain length		composition of oligomers and polymers										
		(n-1)C + 1G	(n-2)C + 2G	(n-3)C + 3G	(n-4)C + 4G	(n-5)C + 5G	(n-6)C + 6G	(n-7)C + 7G	(n-8)C + 8G	(n-9)C + 9G	(n-10)C + 10G	(n-11)C + 11G
2-mer (n=2)	pred	617.12	633.12									
	obsd											
3-mer (n=3)	pred	905.19	921.18	937.18								
	obsd											
4-mer (n=4)	pred	1193.25	1209.25	1225.24	1241.24							
	obsd		1209.35	1225.35	1241.33							
5-mer (n=5)	pred	1481.32	1497.31	1513.31	1529.3	1545.26						
	obsd	1481.40	1497.53	1513.47	1529.47	1545.47						
6-mer (n=6)	pred	1769.38	1785.37	1801.37	1817.36	1833.36	1849.35					
	obsd			1801.58	1817.56	1833.53	1849.52					
7-mer (n=7)	pred	2057.44	2073.44	2089.43	2105.43	2121.42	2137.42	2153.57				
	obsd					2121.50	2137.50	2153.47				
8-mer (n=8)	pred	2345.51	2361.68	2377.5	2393.49	2409.49	2425.48	2441.48	2457.64			
	obsd						2425.48	2441.34	2457.36			
9-mer (n=9)	pred	2633.57	2649.57	2665.56	2681.55	2697.55	2713.54	2729.54	2745.54	2761.73		
	obsd								2745.15	2761.18		
10-mer (n=10)	pred	2921.64	2937.63	2953.62	2969.62	2985.61	3001.61	3017.61	3033.61	3049.61	3065.81	
	obsd								3033.97	3050.96	3064.91	
11-mer (n=11)	pred	3209.7	3225.69	3241.69	3257.68	3273.68	3289.67	3305.67	3321.67	3337.67	3353.67	3369.67
	obsd										3352.51	3370.62

Table 3.9: Predicted and observed monoisotopic *m/z* values from MALDI-TOF MS analysis of the Na$^+$ adduct ions of purified B-type *R. nigrum* leaf (8F2) proanthocyanidins. C: (epi)catechin flavan-3-ol; G: (epi)gallocatechin flavan-3-ol subunits.

chain length		nC	(n-1)C + 1G	(n-2)C + 2G	(n-3)C + 3G	(n-4)C + 4G	(n-5)C + 5G	(n-6)C + 6G	(n-7)C + 7G	(n-8)C + 8G
					composition of oligomers and polymers					
2-mer (n=2)	pred	601.13	617.12	633.12						
	obsd									
3-mer (n=3)	pred	899.19	905.19	921.18	937.18					
	obsd			921.43	937.32					
4-mer (n=4)	pred	1177.26	1193.25	1209.25	1225.24	1241.24				
	obsd					1241.52				
5-mer (n=5)	pred	1465.31	1481.32	1497.31	1513.31	1529.30	1545.26			
	obsd					1529.78	1545.73			
6-mer (n=6)	pred	1753.38	1769.38	1785.37	1801.37	1817.36	1833.36	1849.35		
	obsd						1833.93	1849.87		
7-mer (n=7)	pred	2041.44	2057.44	2073.44	2089.43	2105.43	2121.42	2137.42	2153.57	
	obsd							2137.81	2153.92	
8-mer (n=8)	pred	2329.51	2345.51	2361.68	2377.50	2393.49	2409.49	2425.48	2441.48	2457.65
	obsd								2441.92	2458.06

The smallest PA molecules (trimers) were detected in *R. nigrum* leaf PAs (Table 3.9), whereas the largest (dodecamers) were found in *P. sylvestris* leaf PAs (Table 3.6). *P. sylvestris* also had the widest range of molecules from tetramers to dodecamers. It was noticed that the DP range of some PA mixtures was not reflected by the mDP values determined by thiolysis-HPLC analysis. For example, *S. caprea* leaf PAs (1F2) had an mDP value of 5.3 and the DP from MALDI-TOF-MS ranged from 5 to 11 subunits whereas *C. avellana* pericarp PAs (2F2) had an mDP value of 9.2 and the DP ranged from 3 to 9 subunits. These results showed that mDP values can be misleading and that MALDI-TOF MS analysis has potential to shed some light on PA diversity. Several PA investigations with MALDI-TOF MS studies have also shown that the linear mode enabled the detection of larger PA polymers compared to the reflectron mode [43-46]. This illustrates that the experimental conditions have a large impact on the PA distribution profile. Nevertheless, reflectron mode is often preferred over linear mode due to enhanced signal-to-noise ratio and peak resolution, despite the possible degradation of molecules in the TOF tube as discussed above [18, 23, 32]. Although smaller oligomers tend to be difficult to detect by MALDI-TOF MS [24, 45], the use of sDHB and DHB with Na^+ during the experiments at the University of Reading enabled the detection of dimeric and trimeric homo-and hetero-polymers that were not detected during the analysis at the University of Madison. This variability in PA responses agrees with several reports, which attempted to identify matrix and cationising agent combinations for a more reproducible detection of PAs [24, 45, 47], and thus revealed a particular weakness of this MS method for determining polymerisation ranges.

Therefore, HILIC-DAD-ESI-TOF-MS analysis was used to explore further the degree of polymerisation in these PA samples. This method had originally been developed by Karonen et al. [19] and employed a HILIC column that significantly enhanced PA separation prior to mass spectrometric analysis. Proanthocyanidin homo-polymers generally eluted according to their degrees of polymerisation (Figure 3.15). However, the elution of PAs was more complicated in samples that consisted of both homo- and hetero-polymers even in the relatively resolved area before the polymeric hump. Surprisingly the polymerisation ranges
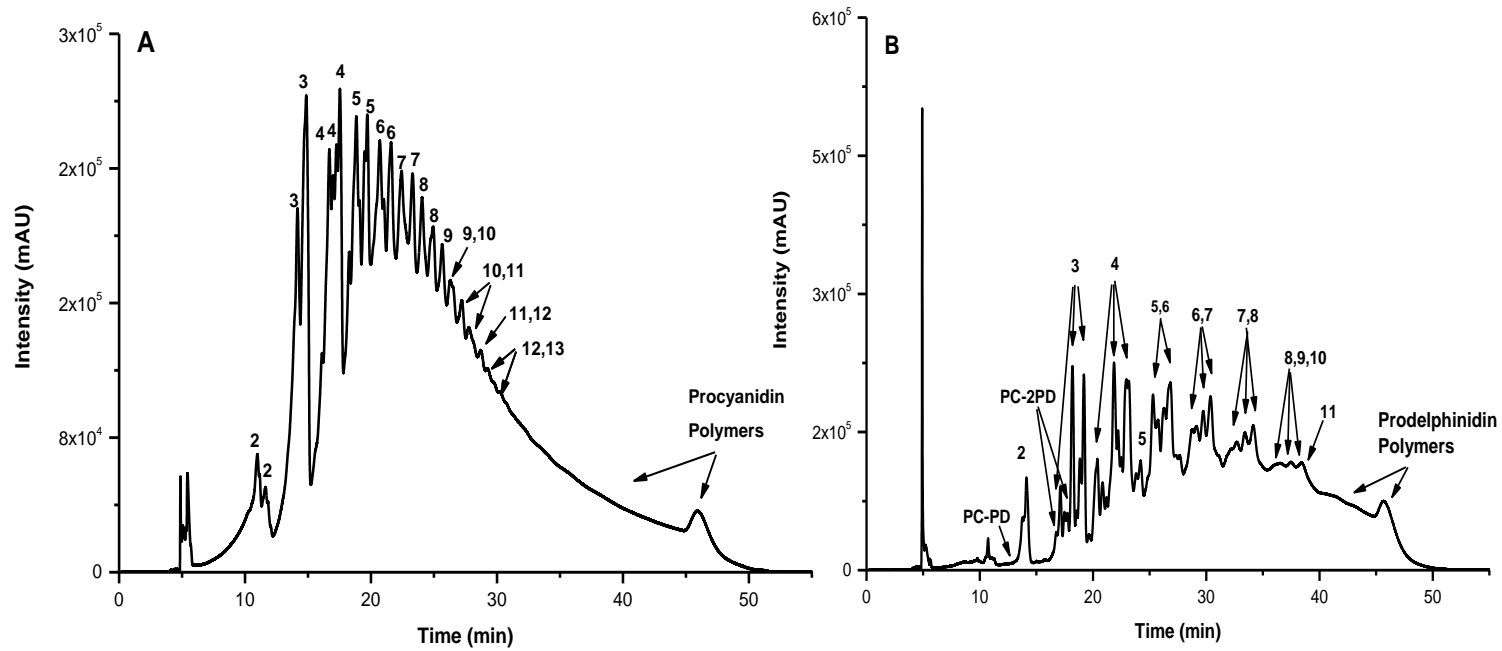
Figure 3.15: *P. sylvestris* bark (A) and *T. repens* flower (B) proanthocyanidin elution profiles according to the polymerisation degree after hydrophilic interaction liquid chromatography (HILIC). The labels indicate the degree of polymerisation of the main proanthocyanidins and the type of the flavan-3-ol subunits (PC: procyanidins, PD: prodelphinidins). The larger polymers elute at the end of the chromatograms.

did not vary as much between these samples (Tables 3.10-3.18) as might have been expected from the mDP values (Table 3.2).

In contrast to the polymerisation ranges obtained by MALDI-TOF MS, smaller oligomers (dimers, trimers and tetramers), up to larger polymers (DP>12) were identified by HILIC-DAD-ESI-TOF-MS analysis in almost all samples. The production of multiply charged ions in the various PA samples revealed a trend: oligomers up to tetramers formed singly charged ions, oligomers up to nonamers produced doubly charged ions and polymers produced triply charged ions. In several cases, ions of different charge states derived from the same compound (Figure 3.16, Tables 3.10-3.18).
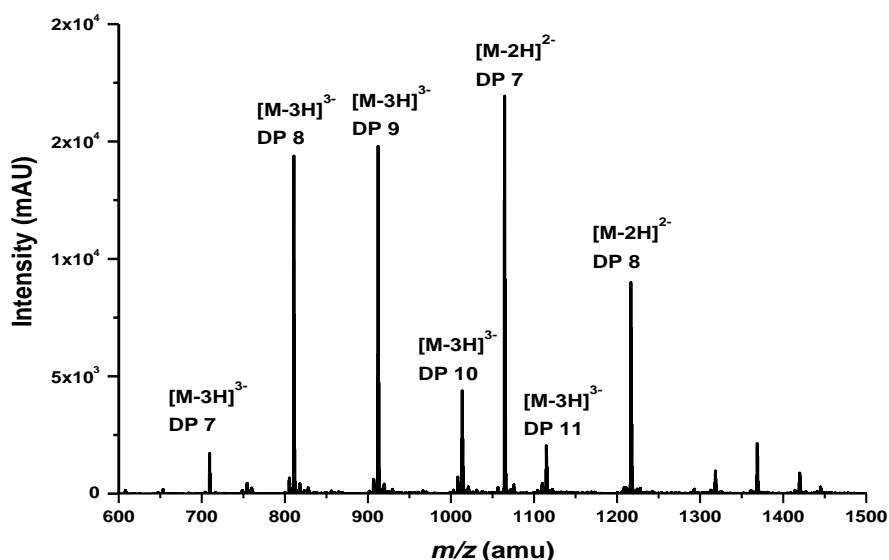
Figure 3.16: Mass spectrum of polymeric prodelphinidins from *T. repens* flower from HILIC-DAD-ESI-MS/MS analysis. Multiply charged ions, $[M-2H]^{2-}$ and $[M-3H]^{3-}$ which correspond to the same polymeric structure allowed the detection of higher molecular weight proanthocyanidins. The peak labels denote the degree of polymerisation (DP: 7-11).

It is known that polymerisation can affect chromatographic retention, peak resolution and ionisation efficiency due to the large number of different isomeric combinations that are possible [19, 35, 48-50]. The overlap of signals from the multiple isomers and multiply-charged ion fragments complicated the peak assignments. It is also not known whether large PA fragments remained stable

until detection or whether they were subjected to further fragmentation due a combination of ionisation and intramolecular events [51, 52]. Despite these reservations, HILIC separations coupled to high resolution ESI-TOF-MS provided some additional information on polymer sizes.

Table 3.10: Composition of *S. caprea* leaf (1F2) proanthocyanidins (PAs) estimated from the ESI-TOF-MS spectra. C: (epi)catechin; G: (epi)gallocatechin; *n*: number of flavan-3-ol subunits

PA composition	$M_{calculated}$	$M_{detected}$	$[M-H]^-$	$[M-2H]^{2-}$	$[M-3H]^{3-}$
2C	578.14	578.14	577.13		
3C	866.21	866.22	865.21		
4C	1154.27	1154.27	1153.26	576.13	
5C	1442.33	1442.34		720.16	
6C	1730.40	1730.38		864.18	
7C	2018.46	2018.46		1008.22	
5C-G	1746.39	1746.38		872.18	
3C-2G	1474.32	1474.32		736.15	
2C-3G	1490.32	1490.34		744.16	
8C	2306.52	2306.52		1152.25	767.83
9C	2594.59	2594.54		1296.26	863.85
4C-2G	1762.39	1762.38		880.18	
10C	2882.65	2882.66		1440.32	959.88
7C-G	2322.52	2322.46		1160.22	
11C	3170.71	3170.72		1584.85	1055.89
12C	3458.78	3458.72			1151.91
9C-G	2898.64	2898.68			965.22
13C	3746.84	3746.78			1247.92
14C	4034.90	4034.90			1343.96
10C-G	3186.71	3186.74			1061.24
11C-G	3474.77	3474.80			1157.26
12C-G	3762.83	3762.77			1253.25
13C-G	4050.90	4050.86			1349.28
15C	4322.97	4322.96			1439.98

Table 3.11: Composition of *C. avellana* pericarp (2F2) proanthocyanidins (PAs) estimated from the ESI-TOF-MS spectra. C: (epi)catechin; G: (epi)gallocatechin; *n*: number of flavan-3-ol units

PA composition	M$_{calculated}$	M$_{detected}$	[M-H]$^{-}$	[M-2H]$^{2-}$	[M-3H]$^{3-}$
2C	578.14	578.15	577.14		
C-G	594.14	594.14	593.13		
3C	866.21	866.21	865.20		
2C-G	882.20	882.21	881.20		
4C	1154.27	1154.28	1153.27	576.13	
3C-G	1170.26	1170.27	1169.26	584.14	
5C	1442.33	1442.36		720.17	
4C-G	1458.33	1458.34		728.16	
6C	1730.40	1730.40		864.19	
3C-2G	1474.32	1474.34		736.16	
5C-G	1746.39	1746.40		872.19	
7C	2018.46	2018.46		1008.22	
4C-2G	1762.39	1762.38		880.18	
6C-G	2034.45	2034.48		1016.23	
8C	2306.52	2306.52		1152.25	763.85
3C-3G	1778.38	1778.38		888.18	
5C-2G	2050.45	2050.44		1024.21	
6C-2G	2338.51	2338.54		1168.26	778.51
3C-5G	2354.51	2354.48		1176.23	783.84
9C	2594.59	2594.60		1296.29	863.85
10C	2882.65	2882.66			959.88
7C-G	2322.52	2322.52		1160.25	773.18
8C-G	2610.58	2610.56			869.18
7C-2G	2626.58	2626.61			874.53
11C	3170.71	3170.75			1055.91
4C-4G	2370.50	2370.53			789.17
4C-3G	2066.44	2066.46		1032.22	
6C-3G	2642.57	2642.58		1320.28	
9C-G	2898.64	2898.65			965.21
11C-2G	3778.83	3778.82			1258.6
10C-G	3186.71	3186.74			1061.24
13C	3746.84	3746.81			1247.93
8C-2G	2914.64	2914.67			970.55
9C-4G	3810.82	3810.83			1269.27
13C-G	4050.90	4050.89			1349.29
14C	4034.90	4034.87			1343.95
5C-4G	2658.57	2658.59			885.19
9C-2G	3202.70	3202.67			1066.55
11C-G	3474.77	3474.74			1157.24
6C-4G	2946.63	2946.59			981.19
13C-G	4354.96	4354.97			1450.65
8C-4G	3522.76	3522.74			1173.24

Table 3.11 *(continued)*

PA composition	$M_{calculated}$	$M_{detected}$	$[M-H]^-$	$[M-2H]^{2-}$	$[M-3H]^{3-}$
7C-3G	2930.63	2930.66			975.88
5C-5G	2962.62	2962.64			986.54
12C-G	3762.83	3762.86			1253.28
8C-3G	3218.70	3218.69			1071.89
10C-G	3490.77	3490.79			1162.59
9C-3G	3506.76	3506.81			1167.93
7C-4G	3234.69	3234.65			1077.21
11C-3G	4082.89	4082.81			1359.93
6C-5G	3250.69	3250.70			1082.56
10C-4G	4098.88	4098.95			1365.31
10C-3G	3794.82	3794.87			1263.95
7C-5G	3538.75	3538.76			1178.58
8C-5G	3826.81	3826.79			1274.59

Table 3.12: Composition of *S. caprea* twig (3F2) proanthocyanidins (PAs) estimated from the ESI-TOF-MS spectra. C: (epi)catechin; G: (epi)gallocatechin; *n*: number of flavan-3-ol subunits

PA composition	$M_{calculated}$	$M_{detected}$	$[M-H]^-$	$[M-2H]^{2-}$	$[M-3H]^{3-}$
2C	578.14	578.15	577.14		
C-G	594.14	594.14	593.13		
3C	866.21	866.21	865.20		
2C-G	882.20	882.21	881.20		
4C	1154.27	1154.28	1153.27	576.13	
5C	1442.33	1442.36	1441.35	720.17	
3C-G	1170.26	1170.27	1169.26	584.14	
4C-G	1458.33	1458.34		728.16	
6C	1730.40	1730.40		864.19	
3C-2G	1474.32	1474.32		736.15	
5C-G	1746.39	1746.38		872.18	
7C	2018.46	2018.46		1008.22	671.82
2C-3G	1490.32	1490.34		744.16	
4C-2G	1762.39	1762.40		880.19	
8C	2306.52	2306.52		1152.25	767.83
C-4G	1506.31	1506.30		752.14	
3C-3G	1778.38	1778.38		888.18	
C-5G	1810.37	1810.38		904.18	
G-6C	2034.45	2034.48		1016.23	
9C	2594.59	2594.60		1296.29	863.87
5C-2G	2050.45	2050.48		1024.23	
10C	2882.65	2882.66			959.88
4C-2G	1794.38	1794.40		896.19	
7C-G	2322.52	2322.52		1160.25	
4C-3G	2066.44	2066.50		1032.24	
11C	3170.71	3170.75			1055.91
12C	3458.78	3458.75			1151.91
C-5G	1810.37	1810.38		904.18	
9C-G	2898.64	2898.71			965.23
10C-G	3186.71	3186.71			1061.23
3C-4G	2082.44	2082.46		1040.22	
2C-5G	2098.43	2098.44		1048.21	
4C-4G	2370.50	2370.50		1184.24	
6C-2G	2338.51	2338.48		1168.23	
11C-G	3474.77	3474.83			1157.27
8C-G	2610.58	2610.56			869.18
8C-2G	2914.64	2914.67			970.55
9C-2G	3202.70	3202.67			1066.55
13C	3746.84	3746.87			1247.95
5C-3G	2354.51	2354.52		1176.25	
7C-3G	2930.63	2930.66			975.88
8C-3G	3218.70	3218.69			1071.89

Table 3.12 *(continued)*

PA composition	$M_{calculated}$	$M_{detected}$	$[M-H]^-$	$[M-2H]^{2-}$	$[M-3H]^{3-}$
3C-5G	2386.50	2386.54		1192.26	
12C-G	3762.83	3762.86			1253.28
9C-3G	3506.76	3506.81			1167.93
7C-4G	3234.69	3234.71			1077.23
6C-4G	2946.63	2946.65			981.21
5C-5G	2962.62	2962.64			986.54
6C-5G	3250.69	3250.70			1082.56
10C-2G	3490.77	3490.79			1162.59
8C-4G	3522.76	3522.74			1173.24

Table 3.13: Composition of *P. sylvestris* bark (4F2) proanthocyanidins (PAs) estimated from the ESI-TOF-MS spectra. C: (epi)catechin; G: (epi)gallocatechin; *n*: number of flavan-3-ol subunits

PA composition	$M_{calculated}$	$M_{detected}$	$[M-H]^-$	$[M-2H]^{2-}$	$[M-3H]^{3-}$
2C	578.14	578.15	577.14		
3C	866.21	866.21	865.20		
4C	1154.27	1154.28	1153.27	576.13	
5C	1442.33	1442.33	1441.32	720.17	
6C	1730.40	1730.40		864.19	
7C	2018.46	2018.46		1008.22	671.82
8C	2306.52	2306.54		1152.26	767.83
9C	2594.59	2594.62		1296.30	863.85
10C	2882.65	2882.64		1440.31	959.89
11C	3170.71	3170.75			1055.91
12C	3458.78	3458.75			1151.91
13C	3746.84	3746.81			1247.93
14C	4034.90	4034.93			1343.97
15C	4322.97	4322.99			1439.99

Table 3.14: Composition of *O. viciifolia* whole plant (5F2) proanthocyanidins (PAs) estimated from the ESI-TOF-MS spectra. C: (epi)catechin; G: (epi)gallocatechin; *n*: number of flavan-3-ol subunits

PA composition	$M_{calculated}$	$M_{detected}$	$[M-H]^-$	$[M-2H]^{2-}$	$[M-3H]^{3-}$
2C	578.14	578.15	577.14		
C-G	594.14	594.14	593.13		
2G	610.13	610.14	609.13		
3C	866.21	866.21	865.20		
2C-G	882.20	882.21	881.20	440.09	
4C	1154.27	1154.28		576.13	
C-2G	898.20	898.20	897.19	448.09	
2C-G	1170.26	1170.27		584.13	
3G	914.19	914.19	913.19	456.09	
5C	1442.33	1442.34		720.16	
3C-G	1186.26	1186.26	1185.25	592.13	
4C-G	1458.33	1458.34		728.16	
C-3G	1202.25	1202.26		600.12	
3C-2G	1474.32	1474.33		736.16	
6C	1730.40	1730.41		864.20	
5C-G	1746.39	1746.40		872.19	
4G	1218.25	1218.26		608.12	
2C-3G	1490.32	1490.33		744.16	
4C-2G	1762.39	1762.39		880.19	
C-4G	1506.31	1506.32		752.15	
3C-3G	1778.38	1778.39		888.19	
8C	2306.52	2306.53		1152.26	767.84
2C-4G	1794.38	1794.39		896.19	
6C-G	2034.45	2034.46		1016.22	677.15
5C-2G	2050.45	2050.46		1024.22	682.48
5G	1522.31	1522.32		760.15	
C-5G	1810.37	1810.38		904.18	
7C-G	2322.52	2322.53			773.17
9C	2594.59	2594.61			863.86
4C-3G	2066.44	2066.46		1032.22	687.82
6C-2G	2338.51	2338.51		1168.25	778.50
8C-G	2610.58	2610.60			869.19
7C-2G	2626.58	2626.59			874.52
6G	1826.37	1826.37		912.18	
5C-3G	2354.51	2354.52			783.83
9C-G	2898.64	2898.67			965.21
3C-4G	2082.44	2082.45		1040.22	693.14
2C-5G	2098.43	2098.43		1048.21	
6C-3G	2642.57	2642.59			879.86
C-6G	2114.43	2114.46		1056.22	
4C-4G	2370.50	2370.50		1184.24	789.16

Table 3.14 *(continued)*

PA composition	$M_{calculated}$	$M_{detected}$	$[M-H]^-$	$[M-2H]^{2-}$	$[M-3H]^{3-}$
8C-2G	2914.64	2914.65			970.54
10C-G	3186.71	3186.72			1061.23
7C-3G	2930.63	2930.65			975.88
9C-2G	3202.70	3202.69			1066.56
3C-5G	2386.50	2386.52		1192.25	794.50
12C	3458.78	3458.78			1151.92
5C-4G	2658.57	2658.58			885.19
11C-G	3474.77	3474.78			1157.25
7G	2130.42	2130.44		1064.21	
8C-3G	3218.70	3218.69			1071.89
4C-5G	2674.56	2674.58			890.52
11C-G	3474.77	3474.78			1157.25
10C-2G	3490.77	3490.78			1162.59
6C-4G	2946.63	2946.64			981.21
5C-5G	2962.62	2962.64			986.54
7C-4G	3234.69	3234.69			1077.22
2C-6G	2402.49	2402.49		1200.24	
3C-6G	2690.56	2690.58			895.85
C-7G	2418.49	2418.51		1208.23	805.16
6C-5G	3250.69	3250.69			1082.56
8G	2434.48	2434.50			810.49
9C-3G	3506.76	3506.77			1167.92
4C-6G	2978.62	2978.63			991.87
8C-4G	3522.76	3522.76			1173.25
5C-6G	3266.68	3266.70			1087.89
C-8G	2722.55	2722.56			906.51
2C-8G	3010.61	3010.64			1002.54
3C-7G	2994.61	2994.63			997.20
4C-7G	3282.68	3282.69			1093.22
7C-5G	3538.75	3538.76			1178.58
3C-8G	3298.67	3298.67			1098.55
9G	2738.54	2738.55			911.84
PC-9G	3026.60	3026.62			1007.87
2C-9G	3314.67	3314.68			1103.88
C-10G	3330.66	3330.66			1109.21
4C-8G	3586.74	3586.73			1194.57
10G	3042.60	3042.61			1013.20
11G	3346.66	3346.66			1114.55

Table 3.15: Composition of *S. babylonica* twig (6F2) proanthocyanidins (PAs) estimated from the ESI-TOF-MS spectra. C: (epi)catechin; G: (epi)gallocatechin; *n*: number of flavan-3-ol subunits

PA composition	$M_{calculated}$	$M_{detected}$	$[M-H]^-$	$[M-2H]^{2-}$	$[M-3H]^{3-}$
C-G	594.14	594.15	593.14		
3C	866.21	866.20	865.19		
2C-G	882.20	882.21	881.20		
C-2G	898.20	898.19	897.18		
3C	1154.27	1154.28	1153.27		
3C-G	1170.26	1170.30		584.14	
4C	1442.33	1442.36		720.17	
2C-2G	1186.26	1186.26		592.12	
4C-G	1458.33	1458.32		728.15	
6C	1730.40	1730.42		864.20	
3C-2G	1474.32	1474.32		736.15	
5C-G	1746.39	1746.38		872.18	
7C	2018.46	2018.46		1008.22	
2C-3G	1490.32	1490.34		744.16	
4C-2G	1762.39	1762.40		880.19	
6C-G	2034.45	2034.44		1016.21	
8C	2306.52	2306.52		1152.25	767.83
3C-3G	1778.38	1778.38		888.18	
5C-2G	2050.45	2050.48		1024.23	
C-4G	1506.31	1506.30		752.14	
7C-G	2322.52	2322.50			773.16
9C	2594.59	2594.57			863.85
4C-3G	2066.44	2066.50		1032.24	
6C-2G	2338.51	2338.49		1168.23	778.49
2C-4G	1794.38	1794.40		896.19	
8C-G	2610.58	2610.56			869.18
10C	2882.65	2882.66			959.88
11C	3170.71	3170.75			1055.91
7C-2G	2626.58	2626.55			874.51
9C-G	2898.64	2898.65			965.21
5C-3G	2354.51	2354.48			783.82
8C-2G	2914.64	2914.67			970.55
3C-4G	2082.44	2082.46		1040.22	
10C-G	3186.71	3186.68			1061.22
4C-4G	2370.50	2370.50		1184.24	789.17
6C-3G	2642.57	2642.60			879.86
9C-2G	3202.70	3202.67			1066.55
7C-3G	2930.63	2930.66			975.88
11C-G	3474.77	3474.83			1157.27
8C-3G	3218.70	3218.69			1071.89
5C-4G	2658.57	2658.59			885.19
6C-4G	2946.63	2946.65			981.21

Table 3.15 *(continued)*

PA composition	$M_{calculated}$	$M_{detected}$	$[M-H]^-$	$[M-2H]^{2-}$	$[M-3H]^{3-}$
10C-2G	3490.77	3490.79			1162.59
7C-4G	3234.69	3234.65			1077.21
9C-3G	3506.76	3506.75			1167.91
8C-4G	3522.76	3522.74			1173.24
6C-5G	3250.69	3250.70			1082.56
11G	3346.66	3346.64			1114.54
10C-3G	3794.82	3794.87			1263.95
5C-6G	3266.68	3266.72			1087.9
12G	3650.72	3650.75			1215.91
7C-5G	3538.75	3538.76			1178.58
8C-5G	3826.81	3826.79			1274.59
C-11G	3634.72	3634.73			1210.57

Table 3.16: Composition of *R. rubrum* leaf (7F2) proanthocyanidins (PAs) estimated from the ESI-TOF-MS spectra. C: (epi)catechin; G: (epi)gallocatechin; *n*: number of flavan-3-ol subunits

PA composition	$M_{calculated}$	$M_{detected}$	$[M-H]^-$	$[M-2H]^{2-}$	$[M-3H]^{3-}$
2C	578.14	578.15	577.14		
C-G	594.14	594.17	593.16		
2G	610.13	610.13	609.12		
3C	866.21	866.21	865.2		
2C-G	882.20	882.21	881.2		
C-2G	898.20	898.19	897.18		
3G	914.19	914.20	913.19		
2C-2G	1186.26	1186.26		592.12	
C-3G	1202.25	1202.27	1201.26	600.12	
4C-G	1458.33	1458.34		728.16	
3C-2G	1474.32	1474.34		736.16	
4G	1218.25	1218.25	1217.24	608.12	
2C-3G	1490.32	1490.32		744.15	
C-4G	1506.31	1506.32		752.15	
5G	1522.31	1522.32		760.15	
C-5G	1810.37	1810.38		904.18	
6G	1826.37	1826.38		912.18	
C-6G	2114.43	2114.42		1056.2	
2C-5G	2098.43	2098.42		1048.2	
7G	2130.42	2130.44		1064.21	
C-7G	2418.49	2418.48		1208.23	805.17
2C-6G	2402.49	2402.52		1200.25	799.83
8G	2434.48	2434.52		1216.25	810.5
2C-7G	2706.61	2706.53			901.17
2C-8G	3010.61	3010.64			1002.54
C-8G	2722.55	2722.52		1360.27	906.5
9G	2738.54	2738.51			911.83
C-9G	3026.60	3026.66			1007.88
2C-9G	3314.67	3314.72			1103.9
2C-10G	3618.73	3618.71			1205.23
C-11G	3634.72	3634.76			1210.58

Table 3.17: Composition of *R. nigrum* leaf (8F2) proanthocyanidins (PAs) estimated from the ESI-TOF-MS spectra. C: (epi)catechin; G: (epi)gallocatechin; *n*: number of flavan-3-ol subunits

PA composition	$M_{calculated}$	$M_{detected}$	$[M-H]^-$	$[M-2H]^{2-}$	$[M-3H]^{3-}$
C-G	594.14	594.14	593.13		
2G	610.13	610.13	609.12		
2C-G	882.20	882.21	881.20		
C-2G	898.20	898.19	897.18		
3G	914.19	914.18	913.17	456.09	
C-3G	1202.25	1202.27	1201.26	600.12	
4G	1218.25	1218.25	1217.24	608.12	
2C-3G	1490.32		1489.31	744.15	
C-4G	1506.31		1505.31	752.15	
5G	1522.31		1521.31	760.15	
C-5G	1810.37		1809.37	904.18	
6G	1826.37		1825.35	912.17	
C-6G	2114.43		2113.41	1056.20	
7G	2130.42		2129.43	1064.21	
C-7G	2418.49		2417.47	1208.23	805.16
8G	2434.48		2433.45	1216.22	810.49
C-8G	2722.55		2721.55	1360.27	906.52
9G	2738.54		2737.51	1368.25	911.85
C-9G	3026.60		3025.66		1007.88
10G	3042.60		3041.59		1013.19
2C-8G	3010.61		3009.64		1002.54
2C-9G	3314.67		3313.69		1103.89
C-10G	3330.66		3329.62		1109.20
11G	3346.66		3345.64		1114.54
2C-10G	3618.73		3617.68		1205.22
C-11G	3634.72		3633.73		1210.57
12G	3650.72		3649.75		1215.91
C-12G	3938.78		3937.80		1311.93
14G	4258.83		4257.88		1418.62

Table 3.18: Composition of *T. repens* flower (9F2) proanthocyanidins (PAs) estimated from the ESI-TOF-MS spectra. C: (epi)catechin; G: (epi)gallocatechin; *n*: number of flavan-3-ol subunits

PA composition	$M_{calculated}$	$M_{detected}$	$[M-H]^-$	$[M-2H]^{2-}$	$[M-3H]^{3-}$
C-G	594.14	594.14	593.13		
2G	610.13	610.13	609.12		
C-2G	898.20	898.19	897.18	448.09	
3G	914.19	914.20	913.19	456.09	
4G	1218.25	1218.25	1217.24	608.12	
5G	1522.31	1522.30	1521.29	760.15	
6G	1826.37	1826.36		912.17	
7G	2130.42	2130.42		1064.20	709.14
8G	2434.48	2434.50		1216.24	810.49
9G	2738.54	2738.50		1368.24	911.84
10G	3042.60	3042.58		1520.28	1013.19
11G	3346.66	3346.64			1114.54
12G	3650.72	3650.72			1215.90

3.3.3 Comparison of methods for analysis of proanthocyanidin composition

Quantitative techniques

Degradation methods, such as thiolysis and the used UPLC-ESI-MS/MS method provided quantitative information on the overall composition of PA mixtures. Thiolytic degradation released (epi)catechin and their BM adducts that allowed calculation of PC contents and (epi)gallocatechin and their BM adducts for PD contents (Figures 3.2-3.10) [13]. The MRM experiments of the UPLC-ESI-MS/MS analysis focussed on the fragmentations of selected precursor-product ion pairs and yielded qualitative and quantitative information on PC and PD terminal and extensions units as well [16]. Results from the two methods showed a very good correlation (R^2=0.99, Figure 3.17A) and demonstrated the ability of the methods to provide quantitative information on PC and PD contents in total PA contents.

Qualitative information on PC and PD contents was obtained by UPLC-DAD (Figure 3.18) and MRM chromatograms (Figure 3.19) of the UPLC-ESI-MS/MS method. The polarity differences between PCs and PDs influenced the elution pattern of the molecules from the reversed-phase chromatographic column. Thus, the UPLC-DAD chromatograms demonstrated clearly the earlier elution of PD-rich PAs (Figures 3.18: 7F2-9F2) compared to the elution of PC-rich PAs (Figures 3.18: 1F2, 4F2) [16]. This difference in retention by the column was also noticeable in the chromatographic humps of PC/PD mixtures (Figure 3.18: 3F2, 5F2, 6F2). The MRM chromatograms provided further information regarding the PA composition and the distribution of terminal and extension units across the total chromatographic hump. For example, the signals of PD units were almost absent in the PC-rich samples as shown in Figures 3.19: 1F2 and 4F2. Similarly, the low intensity of signals for the terminal and extension PCs was clearly presented in the three PD-rich samples (Figures 3.19: 7F2-9F2). In addition, the positioning of separate signals from terminal and extension units across retention time provided some information on the PA composition. For instance, the terminal units of early eluting *R. rubrum*, leaf PAs (7F2) consist mainly of PDs whereas PC terminal units were more evenly distributed within high MW PAs eluting later (Figures 3.19: 7F2).
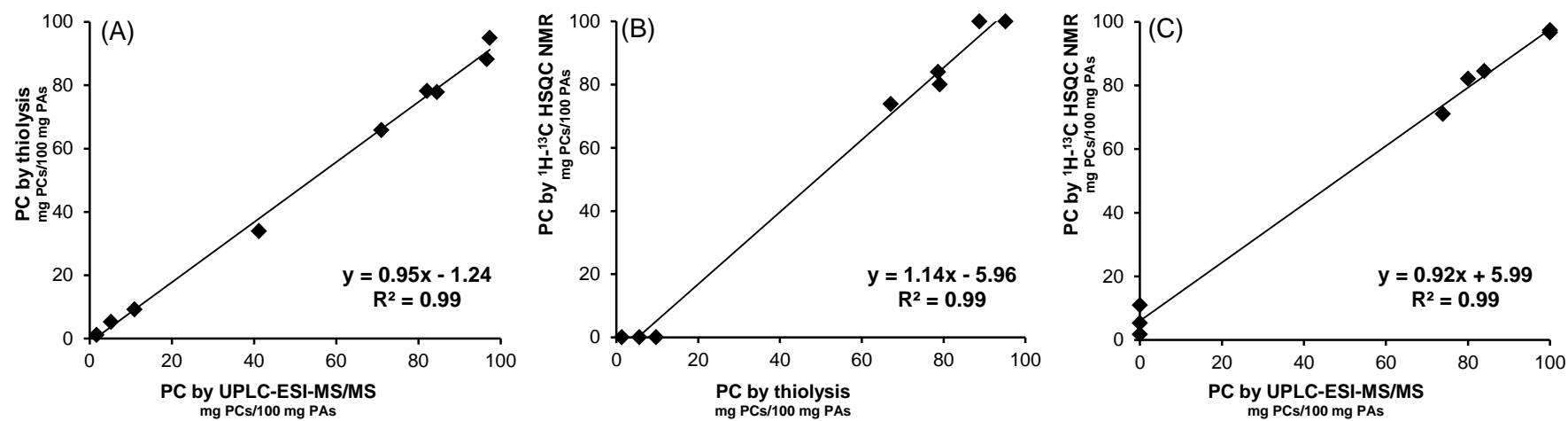
Figure 3.17: Correlations of procyanidin (PC) contents (mg PCs/100 mg PAs) between: (A) thiolysis and UPLC-ESI-MS/MS, (B) ^{1}H-^{13}C HSQC NMR and thiolysis and (C) ^{1}H-^{13}C HSQC NMR and UPLC-ESI-MS/MS.
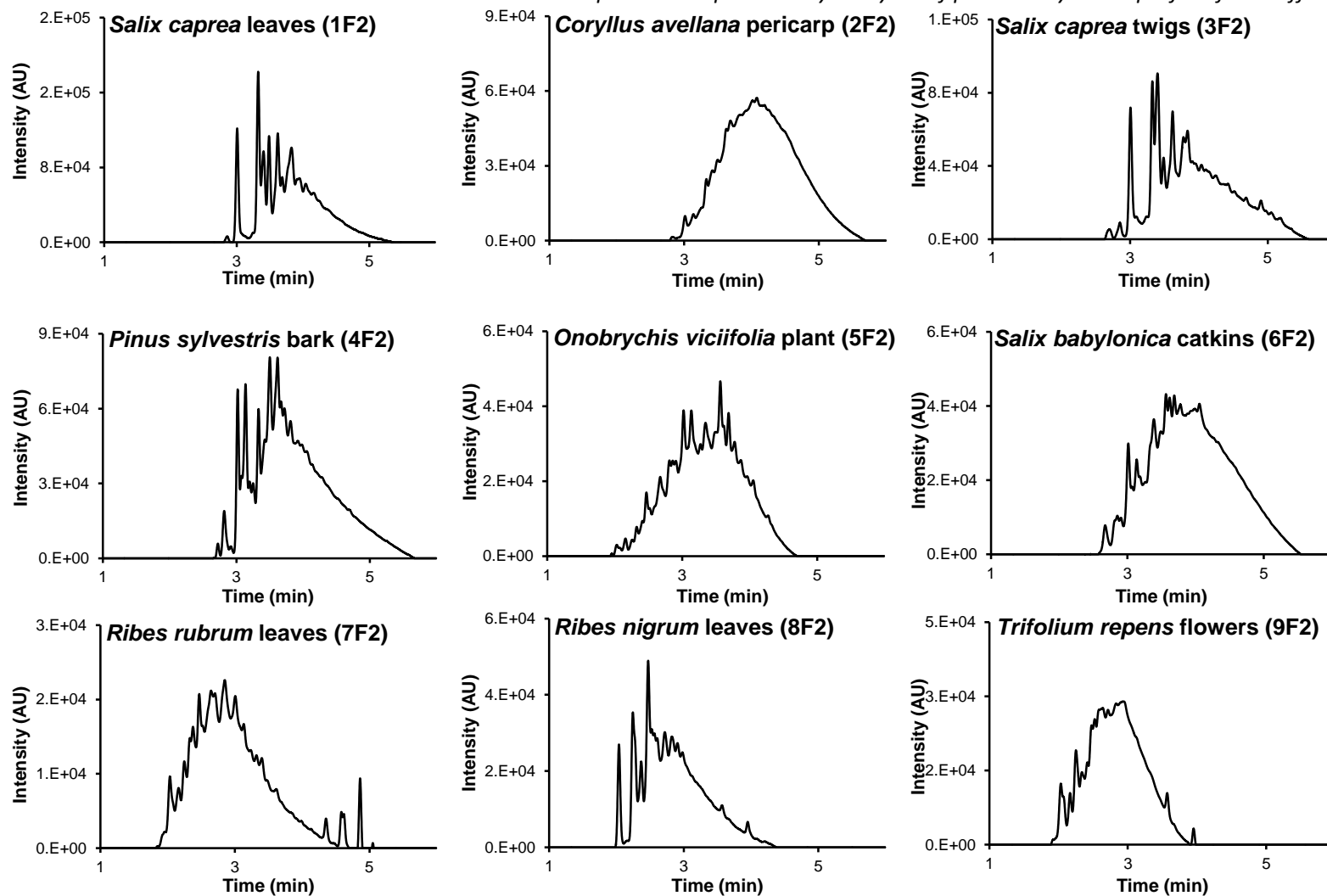
Figure 3.18: UPLC-DAD chromatographic traces of proanthocyanidins from samples 1F2-9F2.
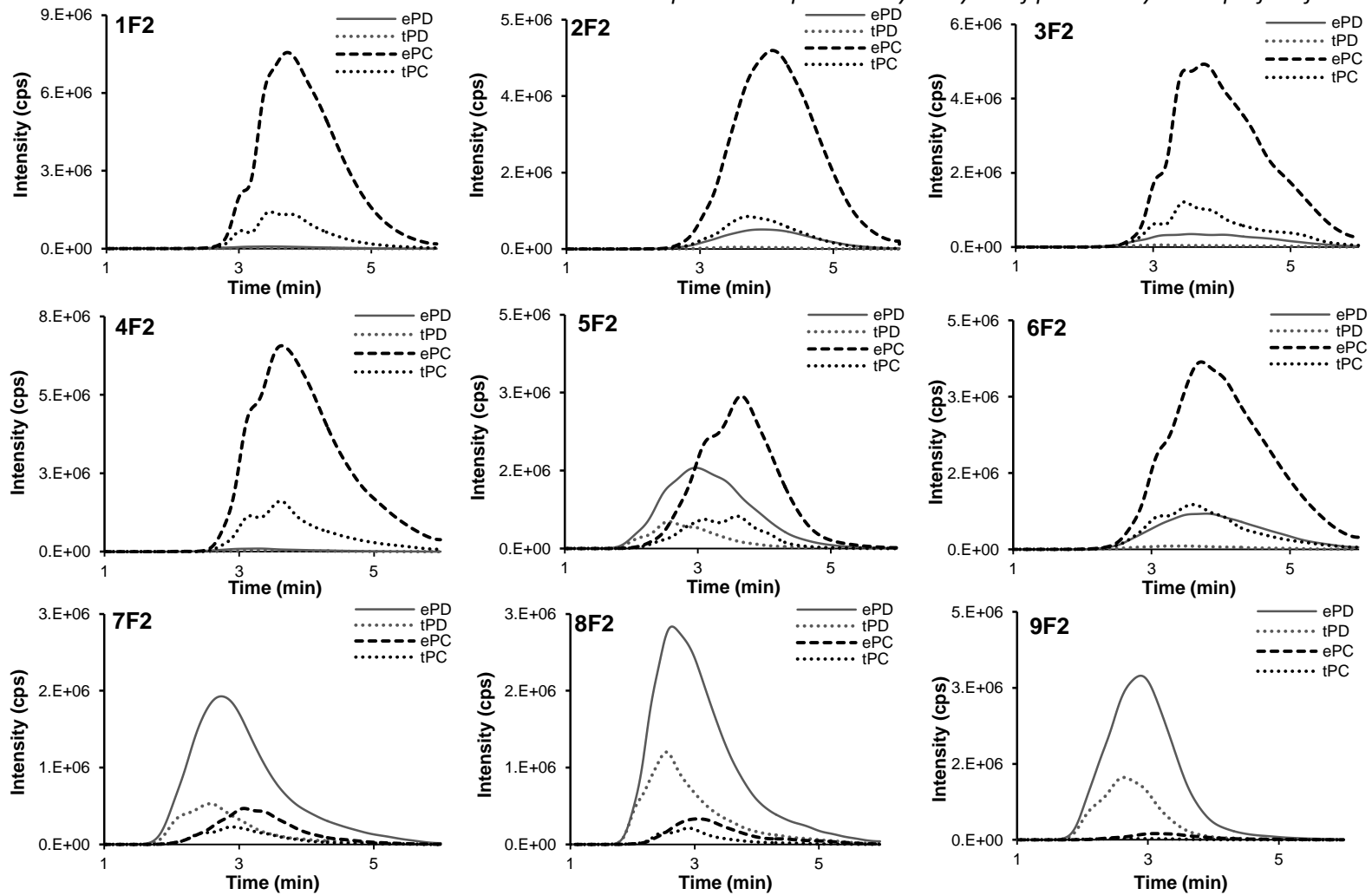
Figure 3.19: MRM chromatograms of proanthocyanidins from samples 1F2-9F2 (for sample identities see Table 3.2); Prodelphinidin extension units (ePD, *m/z* 305→125), prodelphinidin terminal units (tPD, *m/z* 305→125), procyanidin extension units (ePC, *m/z* 287→125) and procyanidin terminal units (tPC, *m/z* 289→245).

Semi-quantitative and qualitative techniques

The ^{1}H-^{13}C HSQC NMR analysis produced distinct spectra that reflected the differences in PC/PD contents of PA samples (Figures 3.12-3.14). The relevant cross-peak signals for PCs and PDs were generated without the need for PA depolymerisation [17]. As explained in section 3.3.2 relaxation times (T1 and T2) and resonance offset effects can pose problems when attempting to relate signal responses to nuclei ratios [17]. As an example, integrations of PC signal intensities from H/C-2′/5′ and H/C-6′ (Figures 3.12B and 3.14B) did not reflect the number of nuclei that produced these signals. Therefore, the determination of PC and PD contents was only possible by comparing the integrations of H/C-6′, and H/C-2′/6′ signals from PCs and PDs, respectively (Figure 3.14). These signals were used for the quantification of PC contents. Moreover, these PC and PD cross-peak contours in the ^{1}H-^{13}C HSQC NMR spectra can distinguish between a PC-rich sample (Figure 3.12), a PD-rich sample (Figure 3.13) and a mixture (Figure 3.15). As a result, PC and PD contents presented excellent linearity between thiolysis-HPLC and ^{1}H-^{13}C HSQC NMR (R^2 = 0.99) (Figure 3.17B) and between UPLC-ESI-MS/MS and ^{1}H-^{13}C HSQC NMR (R^2 = 0.99) (Figure 3.17C). This suggested that the methods produced accurate measurements of PC contents (mg PCs/100 mg PAs).

Differences in the hydroxylation pattern of PCs and PDs are reflected on their mass-to-charge differences and therefore easily identified by MALDI-TOF MS analysis. The signals of Na$^+$, Li$^+$ or Cs$^+$ adducts were assigned to individual PA structures by comparing the theoretical to the measured monoisotopic mass values.

The results of Na$^+$ adducts are summarised in tables that show the predicted and the observed values of B-type PA homo- and hetero-polymers from the various flavan-3-ol combinations (Tables 3.3-3.9). The PC homo-polymers had *m/z* values that differed by 288 amu due to varying numbers of linked (epi)catechin units (Figure 3.20A). The PD homo-polymers differed by 304 amu that derived from varying numbers of linked (epi)gallocatechin units (Figure 3.20B) as explained in section 3.2.10.
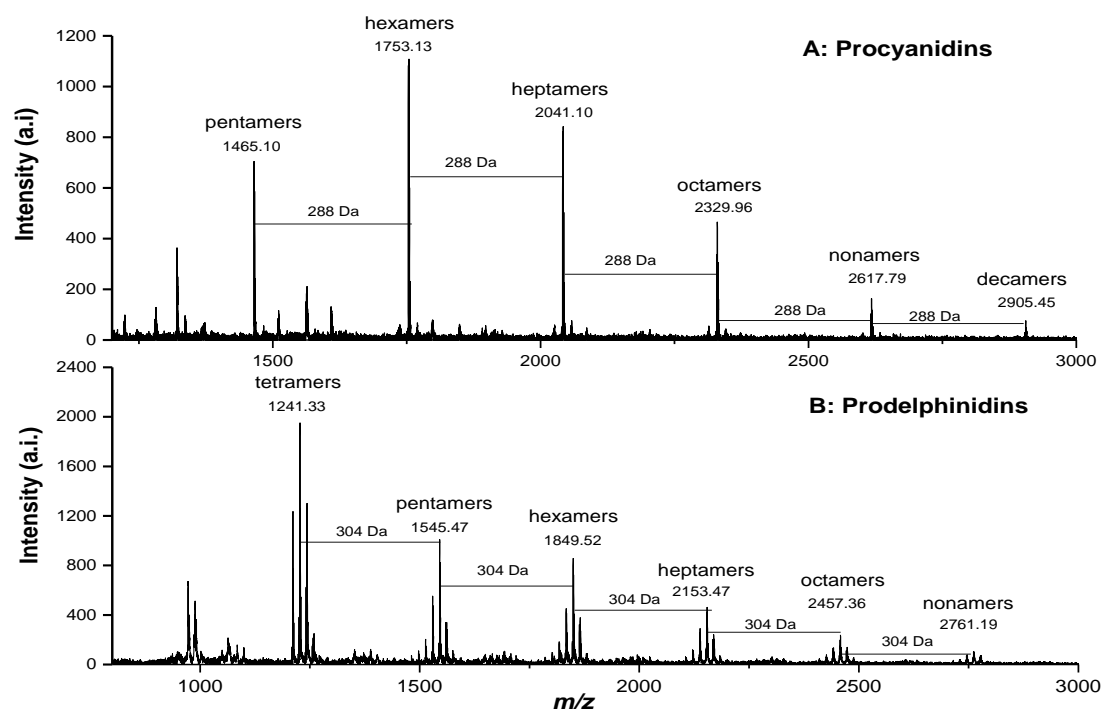
Figure 3.20: Characteristic MALDI-TOF mass spectra which demonstrate the consecutive mass-to-charge value differences between homo-polymers of *S. caprea* leaf procyanidins (A) and *R. rubrum* leaf prodelphinidins (B) with increasing number of (epi)catechin and (epi)gallocatechin units respectively.

Hetero-polymers with the same degree of polymerisation were easily distinguished by a 16 amu difference (i.e. one oxygen atom) (Figure 3.21). This type of information cannot be obtained from the depolymerisation methods or ^{1}H-^{13}C HSQC NMR. The MALDI-TOF MS analysis also revealed how many epi(catechin) and (epi)gallocatechin units occurred per hetero-polymer. Thus, *C. avellana* and *S. caprea* twig PAs had 0 to 2 (epi)gallocatechin units (Table 3.4-3.5); *S. caprea* leaf and *P. sylvestris* PAs had only 0 to 1 such subunits (Table 3.1 and 3.6); *S. babylonica* PAs had 0 to 4 subunits (Table 3.7); *R. rubrum* PAs had 2 to 11 subunits (Table 3.8) and *R. nigrum* had 2 to 8 subunits (Table 3.9). However, MALDI-TOF MS cannot elucidate the composition of extension and terminal units, which would require further fragmentation of selected ions [47].
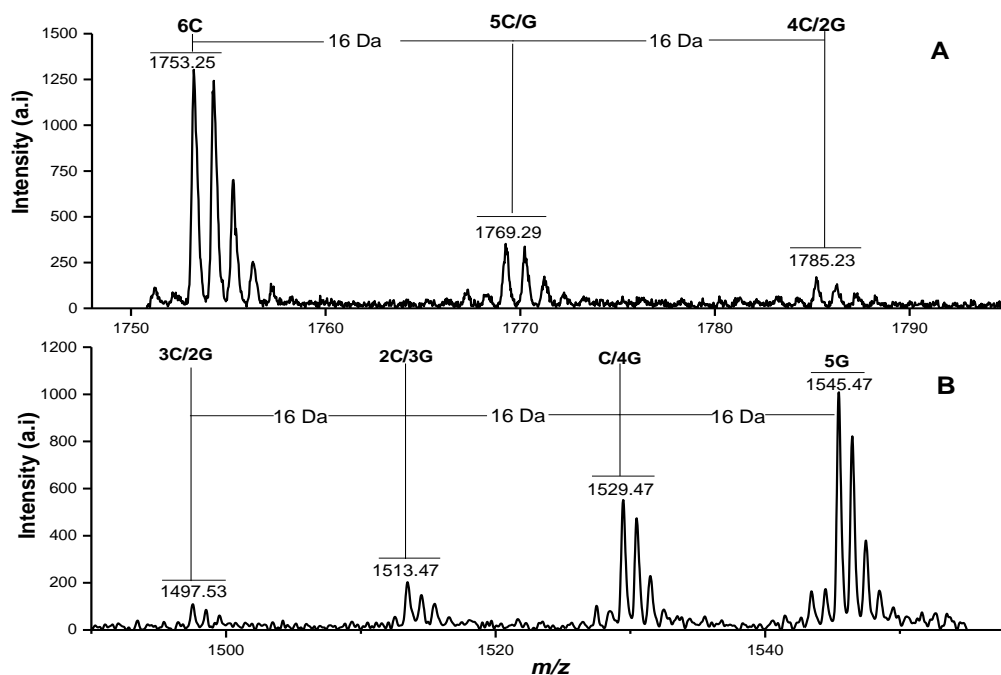
Figure 3.21: Characteristic MALDI-TOF mass spectra that depict the composition of proanthocyanidin hetero-polymers with the same degree of polymerisation. The differences of 16 amu in mass-to-charge values demonstrate the presence of hexameric hetero-polymers in *S. caprea* twigs (A) and pentameric hetero-polymers in *R. rubrum* leaves (B). Peak labels denote the number of (epi)catechin (C) and (epi)gallocatechin (G) constituent units of the homo- and the hetero-polymers.

The ^{1}H-^{13}C HSQC NMR method appeared to be relatively insensitive as it could not detect low quantities of (epi)gallocatechin units in PC-rich samples (1F2, 4F2) or (epi)catechin units in PD-rich samples (7F2 and 8F2) (Table 3.2). Thiolysis and UPLC-ESI-MS/MS proved more sensitive in this respect. This may suggest that the ^{1}H-^{13}C HSQC NMR experimental parameters were not yet optimally adjusted [17]. However, PA characterisation by MALDI-TOF MS was also subject to some method specific issues, as to obtain reproducible spectra was highly dependent on crystallisation and reagents [18, 24]. Moreover, mass detection does not allow the separation of individual PA compounds with the same *m/z* value. The latter can be a concern in the presence of specific isomers [43], the natural presence of alkali metals [24, 43] and combinations of components that may coincidentally form adduct molecules of the same MW weight with the analytes [47]. The extent of complexity of these types of PAs is still unknown, but it could be unravelled by depolymerisation techniques or the inclusion of additional chromatographic steps prior to mass spectral analysis.

A combinatorial assessment of UV spectra, chromatograms and high resolution mass spectra by HILIC-DAD-ESI-TOF-MS analysis also generated interesting information on PA composition. The most prominent fragment ions were produced by the quinone methide cleavage and their mass spectra enabled characterisation of PAs [19]. In general, the PA composition was in agreement with that obtained from the other techniques and the identified PA compounds are presented in Tables 3.10 – 3.18. Comparison of the MALDI-TOF MS and HILIC-DAD-ESI-TOF-MS spectra showed differences in the detection of PA hetero-polymers. For example, the HILIC-DAD-ESI-TOF-MS analysis showed that *P. sylvestris* bark PAs consisted only of (epi)catechin flavan-3-ols (Table 3.13) whereas several peaks of the MALDI-TOF MS spectrum had *m/z* values of hetero-polymeric PAs (Table 3.6). The characterisation of *S. babylonica* catkin PAs by the two methods was another example. The HILIC-DAD-ESI-TOF-MS showed that (epi)gallocatechin units in the PA hetero-polymers ranged from 0 to 6 (Table 3.15) whereas MALDI-TOF MS presented a range of 2 to 4. In general, the HILIC-DAD-ESI-TOF-MS detected much more variable hetero-polymers compared to MALDI-TOF MS. This could be assigned to the fact that higher PA concentrations were used in the HILIC-DAD-ESI-TOF-MS analysis compared to MALDI-TOF MS analysis. This may have allowed the detection of hetero-polymers in very low abundance. Another explanation could be that inhomogeneous crystallisation had a negative impact on the detection of hetero-polymers by MALDI-TOF MS. Also HILIC-DAD-ESI-TOF-MS was capable of detecting PAs of higher MW than MALDI-TOF-MS. Moreover, the possibility that ESI produced variable fragments from larger molecules compared to the softer ionisation of MALDI-TOF MS should not be disregarded.

The large number of possible flavan-3-ol combinations within PA hetero-polymers disturbed the HILIC elution, which normally occurs on a MW basis, and therefore complicated greatly their separation [19, 35]. However, the accurate mass calculations based on the isotopic patterns for each ion provided information on the number of flavan-3-ol units within PAs (Figure 3.22). Selecting the *m/z* values of the lightest carbon and oxygen isotopes prevented the MW weight deviations between observed and calculated values [53]. These mass calculations proved particularly useful for large polymers with long retention times, which

suffered from poor separation and multiply charged ions deriving from the same compound.
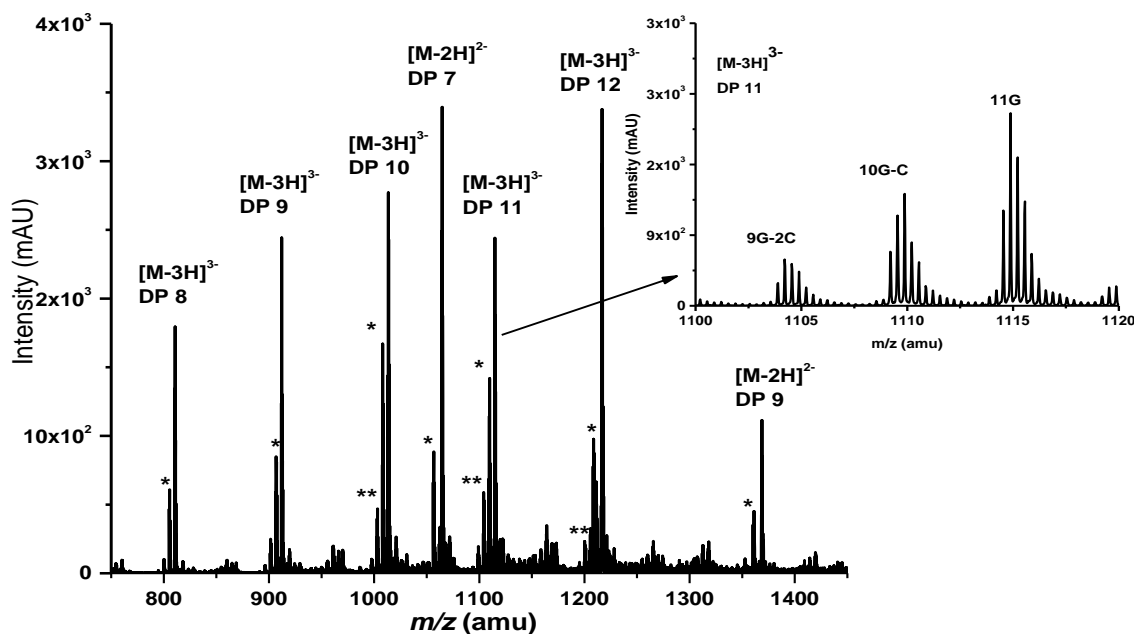
Figure 3.22: High resolution mass spectrum of prodelphinidin polymers eluted from HILIC column at late retention times. The peak labels of the multiply charged ions denote the degree of polymerisation (DP). The number of asterisks denotes the number of (epi)catechin (C) units in prodelphinidin hetero-polymers with the same DP. The inset illustrates the highly resolved isotopic patterns from homo- and hetero-undecamers. The *m/z* value of the lightest isotopes of carbon and oxygen were selected for accurate mass calculations. G: (epi)gallocatechin unit

In addition to these high resolution mass spectra, extracted ion chromatograms (EICs) further facilitated the identification of co-eluting PAs in HILIC-DAD-ESI-TOF-MS [19, 35]. The increase of hydrophilic character and the polymerisation degree had opposing effects on the elution of PA hetero-polymers. As an example, pentameric PAs (PD-rich) from *R. nigrum* leaves (8F2) eluted in the order of 3G+2C < 4G+C < 5G; but pentameric PAs (PC-rich) from *S. caprea* leaves (1F2) eluted in the order of 5C < 3C+2G < 2C+3G (Figure 3.23). The effect was more obvious in PAs that consisted of the PC/PD mixtures (i.e. *S. caprea* twigs, *O. viciifolia* leaves and *S. babylonica* twigs, Tables 3.12, 3.14 and 3.15 respectively).
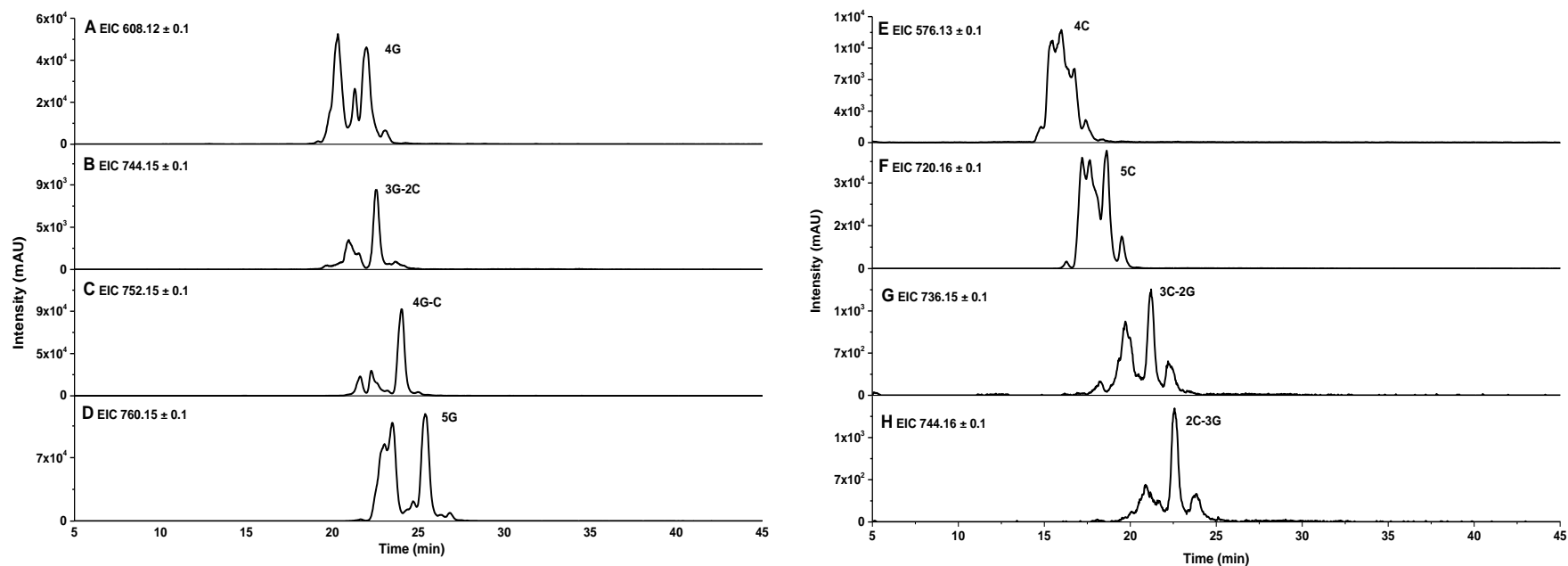
Figure 3.23: Individual extracted ion chromatograms (EICs) denote the different HILIC elution of proanthocyanidins from *R. nigrum*, leaf (A-D) and *S. caprea*, leaf (E-H). The EICs were obtained by using the [M-2H]$^{2-}$ ions and the *m/z* values are presented on the top-left part of the chromatograms. C: (epi)catechin unit, G: (epi)gallocatechin unit

3.3.4 Comparison of methods for analysis of PA stereochemistry

Unlike the MS techniques, thiolysis-HPLC analysis and ^{1}H-^{13}C HSQC NMR spectroscopy are capable of analysing the stereochemistry at the C-ring [13, 17, 28]. Thiolytic depolymerisation of PAs provided quantitative information on *cis*-flavan-3-ol content within total PA content and ranged from 4.3 mg/100 mg PAs in *S. caprea* leaves to 79.1 mg/100 mg PAs in *O. viciifolia* whole plants (Table 3.2). In addition, thiolysis-HPLC analysis can distinguish the *cis*-flavan-3-ols (epigallocatechin: EGC, epicatechin: EC) and the *trans*-flavan-3-ols (gallocatechin: GC, catechin: C) in the terminal and extension units of PAs in a sample (Table 3.19).

Table 3.19: Proanthocyanidin monomer composition and content of Sephadex™ LH-20 acetone/water (1:1 v/v) eluted fractions (F2) (mg/g fraction); GC: gallocatechin, EGC: epigallocatechin, C: catechin, EC: epicatechin; Standard deviation in brackets (*n=2*); nd: not detected

PA origin	Extract type	GC	EGC	C	EC	GC	EGC	C	EC
			Terminal units				Extender units		
Salix caprea (Goat willow; leaves)	1F2	nd	11.3 (1.29)	143 (9.65)	4.73 (0.488)	25.2 (6.94)	5.74 (3.38)	633 (14.3)	14.4 (0.521)
Coryllus avellana (Hazelnut; pericarp)	2F2	3.71 (0.200)	nd	61.4 (1.36)	8.05 (0.962)	78.5 (10.3)	64.8 (1.96)	209 (10.3)	250 (10.4)
Salix caprea (Goat willow; twigs)	3F2	10.8 (2.26)	nd	159 (35.0)	5.41 (0.581)	76.4 (8.93)	118 (23.1)	100 (26.5)	462 (118)
Pinus sylvestris (Scots pine tree; bark)	4F2	2.52 (0.702)	6.10 (0.185)	104 (0.448)	8.66 (0.049)	37.4 (30.1)	48.8 (3.38)	32.9 (9.64)	559 (5.12)
Onobrychis viciifolia (Sainfoin; whole plant)	5F2	33.5 (2.19)	27.5 (2.21)	37.1 (2.50)	31.2 (2.60)	134 (3.18)	555 (45.6)	32.7 (3.58)	285 (19.8)
Salix babylonica (Weeping willow; catkins)	6F2	nd	5.82 (0.669)	67.3 (1.98)	46.8 (1.51)	171 (45.1)	157 (5.04)	176 (0.438)	350 (0.995)
Ribes rubrum (Red currant; leaves)	7F2	43.4 (1.40)	5.07 (0.626)	17.5 (1.05)	1.88 (0.092)	163 (8.03)	408 (24.9)	17.8 (0.319)	25.4 (1.05)
Ribes nigrum (Black currant; leaves)	8F2	126 (3.09)	36.0 (1.09)	22.1 (0.077)	3.28 (0.058)	964 (38.3)	36.2 (1.94)	29.7 (0.190)	9.49 (0.051)
Trifolium repens (White clover; flowers)	9F2	90.4 (3.82)	37.6 (1.68)	1.33 (0.006)	nd	360 (1.79)	613 (40.1)	5.96 (0.140)	6.02 (0.398)

Several NMR spectroscopy experiments have succeeded in providing estimates of *cis/trans* contents within PA mixtures without chemical degradation [17, 39, 40, 54]. However, the sensitivity of the present ^{1}H-^{13}C HSQC NMR experiments was too low for determining *cis*- and *trans*-flavan-3-ol contents. Nevertheless, previous work had shown that *cis/trans* ratios determined by ^{1}H-^{13}C HSQC NMR were in good agreement with the thiolysis values [17].

3.3.5 Comparison of methods for analysis of A-type proanthocyanidins

Quantitative techniques

Proanthocyanidins that contain A-type interflavanyl linkages resist thiolytic degradation; thus terminal units are usually detected as dimers with an A-type bond and extension units as dimeric benzyl mercaptan derivatives [26, 44, 55]. However, a terminal trimer has also been reported [30, 56]. Estimations of A-type molar percentages [26, 30, 57], mDP values [30, 58] and concentrations of A-type thiolytic products in terminal and extension units [30, 59, 60] have been reported, which demonstrates the capacity of the method to provide quantitative information on A-type PAs. Although the present thiolysis-HPLC analysis was not complemented by mass spectrometric analysis which would enable the unambiguous identification and quantification of the A-type thiolytic products, the chromatograms did not have peaks that could be assigned to A-type PAs in the fractions.

Semi-quantitative and qualitative techniques

Several NMR spectroscopy investigations showed the diagnostic features of A-type bonds [61-63]. However, such signals were absent in the current ^{1}H-^{13}C HSQC NMR spectra, although it is possible that the low sensitivity or signal overlap could have hampered the detection of A-type PAs.

Mass spectrometry techniques are capable of detecting A-type PAs. The additional ether bond between the adjacent flavan-3-ol units results in loss of two hydrogen atoms and distinguishes A-type from B-type PAs [24, 43, 55, 58]. It can be seen that several of the MALDI-TOF mass spectra had *m/z* values that could be assigned to A-type PAs. However, the presence of A-type bonds in *C. avellana*

and *P. sylvestris* PAs has not been reported previously [15, 49, 55, 64]. It was also noticed that these signals were weak and very dependent on the matrix, cationising agents, data acquisition parameters and analyst. Furthermore, PA molecules with a flavanone terminal unit can also give rise to this decrease in 2 amu [47]. Behrens et al. suggested that a difference of two mass units could also come from the fragmentation mode [47]. However, another research group stated that MALDI-TOF MS ionisation is softer than ESI and hence quinone methide products sharing the same *m/z* value as A-type PAs should not occur [65]. It is also possible that this mass difference may have derived from oxidation products [33], but this was excluded by Tahata et al. [66]. Stringano et al. also explained that the matrix seemed to influence fragmentation of sainfoin PAs [24]. The A-type PAs were detected with DHB and s-DHB matrices but in some cases the signals disappeared when the sample was mixed with 2, 6-dihydroxyacetophenone (DHAP) and 2, 4, 6-trihydroxyacetophenone (THAP) [24]. Spectral observations in the present study were in agreement with these reports thus, it can be assumed that these peak signals most probably came from structures that were created under these experimental conditions and not from A-type PAs.

Indeed, these conclusions on MALDI-TOF MS analysis of A-type PAs were further supported by the HILIC-DAD-ESI-TOF-MS analysis. The appearance and intensity of peaks, with *m/z* values lacking 2 amu, were random and did not agree with those obtained from the MALDI-TOF MS analysis. This suggested that these signals corresponded to quinone methide cleavage products of larger oligomers or polymers [19, 51]. Several studies have indeed stressed that spectra can become very complex due to the presence of fragment ions, ion adducts and oxidation products [19, 22, 33, 49].

3.3.6 Comparison of methods for analysis of proanthocyanidin substitution patterns (galloylation, etc.)

Quantitative techniques

Thiolysis-HPLC analysis revealed that 2.5% of the flavan-3-ol units in *C. avellana* PAs were galloylated in agreement with previous investigations [64]. All other samples consisted of non-galloylated PAs. The galloylated flavan-3-ols elute with different retention times and have different UV spectra compared to non-

galloylated flavan-3-ols or PA oligomers [67]. Thus their identification [55, 67, 68] is possible after thiolytic degradation but quantification can be hampered due to a lack of standards [69].

Semi-quantitative and qualitative techniques

The ^{1}H-^{13}C HSQC NMR spectra did not contain the characteristic ^{13}C and ^{1}H signals that are typical of galloylated PA structures [70] and thus confirmed the findings from thiolysis-HPLC analysis.

An *m/z* value corresponding to a galloylated PC pentamer was observed in the MALDI-TOF MS spectra of the *C. avellana* pericarp PA sample when mixed with DHB and Na$^+$. However, there was a lack of consistency in the acquired spectra and complementary analysis by thiolysis, MS/MS and UV detection was needed to exclude the possibility of artefact peaks or incorrect assignments [65, 71]. Several researchers cautioned against reported galloylated PAs from MALDI-TOF MS due to the potential presence of numerous other heterogeneous PA isomers [69, 72]. For example, a trimer consisting of two (epi)catechin and one (epi)gallocatechin units possesses the same m/z value (=881 Da) as a galloylated (epi)catechin dimer. Similarly, a tetramer containing three (epi)catechin units and one (epi)gallocatechin unit shares the same m/z value (=1169.5 Da) with a PC trimer di-gallate [73]. Despite these limitations, MALDI-TOF MS studies have identified distinct mass patterns of galloylated PAs from *Delonix regia* [54], pear juice [74], *Diospyros kaki* L. [65], grapes [72], grape seeds [31, 75], *Crataegus pinnatifida* [44] and *Cinnamomum zeylanicum* L. [71].

The HILIC-DAD-ESI-TOF-MS analysis of galloylated PAs suffered from the same limitations as MALDI-TOF MS analysis. However, the HILIC column separated oligomeric PAs according to their MWs, and MS analysis with a high resolution TOF analyser supported the identification of galloylated PA oligomers. Galloylated oligomers eluted later than their non-galloylated oligomers and this together with the accurate masses provided some confidence in the peak assignments [35]. However, UV spectra could not be used due to the low concentration of galloylated PAs.

3.4 Conclusions

This chapter presented the results from several different techniques for PA analysis and discussed the advantages and disadvantages of each method. The information provided by each method and an evaluation of the technical characteristics are summarised in Table 3.20.

Although each method had some distinct advantages, only those that were based on PA depolymerisation, such as thiolysis and UPLC-ESI-MS/MS, provided quantitative information. However, the enormous complexity of PAs still poses challenges for their accurate quantification and characterisation. Selection of quantification standards remains a particularly important issue and despite the recent progress, PA methods still require further improvement. The great complexity of PAs complicates their separation and their structural identification from mass-to-charge values. Technical limitations of the ionisation processes and the TOF analysers also raise the question whether all compounds are detected especially in crude extracts. However, the investigations at the molecular level with state-of-the-art mass spectrometric techniques demonstrated that the determination of average polymer sizes and PC/PD ratios from degradation methods masked some valuable information on PA complexity. Taking into account that PAs in forages (i.e. *O. viciifolia*) occur in mixtures, information on PA complexity may hold the key to probing different PA compositions for their nutritional and animal health benefits.

Ultimately, factors such as availability of instrumentation, expertise, the number of samples to be analysed and most importantly the research purpose will dictate which method to use. The present studies showed that there is no one analytical method that can provide all information on the puzzle of complex PA mixtures. Parallel analysis with an array of different methods is suggested to obtain complementary quantitative and qualitative information, which will pave the way for elucidations of PA related bioactivities.

Table 3.20: Comparison of analytical methods based on features of proanthocyanidin characterisation and technical characteristics; X: denotes the information available per method. Relative ranking of the positive (+) and the negative (-) characteristics is used: +: low, ++: moderate, +++: high, -: low, - -: moderate, - - -: high

Proanthocyanidin Characterisation	Analytical Method				
	Thiolysis	UPLC-ESI-MS/MS	^{1}H-^{13}C HSQC NMR	MALDI-TOF MS	LC-DAD-ESI-TOF-MS
Quantitation	X	X			
Molecular Identification				X	X
mDP	X	X	X		
DP range				X	X
PC/PD ratio	X	X	X		
Cis/trans ratio	X		X		
A-type	X		X	X	X
Galloylation	X		X	X	X
Technical characteristics					
Selectivity	+	+++	++	++	++
Sensitivity	++	+++	+	+++	+
Reproducibility	++	+++	+++	+	+++
Analysis time	- - -	-	- - -	-	- -
Instrumentation costs	-	- - -	- - -	- -	- -

References

1. Aron PM, Kennedy JA: Flavan-3-ols: **Nature, occurrence and biological activity.** *Molecular Nutrition & Food Research* 2008, 52(1):79-104.

2. Hummer W, Schreier P: **Analysis of proanthocyanidins.** *Molecular Nutrition & Food Research* 2008, 52(12):1381-1398.

3. Waghorn G: **Beneficial and detrimental effects of dietary condensed tannins for sustainable sheep and goat production-Progress and challenges.** *Animal Feed Science and Technology* 2008, 147(1-3):116-139.

4. Mueller-Harvey I: **Unravelling the conundrum of tannins in animal nutrition and health.** *Journal of the Science of Food and Agriculture* 2006, 86(13):2010-2037.

5. Wang YX, McAllister TA, Acharya S: **Condensed tannins in sainfoin: Composition, concentration, and effects on nutritive and feeding value of sainfoin forage.** *Crop Science* 2015, 55(1):13-22.

6. McMahon LR, McAllister TA, Berg BP, Majak W, Acharya SN, Popp JD, Coulman BE, Wang Y, Cheng KJ: **A review of the effects of forage condensed tannins on ruminal fermentation and bloat in grazing cattle.** *Canadian Journal of Plant Science* 2000, 80(3):469-485.

7. Hoste H, Martinez-Ortiz-De-Montellano C, Manolaraki F, Brunet S, Ojeda-Robertos N, Fourquaux I, Torres-Acosta JF, Sandoval-Castro CA: **Direct and indirect effects of bioactive tannin-rich tropical and temperate legumes against nematode infections.** *Veterinary Parasitology* 2012, 186(1-2):18-27.

8. Hatew B, Hayot Carbonero C, Stringano E, Sales LF, Smith LMJ, Mueller-Harvey I, Hendriks WH, Pellikaan WF: **Diversity of condensed tannin structures affects rumen *in vitro* methane production in sainfoin (*Onobrychis viciifolia*) accessions.** *Grass and Forage Science* 2015, 70(3):474-490.

9. Reed JD: **Nutritional toxicology of tannins and related polyphenols in forage legumes.** *Journal of Animal Scirnce* 1995, 73(5):1516-1528.

10. Patra AK, Saxena J: **A new perspective on the use of plant secondary metabolites to inhibit methanogenesis in the rumen.** *Phytochemistry* 2010, 71(11-12):1198-1222.

11. Schofield P, Mbugua DM, Pell AN: **Analysis of condensed tannins: A review.** *Animal Feed Science and Technology* 2001, 91(1-2):21-40.

12. Grabber JH, Zeller WE, Mueller-Harvey I: **Acetone enhances the direct analysis of procyanidin- and prodelphinidin-based condensed tannins in *Lotus* species by the butanol-HCl-iron assay.** *Journal of Agricultural and Food Chemistry* 2013, 61(11):2669-2678.

13. Gea A, Stringano E, Brown RH, Mueller-Harvey I: *In situ* **analysis and structural elucidation of sainfoin (*Onobrychis viciifolia*) tannins for high-throughput germplasm screening.** *Journal of Agricultural and Food Chemistry* 2011, 59(2):495-503.

14. Callemien D, Guyot S, Collin S: **Use of thiolysis hyphenated to RP-HPLC-ESI(-)-MS/MS for the analysis of flavanoids in fresh lager beers.** *Food Chemistry* 2008, 110(4):1012-1018.

15. Gu L, Kelm MA, Hammerstone JF, Beecher G, Holden J, Haytowitz D, Prior RL: **Screening of foods containing proanthocyanidins and their structural characterization using LC-**

MS/MS and thiolytic degradation. *Journal of Agricultural and Food Chemistry* 2003, 51(25):7513-7521.

16. Engstrom MT, Palijarvi M, Fryganas C, Grabber JH, Mueller-Harvey I, Salminen JP: **Rapid qualitative and quantitative analyses of proanthocyanidin oligomers and polymers by UPLC-MS/MS.** *Journal of Agricultural and Food Chemistry* 2014, 62(15):3390-3399.

17. Zeller WE, Ramsay A, Ropiak HM, Fryganas C, Mueller-Harvey I, Brown RH, Drake C, Grabber JH: **(1)H-(13)C HSQC NMR spectroscopy for estimating procyanidin/prodelphinidin and *cis*/*trans*-flavan-3-ol ratios of condensed tannin samples: Correlation with thiolysis.** *Journal of Agricultural and Food Chemistry* 2015, 63(7):1967-1973.

18. Monagas M, Quintanilla-Lopez JE, Gomez-Cordoves C, Bartolome B, Lebron-Aguilar R: **MALDI-TOF MS analysis of plant proanthocyanidins.** *Journal of Pharmaceutical and Biomedical analysis* 2010, 51(2):358-372.

19. Karonen M, Liimatainen J, Sinkkonen J: **Birch inner bark procyanidins can be resolved with enhanced sensitivity by hydrophilic interaction HPLC-MS.** *Journal of Separation Science* 2011, 34(22):3158-3165.

20. Kalili KM, de Villiers A: **Off-line comprehensive 2-dimensional hydrophilic interaction x reversed phase liquid chromatography analysis of procyanidins.** *Journal of Chromatography A* 2009, 1216(35):6274-6284.

21. Novobilsky A, Mueller-Harvey I, Thamsborg SM: **Condensed tannins act against cattle nematodes.** *Veterinary Parasitology* 2011, 182(2-4):213-220.

22. Hellstrom J, Sinkkonen J, Karonen M, Mattila P: **Isolation and structure elucidation of procyanidin oligomers from saskatoon berries (*Amelanchier alnifolia*).** *Journal of Agricultural and Food Chemistry* 2007, 55(1):157-164.

23. Feliciano RP, Krueger CG, Shanmuganayagam D, Vestling MM, Reed JD: **Deconvolution of matrix-assisted laser desorption/ionization time-of-flight mass spectrometry isotope patterns to determine ratios of A-type to B-type interflavan bonds in cranberry proanthocyanidins.** *Food Chemistry* 2012, 135(3):1485-1493.

24. Stringano E, Cramer R, Hayes W, Smith C, Gibson T, Mueller-Harvey I: **Deciphering the complexity of sainfoin (*Onobrychis viciifolia*) proanthocyanidins by MALDI-TOF mass spectrometry with a judicious choice of isotope patterns and matrixes.** *Analytical Chemistry* 2011, 83(11):4147-4153.

25. Karonen M, Leikas A, Loponen J, Sinkkonen J, Ossipov V, Pihlaja K: **Reversed-phase HPLC-ESI/MS analysis of birch leaf proanthocyanidins after their acidic degradation in the presence of nucleophiles.** *Phytochemical Analysis : PCA* 2007, 18(5):378-386.

26. Gu L, Kelm M, Hammerstone JF, Beecher G, Cunningham D, Vannozzi S, Prior RL: **Fractionation of polymeric procyanidins from lowbush blueberry and quantification of procyanidins in selected foods with an optimized normal-phase HPLC-MS fluorescent detection method.** *Journal of Agricultural and Food Chemistry* 2002, 50(17):4852-4860.

27. Guyot S, Doco T, Souquet JM, Moutounet M, Drilleau JF: **Characterization of highly polymerized procyanidins in cider apple (*Malus sylvestris* var Kermerrien) skin and pulp.** *Phytochemistry* 1997, 44(2):351-357.

28. Matthews S, Mila I, Scalbert A, Pollet B, Lapierre C, duPenhoat CLMH, Rolando C, Donnelly DMX: **Method for estimation of proanthocyanidins based on their acid depolymerization in the presence of nucleophiles.** *Journal of Agricultural and Food Chemistry* 1997, 45(4):1195-1201.

29. Guyot S, Marnet N, Sanoner P, Drilleau JF: **Variability of the polyphenolic composition of cider apple (*Malus domestica*) fruits and juices.** *Journal of Agricultural and Food Chemistry* 2003, 51(21):6240-6247.

30. Ropiak HM, Ramsay A, Mueller-Harvey I: **Condensed tannins in extracts from European medicinal plants and herbal products.** *Journal of Pharmaceutical and Biomedical analysis* 2016, 121:225-231.

31. Yang Y, Chien MJ: **Characterization of grape procyanidins using high-performance liquid chromatography/mass spectrometry and matrix-assisted laser desorption/ionization time-of-flight mass spectrometry.** *Journal of Agricultural and Food Chemistry* 2000, 48(9):3990-3996.

32. Feliciano RP, Krueger CG, Reed JD: **Methods to determine effects of cranberry proanthocyanidins on extraintestinal infections: Relevance for urinary tract health.** *Molecular Nutrition & Food Research* 2015, 59(7):1292-1306.

33. Reed JD, Krueger CG, Vestling MM: **MALDI-TOF mass spectrometry of oligomeric food polyphenols.** *Phytochemistry* 2005, 66(18):2248-2263.

34. Duval A, Averous L: **Characterization and physicochemical properties of condensed tannins from *Acacia catechu*.** *Journal of Agricultural and Food Chemistry* 2016, 64(8):1751-1760.

35. Kalili KM, Vestner J, Stander MA, de Villiers A: **Toward unraveling grape tannin composition: application of online hydrophilic interaction chromatography x reversed-phase liquid chromatography-time-of-flight mass spectrometry for grape seed analysis.** *Analytical Chemistry* 2013, 85(19):9107-9115.

36. Melone F, Saladino R, Lange H, Crestini C: **Tannin structural elucidation and quantitative (31)P NMR analysis. 2. Hydrolyzable tannins and proanthocyanidins.** *Journal of Agricultural and Food Chemistry* 2013, 61(39):9316-9324.

37. Zhang L, Gellerstedt G: **Quantitative 2D HSQC NMR determination of polymer structures by selecting suitable internal standard references.** *Magnetic Resonance in Chemistry : MRC* 2007, 45(1):37-45.

38. Ayres MP, Clausen TP, MacLean SF, Redman AM, Reichardt PB: **Diversity of structure and antiherbivore activity in condensed tannins.** *Ecology* 1997, 78(6):1696-1712.

39. Czochanska Z, Foo LY, Newman RH, Porter LJ: **Polymeric Proanthocyanidins - stereochemistry, structural units, and molecular-weight.** *Journal of Chemical Society, Perkin Transactions 1* 1980(10):2278-2286.

40. Foo LY, Lu Y, Molan AL, Woodfield DR, McNabb WC: **The phenols and prodelphinidins of white clover flowers.** *Phytochemistry* 2000, 54(5):539-548.

41. Fulcrand H, Mane C, Preys S, Mazerolles G, Bouchut C, Mazauric JP, Souquet JM, Meudec E, Li Y, Cole RB *et al*: **Direct mass spectrometry approaches to characterize polyphenol composition of complex samples.** *Phytochemistry* 2008, 69(18):3131-3138.

42. Vivas N, Nonier MF, de Gaulejac NV, Absalon C, Bertrand A, Mirabel M: **Differentiation of proanthocyanidin tannins from seeds, skins and stems of grapes (*Vitis vinifera*) and heartwood of quebracho (*Schinopsis balansae*) by matrix-assisted laser desorption/ionization time-of-flight mass spectrometry and thioacidolysis/liquid chromatography/electrospray ionization mass spectrometry.** *Analytica Chimica Acta* 2004, 513(1):247-256.

43. Krueger CG, Vestling MM, Reed JD: **Matrix-assisted laser desorption/ionization time-of-flight mass spectrometry of heteropolyflavan-3-ols and glucosylated**

heteropolyflavans in sorghum [*Sorghum bicolor* (L.) Moench]. *Journal of Agricultural and Food Chemistry* 2003(51):538-543.

44. Chai WM, Chen CM, Gao YS, Feng HL, Ding YM, Shi Y, Zhou HT, Chen QX: **Structural analysis of proanthocyanidins isolated from fruit stone of Chinese hawthorn with potent antityrosinase and antioxidant activity.** *Journal of Agricultural and Food Chemistry* 2014, 62(1):123-129.

45. Ohnishi-Kameyama M, Yanagida A, Kanda T, Nagata T: **Identification of catechin oligomers from apple (*Malus pumila* cv. Fuji) in matrix-assisted laser desorption/ionization time-of-flight mass spectrometry and fast-atom bombardment mass spectrometry.** *Rapid Communications in Mass Spectrometry : RCM* 1997, 11(1):31-36.

46. Weber HA, Hodges AE, Guthrie JR, O'Brien BM, Robaugh D, Clark AP, Harris RK, Algaier JW, Smith CS: **Comparison of proanthocyanidins in commercial antioxidants: Grape seed and pine bark extracts.** *Journal of Agricultural and Food Chemistry* 2007, 55(1):148-156.

47. Behrens A, Maie N, Knicker H, Kogel-Knabner I: **MALDI-TOF mass spectrometry and PSD fragmentation as means for the analysis of condensed tannins in plant leaves and needles.** *Phytochemistry* 2003, 62(7):1159-1170.

48. Yanagida A, Murao H, Ohnishi-Kameyama M, Yamakawa Y, Shoji A, Tagashira M, Kanda T, Shindo H, Shibusawa Y: **Retention behavior of oligomeric proanthocyanidins in hydrophilic interaction chromatography.** *Journal of Chromatography A* 2007, 1143(1-2):153-161.

49. Karonen M, Loponen J, Ossipov V, Pihlaja K: **Analysis of procyanidins in pine bark with reversed-phase and normal-phase high-performance liquid chromatography-electrospray ionization mass spectrometry.** *Analytica Chimica Acta* 2004, 522(1):105-112.

50. Tourino S, Fuguet E, Jauregui O, Saura-Calixto F, Cascante M, Torres JL: **High-resolution liquid chromatography/electrospray ionization time-of-flight mass spectrometry combined with liquid chromatography/electrospray ionization tandem mass spectrometry to identify polyphenols from grape antioxidant dietary fiber.** *Rapid Communications in Mass Spectrometry : RCM* 2008, 22(22):3489-3500.

51. Gu L, Kelm MA, Hammerstone JF, Zhang Z, Beecher G, Holden J, Haytowitz D, Prior RL: **Liquid chromatographic/electrospray ionization mass spectrometric studies of proanthocyanidins in foods.** *Journal of Mass Spectrometry : JMS* 2003, 38(12):1272-1280.

52. Mouls L, Mazauric JP, Sommerer N, Fulcrand H, Mazerolles G: **Comprehensive study of condensed tannins by ESI mass spectrometry: Average degree of polymerisation and polymer distribution determination from mass spectra.** *Analytical and Bioanalytical Chemistry* 2011, 400(2):613-623.

53. Moilanen J, Sinkkonen J, Salminen JP: **Characterization of bioactive plant ellagitannins by chromatographic, spectroscopic and mass spectrometric methods.** *Chemoecology* 2013, 23(3):165-179.

54. Chai WM, Shi Y, Feng HL, Qiu L, Zhou HC, Deng ZW, Yan CL, Chen QX: **NMR, HPLC-ESI-MS, and MALDI-TOF MS analysis of condensed tannins from *Delonix regia* (Bojer ex Hook.) Raf. and their bioactivities.** *Journal of Agricultural and Food Chemistry* 2012, 60(19):5013-5022.

55. Hellstrom JK, Mattila PH: **HPLC determination of extractable and unextractable proanthocyanidins in plant materials.** *Journal of Agricultural and Food Chemistry* 2008, 56(17):7617-7624.

56. Yokota K, Kimura H, Ogawa S, Akihiro T: **Analysis of A-Type and B-Type highly polymeric proanthocyanidins and their biological activities as nutraceuticals.** *Journal of Chemistry* 2013, 2013:7.

57. Williams AR, Ramsay A, Hansen TV, Ropiak HM, Mejer H, Nejsum P, Mueller-Harvey I, Thamsborg SM: **Anthelmintic activity of trans-cinnamaldehyde and A- and B-type proanthocyanidins derived from cinnamon (*Cinnamomum verum*).** *Scientific Reports* 2015, 5:14791.

58. Roux EL, Doco T, Sarni-Manchado P, Lozano Y, Cheynier V: **A-type proanthocyanidins from pericarp of *Litchi chinensis*.** *Phytochemistry* 1998, 48(7):1251-1258.

59. Nunes C, Guyot S, Marnet N, Barros AS, Saraiva JA, Renard CM, Coimbra MA: **Characterization of plum procyanidins by thiolytic depolymerization.** *Journal of Agricultural and Food Chemistry* 2008, 56(13):5188-5196.

60. Tarascou I, Mazauric JP, Meudec E, Souquet JM, Cunningham D, Nojeim S, Cheynier V, Fulcrand H: **Characterisation of genuine and derived cranberry proanthocyanidins by LC-ESI-MS.** *Food Chemistry* 2011, 128(3):802-810.

61. Balde AM, Pieters LA, Gergely A, Kolodziej H, Claeys M, Vlietinck AJ: **A-Type proanthocyanidins from stem Bark of *Pavetta owariensis*.** *Phytochemistry* 1991, 30(1):337-342.

62. Idowu TO, Ogundaini AO, Salau AO, Obuotor EM, Bezabih M, Abegaz BM: **Doubly linked, A-type proanthocyanidin trimer and other constituents of *Ixora coccinea* leaves and their antioxidant and antibacterial properties.** *Phytochemistry* 2010, 71(17-18):2092-2098.

63. Foo LY, Lu YR, Howell AB, Vorsa N: **The structure of cranberry proanthocyanidins which inhibit adherence of uropathogenic P-fimbriated *Escherichia coli in vitro*.** *Phytochemistry* 2000, 54(2):173-181.

64. Del Rio D, Calani L, Dall'Asta M, Brighenti F: **Polyphenolic composition of hazelnut skin.** *Journal of Agricultural and Food Chemistry* 2011, 59(18):9935-9941.

65. Li C, Leverence R, Trombley JD, Xu S, Yang J, Tian Y, Reed JD, Hagerman AE: **High molecular weight persimmon (*Diospyros kaki* L.) proanthocyanidin: A highly galloylated, A-linked tannin with an unusual flavonol terminal unit, myricetin.** *Journal of Agricultural and Food Chemistry* 2010, 58(16):9033-9042.

66. Takahata Y, Ohnishi-Kameyama M, Furuta S, Takahashi M, Suda I: **Highly polymerized procyanidins in brown soybean seed coat with a high radical-scavenging activity.** *Journal of Agricultural and Food Chemistry* 2001, 49(12):5843-5847.

67. Bartolome B, Hernandez T, Bengoechea ML, Quesada C, GomezCordoves C, Estrella I: **Determination of some structural features of procyanidins and related compounds by photodiode-array detection.** *Journal of Chromatography A* 1996, 723(1):19-26.

68. Labarbe B, Cheynier V, Brossaud F, Souquet JM, Moutounet M: **Quantitative fractionation of grape proanthocyanidins according to their degree of polymerization.** *Journal of Agricultural and Food Chemistry* 1999, 47(7):2719-2723.

69. Meagher LP, Spencer P, Lane GA, Sivakumaran S, Fraser K: **What do green tea, grapes seeds, and docks have in common?** *Chemistry in New Zealand* 2005, 69(3):6.

70. Lakenbrink C, Engelhardt UH, Wray V: **Identification of two novel proanthocyanidins in green tea.** *Journal of Agricultural and Food Chemistry* 1999, 47(11):4621-4624.

71. Mateos-Martin ML, Fuguet E, Quero C, Perez-Jimenez J, Torres JL: **New identification of proanthocyanidins in cinnamon (*Cinnamomum zeylanicum* L.) using MALDI-TOF/TOF mass spectrometry.** *Analytical and Bioanalytical Chemistry* 2012, 402(3):1327-1336.

72. Flamini R: **Recent applications of mass spectrometry in the study of grape and wine polyphenols.** *ISRN Spectroscopy* 2013, 2013:1-45.

73. Fulcrand H, Remy S, Souquet JM, Cheynier V, Moutounet M: **Study of wine tannin oligomers by on-line liquid chromatography electrospray ionization mass spectrometry.** *Journal of Agricultural and Food Chemistry* 1999, 47(3):1023-1028.

74. Es-Safi NE, Guyot S, Ducrot PH: **NMR, ESI/MS, and MALDI-TOF/MS analysis of pear juice polymeric proanthocyanidins with potent free radical scavenging activity.** *Journal of Agricultural and Food Chemistry* 2006, 54(19):6969-6977.

75. Krueger CG, Dopke NC, Treichel PM, Folts J, Reed JD: **Matrix-assisted laser desorption/ionization time-of-flight mass spectrometry of polygalloyl polyflavan-3-ols in grape seed extract.** *Journal of Agricultural and Food chemistry* 2000, 48(5):1663-1667.

Chapter 4. A comparative study of sainfoin proanthocyanidins by thiolysis-HPLC and UPLC-MS/MS analyses

4.1 Introduction

Sainfoin is a perennial forage legume which possesses several attributes that may contribute to eco-friendly agricultural practices [1]. Sainfoin can support small ruminant production especially in temperate climates [2]. This is possibly based on the observation that proanthocyanidins (PAs, *syn.* condensed tannins) in some forage legumes were shown to increase absorption of dietary amino acids in the small intestine compared to iso-nitrogenous non-PA-containing forages [3-5]. This phenomenon is called "rumen escape protein" and can result in higher live weight gain and fertility, along with increased protein content in milk and higher meat and wool production [2, 6]. Moreover, the voluntary feed intake of sainfoin is higher compared to grasses and other forage legumes, such as red clover or lucerne [5, 7]. Apart from the nutritional benefits of a sainfoin diet, significant reductions in bloat incidents and a better control of gastrointestinal nematode infections have also been reported [2, 6, 8-12]. Several studies have put forward the notion that feeding of sainfoin can contribute to the mitigation of green-house gas emissions, namely nitrous oxide (N_2O) and methane (CH_4) [2, 4, 6, 8, 13-16]. It is thought that the phenolic constituents of sainfoin, especially PAs, may be linked to these positive effects [9, 17-20]. However, sainfoin PAs exhibit a diversity of PA contents and also compositional traits across different accessions and across developmental stages [21-25]. This diversity may account for some of the contradictory findings reported of sainfoin bioactivity [2, 6]. Probing of the relationships between PA content, composition and biological effects requires the characterisation of PAs in extracts and plant samples. This is difficult because of the complexity of PAs and the limitations in analytical methods [26]. Therefore, rapid and accurate profiling and quantification of PAs is required.

This chapter reports the investigation of sainfoin acetone/water extracts by thiolytic degradation coupled with reverse-phase high performance liquid chromatography (RP-HPLC) analysis and by a novel ultra-performance liquid chromatography−tandem mass spectrometry (UPLC-ESI-MS/MS) method. The study aims in particular to:

- Probe the diversity of quantitative and qualitative PA traits in sainfoin accessions that have promising agronomic properties.

- Identify whether trends exist between PA content, structural features and plant parts.

- Compare and evaluate the data acquired by the different methods.

- Draw conclusions on the suitability of the two different methods for the rapid screening of extractable PAs.

4.2 Materials and Methods

4.2.1 Sainfoin samples

Sainfoin samples from 18 different accessions and 2 components (stems and leaves) were collected at Agroscope, (Institute for Sustainability Sciences, Zurich, Switzerland) during November 2012. The majority of plants were at the early flowering stage or just before flowering. The plant tissues were frozen and freeze-dried to minimise any changes in PA concentration or composition. Subsequently, samples were finely ground and ball-milled. Sainfoin was weighed into 15 ml Falcon tubes and stored at -20 °C until PA extraction and analysis.

4.2.2 Extraction of sainfoin PAs

Lyophilised sainfoin tissue (130 mg x 4) was weighed in 10 ml screw-capped glass tubes and macerated in aqueous acetone (9 ml, 8:2 v/v). The mixtures were homogenised for 5 min by vigorous shaking. Samples were stored overnight at 4 °C. The following day samples were mixed again and placed on a reciprocating shaker. Extraction of PAs was performed under vigorous shaking (3 h x 2) and after centrifugation all four supernatants were combined. Acetone was allowed to evaporate overnight at room temperature under slight ventilation in order to concentrate the PAs in the water phase. Samples were centrifuged and supernatant solutions were collected and filtered through 0.2 µm polytetrafluoroethylene filters (VWR, Helsinki, Finland), transferred into plastic tubes, frozen and lyophilised. Stock solutions were prepared by dissolving PA extracts in ultra-pure water (20 mg extract/ml). Aliquots of 0.2 ml were transferred to test tubes in duplicate, frozen and freeze dried for the thiolysis reaction. Freeze

dried PA extracts were also dissolved in ultra-pure water (8 mg/ml) for UPLC-ESI-MS/MS analysis.

4.2.3 Chemicals and reagents

HPLC grade acetonitrile was purchased from Fisher Scientific (Loughborough, UK) and Sigma-Aldrich (Steinheim, Germany). Formic acid was from VWR (Helsinki, Finland). Water purification was performed with a Millipore Synergy water purification system (Merck KGaA, Darmstadt, Germany) and a Milli-Q system (Millipore, Watford, UK). Hydrochloric acid (36%), acetic acid, HPLC grade acetone and HPLC grade methanol were supplied by Fisher Scientific (Loughborough, UK). Benzyl mercaptan and (±)–dihydroquercetin (85%) were obtained from Sigma-Aldrich (Poole, UK). Catechin was from Sigma (Sigma Chemical Co., St. Louis, MO, USA).

4.2.4 Thiolysis-HPLC analysis

The thiolysis reaction was performed according to Novobilský et al. [27] as described in Chapter 2. Briefly, PA extract (4 mg) was weighed into 10 ml screw-capped vials and dissolved in methanol (1.5 ml), acidified with HCl (0.5 ml, 3.3 % in methanol, v/v). The addition of benzyl mercaptan (50 μl) followed and the reaction mixture was stirred at 40 °C for 1 h. The reaction was stopped by adding ultra-pure water (2.5 ml) to the vials at room temperature. Identification and quantification of the thiolysis products was performed by HPLC linked to a diode array detector. The chromatographic conditions and settings of the instrument are described in Section 2.2.6. Content and composition of PAs was determined according to Gea et al. [28].

4.2.5 UPLC-ESI-MS/MS analysis

Information on PA content (mg/g of extract), mean degree of polymerisation (mDP) and PC/PD ratio of the sainfoin extracts was acquired by UPLC-ESI-MS/MS analysis using a new method developed by Engström et al. and described in Chapter 3 [29].

4.2.6 Statistical analysis

The linear correlations of data pairs obtained by the two methods (thiolysis-HPLC and UPLC-ESI-MS/MS) between PA content (mg/g extract), mDP (mol), PC content (mg PCs/100 mg PAs) and *cis*-flavan-3-ol contents (mg *cis*/100 mg PAs) were determined with the Pearson product-moment correlation. A method comparison was performed by computing the limits of agreement (LoA) and determining prediction equations [30, 31] . All data analyses were performed with R software (version 3.2.0).

4.3 Results and discussion

4.3.1 Thiolysis-HPLC and UPLC-ESI-MS/MS analysis of extractable sainfoin PAs

Table 4.1 lists the sainfoin samples that were tested and PA contents (mg/g extract), mDP values and PC contents (mg PCs/100 mg PAs) estimated by the two analytical methods. Determination of the PA subunit composition in terms of *cis*- or *trans*-flavan-3-ol configuration in the C-ring was only possible after thiolytic degradation and HPLC analysis.

In agreement with previous studies [5, 7, 21, 22] sainfoin accessions varied greatly in terms of PA, PC and PD contents (mg/g extract) and PC content within total PAs (mg PCs/100 mg PAs) (Table 4.1, Figures 4.1, 4.3). The results indicated that sainfoin PAs are accession specific. Similarly, there was considerable variation in the concentrations of the four flavan-3-ols (gallocatechin, G; epigallocatechin, EGC; catechin, C and epicatechin, EC) within the terminal and extension units (Table 4.2). The PA content estimated with thiolysis ranged from 5.75 (S10) to 231 (S39) (mg/g extract), whereas the UPLC-ESI-MS/MS data covered a range of 8.50 (S11) to 155 (S39) (mg/g extract) (Table 4.1, Figure 4.1). The average polymer size, expressed as mDP, also varied and ranged from 2.87 (S20) to 23.6 (S31) by thiolysis and from 4.14 to 16.1 (S4 vs. S31) by UPLC-ESI-MS/MS (Table 4.1, Figure 4.2). The PC content within PAs (mg PCs/100 mg PAs) was between 1.36 (S38) and 100 (S10) by thiolysis and between 3.34 (S39) and 89.4 (S4) by UPLC-ESI-MS/MS (Table 4.1, Figure 4.3). The content of flavan-3-ols

with *cis* configuration ranged from 47.3 (S2) to 96.6 (S23) in mg *cis*/100 mg PAs (Table 4.1, Figure 4.4).
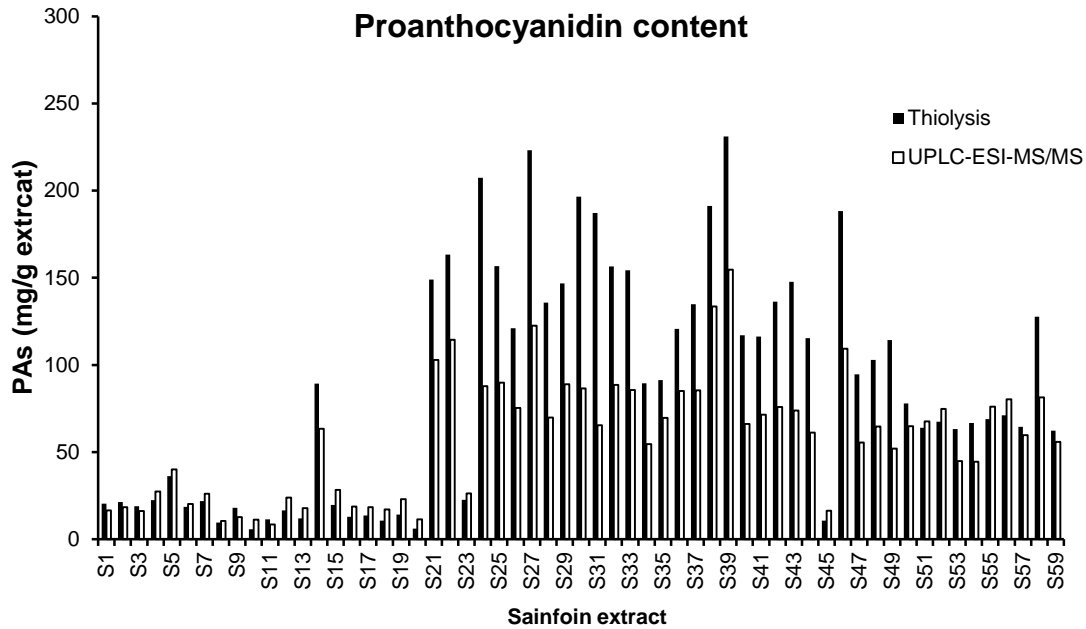
Figure 4.1: Proanthocyanidin (PA) contents (mg/g extract) in sainfoin extracts determined by thiolysis and UPLC-ESI-MS/MS analyses
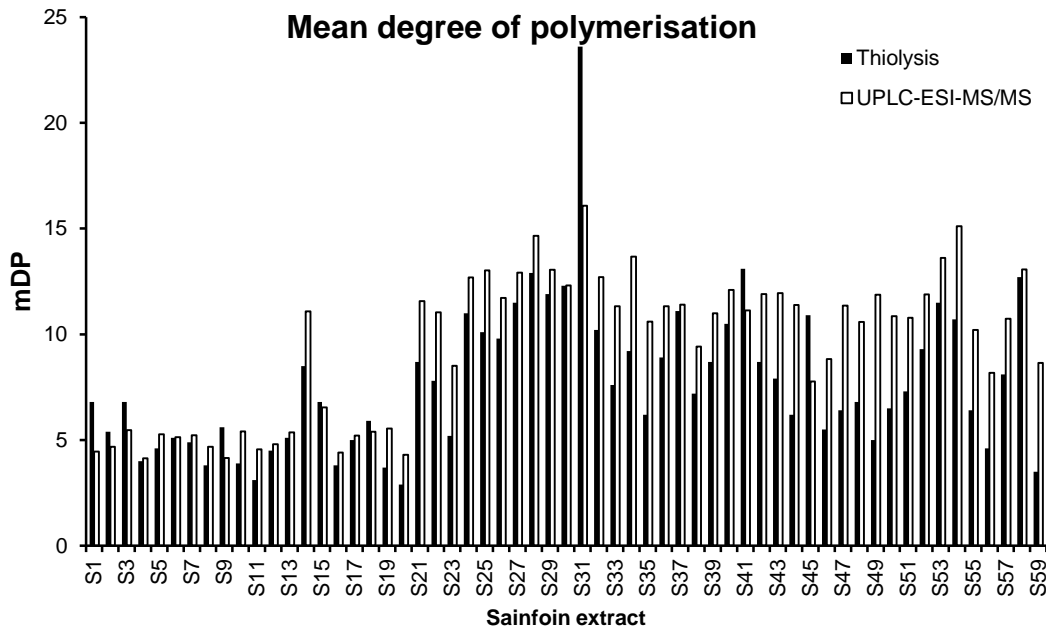
Figure 4.2: Mean degree of polymerisation (mDP) of proanthocyanidins in sainfoin extracts estimated by thiolysis and UPLC-ESI-MS/MS analyses
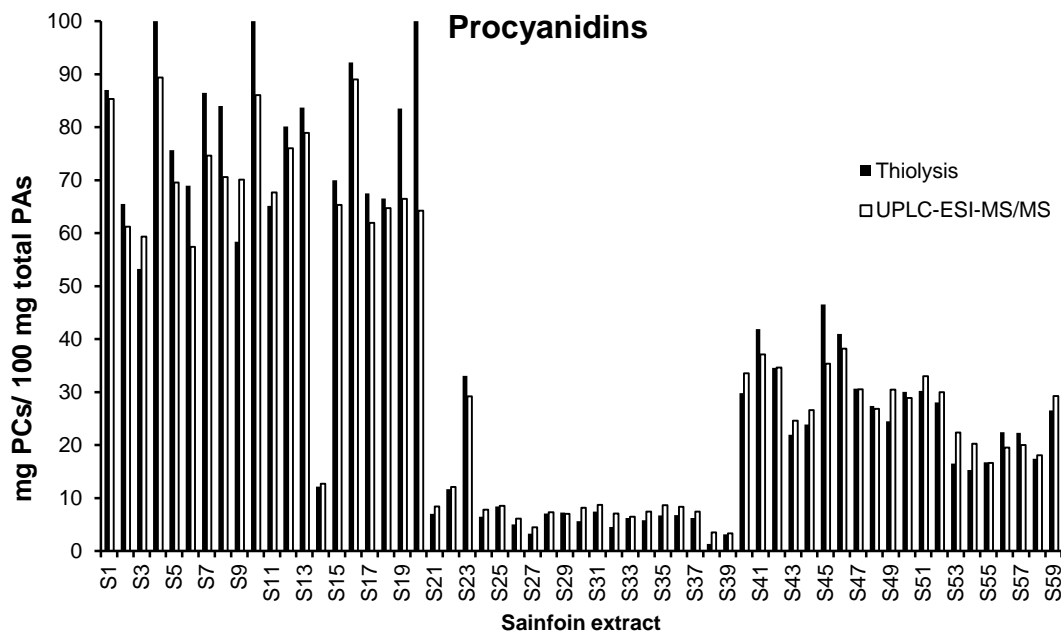
Figure 4.3: Procyanidin (PC) proportions in sainfoin extracts estimated by thiolysis and UPLC-ESI-MS/MS.
PD (mg PDs/100 mg PAs) = 100 − PC
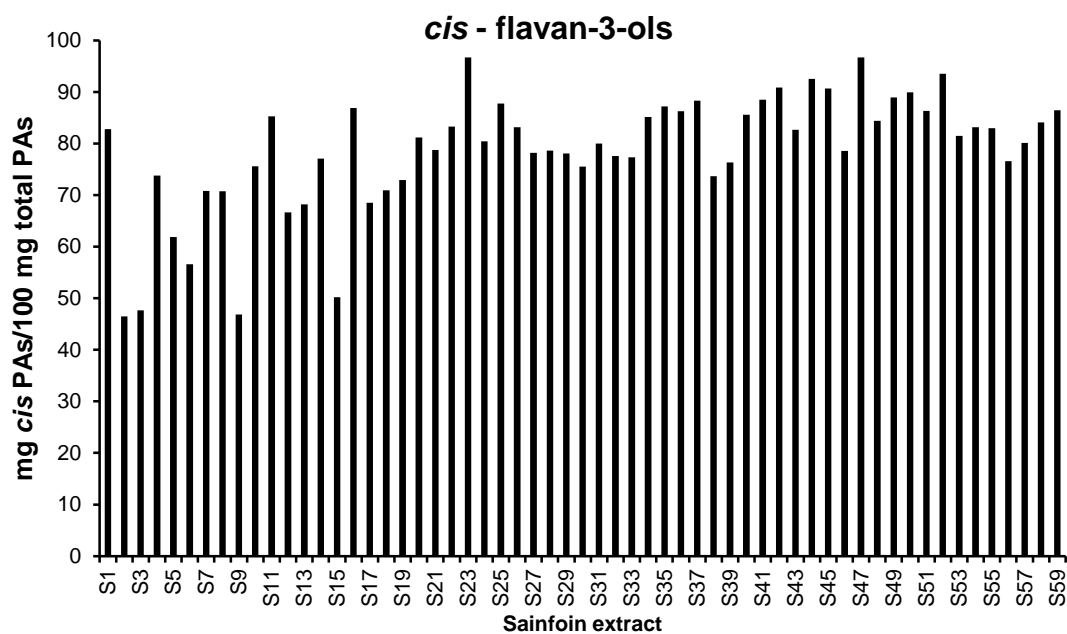
Figure 4.4: *Cis*-flavan-3-ol proportions in sainfoin extracts determined by thiolysis.
trans (mg *trans*/100 mg PAs) = 100 − *cis*

As previously reported [25] sainfoin stems tended to have lower PA contents that consisted mostly of EC and C (Tables 4.1 and 4.2) in terminal and extender units whereas, GC was the next commonly found flavan-3-ol unit only in the extender part of stem PAs (Table 4.2). Interestingly, GC and EGC were only detected in the terminal part of two stem-derived PA extracts (S11, S14) (Table 4.2). However, PAs extracted from leaves displayed higher PA contents and more PDs (Table 4.1, Figure 4.1 and 4.3). Chromatographic separation and analysis of thiolytic reaction products revealed that PA polymers are composed mainly of *cis*-flavan-3-ols in the extension units (Table 4.1, Figure 4.4). These findings accorded with other studies on soluble PAs extracted from sainfoin leaves [25, 33, 35]. This collection of sainfoin extracts was, therefore, characterised by an enormous diversity in PA content, mDP values and PC/PD and *cis/trans* flavan-3-ol ratios. This diversity is likely to impact on their anthelmintic bioactivities and may also affect ruminal fermentation activities [2, 6].

Table 4.1: Characterisation of proanthocyanidins in acetone/water extracts of sainfoin accessions by thiolysis-HPLC and UPLC-ESI-MS/MS methods. Proanthocyanidin (PA) content (mg/g extract), mean degree of polymerisation (mDP), procyanidin (PC) and *cis*-flavan-3-ol content (mg *cis*/100 mg PAs); Standard deviation in brackets (*n=2*); PD (mg PDs/100 mg PAs) = 100 – PC; *trans* (mg *trans*/100 mg PAs) = 100 – *cis*

Sample No	Accession	Plant part	Thiolysis-HPLC				UPLC-ESI-MS/MS		
			PA (mg/g extract)	mDP	PC (mg/100 mg PAs)	*cis* (mg/100 mg PAs)	PA (mg/g extract)	mDP	PC (mg/100 mg PAs)
S1	Perdix	stem	20.6 (5.30)*	6.80 (1.28)	87.0 (2.33)	82.8 (5.83)	16.6	4.46	85.3
S2	Visnovsky	stem	21.5 (0.778)	5.39 (0.069)	65.5 (0.322)	46.5 (1.11)	18.5	4.68	61.2
S3	Esparsette	stem	19.1 (1.06)	6.84 (0.259)	53.3 (0.666)	47.6 (0.528)	16.3	5.47	59.3
S4	Perdix	stem	22.40 (0.707)	4.01 (0.123)	100 (0.000)	73.8 (0.561)	27.5	4.14	89.4
S5	Perly	stem	36.2 (0.141)	4.64 (0.132)	75.6 (0.023)	61.9 (0.151)	40.1	5.27	69.6
S6	Perly	stem	18.6 (1.98)	5.07 (0.266)	69.0 (5.45)	56.6 (5.74)	20.2	5.13	57.4
S7	Perdix	stem	21.9 (0.636)	4.92 (0.124)	86.5 (0.895)	70.8 (0.741)	26.2	5.22	74.7
S8	Taja	stem	9.60 (1.13)	3.75 (0.243)	84.0 (0.079)	70.8 (0.516)	10.5	4.68	70.6
S9	Perdix	stem	18.2 (1.91)	5.58 (0.391)	58.4 (3.47)	46.8 (1.83)	12.8	4.15	70.1
S10	CPI 63854	stem	5.8 (0.212)	3.87 (0.038)	100 (0.000)	75.6 (2.03)	11.2	5.41	86.1
S11	Perly	stem	11.6 (2.47)	3.14 (1.21)	65.2 (7.28)	85.3 (3.72)	8.50	4.55	67.7
S12	Perly	stem	16.6 (1.27)	4.49 (0.246)	81.0 (0.828)	66.7 (0.711)	23.9	4.80	76.1
S13	CPI 63854	stem	12.1 (1.48)	5.4 (0.220)	83.7 (4.23)	68.2 (3.33)	17.9	5.37	79.0
S14	CPI 63854	stem	89.4 (4.45)	8.45 (0.496)	12.1 (1.01)	77.1 (0.129)	63.5	11.1	12.7
S15	Esparsette	stem	19.8 (0.141)	6.79 (0.177)	70.0 (1.66)	50.2 (0.986)	28.4	6.55	65.3
S16	Perly	stem	13.0 (1.41)	3.81 (0.099)	92.2 (0.708)	86.9 (1.17)	18.8	4.41	89.0
S17	Esparsette	stem	13.8 (1.63)	5.04 (0.275)	67.5 (0.914)	68.5 (0.238)	18.4	5.21	62.0
S18	Esparsette	stem	10.7 (0.707)	5.89 (0.082)	66.5 (7.61)	70.9 (2.62)	17.1	5.39	64.7
S19	CPI 63854	stem	14.2 (0.495)	3.71 (0.150)	83.5 (2.42)	72.9 (1.98)	23.1	5.54	66.5

Table 4.1 *(continued)*

Sample No	Accession	Plant part	Thiolysis				UPLC-ESI-MS/MS		
			PA (mg/g extract)	mDP	PC (mg/100 mg PAs)	*cis* (mg/100 mg PAs)	PA (mg/g extract)	mDP	PC (mg/100 mg PAs)
S20	Visnovsky	stem	6.20 (0.990)	2.87 (0.169)	100 (0.000)	81.2 (1.96)	11.4	4.30	64.3
S21	247	leaves	149.1 (9.40)	8.70 (0.303)	7.01 (0.481)	78.7 (1.78)	103	11.6	8.38
S22	CPI 63854	leaves	163 (6.15)	7.76 (0.140)	11.7 (0.622)	83.3 (0.152)	115	11.0	12.1
S23	Esparsette	stem	22.8 (1.20)	5.22 (0.370)	33.0 (0.748)	96.7 (0.237)	26.4	8.51	29.2
S24	Esparsette	leaves	207 (11.2)	11.0 (0.370)	6.49 (0.194)	80.4 (0.240)	87.9	12.7	7.81
S25	La Rippe	leaves	157 (15.98)	10.1 (0.385)	8.40 (0.343)	87.7 (0.132)	89.8	13.0	8.50
S26	CPI 63750	leaves	121 (0.212)	9.80 (0.460)	5.04 (0.301)	83.3 (0.090)	75.4	11.7	6.11
S27	CPI 63750	leaves	223 (21.5)	11.5 (0.059)	3.27 (0.278)	78.2 (0.055)	123	12.9	4.48
S28	CPI 63854	leaves	136 (6.15)	12.9 (0.093)	7.05 (0.486)	78.6 (0.159)	69.9	14.7	7.32
S29	CPI 63854	leaves	147 (16.5)	11.9 (1.24)	7.27 (0.108)	78.0 (0.426)	89.0	13.1	7.02
S30	CPI 63854	leaves	197 (25.2)	12.3 (1.70)	5.64 (0.644)	75.5 (8.71)	86.6	12.3	8.14
S31	CPI 63854	leaves	187 (14.6)	23.6 (0.089)	7.46 (0.460)	80.0 (0.069)	65.4	16.1	8.74
S32	TU86-43-03	leaves	156 (0.636)	10.2 (0.231)	4.56 (0.063)	77.6 (0.379)	88.6	12.7	7.08
S33	Esparsette	leaves	154 (15.9)	7.63 (0.017)	6.21 (0.366)	77.3 (0.310)	85.7	11.3	6.49
S34	Taja	leaves	89.6 (8.84)	9.22 (0.426)	5.82 (0.119)	85.1 (0.780)	54.7	13.7	7.42
S35	Visnovsky	leaves (hay)	91.3 (15.6)	6.17 (0.308)	6.69 (0.075)	87.2 (1.14)	69.7	10.6	8.63
S36	Visnovsky	leaves	121 (3.11)	8.87 (0.111)	6.80 (0.106)	86.3 (0.653)	85.1	11.3	8.36
S37	TU86-43-03	leaves	135 (4.17)	11.1 (2.48)	6.23 (0.203)	88.3 (2.20)	85.4	11.4	7.44
S38	WKT10	leaves	191 (33.4)	7.22 (0.149)	1.36 (0.008)	73.7 (1.89)	134	9.41	3.53
S39	WKT10	leaves	231 (23.8)	8.72 (0.082)	3.17 (0.123)	76.3 (2.56)	155	11.0	3.34
S40	Perly	leaves	117 (29.8)	10.5 (1.19)	29.8 (0.919)	85.6 (0.607)	66.2	12.1	33.6
S41	CPI 63826	leaves	116 (11.5)	13.1 (0.132)	41.9 (1.31)	88.5 (0.291)	71.4	11.1	37.1

Table 4.1 *(continued)*

Sample No	Accession	Plant part	Thiolysis				UPLC-ESI-MS/MS		
			PA mg/g extract	mDP	PC mg/100 mg PAs	*cis* mg/100 mg PAs	PA mg/g extract	mDP	PC mg/100 mg PAs
S42	Rees "A"	leaves	136 (11.1)	8.69 (0.091)	34.6 (0.686)	90.8 (0.333)	75.9	11.9	34.7
S43	Rees "A"	leaves	148 (22.0)	7.88 (0.043)	22.0 (0.094)	82.6 (0.084)	73.9	11.9	24.6
S44	Perdix	leaves (hay)	115 (19.9)	6.17 (0.240)	23.9 (0.036)	92.6 (0.117)	61.3	11.4	26.6
S45	CPI 63854	stem	10.7 (1.77)	10.9 (3.16)	46.6 (4.68)	90.7 (2.72)	16.4	7.77	35.3
S46	Hampshire Common	leaves	188 (18.7)	5.53 (0.048)	41.0 (0.077)	78.6 (0.753)	109	8.83	38.2
S47	Perdix	leaves	94.7 (5.73)	6.39 (0.261)	30.7 (0.781)	96.7 (0.175)	55.6	11.4	30.5
S48	CPI 63854	rosette	103 (13.2)	6.82 (0.155)	27.4 (1.20)	84.4 (0.755)	64.8	10.6	26.8
S49	Perdix	leaves (hay)	114.2 (16.5)	4.97 (0.063)	24.5 (0.057)	88.9 (0.846)	52.1	11.9	30.5
S50	Perly	leaves	77.9 (28.1)	6.53 (0.080)	30.0 (0.002)	89.9 (1.32)	65.0	10.8	28.9
S51	Hampshire Common	leaves	63.9 (1.98)	7.33 (0.165)	30.2 (2.00)	86.3 (0.402)	67.6	10.8	33.0
S52	Hampshire Common	leaves	67.4 (5.66)	9.28 (0.143)	28.1 (0.737	93.5 (0.191)	74.9	11.9	30.0
S53	Perly	leaves	63.2 (5.87)	11.5 (0.218)	16.5 (0.666)	81.5 (0.631)	44.9	13.6	22.4
S54	Perly	leaves	66.8 (13.15)	10.7 (0.362)	15.3 (0.437)	83.1 (0.569)	44.4	15.1	20.3
S55	Buceanskij	leaves	68.9 (15.3)	6.37 (0.144)	16.7 (0.162)	83.0 (1.15)	76.2	10.2	16.6
S56	NA/RCAT 028437	leaves	71.2 (3.46)	4.62 (0.059)	22.4 (1.22)	76.6 (0.012)	80.3	8.18	19.5
S57	CPI 63780	leaves	64.6 (11.6)	8.10 (0.462)	22.3 (2.25)	80.1 (3.11)	59.7	10.7	20.0
S58	247	leaves	128 (0.566)	12.7 (0.508)	17.4 (0.299)	84.1 (0.680)	81.4	13.1	18.1
S59	CPI 63854	leaves	62.3 (5.30)	3.51 (0.333)	26.5 (3.98)	86.5 (7.45)	55.8	8.65	29.2

Table 4.2: Proanthocyanidin monomer composition and content in sainfoin extracts (mg/g extract); GC: gallocatechin, EGC: epigallocatechin, C: catechin, EC: epicatechin. Standard deviation in brackets (*n=2*); nd: not detected

Sample No	GC	EGC	C	EC	GC	EGC	C	EC
		Terminal units				Extender units		
S1	nd	nd	0.868 (0.076)*	2.11 (0.142)	nd	2.60 (0.210)	2.83 (2.04)	12.1 (2.84)
S2	nd	nd	2.97 (0.086)	0.939 (0.005)	7.40 (0.337)	nd	1.11 (0.232)	9.03 (0.117)
S3	nd	nd	1.07 (0.033)	1.65 (0.220)	8.91 (0.623)	nd	nd	7.42 (0.185)
S4	nd	nd	2.12 (0.040)	3.47 (0.308)	nd	nd	3.76 (0.020)	13.1 (0.339)
S5	nd	nd	3.45 (0.133)	4.27 (0.057)	8.82 (0.043)	nd	1.54 (0.089)	18.1 (0.199)
S6	nd	nd	1.57 (0.210)	2.03 (0.025)	5.82 (1.63)	nd	0.736 (0.088)	8.44 (0.079)
S7	nd	nd	1.77 (0.008)	2.64 (0.011)	2.95 (0.110)	nd	1.66 (0.125)	12.8 (0.601)
S8	nd	nd	0.611 (0.044)	1.92 (0.091)	1.53 (0.188)	nd	0.666 (0.148)	4.87 (0.660)
S9	nd	nd	0.963 (0.009)	2.21 (0.115)	5.90 (1.33)	1.69 (0.097)	2.81 (0.028)	4.58 (0.350)
S10	nd	nd	0.738 (0.016)	0.747 (0.054)	nd	nd	0.667 (0.153)	3.60 (0.010)
S11	0.145 (0.205)	2.15 (0.665)	0.487 (0.069)	1.09 (0.072)	0.578 (0.817)	1.24 (1.76)	0.538 (0.114)	5.33 (0.517)
S12	nd	nd	1.25 (0.023)	2.42 (0.503)	3.30 (0.390)	nd	0.992 (0.176)	8.64 (0.227)
S13	nd	nd	1.17 (0.105)	1.16 (0.276)	1.99 (0.751)	nd	0.692 (0.017)	7.03 (0.336)
S14	3.56 (0.327)	3.71 (0.190)	1.12 (0.078)	2.08 (0.302)	14.9 (0.503)	56.3 (4.18)	0.879 (0.003)	6.73 (0.138)
S15	nd	nd	2.87 (0.057)	nd	5.94 (0.370)	nd	1.05 (0.048)	9.93 (0.124)
S16	nd	nd	1.05 (0.102)	2.35 (0.354)	nd	1.01 (0.202)	0.655 (0.067)	7.93 (0.824)
S17	nd	nd	0.988 (0.198)	1.71 (0.298)	2.90 (0.253)	1.56 (0.150)	0.438 (0.029)	6.15 (0.728)
S18	nd	nd	0.962 (0.044)	0.826 (0.107)	1.62 (0.459)	1.94 (0.119)	0.524 (0.341)	4.83 (0.794)
S19	nd	nd	0.803 (0.017)	2.97 (0.008)	2.34 (0.424)	nd	0.698 (0.008)	7.34 (0.089)
S20	nd	nd	0.790 (0.273)	1.38 (0.200)	nd	nd	0.387 (0.036)	3.64 (0.481)
S21	7.86 (0.117)	7.81 (0.373)	1.43 (0.009)	nd	21.8 (4.57)	101 (4.40)	0.712 (0.022)	8.29 (0.027)

Table 4.2 *(continued)*

Sample No	GC	EGC	C	EC	GC	EGC	C	EC
		Terminal units				Extender units		
S22	7.74 (0.060)	7.99 (0.202)	2.27 (0.170)	2.89 (0.096)	16.3 (1.00)	112 (3.27)	1.00 (0.166)	12.9 (1.30)
S23	nd	2.33 (0.326)	0.748 (0.093)	1.26 (0.121)	nd	12.9 (0.309)	nd	5.51 (0.353)
S24	6.60 (0.641)	9.87 (0.522)	nd	2.32 (0.735)	32.9 (1.84)	145 (7.91)	1.09 (0.218)	10.0 (0.843)
S25	2.01 (0.095)	10.9 (0.338)	nd	2.48 (0.536)	17.2 (1.66)	113 (12.0)	nd	10.7 (1.34)
S26	5.28 (0.487)	5.95 (0.039)	nd	1.11 (0.075)	15.1 (0.343)	88.6 (0.346)	nd	5.00 (0.300)
S27	11.2 (1.39)	7.13 (0.481)	1.15 (0.100)	nd	36.3 (3.08)	161 (16.5)	nd	6.11 (0.018)
S27	11.2 (1.39)	7.13 (0.481)	1.15 (0.100)	nd	36.3 (3.08)	161 (16.5)	nd	6.11 (0.018)
S28	5.57 (0.033)	3.45 (0.290)	1.44 (0.072)	nd	21.2 (1.01)	96.0 (5.04)	0.839 (0.015)	7.28 (0.284)
S29	6.90 (1.44)	3.92 (1.09)	1.63 (0.171)	nd	22.8 (2.63)	102 (10.3)	0.896 (0.022)	8.13 (0.852)
S30	7.70 (0.073)	6.72 (0.00)	1.56 (0.101)	nd	39.7 (23.0)	132 (2.06)	0.308 (0.436)	9.13 (0.182)
S31	5.81 (0.311)	nd	2.04 (0.269)	nd	28.4 (2.12)	139 (10.3)	1.20 (0.105)	10.8 (1.58)
S32	8.07 (0.422)	6.22 (0.136)	1.10 (0.002)	nd	25.9 (0.026)	109 (0.820	nd	6.03 (0.130)
S33	7.00 (1.18)	10.2 (1.140)	1.38 (0.083)	1.56 (0.343)	26.6 (2.82)	101 (10.3)	nd	6.62 (0.682)
S34	3.38 (0.092)	5.27 (0.288)	1.03 (0.126)	nd	8.86 (0.396)	66.8 (7.44)	nd	4.19 (0.495)
S35	4.06 (0.387)	9.53 (1.194)	1.15 (0.198)	nd	6.56 (2.44)	65.1 (10.6)	nd	4.95 (0.774)
S36	5.64 (0.335)	6.54 (0.850)	1.40 (0.008)	nd	9.54 (0.033)	90.8 (2.29)	nd	6.81 (0.332)
S37	2.63 (3.02)	8.67 (0.491)	1.13 (0.096)	nd	12.0 (0.447)	103 (6.27)	nd	7.26 (0.110)
S38	14.1 (2.97)	12.5 (2.204)	nd	nd	36.0 (2.19)	126 (25.6)	nd	2.60 (0.438)
S39	15.6 (1.31)	8.87 (0.842)	1.96 (0.321)	nd	36.9 (1.91)	162 (22.5)	nd	5.38 (0.719)
S40	nd	4.81 (0.931)	1.56 (0.471)	4.56 (0.089)	13.6 (3.98)	64.0 (17.1)	1.83 (0.562)	26.8 (6.60)
S41	nd	nd	2.10 (0.149)	6.48 (0.302)	9.03 (0.850)	58.6 (7.34)	2.24 (0.019)	37.8 (2.53)
S42	nd	6.70 (0.008)	2.87 (0.357)	5.94 (0.366)	7.87 (1.00)	74.6 (5.33)	1.80 (0.115)	36.6 (3.57)

Table 4.3 *(continued)*

Sample No	GC	EGC	C	EC	GC	EGC	C	EC
	Terminal units				Extender units			
S43	2.78 (0.211)	8.95 (1.25)	3.94 (0.752)	2.93 (0.282)	16.8 (2.71)	86.8 (13.9)	2.09 (0.193)	23.5 (3.40)
S44	nd	12.8 (1.38)	1.48 (0.253)	4.31 (0.416)	4.78 (0.944)	70.2 (12.8)	2.33 (0.416)	19.4 (3.29)
S45	nd	nd	0.968 (0.125)	nd	nd	5.73 (1.44)	nd	3.95 (0.450)
S46	7.14 (0.736)	10.1 (0.594)	16.7 (1.74)	nd	13.2 (0.240)	80.8 (10.1)	3.25 (0.365)	57.2 (5.43)
S47	nd	7.50 (0.638)	3.14 (0.356)	4.06 (0.248)	nd	58.1 (2.59)	nd	21.8 (1.64)
S48	2.46 (0.471)	6.41 (0.876)	3.07 (0.915)	3.06 (0.002)	9.29 (0.947)	56.6 (8.54)	1.26 (0.504)	20.7 (0.978)
S49	nd	17.9 (2.74)	1.73 (0.251)	3.42 (0.317)	9.17 (0.232)	59.2 (9.46)	1.71 (0.387)	21.1 (2.84)
S50	1.20 (0.505)	5.55 (2.14)	2.17 (0.779)	2.94 (0.499)	3.33 (1.87)	44.4 (15.1)	1.33 (0.702)	16.9 (5.95)
S51	0.891 (0.057)	3.84 (0.040)	1.17 (0.016)	2.75 (0.031)	5.42 (0.104)	34.5 (2.75)	1.26 (0.076)	14.1 (0.802)
S52	nd	3.40 (0.315)	1.57 (0.061)	2.19 (0.058)	2.26 (0.327)	42.8 (3.92)	0.560 (0.109)	14.6 (0.804)
S53	nd	3.25 (0.226)	0.838 (0.025)	1.31 (0.075)	10.2 (1.37)	39.3 (2.88)	0.668 (0.089)	7.63 (1.13)
S54	nd	4.44 (0.625)	0.692 (0.181)	1.04 (0.101)	9.87 (2.23)	42.2 (7.99)	0.741 (0.185)	7.77 (1.74)
S55	2.60 (0.865)	5.59 (1.11)	1.28 (0.342)	1.34 (0.165)	7.16 (1.92)	42.09 (8.77)	0.766 (0.271)	8.14 (1.74)
S56	5.88 (0.017)	4.00 (0.827)	3.60 (0.156)	1.83 (0.062)	6.61 (1.04)	38.7 (1.67)	0.570 (0.109)	9.93 (0.287)
S57	4.19 (0.718)	nd	3.07 (0.252)	0.582 (0.001)	4.64 (0.535)	41.5 (10.3)	0.765 (0.136)	9.85 (1.02)
S58	4.31 (0.086)	nd	3.78 (0.142)	1.75 (0.060)	11.0 (0.511)	90.1 (1.45)	1.21 (0..039)	15.4 (0.017)
S59	1.39 (0.210)	13.0 (0.459)	1.41 (0.069)	2.01 (0.052)	4.10 (5.80)	27.3 (0.828)	1.71 (0.586)	11.3 (0.521)

4.3.2. Relationships between sainfoin PA content and structural features

Proanthocyanidin content (mg/g extract), determined by thiolysis-HPLC analysis, and average polymer size, expressed in mDP values, were significantly and positively correlated ($p<0.01$). This suggested that sainfoin extracts with high PA contents contained larger polymers. A similar correlation was also observed between both parameters when determined by UPLC-ESI-MS/MS ($p<0.01$) (Table 4.3).

Thiolysis results for the PC content within PAs (mg PCs/100 mg PAs) was negatively correlated with PA content (mg/g extract) ($p<0.01$) and an almost identical correlation was found with PC content values from UPLC-ESI-MS/MS analysis (Table 4.3). This means that PDs are more abundant in extracts with high PA contents, whereas PCs tend to dominate in sainfoin extracts with low PA concentrations. This may be associated with low PA concentrations in stems, which consisted mostly of PCs (Table 4.1).

Table 4.3: Pairwise Pearson correlations between proanthocyanidin (PA) content, mean degree of polymerisation (mDP), procyanidin (PC) content (mg PCs/100 mg PAs), *cis*-flavan-3-ol content (mg *cis*/100 mg PAs) of sainfoin extracts

Thiolysis	PA content (mg/g extract)	mDP	PC	*cis*
mDP	0.614***			
PC	−0.806***	−0.624***		
cis	0.324**	0.229*	−0.416***	
UPLC-ESI-MS/MS				
mDP	0.666***			
PC	−0.798***	−0.885***		

* $p < 0.1$
** $p < 0.05$
*** $p < 0.01$

A slightly weaker positive correlation was also observed between PA content (mg/g of extract) and the *cis*-flavan-3-ol content (mg *cis*/100 mg PAs) of extractable PAs ($p<0.05$) (Table 4.3). This was reflected in higher contents of terminal and extender EC units in stem PAs and also in considerable amounts of terminal EC units and terminal and extender EGC units in the majority of the extracts (Table 4.2).

Statistical analysis showed a significant negative correlation ($p<0.01$) between mDP values and PC contents (mg PCs/100 mg PAs) determined by thiolysis. This correlation was also high ($p<0.01$) when mDP and PC content were determined by UPLC-ESI-MS/MS. It appears that PA extracts with high mDP values contained mainly PDs.

The correlation between mDP values and *cis*-flavan-3-ol content (mg *cis*/100 mg PAs) was also positive but not significant ($p<0.1$). The PC content (mg PCs/100 mg PAs) was negatively correlated with *cis*-flavan-3-ols ($p<0.01$) and is linked to the large amounts of mainly EGC but also EC in terminal and extension units.

4.3.3. Correlations and extent of agreement between thiolysis-HPLC and UPLC-ESI-MS/MS results

A comparison of PA contents (mg/g extract) obtained by the two different analytical methods showed that quantification was possible by either method ($R^2=0.85$, Figure 4.5A). The data, using these methods demonstrated their usefulness for estimating PD ($R^2=0.88$, Figure 4.5C) and PC contents ($R^2=0.75$, Figure 4.6B) in mg/mg extract. Thiolysis results for PC content (mg PCs/100 mg PAs) were highly correlated ($R^2=0.96$, Figure 4.5D) with the UPLC-ESI-MS/MS data. Estimation of mDP values proved less accurate as demonstrated by the relatively poor correlation ($R^2=0.59$, Figure 4.5E) compared to the other PA traits.

An evaluation of the agreement between the two methods was also attempted by computing the Bland-Altman plots for PA content (mg/g extract), PC content (mg PCs/100 mg PAs) and mDP values (Figure 4.6). The conversion equations for the two methods revealed relatively large standard deviations. When the differences between both data sets were plotted instead against their mean values, the standard deviations were also large. Therefore, the two methods showed relatively low limits of agreement (LoA) for PA contents, % PC within total PAs and mDP values. However, it can be seen that only a few points were outside an acceptable agreement level in the three plots (Figure 4.6) and this proved that there was a strong linearity between the two methods as previously discussed (Figure 4.5). Bland-Altman plots provide a qualitative assessment of the interchangeable use of different methods [30, 31].
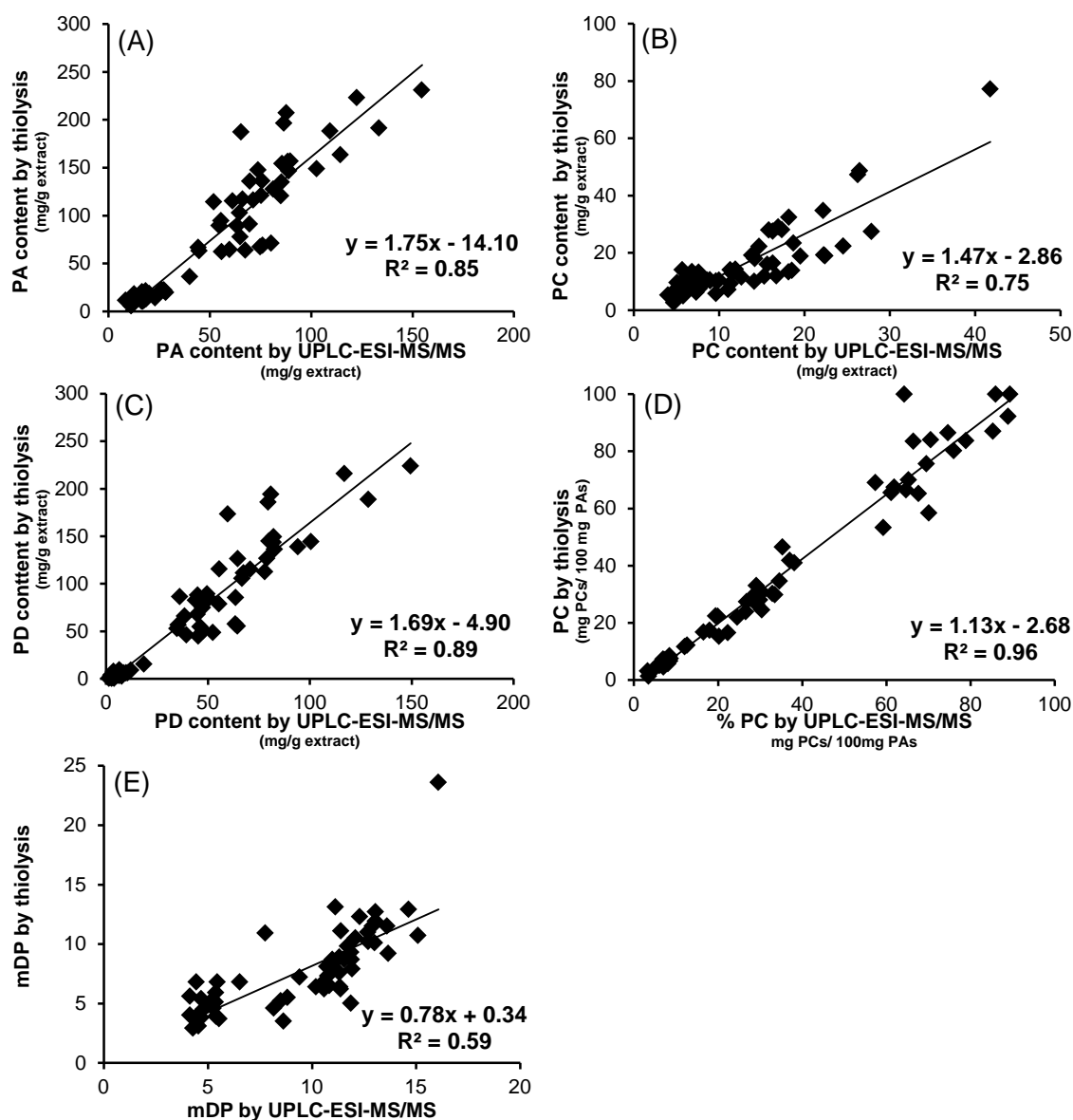
Figure 4.5: Correlations between (A) proanthocyanidin (PA) contents (mg/g extract), (B) procyanidin (PC) contents (mg/g extract), (C) prodelphinidin (PD) contents (mg/g extract), (D) correlation between procyanidin content within PAs (mg PCs/100 mg PAs) and (E) mean degree of polymerisation (mDP) determined by UPLC-ESI-MS/MS and thiolysis methods.
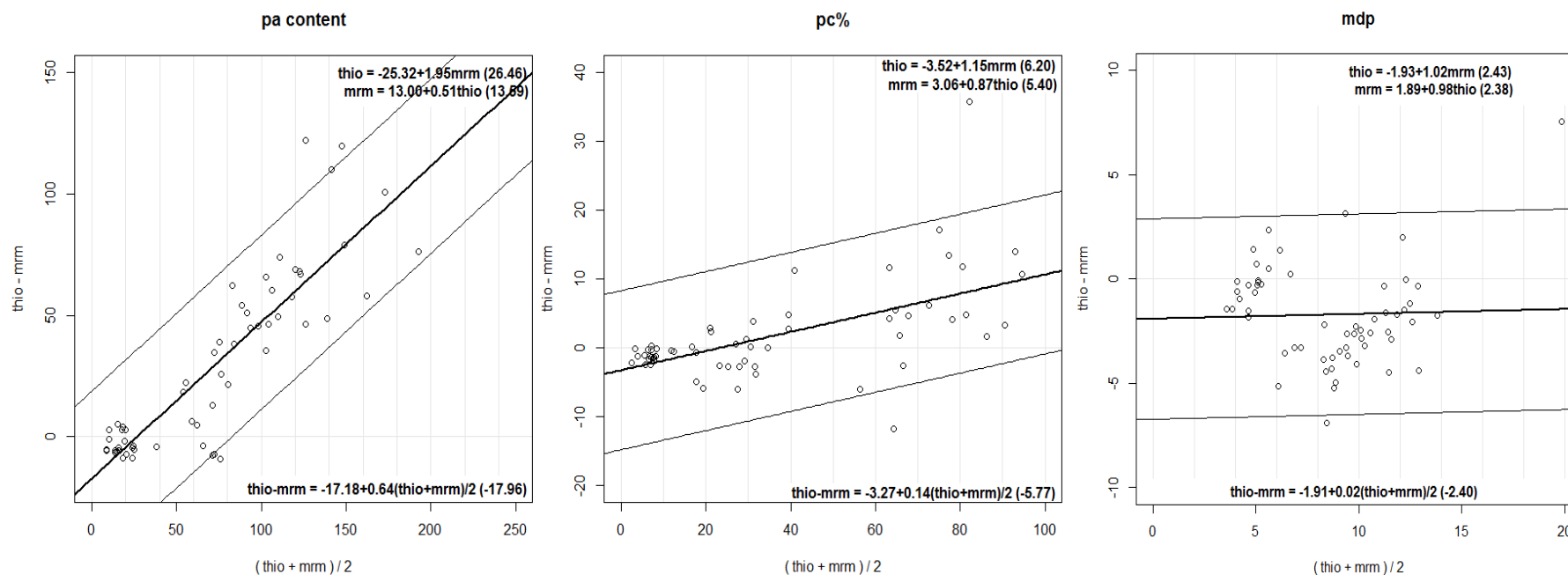
Figure 4.6: Bland-Altman plots with regression lines using the differences between values for PA content (mg/g extract), PC content within PAs (mg PCs/100 mg total PAs) and mDP values against the mean values determined by thiolysis-HPLC (thio) and UPLC-ESI-MS/MS (mrm) methods. Equations on the lower part of the graphs can calculate the difference (thio-mrm) between the two methods based on the mean of values. This equation is represented by the thick lines in the graphs. The values in brackets denote the standard deviation and provide the limits of agreement (LoA) in terms of 95% prediction intervals and are computed by the model as thin lines. The regression of values from thiolysis-HPLC and UPLC-ESI-MS/MS for PA content (mg/g extract), PC content within PAs (mg PCs/100 mg total PAs) and mDP using the linear function of the model, resulted in conversion equations. These are presented in the upper part of the graphs and provide prediction values for one method using values determined by the compared method.

Therefore, a final decision on which method to use can be based on the PA screening objectives. Given the limits of agreement, either method could be used in a sainfoin breeding programme in order to rank accessions for PA content or structural features. However, in cases where PA compositional data are needed for interpreting results from *in vitro* or *in vivo* experiments, then narrower LoA would be required for the interpretation of results. In addition, these low levels of agreement also highlight the necessity for further improvements of current PA analysis methods.

A comparison of the two analytical methods revealed a low correlation level for PA content (mg/g extract) as UPLC-ESI-MS/MS yielded lower values than thiolysis in most samples (Table 4.1, Figure 4.1). It is possible that the sample complexity or the high concentration (mg PAs/g extract) may have compromised ionisation efficiency. Alternatively, if ion formation and accumulation was complete, then perhaps the evaporation in the ESI process was problematic [36]. It is worth noting that this UPLC-ESI-MS/MS method was originally developed and validated with purified PA fractions [29]. However, the current study analysed crude aqueous acetone extracts. It has been reported that extracts of low purity may affect the analyte signal due to ion suppression or enhancement [37, 38]. In addition, Cavaliere et al. emphasised the need for matrix-effect correction, when the aim is to report quantitative results for crude extracts [36]. Several studies have reported that high MW PAs cause problems during the ionisation or vaporisation process and this can lead to suppressed signals [39, 40]. As described in section 4.3.2, extracts with higher PA contents (mg/g extract) tend to have also higher mDP values and this could provide another explanation for the variance between the methods. However, the cone voltages in the ion source were selectively optimised in order to tackle the problematic detection of longer PA polymers [29, 41] and smoothing iterations were also carefully selected to minimise the matrix effect.

Accurate quantification of PAs suffers from a lack of commercially available standards. Such standards would need to cover not only a wide range of PA structures but to offer a wide range of mixtures in order to represent typical compositions in plants as well [26]. Current strategies use purified PAs from the plant species under investigation [29, 42], purified PA fractions from readily

available sources that bear similarities in terms of mDP and flavan-3-ol units [43]
or compounds (i.e. dihydroquercetin and (epi)catechin) that structurally resemble
to the analytes of interest [28, 41, 44, 45]. In the current study external
calibrations using high purity PC- and PD-rich fractions (assessed by thiolysis),
were constructed to enable the quantitation of PCs and PDs in sainfoin extracts
with UPLC-ESI-MS/MS [29]. In contrast, thiolysis-HPLC analysis used
dihydroquercetin as an internal standard to quantify terminal and extension units
as dihydroquercetin equivalents [28, 46]. However, given the heterogeneity of
sainfoin PAs in terms of mDP and flavan-3-ol composition (Table 4.1 and 4.2) [32,
33], reference PAs that had been isolated from different plants, which contained
only PCs or PDs, could have affected the accuracy of the quantitation. It can be
observed that there is a reasonably good correlation (R^2 = 0.88) between PD
content (mg/g extract) analysed by thiolysis and UPLC-ESI-MS/MS; however the
correlation is worse (R^2 = 0.75) for the PC content (mg/g extract). This may
indicate that the model PDs isolated from white clover flowers are more suitable
for quantifying sainfoin PDs than the model PCs, isolated from goat willow leaves,
for quantifying sainfoin PCs. Thiolysis data are also based on assumptions that
are likely to affect the accuracy of PA quantification, i.e. response factors between
several flavan-3-ol BM-adducts and dihydroquercetin are actually not known and
are assumed to be the same as the underivatised flavan-3-ols [25, 26].
Furthermore, if dihydroquercetin is present in the extract, then external calibrations
would need to be performed. Thiolysis subjects PAs to a pre-column derivatisation
into their monomeric flavan-3-ols, which are quantified as individual peaks after
the chromatographic step. This means that co-eluting compounds can interfere
with the quantification of flavan-3-ols. In contrast, the fragmentation of intact PA
polymers in the ESI chamber is a post-column process in the UPLC-ESI-MS/MS
method. The reactions exploit different chemical properties of the PA molecules. In
thiolysis, BM generates a nucleophilic attack at C4 of the C-ring and monomeric
flavan-3-ol units are released as free compounds from the terminal positions or as
BM-adducts when derived from the extension positions. The quinone methide
cleavage mechanism leads to the formation of various *m/z* fragments from the
original molecule: fragments from extender units generate an intermediate
structure that lacks 2H and this *m/z* difference of 2 mass units distinguishes

extension from terminal units in the spectrum [47]. Moreover, detection of PAs in the two methods is based on very different molecular characteristics. The DAD detection is based on the UV absorption spectrum, whereas MRM records selected mass transitions of ion pairs in different channels. Considering the complexity and challenges posed by PA analysis and the fact that both methods are based on rather different detection processes, the observed correlations are promising. On that basis, the two methods enable semi-quantitation of total PAs.

However, poor correlation was obtained for the estimation of average polymer size, in terms of mDP values (Figure 4.5E). This could be due to the presence of monomeric (E)C and/or (E)GC in the plant extracts, which would lead to underestimation of mDP values. Previous studies used thiolytic degradation after isolation and chromatographic purification of sainfoin PAs [29, 33, 48]; this means that free monomeric flavan-3-ols would not have interfered with the mDP measurements. However, other studies did not measure free flavan-3-ols during *in situ* analyses of sainfoin accessions [28, 32] claiming either negligible presence of catechin or absence of free flavan-3-ols. Therefore, the current thiolysis-HPLC analysis also excluded free flavan-3-ol assessments in sainfoin extracts. Determination of free flavan-3-ols doubles the amount of time needed for PA analysis by thiolysis-HPLC.

In contrast to thiolysis, MRM analysis can easily incorporate free flavan-3-ol measurements by applying a range of cone voltages for PA ionisation [29]; the lower (CV1) of the six cone voltages used in the method (see also Table 3.1), detects mainly monomers and some small oligomers depending on the sample [29]. Contrary to the previous thiolysis-based studies [28, 32], screening of the MRM chromatographic fingerprints showed that noticeable amounts of free flavan-3-ols and low MW PAs were detected when CV1 was applied (Figure 4.8). For instance, the S4 extract shows free EC as the main component after fragmentation with CV1 (terminal PCs: tPC, *m/z* 289→245) and a smaller peak for C, whereas the S38 extract had comparable amounts of free GC and EGC (terminal PDs: tPD, *m/z* 305→125). The S49 extract had free EGC and EC and S56 had a combination of all four flavan-3-ols (GC, EGC, C and EC) (Figure 4.7). It can also be seen that CV1 produces less intense signals from PC and PD extension units oligomers (extension PC: ePC, *m/z* 287→125 and extension PD: ePD, *m/z* 303→125).
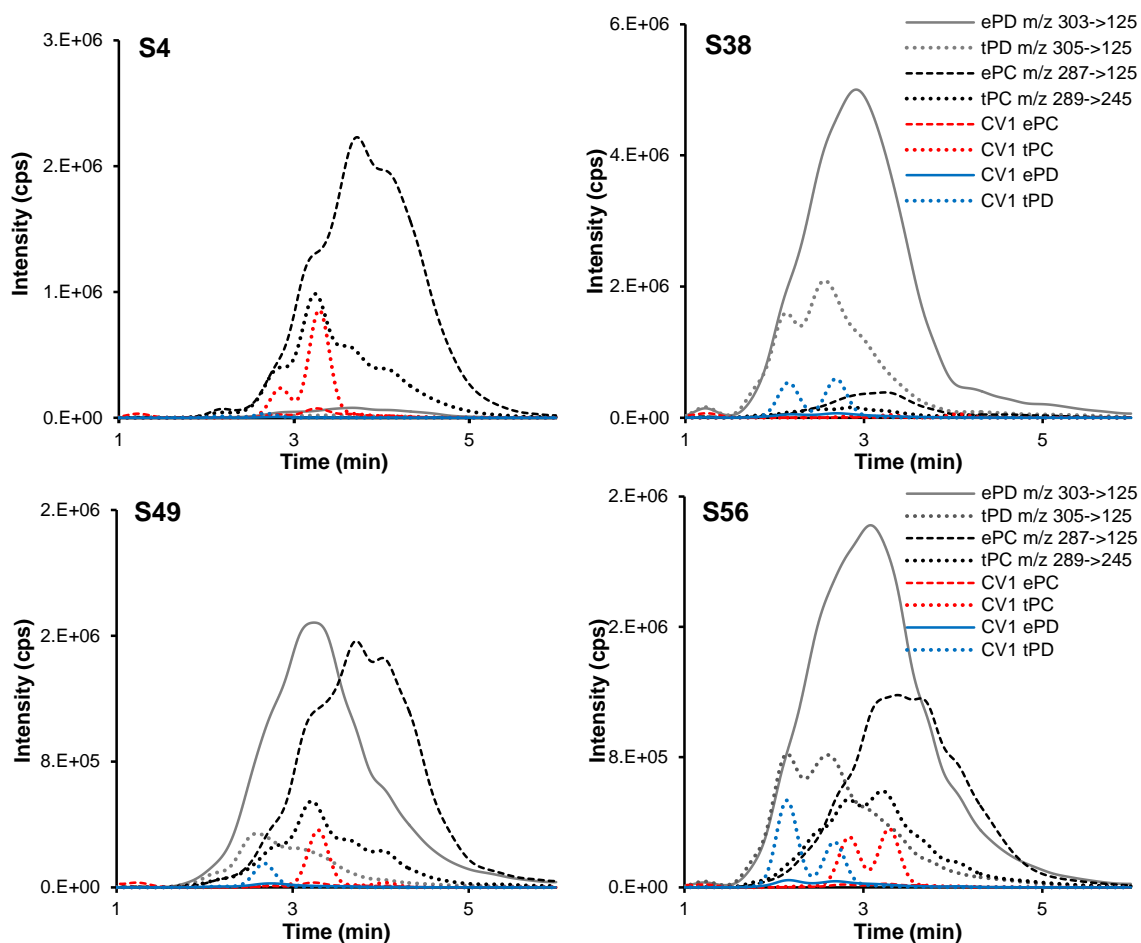
Figure 4.7: MRM chromatograms of procyanidin extension units (ePC, *m/z* 287→125), procyanidin terminal units (tPC, *m/z* 289→245), prodelphinidin extension units (ePD, *m/z* 303→125) and prodelphinidin terminal units (tPD, *m/z* 305→125) from extracts S4, S38, S49, S56. Fragments of monomeric units and small oligomers, produced by the lower cone voltage (CV1), were detected in comparable levels to the signals generated from the 5 higher cone voltages. Red coloured humps depict the total PC response whereas blue coloured humps depict the total PD response when the lower cone voltage was used for proanthocyanidin fragmentation in the ion source.

The MRM method excluded monomers and small oligomers from the PA quantification and mDP estimation. This may account for the lower PA contents and higher mDP values of some of the MRM results compared to the thiolysis results (Table 4.1, Figures 4.5A and E). There is indeed some evidence for this explanation because PC-rich extracts are often likely to contain more free flavan-3-ols (e.g. EC or C) than PD-rich extracts (e.g. free GC or EGC). This can also reflect the lower PC content (mg PC/g extract) correlations (R^2 = 0.75) compared to the PD content (mg PD/g extract) correlations (R^2 = 0.88) between the two methods (Figures 4.5B and C). Apparently, analysis of free flavan-3-ols is critical for the determination of mDP-values and, therefore, the correlation would probably have been improved if free flavan-3-ols had been measured in the extracts before thiolysis, especially in PC-rich PAs (Figures 4.2 and 4.3). In contrast to UV-based HPLC detection methods, where quantification is impeded due to probable co-elution of compounds, MRM methods tend to be much more selective and sensitive.

However, if the results are expressed as a percentage of PCs within PAs (mg PCs/100 mg PAs), then the thiolysis and MRM results are highly correlated (Figure 4.5D; R^2 = 0.96). This graph also reveals that the interference from free flavan-3-ols is more marked in PC-rich PAs and that PD-rich PAs presented an improved linearity.

4.3.4. Comparative and qualitative screening of sainfoin extracts by MRM fingerprints and thiolysis chromatograms

Thiolysis is often used for PA analysis since it provides quantitative information on flavan-3-ol contents, which can be used to calculate total PA content, mDP values, PC content and *cis*-flavan-3-ol content within PAs. Chromatographic separation of individual PA compounds with reversed-phase and normal-phase-HPLC methodologies is extremely challenging [49-54]. Therefore, depolymerisation of PAs is used instead to obtain information on the global flavan-3-ol composition. Several studies have investigated the impact of various reaction parameters on PA degradation and have resulted in established protocols that use phloroglucinol or BM as nucleophiles [21, 28, 33, 40, 43]. These reactions are relatively time-consuming and require a long HPLC gradient for peak resolution. In

contrast, the UPLC-ESI-MS/MS method requires just 10 min per run and thus is more suited for rapid screening of PA extracts.

The dominant constitutive flavan-3-ol units can also be evaluated qualitatively from the MRM chromatograms, which can provide interesting sainfoin fingerprints (Figure 4.8). Signals were recorded from transition states of ion pairs at *m/z* 289→245 and *m/z* 287→125 for PC terminal and extender units, respectively. The ions for PD terminal and extender units were recorded at *m/z* 305→125 and 303→125, respectively. It is apparent from the signal intensity differences that S4 contains mainly PCs, S31 mainly PDs, whereas S45 contains a mixture of PCs and PDs (Figure 4.8C, F and I). These qualitative investigations of the PA polymers were supported independently with detailed quantification of the thiolytic PA degradation products (Table 4.1). The MRM chromatograms provide information on PA composition, which is relatively easy to interpret visually. However, HPLC peaks from thiolysis cannot be interpreted as easily because of the different UV response factors and potential specificity problems (Figure 4.8A, D and G).

The MRM fingerprints provide additional information, which cannot be obtained from the thiolysis method. PAs can be distinguished not only by their PC and PD responses but also from the elution profiles of their PC or PD 'humps' in the MRM fingerprints. Due to their higher polarity PD-rich polymers tend to elute earlier from the analytical column than PC-rich polymers (Figure 4.8C and F, S31 vs S4) [29]. In particular, Figure 4.8 provides representative examples of PD-rich samples (S38, S49 and S56).

The content of extractable PAs can be assessed qualitatively from the UV chromatograms where the size of the unresolved UPLC hump is related to the amounts of total PAs in the extract (e.g. Fig 4.8B, E, H). This information is more easily obtained from the UV rather than the MRM chromatograms; the latter contain four separate PA signals that are difficult to assess visually (Figure 4.8B, E, H).

It is also possible to collect information about PA polymer sizes from the separate MRM signals for terminal and extension units across the elution profile. Samples with large PA polymers will have noticeable differences between the extension and terminal unit signals. This was apparent in the MRM chromatogram
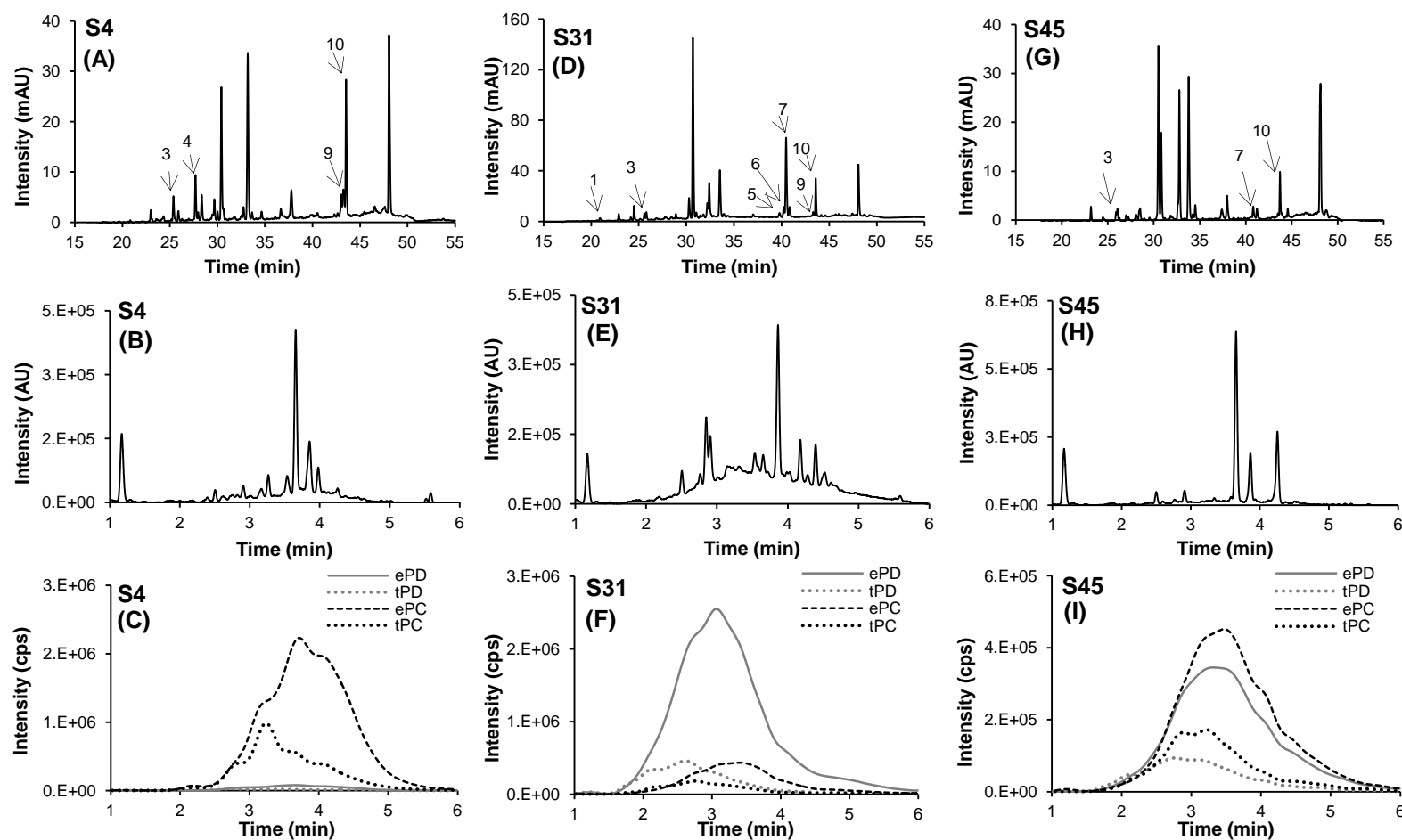
Figure 4.8: HPLC chromatograms after thiolytic degradation (A), UPLC chromatograms (B) and MRM chromatographic fingerprints (C) of sainfoin extracts S4, S31, S45. 1: gallocatechin, 2: epigallocatechin, 3: catechin, 4: epicatechin, 5: gallocatechin BM-adduct (*trans*), 6: gallocatechin BM-adduct (*cis*), 7: epigallocatechin BM-adduct, 8: catechin BM-adduct (*trans*), 9: catechin BM-adduct (*cis*), 10: epicatechin BM-adduct; Prodelphinidin extension units: ePD, prodelphinidin terminal units: tPD, procyanidin extension units: ePC and procyanidin terminal units: tPC

of S31. This extract, presented high levels of PD extension units (m/z 303→125) and low levels of PC and PD terminal units (Figure 4.8F) signifying the presence of large PA polymers across the whole elution profile. In contrast, S4 (Figure 4.8C) had smaller mDP values as shown by the relatively small difference between PA extension and terminal unit signals. This was observed especially for PAs eluting before 3.5 minutes. Another scenario is presented by the S45 extract (Figure 4.8I), which contains a relatively complex mixture of PDs and PCs. It would be more difficult to visually assess the mDP values across this MRM chromatogram. However, in comparison, it is virtually impossible to visually extract this type of information from the thiolysis chromatograms (Figure 4.8A, D, G).

Chromatographic MRM fingerprints can, to some extent, provide information on the complexity of PA mixtures [29] (Figure 4.7 and Figure 4.8). That is the special features (e.g. shoulders and broad peaks) on the PC humps which indicate that these PA mixtures contain distinct groups of smaller (S4) or larger PAs (S49) (Figure 4.7). In contrast, PD humps are generally smoother and this is typical of mixtures that contain closely related polymers which increase the PA complexity. This type of information cannot be obtained from thiolytic degradation and could be valuable when searching for plants with less complex PA mixtures. These plants might be appropriate sources for isolating PA fractions with narrower oligomer or polymer distributions. It would seem that one of the uses of such MRM fingerprints could be for a rapid evaluation of similarities or differences in PA distribution profiles within a plant collection or breeding programmes.

Engström et al. proposed that similarities between MRM chromatographic fingerprints could be used for the identification of reference PA extracts [29] that might enable inter-species quantitative analysis of PAs. In addition, diverse MRM chromatograms could reflect the differences between PA profiles of stem and leaf samples, which originated from the same sainfoin plants (Figure 4.9A). There were clear variations between the PD signal intensity and distribution profiles between the two organs. In contrast, the PC humps for terminal and extension units were proven to be very similar in shape between plant parts, albeit leaf extract generated lower response for PC terminal and extension units than the stem extract (Figure 4.9A). Previous research supports the fact that leaves had more PDs and higher PA contents than stems [25, 55].
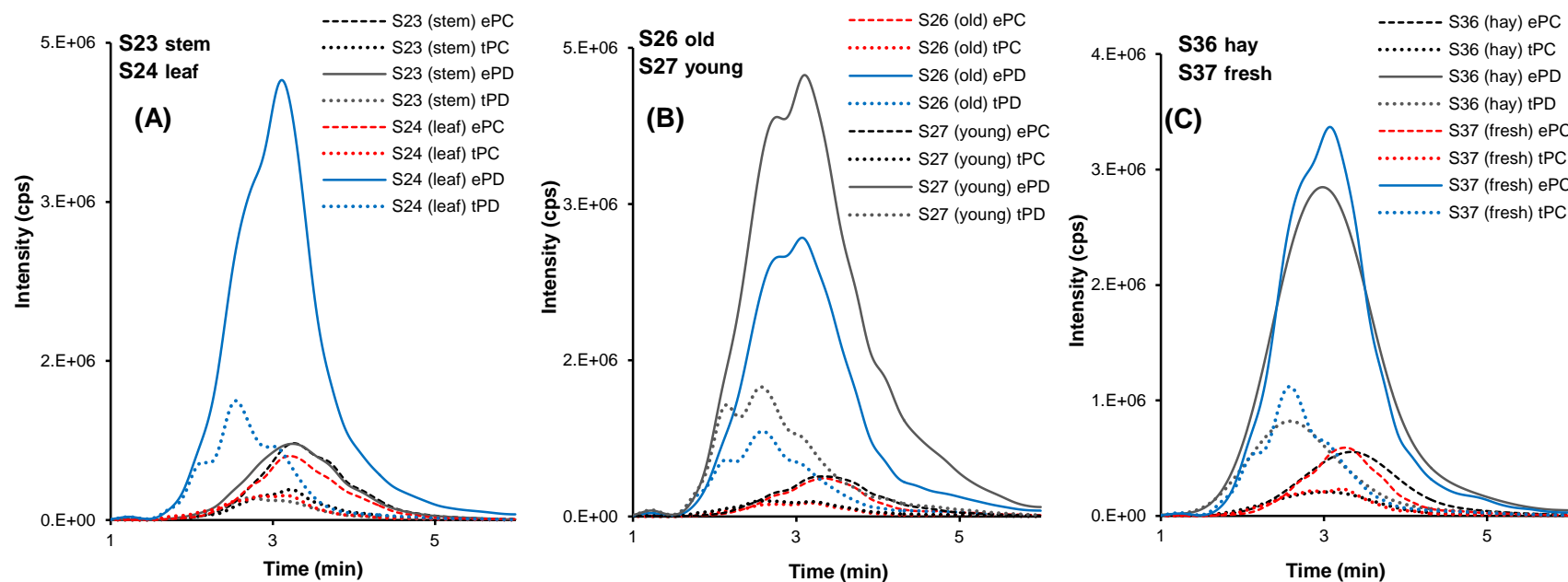
Figure 4.9: Multiple reaction monitoring chromatograms could depict the influence of plant part (A), age of harvest (B) and sample processing (C) on proanthocyanidin profiles. The compared pairs of extracts have derived from the same individual plant (for extract identities see Table 4.1). Stem and leaf signify the sampling plant part, young and old signify the plant age of the sample, hay and fresh signify the difference in processing method. Prodelphinidin extension units: ePD, prodelphinidin terminal units: tPD, procyanidin extension units: ePC and procyanidin terminal units: tPC.

It can also be observed that the mDP values differ greatly between stems and leaves.

In the same principle of PA fingerprint comparisons, MRM chromatograms could illustrate also the possible impact of leaf age on PA content and composition. The influence of sainfoin leaf age on PA content and structures, in terms of mDP, PC content and *cis*-flavan-3-ol content, has been studied previously [21, 24]. In general, PA content in extracts tended to decrease with leaf maturity [21], although some variations have also been reported with extractable and unextractable PAs [24]. Figure 4.9B shows MRM fingerprints of PA extracts from old (S26) and young (S27) leaves from the same plant. It can be observed that hump pairs (old-young) were very similar in shape, for the PC and PD terminal and extension units. However, variance was spotted in intensities of PD terminal units and extension units. These signal differences are reflected to lower PA contents and suggested a little change in mDP values in old compared to young sainfoin leaves. Quantification by thiolysis and UPLC-ESI-MS/MS analysis (Tables 4.1) confirmed these observations since the old leaf extract (S26) had lower PA content value than the young leaf extract (S27). In addition, thiolysis, UPLC-ESI-MS/MS results and MRM chromatograms suggested that leaf age in accession CPI 63750 caused a negligible change on mDP and PA distribution of extension and terminal flavan-3-ols. It has been reported that preservation methods (i.e. drying and ensiling) can alter the PA quantity and composition in sainfoin [15, 55]. These differences can be easily spotted by a rapid qualitative comparison of the MRM chromatograms of extracts from hay (S36) and fresh (S37) samples from the same plant (Figure 4.9C). The humps of PD extension and terminal units, in the fresh sample, presented distinct features. On the contrary the PC and PD humps of the hay sample presented a relatively smoother shape and a dissimilar elution order. Determination of PC percentages within total PAs (mg PCs/100 mg PAs) with thiolysis and UPCL-ESI-MS/MS resulted in similar values (Table 4.1). Flavan-3-ol quantification from thiolysis and PA distribution profiles of MRM chromatograms identified the impact of processing to PA composition and distinguished the samples on that basis.

4.4. Conclusions

Screening of sainfoin polyphenol extracts with thiolysis-HPLC and UPLC-ESI-MS/MS methods confirmed that PA contents and compositions are characterised by a vast diversity among accessions and plant parts. The two methods gave significant positive correlations for PA content (mg/g extract), PD content within PAs (mg PDs/100 mg PAs) and mDP values. Sainfoin stems contained low amounts of PAs that consisted mainly of PCs. In contrast, leaf samples had higher PA contents (mg/g extract), large mDP values and high PD contents. There were good correlations between the two methods for PA content and PC percentages within PAs. UPLC-ESI-MS/MS revealed that free flavan-3-ol monomers were present in sainfoin extracts and this finding may have been responsible for the weak correlation between the mDP values obtained by the two methods. The LoA computed with Bland-Altman plots suggested that the two methods could be used interchangeably in breeding programmes and ranking of samples according to contrasting PA contents and structural characteristics. In case, PA values would be used in bioassays and animal feeding trials, the low LoA would suggest a more critical interpretation of the results.

The recording of selected ion pairs from terminal and extension PA units by MRM enhanced the selectivity and quantification of the UPLC-ESI-MS/MS method. Additional information from the MRM chromatograms produced accession 'fingerprints' or profiles for qualitative comparisons in terms of PA content, PC/PD patterns and approximate differences of mDP values. Accessions could be clearly distinguished by the distribution profiles of different polymers as they eluted from the UPLC column. On that basis, the impact of growth stage, sample processing and plant part on extractable PAs can be assessed within 10 minutes and can complement the individual flavan-3-ol quantification by thiolysis. The UPLC-ESI-MS/MS method is much faster than thiolysis and suitable for the rapid characterisation and for the ranking of extractable PAs. This is likely to prove useful for plant breeding programmes that generate large numbers of plants, require fast screening tools and seek to optimise PA traits, such as PA contents and PCs or PDs. For a selected subset of accession crosses, thiolysis could then

be used to obtain detailed information on the *cis*/*trans* flavan-3-ol isomers in terminal and extension units.

References

1. Hayot Carbonero C, Mueller-Harvey I, Brown TA, Smith L: **Sainfoin (*Onobrychis viciifolia*): A beneficial forage legume.** *Plant Genetic Resources* 2011, 9(01):70-85.

2. Waghorn G: **Beneficial and detrimental effects of dietary condensed tannins for sustainable sheep and goat production-Progress and challenges.** *Animal Feed Science and Technology* 2008, 147(1-3):116-139.

3. Broderick GA: **Desirable characteristics of forage legumes for improving protein utilization in ruminants.** *Journal of Animal Science* 1995, 73(9):2760-2773.

4. Chung YH, Mc Geough EJ, Acharya S, McAllister TA, McGinn SM, Harstad OM, Beauchemin KA: **Enteric methane emission, diet digestibility, and nitrogen excretion from beef heifers fed sainfoin or alfalfa.** *Journal of Animal Science* 2013, 91(10):4861-4874.

5. Waghorn G, Jones W, Shelton I, McNabb W: **Condensed tannins and the nutritive value of herbage.** In: *Proceedings of the New Zealand Grassland Association* 1990: 171-176.

6. Mueller-Harvey I: **Unravelling the conundrum of tannins in animal nutrition and health.** *Journal of the Science of Food and Agriculture* 2006, 86(13):2010-2037.

7. Makkar HPS: **Effects and fate of tannins in ruminant animals, adaptation to tannins, and strategies to overcome detrimental effects of feeding tannin-rich feeds.** *Small Ruminant Research* 2003, 49(3):241-256.

8. Piluzza G, Sulas L, Bullitta S: **Tannins in forage plants and their role in animal husbandry and environmental sustainability: A review.** *Grass and Forage Science* 2014, 69(1):32-48.

9. McMahon LR, Majak W, McAllister TA, Hall JW, Jones GA, Popp JD, Cheng KJ: **Effect of sainfoin on *in vitro* digestion of fresh alfalfa and bloat in steers.** *Canadian Journal of Animal Science* 1999, 79(2):203-212.

10. Hoste H, Jackson F, Athanasiadou S, Thamsborg SM, Hoskin SO: **The effects of tannin-rich plants on parasitic nematodes in ruminants.** *Trends in Parasitology* 2006, 22(6):253-261.

11. Novobilsky A, Stringano E, Hayot Carbonero C, Smith LM, Enemark HL, Mueller-Harvey I, Thamsborg SM: ***In vitro* effects of extracts and purified tannins of sainfoin (*Onobrychis viciifolia*) against two cattle nematodes.** *Veterinary Parasitology* 2013, 196(3-4):532-537.

12. Paolini V, De La Farge F, Prevot F, Dorchies P, Hoste H: **Effects of the repeated distribution of sainfoin hay on the resistance and the resilience of goats naturally infected with gastrointestinal nematodes.** *Veterinary Parasitology* 2005, 127(3-4):277-283.

13. Theodoridou K, Aufrère J, Andueza D, Le Morvan A, Picard F, Pourrat J, Baumont R: **Effects of condensed tannins in wrapped silage bales of sainfoin (*Onobrychis viciifolia*) on *in vivo* and *in situ* digestion in sheep.** *Animal : An International Journal of Animal Bioscience* 2012, 6(02):245-253.

14. Theodoridou K, Aufrere J, Andueza D, Pourrat J, Le Morvan A, Stringano E, Mueller-Harvey I, Baumont R: **Effects of condensed tannins in fresh sainfoin (*Onobrychis viciifolia*) on *in vivo* and *in situ* digestion in sheep.** *Animal Feed Science and Technology* 2010, 160(1-2):23-38.

15. Lorenz MM, Eriksson T, Uden P: **Effect of wilting, silage additive, PEG treatment and tannin content on the distribution of N between different fractions after ensiling of three different sainfoin (*Onobrychis viciifolia*) varieties.** *Grass and Forage Science* 2010, 65(2):175-184.

16. Hatew B, Hayot Carbonero C, Stringano E, Sales LF, Smith LMJ, Mueller-Harvey I, Hendriks WH, Pellikaan WF: **Diversity of condensed tannin structures affects rumenin vitromethane production in sainfoin (*Onobrychis viciifolia*) accessions.** *Grass and Forage Science* 2015, 70(3):474-490.

17. Min BR, Barry TN, Attwood GT, McNabb WC: **The effect of condensed tannins on the nutrition and health of ruminants fed fresh temperate forages: A review.** *Animal Feed Science and Technology* 2003, 106(1-4):3-19.

18. Heckendorn F, Haring DA, Maurer V, Zinsstag J, Langhans W, Hertzberg H: **Effect of sainfoin (*Onobrychis viciifolia*) silage and hay on established populations of *Haemonchus contortus* and *Cooperia curticei* in lambs.** *Veterinary Parasitology* 2006, 142(3-4):293-300.

19. Hoste H, Gaillard L, Le Frileux Y: **Consequences of the regular distribution of sainfoin hay on gastrointestinal parasitism with nematodes and milk production in dairy goats.** *Small Ruminant Research* 2005, 59(2-3):265-271.

20. Patra AK, Saxena J: **A new perspective on the use of plant secondary metabolites to inhibit methanogenesis in the rumen.** *Phytochemistry* 2010, 71(11–12):1198-1222.

21. Koupai-Abyazani MR, McCallum J, Muir AD, Bohm BA, Towers GHN, Gruber MY: **Developmental changes in the composition of proanthocyanidins from leaves of sainfoin (*Onobrychis viciifolia* Scop.) as determined by HPLC analysis.** *Journal of Agricultural and Food Chemistry* 1993, 41(7):1066-1070.

22. Koupai-Abyazani MR, Muir AD, Bohm BA, Towers GHN, Gruber MY: **The proanthocyanidin polymers in some species of *Onobrychis*.** *Phytochemistry* 1993, 34(1):113-117.

23. Stringano E, Cramer R, Hayes W, Smith C, Gibson T, Mueller-Harvey I: **Deciphering the complexity of sainfoin (*Onobrychis viciifolia*) proanthocyanidins by MALDI-TOF mass spectrometry with a judicious choice of isotope patterns and matrixes.** *Analytical Chemistry* 2011, 83(11):4147-4153.

24. Theodoridou K, Aufrere J, Andueza D, Le Morvan A, Picard F, Stringano E, Pourrat J, Mueller-Harvey I, Baumont R: **Effect of plant development during first and second growth cycle on chemical composition, condensed tannins and nutritive value of three sainfoin (*Onobrychis viciifolia*) varieties and lucerne.** *Grass and Forage Science* 2011, 66(3):402-414.

25. Regos I, Urbanella A, Treutter D: **Identification and quantification of phenolic compounds from the forage legume sainfoin (*Onobrychis viciifolia*).** *Journal of Agricultural and Food Chemistry* 2009, 57(13):5843-5852.

26. Hummer W, Schreier P: **Analysis of proanthocyanidins.** *Molecular Nutrition & Food Research* 2008, 52(12):1381-1398.

27. Novobilsky A, Mueller-Harvey I, Thamsborg SM: **Condensed tannins act against cattle nematodes.** *Veterinary Parasitology* 2011, 182(2-4):213-220.

28. Gea A, Stringano E, Brown RH, Mueller-Harvey I: *In situ* **analysis and structural elucidation of sainfoin (*Onobrychis viciifolia*) tannins for high-throughput germplasm screening.** *Journal of Agricultural and Food Chemistry* 2011, 59(2):495-503.

29. Engstrom MT, Palijarvi M, Fryganas C, Grabber JH, Mueller-Harvey I, Salminen JP: **Rapid qualitative and quantitative analyses of proanthocyanidin oligomers and polymers by UPLC-MS/MS.** *Journal of Agricultural and Food Chemistry* 2014, 62(15):3390-3399.

30. Bland JM, Altman DG: **Measuring agreement in method comparison studies.** *Statistical Methods in Medical Research* 1999, 8(2):135-160.

31. Carstensen B: **Comparing methods of measurement: Extending the LoA by regression.** *Staistics in Medicine* 2010, 29(3):401-410.

32. Stringano E, Hayot Carbonero C, Smith LM, Brown RH, Mueller-Harvey I: **Proanthocyanidin diversity in the EU 'HealthyHay' sainfoin (*Onobrychis viciifolia*) germplasm collection.** *Phytochemistry* 2012, 77:197-208.

33. Marais JP, Mueller-Harvey I, Brandt EV, Ferreira D: **Polyphenols, condensed tannins, and other natural products in *Onobrychis viciifolia* (sainfoin).** *Journal of Agricultural and Food Chemistry* 2000, 48(8):3440-3447.

34. Thill J, Regos I, Farag MA, Ahmad AF, Kusek J, Castro A, Schlangen K, Carbonero CH, Gadjev IZ, Smith LM *et al*: **Polyphenol metabolism provides a screening tool for beneficial effects of *Onobrychis viciifolia* (sainfoin).** *Phytochemistry* 2012, 82:67-80.

35. Czochanska Z, Foo LY, Newman RH, Porter LJ: **Polymeric proanthocyanidins - stereochemistry, structural units, and molecular-weight.** *Journal of Chemical Society - Perkin Transactions 1* 1980(10):2278-2286.

36. Cavaliere C, Foglia P, Gubbiotti R, Sacchetti P, Samperi R, Lagana A: **Rapid-resolution liquid chromatography/mass spectrometry for determination and quantitation of polyphenols in grape berries.** *Rapid Communications in Mass Spectrometry : RCM* 2008, 22(20):3089-3099.

37. Fraser K, Harrison SJ, Lane GA, Otter DE, Hemar Y, Quek SY, Rasmussen S: **HPLC-MS/MS profiling of proanthocyanidins in teas: A comparative study.** *Journal of Food Composition and Analysis* 2012, 26(1-2):43-51.

38. Ortega N, Macia A, Romero MP, Trullols E, Morello JR, Angles N, Motilva MJ: **Rapid determination of phenolic compounds and alkaloids of carob flour by improved liquid chromatography tandem mass spectrometry.** *Journal of Agricultural and Food Chemistry* 2009, 57(16):7239-7244.

39. Saenz-Navajas MP, Ferreira V, Dizy M, Fernandez-Zurbano P: **Characterization of taste-active fractions in red wine combining HPLC fractionation, sensory analysis and ultra performance liquid chromatography coupled with mass spectrometry detection.** *Analytica Chimica Acta* 2010, 673(2):151-159.

40. Guyot S, Doco T, Souquet JM, Moutounet M, Drilleau JF: **Characterization of highly polymerized procyanidins in cider apple (*Malus sylvestris* var Kermerrien) skin and pulp.** *Phytochemistry* 1997, 44(2):351-357.

41. Cooper KA, Campos-Gimenez E, Alvarez DJ, Nagy K, Donovan JL, Williamson G: **Rapid reversed phase ultra-performance liquid chromatography analysis of the major cocoa polyphenols and inter-relationships of their concentrations in chocolate.** *Journal of Agricultural and Food Chemistry* 2007, 55(8):2841-2847.

42. Grabber JH, Zeller WE, Mueller-Harvey I: **Acetone enhances the direct analysis of procyanidin- and prodelphinidin-based condensed tannins in *Lotus* species by the butanol-HCl-iron assay.** *Journal of Agricultural and Food Chemistry* 2013, 61(11):2669-2678.

43. Gu L, Kelm M, Hammerstone JF, Beecher G, Cunningham D, Vannozzi S, Prior RL: **Fractionation of polymeric procyanidins from lowbush blueberry and quantification of procyanidins in selected foods with an optimized normal-phase HPLC-MS fluorescent detection method.** *Journal of Agricultural and Food Chemistry* 2002, 50(17):4852-4860.

44. Bartolome B, Monagas M, Garrido I, Gomez-Cordoves C, Martin-Alvarez PJ, Lebron-Aguilar R, Urpi-Sarda M, Llorach R, Andres-Lacueva C: **Almond (*Prunus dulcis* (Mill.) D.A. Webb) polyphenols: From chemical characterization to targeted analysis of phenolic metabolites in humans.** *Archives of Biochemistry and Biophysics* 2010, 501(1):124-133.

45. Kelm MA, Johnson JC, Robbins RJ, Hammerstone JF, Schmitz HH: **High-performance liquid chromatography separation and purification of cacao (*Theobroma cacao* L.) procyanidins according to degree of polymerization using a diol stationary phase.** *Journal of Agricultural and Food Chemistry* 2006, 54(5):1571-1576.

46. Sivakumaran S, Molan AL, Meagher LP, Kolb B, Foo LY, Lane GA, Attwood GA, Fraser K, Tavendale M: **Variation in antimicrobial action of proanthocyanidins from *Dorycnium rectum* against rumen bacteria.** *Phytochemistry* 2004, 65(17):2485-2497.

47. Gu L, Kelm MA, Hammerstone JF, Beecher G, Holden J, Haytowitz D, Prior RL: **Screening of foods containing proanthocyanidins and their structural characterization using LC-MS/MS and thiolytic degradation.** *Journal of Agricultural and Food Chemistry* 2003, 51(25):7513-7521.

48. Koupai-Abyazani MR, McCallum J, Bohm BA: **Identification of the constituent flavanoid units in sainfoin proanthocyanidins by reversed-phase high-performance liquid chromatography.** *Journal of Chromatography A* 1992, 594(1-2):117-123.

49. Adamson GE, Lazarus SA, Mitchell AE, Prior RL, Cao G, Jacobs PH, Kremers BG, Hammerstone JF, Rucker RB, Ritter KA *et al*: **HPLC method for the quantification of procyanidins in cocoa and chocolate samples and correlation to total antioxidant capacity.** *Journal of Agricultural and Food Chemistry* 1999, 47(10):4184-4188.

50. de Pascual-Teresa S, Santos-Buelga C, Rivas-Gonzalo JC: **Quantitative analysis of flavan-3-ols in Spanish foodstuffs and beverages.** *Journal of Agricultural and Food Chemistry* 2000, 48(11):5331-5337.

51. Guyot S, Marnet N, Drilleau J: **Thiolysis-HPLC characterization of apple procyanidins covering a large range of polymerization states.** *Journal of Agricultural and Food Chemistry* 2001, 49(1):14-20.

52. Hammerstone JF, Lazarus SA, Mitchell AE, Rucker R, Schmitz HH: **Identification of procyanidins in cocoa (*Theobroma cacao*) and chocolate using high-performance liquid chromatography mass spectrometry.** *Journal of Agricultural and Food Chemistry* 1999, 47(2):490-496.

53. Karonen M, Hamalainen M, Nieminen R, Klika KD, Loponen J, Ovcharenko VV, Moilanen E, Pihlaja K: **Phenolic extractives from the bark of *Pinus sylvestris* L. and their effects on inflammatory mediators nitric oxide and prostaglandin E2.** *Journal of Agricultural and Food Chemistry* 2004, 52(25):7532-7540.

54. Karonen M, Loponen J, Ossipov V, Pihlaja K: **Analysis of procyanidins in pine bark with reversed-phase and normal-phase high-performance liquid chromatography-electrospray ionization mass spectrometry.** *Analytica Chimica Acta* 2004, 522(1):105-112.

55. Wang YX, McAllister TA, Acharya S: **Condensed tannins in sainfoin: Composition, concentration, and effects on nutritive and feeding value of sainfoin forage.** *Crop Science* 2015, 55(1):13-22.

Chapter 5. Linking contrasting proanthocyanidin structures to *in vitro* anthelmintic activity of *Haemonchus contortus*

5.1 Introduction

During the last decades, gastrointestinal nematodes (GINs) have been identified as one of the most serious threats to livestock, causing anaemia, anorexia, inefficient digestion of nutrients and other parasitic diseases [1, 2]. For many years, synthetic chemical drugs were used to prevent parasitism in animal production [3]. However, the long term administration of these drugs has generated widespread resistance amongst parasitic nematodes [3]. Moreover, high doses can lead to drug residues in the animal products and can constitute a food safety hazard. Therefore, legislators have developed regulations that govern anthelmintic (AH) uses and consumers, nowadays, demand more sustainable and eco-friendly animal husbandry practices [1, 2, 4]. These reasons command the substitution of drug-based helminth control with sustainable alternatives. The use of bioactive forages, with AH properties, has been proposed and its efficacy is currently being investigated [5-8].

The potency of bioactive forages to mitigate parasitism is associated with the presence of proanthocyanidins (PAs) and other secondary metabolites that are abundant in some plants [1, 2, 9]. Several studies have used PA-containing feeds to manage GIN burdens as PAs can have an impact on various GIN life-cycle stages [8, 10-14]. Other attempts focused on *in vitro* assays that tested the efficacy of crude plant extracts or purified fractions of PAs [8, 15-18]. Despite the promising contribution that PAs can make to AH activity, especially in *in vitro* assessments, questions remain concerning their modes of action [3, 9].

PAs occur naturally in many plants in the form of structurally diverse and complex polymeric mixtures [3, 9]. The most important PA structural traits for AH activity appear to be: i) the constitutive flavan-3-ol subunits, especially the presence of prodelphinidins (PDs) [17, 19-23] ii) a high mean degree of polymerisation (mDP), iii) possibly the proportion of *cis* and *trans* monomeric subunits within PAs [20] and interflavanyl linkages (A- vs B-type PAs), and iv) the presence of galloyl groups in PAs [19, 22-24]. Williams et al. reported that cinnamon A-type PAs had similar AH activity to B-type PAs against the swine nematode *Ascaris suum* [25]. There is some evidence that traits can also differ in their efficacies across the various GIN life-cycle stages [20, 26, 27]. In addition, plant extracts often contain substantial amounts of other bioactive plant secondary

metabolites (such as flavonoids) which have been associated to synergistic or antagonistic effects along with PAs [28-30].

Considering what was already mentioned above, it can be concluded that there is a need to establish the fundamental relationships between a structural PA trait and a key life-cycle stage of a specific GIN. Thus, this study focussed on narrowing down the PA parameters that contribute to bioactivity. *Haemonchus contortus* is one of the most deleterious GINs, and therefore it was selected as an experimental model. The evaluation of PA potency against *H. contortus* was evaluated with the *in vitro* Larval Exsheathment Inhibition Assay (LEIA) [16, 17, 31]. The LEIA has been widely used to examine AH activity of flavan-3-ols and PA samples. Moreover, it has proven to be sensitive, reproducible and relevant to *in vivo* processes [32, 33].

Plant samples consisting largely of procyanidins (PCs) or prodelphinidins (PDs) or selected combinations were chosen to critically assess the role of PA structures in the inhibition of *H. contortus* L3 exsheathment. Extracts and partially purified PAs from these plants have already presented *in vitro* anti-parasitic action against *Haemoncus contortus*, *Trichostrongulus colubriformis*, *Oesophagostomum dentatum*, *Ascaris suum*, *Cooperia oncophora*, *Ostertagia ostertagi* and *Hymenolepis diminuta* [16, 17, 20, 26, 34]. However, the optimum PA polymer size for AH activity has remained elusive. Preliminary results showed that it is possible to generate highly pure and well-defined PA sub-fractions with increasing mDP values using semi-preparative reverse-phase (RP) - HPLC. Thus, it was hypothesised that extensive PA purification and sub-fractionation of homo-polymeric PAs (PCs vs PDs) would contribute to:

i) elucidate the relationship between AH activity and mDP values
ii) exploit the diversity in polarities of PA mixtures to obtain sub-fractions by HPLC, with closely related structures, and hence probe their AH potency
iii) the removing of other compounds, which may also have AH activity and may be present in PA samples, after purification procedures

The sub-fractions were characterised with a novel UPLC-DAD-ESI-MS/MS method, which generated information on mDP values and PC/PD contents. It was

hoped that these well-characterised PA sub-fractions would shed light on the structural features that contribute the most in the exsheathment inhibition of *H. contortus* L3 *in vitro*.

5.2   Materials and Methods

5.2.1   Plant samples

Black currant (*Ribes nigrum*) leaves were collected from Hildred PYO farm (Goring-on-Thames, UK) and weeping willow (*Salix babylonica*) catkins from Evesham Road, Emmer Green, UK. Pine tree inner bark (*Pinus sylvestris*) was supplied by Dr Maarit Karonen (University of Turku, Finland). Tilia (*Tilia* x *Europaea*) flowers were purchased from Flos (Mokrsko, Poland). Sainfoin (*Onobrychis viciifolia*, Esparcette var.) was collected from Barham, Kent, UK. Samples were lyophilised or air-dried and subsequently ground to pass through a 1 mm sieve.

5.2.2   Chemicals and reagents

Acetonitrile (HPLC grade) was purchased from Fisher Scientific (Loughborough, UK) and Sigma-Aldrich (Steinheim, Germany). Hydrochloric acid (37%, analytical reagent grade), acetic acid glacial (analytical reagent grade), acetone and methanol (HPLC grade) were supplied by Fisher Scientific (Loughborough, UK). Benzyl mercaptan (BM) was obtained from Sigma-Aldrich (Poole, UK) and (±) – dihydroquercetin (98%) from Apin Chemicals (Abingdon, UK). Catechin was from Sigma (Sigma Chemical Co., St. Louis, MO, USA). Phosphate buffer saline (PBS) was from Biomérieux (Marcy l'Etoile, France) and Sephadex[TM] LH-20 from GE Healthcare (Little Chalfont, UK). Water purification was performed with a Millipore Synergy water purification system (Merck KGaA, Darmstadt, Germany) and a Milli-Q system (Millipore, Watford, UK).

5.2.3   Proanthocyanidin extraction and purification

Extraction and purification of PAs followed the procedure described in Chapter 3. In brief, finely ground plant tissue (50 g) was weighed into a conical

flask. Acetone/water (500 ml, 8:2 v/v) was added and the mixture was vigorously stirred for 1 h. The mixture was filtered under vacuum. The filtrate was further extracted with dichloromethane (250 ml) to remove lipids and chlorophyll. Polyphenols were concentrated in the aqueous phase with a rotary evaporator (T<37.5 °C). This crude extract was diluted in deionised water (2 l) and filtered under vacuum. The filtrate was loaded on a large Sephadex^{TM} LH-20 column. The column was washed with deionised water (2 l) to wash off sugars and small phenolics while PAs were retained on the resin. Gravity elution with acetone/water (3:7, 1:1 and 8:2 v/v) yielded 3 partially purified PA fractions from each plant source. The organic solvent was removed using a rotary evaporator (T<37.5 °C). Fractions containing the PAs were frozen, freeze-dried and stored at -20 °C.

The PA fractions that were collected after the second acetone/water elution step (1:1 v/v), from Sephadex^{TM} LH-20, were subjected to further purification using a semi-preparative HPLC-DAD system. The HPLC-DAD system consisted of a Waters Delta 600 Liquid Chromatograph, a Waters 600 Controller, a Waters 2998 Photodiode Array Detector and a Waters Fraction Collector III. The column was a Gemini C18 column (150 × 21.2 mm, 10 μm, Phenomenex) and the eluents were 0.1% formic acid and acetonitrile. The gradient used was as follows: 0–5 min, 0% B in A; 5–75 min, 0–50% B in A; 75–85 min, 50–70% B in A. The flow rate was 10 ml/min and the sparge rate for the helium flow 100 ml/min. The injection volume was 5 ml and PA concentration ranged from 44 to 50 mg/ml. The photodiode array detector was operating between 190−500 nm, and PAs were detected at 280 nm. All steps in the preparative and semi-preparative purifications were followed by UPLC-DAD-ESI-MS/MS analysis [35]. Closely related fractions were combined to generate sufficient quantities of PA sub-fractions as shown in Figure 5.1, these were concentrated to the water-phase and freeze-dried.

5.2.4 Thiolysis of Sephadex^{TM} LH-20 eluted PAs

Thiolysis reactions on partially purified PA fractions were performed according to Novobilský et al. [7] and as described in Chapter 2. Briefly, PA fraction (4 mg) was weighed into a 10 ml screw-capped vial, dissolved in methanol (1.5 ml) and acidified with HCl (0.5 ml, 3.3% in methanol, v/v). The addition of benzyl mercaptan followed (50 μl) and the reaction mixture was stirred at 40 °C for

1 h. The reaction was ceased by adding ultrapure water (2.5 ml) to the mixtures at room temperature.

5.2.5 HPLC-DAD analysis of thiolysis reaction products

The analysis and quantification of thiolysis reaction products followed the procedures as described by Gea et al. [36] and operating conditions and parameters of HPLC analysis were set as in Williams et al. [20].

5.2.6 UPLC-DAD-ESI-MS/MS analysis of purified PA sub-fractions

After semi-preparative HPLC purification, the determination of mDP values and PC/PD contents of sub-fractions was performed with a UPLC-DAD-ESI-MS/MS method according to Engström et al. [35].

5.2.7 Gastrointestinal nematodes

The recovery of the third-stage larvae (L3) from faecal samples of domesticated donor goats infected monospecifically with AH susceptible strains of *Haemonchus contortus* and their maintenance was carried out as described in Quijada et al. [17]. Larvae concentration of each flask was 1000-1500 L3/ml. At the start of each day, the L3 larvae were examined microscopically to ensure that they were mobile and ensheathed (> 90%) [17].

5.2.8 Larval exsheathment inhibition assay

The capacity of the various PA sub-fractions to inhibit the exsheathment process of L3 larvae was evaluated with the larval exsheathement inhibition assay (LEIA). The experimental procedure was according to Bahuaud et al. [37]. The larvae used for the *in vitro* assays were 2 months old.

A series of dilutions in phosphate buffered saline (PBS, 0.1 M phosphate, 0.05 M NaCl, pH 7.2), for each PA sub-fraction, was prepared at concentrations 600, 300, 150, 75 and 37.5 µg/ml. An aliquot of 1000 larvae in PBS was added to each of the PA solutions. Negative controls (L3 in PBS) were included in each experiment and assessed in parallel. Current AH drugs do not target the

exsheathment process without killing the larvae. Therefore, it was impossible to use a conventional drug as a positive control.

The larvae were incubated with the PA solutions for 3 h under periodic shaking at 20 °C. After incubation, larvae were centrifuged and washed (3x) with PBS. Subsequently larvae were subjected to a controlled exsheathment process by applying sodium hypochlorite (2% w/v) and sodium chloride (16.5% w/v), which had been diluted in PBS. The exsheathment kinetics was assessed in 4 replicates of each PA concentration in 4 time intervals (0, 20, 40, 60 min) by calculating the proportion of the exsheathed larvae after microscopic investigation. The exsheathment percentage was calculated according to the formula:

$$\%Exsheathment = \frac{(number\ of\ exsheathed\ larvae)}{(number\ of\ exsheathed\ larvae\ +\ number\ of\ ensheathed\ larvae)} \times 100$$

5.2.9 Statistical analyses

The calculation of the EC_{50} value (effective concentration that inhibits the exsheathment by 50% in µg/ml) for each PA sub-fraction was performed at 40 or 60 min using the Pobit PoloPlus® software. Initially, the relationship between structural traits (mDP and PC/PD contents) was evaluated and then the *in vitro* AH activity was correlated to structural traits, using a pairwise Spearman nonparametric correlation. This statistical analysis was performed with Systat® 9 software (SPSS Ltd).

5.3 Results and discussion

5.3.1 Chemical characterisation of proanthocyanidins in fractions and sub-fractions and relationships between structural parameters

Extensive PA purification and sub-fractionation yielded a total of 38 sub-fractions; 6 sub-fractions from pine bark; 10 sub-fractions, from Tilia; 8 sub-fractions from weeping willow; 8 sub-fractions from sainfoin and 6 sub-fractions from black currant (Figure 5.1). Sufficient quantities of purified PAs were collected from 32 sub-fractions for AH activity tests against L3 larvae of *H. contortus*. An additional sample for each PA source was generated by combining a small

amount (10% of total yield, w/w) from each sub-fraction in order to prepare an artificial mixture of PAs.
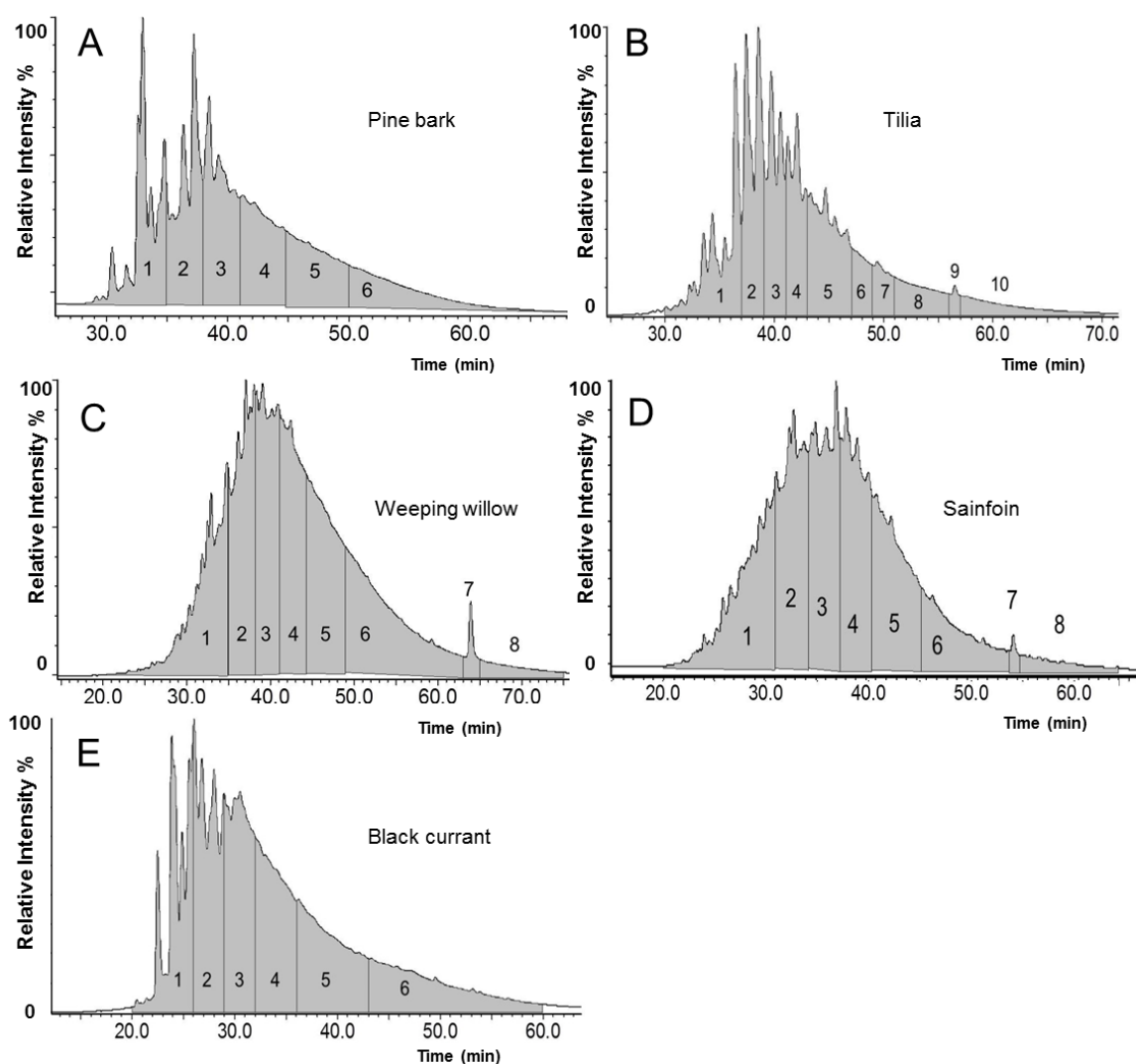
Figure 5.1: UV chromatograms (280 nm) obtained from semi-preparative reverse-phase HPLC of Sephadex[TM] LH-20 fractions (see Table 5.1) from A: Pine bark, B: Tilia, C: Weeping willow, D: Sainfoin and E: Black currant. The numbers in the individual chromatograms denote the time-slices for the PA sub-fractions. Flavonoid impurities were detected, but not identified, in fractions B9, C7 and D7 by UPLC-DAD-ESI-MS/MS

5.3.1.1 Sephadex[TM] LH-20 fractions

Thiolysis of PAs in the fractions that eluted from the Sephadex[TM] LH-20 column with acetone/water (1:1 v/v) and subsequent HPLC analysis of the reaction products provided information on PA content (mg/g fraction), mDP, PC and *cis*-flavan-3-ol contents in total PAs (Table 5.1). The PA content ranged from 611 (weeping willow) to 945 mg/g fraction (sainfoin); mDP values ranged from 6.15

(pine bark) to 10.4 (sainfoin); PC contents within PAs ranged from 5.37 mg PCs/100 mg PAs in black currant to 98.0 mg PCs/100 mg PAs in Tilia and finally, the *cis*-flavan-3-ol percentages ranged from 12.1 mg *cis*-flavan-3-ols/100 mg PAs in black currant to 94.0 mg *cis*-flavan-3-ols/100 mg PAs in Tilia. The PA fractions consisted of two PC-rich samples (pine bark and Tilia), two contrasting PC/PD mixtures (sainfoin and weeping willow) and one PD-rich sample (black currant) (Table 5.1). The flavan-3-ol composition of PA terminal and extension units was very diverse (Table 5.2). The PC-rich fractions differed mostly in their terminal units. Pine bark had mostly catechin (C) (89.4 mg/g fraction) whereas Tilia had mostly epicatechin (EC) (81.7 mg/g fraction). Weeping willow terminal units contained mostly C (34.9 mg/g fraction) and EC (28.2 mg/g fraction) but sainfoin contained comparable amounts of C, EC, gallocatechin (GC) and epigallocatechin (EC) (~20 mg/g fraction). The extension parts of pine bark, Tilia and weeping willow contained mostly EC (462, 518, 265 mg/g fraction respectively) whereas sainfoin contained EGC (482 mg/g fraction) and black currant contained GC (614 mg/g fraction).

These findings suggested a large diversity of PA characteristics. Therefore, it was hypothesised that this particular sample set would facilitate the elucidation structure-activity relationships.

Table 5.1: Proanthocyanidin (PA) content and composition of Sephadex LH-20 fractions that were eluted with acetone/water (1:1 v/v) and analysed by thiolytic degradation; Standard deviation in brackets (*n=2*); PC: procyanidin; PD (mg PDs/100 mg PAs) = 100 - PC; *trans* (mg *trans*-flavan-3-ols/100 mg total flavan-3-ols) = 100 - *cis*

Plant source	PA content (mg/g fraction)	mDP	PC (mg PCs/100 mg PAs)	*cis* (mg *cis*/100 mg PAs)
Scots pine bark (*Pinus sylvestris*)	621 (17.4)	6.15 (0.000)	96.9 (0.315)	77.9 (0.046)
Tilia flowers (*Tilia* x *europaea*)	649 (1.51)	6.63 (0.078)	98.0 (0.249)	94.0 (0.072)
Weeping willow catkins (*Salix babylonica*)	611 (12.6)	8.71 (0.170)	68.9 (0.856)	68.2 (0.295)
Sainfoin whole plant (*Onobrychis viciifolia*)	945 (7.41)	10.4 (0.566)	34.3 (1.30)	81.6 (0.053)
Black currant leaves (*Ribes nigrum*)	830 (17.6)	6.90 (0.028)	5.37 (0.107)	12.0 (0.296)

Table 5.2: Flavan-3-ol content of proanthocyanidins (mg/g fraction) in Sephadex™ LH-20 fractions (see Table 5.1); GC: gallocatechin, EGC: epigallocatechin, C: catechin, EC: epicatechin; Standard deviation in brackets (*n=2*); nd: not detected

Plant source	GC	EGC	C	EC	GC	EGC	C	EC
		Terminal units				Extender units		
Scots pine bark (*Pinus sylvestris*)	nd	5.93 (0.311)	89.4 (2.53)	5.77 (0.021)	3.28 (1.20)	10.2 (0.984)	44.4 (0.393)	462 (12.1)
Tilia flowers (*Tilia* x *Europaea*)	nd	1.44 (0.059)	14.9 (0.464)	81.7 (0.830)	2.31 (0.252)	9.02 (1.33)	21.9 (0.158)	518 (1.27)
Weeping willow catkins (*Salix babylonica*)	3.11 (0.302)	3.01 (0.247)	34.9 (0.104)	28.3 (0.026)	63.1 (1.02)	121 (8.17)	93.0 (1.37)	265 (1.98)
Sainfoin plant (*Onobrychis viciifolia*)	23.3 (1.11)	18.5 (0.478)	26.3 (1.52)	22.4 (1.13)	97.8 (5.72)	482 (13.0)	26.4 (1.22)	249 (5.84)
Black currant leaves (*Ribes nigrum*)	82.2 (1.93)	20.2 (0.588)	15.0 (0.369)	2.27 (0.073)	614 (14.6)	69.0 (1.36)	19.1 (1.03)	8.23 (0.362)

5.3.1.2 Proanthocyanidin sub-fractions

The above fractions from Sephadex™ LH-20 column chromatography were then separated further using semi-preparative RP-HPLC. Their mDP values and PC contents (in mg PCs/100 mg PAs) are presented in Table 5.3. Surprisingly, little variation was found between mDP values of PC-rich sub-fractions from pine bark (from 4 to 5) and Tilia (4 to 8). A flavonoid impurity was detected in sub-fraction B9 from Tilia (Figure 5.1, Table 5.3), whereas all sub-fractions from pine bark consisted of PAs only. The artificial mixtures prepared from pine bark and Tilia sub-fractions both had 98 mg PCs/100 mg PAs and mDP values of 4 and 6, respectively. Weeping willow sub-fractions had from 67% to 76% PCs and mDP values from 4 to 15. Sub-fraction C7 (Figure 5.1, Table 5.3) contained a flavonoid impurity, which could not be identified, and the artificial mixture had an mDP value of 8 and 74% PCs within PAs. Sainfoin sub-fractions showed a range of mDP values between 8 and 14 and PCs within PAs ranged from 16% to 61%. An unidentified flavonoid was detected in sub-fraction D7 (Figure 5.1, Table 5.3) and the artificial mixture had mDP and PC content values of 9 and 42, respectively. Finally, mDP values of black currant ranged from 8 to 10 and PCs from 3% to 9%. The artificial mixture had an mDP value of 9 and contained mostly PDs (PC = 5 mg PCs/100 mg PAs). As expected, the mDP range in the sub-fractions from the same plant source demonstrated that the mDP values of the Sephadex™ LH-20 fractions masked the true PA complexity, which had made it difficult previously to

Table 5.3: Procyanidin (PC) contents of proanthocyanidins (PAs) in mg PCs/100 mg PAs and mean degree of polymerisation (mDP) of sub-fractions obtained by semi-preparative reversed-phase HPLC, which were characterised with UPLC-DAD-ESI-MS/MS; PD (mg PDs/100 mg PAs) = 100 - PC.

Sub-fraction no	Pine bark (A)		Tilia (B)		Weeping willow (C)		Sainfoin (D)		Black currant (E)	
	PC	mDP	PC	mDP	PC	mDP	PC	mDP	PC	mDP
1	98	4	96	4	67	7	16	8	3	8
2	98	4	98	5	74	7	35	9	5	8
3	98	4	98	6	76	8	51	10	8	9
4	97	5	98	6	76	8	60	11	9	10
5	97	4	98	7	72	10	61	12	8	10
6	97	5	97	7	70	11	54	14	8	9
7*,**			96	7	68	14	60	12		
8*			98	7	69	15	63	11		
9*,**			98	7						
10*			97	8						
Artificial mixture***	98	4	98	6	74	8	42	9	5	9

*Signifies sub-fractions (B9, B10, C7, C8, D7 and D8) with too low yields; thus these fractions could not be tested with the Larval Exsheathment Inhibition Assay (see Figure 5.1).

**Signifies sub-fractions (B9, C7 and D7), which contained flavonoid impurities (see Figure 5.1).

***Signifies the artificial mixture, which was prepared by combining 10% from each sub-fraction by weight (w/w).

establish the main factor for AH activity in the LEIA. Thus, further purification and separation of PAs by semi-preparative RP-HPLC added new information on their overall complexity. For example, the sharp chromatographic peaks of the early eluting PAs from PC- and PD-rich samples denoted the presence of distinct PA groups (Figure 5.1 A, B, E). However, more complex polymeric mixtures are eluted at later retention times and are indicated by the smooth and broad shape of the chromatographic humps (Figure 5.1); this complexity may stem from an increase of PA size or from an increase of PC over PD sub-units. These PA differences between sub-fractions were also illustrated in the multiple reaction monitoring (MRM) chromatograms after UPLC-DAD-ESI-MS/MS analysis (Figure 5.2).
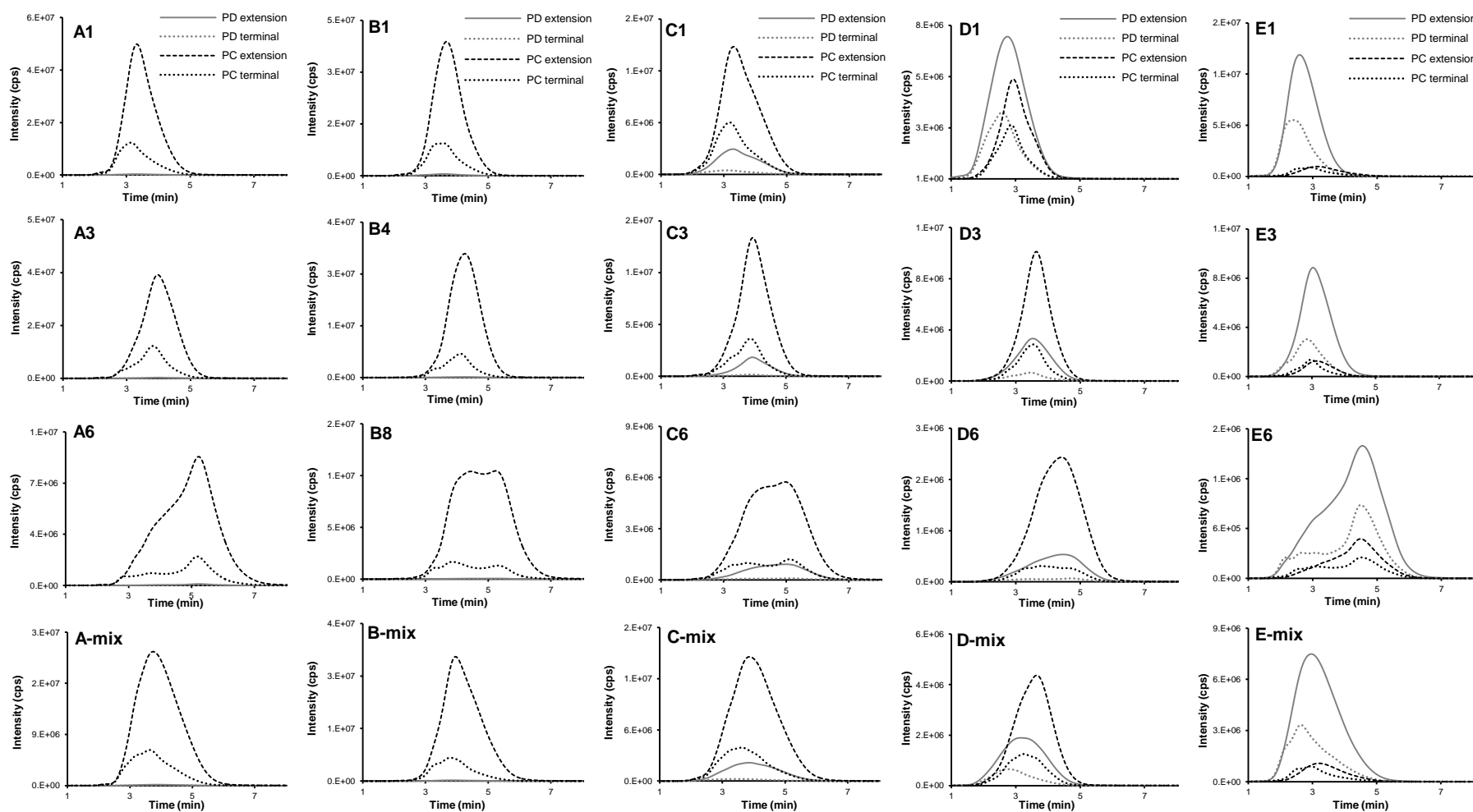
Figure 5.2: Chromatographic fingerprints of proanthocyanidin sub-fractions obtained by multiple reaction monitoring experiments (for sub-fraction identity, see Table 5.3). Selected signals are recorded from precursor-daughter ion transitions for procyanidin extension units (m/z 287→125, PC extension), procyanidin terminal units (m/z 289→125, PC terminal), prodelphinidin extension units (m/z 303→125, PD extension), prodelphinidin terminal units (m/z 305→125, PD terminal).

The method used a range of MRM experiments that enabled selective detection and quantification of PC, PD terminal and extension units in each sub-fraction. The MRM chromatograms are synthesised by unique combinations of signals for PC and PD terminal and extension units that could also be used as fingerprints for distinguishing PA samples that share the same characteristics. According to Engström et al, PAs that elute early and have narrow width of the chromatographic humps corresponded to relatively simple oligomers whereas more complex PA oligomers and polymers eluted later and had a broader distribution along the retention time axis (Figure 5.2) [35].

In addition, the artificial mixtures that were made from the combined sub-fractions could partially simulate the Sephadex^{TM} LH-20 semi-purified fractions, prior to semi-preparative purification, and consequently evaluate and compare their AH potency. Moreover, as the low yields of impure sub-fractions (Figure 5.1) did not allow their actual testing, the artificial mixtures could provide information on the AH potency of flavonoid impurities. Therefore, it was hoped that these PA sub-fractions and their statistical analysis in groups would provide further information on structural PA features that cause the *in vitro* AH activity via the LEIA.

5.3.1.3   Relationships between structural parameters

Calculation of Spearman correlation coefficients for all sub-fractions, with or without the artificial mixtures, showed a positive and significant relationship between mDP and PDs ($r = 0.76$ or $r = 0.75$, $p < 0.001$, df = 37 or df = 32, Table 5.4). This correlation complied with previous reports on PAs from grapes [38, 39], hops [39] and sainfoin [16]. However, the statistical analysis of diverse semi-purified PA fractions, from similar plant sources to ours, showed weak relationships between PDs and polymer size [17, 40]. This suggested that particular grouping of variables, in statistical analysis, could often result in confounding conclusions. Therefore, we separately assessed the relationships between mDP and PDs of sub-fraction groups with similar or diverse PD contents (Table 5.4). A positive and significant relationship was generated when only the PC- and PD-rich sub-fractions (Tilia, pine bark and black currant) were assessed ($r = 0.67$ or $r = 0.65$, $p < 0.001$ and $p < 0.01$; df = 23 or df = 20, Table 5.4). When the Spearman correlation test was applied to two PC-rich plus the weeping willow sub-

Table 5.4: Spearman's correlation coefficients for mean degree of polymerisation and prodelphinidins (mg PD/100 mg PAs) in all sub-fractions and in selected proanthocyanidin groups with and without the artificial proanthocyanidin mixtures

	mean Degree of Polymerisation													
	All sub-fractions		Group 1:		Group 2:		Group 3:		Group 4:		Group 5:		Group 6:	
			Tilia		Tilia		Tilia		Sainfoin		Black currant		Black currant	
			Pine bark		Pine bark		Pine bark		Weeping willow		Sainfoin		Sainfoin	
			Black currant				Weeping willow				Weeping willow			
	(df = 37)		(df = 23)		(df = 16)		(df = 23)		(df = 14)		(df = 21)		(df=14)	
Variable	*r* value	*p* value	*r* value	*p* value	*r* value	*p* value	*r* value	*p* value	*r* value	*p* value	*r* value	*p* value	*r* value	*p* value
PD	0.76^{a}	0.53	0.67^{a}	0.65	0.04	0.43	0.64^{b}	0.53	0.34	0.46	0.09	0.37	-0.71^{b}	0.68
	(df =32)		(df = 20)		(df =14)		(df =20)		(df =12)		(df =18)		(df=12)	
PD	0.75^{a}	0.56	0.65^{b}	0.57	0.01	0.46	0.61^{b}	0.57	0.33	0.50	0.04	0.40	-0.74^{b}	0.50

$^{a}p < 0.001$ $^{b}p < 0.01$ $^{c}p < 0.05$ $^{d}p < 0.1$

fractions, a significant relationship between mDP and PD content was also identified ($r = 0.64$ or $r = 0.61$, $p < 0.01$, df = 23 or df = 20; Table 5.4). The PD-rich sub-fractions (Black currant and Sainfoin) generated a significant negative relationship between mDP and PD values ($r = -0.71$ or $r = -0.74$, $p < 0.01$, df = 14 or df = 12, Table 5.4). This result can be explained by the fact that early eluting PAs from sainfoin and black currant were characterised by higher PD content but lower mDP values compared to PAs that eluted later (Table 5.3). The correlation between mDP and PDs in this sub-fraction group contradicted the mDP - PD patterns identified in the other sub-fraction groups and the reported patterns in PAs from black currants [41] and sainfoin [16]. This suggested that sub-fractionation of PA samples partially unravelled the complexity of Sephadex^{TM} LH-20 fractions and that statistical analysis of PA variables can complicate interpretations.

5.3.2 Anthelmintic activity

5.3.2.1 Proanthocyanidin sub-fractions

The PA sub-fractions inhibited the exsheathment of *H. contortus* L3 in a dose-dependent manner as reported previously [17, 30, 42]. The AH effect of each PA sub-fraction was measured in terms of EC_{50} values (µg/ml) (Table 5.5).

Table 5.5: EC_{50} values (µg PAs/ml) with 95% confidence intervals of each sub-fraction tested against *Haemonchus contortus* with the LEIA; nt: not tested.

Sub-fraction no	*Haemonchus contortus* EC_{50} (µg PAs/ml)				
	Pine bark (A)	Tilia (B)	Weeping willow (C)	Sainfoin (D)	Black currant (E)
1	46.9 (23.6-67.1)	139 (77-211)	373 (232-1130)	215 (172-267)	199 (114-383)
2	178 (87.4-247)	79.0 (31.8-128)	170 (121-245)	149 (117-188)	125 (72.9-211)
3	266 (197-376)	75.1 (55.7-97.7)	145 (108-191)	148 (120-187)	115 (88.4-144)
4	246 (136-393)	116 (71.3-178)	231 (182-298)	118 (96.8-142)	114 (77.5-159)
5	192 (131-287)	82.7 (65.2-102)	256 (175-404)	160 (125-200)	72.1 (49.1-96.8)
6	95.0 (72.4-120)	73.7 (53.8-92.4)	135 (69.3-242)	<37.5* (17.1-42.4)*	<37.5* (7.07-56.4)*
7		74.3 (38.2-111)	nt	nt	
8		61.2 (39.8-83.5)	nt	nt	
9		nt			
10		nt			
Calculated average of sub-fractions**	171 (128-214)	87.6 (74.6-101)	218 (173-263)	137 (106-168)	110 (82.2-138)
Artificial mixture	209 (182-243)	106 (59.4-137)	67.0 (42.8-90.4)	133 (104-167)	111 (86-141)

*Determination of EC_{50} values with PoloPlus software generated the following values: black currant sub-fraction E6 = 33.5 µg/ml and sainfoin sub-fraction D6 = 29.9 µg/ml.

**Average EC_{50} values are calculated from the individual sub-fractions and did not include the artificial mixture.

Figure 5.3 reveals a trend, i.e. late eluting PA sub-fractions were the most active against *H. contortus* L3 (Table 5.5).
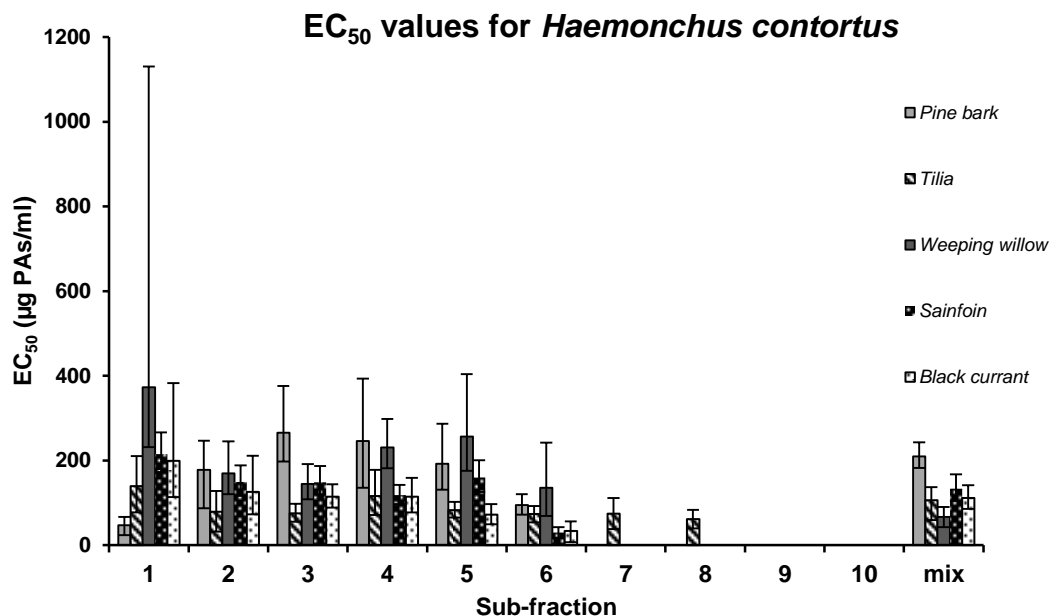
Figure 5.3: EC_{50} values (µg PAs/ml) and 95% confidence intervals (CI) of individual sub-fractions (see Table 5.6) from each plant source against *in vitro* exsheathment of *Haemonchus contortus* L3.

This was observed in almost all series of PA sub-fractions irrespectively of the plant source. Two sainfoin and black currant sub-fractions (D6 and E6) were particularly active with EC_{50} values of <37.5 µg/ml. However, sub-fraction A1 from Pine bark bucked this trend (EC_{50} = 46.9 µg/ml). It was also noted that some sub-fractions presented different potency against H. contortus despite the fact that they shared the same mDP and PD values (Table 5.3). For instance, PAs from sub-fraction E6 were more anthelmintic compared to PAs from sub-fraction E3 in black currant (Table 5.5) although they had same mPD and PD content values (Table 5.3). It is conceivable that in such cases, MRM chromatographic fingerprints may provide qualitative information on PA distribution profiles that could help to explain such discrepancies. Indeed, their chromatographic fingerprints showed clearly that late eluting sub-fractions contained very complex PA structures (Figure 5.2). This was illustrated by the broad shape of the chromatographic humps and the wide distribution across retention times compared to earlier collected sub-fractions. These qualitative comparisons were easily made with sub-fractions, governed by

oligomers of homopolymeric PAs but complicated PA mixtures generated MRM fingerprints which were more difficult to interpret.

The AH activity of the artificial mixtures followed the order: Weeping willow, Tilia, Black currant, Sainfoin and Pine Bark (Table 5.5, Figure 5.4).
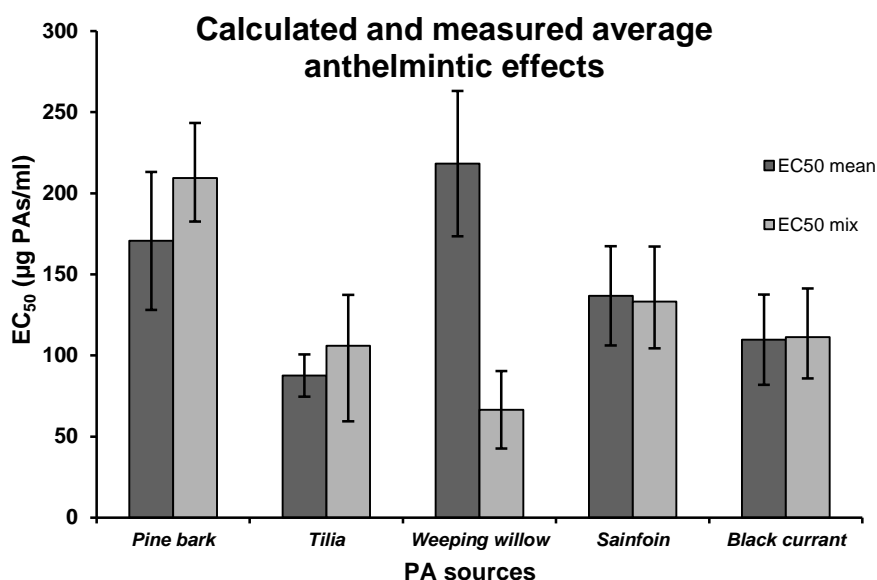
Figure 5.4: Calculated and measured EC_{50} values of PAs in the *in vitro* larval exsheathment inhibition assay against L3 larvae of *Haemonchus contortus*. Calculated means (dark bars) stem from the EC_{50} values of the sub-fractions. Measured average AH effect (light bars) stem from the EC_{50} values of the artificial mixtures (mix) (see Table 5.5).

Research from Quijada et al. on Sepahdex^{TM} LH-20 fractions from similar plant sources, generated comparable EC_{50} values to our mean EC_{50} and measured EC_{50} values of the artificial mixtures [17]. Interestingly, the artificial mixtures produced similar EC_{50} values to the mean EC_{50} values calculated from individually tested sub-fractions (Figure 5.4) with one exception: the artificial weeping willow mixture was unexpectedly more active (EC_{50} = 67.0 µg/ml) (Table 5.5, Figure 5.3) than the calculated EC_{50} average of 218 µg/ml (Table 5.5). This could be associated to the impurity of sub-fraction C7 of weeping willow (Table 5.3, Figure 5.1). Some researchers have suggested that the presence of non-PA compounds could contribute to AH activity [19-21]. Quercetin and luteolin have generated AH effects that interacted synergistically with PAs [29]. However, antagonistic effects between PAs and other naturally occurring polyphenols in foliages and by-

products of cacao have also been presented [30]. Finally, flavonol glycosides from *Vicia pannonica* might also have contributed to an observed AH effect [43].

5.3.2.2 Relationships between proanthocyanidin structural traits and anthelmintic effect

At a first glance, the results of 2 by 2 calculations of Spearman correlations in the whole sample population indicated that mDP had no influence on the AH effect (Table 5.6). However, when the various sub-fraction sets were analysed in groups, e.g. in PC-rich, PD-rich and mixed groups (Table 5.6), 4 out of 6 selected PA sub-fraction groups revealed a mDP contribution to AH activity, especially when the artificial mixtures were excluded from the analysis. Thus a significant negative correlation emerged between mDP and EC_{50} values (r = -0.59 or -0.56, p < 0.05, df = 16 or df = 14) for the PC-rich Tilia and pine bark series (Table 5.6). By adding the PD-rich black currant sub-fractions this was reduced to a negative trend (r = -0.39, p < 0.1, df = 23, Table 5.6) and no trend was found excluding the artificial mixtures (Table 5.6). Two other groups also generated a negative trend: the sainfoin and weeping willow sets (r = -0.49, p < 0.1, df = 14), and the sainfoin/weeping willow/black currant sets (r = -0.40, p < 0.1, df = 21, Table 5.5). Both trends were changed into significant negative correlations by excluding the artificial mixtures (r = -0.66 and r = -0.52, p < 0.05, df = 12 or df = 18 respectively). These findings agreed with reports that linked mDP values to *in vitro* AH activity against lamb (*H. contortus*) or bovine (*O. ostertagi* and *C. oncophora*) nematodes using the LEIA [17] and the Larval Feeding Inhibition Assay (LFIA) [16, 40], respectively.

Several *in vitro* and *in vivo* studies have shown that PD-rich PAs had higher efficacy against GINs than PC-rich PAs [16, 17, 22]. Quijada et al. showed that exsheathment inhibition of *H. contortus* L3 was mainly related to % PD within PAs [17, 22]. Similarly, PD-rich polymers isolated from sainfoin were also associated with the *in vitro* suppression of cattle nematode feeding [16]. Flavan-3-ols (GC and EGC) that give rise to PDs were found to be more inhibitory to *in vitro* motility and migration of *A. suum* L3 than C and EC [20, 21]. In addition, it has been also suggested that the additional OH groups in the B-ring of prodelphinidins promoted

Table 5.6: Spearman's correlation coefficients for anthelmintic activity in relation to proanthocyanidin structural parameters in all sub-fractions and in selected PA groups with and without the artificial PA mixtures

	Haemonchus contortus EC_{50} (µg/ml)													
	All sub-fractions		**Group 1:**		**Group 2:**		**Group 3:**		**Group 4:**		**Group 5:**		**Group 6:**	
			Tilia		Tilia		Tilia		Sainfoin		Black currant		Black currant	
			Pine bark		Pine bark		Pine bark		Weeping willow		Sainfoin		Sainfoin	
			Black currant				Weeping willow				Weeping willow			
	(df = 37)		(df = 23)		(df = 16)		(df = 23)		(df = 14)		(df = 21)		(df=14)	
Variable	*r* value	*p* value	*r* value	*p* value	*r* value	*p* value	*r* value	*p* value	*r* value	*p* value	*r* value	*p* value	*r* value	*p* value
mDP	-0.13	0.28	-0.39[d]	0.35	-0.59[c]	0.50	-0.08	0.35	-0.49[d]	0.46	-0.40[d]	0.37	-0.42	0.46
PD	0.05	0.28	0.03	0.35	0.05	0.43	0.32	0.35	-0.15	0.46	-0.36	0.37	-0.13	0.68
	(df =32)		(df = 20)		(df =14)		(df =20)		(df =12)		(df =18)		(df=12)	
mDP	-0.11	0.30	-0.37	0.38	-0.56[c]	0.50	0.03	0.38	-0.66[c]	0.59	-0.52[c]	0.47	-0.46	0.50
PD	0.08	0.30	0.07	0.38	0.13	0.46	0.47[c]	0.45	-0.23	0.50	-0.45[d]	0.40	-0.05	0.50

[a] $p < 0.001$ [b] $p < 0.01$ [c] $p < 0.05$ [d] $p < 0.1$

interactions with proteins of the parasite cuticle (sheath), and generated, therefore, a stronger AH effect [2, 21]. Surprisingly, our analysis showed no correlations between EC_{50} values and PD content (mg PDs/100 mg PAs) when all sub-fractions and artificial mixtures were examined. Only a negative trend (r = -0.45, p < 0.1, df = 18) of EC_{50} values with PD emerged in the black currant/sainfoin/weeping willow group was aligned with previous findings. On the contrary, a positive relationship (r = 0.47, p < 0.05, df = 20) between EC_{50} values and PD was found for the PC-rich sub-fractions of Tilia, pine bark and weeping willow, when the artificial mixtures were excluded (Table 5.6). The contribution of PC content to AH effect has been previously reported as the same PC-based PAs from Tilia exerted *in vitro* AH effects against *O. dentatum* [26] and PCs from pine bark against *A. suum* [20].

5.4 Conclusions

A novel purification scheme was applied to yield several highly pure PA sub-fractions from the same plant material. It was hypothesised that PA sub-fractions with a narrow distribution of structural features (e.g. mDP or PD contents) could be used to finally identify, which PA features mostly affected the *in vitro* exsheathment process of *H. contortus* L3 larvae. Fractionation of PAs according to increasing mDP was achieved, more with hetero-polymeric than with homo-polymeric PAs. Several of the resulting PC- and PD-polymer fractions differed from the original PA mixtures in terms of mDP and PC content.

Although all PA sub-fractions displayed AH activity in a dose-related manner, overall analysis revealed no clear link between a specific structural feature and AH activity. Therefore, several PA sub-fractions were subjected to separate statistical analysis which revealed some significant negative correlations between EC_{50} values and mDP. This was particularly evident with PC-rich polymers and with PA hetero-polymers and denoted that large molecules were more effective in *in vitro* exsheathment inhibition of *H. contortus* L3 larvae. Thus, it can be concluded that the mDP was the main structural factor responsible for the bio-activity of PAs in the LEIA. It is also of note that these results have emerged from a relatively small range of mDP values (i.e. 4 to 14) in these sub-fractions from PC- and PD-rich sources (Table 5.3). It would be interesting to explore

whether there is an optimum mDP for inhibiting larval exsheathment *in vitro* and *in vivo*.

It was observed that late eluting PAs generated lower EC_{50} values, thus stronger AH impact within sub-fractions of the same origin. Retention properties of RP-HPLC column resulted in late eluting PC-rich polymers, therefore the AH activity was not correlated with the PD content in the PA sub-fractions (Table 5.6). This suggests that further research should focus on optimal PA sizes that include a wide range of PD-contents.

An attempt was made to evaluate the AH potency of the unidentified flavonoid impurities by comparing the measured EC_{50} values from the artificial mixtures and the calculated mean EC_{50} values from the tested sub-fractions. Given the similarities, there was no evidence of synergistic or antagonistic interactions of PAs and the unidentified flavonoids. However, one impure PA sample from weeping willow mixture had a low EC_{50} value, which might be linked to the flavonoids and this might be worth further investigation.

Finally, the results presented here suggest that average values of PA characteristics in complex, mixed samples isolated from plants may lead to misinterpretation of AH outcomes. Therefore, fractionation into highly pure PA sub-fractions may be required to fully unravel *in vitro* structure-activity relationships. It would also be important to test these sub-fractions in different bioassays, as the AH mechanisms are likely to differ across the various life stages of gastro-intestinal parasites.

References

1. Athanasiadou S, Kyriazakis I: Plant secondary metabolites: **Antiparasitic effects and their role in ruminant production systems.** *Proceedings of the Nutrition Society* 2007, 63(04):631-639.

2. Hoste H, Martinez-Ortiz-De-Montellano C, Manolaraki F, Brunet S, Ojeda-Robertos N, Fourquaux I, Torres-Acosta JF, Sandoval-Castro CA: **Direct and indirect effects of bioactive tannin-rich tropical and temperate legumes against nematode infections.** *Veterinary Parasitology* 2012, 186(1-2):18-27.

3. Hoste H, Jackson F, Athanasiadou S, Thamsborg SM, Hoskin SO: **The effects of tannin-rich plants on parasitic nematodes in ruminants.** *Trends in Parasitology* 2006, 22(6):253-261.

4. Min BR, Hart SP: **Tannins for suppression of internal parasites.** *Journal of Animal Science* 2003, 81(14_suppl_2):E102-E109.

5. Molan AL, Waghorn GC, Min BR, McNabb WC: **The effect of condensed tannins from seven herbages on *Trichostrongylus colubriformis* larval migration *in vitro*.** *Folia Parasitolologica* 2000, 47(1):39-44.

6. Terrill TH, Miller JE, Burke JM, Mosjidis JA, Kaplan RM: **Experiences with integrated concepts for the control of *Haemonchus contortus* in sheep and goats in the United States.** *Veterinary Parasitology* 2012, 186(1-2):28-37.

7. Novobilsky A, Mueller-Harvey I, Thamsborg SM: **Condensed tannins act against cattle nematodes.** *Veterinary Parasitology* 2011, 182(2-4):213-220.

8. Manolaraki F, Sotiraki S, Stefanakis A, Skampardonis V, Volanis M, Hoste H: **Anthelmintic activity of some Mediterranean browse plants against parasitic nematodes.** *Parasitology* 2010, 137(4):685-696.

9. Mueller-Harvey I: **Unravelling the conundrum of tannins in animal nutrition and health.** *Journal of the Science of Food and Agriculture* 2006, 86(13):2010-2037.

10. Athanasiadou S, Tzamaloukas O, Kyriazakis I, Jackson F, Coop RL: **Testing for direct anthelmintic effects of bioactive forages against *Trichostrongylus colubriformis* in grazing sheep.** *Veterinary Parasitology* 2005, 127(3-4):233-243.

11. Githiori JB, Athanasiadou S, Thamsborg SM: **Use of plants in novel approaches for control of gastrointestinal helminths in livestock with emphasis on small ruminants.** *Veterinary Parasitology* 2006, 139(4):308-320.

12. Heckendorn F, Haring DA, Maurer V, Senn M, Hertzberg H: **Individual administration of three tanniferous forage plants to lambs artificially infected with *Haemonchus contortus* and *Cooperia curticei*.** *Veterinary Parasitology* 2007, 146(1-2):123-134.

13. Joshi BR, Kommuru DS, Terrill TH, Mosjidis JA, Burke JM, Shakya KP, Miller JE: **Effect of feeding sericea lespedeza leaf meal in goats experimentally infected with *Haemonchus contortus*.** *Veterinary Parasitology* 2011, 178(1-2):192-197.

14. Niezen JH, Charleston WA, Robertson HA, Shelton D, Waghorn GC, Green R: **The effect of feeding sulla (*Hedysarum coronarium*) or lucerne (*Medicago sativa*) on lamb parasite burdens and development of immunity to gastrointestinal nematodes.** *Veterinary Parasitology* 2002, 105(3):229-245.

15. Brunet S, Fourquaux I, Hoste H: **Ultrastructural changes in the third-stage, infective larvae of ruminant nematodes treated with sainfoin (*Onobrychis viciifolia*) extract.** *Parasitology International* 2011, 60(4):419-424.

16. Novobilsky A, Stringano E, Hayot Carbonero C, Smith LM, Enemark HL, Mueller-Harvey I, Thamsborg SM: **In vitro effects of extracts and purified tannins of sainfoin (Onobrychis viciifolia) against two cattle nematodes**. *Veterinary Parasitology* 2013, **196**(3-4):532-537.

17. Quijada J, Fryganas C, Ropiak HM, Ramsay A, Mueller-Harvey I, Hoste H: **Anthelmintic Activities against Haemonchus contortus or Trichostrongylus colubriformis from Small Ruminants Are Influenced by Structural Features of Condensed Tannins**. *Journal of Agricultural and Food Chemistry* 2015, **63**(28):6346-6354.

18. Naumann HD, Armstrong SA, Lambert BD, Muir JP, Tedeschi LO, Kothmann MM: **Effect of molecular weight and concentration of legume condensed tannins on in vitro larval migration inhibition of Haemonchus contortus**. *Veterinary Parasitology* 2014, **199**(1-2):93-98.

19. Molan AL, Sivakumaran S, Spencer PA, Meagher LP: **Green tea flavan-3-ols and oligomeric proanthocyanidins inhibit the motility of infective larvae of Teladorsagia circumcincta and Trichostrongylus colubriformis in vitro**. *Research in Veterinary Science* 2004, **77**(3):239-243.

20. Williams AR, Fryganas C, Ramsay A, Mueller-Harvey I, Thamsborg SM: **Direct anthelmintic effects of condensed tannins from diverse plant sources against Ascaris suum**. *PLoS One* 2014, **9**(5):e97053.

21. Brunet S, Hoste H: **Monomers of condensed tannins affect the larval exsheathment of parasitic nematodes of ruminants**. *Journal of Agricultural and Food Chemistry* 2006, **54**(20):7481-7487.

22. Molan AL, Meagher LP, Spencer PA, Sivakumaran S: **Effect of flavan-3-ols on in vitro egg hatching, larval development and viability of infective larvae of Trichostrongylus colubriformis**. *International Journal for Parasitology* 2003, **33**(14):1691-1698.

23. Brunet S, Jackson F, Hoste H: **Effects of sainfoin (Onobrychis viciifolia) extract and monomers of condensed tannins on the association of abomasal nematode larvae with fundic explants**. *International Journal for Parasitology* 2008, **38**(7):783-790.

24. Katiki LM, Ferreira JF, Gonzalez JM, Zajac AM, Lindsay DS, Chagas AC, Amarante AF: **Anthelmintic effect of plant extracts containing condensed and hydrolyzable tannins on Caenorhabditis elegans, and their antioxidant capacity**. *Veterinary Parasitology* 2013, **192**(1-3):218-227.

25. Williams AR, Ramsay A, Hansen TV, Ropiak HM, Mejer H, Nejsum P, Mueller-Harvey I, Thamsborg SM: **Anthelmintic activity of trans-cinnamaldehyde and A- and B-type proanthocyanidins derived from cinnamon (Cinnamomum verum)**. *Scientific Reports* 2015, **5**:14791.

26. Williams AR, Ropiak HM, Fryganas C, Desrues O, Mueller-Harvey I, Thamsborg SM: **Assessment of the anthelmintic activity of medicinal plant extracts and purified condensed tannins against free-living and parasitic stages of Oesophagostomum dentatum**. *Parasites & Vectors* 2014, **7**(1):518.

27. Hounzangbe-Adote MS, Paolini V, Fouraste I, Moutairou K, Hoste H: **In vitro effects of four tropical plants on three life-cycle stages of the parasitic nematode, Haemonchus contortus**. *Research in Veterinary Science* 2005, **78**(2):155-160.

28. Barrau E, Fabre N, Fouraste I, Hoste H: **Effect of bioactive compounds from Sainfoin (Onobrychis viciifolia Scop.) on the in vitro larval migration of Haemonchus contortus: role of tannins and flavonol glycosides**. *Parasitology* 2005, **131**(Pt 4):531-538.

29. Klongsiriwet C, Quijada J, Williams AR, Mueller-Harvey I, Williamson EM, Hoste H: **Synergistic inhibition of *Haemonchus contortus* exsheathment by flavonoid monomers and condensed tannins.** *International Journal for Parasitology Drugs and Drug Resistance* 2015, 5(3):127-134.

30. Vargas-Magana JJ, Torres-Acosta JF, Aguilar-Caballero AJ, Sandoval-Castro CA, Hoste H, Chan-Perez JA: **Anthelmintic activity of acetone-water extracts against *Haemonchus contortus* eggs: Interactions between tannins and other plant secondary compounds.** *Veterinary Parasitology* 2014, 206(3-4):322-327.

31. Moreno-Gonzalo J, Manolaraki F, Frutos P, Hervas G, Celaya R, Osoro K, Ortega-Mora LM, Hoste H, Ferre I: ***In vitro* effect of heather extracts on *Trichostrongylus colubriformis* eggs, larvae and adults.** *Veterinary Parasitology* 2013, 197(3-4):586-594.

32. Alonso-Diaz MA, Torres-Acosta JF, Sandoval-Castro CA, Hoste H: **Comparing the sensitivity of two *in vitro* assays to evaluate the anthelmintic activity of tropical tannin rich plant extracts against *Haemonchus contortus*.** *Veterinary Parasitology* 2011, 181(2-4):360-364.

33. Brunet S, Aufrere J, El Babili F, Fouraste I, Hoste H: **The kinetics of exsheathment of infective nematode larvae is disturbed in the presence of a tannin-rich plant extract (sainfoin) both *in vitro* and *in vivo*.** *Parasitology* 2007, 134(Pt 9):1253-1262.

34. Dhakal S, Meyling NV, Williams AR, Mueller-Harvey I, Fryganas C, Kapel CM, Fredensborg BL: **Efficacy of condensed tannins against larval *Hymenolepis diminuta* (Cestoda) *in vitro* and in the intermediate host *Tenebrio molitor* (Coleoptera) *in vivo*.** *Veterinary Parasitology* 2015, 207(1-2):49-55.

35. Engstrom MT, Palijarvi M, Fryganas C, Grabber JH, Mueller-Harvey I, Salminen JP: **Rapid qualitative and quantitative analyses of proanthocyanidin oligomers and polymers by UPLC-MS/MS.** *Journal of Agricultural and Food Chemistry* 2014, 62(15):3390-3399.

36. Gea A, Stringano E, Brown RH, Mueller-Harvey I: ***In situ* analysis and structural elucidation of sainfoin (*Onobrychis viciifolia*) tannins for high-throughput germplasm screening.** *Journal of Agricultural and Food Chemistry* 2011, 59(2):495-503.

37. Bahuaud D, Martinez-Ortiz de Montellano C, Chauveau S, Prevot F, Torres-Acosta F, Fouraste I, Hoste H: **Effects of four tanniferous plant extracts on the *in vitro* exsheathment of third-stage larvae of parasitic nematodes.** *Parasitology* 2006, 132(Pt 4):545-554.

38. Labarbe B, Cheynier V, Brossaud F, Souquet JM, Moutounet M: **Quantitative fractionation of grape proanthocyanidins according to their degree of polymerization.** *Journal of Agricultural and Food Chemistry* 1999, 47(7):2719-2723.

39. Kennedy JA, Taylor AW: **Analysis of proanthocyanidins by high-performance gel permeation chromatography.** *Journal of Chromatography A* 2003, 995(1-2):99-107.

40. Desrues O, Fryganas C, Ropiak HM, Mueller-Harvey I, Enemark HL, Thamsborg SM: **Impact of chemical structure of flavanol monomers and condensed tannins on *in vitro* anthelmintic activity against bovine nematodes.** *Parasitology* 2016, 143(4):444-454.

41. Laaksonen OA, Salminen JP, Makila L, Kallio HP, Yang B: **Proanthocyanidins and their Contribution to sensory attributes of black currant juices.** *Journal of Agricultural and Food Chemistry* 2015, 63(22):5373-5380.

42.   Moreno-Gonzalo J, Manolaraki F, Frutos P, Hervas G, Celaya R, Osoro K, Ortega-Mora LM, Hoste H, Ferre I: ***In vitro* effect of heather (*Ericaceae*) extracts on different development stages of *Teladorsagia circumcincta* and *Haemonchus contortus*.** *Veterinary Parasitology* 2013, 197(1-2):235-243.

43.   Kozan E, Anul SA, Tatli, II: ***In vitro* anthelmintic effect of *Vicia pannonica* var. Purpurascens on trichostrongylosis in sheep.** *Experimental Parasitology* 2013, 134(3):299-303.

Chapter 6. Evaluation of carbon 13 cross polarisation magic angle spinning nuclear magnetic resonance for measuring proanthocyanidin content and the procyanidin to prodelphinidin ratio in sainfoin tissues

6.1 Introduction

Feeding sainfoin (*Onobrychis viciifolia*) to ruminants prevents animals suffering from bloat [1, 2], can lower gastrointestinal nematode burdens [3, 4] and reduces urinary nitrogen excretion [5, 6]. Adding sainfoin to common forage legumes, such as lucerne, has also shown some potential for decreasing enteric methanogenesis [7]. Another interesting investigation demonstrated that a sainfoin diet increased the polyunsaturated fatty acid content of dairy products, without altering desirable organoleptic characteristics, thus extending its beneficial impact also on human nutrition [8].

Although sainfoin contains a vast array of phenolic compounds [9, 10], its bioactivity has been mainly linked to a specific class of polymeric polyphenols that are called proanthocyanidins (PAs) [2, 6]. Sainfoin PAs vary enormously in composition and concentrations between accessions and different plant organs [10, 11]. Some of these PA features have been linked to biological effects. Thus, many parasites are negatively affected by prodelphinidin (PD)-rich PAs [3] (Figure 6.1) and larger PAs are also potent against some parasite species [12-14].

Similarly, PA features can also impact on the nutritive value of animal feeds. The same PA features, namely PD content and size, were negatively correlated to methane production [15]. However, a few procyanidin (PC)-rich PAs (Figure 6.1) appear to protect dietary proteins from ruminal degradation and release these at the small intestine in contrast to PD-rich PAs. This means that PC-rich PAs can enhance the nutritive values of few animal feeds [2]. There is still lack of information on the optimal concentration range for making best use of PAs for both animal nutrition and health [2]. Thus, farmers and plant breeders would benefit from rapid methods that can correctly measure PA content and composition in large numbers of sainfoin samples.

The occurrence of PAs as complex polymeric mixtures in plant matrices complicates their accurate quantification and characterisation [16, 17]. Chromatographic and mass spectrometric methods can only provide qualitative information on extracted or purified PAs. Recently, a mass spectrometer with a triple quadrupole, operating in multiple reaction monitoring (MRM) mode allowed determination of PA content, mean degree of polymerisation (mDP) and PC/PD ratio in plant extracts [18]. However, mass spectrometry does not provide

information on *cis/trans* ratios. In addition, extraction and purification are time-consuming and extraction is often incomplete as many plants contain large quantities of unextractable PAs, resulting in PA underestimations [19-21]. Therefore, *in situ* PA depolymerisation with HCl-butanol, or thiolysis with benzyl mercaptan are widely used. Unfortunately, these methods also suffer from serious limitations [16, 17]. It has been shown that the HCl-butanol reagent does not interact quantitatively with PAs [22] and several matrices may contain degradation-resistant PAs [23] or components that alter the thiolysis reaction [24]. Moreover, the HCl-butanol assay determines PA content but cannot provide information on structural characteristics. In contrast, derivatisation with nucleophiles (benzyl mercaptan and phloroglucinol) makes this information available by cleaving PAs into their monomeric flavan-3-ols and by preserving stereochemical features [25, 26].

Solution-state ^{13}C NMR spectroscopy has been used previously to obtain information on PC/PD [27-31] and *cis/trans* ratios [27-29, 31, 32], mDP values [27-29, 31, 32] of extracted or isolated PAs. However, these NMR techniques have been often complemented with other established techniques due to problematic signal-to-noise ratios and peak resolution. Two dimensional NMR techniques do not fully overcome signal limitations such as poor signal-to-noise ratio and poor resolution from significant peak overlap. In addition, they can only estimate PC/PD and *cis/trans* ratios [33], determine PA presence in PA extracts and isolates [34] or evaluate their purity [35]. Two dimensional gel-state NMR was used to successfully assess PA presence and composition directly in ground *Lotus* tissues [34], but our preliminary analysis with sainfoin tissue showed that these NMR spectra suffered from weak resolution and matrix interferences.

In contrast to solution-state NMR, solid-state NMR studies have been widely used for direct analysis of plant materials. In particular, cross-polarisation magic angle spinning (CPMAS) techniques have enabled investigations into extraction efficiency, identification of predominant flavan-3-ol structures and qualitative comparison of PA contents in barks [36, 37], humus extracts [38] and nutshell types [39]. Additionally, differences in fingerprint PA spectra could distinguish between the various tanning transformations on leather PAs [40], diverse dietary fibre powders [41] and levels of PA degradation induced by fungi [42].

The significant advantage of a solid-state NMR experiment is that it minimises effects from chemical manipulation or contamination of samples and provides relatively unaffected PA spectra [40]. However, the presence of large carbon numbers in different environments can cause complex signal overlaps in the solid-state NMR spectra and thus complicate the estimation of PA content, mDP values and PC/PD ratios [36], therefore other established chemical techniques are required to validate the findings.

This work aimed to develop a ^{13}C CPMAS NMR method that would allow estimation of PA concentration, as well as, mDP and PC/PD ratio values directly from a few milligrams of milled freeze-dried sainfoin tissue. The results obtained from the ^{13}C CPMAS NMR analysis were compared to those obtained from other established chemical techniques such as thiolysis-HPLC analysis and the HCl-butanol assay in order to assess the validity of the proposed procedure.

6.2   Materials and methods

6.2.1   Plant samples

Black currant (*Ribes nigrum*) leaves were collected from Hildred PYO farm (Goring-on-Thames, UK). Tilia (*Tilia* x *Europaea*) flowers were purchased from Flos (Mokrsko, Poland). Sainfoin (*Onobrychis viciifolia*) leaves and stems, from various accessions, were collected from the National Institute of Agricultural Botany (Cambridge, UK). Black currant and Tilia leaf samples were lyophilised or air-dried and subsequently ground and ball-milled. Sainfoin samples were collected in liquid nitrogen, lyophilised and ball-milled.

6.2.2   Chemicals and reagents

Hydrochloric acid (36%), formic acid, acetic acid, butan-1-ol, HPLC-grade acetone, HPLC-grade methanol, HPLC-grade dichloromethane, HPLC-grade hexane, HPLC-grade acetonitrile and ammonium chloride were purchased from Fisher Scientific (Loughborough, UK). (±) – Dihydroquercetin (98%) was from Apin Chemicals (Abingdon, UK). Benzyl mercaptan and acetone-d_6 (99.9%) was supplied from Sigma-Aldrich (Poole, UK). Deuterium oxide (D_2O) was from CK

Isotopes (Ibstock, UK). Sephadex[TM] LH-20 was purchased from GE Healthcare (Little Chalfont, UK). Deionised water was purified with a Milli-Q system (Millipore, Watford, UK).

6.2.3 Proanthocyanidin extraction and purification

Extraction and purification of black currant and Tilia PAs followed the procedure described in Chapter 3. In brief, finely ground plant tissue (50 g) was weighed into a conical flask. Acetone/water (500 ml, 7:3 v/v) was added and the mixture was vigorously stirred for 1 h. The mixture was filtered under vacuum. The filtrate was further extracted with dichloromethane (250 ml) to remove lipids and chlorophyll. Polyphenols were concentrated in the aqueous phase with a rotary evaporator (T<37.5 °C). This crude extract was diluted in deionised water (2 l) and filtered under vacuum. The filtrate was loaded on a large Sephadex[TM] LH-20 column. The column was washed with deionised water (2 l) to wash off sugars and small phenolics while PAs were retained by the resin. Gravity elution with acetone/water (3:7, 1:1 and 8:2, v/v) yielded 3 purified PA fractions from each plant source. The organic solvent was removed using a rotary evaporator (T<37.5 °C). Fractions containing the PAs were frozen, freeze-dried and stored at -20 °C.

6.2.4 Thiolysis of proanthocyanidins

6.2.4.1 Thiolysis of purified proanthocyanidin fractions

Thiolysis reactions on purified PA fractions that eluted with acetone/water (1:1 v/v) were performed according to Novobilský et al. [43] and as described in Chapter 2. Briefly, PA fraction (4 mg) was weighed in 10 ml screw-capped vials, dissolved in methanol (1.5 ml) and acidified with HCl (0.5 ml, 3.3% in methanol, v/v). The addition of benzyl mercaptan followed (50 µl) and the reaction mixture was stirred (1 h) at 40 °C. The reaction was ceased by adding ultrapure water (2.5 ml) to the mixtures at room temperature. The analysis and quantification of thiolysis reaction products were performed with reverse-phase HPLC as described in section 2.2.7. and according to Gea et al. [25]. The operating conditions and parameters of HPLC analysis were set as in Williams et al. [14] and were thoroughly described in section 2.2.6.

6.2.4.2   *In situ* thiolysis of sainfoin proanthocyanidins

Milled sainfoin material was weighed (200 mg) in 10 ml screw-capped vials, dissolved in methanol (2 ml) and acidified with HCl (1 ml, 3.3% in methanol, v/v). The addition of benzyl mercaptan followed (100 µl) and the reaction mixture was stirred (1 h) at 40 °C. The reaction was ceased by adding 1 % formic acid in ultrapure water (9 ml) to the mixtures at room temperature. The samples were centrifuged (3000 rpm, 3 min) and 1 ml of the mixtures was added to HPLC vials for LC-MS analysis. Flavan-3-ols and their benzyl mercaptan adducts were quantified using published response factors against dihydroquercetin [25, 44].

Samples (5 µl) were injected into an HPLC Agilent 1100 series system connected to an ACE super C-18 column (5 µm; 150 x 3 mm; Hichrom Ltd; Theale; UK) fitted to an ACE guard column. The column temperature was set at 60 °C. The HPLC system consisted of a G1379A degasser, a G1312A binary pump, a G1313A ALS autoinjector, a G1314A VWD UV detector and a G1316A column oven and an API-ES instrument Hewlett Packard 1100 MSD Series (Agilent Technologies, Waldbronn, Germany). Data were acquired and processed with ChemStation software (version A 10.01 Rev. B.01.03). The flow rate was 0.4 ml/min using formic acid (1%) in water containing 100 mg/l ammonium chloride (solvent A) and HPLC-grade acetonitrile (solvent B). The thiolysis reaction products eluted with the following gradient: 0-7 min, 2.5% B; 7-15 min, 2.5-5% B; 15-22 min, 5-10% B; 22-40 min, 10-40% B; 40-45 min, 40-100% B; 45-49, 100-2.5% B; 49-60, 2.5% B. Flavan-3-ol terminal and extension units were identified by their retention times and ultraviolet-visible (UV) spectra between 210 and 280 nm. Mass spectra were recorded in the negative ionisation scan mode between *m/z* 100 and 1000. The mass spectrometer operating conditions were as follows: 3000 V for capillary voltage, nebuliser gas pressure at 35 psi, drying gas at 12 ml/min and dry heater temperature at 350 °C. Terminal and extension units were identified by their retention times and molecular masses.

6.2.4.3   *In situ* sainfoin proanthocyanidin analysis with the HCl - butanol assay

The HCl-butanol assay followed the procedure as described by Grabber et al. [34] with minor modifications. Briefly, lyophilised sainfoin tissue was weighed

(10 mg) in 10 ml screw-capped vials. A reagent mixture was prepared by mixing ammonium ferric sulphate (150 mg) in ultrapure water (3.3 ml), hydrochloric acid (12M, 5 ml), butan-1-ol (42 ml) and acetone (50 ml). An aliquot of the reagent (10 ml) was added to the sainfoin samples. The samples were left at room temperature (1 h) to evaluate the presence of flavan-4-ols and flavan-3,4-diols as these generate false positives. Tubes were then placed on a stirring heating block (70 °C, 2.5 h). Samples were left to room temperature and centrifuged (3000 rpm, 1 min). Absorbance of the supernatants was recorded at 555 nm in a CE 2040-2000 series UV/visible spectrophotometer (Cecil, London, UK). The acetone-butanol-HCl reagent was used as a blank, and all samples were run in duplicate. A sainfoin sample of known PA content and composition was used as a quality control for the HCl-butanol assay.

6.2.5 Analysis of proanthocyanidins with nuclear magnetic resonance spectroscopy

6.2.5.1 13-Carbon cross polarisation and magic angle spinning nuclear magnetic resonance analysis

The ^{13}C solid state cross polarisation magic angle spinning (CPMAS) NMR spectra were recorded on a Bruker Avance III spectrometer operating at Larmor frequency of 125.78 MHz (11.75T). Crude and purified extracts from Tilia, black currant and ball-milled Tilia, black currant and sainfoin leaves (~80 mg) were compressed into standard 4 mm zirconia rotors prior to analysis. The standard bore 4 mm MAS probe was used and rotors were spun at 10 kHz rate. The proton 90° pulse width was 3.7 µs at the power level of 32 W. The variable amplitude CP ramp (90-100) was used with the contact time of 1.0 ms. In total, 4096 signal transients were averaged into each spectrum with a 6 s relaxation delay at ambient temperature. All spectra were referenced to an external adamante signal (frequency peak at 38.5 ppm with respect to TMS) as a secondary reference.

Dipolar dephasing experiments were run with identical parameters to ^{13}C CPMAS NMR experiments and dephasing filter time (t_{dd}) of 45 µs was optimised to attenuate the signals of all non-quaternary carbons.

6.2.5.2 ^{1}H-^{13}C heteronuclear single quantum coherence nuclear magnetic resonance analysis

The purified PA fractions (20 mg) were transferred into a 1.5 ml Eppendorf tubes and dissolved in deuterium oxide/acetone-d_6 mixture (1 ml, 4:1 v/v). Samples were vigorously mixed and transferred into standard NMR tubes (5 mm diameter). The ^{1}H-^{13}C heteronuclear single quantum coherence (HSQC) spectra were recorded on a Bruker Avance III 500 spectrometer and experimental settings were described in Section 3.2.8.

The integrals of characteristic cross peak resonances from H/C-6´ signals from PCs and H/C-2´/6´ signals from PDs (Figure 6.1) were used to estimate the PC/PD ratio in the purified PA mixtures as described by Zeller et al. [33]. The percentage of PCs in total PAs of the sample was calculated using the following equation:

$$\%PC = PC\text{-}6'/[(PD\text{-}2'6'/2) + PC\text{-}6'] \times 100$$

where $PC\text{-}6'$ is the integral of the contour for the H/C-6´ cross peak of the PC subunits and $PD\text{-}2'6'$ is the integral of the contour for the cross peak of the PD subunits. The $PD\text{-}2'6'$ value was divided by 2 because the signal was generated by 2 sets of correlated nuclei. Integration of the peaks/signals was performed using the TopSpin software.

6.3   Results and discussion

6.3.1   Peak assignments

The ^{13}C CPMAS NMR analysis of the purified PA fractions from Tilia and black currant leaves produced several PA fingerprint signals (Figure 6.1). Each spectrum consisted of approximately 10 resolved resonances centred between 170 ppm and 0 ppm. Characteristic resonances at 155, 144 and 132 ppm were clearly observed in the spectra of all samples, including plants and crude extracts (Figure 6.2). The signal at 155 ppm originated from the carbons C5, C7, C8a of the flavan-3-ol structure (Figure 6.1). The signal at 144 ppm was generated from

the resonance of carbons C3´, C5´ of black currant PAs and carbons C3´, C4´ of Tilia PAs (Figure 6.1). The most distinctive peak at 132 ppm originated from the carbons C1´, C4´ in black currant PAs but only from carbon C1´ in Tilia PAs (Figure 6.1).

In order to confirm these assignments, the dipolar dephasing NMR experiments were also performed on the purified PA fractions from Tilia and black currant leaves (Figure 6.1). The experimental parameters were optimised to detect signals from non-protonated carbons only. The resulting data agreed with the identification of the non-protonated carbons justifying the peak assignments in the area of 160-90 ppm (Figure 6.1). Our assignments were also in good agreement with previously observed spectra in reports on pecan nutshell PDs and *Photinia* leaf PCs [39, 45]. The rest of the signals derived from miscalibration of the dephasing parameters for some functional groups (i.e. fast relaxation of CH_3 groups).
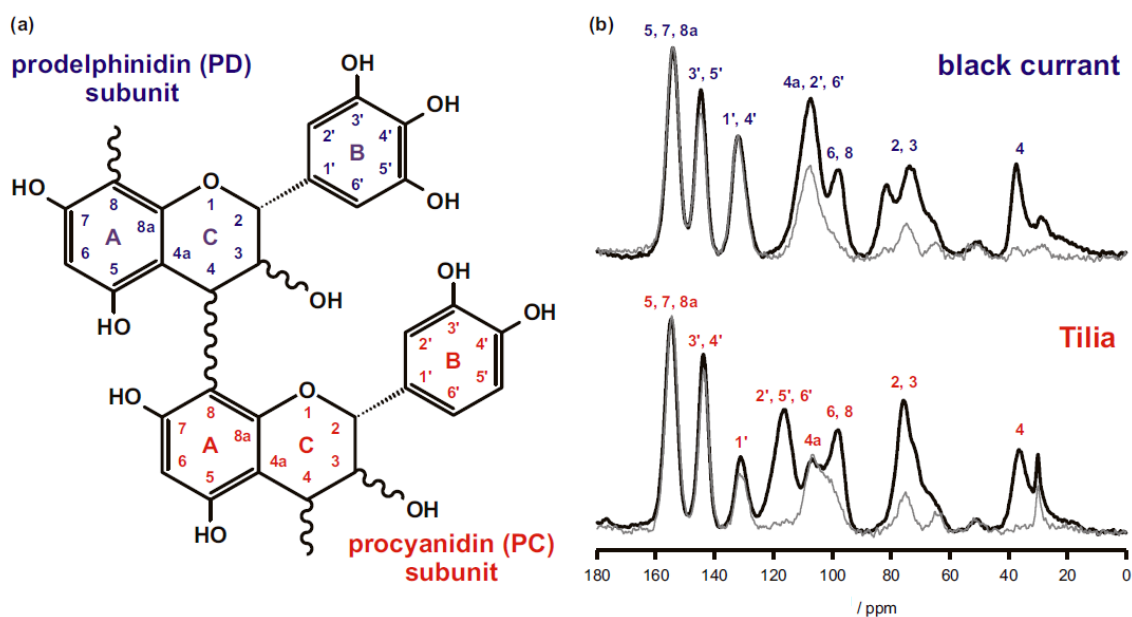
Figure 6.1: (a) Schematic representation of a proanthocyanidin structure consisting of a prodelphidin (top) subunit and a procyanidin (bottom) subunit. Black currant proanthocyanidins are dominated by prodelphinidin (PD) subunits whereas Tilia proanthocyanidins consist mainly of procyanidin (PC) subunits. (b) ^{13}C CPMAS NMR spectra (black solid line) of black currant (upper) and Tilia (lower) purified proanthocyanidin samples. Peak assignments are consistent with the labelled carbon positions of the proanthocyanidin structure. The grey lines depict the corresponding dipolar dephased NMR spectra which were optimised to detect only non-protonated carbons.
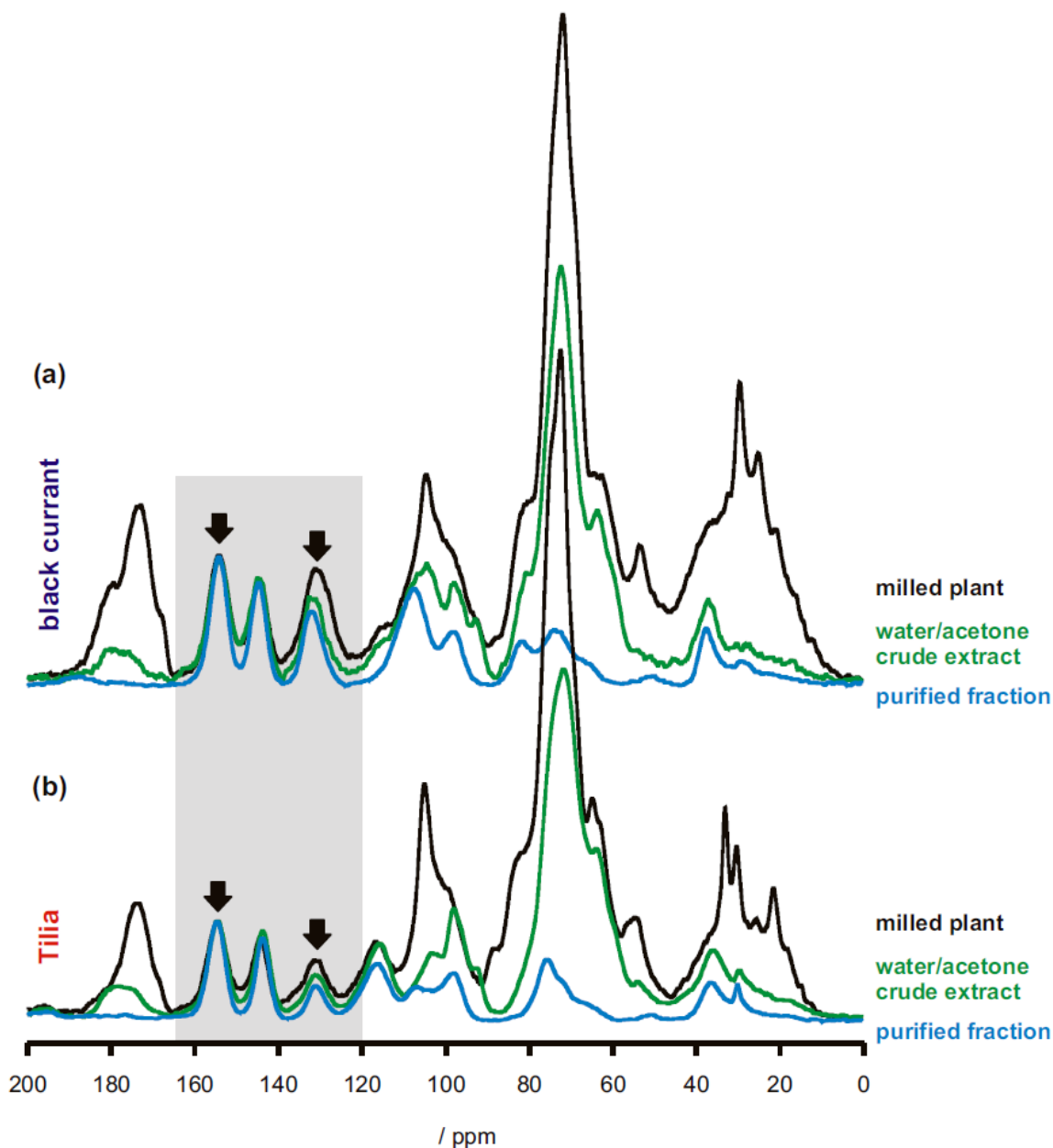
Figure 6.2: Comparison of ^{13}C CPMAS NMR spectra of milled plant (black line), acetone/water crude extract (green line) and purified proanthocyanidin fraction (blue line) from black currant (a) and Tilia (b). Black arrows depict the peaks at 155 and 132 ppm. All spectra were normalised to the amplitude of peak at 155 ppm to evaluate interferences from other plant components in the area of interest (160-120 ppm, highlighted in grey colour).

The different hydroxylation pattern between PC and PD subunits generated distinct bands in the 160-130 ppm region and different peak overlap between 120 ppm and 90 ppm (Figure 6.1). Peak assignments in the 120-20 ppm region of the plant and crude extract spectra proved more difficult in comparison to the purified PA spectra (Figure 6.2). This was due to interferences from other plant

components such as lignin, pectin, cutin, cellulose and hemicellulose as has been previously reported [36, 39, 40, 46].

6.3.2 Estimation of proanthocyanidin content

Several publications on solid-state NMR have expressed caution when quantifying PAs due to possible lignin or lignin-PA complex contributions to the peak signals in the 160-120 ppm region [36, 39, 47]. In particular, Wawer et al. postulated that the intense peak resonance of 155 and 144 ppm in ^{13}C CPMAS NMR dipolar dephased spectra from aronia and black currant fibre powders could include responses from C3, 5-OMe and C4-OH carbons of lignin [41]. However, lignin is insoluble in acetone/water, suggesting that the characteristic peak at 155 ppm in the spectra from purified fractions derived from PAs only [41]. In addition, this signal did not seem to suffer from any significant peak overlap in the spectra collection from purified PA fractions, crude extracts and plant samples as shown in Figures 6.1 and 6.2. Therefore, this particular signal was selected as a potential signature peak to estimate PA contents in unknown samples.

Initially, the experimental spectrum was fitted with a theoretical spectrum that was constructed from the sum of Gaussian peaks. Numbers and positions of peaks in the theoretical spectrum corresponded directly to the number and positions of peaks in the experimental spectrum. Width, amplitude and position of each peak in the theoretical spectrum were allowed to vary, in order to minimise the discrepancy between spectra and obtain the best agreement. A home written Matlab routine procedure based on the least square method was used. A number of initial parameters were tested and the sets with the smallest discrepancy led to final results with a narrow range of the fitting error. Once the width and the amplitude of the fitted peak at 155 ppm were known, the intensity of this peak was calculated.

The PA content of sainfoin samples was then estimated by comparing peak intensity to a reference peak (IR_{155}) at 155 ppm of the purified PA fraction from Tilia (PA content, [PA] = 95 g / 100 g of purified fraction, determined by thiolysis), using the following equation [37, 40]:

$$\text{PA (g/100 g plant or extract)} = \frac{I_{155} \times [PA]}{(IR^{\alpha}_{155} + IR^{\beta}_{155})/2}$$

where I_{155} is the intensity of the 155 ppm peak in spectra of unknown samples and $(IR^{\alpha}_{155} + IR^{\beta}_{155})/2$ is the average intensity of the reference peak obtained in two separate fitting procedures.

The calculation of experimental error involved three factors: i) the CP and relaxation parameters, ii) the small variation in setting hardware parameters, such as tuning and matching of the probe and iii) the intensity calculation after fitting of the spectra. The recording of 2-3 spectra of the same sample with slightly different settings regarding the first two parameters resulted in an error of ca 2 %. The discrepancies of the spectra acquired with different parameters introduced an additional error of ca 2% after the fitting process. This accounted for a total error of ca 4% for the intensity measurements. The PA concentration was calculated by comparing the reference peak intensity to the intensity of the sample of interest. Therefore the total experimental error, ca 8%, derived from the sum of the intensity errors between reference and sample intensity. However, it should not be disregarded that ^{13}C CPMAS NMR is not quantitative therefore the discrepancies could have exceeded the range of the estimated experimental error.

For an initial assessment of this method, the PA content of a crude acetone/water extract from black currant was estimated with this ^{13}C CPMAS NMR method and compared to the thiolysis-HPLC result. The PA content was 29.2 g PAs/100 g of crude extract as determined by thiolysis-HPLC and 39.7 g PAs/100 g of crude extract as determined by ^{13}C CPMAS NMR. Thus, the ^{13}C CPMAS NMR method held promise for PA estimations. However, possible impurity presence should not be disregarded since a study on humus have reported the lignin presence in aqueous and emulsified purified PA fractions [38].

6.3.3 Estimation of mean degree of polymerisation

The mean degree of polymerisation (mDP) can be obtained by integration of the C3 signals from PA extension units at 73 ppm and the corresponding signals of PA terminal units at 67 ppm [30, 38]. However, peak overlaps from other

plant constituents (Figure 6.2) [38] and poor resolution in the ^{13}C CPMAS NMR spectra of purified PA fractions (Figure 6.2) prevented the estimation of mDP values.

6.3.4 Estimation of procyanidin/prodelphinidin ratios

The procedure to estimate PC/PD proportions within total PAs was based on the different hydroxylation patterns of PCs and PDs. This was clearly illustrated by the ^{13}C CPMAS NMR spectra of the 140-100 ppm region (Figure 6.1). The resonance peak at 132 ppm was assigned to C1′ and C4′carbons of PD-type PAs from black currant (Figure 6.1 b). However, in Tilia PCs this resonance peak was assigned only to the C1′ carbon and had half the intensity of the PD peak [39, 45] (Figure 6.1 b). This difference in the 132 ppm peak intensity directly reflected the PD-PC composition as the PA contents were comparable (i.e. 87 g PAs/100 g of purified fraction for the black currant PA fraction and 95 g PAs/ 100 g of purified fraction for the Tilia purified PA fraction) and the molar percentages by thiolysis were 94% PDs and 97.4% PCs for the black currant and Tilia PAs respectively. Thus, we hypothesised that the ratio of peak intensities at 132 and 155 ppm (I_{132}/I_{155}) could provide information on the PD proportion within total PAs of purified PA fractions but more importantly of milled plants [37, 39, 40].

The Tilia and black currant purified PA fractions were initially analysed by ^{1}H-^{13}C HSQC NMR for their PC/PD ratios within total PAs [62]. This analysis showed that Tilia PAs consisted of 100% PCs and black currant PAs of 88.9% PDs (Figure 6.3) and confirmed the high purity of the purified PA fractions as determined by thiolysis (Tilia PAs = 95 g/100 g of purified fraction, black currant PAs = 86.6 g/100 g of purified fraction). Therefore, we assumed that the creation of artificial contrasting PC/PD mixtures (i.e. 10/0, 7/3, 5/5, 3/7 and 0/10) of purified PA fractions from Tilia and black currant would validate the intensity changes across the expected range of PC/PD ratios in the ^{13}C CPMAS NMR spectra. A similar approach with sainfoin plant mixtures was used previously for assessing the validity of the *in situ* thiolysis reaction and revealed only small differences between calculated and measured PA values [48].
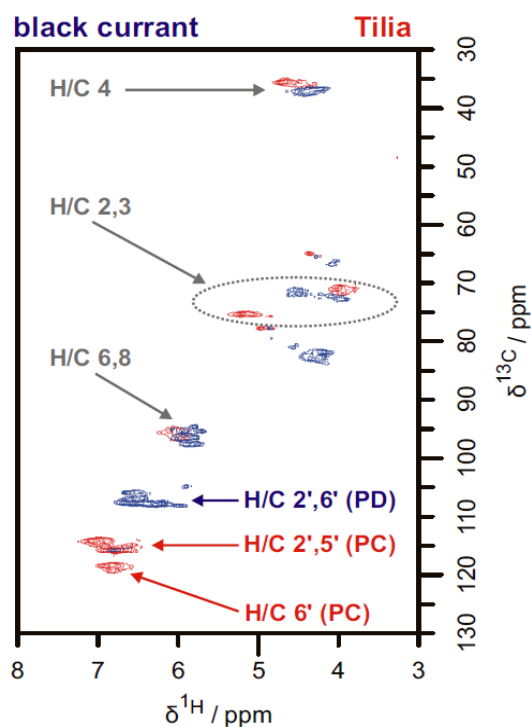
Figure 6.3: Signal assignments for the ^{1}H-^{13}C HSQC NMR spectrum (sample in deuterium oxide/acetone-d_6 solution) of purified proanthocyanidin fractions from Tilia (red) and black currant (blue). The absence of response in the procyanidin (PC) region is apparent for the prodelphinidin (PD)-rich black currant fraction. Accordingly, Tilia procyanidin-rich proanthocyanidins are not detected in the prodelphinidin region.

These artificial mixtures were prepared by combining the following quantities of black currant and Tilia purified PA fractions: 152:0 mg, 36:83 mg, 45:38 mg, 63:25 mg, 0:157 mg respectively. The calculated PC and PD contents within total PAs (in g PCs or PDs/100 g PAs) were based on the PC and PD contents from thiolysis (Tilia: 92.5 g PCs/100 g of purified fraction and black currant: 82.2 g PDs/100 g of purified fraction). These mixtures were analysed with ^{1}H-^{13}C HSQC NMR and as expected the measured and calculated PC and PD values of the mixtures, were highly correlated (R^2=0.99) (Figure 6.4). The strong correlation and linearity confirmed that the PC/PD mixtures covered the expected range of PD content within PAs. Hence, it was hypothesised that it could also reflect the intensity changes from diverse PD content within PAs in the ^{13}C CPMAS NMR analysis. The artificial mixtures of purified PA fractions were then analysed by ^{13}C CPMAS NMR and the I_{132}/I_{155} ratio gave a linear response with the PD content within total PAs (Figure 6.5 b).
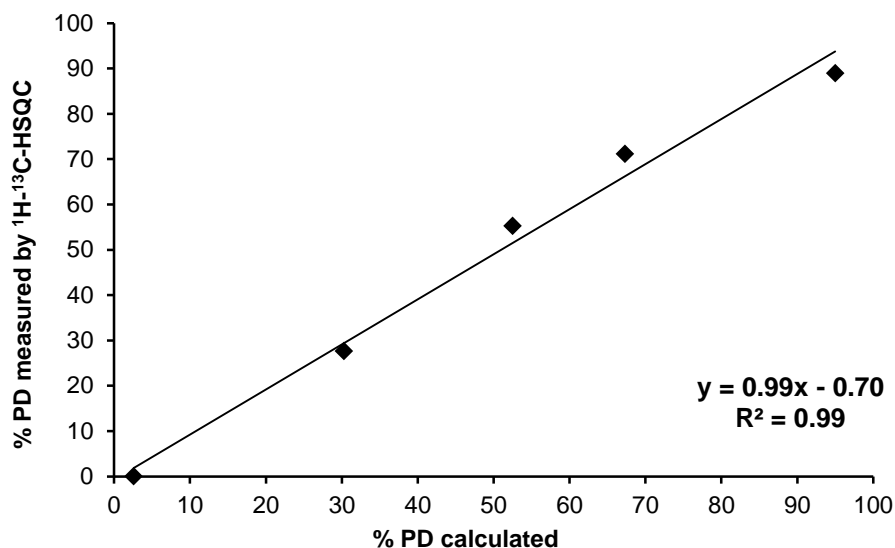
Figure 6.4: Correlation between calculated and measured values of % prodelphinidin (PD) within proanthocyanidins by ^1H-^{13}C HSQC NMR in the PC/PD mixtures. The PC/PD mixtures were prepared from purified Tilia (PC-rich) and purified black currant (PD-rich) PAs with fixed ratios (10/0, 7/3, 1/1, 3/7, 0/10) in mg of total PAs. (%PC = 100 - %PD)

However, the experimental error which was calculated as explained in Section 6.3.2 was ca 16%. It is possible that the overlap of the lines during fitting could have resulted in a larger error. Since, the aim of this study was to estimate PC/PD ratios within total PAs directly in plant tissue, mixtures of Tilia and black currant leaves, of unknown PC/PD proportions, were prepared on a plant weight (mg) basis. It was assumed that extraction and purification would not alter their PC/PD proportions within total PAs (Chapter 3, Appendix). Thus, these plant mixtures could construct a calibration curve for the quantification of PC/PD contents within total PAs in plant matrix with ^{13}C CPMAS NMR.

The ^{13}C CPMAS NMR analysis showed that the I_{132}/I_{155} ratios of the milled plant mixtures were considerably larger than those of the purified PA fractions (Figure 6.5). It appeared that there were no matrix interferences in the 155 ppm peak area (Figure 6.2 and 6.5 a) but the 132 ppm peaks of the plant mixtures were noticeably broader than the purified PA fractions which may account for the difference in intensity ratios I_{132}/I_{155} (Figure 6.5 a). The peak broadening in ^{13}C-NMR spectra usually derives from rotational restrictions of the interflavanyl
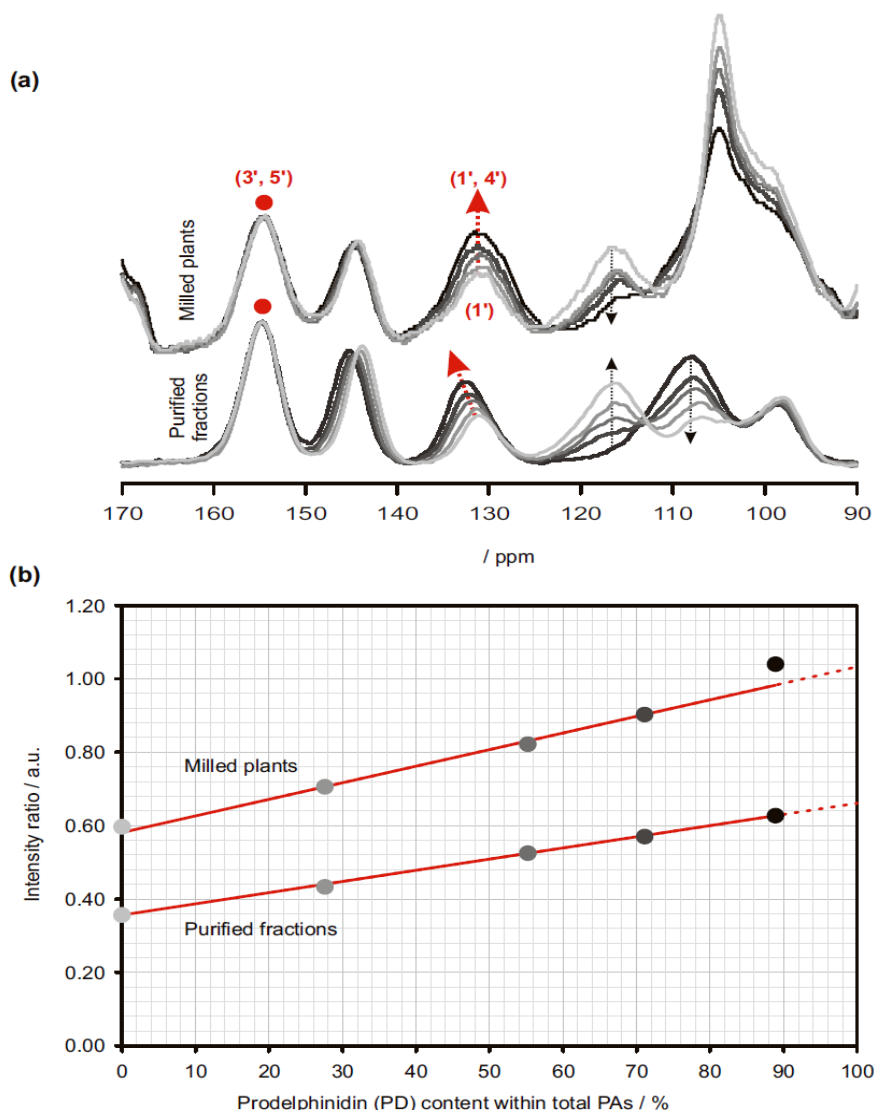
Figure 6.5: (a) Comparison of the selected region of ^{13}C CPMAS NMR spectra recorded for procyanidin (PC) - prodelphinidin (PD) mixtures of purified fractions (bottom) and milled plants (top). The mixtures of purified fractions were prepared from purified Tilia (PC-rich) and Black currant (PD-rich) PAs in fixed PC/PD contents within total (10/0, 7/3, 1/1, 3/7, 0/10). The plant mixtures were prepared by mixing Tilia and black currant milled leaves in fixed amounts (10/0, 7/3, 1/1, 3/7, 0/10 w/w). The increase in the colour intensity of lines (light grey to black), denotes the increase of prodelphinidin content. The signature peak at 132 ppm reflects the changes in prodelphinidin content and a small change in chemical shift (indicated by the red arrows). The black arrows depict other peaks that also reflect spectral differences but are less reliable due to peak overlaps. All signals were normalised to the amplitude of the peak at 155 ppm (red dot) which remains stable in intensity and position and does not suffer from any significant peak overlaps (see Figure 6.1 for structure). (b) The relation between the intensity ratio I_{132}/I_{155} and PD content for the mixtures of purified PA fractions and milled plants. The intensity was calculated as the area under the corresponding peak (I132 or I155) by fitting the Gaussian lines to the recorded ^{13}C CPMAS NMR spectrum (see Figure 6.6). The dots denote the experimental points and the red lines show fitted linear dependence.

linkages and is indicative of large degrees of polymerisation [41]. It has been reported previously that PAs in some plant extracts have lower mDP values than plant PAs [16, 48]. Thus, the differences in peak width between purified and plant PA spectra could also be explained by plant PAs having larger polymers than the extracted or purified PAs. Peak broadening is also often linked to heterogeneity deriving from partial or complete molecular disorder [40]. At this stage it is not possible to estimate how mDP or heterogeneity has affected peak widths in purified PA and milled plant spectra. According to Preston et al., packing differences of milled plant and purified PAs could also account for broadening of peak shapes in particular from carbons near to linkage points [39]. Moreover, the peak shift towards 130 ppm in purified PA fractions was linked to the increase of PC content within PAs, but this was not apparent in plant sample spectra (Figure 6.5 a). This may indicate that other plant compounds, such as lignin, could have affected this PA peak at 132 ppm [37, 41]. The above issues and the experimental error could lead to the conclusion that estimation of PC/PD contents within total PAs by solid state NMR remains a challenge. However, despite the peak broadening and the background interferences, the trend of calibration curve for the milled plant mixtures was the same as for the artificial mixtures of purified PAs. Consequently there is some potential for ranking sainfoin samples according to PC/PD contents within total PAs by ^{13}C CPMAS NMR.

6.3.5 Analysis of sainfoin tissues with ^{13}C CPMAS NMR

The above method was then used to estimate PA concentrations and PC/PD contents within PAs of different sainfoin samples. The results were compared to those obtained by *in situ* thiolysis and the HCl-butanol assay in order to evaluate this newly developed ^{13}C CPMAS NMR method for PA analysis.

6.3.5.1 Estimation of proanthocyanidin content

The results for PA contents from the three methods are presented in Table 6.1. In brief, proanthocyanidin contents determined by ^{13}C CPMAS NMR ranged from 143 (S7, Perly) to 214 mg PAs/g plant (S3, Cholderton). Proanthocyanidin contents obtained from thiolysis-HPLC analysis ranged from 5.33 (S7, Perly) to 99.8 mg PAs/g plant (S3, Cholderton) and the HCl-butanol results from 42.9 (S6,

Zeus) to 87.7 mg PAs/g plant (S3, Cholderton). Whilst PA contents from thiolysis and HCl-butanol assays were highly correlated (R^2 = 0.90), they were very different from ^{13}C CPMAS NMR results (Table 6.1) and PA contents also differed between thiolysis and HCl-butanol assay [49]. In general, higher PA contents were determined by ^{13}C CPMAS NMR followed by HCl-butanol and thiolysis results.

Table 6.1: Proanthocyanidin (PA) contents (mg/g plant) and procyanidin proportions (PC) within total proanthocyanidins determined by ^{13}C CPMAS NMR, thiolysis-HPLC analysis and the HCl-butanol assay. Standard deviation in brackets (*n=2*); the experimental error in the ^{13}C CPMAS NMR values was ± 80 mg/g for the proanthocyanidin content and ± 20 mg PCs/100 mg of PAs for the procyanidin content within total proanthocyanidins; nt: not tested.

Sainfoin sample	Accession	PA mg/g of plant			PC mg/100 mg PAs	
		^{13}C CPMAS NMR	Thiolysis	HCl-butanol	^{13}C CPMAS NMR	Thiolysis
S1	Zeus	155	15.3 (0.601)	49.5 (1.56)	20.0	23.0 (3.08)
S2	Zeus	159	33.8 (2.55)	52.7 (1.56)	30.0	17.5 (0.055)
S3	Cholderton	214	99.8 (0.530)	87.7 (3.21)	50.0	18.6 (0.031)
S4	Hampshire	137	51.6 (2.40)	70.8 (2.69)	30.0	19.2 (0.061)
S5	Ambra	182	52.2 (3.98)	nt	30.0	18.8 (0.069)
S6	Zeus	145	17.2 (0.403)	42.9 (1.28)	10.0	17.5 (0.131)
S7	Perly	143	5.33 (0.064)	50.8 (0.901)	20.0	17.8 (0.759)
S8	Cotswold Common	188	41.9	nt	20.0	18.8

Previous studies suggested that the limitations of ^{13}C CPMAS NMR spectroscopy usually do not allow for the accurate quantification of PAs [36, 40]. The polymeric nature of plant PAs hampers the direct correlation of signal intensity to fixed carbon atom amounts [36]. The technique of CP depends on proton abundance of the neighbouring environment for improving the ^{13}C signal [36, 40]. However, the efficiency of this enhancement depends strongly on molecular dynamics and relaxation behaviour, which are difficult to fully control in NMR experiments. These factors are unlikely to be the same for all carbons at sample

and will also vary between different plant matrices. As an example, quaternary and methyl carbons, as well as very mobile structures have shown less efficient CP [36, 40, 46]. In addition, an optimal relationship between CP dynamics and relaxation time cannot be anticipated for all carbons [36]. It is possible that the proton environment of the more complex and possibly larger sainfoin PAs may have resulted in a signal enhancement compared to the purified PC-rich Tilia PAs and this could account for the PA concentration differences between ^{13}C CPMAS NMR and HCl-butanol or thiolysis results.

Although the dipolar-dephasing experiments showed no overlap from impurities at 155 ppm, several studies have expressed caution when quantifying PAs as cutin [42, 50] but more importantly lignin may interfere with peaks assigned to phenolic PA rings [38, 39, 41]. A resolved peak at 56 ppm of the sainfoin ^{13}C CPMAS NMR spectra (Figure 6.6) was previously assigned to OCH_3 group of lignin [36, 39, 50] and indicated the possibility of lignin presence in sainfoin samples but also in the plant samples from Tilia and Black currant (Figures 6.2). This could indicate a lignin contribution to the peak signal at 155 ppm despite our initial assessments and could suggest another reason of the discrepancies of these different PA quantification methods.

However, another reason for these discrepancies in PA contents of the three methods may stem from the limitations of the thiolysis and HCl-butanol assays in quantifying PAs directly in plant tissue as well [16, 17]. It was shown that longer reaction times with benzyl mercaptan (up to 24 hours rather than an hour) resulted in considerably higher concentrations [25]. It is well known that free flavan-3-ols interfere with PA quantification by thiolysis [51] but these were not analysed due to the negligible amounts reported in mature sainfoin plants [25]. In addition, some evidence exists for thiolysis resistant PAs [19, 52]. Therefore, lower PA contents by thiolysis than ^{13}C CPMAS NMR are to be expected.

Despite its wide use, the HCl-butanol assay often underestimates total PA content when the reagent is applied directly to plant material or extraction residues [22, 53]. This limitation derives mainly from the inefficiency of the reagent to quantitatively interact with bound and insoluble PAs [22]. Other assay parameters have also been reported to impede accurate PA quantification [17]. A thorough study by Grabber et al. investigated recently the impact of a co-solvent, iron concentration, heating temperature and time on total PA content of leaves and

herbages from two *Lotus* species with contrasting PAs [34]. The addition of acetone as a co-solvent in the reaction solution improved the assay performance over the conventional assay. The use of purified *Lotus* PAs as standards was also important for quantification. Collection of ^{13}C gel-state and ^{1}H-^{13}C HSQC NMR spectra from the residues after the HCl-butanol-acetone reaction demonstrated the complete degradation of insoluble PAs into anthocyanidins [34]. Therefore, this particular HCl-butanol method was used to compare total PA contents with results from ^{13}C CPMAS NMR and thiolysis. The large discrepancies between these results may perhaps point to the occurrence of more diverse PA mixtures in sainfoin compared to *Lotus* species and considerable amounts of insoluble PAs. In addition, Grabber et al. [34] isolated PA standards from the same *Lotus* sample which improved quantification but this approach was not followed in the present study. Regarding that PA composition is cultivar specific [26] and that PDs yield more colour than PCs [34] the use of one standard for samples from various accessions, may also have contributed to these PA differences.

6.3.5.2 Estimation of procyanidin proportions within total proanthocyanidins

The PC proportions within total PAs in sainfoin samples ranged from 17.5 mg PCs/100 mg PAs (S2, S6 Zeus) to 23.0 mg PCs/100 mg PAs (S1, Zeus) as determined by thiolysis, and from 10.0 mg PCs/100 mg PAs (S6 Zeus) to 50.0 mg PCs/100 mg PAs (S3, Cholderton) as determined by ^{13}C CPMAS NMR (Table 6.1).

The discussion in Section 6.3.3 described the factors that could have contributed to peak broadening at 132 ppm and would have affected the intensity ratio I_{132}/I_{155} that was used to estimate the PC content within PAs. This resulted in an experimental error of ca. 16% for ^{13}C CPMAS NMR analysis and could reflect the PC content differences between the methods.

Broadening of the resonances in the milled plant spectra could also be due to the presence of high MW PAs [27, 34]. Peak signals from C6 and C8 sites at 97-98 ppm were less intense and better resolved in the artificial purified PA mixtures in contrast to the milled plant spectra where they appeared as a shoulder of the peak at 105-103 ppm from the sites C4-C6 and C4a [54] (Figure 6.2)

denoting the presence of high MW PAs. It is possible that such peak broadening could explain why the largest PC content difference was observed for S3 (Table 6.1) which had the highest PA content and mDP value. However, another cause could be the PA differences between sainfoin samples (Figure 6.6 a) and milled plants of Tilia and black currant that were used as model standards (Figure 6.2).
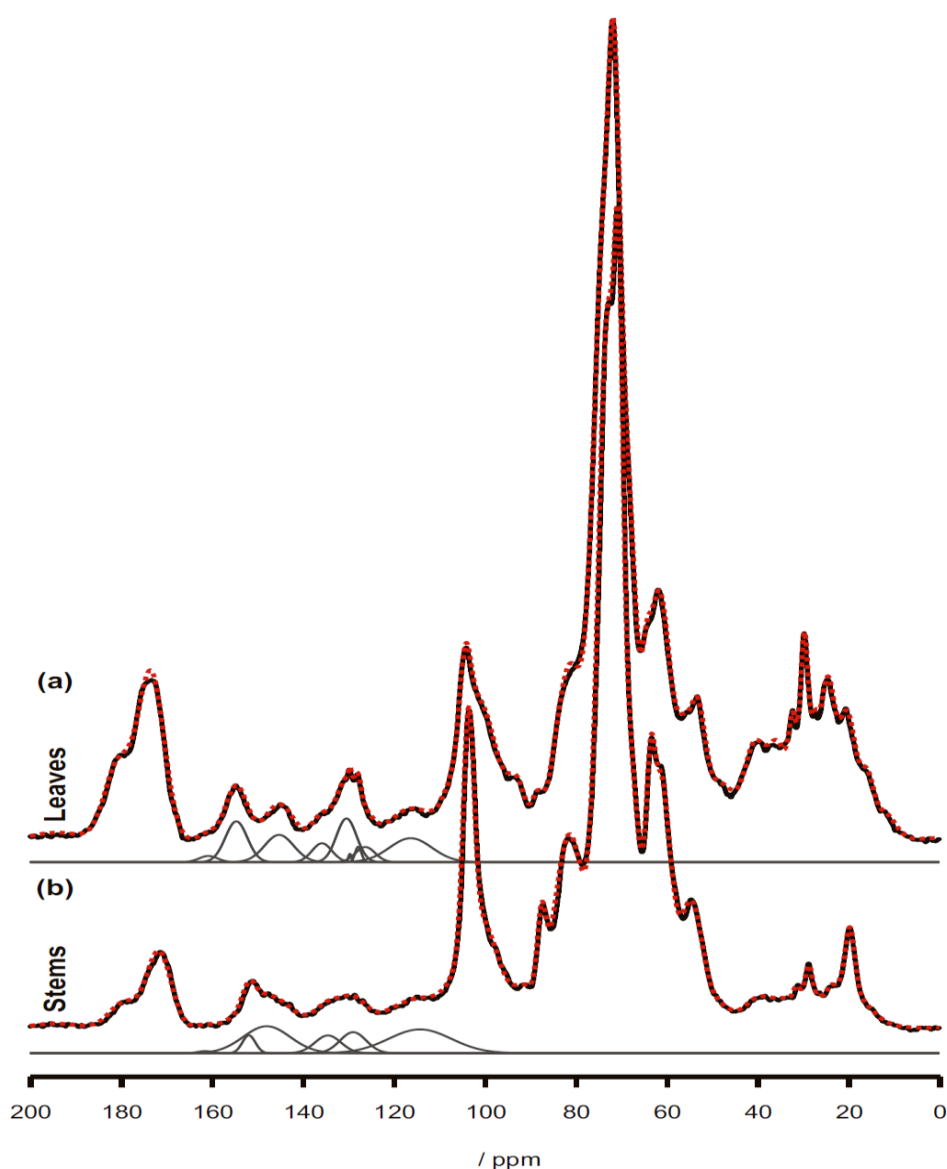
Figure 6.6: Fingerprint ^{13}C CPMAS NMR spectra from sainfoin leaves (a) and stems (b). Both spectra were fitted using the sum of Gaussian shape lines. All lines were centred at the peak positions of the recorded ^{13}C CPMAS NMR spectrum. The result of the fit is superimposed on the original spectrum (red dotted lines). The grey lines below show Gaussian lines used to fit the corresponding region of the spectrum. The peak intensities from this region were used to estimate proanthocyanidin concentration and procyanidin/prodelphinidin contents with PAs.

Problematic thiolytic degradation of PAs has been often linked with structural characteristics, such as polymer size and PD presence [11, 25]. Time course studies of *in situ* thiolysis on sainfoin, presented an increase in PD contents within total PAs after long reaction times and was correlated with high MW PAs [23, 25]. This observation suggested that the benzyl mercaptan could not easily react with large polymers that consisted of PD-type flavan-3-ols. However, in this study, the *in situ* thiolysis yielded actually higher PD content values (i.e. lower PC content values) than the ^{13}C CPMAS NMR experiments.

Previous work on sainfoin showed that stems contain lower PA amounts compared to leaves (Chapter 4, [10, 55]). This information could be also gained by a rapid qualitative assessment of the ^{13}C CPMAS NMR spectra (Figure 6.6 b). The stem spectra showed poor resolution of peaks at 155 and 144 ppm and a broad peak at 132 ppm denoting a lower PA content and possibly also a different PA composition than leaves. This peak broadening prevented the estimation of PC/PD contents within total PAs. These results indicated that the ^{13}C CPMAS NMR method may enable the discrimination of different plant organs based on their PA spectra; however, further work would be needed to confirm these observations.

6.4 Conclusions

This chapter reported a first attempt to develop a ^{13}C CPMAS NMR method for the direct screening of PAs in sainfoin plant tissues. By using contrasting signature PA spectra from black currant and Tilia leaves, peak assignments could be made and a calibration for PAs was developed based on signal intensities. However, there were surprisingly large discrepancies between the PA concentrations obtained by thiolysis or the HCl-butanol assay and the ^{13}C CPMAS NMR method. These discrepancies may have arisen from the presence of interfering plant components (i.e. flavonoids). It is also possible that the differences in size and mobility between model and sainfoin PAs could account for these differences. Nevertheless, preliminary evidence was indeed obtained for the latter as a sainfoin sample with large MW PAs also gave rise to the largest difference. Future work will need to evaluate the impact of constituents with similar structures on PA quantification and estimation of PC/PD contents within PAs and refine the method. The present study used PC- and PD-rich samples with a

relatively narrow range of average polymer size as standards which could have had a negative influence on the quantification of the highly complex sainfoin PAs. However, the large differences between thiolysis, HCl-butanol assay and the ^{13}C CPMAS NMR method together with the recognised limitations of both chemical assays, highlighted continuing challenges of PA analysis and the need to review the established chemical methods.

To our knowledge this is the first time ^{13}C CPMAS NMR has been used to evaluate PA contents and compositions in sainfoin tissues. The results indicate that this method should be used with caution for quantitative PA analysis as further investigations will be necessary and that a wide range of purified PA fractions and milled plant samples will need to be used. This study indicated that the NMR technique may allow the discrimination of different sainfoin organs, PD-rich accessions and the ranking of PA concentrations. Libraries with contrasting signature PA spectra may allow widening the use of ^{13}C CPMAS NMR to other plant materials. Thus, this method has potential to provide a new approach to analyse PAs in whole plants rather than extracts and this could be of interest in future research as unextractable PAs may have biological activities that are not been yet recognised in the digestive tract.

References

1.   Sottie ET, Acharya SN, McAllister T, Thomas J, Wang Y, Iwaasa A: **Alfalfa pasture bloat can be eliminated by intermixing with newly-developed sainfoin population.** *Agronomy Journal* 2014, 106(4):1470-1478.

2.   Mueller-Harvey I: **Unravelling the conundrum of tannins in animal nutrition and health.** *Journal of the Science of Food and Agriculture* 2006, 86(13):2010-2037.

3.   Hoste H, Martinez-Ortiz-De-Montellano C, Manolaraki F, Brunet S, Ojeda-Robertos N, Fourquaux I, Torres-Acosta JF, Sandoval-Castro CA: **Direct and indirect effects of bioactive tannin-rich tropical and temperate legumes against nematode infections.** *Veterinary Parasitology* 2012, 186(1-2):18-27.

4.   Manolaraki F, Sotiraki S, Stefanakis A, Skampardonis V, Volanis M, Hoste H: **Anthelmintic activity of some Mediterranean browse plants against parasitic nematodes.** *Parasitology* 2010, 137(4):685-696.

5.   Chung YH, Mc Geough EJ, Acharya S, McAllister TA, McGinn SM, Harstad OM, Beauchemin KA: **Enteric methane emission, diet digestibility, and nitrogen excretion from beef heifers fed sainfoin or alfalfa.** *Journal of Animal Science* 2013, 91(10):4861-4874.

6.   Wang YX, McAllister TA, Acharya S: **Condensed tannins in sainfoin: Composition, concentration, and effects on nutritive and feeding value of sainfoin forage.** *Crop Science* 2015, 55(1):13-22.

7.   McMahon LR, Majak W, McAllister TA, Hall JW, Jones GA, Popp JD, Cheng KJ: **Effect of sainfoin on *in vitro* digestion of fresh alfalfa and bloat in steers.** *Canadian Journal of Animal Science* 1999, 79(2):203-212.

8.   Girard M, Dohme-Meier F, Wechsler D, Goy D, Kreuzer M, Bee G: **Ability of 3 tanniferous forage legumes to modify quality of milk and Gruyere-type cheese.** *Journal of Dairy Science* 2016, 99(1):205-220.

9.   Regos I, Urbanella A, Treutter D: **Identification and quantification of phenolic compounds from the forage legume sainfoin (*Onobrychis viciifolia*).** *Journal of Agricultural and Food Chemistry* 2009, 57(13):5843-5852.

10.   Malisch CS, Luscher A, Baert N, Engstrom MT, Studer B, Fryganas C, Suter D, Mueller-Harvey I, Salminen JP: **Large variability of proanthocyanidin content and composition in sainfoin (*Onobrychis viciifolia*).** *Journal of Agricultural and Food Chemistry* 2015, 63(47):10234-10242.

11.   Stringano E, Hayot Carbonero C, Smith LM, Brown RH, Mueller-Harvey I: **Proanthocyanidin diversity in the EU 'HealthyHay' sainfoin (*Onobrychis viciifolia*) germplasm collection.** *Phytochemistry* 2012, 77:197-208.

12.   Quijada J, Fryganas C, Ropiak HM, Ramsay A, Mueller-Harvey I, Hoste H: **Anthelmintic activities against *Haemonchus contortus* or *Trichostrongylus colubriformis* from small ruminants are influenced by structural features of condensed tannins.** *Journal of Agricultural and Food Chemistry* 2015, 63(28):6346-6354.

13.   Novobilsky A, Stringano E, Hayot Carbonero C, Smith LM, Enemark HL, Mueller-Harvey I, Thamsborg SM: ***In vitro* effects of extracts and purified tannins of sainfoin (*Onobrychis viciifolia*) against two cattle nematodes.** *Veterinary Parasitology* 2013, 196(3-4):532-537.

14. Williams AR, Fryganas C, Ramsay A, Mueller-Harvey I, Thamsborg SM: **Direct anthelmintic effects of condensed tannins from diverse plant sources against *Ascaris suum*.** *PLoS One* 2014, 9(5):e97053.

15. Hatew B, Hayot Carbonero C, Stringano E, Sales LF, Smith LMJ, Mueller-Harvey I, Hendriks WH, Pellikaan WF: **Diversity of condensed tannin structures affects rumenin vitromethane production in sainfoin (*Onobrychis viciifolia*) accessions.** *Grass and Forage Science* 2015, 70(3):474-490.

16. Hummer W, Schreier P: **Analysis of proanthocyanidins.** *Molecular Nutrition & Food Research* 2008, 52(12):1381-1398.

17. Schofield P, Mbugua DM, Pell AN: **Analysis of condensed tannins: A review.** *Animal Feed Science and Technology* 2001, 91(1-2):21-40.

18. Engstrom MT, Palijarvi M, Fryganas C, Grabber JH, Mueller-Harvey I, Salminen JP: **Rapid qualitative and quantitative analyses of proanthocyanidin oligomers and polymers by UPLC-MS/MS.** *Journal of Agricultural and Food Chemistry* 2014, 62(15):3390-3399.

19. Matthews S, Mila I, Scalbert A, Donnelly DMX: **Extractable and non-extractable proanthocyanidins in barks.** *Phytochemistry* 1997, 45(2):405-410.

20. Dalzell SA, Kerven GL: **A rapid method for the measurement of *Leucaena* spp proanthocyanidins by the proanthocyanidin (butanol/HCl) assay.** *Journal of the Science of Food and Agriculture* 1998, 78(3):405-416.

21. Perez-Jimenez J, Arranz S, Saura-Calixto F: **Proanthocyanidin content in foods is largely underestimated in the literature data: An approach to quantification of the missing proanthocyanidins.** *Food Research International* 2009, 42(10):1381-1388.

22. Makkar HPS, Gamble G, Becker K: **Limitation of the butanol-hydrochloric acid-iron assay for bound condensed tannins.** *Food Chemistry* 1999, 66(1):129-133.

23. Callemien D, Guyot S, Collin S: **Use of thiolysis hyphenated to RP-HPLC-ESI(-)-MS/MS for the analysis of flavanoids in fresh lager beers.** *Food Chemistry* 2008, 110(4):1012-1018.

24. Wayne McGraw G, Steynberg JP, Hemingway RW: **Condensed tannins: A novel rearrangement of procyanidins and prodelphinidins in thiolytic cleavage.** *Tetrahedron Letters* 1993, 34(6):987-990.

25. Gea A, Stringano E, Brown RH, Mueller-Harvey I: ***In situ* analysis and structural elucidation of sainfoin (*Onobrychis viciifolia*) tannins for high-throughput germplasm screening.** *Journal of Agricultural and Food chemistry* 2011, 59(2):495-503.

26. Marais JP, Mueller-Harvey I, Brandt EV, Ferreira D: **Polyphenols, condensed tannins, and other natural products in *Onobrychis viciifolia* (sainfoin).** *Journal of Agricultural and Food chemistry* 2000, 48(8):3440-3447.

27. Czochanska Z, Foo LY, Newman RH, Porter LJ, Thomas WA, Jones WT: **Direct proof of a homogeneous polyflavan-3-ol structure for polymeric proanthocyanidins.** *Journal of the Chemical Society, Chemical Communications* 1979(8):375-377.

28. Czochanska Z, Foo LY, Newman RH, Porter LJ: **Polymeric proanthocyanidins - stereochemistry, structural units, and molecular-weight.** *Journal of the Chemical Society, Perkin Transactions 1* 1980(10):2278-2286.

29. Foo LY, Lu Y, Molan AL, Woodfield DR, McNabb WC: **The phenols and prodelphinidins of white clover flowers.** *Phytochemistry* 2000, 54(5):539-548.

30. Qaadan F, Nahrstedt A, Schmidt M, Mansoor K: **Polyphenols from *Ginkgo biloba*.** *Scientia Pharmaceutica* 2010, 78(4):897-907.

31.   Chai WM, Shi Y, Feng HL, Qiu L, Zhou HC, Deng ZW, Yan CL, Chen QX: **NMR, HPLC-ESI-MS, and MALDI-TOF MS analysis of condensed tannins from *Delonix regia* (Bojer ex Hook.) Raf. and their bioactivities.** *Journal of Agricultural and Food Chemistry* 2012, 60(19):5013-5022.

32.   Zhang LL, Lin YM, Zhou HC, Wei SD, Chen JH: **Condensed tannins from mangrove species *Kandelia candel* and *Rhizophora mangle* and their antioxidant activity.** *Molecules* 2010, 15(1):420-431.

33.   Zeller WE, Ramsay A, Ropiak HM, Fryganas C, Mueller-Harvey I, Brown RH, Drake C, Grabber JH: **(1)H-(13)C HSQC NMR spectroscopy for estimating procyanidin/prodelphinidin and cis/trans-flavan-3-ol ratios of condensed tannin samples: Correlation with thiolysis.** *Journal of Agricultural and Food Chemistry* 2015, 63(7):1967-1973.

34.   Grabber JH, Zeller WE, Mueller-Harvey I: **Acetone enhances the direct analysis of procyanidin- and prodelphinidin-based condensed tannins in *Lotus* species by the butanol-HCl-iron assay.** *Journal of Agricultural and Food Chemistry* 2013, 61(11):2669-2678.

35.   Hellstrom J, Sinkkonen J, Karonen M, Mattila P: **Isolation and structure elucidation of procyanidin oligomers from saskatoon berries (*Amelanchier alnifolia*).** *Journal of Agricultural and Food Chemistry* 2007, 55(1):157-164.

36.   Reid DG, Bonnet SL, Kemp G, van der Westhuizen JH: **Analysis of commercial proanthocyanidins. Part 4: solid state (13)C NMR as a tool for *in situ* analysis of proanthocyanidin tannins, in heartwood and bark of quebracho and acacia, and related species.** *Phytochemistry* 2013, 94(0):243-248.

37.   Grigsby WJ, Hill SJ, McIntosh CD: **NMR estimation of extractables from bark: Analysis method for quantifying tannin extraction from bark.** *Journal of Wood Chemistry and Technology* 2003, 23(2):179-195.

38.   Lorenz K, Preston CM: **Characterization of high-tannin fractions from humus by carbon-13 cross-polarization and magic-angle spinning nuclear magnetic resonance.** *Journal of Environmental Quality* 2002, 31(2):431-436.

39.   Preston CM, Sayer BG: **What's in a nutshell: An investigation of structure by carbon-13 cross-polarization magic-angle spinning nuclear magnetic resonance spectroscopy.** *Journal of Agricultural and Food Chemistry* 1992, 40(2):206-210.

40.   Romer FH, Underwood AP, Senekal ND, Bonnet SL, Duer MJ, Reid DG, van der Westhuizen JH: **Tannin fingerprinting in vegetable tanned leather by solid state NMR spectroscopy and comparison with leathers tanned by other processes.** *Molecules* 2011, 16(2):1240-1252.

41.   Wawer I, Wolniak M, Paradowska K: **Solid state NMR study of dietary fiber powders from aronia, bilberry, black currant and apple.** *Solid State Nuclear Magnetic Resonance* 2006, 30(2):106-113.

42.   Gamble GR, Akin DE, Makkar HP, Becker K: **Biological degradation of tannins in sericea lespedeza (*Lespedeza cuneata*) by the white rot fungi *Ceriporiopsis subvermispora* and *Cyathus stercoreus* analyzed by solid-state (13)C nuclear magnetic resonance spectroscopy.** *Applied and Environmental Microbiology* 1996, 62(10):3600-3604.

43.   Novobilsky A, Mueller-Harvey I, Thamsborg SM: **Condensed tannins act against cattle nematodes.** *Veterinary Parasitology* 2011, 182(2-4):213-220.

44.   Ropiak HM, Ramsay A, Mueller-Harvey I: **Condensed tannins in extracts from European medicinal plants and herbal products.** *Journal of Pharmaceutical and Biomedical Analysis* 2016, 121:225-231.

45.   Newman R, Porter L: **Solid state 13(C) NMR studies on condensed tannins.** In: *Plant Polyphenols.* Edited by Hemingway R, Laks P, vol. 59: Springer US; 1992: 339-347.

46.   Maie N, Behrens A, Knicker H, Kogel-Knabner I: **Changes in the structure and protein binding ability of condensed tannins during decomposition of fresh needles and leaves.** *Soil Biology & Biochemistry* 2003, 35(4):577-589.

47.   Quideau SA, Graham RC, Oh SW, Hendrix PF, Wasylishen RE: **Leaf litter decomposition in a chaparral ecosystem, Southern California.** *Soil Biology & Biochemistry* 2005, 37(11):1988-1998.

48.   Stringano E: **Analysis of sainfoin (*Onobrychis viciifolia*) proanthocyanidins by complementary and newly developed techniques.** *PhD thesis*, University of Reading; 2011.

49.   Azuhnwi BN, Boller B, Dohme-Meier F, Hess HD, Kreuzer M, Stringano E, Mueller-Harvey I: **Exploring variation in proanthocyanidin composition and content of sainfoin (*Onobrychis viciifolia*).** *Journal of the Science of Food and Agriculture* 2013, 93(9):2102-2109.

50.   Parfitt RL, Newman RH: **13(C) NMR study of pine needle decomposition.** *Plant and Soil* 2000, 219(1/2):273-278.

51.   Guyot S, Marnet N, Sanoner P, Drilleau J-F: **Direct thiolysis on crude apple materials for high-performance liquid chromatography characterization and quantification of polyphenols in cider apple tissues and juices.** In: *Methods in Enzymology.* Edited by Lester P, vol. Volume 335: Academic Press; 2001: 57-70.

52.   Matthews S, Mila I, Scalbert A, Pollet B, Lapierre C, duPenhoat CLMH, Rolando C, Donnelly DMX: Method for estimation of proanthocyanidins based on their acid depolymerization in the presence of nucleophiles. *Journal of Agricultural and Food Chemistry* 1997, 45(4):1195-1201.

53.   **Wolfe RM, Terrill TH, Muir JP: Drying method and origin of standard affect condensed tannin (CT) concentrations in perennial herbaceous legumes using simplified butanol-HCl CT analysis.** *Journal of the Science of Food and Agriculture* 2008, 88(6):1060-1067.

54.   Hoong YB, Pizzi A, Md. Tahir P, Pasch H: **Characterization of *Acacia mangium* polyflavonoid tannins by MALDI-TOF mass spectrometry and CP-MAS 13(C) NMR.** *European Polymer Journal* 2010, 46(6):1268-1277.

55.   Theodoridou K, Aufrere J, Andueza D, Pourrat J, Le Morvan A, Stringano E, Mueller-Harvey I, Baumont R: **Effects of condensed tannins in fresh sainfoin (*Onobrychis viciifolia*) on *in vivo* and *in situ* digestion in sheep.** *Animal Feed Science and Technology* 2010, 160(1-2):23-38.

Chapter 7. General discussion and conclusions

The first section of this chapter (Section 7.1) summarises the most important findings of proanthocyanidin (PA) analysis in acetone/water extracts and purified fractions from various plant sources, using several analytical techniques. For the sainfoin extracts, it also includes a comparison between the thiolysis-HPLC and UPLC-ESI-MS/MS methods for the PA characterisation. Finally it describes the development of a new method for screening sainfoin PAs with ^{13}C CPMAS NMR directly in plant tissues.

Collaborating studies, in the "LegumePlus" and related projects, used these well-characterised acetone/water extracts and fractions in order to develop novel methods for PA analysis and the key findings are presented in the second section (Section 7.2). Section 7.3 summarises the highlights from the key biological effects that were obtained with these model PA samples during my parasitology secondment in INRA/ENVT (Toulouse, France) and through collaborations in the "LegumePlus" and other projects.

7.1 Analysis of model and sainfoin proanthocyanidins

An initial screening with HCl-butanol assay identified potentially useful sources for PAs, and the subsequent thiolysis-HPLC analysis of acetone/water extracts, prepared from these samples, enabled the selection of seeds and plants with wide a range of PA contents and compositions. The final set of plants was selected based on PA content, contrasting structural features, availability of resources and simplicity of sample preparation. All acetone/water extracts and two purified PA fractions, which were eluted from Sephadex^{TM} LH-20 columns, were analysed by thiolysis-HPLC. This demonstrated that these PA samples covered a wide range of concentrations and compositions in terms of mDP, PC/PD and *cis/trans* ratios in agreement with the literature (Tables A.1 and A.2, Chapter 2-3) [1-3]. These PA samples had mDP values that ranged from 2 to 10, PC contents ranged from 1.2 to 96 mg PCs/100 mg PAs (with the rest being PDs) and *cis*-flavan-3-ol contents ranged from 2.8 to 80 mg *cis* flavan-3-ols/100 mg PAs (with the rest being *trans*-flavan-3-ols) whilst the PA concentration ranged from 116 to 1000 mg PAs/g extract. Therefore, these model PA samples were used for the development of analytical methods, for instrument calibrations and bioactivity studies.

Several studies have pointed out the limitations of some of the widely used methods for PA analysis to elucidate the complexity of PA polymers in terms of PA contents, degree of polymerisation, composition and stereochemistry of their flavan-3-ol subunits and also to provide information on distribution profiles of individual PA molecules [4-9]. Therefore, some authors have recommended the use of several analytical techniques that can provide complementary information on PAs [10-13]. Chapter 3 characterised purified fractions of model PAs with several analytical methods and critically evaluated the results and the pros and cons of each method. In general, results from the thiolysis-HPLC, UPLC-ESI-MS/MS and ^{1}H-^{13}C HSQC NMR analyses correlated very well (see Chapter 3). The total PC and PD contents (in mg/g fraction) determined by thiolysis-HPLC and UPLC-ESI-MS/MS showed excellent correlations (R^2=0.93 and 0.98, respectively). Some content deviations between the thiolysis-HPLC and UPLC-ESI-MS/MS stressed that the selection of quantification standards can still pose problems in PA analysis. A good correlation of mDP values was also obtained by thiolysis and UPLC-ESI-MS/MS analysis (R^2=0.76). However, the small number of samples led to lower correlations for the mDP values between ^{1}H-^{13}C HSQC NMR and the other two quantitative methods (thiolysis vs ^{1}H-^{13}C HSQC NMR, R^2=0.67 and UPLC-ESI-MS/MS vs ^{1}H-^{13}C HSQC NMR, R^2=0.47). In contrast, PC and PD contents within total PAs presented excellent correlations between methods (thiolysis vs ^{1}H-^{13}C HSQC NMR, R^2=0.99, UPLC-ESI-MS/MS vs ^{1}H-^{13}C HSQC NMR, R^2=0.99 and thiolysis vs UPLC-ESI-MS/MS, R^2=0.99). However, information on *cis/trans* flavan-3-ols was only available via thiolysis-HPLC. The MALDI-TOF MS and HILIC-DAD-ESI-TOF-MS analyses complemented the information from thiolysis-HPLC and UPLC-ESI-MS/MS methods on PC/PD ratios by detecting individual oligomers and polymers. However, both methods currently do not provide quantitative data on individual PA compounds. It was also noticed that PA hetero-polymers did not necessarily elute from the HILIC column on a MW basis. Matrix interferences also affected the detection of PAs with mass spectrometry techniques and ^{1}H-^{13}C HSQC NMR. To my knowledge this is the first time that these state-of-the-art analytical tools were compared for their suitability to characterise a wide range of PA samples in terms of PA contents and compositions.

Acetone/water extracts from sainfoin were analysed with thiolysis-HPLC and UPLC-ESI-MS/MS (Chapter 4) and demonstrated considerable quantitative and qualitative diversity of PAs among sainfoin accessions and plant parts. The high PA contents, determined by the two methods, were positively correlated with high PD contents (P<0.01) and high mDP values (P<0.01). Leaf extracts contained much higher PA contents than stem extracts. The PA contents in leaves, ranged from 63 to 231 mg PAs/g of extract, determined by thiolysis, and from 45 to 155 mg PAs/g of extract determined by UPLC-ESI-MS/MS. The PA contents in stems ranged from 5.8 to 89.4 mg PAs/g of extract when determined by thiolysis and from 8.5 to 63.5 mg PAs/g of extract when determined by UPLC-ESI-MS/MS. A positive correlation (P<0.01) was also found between PD contents (mg PDs/100 mg of PAs) and mDPs. In general, leaves consisted of complex mixtures of large PD-based PA structures. Thiolysis results for the PC contents ranged from 3.2 to 47 mg PCs/100 mg of PAs whereas the UPLC-ESI-MS/MS results ranged from 3.3 to 37 mg PCs/100 mg of PAs. Stems, in contrast, tended to have higher proportions of PCs. The PC content in stems ranged from 12 to 100 mg PCs/100 mg of PAs, determined by thiolysis and from 12.7 to 89 mg PCs/100 mg determined by UPLC-ESI-MS/MS. Both methods generated good correlations for PA contents (R^2=0.85) and PC, PD proportions within total PAs (R^2=0.96). The computing of Bland-Altman plots suggested that sample matrices continue to pose analytical challenges and thus the currently available methods do need further refinement. It is apparent that none of these PA analysis methods are robust enough to be used on their own. The low limits of agreement (LoA), therefore, suggested that the selection of an analytical method needs to be based on the research purpose. For example, the rapid data acquisition by the new UPLC-ESI-MS/MS method suggested that it would be suitable for the high throughput screening of extractable PAs. In addition, this MS/MS method provided information on the distribution of PA terminal and extension units via multiple reaction monitoring (MRM) chromatograms, which allowed a visual differentiation between diverse PAs that resulted from different growth stages, sample processing methods and plant parts. Further analysis of these unique extracts by thiolysis-HPLC could complement the information on PA composition by providing information on the stereochemistry of flavan-3-ol subunits and could be used to validate the quantitative results.

It is possible that animal nutrition and health and, therefore, plant breeding might benefit from information on both extractable and insoluble PAs in plant tissues as animals eat whole plants and not just solvent extractable compounds. However, the HCl-butanol and thiolysis that are currently used for *in situ* PA analysis suffer from limitations [4, 9]. For instance, the HCl-butanol assay does not provide information on structural characteristics and some bound PAs can be thiolysis resistant [14, 15]. For these reasons, the feasibility of developing a method that could deliver quantitative data on PA contents and compositions directly from plant tissues was explored. Chapter 6 described the development of a ^{13}C CPMAS NMR method, which also used purified model PAs as standards in order to determine PA contents and compositions directly in milled sainfoin samples. The results indicated that the method could be used to distinguish between plant organs, i.e. leaves and stems, to rank accessions according to PA contents with an experimental error up to 8% and to identify those with diverse PC and PD proprotions within total PAs with an experimental error up to 16%. However, PA quantitation by ^{13}C CPMAS NMR strongly depended on the suitability of the model PAs used for signal calibrations and on interferences from matrix constituents with the signature PA peaks in the spectra. Nevertheless, this method may hold promise for the analysis of total PAs in plants, as it is should be able to detect extractable and unextractable PAs that may also impact on bioactivity.

7.2   Collaborative studies on proanthocyanidin analysis

Purified PA samples from goat willow leaves and white clover flowers (Table 3.2) were used to construct calibration curves for quantification of PCs and PDs with a new UPLC-ESI-MS/MS method developed by colleagues at the University of Turku (Turku, Finland) (Appendix B) [16]. The method optimised cone voltage ionisations in order to fragment the PAs. Subsequent fragmentation in the collision cell and the recording of precursor-daughter ions in a range of MRM experiments provided quantitative information on mDP values, contents of PAs, PC and PD, terminal and extension units. It also profiled the distribution of terminal and extension units along the chromatographic hump, which was produced from polymeric PAs. The development of this method then proceeded to utilise my

model PA fractions in order to validate the method for quantification of soluble PAs. In addition, the PA contents, mDP values and PC/PD ratios from the UPLC-ESI-MS/MS analysis were compared to the thiolysis-HPLC data (Table A.1). The correlation between PA contents was good (R^2=0.82) and excellent between mDP values (R^2=0.90) and PC/PD ratios (R^2=0.98) suggesting, for the first time, that a mass spectrometric approach can accurately determine PA contents, average polymer sizes and PC/PD ratios without pre-column PA degradation (i.e. thiolysis). Moreover, the MRM chromatographic fingerprints could also assist the rapid fingerprinting of diverse soluble plant PAs. Therefore, this method can now be added to the analytical tools for determining PA contents and compositions.

Apart from this UPLC-ESI-MS/MS method, my model fractions were also used for the development of a ^{1}H-^{13}C HSQC NMR method (Appendix C) in collaboration with the U.S. Dairy Forage Research Center (Madison, USA). Integrations of selected resonance peaks allowed the determination of PC/PD ratios and *cis/trans*-flavan-3-ol ratios. The results were highly correlated with those obtained from thiolysis-HPLC (R^2=0.99 and R^2=0.89, respectively). This suggested that the ^{1}H-^{13}C HSQC NMR method can be used to validate information on PA structures obtained from thiolysis and added a non-depolymerisation technique to the tools for PA analysis [17].

7.3   Biological effects of different types of proanthocyanidins

7.3.1   Anthelmintic activity of proanthocyanidins

Several of my model PA fractions were also shared with "LegumePlus" partners in order to evaluate their *in vitro* anthelmintic (AH) efficacy against important nematodes from the gastrointestinal tracts of ruminant and monogastric animals (Tables 3.2 and A.1). INRA/ENVT (Toulouse, France) investigated the structure-activity relationships of these fractions with an *in vitro* exsheathment assay of L3 larvae from *Haemonchus contortus* and *Trichostrongylus colubriformis* (Appendix D) [18]. The data showed that lower PA concentrations needed for the exsheathement inhibition of *H. contortus* compared to *T. colubriformis*. This demonstrated that the abomasal *H. contortus* was more susceptible to PAs than the intestinal *T. colubriformis* and suggested different mechanisms of action. As

expected, fractions with higher PA content were more active against L3 from both nematode species. In addition, PD-rich PAs were significantly more potent against the nematodes confirming previous observations [19-21]. However, PA fractions with higher mDP values inhibited *H. contortus* L3 but not *T. colubriformis* L3 exsheathment.

In collaboration with the University of Turku (Turku, Finland), we developed a new purification scheme to prepare a series of PA sub-fractions with narrow ranges of polymer sizes and PD contents (Chapter 5). It was hypothesised that these samples would help to shed light on the structural features that were most important for conferring AH activity. This was important, because previous studies had used highly complex PA mixtures, which had been analysed by thiolysis for average flavan-3-ol subunit compositions [18, 22-26]. This approach did not take account of the multitude of different PA molecules in these mixtures. It is possible that mixtures with the same average values may have very different PA distribution profiles and this could account for different AH effects.

The UPLC-ESI-MS/MS analysis of these sub-fractions showed considerable differences in mDP values compared to the original PA fractions. For instance, the original fractions of weeping willow catkins and sainfoin had mDP values of 8.7 and 10.4 respectively. However, the mDP values ranged from 7 to 15 in the sub-fractions of weeping willow catkin PAs and from 8 to 14 in the sub-fractions of sainfoin PAs. In addition, PCs within total PAs in the original sainfoin fraction was 34 mg PCs/100 mg PAs, but in the sub-fractions the range was from 16 to 63 mg PCs/100 mg PAs. The AH activity of these highly pure PA sub-fractions was then tested *in vitro* against *H. contortus* L3 with the larval exsheathment inhibition assay. Results showed a significant positive relationship between mDP and AH activity in the PC homo-polymeric sample group (P<0.05) and in some PA hetero-polymeric sample groups (P<0.05 and P<0.1) (Chapter 5). This is thus the first time that it could be demonstrated, in the absence of any confounding effects from PDs, that larger PAs had higher AH activity in this assay. Future research should now focus on identifying the optimal polymer sizes and also a wider PD range through further fractionation of PA samples. Investigations into synergistic or antagonistic effect with other plant compounds may also be warranted.

Colleagues at the University of Copenhagen (Copenhagen, Denmark) utilised several of my PA samples (crude extracts and purified fractions) to investigate their efficacy against cattle and pig nematodes. The purified PA fractions showed diverse *in vitro* larval feeding inhibition against the two cattle nematodes, as *Ostertagia ostertagi* L1 were more susceptible than *Cooperia oncophora* L1 (Appendix E) [22]. In agreement with the above results against *H. contortus*, larger PAs and PDs were most effective at inhibition of feeding in both nematode species. However, the motility of larvae and adult worms was significantly reduced and was solely influenced by the PD content within PAs as mDP and *cis* content within PAs had no effect. These findings suggested that there were differences in how PAs acted on nematode motility and feeding. It is thought that different degree of PA aggregation on the surface of the feeding source (*Escherichia coli*) is possibly related to PA size and may have affected differently the feeding patterns of the nematodes [22, 27]. The interactions between PAs and proline-rich proteins of the parasite cuticle and the digestive tract have been also assumed to be critical for AH activity [24, 25, 28]. Studies have shown that PA structural features such as size and hydroxylation are important for PA affinity to proteins [29-32] and that carbohydrates can also affect PA-protein binding [33, 34] and therefore, could have an impact on AH activity.

An array of *in vitro* studies with crude extracts and purified fractions also probed PA structure-activity relationships using the swine nematodes, *Ascaris suum* and *Oesophagostomum dentatum*, at the University of Copenhagen. These extracts and fractions showed direct AH activity by significantly reducing the migratory ability of L3 and the motility of L4 larvae of *A. suum* (Appendix F) [25]. These effects were also correlated positively with the average polymer size and PD contents. Transmission electron microscopy showed lesions at the cuticle and in the digestive tissues of the larvae. These extracts and fractions strongly inhibited (>90%) the development of non-parasitic stages (L1 to infective L3) of *O. dentatum* (Appendix G). Interestingly, the parasitic forms were either not very susceptible (L4) or unaffected (L3) [24]. This means that PAs have potential to disrupt at least one stage in the *O. dentatum* life-cycle. This was one of the few studies that discovered that PC-rich PAs were more potent than PD-rich PAs against a parasitic nematode. Taken together, these findings have provided conclusive evidence for the type of PAs that can best confer anthelmintic activity

and can now be used as guidelines for plant breeders. In addition, information on the most active PAs should also enable future *in vitro* and *in vivo* studies aimed at elucidating the various AH mechanisms against the different nematode species.

Other studies from University of Copenhagen exposed cysticercoids from *Hymenolepis diminuta* (rat tapeworm) to my crude extracts from hazelnut pericarp, pine tree bark and white clover flowers (Appendix H) [23]. It was possible to establish that there was a dose-dependent *in vitro* inhibition by PAs of cysticercoid excystation. These results showed that PAs can also have an AH effect against other types of helminths. The PAs from hazelnut pericarp had also a high AH effect (P<0.0002) *in vivo* as development *of H. diminuta* cysticercoids was inhibited in infected beetles (*Tenebrio molitor*). It would thus be of interest to test the same model PAs against other key life cycle stages of *H. diminuta* and to elucidate the structure-activity relationships and mechanisms of action against this tapeworm. It could be possible that PAs can indirectly promote AH activity by increasing host resistance [35]. Thus, this activity of PAs against *H. diminuta* in invertebrates could pave the way for future studies on other tapeworms in vertebrates.

The AH activity of PAs is generally assumed to be linked to their capacity to interact with proteins [22, 25, 36-38]. Therefore, the hypothesis that PAs may interfere with key enzyme functions was tested by University of Copenhagen using two of the model PA fractions from pine tree bark and white clover flowers (Appendix I). Glutathione-S-transferase is an important enzyme in parasites due to its ability to protect the organism from toxic compounds. Results showed an significant inhibition of glutathione-S-transferase activity in *A. suum* by pine tree bark and white clover flower PAs [39]. In addition, the half maximal inhibitory concentrations (IC_{50}) of levamisole and ivermectin were reduced by factor 4.6 and 3.2 respectively in the presence of purified PAs from pine tree bark. Thus, these assays revealed a synergistic activity of PAs with the widely used synthetic AH drugs. This confirmed the hypothesis that PA-protein interactions may have contributed to an anti-parasitic mode of action and may warrant further investigations.

7.3.2 Effect of proanthocyanidins on ruminal fermentation and methanogenesis

"LegumePlus" partners from Wageningen University (Wageningen, the Netherlands) also used several of my crude extracts in order to study the influence of contrasting PAs on ruminal *in vitro* fermentation and methane production [40, 41]. These studies tested a wide range of PA types and found that they exerted different effects on the extent and the rate of total gas and of methane production. The results showed that PAs significantly reduced methane production ($P<0.0001$) and total methane concentration ($P<0.0001$). Statistical correlations indicated that lower gas and methane production were associated with high PA contents (g PAs/100 g extract) and high molar percentages of PDs. The total volatile fatty acid production was negatively affected by high PA contents and the reductions in ammonia concentration were associated with high mDP values. These findings showed that diverse structural characteristics may have influenced differently the fermentation end-products.

Another study in Wageningen University utilised the same PA extracts in order to evaluate their effects on ruminal fermentation and bio-hydrogenation of unsaturated fatty acids *in vitro* [41, 42]. The bio-hydrogenation rate of C18:3n-3 and the proportion of C18:0, *cis*-9-C18:1; *cis*-9, *cis*-12-C18:2; *cis*-9, *cis*-12, *cis*-15-C18:3 fatty acids was not affected by PAs. However, a 24 h incubation of PA extracts in the rumen fluid caused significant reductions in ammonia, total volatile fatty acid (tVFA) concentrations and the proportion of branched chain VFA. The mDP negatively affected the tVFA concentrations ($P<0.05$) whereas the molar percentages of PDs positively affected propionic acid concentrations and the *cis*-flavan-3-ol molar percentages negatively affected acetic acid concentrations.

Similar *in vivo* investigations will now be needed to evaluate feeds that also contain PAs with contrasting compositions in order to validate these *in vitro* observations. Obviously, whole animal studies will be much more complicated, as they will include not only the impact of PAs on microorganism populations of the rumen, but also tissue effects and cell responses all along the digestive tract.

7.3.3 Interesting developments in the contributions of proanthocyanidins on animal health

Recent studies have made some very interesting discoveries: PAs can activate ruminant γδ T-cells *in vitro* and hence trigger mechanisms of innate immunity [43]. Feeding trials showed an increase in numbers of peripheral γδ T-cells when willow fodder blocks were administered to sheep [44]. Therefore, another study at University of Copenhagen assessed the ability of PAs to prime porcine γδ T-cells (Appendix J) [45]. This *in vitro* study used two PA fractions from hazelnut pericarp and from black currant leaves and showed that both sets of PA fractions were effective priming agents for the γδ T-cells and that the mDP value was the critical factor. More effective priming of γδ T-cells was achieved by the PA fractions with mDP values > 6 rather than by the PA fractions with mDP < 6. However, more experiments with a wider range of PA samples will be necessary to identify the optimal structural features for boosting innate immunity via stimulation of γδ T-cells and this will need to be validated with *in vivo* studies.

Another *in vitro* study evaluated the ability of PAs to modulate the activity of human dendritic cells [46]. Purified PA fractions from white clover flowers (PD-rich PAs), cocoa (PC-rich PAs) and cinnamon (PCs with A-type linkages) induced a Th2 type immunity in human dendritic cells. This profound PA activity was linked to fractions with higher mDP values and higher PD contents PAs. Interestingly, secreted products from the swine parasite *Trichuris suis* and PAs synergistically influenced Th1 and Th2 immune responses. The *in vivo* evaluations of synergistic effects between PAs and intestinal parasites would elucidate further the impact of dietary PAs on immunity functions.

In conclusion, the studies presented in this thesis demonstrated that analysis of PAs still poses many challenges that will need to be overcome in order to probe structure-activity relationships across a wide range of plant matrices and PA types. This research involved new purification and analytical techniques that supported collaborative studies on PAs and made considerable progress in the fields of analytical chemistry, parasitology, and sustainable animal production. This interdisciplinary research within the "LegumePlus" project produced new knowledge on the contributions that PA-containing legumes can make in modern farming systems, animal welfare and quality of animal products. It is hoped that

the promising results from this EU "LegumePlus" network and related research programmes will enable targeted breeding of new sainfoin varieties and support new farming practices that will improve animal health and the quality of end products with a lower environmental footprint and without economic losses.

References

1.   Gu L, Kelm M, Hammerstone JF, Beecher G, Cunningham D, Vannozzi S, Prior RL: **Fractionation of polymeric procyanidins from lowbush blueberry and quantification of procyanidins in selected foods with an optimized normal-phase HPLC-MS fluorescent detection method.** *Journal of Agricultural and Food Chemistry* 2002, 50(17):4852-4860.

2.   Santos-Buelga C, Scalbert A: **Proanthocyanidins and tannin-like compounds - Nature, occurrence, dietary intake and effects on nutrition and health.** *Journal of the Science of Food and Agriculture* 2000, 80(7):1094-1117.

3.   Porter LJ: **Flavans and proanthocyanidins. In: *The Flavonoids: Advances in Research since 1980.*** Edited by Harborne JB. Boston, MA: Springer US; 1988: 21-62.

4.   Hummer W, Schreier P: **Analysis of proanthocyanidins.** *Molecular Nutrition & Food Research* 2008, 52(12):1381-1398.

5.   Yang Y, Chien MJ: **Characterization of grape procyanidins using high-performance liquid chromatography/mass spectrometry and matrix-assisted laser desorption/ionization time-of-flight mass spectrometry.** *Journal of Agricultural and Food chemistry* 2000, 48(9):3990-3996.

6.   Ignat I, Volf I, Popa VI: **A critical review of methods for characterisation of polyphenolic compounds in fruits and vegetables.** *Food Chemistry* 2011, 126(4):1821-1835.

7.   Flamini R: **Recent applications of mass spectrometry in the study of grape and wine polyphenols.** *ISRN Spectroscopy* 2013, 2013:1-45.

8.   Fulcrand H, Mane C, Preys S, Mazerolles G, Bouchut C, Mazauric JP, Souquet JM, Meudec E, Li Y, Cole RB, Cheynier V: **Direct mass spectrometry approaches to characterize polyphenol composition of complex samples.** *Phytochemistry* 2008, 69(18):3131-3138.

9.   Schofield P, Mbugua DM, Pell AN: **Analysis of condensed tannins: A review.** *Animal Feed Science and Technology* 2001, 91(1-2):21-40.

10. Kallio H, Yang W, Liu P, Yang B: **Proanthocyanidins in wild sea buckthorn (*Hippophae rhamnoides*) berries analyzed by reversed-phase, normal-phase, and hydrophilic interaction liquid chromatography with UV and MS detection.** *Journal of Agricultural and Food Chemistry* 2014, 62(31):7721-7729.

11. Taylor AW, Barofsky E, Kennedy JA, Deinzer ML: **Hop (*Humulus lupulus* L.) proanthocyanidins characterized by mass spectrometry, acid catalysis, and gel permeation chromatography.** *Journal of agricultural and food chemistry* 2003, 51(14):4101-4110.

12. Vivas N, Nonier MF, de Gaulejac NV, Absalon C, Bertrand A, Mirabel M: **Differentiation of proanthocyanidin tannins from seeds, skins and stems of grapes (*Vitis vinifera*) and heartwood of quebracho (*Schinopsis balansae*) by matrix-assisted laser desorption/ionization time-of-flight mass spectrometry and thioacidolysis/liquid chromatography/electrospray ionization mass spectrometry.** *Analytica Chimica Acta* 2004, 513(1):247-256.

13. Weber HA, Hodges AE, Guthrie JR, O'Brien BM, Robaugh D, Clark AP, Harris RK, Algaier JW, Smith CS: **Comparison of proanthocyanidins in commercial antioxidants: Grape seed and pine bark extracts.** *Journal of Agricultural and Food Chemistry* 2006, 55(1):148-156.

14. Makkar HPS, Gamble G, Becker K: **Limitation of the butanol-hydrochloric acid-iron assay for bound condensed tannins.** *Food Chemistry* 1999, 66(1):129-133.

15. Callemien D, Guyot S, Collin S: **Use of thiolysis hyphenated to RP-HPLC-ESI(-)-MS/MS for the analysis of flavanoids in fresh lager beers.** *Food Chemistry* 2008, 110(4):1012-1018.

16. Engstrom MT, Palijarvi M, Fryganas C, Grabber JH, Mueller-Harvey I, Salminen JP: **Rapid qualitative and quantitative analyses of proanthocyanidin oligomers and polymers by UPLC-MS/MS.** *Journal of Agricultural and Food Chemistry* 2014, 62(15):3390-3399.

17. Zeller WE, Ramsay A, Ropiak HM, Fryganas C, Mueller-Harvey I, Brown RH, Drake C, Grabber JH: **(1)H-(13)C HSQC NMR spectroscopy for estimating procyanidin/prodelphinidin and cis/trans-flavan-3-ol ratios of condensed tannin samples: Correlation with thiolysis.** *Journal of Agricultural and Food Chemistry* 2015, 63(7):1967-1973.

18. Quijada J, Fryganas C, Ropiak HM, Ramsay A, Mueller-Harvey I, Hoste H: **Anthelmintic activities against *Haemonchus contortus* or *Trichostrongylus colubriformis* from small ruminants are influenced by structural features of condensed tannins.** *Journal of Agricultural and Food Chemistry* 2015, 63(28):6346-6354.

19. Brunet S, Jackson F, Hoste H: **Effects of sainfoin (*Onobrychis viciifolia*) extract and monomers of condensed tannins on the association of abomasal nematode larvae with fundic explants.** *International Journal for Parasitology* 2008, 38(7):783-790.

20. Molan AL, Meagher LP, Spencer PA, Sivakumaran S: **Effect of flavan-3-ols on *in vitro* egg hatching, larval development and viability of infective larvae of *Trichostrongylus colubriformis*.** *International Journal for Parasitology* 2003, 33(14):1691-1698.

21. Novobilsky A, Stringano E, Hayot Carbonero C, Smith LM, Enemark HL, Mueller-Harvey I, Thamsborg SM: ***In vitro* effects of extracts and purified tannins of sainfoin (*Onobrychis viciifolia*) against two cattle nematodes.** *Veterinary Parasitology* 2013, 196(3-4):532-537.

22. Desrues O, Fryganas C, Ropiak HM, Mueller-Harvey I, Enemark HL, Thamsborg SM: **Impact of chemical structure of flavanol monomers and condensed tannins on *in vitro* anthelmintic activity against bovine nematodes.** *Parasitology* 2016, 143(4):444-454.

23. Dhakal S, Meyling NV, Williams AR, Mueller-Harvey I, Fryganas C, Kapel CM, Fredensborg BL: **Efficacy of condensed tannins against larval *Hymenolepis diminuta* (Cestoda) in vitro and in the intermediate host *Tenebrio molitor* (Coleoptera) *in vivo*.** *Veterinary Parasitology* 2015, 207(1-2):49-55.

24. Williams AR, Ropiak HM, Fryganas C, Desrues O, Mueller-Harvey I, Thamsborg SM: **Assessment of the anthelmintic activity of medicinal plant extracts and purified condensed tannins against free-living and parasitic stages of *Oesophagostomum dentatum*.** *Parasites & Vectors* 2014, 7(1):518.

25. Williams AR, Fryganas C, Ramsay A, Mueller-Harvey I, Thamsborg SM: **Direct anthelmintic effects of condensed tannins from diverse plant sources against *Ascaris suum*.** *PLoS One* 2014, 9(5):e97053.

26. Klongsiriwet C, Quijada J, Williams AR, Mueller-Harvey I, Williamson EM, Hoste H: **Synergistic inhibition of *Haemonchus contortus* exsheathment by flavonoid monomers and condensed tannins.** *International Journal for Parasitology Drugs and Rrug Resistance* 2015, 5(3):127-134.

27. Verhelst R, Schroyen M, Buys N, Niewold TA: ***E. coli* heat labile toxin (LT) inactivation by specific polyphenols is aggregation dependent.** *Veterinary Microbiology* 2013, 163(3-4):319-324.

28. Brunet S, Hoste H: **Monomers of condensed tannins affect the larval exsheathment of parasitic nematodes of ruminants.** *Journal of Agricultural and Food Chemistry* 2006, 54(20):7481-7487.

29. Poncet-Legrand C, Edelmann A, Putaux JL, Cartalade D, Sarni-Manchado P, Vernhet A: **Poly(L-proline) interactions with flavan-3-ols units: Influence of the molecular structure and the polyphenol/protein ratio.** *Food Hydrocolloids* 2006, 20(5):687-697.

30. Hagerman AE, Butler LG: **The specificity of proanthocyanidin-protein interactions.** *The Journal of Biological Chemistry* 1981, 256(9):4494-4497.

31. Huang XD, Liang JB, Tan HY, Yahya R, Long R, Ho YW: **Protein-binding affinity of leucaena condensed tannins of differing molecular weights.** *Journal of Agricultural and Food Chemistry* 2011, 59(19):10677-10682.

32. Zeller WE, Sullivan ML, Mueller-Harvey I, Grabber JH, Ramsay A, Drake C, Brown RH: **Protein precipitation behavior of condensed tannins from *Lotus pedunculatus* and *Trifolium repens* with different mean degrees of polymerization.** *Journal of Agricultural and Food Chemistry* 2015, 63(4):1160-1168.

33. Asquith TN, Uhlig J, Mehansho H, Putman L, Carlson DM, Butler L: **Binding of condensed tannins to salivary proline-rich glycoproteins - the role of carbohydrate.** *Journal of Agricultural and Food Chemistry* 1987, 35(3):331-334.

34. Mateus N, Carvalho E, Luis C, de Freitas V: **Influence of the tannin structure on the disruption effect of carbohydrates on protein-tannin aggregates.** *Analytica Chimica Acta* 2004, 513(1):135-140.

35. Hoste H, Jackson F, Athanasiadou S, Thamsborg SM, Hoskin SO: **The effects of tannin-rich plants on parasitic nematodes in ruminants.** *Trends in Parasitology* 2006, 22(6):253-261.

36. Hoste H, Martinez-Ortiz-De-Montellano C, Manolaraki F, Brunet S, Ojeda-Robertos N, Fourquaux I, Torres-Acosta JF, Sandoval-Castro CA: **Direct and indirect effects of bioactive tannin-rich tropical and temperate legumes against nematode infections.** *Veterinary Parasitology* 2012, 186(1-2):18-27.

37. Athanasiadou S, Kyriazakis I, Jackson F, Coop RL: **Direct anthelmintic effects of condensed tannins towards different gastrointestinal nematodes of sheep: *In vitro* and *in vivo* studies.** *Veterinary Parasitology* 2001, 99(3):205-219.

38. Brunet S, Fourquaux I, Hoste H: **Ultrastructural changes in the third-stage, infective larvae of ruminant nematodes treated with sainfoin (*Onobrychis viciifolia*) extract.** *Parasitology International* 2011, 60(4):419-424.

39. Hansen TV, Fryganas C, Acevedo N, Caraballo L, Thamsborg SM, Mueller-Harvey I, Williams AR: **Proanthocyanidins inhibit *Ascaris suum* glutathione-S-transferase activity and increase susceptibility of larvae to levamisole *in vitro*.** *Parasitology International* 2016, 65(4):336-339.

40. Huyen NT, Fryganas C, Uittenbogaard G, Mueller-Harvey I, Verstegen MWA, Hendriks WH, Pellikaan WF: **Structural features of condensed tannins affect *in vitro* ruminal methane production and fermentation characteristics.** *Journal of Agricultural Science (accepted)* 2016.

41. Huyen NT: **Sainfoin (*Onobrychis viciifolia*): A forgotten crop for dairy cows with future potential.** *PhD thesis,* Wageningen University; 2016.

42. Huyen NT, Fryganas C, Mueller-Harvey I, Verstegen MWA, Van Laar-Van Schuppen S, Hendriks WH, Pellikaan WF: **Structural features of condensed tannins affect in vitro**

rumen C18:3n-3 biohydrogenation in dairy cows. *Animal Feed Science and Technology (submitted)* 2016.

43. Tibe O, Pernthaner A, Sutherland I, Lesperance L, Harding DR: **Condensed tannins from Botswanan forage plants are effective priming agents of gammadelta T cells in ruminants.** *Veterinary Immunology and Immunopathology* 2012, 146(3-4):237-244.

44. Ramirez-Restrepo CA, Pernthaner A, Barry TN, Lopez-Villalobos N, Shaw RJ, Pomroy WE, Hein WR: **Characterization of immune responses against gastrointestinal nematodes in weaned lambs grazing willow fodder blocks.** *Animal Feed Science and Technology* 2010, 155(2-4):99-110.

45. Williams AR, Fryganas C, Reichwald K, Skov S, Mueller-Harvey I, Thamsborg SM: **Polymerization-dependent activation of porcine gammadelta T-cells by proanthocyanidins.** *Research in Veterinary Science* 2016, 105:209-215.

46. Williams AR, Klaver EJ, Laan LC, Ramsay A, Fryganas C, Diborg R, Kringel H, Reed JD, Mueller-Harvey I, Skov S, van Die I, Thamsborg SM: **Co-operative suppression of inflammatory responses in human dendritic cells by proanthocyanidins and helminth products.** *Immunology (submitted)* 2016.

Appendix A

Supporting information on proathocyanidin characterisation in acetone/water extracts and SephadexTM LH-20 (3:7 v/v) eluted fractions from model plant species.

Table A.1: Characterisation of proanthocyanidins (PAs) in acetone/water (7:3, v/v) extracts (Ao) and Sephadex^TM LH-20 acetone/water (3:7, v/v) eluted fractions (F1) by thiolysis-HPLC and UPLC-ESI-MS/MS methods. PA content (mg/g extract), mean degree of polymerisation (mDP) values, procyanidin (PC) and *cis* contents (mg/100 mg PAs) within total PAs. Standard deviation in brackets (*n=2*).

PA origin	Extract type	Thiolysis				UPLC-ESI-MS/MS		
		PA mg/g extract	mDP	PC (mg/100 mg PAs)	*cis* (mg/100 mg of PAs)	PA mg/g extract	mDP	PC (mg/100 mg PAs)
Salix caprea (Goat willow; leaves)	1Ao	300 (82.3)	3.87 (0.049)	96.5 (0.784)	2.80 (0.147)	286	4.93	96.9
	1F1	515 (1.38)	2.05 (0.035)	93.9 (0.652)	6.96 (0.603)	405	2.88	96.4
Coryllus avellana (Hazelnut; pericarp)	2Ao	709 (39.0)	9.59 (0.163)	78.6 (0.018)	49.7 (0.157)	599	10.0	81.4
	2F1	491 (22.7)	4.58 (0.170)	80.9 (1.86)	41.0 (0.211)	513	5.03	83.4
Salix caprea (Goat willow; twigs)	3Ao	538 (41.6)	4.31 (0.049)	73.9 (0.343)	52.7 (0.133)	459	4.99	83.3
	3F1	720 (22.8)	2.11 (0.000)	83.7 (1.79)	40.6 (0.283)	480	2.56	84.4
Pinus sylvestris (Scots pine tree; bark)	4Ao	492 (17.03)	2.54 (0.021)	62.9 (1.32)	79.7 (0.575)	422	5.19	97.0
	4F1	540 (39.6)	2.27 (0.021)	84.2 (1.06)	47.9 (0.098)	563	2.40	96.4
Onobrychis viicifolia (Sainfoin; plant)	5Ao	126 (12.0)	5.53 (0.078)	24.3 (1.55)	80.2 (0.297)	47.1	10.7	43.1
	5F1	372 (91.6)	2.73 (0.014)	27.0 (0.462)	66.7 (0.404)	119	2.33	45.8
Salix babylonica (Weeping willow; catkins)	6Ao	253 (8.00)	2.34 (0.071)	42.9 (0.224)	77.9 (0.479)	122	7.43	70.3
	6F1	402 (55.5)	2.90 (0.00)	74.3 (0.249)	55.5 (0.483)	346	3.78	76.5
Ribes rubrum (Red currant; leaves)	7Ao	245 (28.1)	9.83 (0.311)	5.71 (0.464)	77.3 (0.123)	98.8	17.8	8.88
	7F1	577 (181)	4.90 (0.007)	13.6 (0.654)	44.5 (2.18)	635	6.45	15.0
Ribes nigrum (Black currant; leaves)	8Ao	292 (24.1)	5.44 (0.665)	5.56 (0.247)	9.03 (2.39)	306	9.56	5.66
	8F1	598 (26.1)	2.47 (0.007)	6.01 (0.106)	12.8 (0.612)	580	3.15	6.91
Trifolium repens (White clover; flowers)	9Ao	338 (21.7)	4.38 (0.148)	0.757 (0.033)	65.7 (0.183)	191	10.6	2.03
	9F1	116 (8.40)	1.77 (0.007)	1.62 (0.610)	17.8 (0.251)	150	2.24	2.82

Table A.2: Proanthocyanidin (PA) monomer composition and content (mg/g extract) acetone/water extracts (Ao) and Sephadex^{TM} LH-20 acetone/water (3:7, v/v) eluted fractions (F1). GC: gallocatechin, EGC: epigallocatechin, C: catechin, EC: epicatechin; standard deviation in brackets (*n=2*); nd: not detected.

PA Origin	Extract type	GC	EGC	C	EC	GC	EGC	C	EC
		Terminal units				Extender units			
Salix caprea (Goat willow; leaves)	1Ao	2.69 (1.21)	nd	72.2 (20.5)	2.84 (0.625)	8.01 (3.99)	nd	209 (54.8)	5.49 (1.23)
	1F1	3.10 (0.510)	19.5 (3.50)	221 (0.658)	8.15 (0.218)	8.80 (0.732)	nd	246 (3.51)	8.25 (0.704)
Coryllus avellana (Hazelnut; pericarp)	2Ao	4.06 (0.036)	nd	59.7 (4.57)	9.55 (0.611)	75.0 (4.65)	72.7 (3.53)	217 (11.4)	270 (14.1)
	2F1	4.74 (0.183)	nd	87.7 (7.72)	14.2 (1.12)	51.1 (1.59)	37.8 (3.38)	146 (8.14)	150 (10.6)
Salix caprea (Goat willow; twigs)	3Ao	9.47 (1.05)	nd	111 (6.59)	3.80 (0.547)	85.5 (7.78)	45.6 (3.90)	48.7 (4.97)	234 (16.8)
	3F1	18.6 (0.176)	nd	310 (9.36)	10.4 (1.27)	42.4 (4.46)	55.8 (4.90)	56.1 (6.84)	226 (14.5)
Pinus sylvestris (Scots pine tree; bark)	4Ao	nd	147 (7.08)	47.7 (1.60)	3.25 (0.075)	35.3 (5.70)	0.00 (0.00)	17.2 (1.02)	241 (3.73)
	4F1	2.55 (0.275)	11.2 (0.458)	210 (19.0)	13.4 (0.623)	62.6 (0.947)	8.70 (1.17)	6.09 (0.927)	226 (18.5)
Onobrychis viciifolia (Sainfoin; plant)	5Ao	4.03 (0.013)	14.6 (2.22)	2.23 (0.041)	2.09 (0.252)	15.2 (2.48)	61.6 (2.42)	3.58 (0.221)	22.9 (4.36)
	5F1	34.6 (8.64)	51.6 (14.9)	21.6 (6.09)	28.4 (7.99)	59.7 (12.4)	126 (29.2)	8.11 (1.84)	42.6 (10.6)
Salix babylonica (Weeping willow; catkins)	6Ao	nd	88.0 (0.337)	12.0 (0.042)	9.49 (0.022)	21.9 (1.99)	34.7 (1.67)	22.0 (1.02)	64.9 (3.00)
	6F1	nd	9.78 (1.26)	77.1 (10.9)	50.5 (6.66)	43.1 (7.80)	50.3 (6.21)	58.6 (7.97)	112 (14.5)
Ribes rubrum (Red currant; leaves)	7Ao	7.11 (1.46)	13.9 (2.81)	3.05 (0.548)	0.805 (1.14)	42.6 (3.76)	167 (19.6)	2.75 (0.295)	7.32 (0.761)
	7F1	65.4 (18.1)	13.0 (8.31)	33.4 (8.77)	4.90 (1.32)	195 (54.7)	226 (79.3)	24.2 (6.41)	15.1 (4.28)
Ribes nigrum (Black currant; leaves)	8Ao	28.9 (1.48)	17.9 (7.75)	6.16 (1.38)	1.15 (0.360)	225 (11.9)	4.35 (0.883)	5.65 (0.219)	3.29 (0.178)
	8F1	168 (8.48)	53.0 (2.55)	17.3 (0.346)	4.16 (0.130)	326 (9.89)	15.0 (4.25)	10.1 (0.390)	4.38 (0.071)
Trifolium repens (White clover; flowers)	9Ao	22.8 (1.81)	54.6 (5.78)	nd	nd	91.9 (5.04)	166 (8.97)	1.10 (0.042)	1.45 (0.069)
	9F1	45.3 (3.34)	20.30 (1.753)	0.334 (0.472)	nd	48.9 (3.88)	0.00 (0.00)	1.040 (0.139)	0.483 (0.037)

Appendix B

Original publication:

Rapid Qualitative and Quantitative Analyses of Proanthocyanidin Oligomers and Polymers by UPLC-MS/MS

Marica T. Engström, Maija Pälijärvi, Christos Fryganas, John H. Grabber, Irene Mueller-Harvey, and Juha-Pekka Salminen

Rapid Qualitative and Quantitative Analyses of Proanthocyanidin Oligomers and Polymers by UPLC-MS/MS

Marica T. Engström,[*,†] Maija Pälijärvi,[†] Christos Fryganas,[‡] John H. Grabber,[§] Irene Mueller-Harvey,[‡] and Juha-Pekka Salminen[†]

[†]Laboratory of Organic Chemistry and Chemical Biology, Department of Chemistry, University of Turku, FI-20014 Turku, Finland

[‡]Chemistry and Biochemistry Laboratory, Food Production and Quality Division, School of Agriculture, Policy and Development, University of Reading, P.O. Box 236, 1 Earley Gate, Reading RG6 6AT, United Kingdom

[§]U.S. Dairy Forage Research Center, Agricultural Research Service, U.S. Department of Agriculture, 1925 Linden Drive West, Madison, Wisconsin 53706, United States

Ⓢ *Supporting Information*

ABSTRACT: This paper presents the development of a rapid method with ultraperformance liquid chromatography–tandem mass spectrometry (UPLC-MS/MS) for the qualitative and quantitative analyses of plant proanthocyanidins directly from crude plant extracts. The method utilizes a range of cone voltages to achieve the depolymerization step in the ion source of both smaller oligomers and larger polymers. The formed depolymerization products are further fragmented in the collision cell to enable their selective detection. This UPLC-MS/MS method is able to separately quantitate the terminal and extension units of the most common proanthocyanidin subclasses, that is, procyanidins and prodelphinidins. The resulting data enable (1) quantitation of the total proanthocyanidin content, (2) quantitation of total procyanidins and prodelphinidins including the procyanidin/prodelphinidin ratio, (3) estimation of the mean degree of polymerization for the oligomers and polymers, and (4) estimation of how the different procyanidin and prodelphinidin types are distributed along the chromatographic hump typically produced by large proanthocyanidins. All of this is achieved within the 10 min period of analysis, which makes the presented method a significant addition to the chemistry tools currently available for the qualitative and quantitative analyses of complex proanthocyanidin mixtures from plant extracts.

KEYWORDS: *proanthocyanidin, procyanidin, prodelphinidin, tannins, mass spectrometry, MRM*

■ INTRODUCTION

Proanthocyanidins (syn. condensed tannins) are oligomers or polymers of flavan-3-ols consisting of one terminal unit and one or more extension units that are primarily linked by C–C bonds (Figure 1A). Proanthocyanidins are divided into subtypes on the basis of their stereochemistry at C2 and C3 and the hydroxylation pattern of the B-ring. The most common proanthocyanidins are 3',4'-dihydroxy-substituted procyanidins and 3',4',5'-trihydroxy-substituted prodelphinidins. Proanthocyanidins containing both procyanidin and prodelphinidin units are common in plants. Due to differences in procyanidin and prodelphinidin composition, relative stereochemistry, and degree of polymerization, proanthocyanidins are a highly complex and exceptionally diverse group of compounds.[1−3]

Proanthocyanidins are present in roots, wood, bark, leaves, fruits, and seeds of many herbaceous and woody plants, where they are believed to confer resistance against herbivores, seed predators, and pathogens.[3−5] These polyphenols also give flavor and astringency to beverages such as wine, fruit juices, and teas, and some have beneficial effects on human health.[3−5] Other studies have shown that feeding of some species of proanthocyanidin-containing forages can significantly improve the utilization of dietary protein by ruminant livestock and reduce the excretion of labile forms of nitrogen in manure that contribute to environmental pollution from farms.[6] Many proanthocyanidin-containing forages also lower intestinal

parasite burdens of several ruminant species.[7−9] In general, higher proanthocyanidin and prodelphinidin contents and higher average polymer sizes have been associated with stronger anthelmintic activities.[10−12]

To select or develop new plant varieties with desirable proanthocyanidin properties, plant breeders require rapid and specific methods for proanthocyanidin analysis. Unfortunately, full characterization of complex proanthocyanidins in plant tissues typically requires a combination of laborious analytical methods. Most approaches include time-consuming isolation, purification, and depolymerization steps prior to HPLC analysis. Currently, thiolysis and phloroglucinolysis are the most commonly used depolymerization methods for collecting qualitative and quantitative information on proanthocyanidin content, composition, and mean degree of polymerization (mDP).[2,13−17] However, these depolymerization methods do not enable characterization of the polymer distribution profiles in plant samples because all proanthocyanidins are cleaved into monomer units and, thus, all information on individual oligomers or polymers is lost.[15] Moreover, due to their insensitivity, these degradation methods typically require
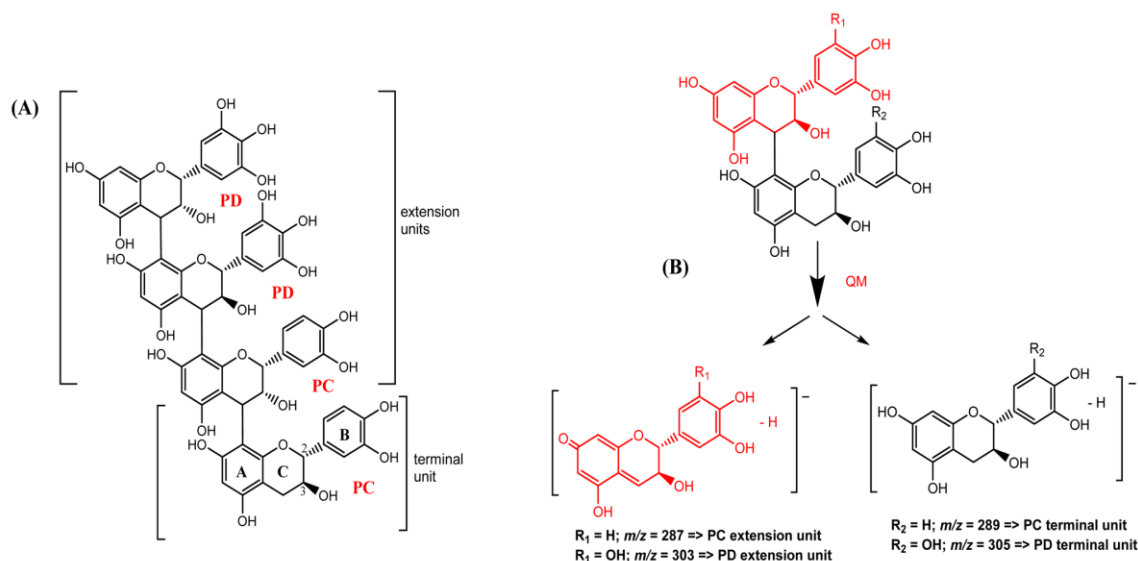
Figure 1. Model structure of a proanthocyanidin tetramer containing two prodelphinidin (PD) and two procyanidin (PC) units (A) and quinone methide fragmentation of proanthocyanidin dimer in negative ion mode ESI-MS (B).

relatively large amounts of plant tissue, in the range of hundreds of milligrams, for analysis.[17−19]

The development in LC-MS/MS instruments has been vast in recent years,[20−22] and the use of ultraperformance liquid chromatography combined with a mass spectrometer (UPLC-MS/MS) is becoming common also in proanthocyanidin studies.[23] UPLC enables rapid chromatography of different kinds of proanthocyanidin oligomers, whereas MS/MS fragments compounds into proanthocyanidin-specific precursor and product ions for detection with multiple reaction monitoring (MRM) methods. Specific fragmentations, that is, compound-specific methods, have been widely used for the identification and quantitation of relatively small proanthocyanidin oligomers.[23−25] However, no compound-specific methods have been reported for larger oligomers or proanthocyanidin polymers as the limit has been with tetramers.[23−26] Furthermore, to our knowledge, no group-specific method for the qualitative and quantitative determination of all proanthocyanidin sizes in plant samples has been reported. The present study explored the potential of UPLC combined with a triple-quadrupole mass spectrometer (TQ-MS) for the rapid qualitative and quantitative analyses of proanthocyanidins. Our main interest was in establishing a fast, sensitive, and selective method for the analysis of the two most common proanthocyanidin types: procyanidins and prodelphinidins.

■ MATERIALS AND METHODS

Chemicals and Reagents. LC-MS grade acetonitrile used in the UPLC analyses was from Sigma-Aldrich (Steinheim, Germany). Formic acid was from VWR (Helsinki, Finland). Water was purified with a Millipore Synergy water purification system (Merck KGaA, Darmstadt, Germany). Catechin was from Sigma (Sigma Chemical Co., St. Louis, MO, USA) and epigallocatechin from ExtraSynthese (Genay, France).

Materials. Pure compounds gallocatechin gallate, proanthocyanidin dimers and trimers, mixture of oligomers, and mixture of polymers (not fractions 1-F−13-F) used in optimization of cone voltages and collision energies were produced as described in Karonen et al.[17] Proanthocyanidin fractions 1-F−13-F were extracted from different plant materials with 70% aqueous acetone and subjected to Sephadex

LH-20 column chromatography. F1 fractions were eluted with acetone/water (30:70, v/v) and F2 fractions with acetone/water (50:50, v/v). The procyanidin proportions of the fractions varied from 1 to 95% and the mDP from 2 to 14 (by thiolysis). The plant materials, fractions, and results from thiolysis are listed in Table 1.

Thiolysis. Thiolysis was carried out as described in Gea et al.[18]

HCl-Butanol Assay. A 0.1 mL aqueous solution of fractions 5F−13F (0.5 mg/mL) was added to 0.5 mL of a freshly prepared mixture of 1-butanol/hydrochloric acid (95:5 v/v) in 1.5 mL Eppendorf tubes. Tubes were locked with Eppendorf tube locks and vigorously mixed by hand. After mixing, tubes were placed in an oven at 95 °C for 2.5 h. Tubes were then cooled to room temperature, and the absorbance at 550 nm was measured using a Multiskan Ascent microplate photometer (Thermo Fisher Scientific, Shanghai, China). Standard curves were constructed using known concentrations of procyanidin-rich sample 1-F2 and prodelphinidin-rich sample 9-F2 in H_2O. Dilution range was from 5.0 to 0.1 mg/mL. Five replicates of each sample were run. Because the HCl-butanol assay measures only total proanthocyanidins and cannot separate procyanidins from prodelphinidins, the results were calculated by using the average calibration curve obtained from procyanidin and prodelphinidin standards separately.

UPLC-MS/MS Analysis. Sample analysis was carried out with an Acquity UPLC system (Waters Corp., Milford, MA, USA) coupled with a Xevo TQ triple-quadrupole mass spectrometer (Waters Corp., Milford, MA, USA). The UPLC system consisted of a sample manager, a binary solvent manager, a column, and a diode array detector. The column used was a 100 mm × 2.1 mm i.d., 1.7 μm, Acquity UPLC BEH Phenyl column (Waters Corp., Wexford, Ireland). The flow rate of the eluent was 0.5 mL/min. The elution profile used two solvents, acetonitrile (A) and 0.1% aqueous formic acid (B): 0−0.5 min, 0.1% A in B; 0.5−5.0 min, 0.1−30% A in B (linear gradient); 5.0−6.0 min, 30−35% A in B (linear gradient); 6.0−9.5 min, column wash and stabilization. UV and MS data were collected from 0 to 6 min. Negative ionization mode was used for MS analyses. ESI conditions were as follows: capillary voltage, 2.4 kV; desolvation temperature, 650 °C; source temperature, 150 °C; desolvation and cone gas (N_2), 1000 and 100 L/h, respectively; and collision gas, argon. Catechin (1 μg/mL) was used to monitor the stability of the ionization efficiency of the mass spectrometer.

Optimization of Cone Voltages and Collision Energies. When optimizing the cone voltages and the collision energies for the selected compounds and fractions, aqueous solutions of different proantho-

3391

dx.doi.org/10.1021/jf500745y | J. Agric. Food Chem. 2014, 62, 3390−3399

255

Table 1. Plant Materials and Fractions Used in the Present Work[a]

sample	plant species	% PC	mDP
1-F1	*Onobrychis viciifolia* (sainfoin: Nova var.), leaves	28	6
1-F2	*Onobrychis viciifolia* (sainfoin: Nova var.), leaves	18	12
2-F1	*Lotus corniculatus* (birdsfoot trefoil: Rodeo var.), leaves	79	4
2-F2	*Lotus corniculatus* (birdsfoot trefoil: Rodeo var.), leaves	68	11
3-F1	*Lotus uliginosus* (big trefoil: ARS-1221 var.), leaves	31	4
3-F1b	*Lotus uliginosus* (big trefoil: ARS-1221 var.), leaves	26	7
3-F2	*Lotus uliginosus* (big trefoil: ARS-1221 var.), leaves	25	11
4-F1	*Securigera varia* (crownvetch: Emerald var.), leaves	12	11
4-F2	*Securigera varia* (crownvetch: Emerald var.), leaves	18	14
5-F1	*Salix caprea* (goat willow), leaves	94	2
5-F2	*Salix caprea* (goat willow), leaves	95	5
6-F1	*Coryllus avellana* (hazelnut), pericarp membrane	82	5
6-F2	*Coryllus avellana* (hazelnut), pericarp membrane	79	9
7-F1	*Salix caprea* (goat willow), twigs	84	2
7-F2	*Salix caprea* (goat willow), twigs	79	5
8-F1	*Pinus sylvestris* L. (scots pine tree), inner bark	85	2
8-F2	*Pinus sylvestris* L. (scots pine tree), inner bark	91	7
9-F1	*Onobrychis viciifolia* (sainfoin; Esparsette var.), whole plant	28	3
9-F2	*Onobrychis viciifolia* (sainfoin; Esparsette var.), whole plant	35	9
10-F1	*Salix babylonica* (weeping willow), catkins	75	3
10-F2	*Salix babylonica* (weeping willow), catkins	67	8
11-F1	*Ribes rubrum* (red currant), leaves	14	5
11-F2	*Ribes rubrum* (red currant), leaves	10	10
12-F1	*Ribes nigrum* (black currant), leaves	6	3
12-F2	*Ribes nigrum* (black currant), leaves	6	7
13-F1	*Trifolium repens* (white clover), flowers	2	2
13-F2	*Trifolium repens* (white clover), flowers	1	9

[a]F1 fractions were eluted with acetone/water (30:70; v/v) and F2 fractions with acetone/water (50:50; v/v); sample 3-F1 was passed through the Sephadex column twice; F1b after the second Sephadex purification. % PC, procyanidin concentration from total proanthocyanidin concentration as percent by thiolysis; mDP, mean degree of polymerization by thiolysis.

cyanidins were directly infused into the ESI source with a syringe pump at a flow rate of 5−40 μL/min. The concentrations of the aqueous proanthocyanidin solutions were 40 μg/mL for pure compounds and 2 mg/mL for proanthocyanidin-rich fractions. The ranges of cone voltage and collision energy varied between 10 and 170 V and between 5 and 50 eV, respectively.

Calibration Curves for Procyanidin and Prodelphinidin Contents. Solutions for calibration curves were produced from stock solutions (1.0 mg/mL) of procyanidin-rich sample 5-F2 (procyanidin content = 95%, determined by thiolysis) and prodelphinidin-rich sample 13-F2 (prodelphinidin content = 98%, determined by thiolysis) by dilution with acetonitrile/water (20:80, v/v). The dilution range was from 1.0 to 0.01 mg/mL.

Limit of Detection, Limit of Quantitation, and Linearity. Procyanidin and prodelphinidin dimers were used for determination of the limit of detection (LOD) and limit of quantitation (LOQ) for the presented MRM method at signal-to-noise ratios (S/N) >3 and >10, respectively. Dilution series were prepared from stock solutions of 40 μg/mL and diluted with H_2O. The dilution range was from 40 μg/mL to 0.019 ng/mL. Three replicates of each sample were run.

■ RESULTS AND DISCUSSION

Optimization of the MRM Methods. On the basis of the quinone methide cleavage theory (Figure 1B), both terminal and extension units of procyanidins and prodelphinidins yield different fragments,[4,27,28] and it was hypothesized that it would be possible to develop separate MRM methods for the specific detection of these fragments. To optimize MRM methods for the qualitative and quantitative analyses of procyanidin and prodelphinidin units of proanthocyanidins, direct flow injection experiments of the reference compounds were performed in both positive-ion and negative-ion modes. The reference compounds consisted of different proanthocyanidin monomers and oligomers, as well as semipurified mixtures of proanthocyanidin oligomers and polymers (fractions 1-F1−4-F2) (Table 1). Negative mode was superior to positive mode in terms of sensitivity, particularly for the terminal units (Figure 2) and, thus, negative-ion mode was selected to be used in the MRM methods.

As previously reported,[4,27,29,30] both procyanidin and prodelphinidin units of proanthocyanidins yielded two different types of ions in the collision-induced MS analysis depending on whether they represented the extension or terminal units of the
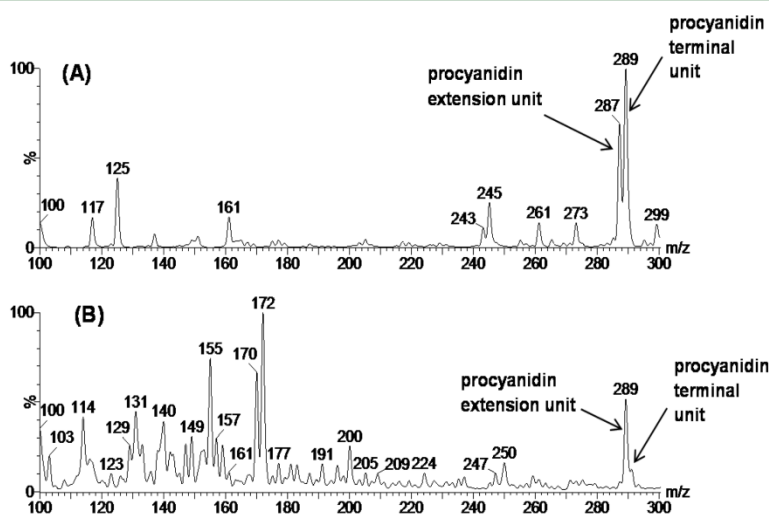
Figure 2. Detection of extension and terminal units of procyanidin trimer with negative-ion mode (A) and positive-ion mode (B).
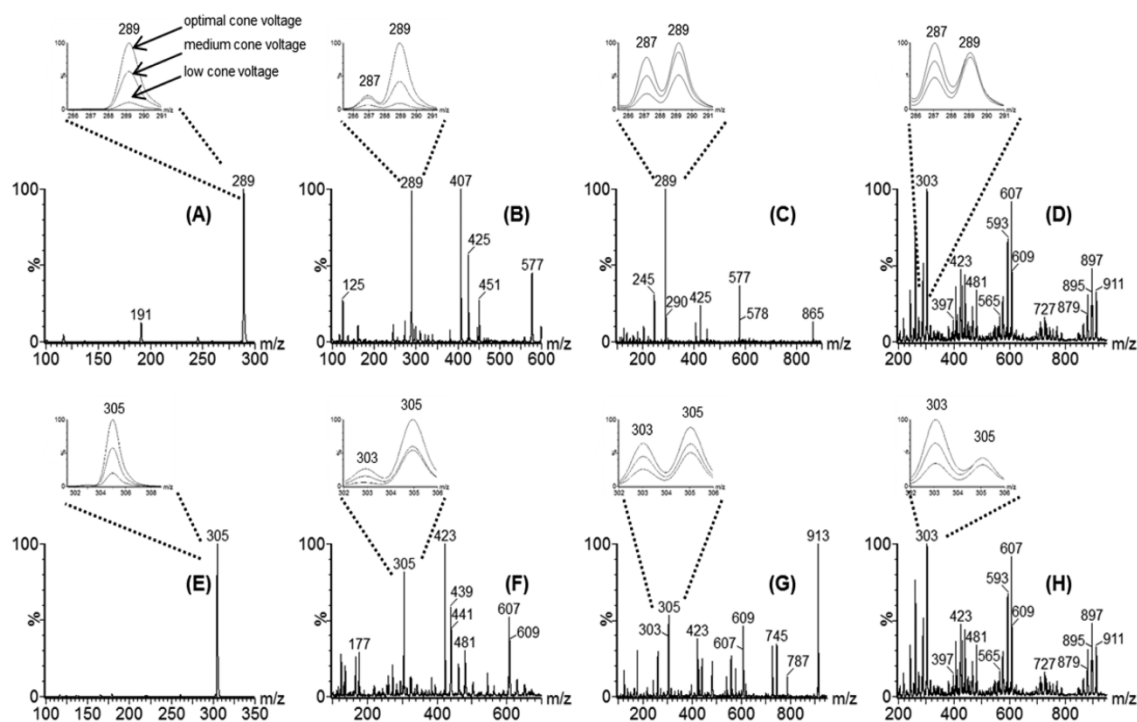
Figure 3. Mass spectra of proanthocyanidin monomers, dimers, trimers, and polymers obtained by in-source fragmentation: (A) catechin; (B) procyanidin dimer; (C) procyanidin trimer; (D) sample 1-F2; (E) epigallocatechin; (F) prodelphinidin dimer; (G) prodelphinidin trimer; (H) sample 1-F2. The insets show how the intensities of the extension units (m/z 287 and 303) and terminal units (m/z 289 and 305) change due to shifts in cone voltage. See Table 1 for fraction identities.

corresponding proanthocyanidin molecule (Figure 1B). For procyanidins the characteristic ions formed via quinone methide cleavage were m/z 287 and 289 and for prodelphinidins m/z 303 and 305, respectively. Also, ions formed by retro-Diels−Alder and heterocyclic ring fission mechanisms were detected at low intensity, but because these do not give specific information of proanthocyanidin extension and terminal units, they were not included in the MRM development section.

Figure 3 shows a comparison of the mass spectra of monomeric, dimeric, and trimeric procyanidins and prodelphinidins and oligomeric procyanidin/prodelphinidin mixture (sample 1-F2) with direct flow infusion into the MS. The zoomed m/z areas present results obtained with low, medium, and optimal cone voltages. In all cases the optimal cone voltage resulted in highest response and, correspondingly, the low cone voltage in lowest response. Catechin and epigallocatechin monomers yielded only ions at m/z 289 and 305, respectively. The other proanthocyanidin samples yielded ions at both m/z 287 and 289 for procyanidins and m/z 303 and 305 for prodelphinidins. The intensity of ions at m/z 287 and 303 increased as the degree of polymerization of the proanthocyanidin molecule increased, suggesting that the intensity of these ions in MS analysis was related to the number of extension units present in the original proanthocyanidin structure.

The cone voltage optimization experiments revealed that the larger the proanthocyanidin, the higher the cone voltage required to produce maximal ion intensities for the proanthocyanidin fragments. For monomers the optimal cone voltage was 30 V for ions at m/z 289 and 305. For dimers the optimal cone voltages were 50, 60, 60, and 55 V for ions m/z

287, 289, 303, and 305, respectively. Similar cone voltages have been also previously proposed for these fragmentations of the proanthocyanidin dimers and trimers.[31] For the proanthocyanidin fractions containing both oligomers and polymers, the optimal cone voltages ranged from 100 to 150 V. In general, the optimal cone voltage required for prodelphinidins was higher than that for procyanidins and higher for extension units (ions at m/z 287 and 303) than for terminal units (ions at m/z 289 and 305). These results indicate differences in the collision-induced dissociation of different types of proanthocyanidin molecules and that high energy is required to fragment as many extension units as possible.

The results from these experiments suggested that a single cone voltage cannot be used for the optimal detection of all types of proanthocyanidins. Therefore, the choice of an optimal cone voltage is not straightforward; the ideal cone voltage is highly dependent upon the size, composition, and structure of the analytes of interest. For example, when only small proanthocyanidins are studied, increasing the cone voltages beyond the optimum induces fragmentation before the ions enter the mass filter, resulting in a decrease in sensitivity. In contrast, when proanthocyanidin oligomers and polymers are studied, use of a too low cone voltage would lead to poor fragmentation of the original molecule and thus low sensitivity for the detection of the terminal and especially extension units. This in turn would cause underestimation of the concentrations of the oligomers and polymers.

Enhanced selectivity and sensitivity of the method is achieved by collision energies separately optimized for product ions of the specific procyanidin and prodelphinidin units. Such an approach allows the accurate qualitative and quantitative

Table 2. Cone Voltages and Collision Energies in the New MRM Method for the Detection of Procyanidin (PC) and Prodelphinidin (PD) Terminal and Extension Units

unit	precursor ion (m/z)	CV^a 1 (V)	CV 2 (V)	CV 3 (V)	CV 4 (V)	CV 5 (V)	CV 6 (V)	fragment ion (m/z)	collision energy (eV)
PC extension unit	287	30	50	75	85	110	140	125	15
PC terminal unit	289	30	50	75	85	110	140	245	15
PD extension unit	303	30	55	80	110	130	150	125	20
PD terminal unit	305	30	55	80	110	130	150	125	20

^{a}CV, cone voltage.
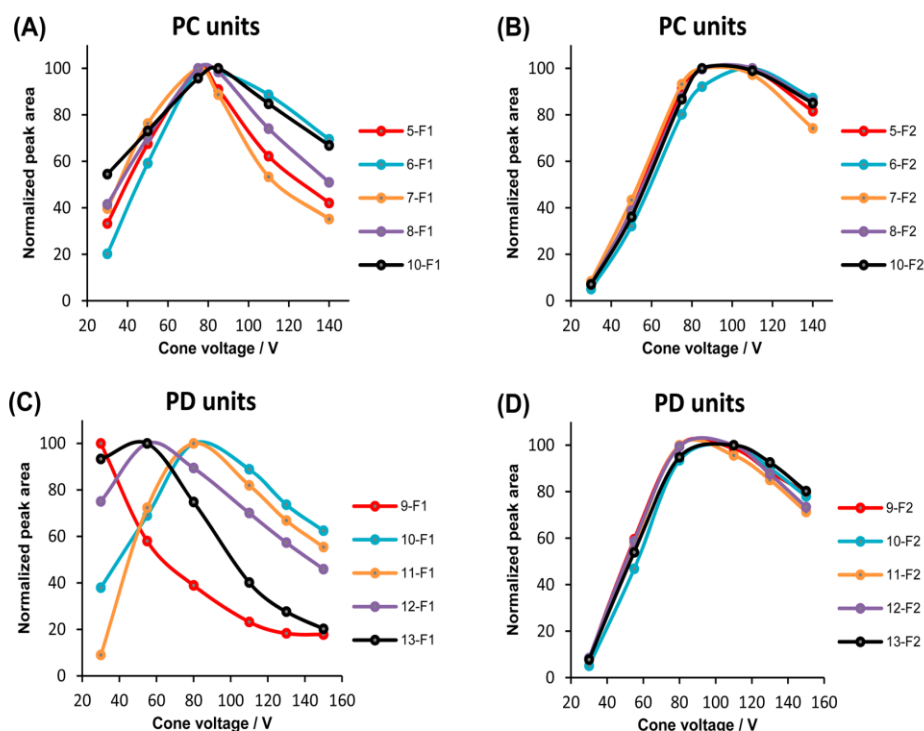
Figure 4. Normalized peak areas from the MRM chromatograms of procyanidin (PC) units (sum of procyanidin terminal and extension units) and prodelphinidin (PD) units (sum of prodelphinidin terminal and extension units) obtained with F1 fractions containing smaller proanthocyanidins (A, C) and F2 fractions containing larger proanthocyanidins (B, D). See Table 1 for fraction identities.

analyses of complex proanthocyanidins directly from plant crude extracts. In contrast to identifying optimal cone voltages, the choice of optimal collision energy was straightforward. The product ions produced from the ions derived from terminal and extension units always had the same optimal collision energy. The optimal collision energy for both transitions m/z 287 → 125 and 289 → 245 was 15 eV. For both transitions of m/z 303 → 125 and 305 → 125 the optimal collision energy was 20 eV. On the basis of the results from cone voltage and collision energy optimizations, one MRM method containing six different cone voltages for each terminal and extension unit ion and one optimal collision energy for the accumulation of the unit-specific product ions was developed (Table 2).

In previous studies, cone voltages and collision energies have been used for the optimization of separate MRM methods for small proanthocyanidin oligomers[32,32−36] and for studying the fragmentation patterns of proanthocyanidins.[22,37,38] No compound-specific MRM methods have been reported for larger proanthocyanidin oligomers or polymers as the limit has been with tetramers.[23−25,31] This highlights the novelty of our approach: to our knowledge, no previous study has used

UPLC-MS/MS with a range of cone voltages and optimized collision energies for the detection of extension and terminal units and thus for the detection of total oligomeric and polymeric proanthocyanidins.

Effect of Optimized Cone Voltages and Sample Composition on Peak Areas. After optimization of MRMs, the new method was rigorously tested with an independent set of 18 structurally diverse proanthocyanidin fractions (5-F1−13-F2) prepared from nine plant species; the proportion of procyanidin units in these fractions ranged from 1 to 95% and mDP ranged from 2 to 10 (Table 1). Figure 4 shows the normalized peak areas for all 18 proanthocyanidin fractions plotted as a function of cone voltage. For better visual clarity, peak areas (a sum of terminal and extension units) for procyanidin-derived ions are shown for only the five procyanidin-richest fractions in Figure 4A,B. Similarly, peak areas (a sum of terminal and extension units) for prodelphinidin-derived ions are shown for the five prodelphinidin-richest fractions in Figure 4C,D.

For every F1 fraction, the largest procyanidin peak areas were detected with 75−80 V (Figure 4A). However, the profiles of
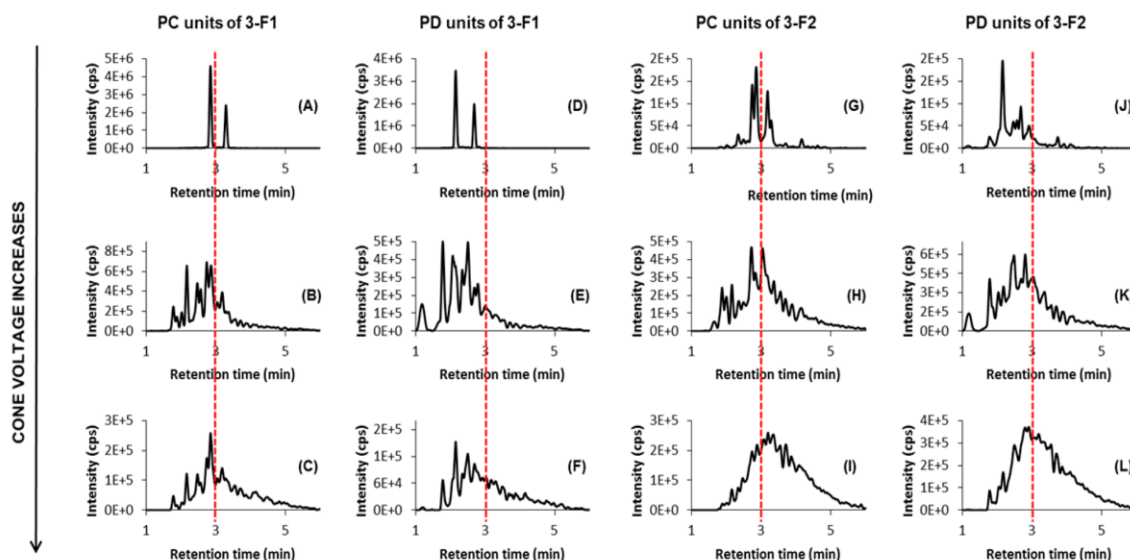
Figure 5. MRM chromatograms of procyanidin (PC) and prodelphinidin (PD) units for samples 3-F1 and 3-F2 (see Table 1) obtained with cone voltages of 30 V (A, D, G, J), 80 V (B, E, H, K), and 140 V (C, F, I, L).

the plots differed a little. In general, when the cone voltage increased beyond the optimal, the peak areas decreased more rapidly with samples having low mDP. This is in agreement with the earlier findings showing that smaller proanthocyanidins require lower cone voltages for their optimal detection.[31] In contrast, the procyanidin response of the larger proanthocyanidins of the F2 fractions did not significantly decrease even though the cone voltage was increased from 80 to 140 V (Figure 4B). This again confirmed the presence of larger proanthocyanidins in these samples.

The plots for prodelphinidin-richest F1 fractions were the most diverse compared to all other fractions (Figure 4C). The mDP values from thiolysis ranged from two to five and a qualitative comparison of the chromatograms revealed differences in the prodelphinidin composition of these fractions (data not shown). For example, fractions 9-F1 and 10-F1 both had an mDP of 3, but the prodelphinidin profiles differed. Detection with low cone voltage suggested that the 9-F1 sample contained a lot of monomers, which caused the sharp decrease in peak area with increasing cone voltage. The 10-F1 sample had a lot of oligomers in addition to monomers, and this explained the increasing peak area with increasing cone voltage. Similarly to the procyanidin detection (Figure 4B), the prodelphinidin-richest F2 fractions showed largest peak areas with cone voltages of 80–100 V. Also, the profiles of the two plots were similar (Figure 4B,D). The similarity among the F2 fractions was due to the absence of smaller proanthocyanidins, as these eluted generally in F1 fractions. Again, these results suggested that the developed MRM method is able to reveal whether the analyzed sample contains mainly small or large proanthocyanidins.

Qualitative Comparison of the MRM Chromatograms. The number of proanthocyanidin isomers increases with increasing degree of polymerization.[39] As a result, proanthocyanidin samples with high mDP generate a large unresolved hump in RP-LC.[40−43] However, a qualitative comparison of the chromatograms showed that higher cone voltages caused a shift in the detected proanthocyanidin hump to the right, that is, to later retention times and larger proanthocyanidins. When the

chromatograms obtained with cone voltages of 30, 80, and 140 V are compared, a clear shift in the detected hump can be seen for both procyanidins (Figure 5A−C,G−I) and prodelphinidins (Figure 5D−F,J−L). A vertical line is shown that crosses the x-axis at 3 min to highlight these shifts. The lowest cone voltage detected mainly monomers and some smaller oligomers that are witnessed as sharp chromatographic peaks. Higher cone voltages also detected the proanthocyanidin hump characteristic for larger oligomers and polymers. In general, prodelphinidins eluted at earlier retention times than corresponding procyanidins. This can be seen when the chromatogram pairs A and D, B and E, C and F, G and J, H and K, and I and L in Figure 5 are compared. The elution time of compounds from reverse phase columns tends to be inversely related to their polarity; thus, shorter retention times of prodelphinidins would be expected because of their greater polarity associated with more extensive hydroxylation of the B-ring.[44]

In addition to the distribution of procyanidins and prodelphinidins along the chromatographic hump, the distribution of procyanidin and prodelphinidin extension and terminal units can be investigated by examining their MRM chromatograms. For example, the MRM chromatograms of extension units and terminal units of samples 1-F2 and 2-F2 are presented in Figure 6. To focus mainly on larger oligomers and polymers, MRM chromatograms with a cone voltage of 140 V were compared. In the 1-F2 sample, the MRM chromatographic hump of procyanidin extension units eluted later than prodelphinidin extension units and procyanidin and prodelphinidin terminal units (Figure 6A). This suggests that procyanidin extension units were most abundant in late-eluting proanthocyanidin molecules. It could also be seen that the chromatographic hump of terminal prodelphinidin units eluted earlier than terminal procyanidin units. This indicates that prodelphinidin terminal units were most abundant in earlier eluting proanthocyanidin molecules. In contrast, the shape of the chromatographic hump of procyanidin terminal units suggests that they were distributed fairly evenly among the proanthocyanidins. In contrast to the 1-F2 sample, the 2-F2
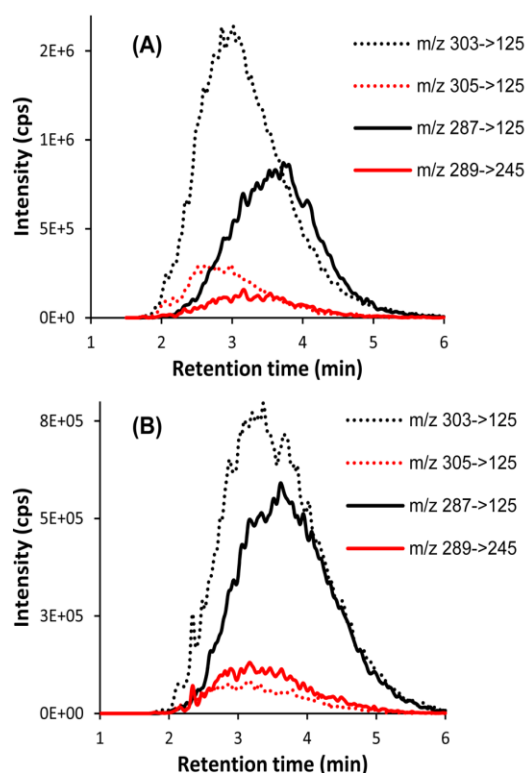
Figure 6. MRM chromatograms of procyanidin extension units (m/z 287 → 125), procyanidin terminal units (m/z 289 → 245), prodelphinidin extension units (m/z 303 → 125), and prodelphinidin terminal units (m/z 305→ 125) for samples 1-F2 (A) and 2-F2 (B). See Table 1 for fraction identities.

sample (Figure 6B) had a more uniform distribution of all procyanidin and prodelphinidin terminal and extension units, which would indicate a relatively homogeneous distribution of these units in the proanthocyanidins of this particular sample. The same kind of comparisons can be made at lower cone voltages to provide information on how the extension and terminal units of procyanidin and prodelphinidin are distributed across smaller oligomeric proanthocyanidins.

Determination of Proanthocyanidin Contents and Procyanidin/Prodelphinidin Ratios. To determine the total content of proanthocyanidins and procyanidin/prodelphinidin ratios, calibration curves were produced for the developed MRM method with pure procyanidins (fraction 5-F2) and pure prodelphinidins (fraction 13-F2). The five highest cone voltages were used for detection, and resulting peak areas were summed. The lowest cone voltage was not used to avoid monomer detection, because they are not classified as proanthocyanidins. These calibration curves were then used for estimation of procyanidin and prodelphinidin concentrations in all 18 proanthocyanidin fractions (5-F1−13-F2). The resulting proanthocyanidin contents were compared to proanthocyanidin contents estimated by thiolysis and HCl-butanol assay. Procyanidin/prodelphinidin ratios were then compared to procyanidin/prodelphinidin ratios estimated by thiolysis. A good correlation for proanthocyanidin contents with both thiolysis (R^2 = 0.82) and HCl-butanol assay (R^2 = 0.86) was achieved as was an excellent agreement for procyanidin/prodelphinidin ratios between the thiolysis and

MRM results (R^2 = 0.98). These results suggest that our MRM approach allows both qualitative and quantitative analyses of complex proanthocyanidins directly from plant extracts.

Estimating the Mean Degree of Polymerization. On the basis of the quinone methide cleavage theory[4,27] (Figure 1B), it was hypothesized that an equation could be empirically developed to calculate the mDP of proanthocyanidins from total peak areas obtained for procyanidin and prodelphinidin extension and terminal units. A preliminary equation using estimated coefficients for each MRM transition was developed by comparing the thiolysis and MRM results from the 18 procyanidin- and prodelphinidin-rich fractions (5-F1−13-F2). Initially equations were developed individually for each cone voltage, but finally only one equation was developed by using the total peak area from the five highest cone voltages: 50, 75, 85, 110, and 140 V for procyanidins and 55, 80, 110, 130, and 150 V for prodelphinidins. The lowest cone voltage (30 V) was not used to avoid detection of monomers because monomers cause underestimation of the mDP. The resulting equation is as follows:

$$mDP = \frac{0.37A_{287} + 0.42A_{289} + 2.15A_{303} + 0.68A_{305}}{0.42A_{289} + 0.68A_{305}}$$

A_{287}, A_{289}, A_{303}, and A_{305} are the sums of peak areas determined from MRM chromatograms of procyanidin extension units (m/z 287 → 125), procyanidin terminal units (m/z 289 → 245), prodelphinidin extension units (m/z 303 → 125), and prodelphinidin terminal units (m/z 305→ 125), respectively, with the five highest cone voltages (Table 2). The coefficients of the four ions differ due to the differing propensities of procyanidin/prodelphinidin extension and terminal units to undergo ionization. It should be noted that ionization coefficients could differ among UPLC-MS/MS instruments. Therefore, the correct ionization coefficients should be individually checked for each instrument. When this is done, the samples used should cover a wide range of proanthocyanidin types with various features (procyanidin/prodelphinidin ratio, mDP). In this study, 18 was a sufficient number of varying proanthocyanidin samples for adjusting these coefficients.

For the 18 samples used in the calibration, the mDPs estimated by the equation were naturally related (R^2 = 0.94) to results obtained by thiolysis. The equation was then independently tested with nine additional proanthocyanidin-rich fractions (1-F1−4-F2) to prove that it functions well also with other independent samples (R^2 = 0.90). Together these 27 fractions represented a diverse set of proanthocyanidins, with mDP values ranging from 2 to 15 and compositions varying from 95% procyanidin to 99% prodelphinidin. Therefore, these results indicated that the developed MRM method accompanied by this equation can reliably estimate the mDP of a wide variety of proanthocyanidins.

Previously, thiolysis and phloroglucinolysis have been the most commonly used tools for achieving information of proanthocyanidin content, procyanidin/prodelphinidin distribution, and mDP from plant extracts.[2,13−17] However, in these methods, proanthocyanidins are cleaved into monomer units before analysis, and all information of the individual oligomers and polymers is lost. Therefore, these methods lack the possibility to characterize the original oligomer and polymer fingerprint. In the presented UPLC-MS/MS method, the proanthocyanidin fragmentation takes place after the chromato-

260

graphic step, and therefore it is possible to estimate how the different proanthocyanidins, in terms of their procyanidin and prodelphinidin composition and mDP, are distributed along the chromatographic hump typically produced by large proanthocyanidin oligomers and polymers. Another advantage of the presented UPLC-MS/MS method is its sensitivity. It can be used to analyze samples produced from as little as 1 mg of plant powder, whereas thiolysis and phloroglucinolysis typically require relatively large amounts of plant tissue, in the range of hundreds of milligrams, for analysis.[17−19]

Repeatability of the UPLC-MS/MS Mthod. The repeatability of the method was determined using Student's t test at the 95% confidence interval. Five replicates of nine different proanthocyanidin fractions (1-F1−4-F2) were analyzed with the MRM method containing six different cone voltages and one optimal collision energy for each terminal and extension unit (Table 2). Results were presented as confidence intervals of the sums of peak areas obtained with different cone voltages and concentrations for procyanidins and prodelphinidins, procyanidin/prodelphinidin ratios, and mDP values. The procyanidin and prodelphinidin concentrations were calculated as milligrams per gram in fractions and procyanidin/prodelphinidin ratios as percent procyanidin. The relative standard deviation (RSD) for all nine samples with five replicates was determined from these results. The results showed that the quantitative determination of procyanidins is generally slightly less accurate than that for prodelphinidins (RSD = 3.5 and 2.1%, respectively). The RSDs for procyanidin/prodelphinidin ratio and mDP were small (0.6 and 1.4%, respectively), which demonstrates the pronounced reliability of this method for these qualitative measurements.

Limit of Detection, Limit of Quantitation, and Linearity. LOD, LOQ, and linearity were determined with the presented method for procyanidin and prodelphinidin dimers. LOD for procyanidin dimer was 16 ng/mL, whereas LOQ was 23 ng/mL. For prodelphinidin dimer, the corresponding values were 170 and 190 ng/mL, respectively. There was a difference in the efficiency of detection of procyanidin terminal and extension units; procyanidin terminal units were detected at 8 times lower concentration than the extension units. For prodelphinidins the difference was smaller; prodelphinidin terminal units were detected at 2 times lower concentration than prodelphinidin extension units. The linear areas were 0.04−2.5 μg/mL for procyanidins and 0.5−10 μg/mL for prodelphinidins. However, because the methodology presented is group-specific, that is, it is used for the analysis of the total amount of proanthocyanidins, values determined with pure dimers do not truly illustrate the limits of the method. Depending on the analyzed samples, different types of proanthocyanidins are detected from very small concentrations, whereas other proanthocyanidins can be detected only from more concentrated samples. In this study, it was not possible to determine the limits of detection of all possible individual proanthocyanidin compounds, and this will have to wait until pure oligomers and polymers of procyanidin and prodelphinidin compounds become available.

Use of the Method for Proanthocyanidin Characterization. Plants produce complex and often heterogeneous mixtures of procyanidins and prodelphinidins and, apart from small oligomers, it is practically impossible to purify large procyanidin and prodelphinidin oligomers or polymers individually.[6,14,45] For this reason the current research utilized a mixture of oligo- and polymeric quantitation standards that

were chosen on the basis of their procyanidin and prodelphinidin purities. Naturally, the best quantitation results are expected with proanthocyanidin standards that are isolated from the very same species that is investigated for its proanthocyanidin content. This approach lowers the risk of utilization of wrong types of quantitation standards, but is too laborious with investigations that include hundreds of species, for example. In such cases, our MRM method offers a practical solution to significantly narrow the need for hundreds of standards.

We have used the method for the analysis of crude extracts of over 1000 plant species and found that the MRM chromatographic proanthocyanidin profiles (chromatographic fingerprint of the procyanidin and prodelphinidin extension and terminal units) (Figure 6) are not different with all of the species. Instead, it is possible to find several species clusters that share similar proanthocyanidin profiles (Salminen, unpublished observations). Thus, it would be sufficient to isolate one well-characterized proanthocyanidin standard per a given species cluster as proanthocyanidin fingerprints do not differ significantly within the cluster. Such an approach would allow the production of a library of proanthocyanidin standards, and each time the most correct standard could be chosen for any new plant species that was analyzed for its proanthocyanidin fingerprint during the 10 min analysis with the developed MRM method.

The present method can be used for both qualitative and quantitative analyses of complex proanthocyanidins directly from plant crude extracts. Instead of time-consuming degradation required by thiolysis or phloroglucinolysis, the present method describes in-source fragmentation of the UPLC-separated proanthocyanidin molecules by cone voltages optimized for terminal and extension units of procyanidins and prodelphinidins. UPLC enables rapid chromatography of different kinds of proanthocyanidins, whereas TQ-MS fragments compounds into proanthocyanidin-specific precursor and product ions for detection with MRM methods. The selective nature of the method enables the estimation of both the procyanidin/prodelphinidin ratio and mDP for the proanthocyanidins during the 10 min MS/MS analysis. Furthermore, because the proanthocyanidin fragmentation takes place after the chromatographic step, it is possible to estimate how the different proanthocyanidins in terms of their procyanidin and prodelphinidin composition and mDP are distributed along the chromatographic hump typically produced by large proanthocyanidin polymers. The UPLC-MS/MS method is able to handle 140 extracts, produced from as little as 1 mg of plant powder, in a day, and it offers a user-friendly, robust, and fast addition to the chemistry tools currently used for the qualitative and quantitative screening of large numbers of proanthocyanidin-containing plants for their bioactive proanthocyanidin types and content.

■ ASSOCIATED CONTENT

ⓢ Supporting Information

UPLC traces of the fractions used in the present work (Figure S1−S7). HCl-butanol calibration curves used for quantitation of proanthocyanidin contents in the present work (Figure S8). UPLC-MS/MS calibration curves used for quantitation of procyanidins and prodelphinidins in the present work (Figure S9). Cone voltage optimization plots for the accumulation of precursor ions presenting procyanidin and prodelphinidin extension and terminal units (Figure S10). Collision energy

3397

dx.doi.org/10.1021/jf500745y | J. Agric. Food Chem. 2014, 62, 3390−3399

261

optimization plots for the accumulation of product ions presenting procyanidin and prodelphinidin extension and terminal units (Figure S11). Correlations between proanthocyanidin content determined by the MRM and thiolysis and MRM and HCl-butanol methods, correlation between procyanidin percentage of total proanthocyanidin content and correlation between mean degree of polymerization determined by the MRM and thiolysis methods for proanthocyanidin-rich fractions used in the present work (Figure S12). The effect of cone voltage to the peak areas of fractions 1-F1 to 13-F2 (Figure S13). Repeatability data of the presented MRM method determined with the Student's t test at 95% confidence interval (Table S1). This material is available free of charge via the Internet at http://pubs.acs.org.

■ AUTHOR INFORMATION

Corresponding Author

*(M.T.E.) Phone: +358 2 333 6755. E-mail: marica.engstrom@utu.fi.

Notes

The authors declare no competing financial interest.

■ ACKNOWLEDGMENTS

■ ABBREVIATIONS USED

UPLC, ultrahigh-performance liquid chromatography; TQ-MS, triple-quadrupole mass spectrometer; MRM, multiple reaction monitoring; mDP, mean degree of polymerization; ESI, electrospray ionization; LOD, limit of detection; LOD, limit of quantitation; S/N, signal-to-noise ratio; RSD, relative standard error

■ REFERENCES

(1) Haslam, E. Proanthocyanidins. In *Plant Polyphenols: Vegetable Tannins Revisited*; Cambridge University Press: Cambridge, UK, 1989; pp 14–79.

(2) Hemingway, R. W. Structural variation in proanthocyanidins and their derivatives. In *Chemistry and Significance of Condensed Tannins*; Hemingway, R. W., Karchesy, J. J., Eds.; Plenum Press: New York, 1989; pp 83–107.

(3) Porter, L. J. Tannins. In *Methods in Plant Biochemistry*; Dey, P. M., Harborne, J. B., Eds.; Academic Press: New York, 1989; Vol. 1, pp 389–419.

(4) Gu, L.; Kelm, M. A.; Hammerstone, J. F.; Beecher, G.; Holden, J.; Haytowitz, D.; Prior, R. L. Screening of foods containing proanthocyanidins and their structural characterization using LC-MS/MS and thiolytic degradation. *J. Agric. Food Chem.* **2003**, *51*, 7513–7521.

(5) Dixon, R. A.; Xie, D.-Y.; Sharma, S. B. Proanthocyanidins− a final frontier in flavonoid research? *New Phytol.* **2005**, *165*, 9–28.

(6) Mueller-Harvey, I. Unravelling the conundrum of tannins in animal nutrition and health. *J. Sci. Food Agric.* **2006**, *86*, 2010–2037.

(7) Hoste, H.; Jackson, F.; Athanasiadou, S.; Thamsborg, S. M.; Hoskin, S. O. The effects of tannin-rich plants on parasitic nematodes in ruminants. *Trends Parasitol.* **2006**, *22*, 253–261.

(8) Brunet, S.; Jackson, F.; Hoste, H. Effects of sainfoin (*Onobrychis viciifolia*) extract and monomers of condensed tannins on the association of abomasal nematode larvae with fundic explants. *Int. J. Parasitol.* **2008**, *38*, 783–790.

(9) Novobilský, A.; Mueller-Harvey, I.; Thamsborg, S. M. Condensed tannins act against cattle nematodes. *Vet. Parasitol.* **2011**, *182*, 213–220.

(10) Novobilský, A.; Stringano, E.; Carbonero, C. H.; Smith, L. M. J.; Enemark, H. L.; Mueller-Harvey, I.; Thamsborg, S. M. *In vitro* effects of extracts and purified tannins of sainfoin (*Onobrychis viciifolia*) against two cattle nematodes. *Vet. Parasitol.* **2013**, *196*, 532–537.

(11) Molan, A. L.; Waghorn, G. C.; Min, B. R.; McNabb, W. C. The effect of condensed tannins from seven herbages on *Trichostrongylus colubriformis* larval migration *in vitro*. *Folia Parasitol.* **2000**, *47*, 39–44.

(12) Manolaraki, F.; Sotiraki, S.; Skampardonis, V.; Volanis, M.; Stefanakis, A.; Hoste, H. Anthelmintic activity of some Mediterranean browse plants against parasitic nematodes. *Parasitology* **2010**, *137*, 685–696.

(13) Cheynier, V.; Fulcrand, H. Analysis of polymeric proanthocyanidins and complex polyphenols. In *Methods in Polyphenol Analysis*; Santos-Buelga, C., Williamson, G., Eds.; Royal Society of Chemistry: Cambridge, UK, 2003; pp 284–313.

(14) Hümmer, W.; Schreier, P. Analysis of proanthocyanidins. *Mol. Nutr. Food Res.* **2008**, *52*, 1381–1398.

(15) Gu, L. Analysis methods of proanthocyanidins. In *Analysis of Antioxidant-Rich Phytochemicals*; Xu, Z., Howard, L. R., Eds.; Wiley-Blackwell: Oxford, UK, 2012; pp 247–274.

(16) Thompson, R. S.; Jacques, D.; Haslam, E.; Tanner, R. J. N. Plant proanthocyanidins. Part I. Introduction; the isolation, structure, and distribution in nature of plant procyanidins. *J. Chem. Soc., Perkin Trans. 1* **1972**, *11*, 1387–1399.

(17) Karonen, M.; Leikas, A.; Loponen, J.; Sinkkonen, J.; Ossipov, V.; Pihlaja, K. Reversed-phase HPLC-ESI/MS analysis of birch leaf proanthocyanidins after their acidic degradation in the presence of nucleophiles. *Phytochem. Anal.* **2007**, *18*, 378–386.

(18) Gea, A.; Stringano, E.; Brown, R. H.; Mueller-Harvey, I. In situ analysis and structural elucidation of sainfoin (*Onobrychis viciifolia*) tannins for high-throughput germplasm screening. *J. Agric. Food Chem.* **2011**, *59*, 495–503.

(19) Hellström, J. K.; Törrönen, A. R.; Mattila, P. H. Proanthocyanidins in common food products of plant origin. *J. Agric. Food Chem.* **2009**, *57*, 7899–7906.

(20) Guillarme, D.; Schappler, J.; Rudaz, S.; Veuthey, J.-L. Coupling ultra-high-pressure liquid chromathography with mass spectrometry. *Trends Anal. Chem.* **2010**, *29*, 15–27.

(21) Motilva, M.-J.; Serra, A.; Macià, A. Analysis of food polyphenols by ultra high-performance liquid chromatography coupled to mass spectrometry: an overview. *J. Chromatogr., A* **2013**, *1292*, 66–82.

(22) Rodríguez-Aller, M.; Gurny, R.; Veuthey, J.-L.; Guillarme, D. Coupling ultra high-pressure liquid chromatography with mass spectrometry: constraints and possible applications. *J. Chromatogr., A* **2013**, *1292*, 2–18.

(23) Valls, J.; Millán, S.; Martí, M. P.; Borràs, E.; Arola, L. Advanced separation methods of food anthocyanins, isoflavones and flavanols. *J. Chromatogr., A* **2009**, *1216*, 7143–7172.

(24) Prasain, J. K.; Wang, C.-C.; Barnes, S. Mass spectrometric methods for the determination of flavonoids in biological samples. *Free Radical Biol. Med.* **2004**, *37*, 1324–1350.

(25) Prasain, J. K.; Barnes, S. Uptake and metabolism of dietary proanthocyanidins. In *Polyphenols in Human Health and Disease*; Watson, R. R., Preedy, V. R., Zibadi, S., Eds.; Academic Press: London, UK, 2014; Vol. 1, pp 553–560.

3398
dx.doi.org/10.1021/jf500745y | *J. Agric. Food Chem.* 2014, 62, 3390–3399

262

Article

(26) Benavides, A.; Montoro, P.; Bassarello, C.; Piacente, S.; Pizza, C. Catechin derivatives in *Jatropha macrantha* stems: characterisation and LC/ESI/MS/MS quali-quantitative analysis. *J. Pharm. Biomed. Anal.* **2006**, *40*, 639–647.

(27) Friedrich, W.; Eberhardt, A.; Galensa, R. Investigation of proanthocyanidins by HPLC with electrospray ionization mass spectrometry. *Eur. Food Res. Technol.* **2000**, *211*, 56–64.

(28) Mari, A.; Eletto, D.; Pizza, C.; Montoro, P.; Piacente, S. Integrated mass spectrometry approach to profile proanthocyanidins occurring in food supplements: analysis of *Potentilla erecta* L. rhizomes. *Food Chem.* **2013**, *141*, 4171–4178.

(29) Flamini, R. Recent applications of mass spectrometry in the study of grape and wine polyphenols. *ISRN Spectrosc.* **2013**, *2013*, 1–45, article ID 813563; http://dx.doi.org/10.1155/2013/813563 (accessed Jan 9, 2014).

(30) Rebello, L. P. G.; Lago-Vanzela, E. S.; Barcia, M. T.; Ramos, A. M.; Stringheta, P. C.; Da-Silva, R.; Castillo-Muñoz, N.; Gómez-Alonso, S.; Hermosín-Gutiérrez, I. Phenolic composition of the berry parts of hybrid grape cultivar BRS Violeta (BRS Rubea × IAC 1398-21) using HPLC-DAD-ESI-MS/MS. *Food Res. Int.* **2013**, *54*, 354–366.

(31) Zywicki, B.; Reemtsma, T.; Jekel, M. Analysis of commercial vegetable tanning agents by reversed-phase liquid chromatography–electrospray ionization–tandem mass spectrometry and its application to wastewater. *J. Chromatogr., A* **2002**, *970*, 191–200.

(32) Monagas, M.; Garrido, I.; Lebrón-Aguilar, R.; Bartolomé, B.; Gómez-Cordovés, M. C. Almond (*Prunus dulcis* (Mill.) D.A. Webb) skins as a potential source of bioactive polyphenols. *J. Agric. Food Chem.* **2007**, *55*, 8498–8507.

(33) Touriño, S.; Fuguet, E.; Jáuregui, O.; Saura-Calixto, F.; Cascante, M.; Torres, J. L. High-resolution liquid chromatography/electrospray ionization time-of-flight mass spectrometry combined with liquid chromatography/electrospray ionization tandem mass spectrometry to identify polyphenols from grape antioxidant dietary fiber. *Rapid Commun. Mass Spectrom.* **2008**, *22*, 3489–3500.

(34) Callemien, D.; Collin, S. Use of RP-HPLC-ESI (−)-MS/MS to differentiate various proanthocyanidin isomers in lager beer extracts. *J. Am. Soc. Brew. Chem.* **2008**, *66*, 109–115.

(35) Monagas, M.; Garrido, I.; Lebrón-Aguilar, R.; Gómez-Cordovés, M. C.; Rybarczyk, A.; Amarowicz, R.; Bartolomé, B. Comparative flavan-3-ol profile and antioxidant capacity of roasted peanut, hazelnut, and almond skins. *J. Agric. Food Chem.* **2009**, *57*, 10590–10599.

(36) Fraser, K.; Harrison, S. J.; Lane, G. A.; Otter, D. E.; Hemar, Y.; Quek, S.-Y.; Rasmussen, S. HPLC–MS/MS profiling of proanthocyanidins in teas: a comparative study. *J. Food Compos. Anal.* **2012**, *26*, 43–51.

(37) Sarnoski, P. J.; Johnson, J. V.; Reed, K. A.; Tanko, J. M.; O'Keefe, S. F. Separation and characterisation of proanthocyanidins in Virginia type peanut skins by LC–MS^n. *Food Chem.* **2012**, *131*, 927–939.

(38) Ojwang, L. O.; Yang, L.; Dykes, L.; Awika, J. Proanthocyanidin profile of cowpea (*Vigna unguiculata*) reveals catechin-O-glucoside as the dominant compound. *Food Chem.* **2013**, *139*, 35–43.

(39) Wilson, E. L. High-pressure liquid chromatography of apple juice phenolic compounds. *J. Sci. Food Agric.* **1981**, *32*, 257–264.

(40) Guyot, S.; Doco, T.; Souquet, J.-M.; Moutounet, M.; Drilleau, J.-F. Characterization of highly polymerized procyanidins in cider apple (*Malus sylvestris* var. *kermerrien*) skin and pulp. *Phytochemistry* **1997**, *44*, 351–357.

(41) Roux, E. L.; Doco, T.; Sarni-Manchado, P.; Lozano, Y.; Cheynier, V. A-type proanthocyanidins from pericarp of *Litchi sinensis*. *Phytochemistry* **1998**, *48*, 1251–1258.

(42) Adamson, G. E.; Lazarus, S. A.; Mitchell, A. E.; Prior, R. L.; Cao, G.; Jacobs, P. H.; Kremers, B. G.; Hammerstone, J. F.; Rucker, R. B.; Ritter, K. A.; Schmitz, H. H. HPLC method for the quantification of procyanidins in cocoa and chocolate samples and correlation to total antioxidant capacity. *J. Agric. Food Chem.* **1999**, *47*, 4184–4188.

(43) Karonen, M.; Loponen, J.; Ossipov, V.; Pihlaja, K. Analysis of procyanidins in pine bark with reversed-phase and normal-phase high-performance liquid chromatography-electrospray ionization mass spectrometry. *Anal. Chim. Acta* **2004**, *522*, 105–112.

(44) Koupai-Abyazani, M. R.; McCallum, J.; Bohm, B. A. Identification of the constituent flavanoid units in sainfoin proanthocyanidins by reverse-phase liquid chromatography. *J. Chromatogr.* **1992**, *594*, 117–123.

(45) Santos-Buelga, C.; Scalbert, A. Proanthocyanidins and tannin-like compounds − nature, occurrence, dietary intake and effects on nutrition and health. *J. Sci. Food Agric.* **2000**, *80*, 1094–1117.

Appendix C

Original publication:

1H–13C HSQC NMR Spectroscopy for Estimating Procyanidin/Prodelphinidin and cis/trans-Flavan-3-ol Ratios of Condensed Tannin Samples: Correlation with Thiolysis

Wayne E. Zeller, Aina Ramsay, Honorata M. Ropiak, Christos Fryganas, Irene Mueller-Harvey, Ronald H. Brown, Chris Drake, and John H. Grabber

¹H–¹³C HSQC NMR Spectroscopy for Estimating Procyanidin/Prodelphinidin and *cis/trans*-Flavan-3-ol Ratios of Condensed Tannin Samples: Correlation with Thiolysis

Wayne E. Zeller,*,[†] Aina Ramsay,[§] Honorata M. Ropiak,[§] Christos Fryganas,[§] Irene Mueller-Harvey,[§] Ronald H. Brown,[§] Chris Drake,[§] and John H. Grabber[†]

[†]U.S. Dairy Forage Research Center, Agricultural Research Service, U.S. Department of Agriculture, 1925 Linden Drive West, Madison, Wisconsin 53706, United States

[§]Chemistry and Biochemistry Laboratory, Food Production and Quality Division, School of Agriculture, Policy and Development, University of Reading, P.O. Box 236, 1 Earley Gate, Reading RG6 6AT, United Kingdom

ABSTRACT: Studies with a diverse array of 22 purified condensed tannin (CT) samples from nine plant species demonstrated that procyanidin/prodelphinidin (PC/PD) and *cis/trans*-flavan-3-ol ratios can be appraised by ¹H–¹³C HSQC NMR spectroscopy. The method was developed from samples containing 44–~100% CT, PC/PD ratios ranging from 0/100 to 99/1, and *cis/trans* ratios ranging from 58/42 to 95/5 as determined by thiolysis with benzyl mercaptan. Integration of cross-peak contours of H/C-6′ signals from PC and of H/C-2′,6′ signals from PD yielded nuclei-adjusted estimates that were highly correlated with PC/PD ratios obtained by thiolysis ($R^2 = 0.99$). *cis/trans*-Flavan-3-ol ratios, obtained by integration of the respective H/C-4 cross-peak contours, were also related to determinations made by thiolysis ($R^2 = 0.89$). Overall, ¹H–¹³C HSQC NMR spectroscopy appears to be a viable alternative to thiolysis for estimating PC/PD and *cis/trans* ratios of CT if precautions are taken to avoid integration of cross-peak contours of contaminants.

KEYWORDS: *condensed tannins, proanthocyanidins, procyanidins, prodelphinidins, nuclear magnetic resonance spectroscopy, NMR, thiolysis*

■ INTRODUCTION

Condensed tannins (CTs) (also referred to as proanthocyanidins or PACs) represent a class of polyphenolic plant secondary metabolites that are composed of oligomers and polymers of flavan-3-ols.[1,2] These structures vary not only in flavan-3-ol subunit composition but also in interflavan-3-ol bond connectivity and mean degree of polymerization (mDP). Condensed tannins are most commonly composed of procyanidin (PC) subunits derived from catechin and epicatechin and of prodelphinidin (PD) subunits derived from gallocatechin and epigallocatechin. Substituents at C-2 and C-3 in the C-ring of epicatechin and epigallocatechin have a *cis* configuration, whereas catechin and gallocatechin possess a *trans* stereochemical orientation (Figure 1). These subunits are typically interconnected by C4–C8 interflavan-3-ol linkages (classified as a B-type linkage, Figure 1), but other less common interunit linkages such as C4–C6 also occur in CTs.

A major point of interest in CTs stems from the potential positive impact they could bring to the agricultural industry because of their ability to modulate proteolysis during forage conservation and ruminal digestion,[3–7] to prevent bloat,[8] to reduce intestinal parasite burdens,[9] and to lessen methane emissions from ruminants.[10,11] It is thought that the CT composition may play a role in how effectively they impart their biological effects on each of these outcomes, improving both the economical and environmental sustainability of ruminant farm operations. Thus, results from in vitro and in vivo experiments in which CT content is known and the composition is well-defined should reveal CT types and levels that are required for optimizing ruminant health and productivity. Such information would help plant breeders with selection for CT content and structure and also help identify plant varieties that are good candidates for genetic modification.

Analytical techniques allowing for the rapid assessment of chemical structures of CT mixtures within and isolated from plant materials remain a high priority.[1,2] Development of robust analytical methods is required to gain a better understanding of how CTs affect the interdependency of CT/protein structure–activity relationships. Owing to the structural complexity of CTs, novel approaches are needed for their analysis, including new techniques to corroborate data from existing methods. These analytical techniques are needed for analyzing CT mixtures as these are relevant, and applicable to, nutritional and health research on CTs for both humans[13] and animals.[14]

A variety of analytical techniques have been developed for the characterization and analysis of condensed tannins. Thiolysis with benzyl mercaptan[15,16] is one of the most common methods to obtain compositional and structural data on in situ or isolated CTs.[17] This method involves acid-catalyzed degradation of CT polymers into reactive monomeric cationic subunits, which are subsequently trapped with nucleophiles, such as benzyl mercaptan, providing stable
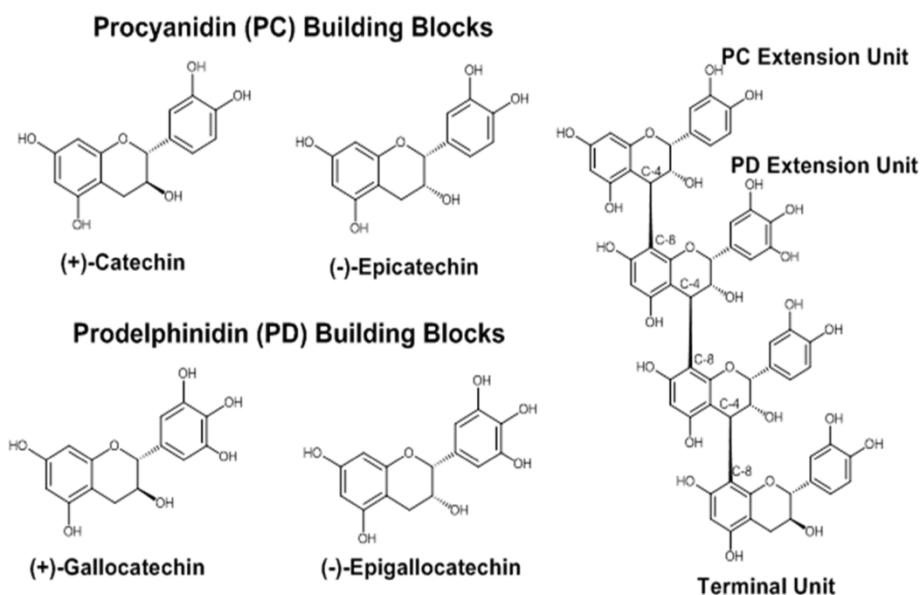
Figure 1. Structures of common flavan-3-ol monomeric subunits found in condensed tannins (left) and a condensed tannin tetramer (right) showing C4−C8 (B-type) linkages, PC and PD extension units, and a terminal unit.

monomeric flavan-3-ol adducts. In this method, extension units are converted into stable C-4 thio ethers, whereas terminal units of the polymers are liberated as intact flavan-3-ol monomers. HPLC analysis of the mixtures obtained from these depolymerization studies allows qualitative and quantitative assessment of CT composition in terms of ratios of PC/PD and *cis/trans* subunits and overall mDP. It can thus be used to calculate the purity of isolated CT samples on the basis of the total flavan-3-ol yield. Currently, thiolysis represents one of the most useful techniques available for the analysis of CT composition.

One-dimensional (1D) NMR spectroscopic studies have been used previously to determine the compositional aspects of isolated condensed tannin samples by either solution state ^{13}C NMR spectroscopy[18−27] or cross-polarization magic angle spinning (CPMAS) solid state ^{13}C NMR spectroscopy.[28−31] Solution state ^{13}C NMR spectroscopy has been utilized for the determination of PC/PD[18−20,22−27] and *cis/trans* ratios,[18,19,22,24−27] estimations of mDP,[18−20,22,24,26,27] and the identification of C4−C6 and C4−C8 linkages.[20,21] These NMR techniques, however, suffer from broad and often unresolved signals, long acquisition times, and low signal-to-noise ratios, which hamper an accurate assessment of CT composition. Solid phase studies of CT-containing plant material have been conducted using ^{13}C CPMAS NMR techniques.[28−31] Although this technique provides good signal-to-noise ratios, signals in the spectra are still broad and frequently overlap with non-CT signals. In addition, ^{13}C CPMAS requires the use of highly specialized equipment.

By contrast, common two-dimensional (2D) NMR techniques have not been extensively explored for assessing the composition of either purified CTs or CTs present in whole plant materials.[32] Here we report the use of [1]H−^{13}C HSQC NMR spectroscopy as a means to determine PC/PD and *cis/trans* ratios of isolated CT samples.

MATERIALS AND METHODS

General Procedure for the Purification and Characterization of Condensed Tannins. Condensed tannins were purified from dried and milled plant material and analyzed for CT composition and purity as previously described.[15,16] Briefly, dried plant material was milled (typically using a cyclone mill) containing a 1 or 0.5 mm screen, and the resulting ground material was extracted with 7:3 acetone/water (3 × 10 mL/g of dried material) and filtered. The combined filtrates were concentrated on a rotary evaporator (<40 °C) to remove acetone, and the resulting aqueous layer was extracted with a half volume of dichloromethane (2 times) and was freeze-dried. The freeze-dried residue was purified in one of two ways. The first method involved dissolving the freeze-dried residue in water and applying the resulting mixture to the top of a Sephadex LH-20 column prepacked in water. The column was eluted with water, removing a majority of the carbohydrates present. Column elution was continued with 3:7 acetone/water (providing sample fraction 1) followed by elution of the column with 1:1 acetone/water to give sample fraction 2, which typically contained CTs of highest purity. Alternatively, the dried extraction residue is adsorbed onto Sephadex LH-20 as a 1:1 methanol/water solution to provide a mixture with the consistency of wet sand. This material is then placed in a Buchner funnel and consecutively rinsed with methanol/water (1:1) followed by a series of acetone/water mixtures (1:1, 7:3, 9:1) with each rinsing conducted three times with 5 mL of solvent per gram of Sephadex LH-20. The three rinse filtrates for each solvent were pooled, concentrated on a rotary evaporator (<40 °C) to remove the volatile solvent, and freeze-dried. In both purification methods, the freeze-dried samples were analyzed by [1]H−^{13}C HSQC NMR spectroscopy to assess relative purity and/or thiolysis to provide a numerical purity.

NMR Spectroscopy. ^{1}H, ^{13}C, and [1]H−^{13}C HSQC NMR spectra were recorded at 27 °C on a BrukerBiospin DMX-500 ([1]H 500.13 MHz, [13]C 125.76 MHz) instrument equipped with TopSpin 2.1 software and a cryogenically cooled 5 mm TXI ^{1}H/^{13}C/^{15}N gradient probe in inverse geometry. Spectra were recorded in DMSO-d_6/pyridine-d_5 (4:1) mixtures and were referenced to the residual signals of DMSO-d_6 (2.49 ppm for ^{1}H and 39.5 ppm for ^{13}C spectra). ^{13}C NMR spectra were obtained using 5000 scans (acquisition time of 4 h and 30 min each). For [1]H−^{13}C HSQC experiments, spectra were obtained using 128 scans (acquisition time of 18 h 30 min each) obtained using the standard Bruker pulse program (hsqcegtpsi) with

266

Table 1. Comparison of Data from Thiolysis and ^{1}H–^{13}C HSQC NMR Determinations for 22 Condensed Tannin (CT) Samples[a]

CT sample	plant species	CT content (thiolysis) (%)*	SD	% PC (thiolysis)	SD	% PC (NMR)	SD	% cis (thiolysis)	SD	% cis (NMR)	SD
1	Lespedeza cuneata	96.3	0.08	5.9	0.06	4.9	0.06	79.2	0.26	73.2	1.19
2	Lotus corniculatus	92.5	0.03	54.0	0.62	55.6	1.17	93.3	0.58	86.8	0.59
3	Lotus corniculatus	78.1	0.40	68.0	0.35	70.9	0.19	87.5	0.15	88.7	1.17
4	Lotus corniculatus	75.3	0.01	57.1	0.12	60.8	0.32	91.3	0.13	87.0	1.58
5	Lotus pedunculatus	108.0	0.01	16.0	0.07	14.6	0.80	81.7	0.22	69.3	1.63
6	Lotus pedunculatus	91.3	0.35	25.9	0.29	23.7	0.28	78.7	0.23	75.4	1.22
7	Lotus pedunculatus	85.8	0.01	17.5	0.06	17.5	0.50	79.5	0.05	71.7	0.45
8	Lotus pedunculatus	80.3	0.41	28.1	0.17	29.0	1.02	74.4	0.15	71.0	1.79
9	Onobrychis viciifolia	102.2	8.13	37.3	0.29	39.1	3.23	82.9	0.27	84.4	5.05
10	Onobrychis viciifolia	93.7	4.55	19.2	0.06	19.1	0.28	83.3	0.21	77.9	1.96
11	Onobrychis viciifolia	82.4	1.10	51.7	0.32	56.7	0.62	83.5	0.10	79.7	0.90
12	Onobrychis viciifolia	44.3	0.17	57.3	0.07	59.0	1.45	68.7	0.00	64.9	1.10
13	Securigera varia	56.6	n = 1	18.2	n = 1	22.5	0.17	89.7	n = 1	87.6	0.56
14	Sorghum bicolor	58.8	0.02	100.0	0.00	100.0	0.00	85.5	0.09	87.1	2.60
15	Theobroma cacao	63.8	n = 1	100.0	n = 1	100.0	nd	93.4	n = 1	100.0	nd
16	Theobroma cacao	49.0	0.01	100.0	0.0	100.0	0.00	90.1	0.12	88.7	2.06
17	Tilia sp.	92.7	0.04	98.5	0.05	99.2	0.19	95.5	0.09	91.2	0.15
18	Tilia sp.	61.1	0.47	98.1	0.14	99.2	0.47	89.4	0.11	89.1	0.73
19	Trifolium repens	120.6	0.01	0.8	0.00	0.0	nd	69.3	0.07	61.1	1.01
20	Trifolium repens	111.4	4.80	1.3	0.00	0.0	nd	58.9	1.27	56.3	0.75
21	Trifolium repens	106.6	5.08	0.9	0.04	0.0	nd	58.3	0.24	50.6	1.22
22	Trifolium repens	97.6	0.01	1.1	0.04	0.0	nd	69.8	0.02	56.1	1.60

[a]% purity refers to g tannins/100 g fraction; % PD = 100 − % PC; % trans = 100 − % cis. nd, not detected.

the following parameters: acquisition, TD 1024 (F2), 320 (F1); SW, 10.0 ppm (F2), 160 ppm (F1); O1, 2500.65 Hz; O2, 11,318.20 Hz; D1 = 1.50 s; CNST2 = 145; acquisition time, F2 channel, 102.55 ms; F1 channel, 7.9511 ms; processing, SI = 1024 (F2, F1), WDW = QSINE, LB = 1.00 Hz (F2), 0.30 Hz (F1); PH_mod = pk; baseline correction ABSG = 5 (F2, F1), BCFW = 1.00 ppm, BC_mod = quad (F2), no (F1); linear prediction = no (F2), LPfr (F1). Samples sizes used for these spectra ranged from 10 to 15 mg providing NMR sample solutions with concentrations of 20–30 mg/mL.

Calculating Procyanidin/Prodelphinidin (PC/PD) and cis/trans-Flavan-3-ol Ratios. The percentage of PCs in the CT sample was calculated using eq 1

$$\%PC = PC\text{-}6' / [(PD\text{-}2'6'/2) + PC\text{-}6'] \times 100 \qquad (1)$$

where PC-6′ is the integration of the contour for the H/C-6′cross-peak of the PC units and PD-2′6′ is the integration of the contour for the H/C-2′,6′ cross-peak of the PD units. The PD-2′6′ value is divided by 2 to account for the signal arising from two sets of correlated nuclei. The percentage of cis isomers present in the CT sample was calculated through integration of the respective H/C-4 cis- and trans-flavan-3-ol cross-peak contours centered around ^{1}H/^{13}C chemical shifts of 4.5–4.8/36.0 and 4.4–4.65/37.5 ppm, respectively, and used in eq 2:

$$\%cis\text{-flavan-3-ols} = cis\text{-flavan-3-ols} / [cis\text{-flavan-3-ols}$$
$$+ trans\text{-flavan-3-ols}] \times 100 \qquad (2)$$

Integrations of cross-peaks were performed in triplicate, and the values were averaged. Integration of the peaks was performed using Topspin 2.1 software.

■ RESULTS AND DISCUSSION

We have recently shown that ^{1}H–^{13}C HSQC NMR spectroscopy can be a useful tool when assessing the presence of CT in forages and detection of CT left in residues after HCl–butanol treatment,[16] demonstrating the power of 2D NMR techniques. The current study included examining the ^{1}H–^{13}C HSQC NMR spectra of 22 purified CT samples prepared from 9 different plant species. The CT samples had PC/PD ratios ranging from 0/100 to 99/1, cis/trans ratios ranging from 58/42 to 95/5, and a CT content of 44–~100% as determined by thiolysis (Table 1). As an example, the ^{1}H–^{13}C HSQC NMR spectrum of CT purified from Lotus pedunculatus (big trefoil, sample 6, Table 1) is given in Figure 2A along with cross-peak assignments. The absence of significant cross-peak NMR signals from non-CT organic compounds in this spectrum also confirms a high degree of purity of this sample.

Determination of PC/PD Ratios. Quantification of signals arising from polymeric materials by ^{1}H–^{13}C HSQC NMR spectroscopy is often hampered by nuclei having differing $T1$ and $T2$ relaxation times and differences in coupling constants and resonance offset effects.[33] The presence of these effects results in skewing of cross-peak signal contour volumes and thus typically limits the utility of these contours for quantifying structural information. Usually these effects require special spectroscopic treatments and alterations in NMR acquisition parameters, such as changes in pulse sequences or increased relaxation delays, before reliable quantification can be made.[34−36]
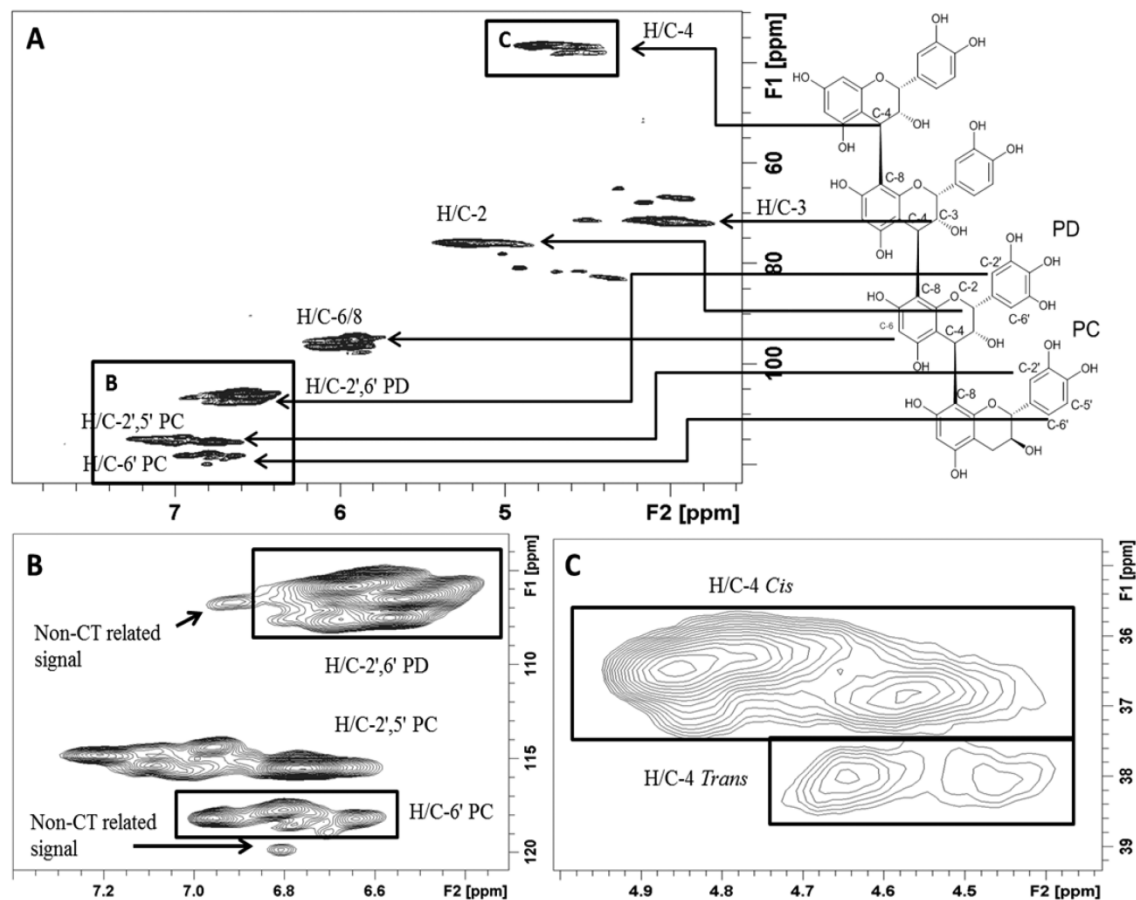
Figure 2. (A) Signal assignments for the ^{1}H–^{13}C HSQC NMR spectrum (500/125 MHz, DMSO-d_6/pyridine-d_5, 4:1) of purified condensed tannin sample (Table 1, sample 6) from *Lotus pedunculatus* (big trefoil) leaves. (B) B-Ring aromatic region cross-peak signals including H/C-2′,6′ PD signal and the H/C-2′,5′ and 6′ signals from procyanidin units. (C) H/C-4 *cis*- and *trans*-flavan-3-ol cross-peak signals. Contours were integrated as indicated by boxes. Non-tannin-related signals arising from impurities are noted and are not included in the integration.
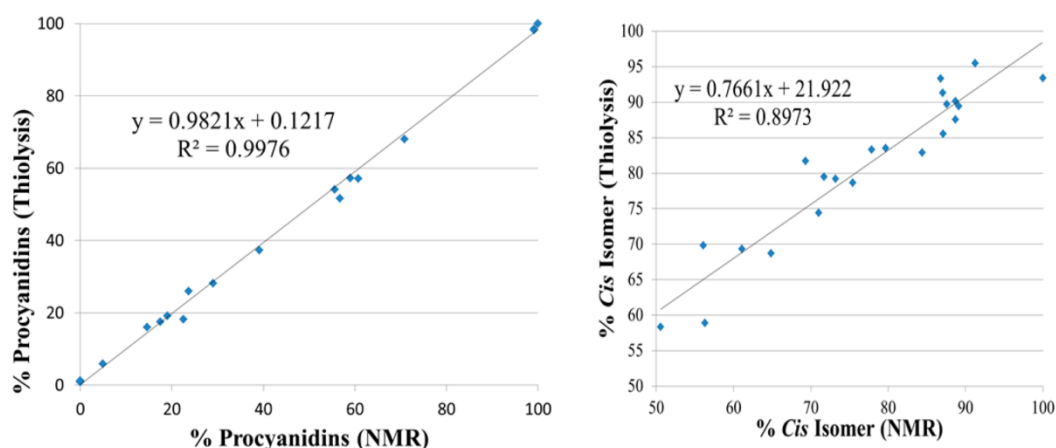
Figure 3. Proportion of procyanidin subunits (left) and *cis* subunits (right) *cis* subunits in 22 isolated condensed tannin samples as determined by thiolysis versus ^{1}H–^{13}C HSQC NMR.

In the ^{1}H–^{13}C HSQC NMR spectra of these samples, a combination of the nuclei *T1* and *T2* relaxation and resonance offset effects can be observed for most cross-peak signals. The results of these effects lead to cross-peak contours in the spectra the volumes of which are not proportional to the corresponding nuclei ratios. As a prime example, integration of the contours for signals arising from H/C-2′,5′ of PC units versus those from H/C-6′ of PC units would normally provide a ratio of 2:1 if

268

Table 2. Comparison of Duplicate NMR Data with Thiolysis Data Obtained from Condensed Tannin (CT) Samples[a]

CT sample	% PC (thiolysis)	SD	% PC (NMR)	SD	% cis (thiolysis)	SD	% cis (NMR)	SD
3	68.0	0.35	70.0	0.49	87.5	0.15	88.6	1.32
3			71.1	0.50			88.6	0.68
4	57.1	0.12	60.4	0.41	91.3	0.13	89.8	0.53
4			59.7	0.53			91.1	0.50
6	26.0	0.29	24.4	0.35	78.7	0.23	75.4	1.02
6			23.7	0.17			75.1	0.99
7	17.5	0.06	17.5	0.50	79.5	0.05	71.6	0.45
7			18.6	0.47			71.8	2.20
11	51.7	0.32	56.9	0.42	83.5	0.10	79.5	1.20
11			55.5	0.13			80.9	0.68

[a] % PC = percentage of procyanidins in CT sample; % cis = percentage of cis-flavan-3-ols in CT sample. Percentages for prodelphinidins (PD) and trans-flavanols are not shown as % PD = 100 − % PC and % trans = 100 − % cis.

none of the above-mentioned effects were observed (Figure 2B). However, the integration ratios of H/C-2′,5′ versus H/C-6′ cross-peak contours in PC containing samples from this study showed wide variability with a range from 2.37:1 to 3.86:1 (n = 17, av = 3.15, SD ±0.48). Most of the signals in the $^{1}H-^{13}C$ HSQC NMR spectra of these purified CT samples followed this trend. A comparison of integration values obtained from the cross-peak contours could not be directly correlated with theoretical relative intensities of the nuclei giving rise to the signal. Similarly, in an attempt to assess the mDP of these samples, integration of the terminal methylene unit versus any of the other CT cross-peak signals in the spectra also led to no obvious correlation with the thiolysis data of this study. It is worth noting that even integrations of the C-4 methylene units of the flavan-3-ol monomers catechin, epicatechin, and epigallocatechin under identical conditions only integrate, on average, to 72% of other signals present in the $^{1}H-^{13}C$ NMR spectrum.

However, integration ratios of H/C-6′ cross-peak signals from PC units and the H/C-2′,6′ cross-peak signal from PD units did show an extremely strong and unbiased relationship with PC/PD estimates from thiolysis determinations (Figure 3). Thus, this is the first time that $^{1}H-^{13}C$ HSQC NMR data from purified CT samples have been corroborated with data from an alternative method (thiolysis) to quantify compositional characteristics of CTs. Separate NMR analyses conducted on a limited set of other purified CT samples at the University of Reading confirmed this method as providing reliable PC/PD ratios.

It is not clear how all of the parameters controlling contour intensities are interrelated: Do the nuclei involved impart the same or similar $T1$ and $T2$ relaxation times, coupling constants, and resonance offset effects, allowing for accurate comparison of the two contours, or is this simply a coincidence of cancellation of the effects? Answers to these questions remain to be determined.

To test for variability in sample-to-sample preparation and data acquisition, we prepared duplicate NMR solutions from the same CT samples and obtained NMR spectra of these preparations on different days. These results are given in Table 2. As shown, there is excellent reproducibility of the method between these duplicate runs. In all, these experiments prove that this is a robust method for the estimation of PC/PD ratios in purified CT samples.

Determination of cis/trans-Flavan-3-ol Ratios. To assess cis- and trans-flavan-3-ol ratios (i.e., ratio of epicatechin and epigallocatechin versus catechin and gallocatechin) in these

samples, we focused on the H/C-4 cross-peak signal (Figure 2C). It has been reported[32] that this signal is segregated into two cross-peaks with $^{1}H/^{13}C$ chemical shifts of ~4.5−4.8/36.0 and ~4.4−4.65/37.5 ppm for the cis- and trans-flavan-3-ol subunits, respectively. The integration of cross-peak signals in $^{1}H-^{13}C$ HSQC NMR spectra of the same nuclei with the same connectivity in nearly identical electronic environments should be straightforward as they should possess similar, if not identical, $T1$ and $T2$ relaxation times and pose little or no differences in coupling constants and resonance offset effects. Thus, we should be able to use the data obtained from these $^{1}H-^{13}C$ HSQC NMR spectra to directly measure this structural element of isolated CTs. The percentage of cis isomers present in the CT sample was calculated through integration of the respective H/C-4 cis and trans cross-peak contours (Figure 2C). Integration ratios from these contours provided strongly related but biased estimates of cis/trans ratios relative to thiolysis (Figure 3). A literature search revealed that this segregation of the cis and trans signals of flavan-3-ol moieties is most likely not absolute, and this could provide an explanation for the bias in cis/trans estimates relative to thiolysis. NMR spectroscopic data from epicatechin (cis) oligomers report ^{13}C chemical shift in the range of 37.5 ppm, overlapping into the previously designated "trans" signal region.[37,38] The lack of signal segregation is more pronounced in structures containing C4−C6 interflavanyl linkages.[38,39] Thus, overlapping of signals from cis- and trans-flavan-3-ol subunits is the most likely contributing factor for slightly larger discrepancies between the thiolysis/NMR correlations for cis/trans-flavan-3-ol subunit assessments and may also be responsible for the biased regression fit (Figure 3).

Precautions. The first issue here, as with most analytical techniques, is to obtain a spectrum with strong signal-to-noise ratio before the integration of data is attempted. If sample size is limited, extended acquisition times need to be considered. When using this technique on samples of low purity, it is imperative that the user be able to recognize any non-CT impurity signals present and avoid incorporating them into the integration values. For PC/PD ratio evaluations, we have found that the signals indicated in Figure 2B are the most common impurity signals which may interfere in obtaining reliable results. These signals most likely arise from trace amounts of non-CT polyphenols present in the sample. For the assessment of cis/trans ratios, the problem of integration of non-CT impurities does not seem to be an issue. The H/C-4 cross-peak signals appear, even in spectra of whole plant material, in an area void of other non-CT signals. The major issue in the cis/

trans ratio assessment is the resolution of the two signals. In some cases these signals are not well resolved (Figure 2C), and care needs to be taken in selecting the integration areas.

In conclusion, the method developed now permits analytical assessment, via 2D ^{1}H$-$^{13}C HSQC NMR spectroscopy, of two specific chemical properties of purified CT samples: PC/PD and *cis/trans* ratios. The purified CT samples examined encompass the entire range of procyanidin/prodelphinidin ratios from 0/100 to 99/1 and a substantial range of *cis/trans*-flavan-3-ol ratios from 58:42 to 95.5:4.5. The observations outlined here also provide validation of thiolysis data for analysis of CT composition. In contrast to thiolysis, NMR spectroscopy represents a nondestructive analytical tool, which can be important when sample quantities are limited. Thiolysis requires ca. 4 mg for a single determination, whereas NMR analysis requires only 10 mg for an 18 h acquisition time using the described instrumentation. No additional straightforward correlations were found upon examination of other cross-peak signals in these ^{1}H$-$^{13}C HSQC NMR spectra. Additional spectroscopic examination of these samples is warranted to investigate whether other significant structural information can be obtained using quantitative ^{1}H$-$^{13}C HSQC NMR data[34−36] or alternative NMR techniques.

■ AUTHOR INFORMATION

Corresponding Author

*(W.E.Z.) E-mail: wayne.zeller@ars.usda.gov. Phone: (608) 890-0071. Fax: (608) 890-0076.

Notes

The authors declare no competing financial interest.

■ ACKNOWLEDGMENTS

■ ABBREVIATIONS USED

^{1}H$-$^{13}C HSQC, proton−carbon-13 heteronuclear single-quantum coherence; NMR, nuclear magnetic resonance; PC, procyanidin; PD, prodelphinidin; *cis*, 2,3-*cis*; *trans*, 2,3-*trans*; CT, condensed tannins; mDP, mean degree of polymerization; ^{13}C, carbon-13; CPMAS, cross-polarization magic angle spinning; 1D, one-dimensional; 2D, two-dimensional; 5K, five thousand; DMSO-d_6, perdeuterated dimethyl sulfoxide

■ REFERENCES

(1) Hagerman, A. E. *Tannin Handbook*; Miami University: Oxford, OH, USA, 2002; available at http://www.users.muohio.edu/hagermae/.

(2) Schofield, P.; Mbugua, D. M.; Pell, A. N. Analysis of condensed tannins: a review. *Anim. Feed Sci. Technol.* **2001**, *91*, 21−40.

(3) Min, B. R.; Barry, T. N.; Attwood, G. T.; McNabb, W. C. The effect of condensed tannins on the nutrition and health of ruminants fed fresh temperate forages: a review. *Anim. Feed Sci. Technol.* **2003**, *106*, 3−19.

(4) Waghorn, G. C.; Douglas, G. B.; Niezen, J. H.; McNabb, W. C.; Foote, A. G. Forages with condensed tannins − their management and nutritive value for ruminants. *Proc. N. Z. Grassl. Assoc.* **1998**, *60*, 89−98.

(5) Barry, T. N.; McNabb, W. C. The implications of condensed tannins on the nutritive value of temperate forages fed to ruminants. *Br. J. Nutr.* **1999**, *81*, 263−272.

(6) Albrecht, K. A.; Muck, R. E. Proteolysis in ensiled forage legumes that vary in tannin concentration. *Crop Sci.* **1991**, *31*, 464−469.

(7) Coblentz, W. K.; Grabber, J. H. *In situ* protein degradation of alfalfa and birdsfoot trefoil hays and silages as influenced by condensed tannin concentration. *J. Dairy Sci.* **2013**, *96*, 3120−3137.

(8) McMahon, L. R.; McAllister, T. A.; Berg, B. P.; Majak, W.; Acharya, S. N.; Popp, J. D.; Coulman, B. E.; Wang, Y.; Cheng, K.-J. A review of the effects of forage condensed tannins on ruminal fermentation and bloat in grazing cattle. *Can. J. Plant Sci.* **2000**, *80*, 469−485.

(9) Hoste, H.; Jackson, F.; Athanasiadou, S.; Thamsborg, S. M.; Hoskin, S. O. The effects of tannin-rich plants on parasitic nematodes in ruminants. *Trends Parasitol.* **2006**, *22*, 253−261.

(10) Patra, A. K.; Saxena, J. A new perspective on the use of plant secondary metabolites to inhibit methanogenesis in the rumen. *Phytochemistry* **2010**, *71*, 1198−1222.

(11) Pellikaan, W. F.; Stringano, E.; Leenaars, J.; Bongers, D. J. G. M.; van Laar-van Schuppen, S.; Plant, J.; Mueller-Harvey, I. Evaluating effects of tannins on extent and rate of in vitro gas and CH$_4$ production using an automated pressure evaluation system (APES). *Anim. Feed Sci. Technol.* **2011**, *166−167*, 377−390.

(12) Hümmer, W.; Schreier, P. Analysis of proanthocyanidins. *Mol. Nutr. Food Res.* **2008**, *52*, 1381−1398.

(13) Santos-Buelga, C.; Scalbert, A. Proanthocyanidins and tannin-like compounds − nature, occurrence, dietary intake and effects on nutrition and health. *J. Sci. Food Agric.* **2000**, *80*, 1094−1117.

(14) Patra, A. K.; Saxena, J. Exploitation of dietary tannins to improve rumen metabolism and ruminant nutrition. *J. Sci. Food Agric.* **2011**, *91*, 24−37.

(15) Gea, A.; Stringano, E.; Brown, R. H.; Mueller-Harvey, I. In situ analysis and structural elucidation of sainfoin (*Onobrychis viciifolia*) tannins for high-throughput germplasm screening. *J. Agric. Food Chem.* **2011**, *59*, 495−503.

(16) Grabber, J. H.; Zeller, W. E.; Mueller-Harvey, I. Acetone enhances the direct analysis of procyanidin- and prodelphinidin-based condensed tannins in *Lotus* species by the butanol−HCl−iron assay. *J. Agric. Food Chem.* **2013**, *61*, 2669−2678.

(17) Stringano, E.; Hayot Carbonero, C.; Smith, L. M. J.; Brown, R. H.; Mueller-Harvey, I. Proanthocyanidin diversity in the EU 'HealthyHay' sainfoin (*Onobrychis viciifolia*) germplasm collection. *Phytochemistry* **2012**, *77*, 197−208.

(18) Czochanska, Z.; Foo, L. Y.; Newman, R. H.; Porter, L. J.; Thomas, W. A. Direct proof of a homogeneous polyflavan-3-ol structure for polymeric proanthocyanidins. *J. Chem. Soc., Chem. Comm.* **1979**, 375−377.

(19) Czochanska, Z.; Foo, L. Y.; Newman, R. H.; Porter, L. J. Polymeric proanthocyanidins. Stereochemistry, structural units, and molecular weight. *J. Chem. Soc., Perkin Trans. 1* **1980**, 2278−2286.

(20) Pizzi, A.; Stephanou, A. A comparative ^{13}C NMR study of polyflavonoid tannin extracts for phenolic polycondensates. *J. Appl. Polym. Sci.* **1993**, *50*, 2105−2113.

(21) Newman, R. H.; Porter, L. J.; Foo, L. Y.; Johns, S. R.; Willing, R. I. High-resolution ^{13}C NMR studies of proanthocyanidin polymers (condensed tannins). *Magn. Reson. Chem.* **1987**, *25*, 118−124.

(22) Foo, L. Y.; Lu, Y.; Molan, A. L.; Woodfield, D. R.; McNabb, W. C. The phenols and prodelphinidins of white clover flowers. *Phytochemistry* **2000**, *54*, 539−548.

(23) Ossipova, S.; Ossipov, V.; Haukioja, E.; Loponen, J.; Pihlaja, K. Proanthocyanidins of mountain birch leaves: quantification and properties. *Phytochem. Anal.* **2001**, *12*, 128–133.

(24) Kraus, T. E. C.; Yu, Z.; Preston, C. M.; Dahlgren, R. A.; Zasoski, R. J. Linking chemical reactivity and protein precipitation to structural characteristics of foliar tannins. *J. Chem. Ecol.* **2003**, *29*, 703–730.

(25) Qa'dan, F.; Nahrstedt, A.; Schmidt, M.; Mansoor, K. Polyphenols from *Ginkgo biloba*. *Sci. Pharm.* **2010**, *78*, 897–907.

(26) Zhang, L.-L.; Lin, Y.-M.; Zhou, H.-C.; Wei, S.-D.; Chen, J.-H. Condensed tannins from mangrove species *Kandelia candel* and *Rhizophora mangle* and their antioxidant activity. *Molecules* **2010**, *15*, 420–431.

(27) Chai, W.-M.; Shi, Y.; Feng, H.-L.; Qiu, L.; Zhou, H.-C.; Deng, Z.-W.; Yan, C.-L.; Chen, Q.-X. NMR, HPLC-ESI-MS, and MALDI-TOF MS analysis of condensed tannins from *Delonix regia* (Bojer ex Hook.) Raf. and their bioactivities. *J. Agric. Food Chem.* **2012**, *60*, 5013–5022.

(28) Hoong, Y. B.; Pizzi, A.; Tahir, P. Md.; Pasch, H. Characterization of *Acacia mangium* polyflavonoid tannins by MALDI-TOF mass spectrometry and CP-MAS ^{13}C NMR. *Eur. Polym. J.* **2010**, *46*, 1268–1277.

(29) Reid, D. G.; Bonnet, S. L.; Kemp, G.; Van der Westhuizen, J. H. Analysis of commercial proanthocyanidins. Part 4: Solid state ^{13}C NMR as a tool for in situ analysis of proanthocyanidin tannins, in heartwood and bark of quebracho and acacia, and related species. *Phytochemistry* **2013**, *94*, 243–248.

(30) Romer, F. H.; Underwood, A. P.; Senekal, N. D.; Bonnet, S. L.; Duer, M. J.; Reid, D. G.; Van der Westhuizen, J. H. Tannin fingerprinting in vegetable tanned leather by solid state NMR spectroscopy and comparison with leathers tanned by other processes. *Molecules* **2011**, *16*, 1240–1252.

(31) Lorenz, K.; Preston, C. M. Characterization of high-tannin fractions from humus by carbon-13 cross-polarization and magic-angle spinning nuclear magnetic resonance. *J. Environ. Qual.* **2002**, *31*, 431–436.

(32) Zhang, L.; Gellerstedt, G. 2D Heteronuclear (^{1}H–^{13}C) single quantum correlation (HSQC) NMR analysis of norway spruce bark components. In *Characterization of Lignocellulosic Materials*, 1st ed.; Hu, T. Q., Ed.; Blackwell Publishing: Oxford, UK, 2008; Vol. 1, pp 3–16.

(33) Zhang, L.; Gellerstedt, G. Quantitative 2D HSQC NMR determination of polymer structures by selecting suitable internal standard references. *Magn. Reson. Chem.* **2007**, *45*, 37–45.

(34) Sette, M.; Lange, H.; Crestini, C. Quantitative HSQC analyses of lignin: a practical comparison. *Comput. Struct. Biotechnol. J.* **2013**, *6*, No. e201303016.

(35) Hu, K.; Westler, W. M.; Markley, J. L. Simultaneous quantification and identification of individuals chemicals in metabolite mixtures by two-dimensional extrapolated time-zero ^{1}H-^{13}C HSQC (HSQC$_0$). *J. Am. Chem. Soc.* **2011**, *133*, 1662–1665.

(36) Heikkinen, S.; Toikka, M. M.; Karhunen, P. T.; Kilpeläinen, I. A. Quantitative 2D HSQC (Q-HSQC) via suppression of *J*-dependence of polarization transfer in NMR spectroscopy: application to wood lignin. *J. Am. Chem. Soc.* **2003**, *125*, 4362–4367.

(37) Shoji, T.; Mutsuga, M.; Nakamura, T.; Kanda, T.; Akiyama, H.; Goda, Y. Isolation and structural elucidation of some procyanidins from apple by low-temperature nuclear magnetic resonance. *J. Agric. Food Chem.* **2003**, *51*, 3806–3813.

(38) Nakashima, S.; Oda, C.; Masuda, S.; Tagashira, M.; Kanda, T. Isolation and structure elucidation of tetrameric procyanidins from unripe apples (*Malus pumila* cv. Fuji) by NMR spectroscopy. *Phytochemistry* **2012**, *83*, 144–152.

(39) Cui, C.-B.; Tezuka, Y.; Yamashita, H.; Kikuchi, T.; Nakano, H.; Tamaoki, T.; Park, J.-H. Constituents of a fern, *Davallia mariesii* Moore. V. Isolation and structures of davallin, a new tetrameric proanthocyanidin, and two new phenolic glycosides. *Chem. Pharm. Bull.* **1993**, *41*, 1491–1497.

271

Appendix D

Original publication:

Anthelmintic Activities against *Haemonchus contortus* or *Trichostrongylus colubriformis* from Small Ruminants Are Influenced by Structural Features of Condensed Tannins

Jessica Quijada, Christos Fryganas, Honorata M. Ropiak, Aina Ramsay, Irene Mueller-Harvey, and Hervé Hoste

Anthelmintic Activities against *Haemonchus contortus* or *Trichostrongylus colubriformis* from Small Ruminants Are Influenced by Structural Features of Condensed Tannins

Jessica Quijada,[†,‡] Christos Fryganas,[§] Honorata M. Ropiak,[§] Aina Ramsay,[§] Irene Mueller-Harvey,[§] and Hervé Hoste*[,†,‡]

[†]INRA, UMR 1225 IHAP, 23 Chemin des Capelles, Toulouse F-31076, France

[‡]Université de Toulouse, ENVT, 23 Chemin des Capelles, Toulouse F-31076, France

[§]School of Agriculture, Policy and Development, University of Reading, 1 Earley Gate, P.O. Box 236, Reading RG6 6AT, United Kingdom

ABSTRACT: Plants containing condensed tannins (CTs) may hold promise as alternatives to synthetic anthelmintic (AH) drugs for controlling gastrointestinal nematodes (GINs). However, the structural features that contribute to the AH activities of CTs remain elusive. This study probed the relationships between CT structures and their AH activities. Eighteen plant resources were selected on the basis of their diverse CT structures. From each plant resource, two CT fractions were isolated and their in vitro AH activities were measured with the larval exsheathment inhibition assay, which was applied to *Haemonchus contortus* and *Trichostrongylus colubriformis*. Calculation of mean EC_{50} values indicated that *H. contortus* was more susceptible than *T. colubriformis* to the different fractions and that the F1 fractions were less efficient than the F2 ones, as indicated by the respective mean values for *H. contortus*, F1 = 136.9 ± 74.1 μg/mL and F2 = 108.1 ± 53.2 μg/mL, and for *T. colubriformis*, F1 = 233 ± 54.3 μg/mL and F2 = 166 ± 39.9 μg/mL. The results showed that the AH activity against *H. contortus* was associated with the monomeric subunits that give rise to prodelphinidins ($P < 0.05$) and with CT polymer size ($P < 0.10$). However, for *T. colubriformis* AH activity was correlated only with prodelphinidins ($P < 0.05$). These results suggest that CTs have different modes of action against different parasite species.

KEYWORDS: *proanthocyanidins, larval exsheathment inhibition assay (LEIA), nematodes, ruminants, structure–activity relationships*

INTRODUCTION

Gastrointestinal nematodes (GINs) represent a major threat for the breeding and production of grazing ruminants. Up to now, their control has been based mainly on the repeated use of synthetic anthelmintic (AH) drugs. However, worm populations in small ruminants have consistently developed resistance against all AH drugs.[1] Therefore, the search for alternative solutions to such drug treatments is now a necessity for a more sustainable control of these parasites.[2] The past two decades have provided evidence that some plants possess natural AH bioactivity, which is based on the presence of condensed tannins (CTs) and flavonoids. Such plants, therefore, represent a promising alternative to chemotherapy, especially when used as nutraceuticals that combine beneficial effects on health and nutrition in small and large ruminants.[3–6]

The involvement of CTs in the observed AH effects against parasitic nematodes has been suggested from several results acquired in vitro using either plant extracts or purified CT fractions[7–10] and from in vivo studies with tannin-containing resources.[11–15]

Differences in AH effects have repeatedly been noted between abomasal and intestinal nematode species of both small ruminant and cattle parasites.[12] These observations have been made in in vitro[9,10,16] and in vivo studies with the same CT resources.[13,15,17,18]

Some authors have suggested that different structural features of CTs are involved in their AH effects, namely, (i) CT size;[7,10,19,20] (ii) the type of flavan-3-ol subunits that give rise to either prodelphinidin (PD) or procyanidin tannins (PC);[8,20–22] or (iii) the stereochemistry of the C-ring in these subunits (i.e., *trans* vs *cis* flavan-3-ols).[19,22] Taken together, these observations led us to hypothesize that there are quantitative and qualitative differences between CTs, which determine their activity against parasitic nematodes. There is thus a need to evaluate the structure–activity relationship between tannins and GINs. A better understanding of these plant compounds is also required for a more rational use of these nutraceutical feeds under farm conditions.

Therefore, the objectives of the current study were (i) to examine the relationship between tannin structures and their anthelmintic activities by using 36 different tannin fractions that span CTs with a wide range of sizes and prodelphinidin/procyanidin and *trans/cis* flavan-3-ol ratio and (ii) to evaluate whether responses toward CTs differ between abomasal and intestinal small ruminant nematode species.

MATERIALS AND METHODS

Chemicals. Hydrochloric acid (37%, analytical reagent grade), butan-1-ol, acetic acid glacial (analytical reagent grade), acetone

(analytical reagent grade), acetonitrile (HPLC grade), dichloromethane (laboratory reagent grade), hexane (GLC, pesticide residue grade), and methanol (HPLC grade) were obtained from Thermo-Fisher Scientific (Loughborough, UK); benzyl mercaptan (BM) was from Sigma-Aldrich (Poole, UK); phosphate buffered saline (PBS) was from Biomérieux (Marcy l'Etoile, France); Sephadex LH-20 was from GE Healthcare (Little Chalfont, UK); and ultrapure water (MQ H₂O) was from a Milli-Q Plus system (Millipore, Watford, UK).

Preparation of Plant Extracts and Tannin Fractions. Eighteen different plant materials were used: aerial plants of *Onobrychis viciifolia* (OV) were collected on June 7, 2012 (Barham, Kent, UK); *Trifolium repens* flowers were collected from at NIAB (Cambridge, UK; sample TRa) or purchased from Zioła z Kurpi (Jednorożec, Poland; sample TRb); *Lespedeza cuneata* (LC) pellets were from Sims Brothers Seed Co. (Union Springs, AL, USA); *Betulae folium* leaves (*Betula pendula* Roth and/or *Betula pubescens* Ehrh.; BP), *Tilia inflorescentia* flowers (T; a mixture of *Tilia cordata*, *Tilia platyphyllos*, and *Tilia vulgaris* L), *Salicis cortex* bark (SA) from various *Salix* spp. (including *Salix purpurea* L.; *Salix daphnoides* Vill.; *Salix fragilis* L.), and *Ribes nigrum* leaves (sample RNb) were from Flos (Mokrsko, Poland); *Corylus avellana* (CA) pericarp was from Société Inovfruit (Musidan, France); *Juglandis folium* leaves of *Juglans regia* L. (JR) were from Kawon (Gostyń, Poland); inner bark of *Pinus sylvestris* (PS) was from University of Turku (Turku, Finland); *Salix babylonica* catkins (SB) were collected on May 26, 2012 (Emmer Green, UK); *Salix caprea* (SCL and SCT) leaves and twigs were harvested on June 19, 2012 (Goring-on-Thames, UK); *Ribes nigrum* leaves (sample RNa) and *Ribes rubrum* leaves (RR) were collected on August 13, 2012, from Hildred PYO farm (Goring-on-Thames, UK); *Theobroma cacao* beans (TC) were from Peru (imported by "Detox your world" Inc., Norfolk, UK); and *Vitellaria paradoxa* (VP) meal (i.e., residue of VP nuts after fat extraction) was from AarhusKarlshamm Sweden AB, Sweden. Samples OV and TRa were lyophilized; samples PS, CA, SCL, SCT, RNa, and RR were dried at room temperature for <10 days and then stored at room temperature. The different botanical families[23] of each plant are indicated in Table 2.

Extracts were prepared according to the method of Stringano et al.[24] with a few modifications. Plant samples (50 g; <1 mm sieve) were extracted with 70% acetone/H₂O (500 mL, 7:3, v/v) and filtered under vacuum. Chlorophyll and lipids were removed with dichloromethane (125 mL) by liquid–liquid extraction. The remaining solvents were removed from the aqueous phase on a rotary evaporator at 35 °C. The aqueous extracts were centrifuged for 3 min at 4500 rpm (Jouan CR3i multifunction centrifuge) to remove the remaining chlorophyll, insoluble particles, and some precipitates. Extracts were freeze-dried and stored at −20 °C.

Extracts were purified on Sephadex LH-20 chromatographic columns to remove impurities (mainly sugars and small phenolics) with water. Elution with acetone/H₂O (3:7, v/v) yielded fraction 1 CTs (F1); a second elution with acetone/H₂O (1:1, v/v) yielded fraction 2 CTs (F2). In total 36 (18 F1 and 18 F2) fractions were tested using *H. contortus* and *T. colubriformis* infective third-stage larvae (L3).

Tannin Analysis by Thiolytic Degradation and HPLC. The purified CT fractions were subjected to thiolytic degradation as described by Gea et al.[25] with some changes for the analysis of CT contents (% CT) and features (size in terms of mean degree of polymerization, mDP; percentage of prodelphinidins and procyanidins within CTs, % PD and % PC; and percentage of *trans* vs *cis* flavanols, % *trans*, and % *cis*). Freeze-dried samples (4 mg) were weighed into 10 mL glass tubes, and methanol (1.5 mL) was added, followed by acidified methanol (0.5 mL of 3.3% HCl/in MeOH), benzyl mercaptan (50 μL), and a magnetic stirrer. The tube was capped and heated at 40 °C for 1 h in a water bath. Water (2.5 mL) was added to stop the reaction, and the internal standard (0.5 mL of taxifolin: 0.05 mg/mL) was added. Samples were analyzed within 48 h by RP-HPLC.[25]

Gastrointestinal Nematodes. The third-stage larvae (L3) were obtained from feces of donor goats, kept indoors and infected monospecifically, with AH susceptible strains of either *H. contortus* or *T. colubriformis*. The facilities hosting the animals and trial perform-ance met French ethical and welfare rules (agreement C 31 555 27 of August 19, 2010).

Coproculture were maintained for 12 days at 23 °C to obtain the third-stage larvae. Larvae were then recovered from feces using the Baerman technique and stored at 4 °C in a horizontally vented cap flask at a concentration of 1000–1500 L3/mL. Prior to use, the larvae were checked to ensure that at least 90% of them were mobile and ensheathed.

Larval Exsheathment Inhibition Assay (LEIA). The larval exsheathment inhibition assay was performed as described by Bahuaud et al.[26] to compare the inhibitory effects of the various tannin fractions (F1 and F2) on the exsheathment process of *H. contortus* and *T. colubriformis*. For both nematode species a batch of 2-month-old larvae was used to perform the in vitro assays.

Briefly, 1000 ensheathed L3 larvae (*H. contortus* or *T. colubriformis*) were first incubated for 3 h at 20 °C with one of the fractions at serial dilutions from 600, 300, 150, 75, to 37.5 μg/mL in PBS (0.1 M phosphate, 0.05 M NaCl, pH 7.2). In addition to all of the tested fractions, negative controls (L3 in PBS) were run in parallel. After incubation, the larvae were washed and centrifuged, three times in PBS, and then submitted to the artificial exsheathment process by contact with a solution containing sodium hypochlorite (2% w/v) and sodium chloride (16.5% w/v), which had been diluted 1 to 350 in PBS. The exsheathment kinetics were measured under a microscope at ×200 magnification by identifying the proportion of exsheathed larvae. Regular examination was performed at 0, 20, 40, and 60 min after contact with the exsheathment solution. The exsheathment percentage was calculated according to the formula (number of exsheathed larvae) × 100/(number of exsheathed larvae + ensheathed larvae). For each fraction, four replicates were run per concentration and observation time to examine the exsheathment kinetics.

Statistical Analyses of the Results. The effective concentration that causes 50% exsheathment inhibition (EC₅₀) for each tannin fraction was calculated at 60 min (using the software Probit Polo Plus). First, a nonparametric rank correlation of Spearman was calculated using a 2 by 2 correlation to evaluate the relationship between the structural parameters characterizing the tannin fractions and also the relationship between the in vitro AH activity (EC₅₀ of each fraction) and quantitative (% CT) and qualitative parameters (mDP, % PD and *trans*) of the respective F1, F2, and combined F1 and F2 (F1+F2) fractions. Significant values (*P* < 0.05) and (close to significance) values (*P* < 0.10) are reported.

Then multivariate analyses, principal component analyses (PCA), were performed separately for each nematode species on the basis of the combined data of F1+F2 to obtain an overall synthesis of the relationships between the effects on larval exsheathment and the main CT features. The five variables composing the column of the two PCA matrices included quantitative (% CT) and qualitative parameters (mDP, % PD and % *trans* values) plus the EC₅₀ per species. The 36 rows of the matrix corresponded to the F1 and F2 data of the 18 plant samples. All statistical analyses were performed using Systat 9 software (SPSS Ltd.).

■ RESULTS

Tannin Analysis and Relationships between Structural Parameters. The parameters that characterized the 18 CT samples are provided in Table 1. The average % CT, mean degree of polymerization (mDP), and % prodelphinidins (PD) values were higher in the F2 compared with the F1 fraction, whereas the mean % *trans* values were lower for F2. The Spearman correlation coefficients were positive and significant between the F1 and F2 fractions for mDP (*r* = 0.583, *P* < 0.05, df = 16), % PD (*r* = 0.975, *P* < 0.01, df = 16), and % *trans* (*r* = 0.728, *P* < 0.05, df = 16), which is due to the fact that these 15 plant species produce different CT types. There was no correlation for the % CT in both fractions (*r* = 0.082, NS, df = 16).

When the Spearman correlation test was applied to the combined F1+F2 data (*n* = 36 samples), there were positive

Table 1. Chemical Characterization of Two Tannin Fractions from 18 Plant Resources (F1 and F2 Fractions; % PC = 100 − % PD; % cis = 100 − % trans)

scientific name	family[23]	common name/sample	% CT ± SD F1	% CT ± SD F2	mDP ± SD F1	mDP ± SD F2	% PD ± SD F1	% PD ± SD F2	% trans ± SD F1	% trans ± SD F2
Onobrychis viciifolia[a]	Leguminosae	sainfoin/whole plant	37.2 ± 4.5	100 ± 4.1	2.8 ± 0.1	8.7 ± 0.0	72.0 ± 0.3	64.9 ± 0.1	33.3 ± 0.2	20.9 ± 0.3
Trifolium repens[a]	Leguminosae	white clover/flower	11.7 ± 0.4	100 ± 2.4	1.8 ± 0.0	8.6 ± 0.0	98.3 ± 0.3	98.7 ± 0.0	82.2 ± 0.1	41.1 ± 0.6
Trifolium repens[b]	Leguminosae	white clover/flower	13.4 ± 0.4	82.4 ± 2.0	3.1 ± 0.1	12.7 ± 0.0	98.1 ± 0.1	98.8 ± 0.0	74.2 ± 0.2	38.2 ± 0.0
Lespedeza cuneata	Leguminosae	sericea lespedeza/pellets	42.1 ± 0.2	82.6 ± 1.4	5.0 ± 0.0	11.3 ± 0.3	92.4 ± 0.1	92.3 ± 0.0	34.7 ± 0.0	24.8 ± 0.2
Betula spp.	Betulaceae	birch/leaf	12.9 ± 0.3	63.6 ± 2.5	2.2 ± 0.0	8.3 ± 0.1	44.7 ± 0.1	58.9 ± 0.1	59.3 ± 0.1	29.3 ± 0.1
Corylus avellana	Corylaceae	hazelnut/pericarp	49.2 ± 1.1	67.5 ± 0.6	4.6 ± 0.1	9.2 ± 0.1	18.3 ± 0.9	20.9 ± 0.8	59.0 ± 0.11	52.2 ± 0.35
Juglans regia L.	Juglandaceae	walnut/leaf	21.8 ± 1.4	69.0 ± 1.7	2.9 ± 0.0	12.3 ± 0.1	9.3 ± 0.4	30.9 ± 0.0	56.1 ± 0.0	23.7 ± 0.0
Pinus sylvestris L.	Pinaceae	pine/inner bark	54.0 ± 2.0	79.0 ± 2.4	2.3 ± 0.0	6.6 ± 0.2	15.1 ± 0.6	11.2 ± 1.7	51.9 ± 0.7	21.9 ± 1.8
Tilia L.	Tiliaceae	lime tree/flower	47.5 ± 2.8	91.7 ± 3.8	2.0 ± 0.0	7.9 ± 0.1	1.1 ± 0.0	0.9 ± 0.1	16.4 ± 0.0	4.4 ± 0.1
Salix spp	Salicaceae	white willow/bark	23.1 ± 1.7	83.3 ± 0.6	2.0 ± 0.1	9.9 ± 0.0	0.0 ± 0.0	6.0 ± 0.0	63.0 ± 0.2	21.9 ± 0.0
Salix babylonica	Salicaceae	weeping willow/catkins	40.2 ± 2.8	97.4 ± 2.2	2.9 ± 0.0	8.0 ± 0.3	24.6 ± 0.1	33.0 ± 1.7	44.5 ± 0.2	42.3 ± 1.2
Salix caprea	Salicaceae	goat willow/leaf	51.5 ± 0.1	83.8 ± 1.8	2.1 ± 0.1	5.3 ± 0.1	5.8 ± 0.3	4.8 ± 0.6	93.2 ± 0.3	95.8 ± 0.2
Salix caprea	Salicaceae	goat willow/twigs	72.0 ± 1.1	93.2 ± 11	2.1 ± 0.0	5.3 ± 0.1	15.6 ± 0.9	21.3 ± 0.71	59.4 ± 0.1	37.2 ± 0.4
Ribes nigrum[a]	Grossulariaceae	black currant/leaf	59.8 ± 1.3	100.0 ± 1.7	2.5 ± 0.0	6.5 ± 0.1	93.7 ± 0.07	94.5 ± 0.11	87.2 ± 0.1	93.0 ± 0.1
Ribes nigrum[b]	Grossulariaceae	black currant/leaf	55.5 ± 3.2	77.1 ± 3.9	3.8 ± 0.0	11.8 ± 0.1	94.0 ± 0.0	95.3 ± 0.0	91.5 ± 0.1	81.2 ± 0.1
Ribes rubrum	Grossulariaceae	red currant/leaf	57.7 ± 9.1	68.2 ± 1.1	4.9 ± 0.0	10.0 ± 0.1	85.8 ± 0.4	90.4 ± 0.1	55.7 ± 1.1	35.6 ± 0.9
Theobroma cacao	Malvaceae	cocoa/seed	58.5 ± 2.9	75.5 ± 8.1	2.3 ± 0.0	5.4 ± 0.1	0.0 ± 0.2	0.0 ± 0.0	8.7 ± 0.2	3.7 ± 0.1
Vitellaria paradoxa	Sapotaceae	shea/meal	33.0 ± 0.6	44.9 ± 0.8	2.2 ± 0.1	4.1 ± 0.1	76.3 ± 0.1	72.5 ± 0.1	41.4 ± 0.3	40.2 ± 0.1
		mean value	40.2 ± 9.2	81.1 ± 7.4	2.8 ± 0.5	8.4 ± 1.3	44.6 ± 20.2	49.7 ± 19.4	56.2 ± 12.4	39.3 ± 13.3

[a]Sample a. [b]Sample b.

275

Table 2. EC$_{50}$ Values by Parasite and by Fraction (F1 or F2) from Each Tannin-Containing Resource Tested

plant	abbreviation	family[26]	H. contortus EC$_{50}$ (95% CI) (µg/mL)		T. colubriformis EC$_{50}$ (95% CI) (µg/mL)	
			F1	F2	F1	F2
Onobrychis viciifolia	OVF1/OV2	Leguminosae	62.7 (49.9–76.5)	212 (182–250)	203 (131–322)	147 (99–230)
Trifolium repens (a)	TRaF1/TRaF2	Leguminosae	287 (249–328)	177 (131–239)	110 (82.1–145)	152 (109–210)
Trifolium repens (b)	TRbF1/TRbF2	Leguminosae	37.5 < (0.7–74.4)^a	37.5 < (0.08–42.4)^a	132 (92.3–186)	110 (63.2–166)
Lespedeza cuneata	LCF1/LCF2	Leguminosae	78.2 (28.1–157)	37.5 <(2.5–55.3)^a	198 (108–366)	94.9 (50.5–140)
Corylus avellana	CAF1/C1F2	Corylaceae	166 (82.5–441)	143 (104–170)	351 (287–441)	329 (209–671)
Juglans regia L.	JRF1/JRF2	Juglandaceae	94.7 (65.5–115)	70.6 (46.9–106)	258 (130–386)	243 (169–384)
Betula spp.	BPF1/BPF2	Betulaceae	62.8 (58.6–82)	62.6 (19.0–90.3)	226 (163–335)	125 (86.7–169)
Pinus sylvestris L.	PSF1/PSF2	Pinaceae	236 (192–290)	144 (125–167)	184 (121–305)	135.9 (112–163)
Tilia L. spp.	TF1/TF2	Tiliaceae	113 (82–157)	88.7 (66.1–107)	459 (353–660)	297 (258–335)
Salix spp.	SAF1/SAF2	Salicaceae	188 (137–241)	138 (117–154)	300 (271–333)	191 (126–294)
Salix babylonica	SBF1/SBF2	Salicaceae	174 (120–206)	128 (69.8–166)	181 (152–214)	108 (83.8–132)
Salix caprea (twigs)	SCTF1/SCTF2	Salicaceae	195 (142–266)	132 (97.6–184)	385 (296–459)	125 (94.9–159)
Salix caprea (leaves)	SCLF1/SCLF2	Salicaceae	196 (86–217)	161 (133–191)	377 (316–435)	316 (243–420)
Ribes nigrum (sample a)	RNaF1/RNaF2	Grossilariaceae	145 (85–259)	157 (124–203)	145 (123–169)	89.5 (70.1–111)
Ribes nigrum (sample b)	RNbF2/RNbF2	Grossilariaceae	48.7 (78.1–158)	59.2 (18.5–111)	315 (212–592)	209 (140–344)
Ribes rubrum	RRF1/RRF2	Grossilariaceae		97.8 (85.4–305)	130 (84.5–199)	124 (99.5–152)
Theobroma cacao	TCF1/TCF2	Malvaceae	208 (168–246)	65.2 (34.1–95.7)	76.1 (24.3–130)	122 (94.8–200)
Vitellaria paradoxa	VP1/VP2	Sapotaceae	37.5 < (0.7–29.1)^a	37.5 < (0.48–36.5)^a	169 (115–288)	76.0 (65.7–86.7)
	mean values		136.9 ± 74.1	108.1 ± 53.2	233 ± 54.3	166 ± 39.9

^{a}Calculation of the EC$_{50}$ values relying on the Polo Plus software gave the following values for the effects against H. contortus for T. repens (b), fraction F1 = 33.2 µg/mL and fraction F2 = 14.5 µg/mL; for L. cuneate, fraction F2 = 29.4 µg/mL; and for V. paradoxa, fraction F1 = 13.6 µg/mL and fraction F2 = 16.5 µg/mL.

correlation coefficients between % CT and mDP values ($r = 0.696$; $P < 0.01$; df = 34). A nonsignificant negative correlation existed between % CT and % trans ($r = -0.261$; NS; df = 34) and between % PD and mDP values ($r = 0.270$; NS; df = 34). This absence of a link between % PD and mDP is important because column chromatography of CTs from the same plant material tends to lead to fractions, where % PD and mDP are positively correlated (unpublished observations). Therefore, these F1 and F2 fractions enable the investigation of relationships between CT structures and AH activities. Trends were observed for % PD and % trans ($r = 0.300$; $P < 0.08$; df = 34).

Anthelmintic Activity. The different fractions affected the larval exsheathment process in a dose-dependent way. The EC$_{50}$ values for each of the F1 and F2 fractions per plant sample were used to characterize the AH activity and are shown for H. contortus and T. colubriformis in Table 2. For both parasites, EC$_{50}$ values were generally lower with F2 than with F1 fractions. In addition, overall, EC$_{50}$ values calculated for H. contortus were lower than those of T. colubriformis, suggesting that H. contortus was more susceptible to these fractions. Thus, the calculation of Spearman's correlation coefficients between EC$_{50}$ values, obtained respectively for F1 and F2, showed significant and positive values for both species separately, that is, H. contortus ($r = 0.642$; $P < 0.05$; df = 15) and T. colubriformis ($r = 0.688$; $P < 0.01$; df = 16). However, there were no correlations between the EC$_{50}$ values of the F1 fractions between H. contortus and T. colubriformis ($r = -0.056$; NS; df = 15) and also not for the F2 fractions ($r = 0.397$; NS; df = 16). Finally, there were also no correlations between the EC$_{50}$ values of both parasite species with the F1+F2 combined data ($r = 0.164$; NS; df = 33).

Figure 1 shows the EC$_{50}$ score values in rank order for H. contortus and T. colubriformis, respectively. The 25% of the most effective plants against both GIN species (i.e., lowest EC$_{50}$ values) were Vitellaria paradoxa, Trifolium repens, Lespedeza

cuneata, Ribes nigrum, Theobroma cacao, and Betula spp. In addition, Onobrychis viciifolia was active against H. contortus, and Ribes rubrum and Salix babylonica were active against T. colubriformis.

Table 3 presents the Spearman's correlation coefficients between the EC$_{50}$ values and the various CT parameters for both nematode species in terms of the F1, F2, and the combined (F1+F2) data. For H. contortus, there were negative trends between EC$_{50}$ and mDP and % PD of the F1 fraction and between EC$_{50}$ and mDP of the F1+F2 data. The correlation between EC$_{50}$ and % PD was negative and significant for the F1+F2 data. Somewhat surprisingly, a significant positive correlation was noted for EC$_{50}$ values and % CT of the F2 fractions.

In contrast, for T. colubriformis there were no correlations with mDP or % CT. Instead, negative correlation coefficients between EC$_{50}$ and % PD were close to significance for F1 ($r = -0.453$; $P < 0.10$; df = 16) and F2 ($r = -0.439$; $P < 0.10$; df = 16) and were significant for the combined (F1+F2) fractions ($r = -0.403$; $P < 0.05$; df = 34).

When PCA was applied separately to either H. contortus or T. colubriformis, the two main components of axis 1 were mDP and % CT. For axis 2, % PD appeared as the key component. The plane defined by the combination of axes 1 and 2 (Figure 2) represented 67% of the overall variability for H. contortus and close to 70% for T. colubriformis.

The main objective of the PCA was to analyze the overall combined relationships between the different variables and the effects on exsheathment as assessed by the EC$_{50}$ values (Figure 2). Variables that are positively related are located on the same side of the plane. In contrast, variables that are negatively related are located in diagonally opposed quadrants. Analyses of these planes for both GIN species tend to confirm the 2 by 2 Spearman's correlation results. For Haemonchus, the EC$_{50}$ values were in opposition to % PD and mDP values and, to a lesser
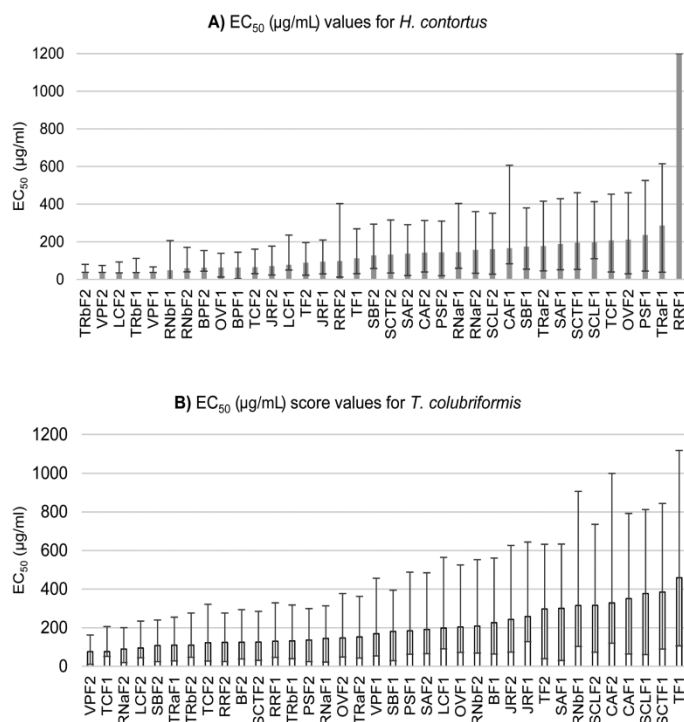
276

Figure 1. EC$_{50}$ values (and 95% confidence interval) scores for (A) *Haemonchus contortus* and (B) *Trichostrongylus colubriformis* using F1 and F2 fractions from the 18 tannin-containing plant resources.

Table 3. Spearman's Correlation Coefficients for Anthelmintic Activity by Nematode Species According to Tannin Content and Structural Parameters in F1 and/or F2 Fractions

| | *Haemonchus contortus* EC$_{50}$ (μg/mL) | | | | | | *Trichostrongylus colubriformis* EC$_{50}$ (μg/mL) | | | | | |
| | F1 (df = 15) | | F2 (df = 16) | | F1+F2 (df = 33) | | F1 (df = 16) | | F21 (df = 16) | | F1+F2 (df = 34) | |
variable	r value	P value	r value	P value	r value	P value	r value	P value	r value	P value	r value	P value
% CT	0.30	0.44	0.61[a]	0.50	0.12	0.29	0.10	0.43	0.01	0.43	−0.22	0.28
mDP	−0.46[b]	0.44	−0.28	0.43	−0.33[b]	0.29	−0.17	0.43	0.19	0.43	−0.26	0.28
% PD	−0.44[b]	0.44	−0.22	0.43	−0.35[a]	0.34	−0.46[b]	0.43	−0.43[b]	0.43	−0.40[a]	0.34
% trans	0.08	0.44	0.12	0.43	0.18	0.29	0.12	0.43	−0.01	0.43	0.24	0.28

[a]$P < 0.05$. [b]$P < 0.10$.

extent, to the % CT. For *Trichostrongylus*, the EC$_{50}$ values were mainly in opposition to % PD.

■ DISCUSSION

The study evaluated 36 CT fractions from 18 sources (15 plant species). These plants were chosen because they present a wide range of different CT features in terms of mDP, % PD, and % *trans* values. It was expected that this variation would allow exploring the relationships between CTs and their AH activities. These particular CT parameters have been described previously as being involved in their biological activities.[10,19,20,22,27−29] From these 15 plant species 18 tannin extracts were obtained that yielded two related CT fractions (i.e., F1 and F2 fractions). These 36 samples were used to test the effects of quantitative and qualitative differences between CTs. The range of CT concentrations tested with these fractions was chosen on the basis of previous in vitro data, which had been obtained with plant extracts of known CT concentrations.[16,26,27]

Three in vitro assays are available to explore the interactions between tannins and infective third-stage larvae of gastro-intestinal nematodes;[30] these are the larval migration inhibition assay (LMIA), the larval feeding inhibition assay (LFIA), and the LEIA, which has been used in the current study. The LEIA has been widely used to screen the AH activity of either plant extracts,[26,30] tannin fractions,[8,10] or flavan-3-ol monomers.[21,22] The LEIA has proved to be simple and reproducible and, like the LFIA, it also has the advantage that it allows calculation of EC$_{50}$ values, which is rarely the case for the LMIA. Moreover, LEIA has been related to similar in vivo processes.[31] The LEIA was performed with 2-month-old larvae for both nematode species to allow comparison of EC$_{50}$ values obtained with the F1 and F2 fractions of each plant sample and between the two nematodes species.

Overall, CT contents (% CT) were higher in the F2 than in the F1 fractions, and the EC$_{50}$ values for F2 calculated for both nematodes were, in most cases, lower than for F1 fractions. This suggests a role for the % CT in the antiparasitic effect. Similar results were obtained by Williams et al.[20] for the AH
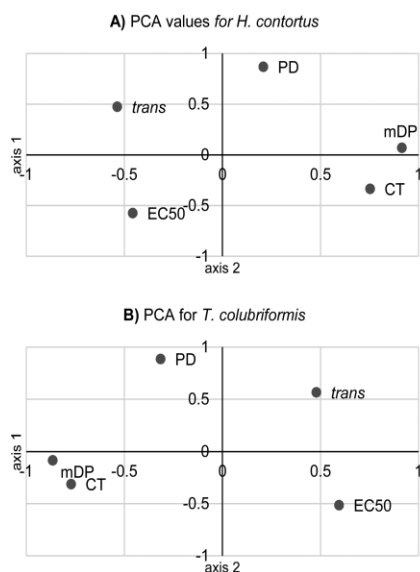
Figure 2. Multivariate principal component analyses (PCA) explained to condensed tannins for each parasite species: (A) *H. contortus*; (B) *T. colubriformis*. For both nematode species, the matrix was composed of 5 variables and 36 lines corresponding to 2 fractions (F1 and F2) of a range of 18 tannin-containing samples. Abbreviations: EC_{50} values based on LEIA (low values reflect high anthelmintic activities), CT (condensed tannins content, units g CT/100 g fraction); mDP (mean degree of polymerization of tannins); PD (% of prodelphinidins) *trans* (% of *trans* flavan-3-ols). The planes represent 67% of the variability for *H. contortus* and 70% for *T. colubriformis*, respectively.

effects against *Ascaris suum* with a subset of these F1 and F2 fractions. Many studies, based on different in vitro tests, have reported a dose-dependent AH effect when using tannin-containing plant extracts. For example, for some legume forages such dose-dependent effects have been described for (i) *O. viciifolia* (sainfoin) with the larval migration inhibition assay (LMIA),[7] LEIA,[31] egg hatch assay (EHA),[28] and larval development inhibition assay (LDIA);[28] and for (ii) *L. pedunculatus* and *L. corniculatus* extracts with the LMIA and LDIA,[27,28] the larval feeding inhibition assay (LFIA), and LEIA.[9] Although, surprisingly, there was a significant positive correlation between CT content and AH activity of the F2 fractions for *H. contortus*, there was no significant correlation when the F1+F2 data were combined. Similarly, Naumann et al.[19] also found no relationship between CT content and the AH activity against *H. contortus* L3 when comparing fractions from three legumes (*Lespedeza stuevei*, *L. cuneata*, and *Arachis glabrata*). Novobilský et al.[10] compared the effects of different CT fractions from *O. viciifolia* on cattle nematodes of either the abomasum (*Ostertagia ostertagi*) or the small intestine (*Cooperia oncophora*). These authors also did not obtain consistent correlations between the CT contents and the in vitro AH activity as measured by LFIA.

This discrepancy in relationship between dose and AH activity obtained with either CT-containing extracts or fractions could perhaps be related to other compounds that are also present in extracts.[7,21] Indeed, Molan et al.[22] also reported deleterious effects of flavan-3-ol monomers against *T. colubriformis* at different life cycle stages, that is, eggs (EHA) and larvae (LDIA, LMIA). The highest AH effect occurred with the epigallocatechin gallate (EGCG) monomer. This observation was confirmed by further studies with green tea fractions

that were tested against *Teladorsagia circumcincta* and *T. colubriformis*, where higher EGCG content was linked with a higher AH effect.[8] Similarly, when monomeric subunits of CT were tested in the LEIA on *H. contortus* and *T. colubriformis*,[21] a higher AH activity was observed with (i) the monomeric subunits of PDs (i.e., gallocatechin, epigallocatechin) and (ii) the galloyl derivatives of both PDs and procyanidins.

Besides the possible contribution of CT concentration toward explaining antiparasitic activities, several authors have also suggested that CT structures (or quality) could explain some of the observations.[8−10,19,20,22] For instance, it has been proposed that the biological activity is affected by the hydroxylation at the B-ring in flavan-3-ol monomers and in polymers, where the presence of an additional hydroxyl group (OH) increases the interaction with proteins. This could explain the generally higher activity of PDs compared to PCs. In addition, activity is also increased when galloyl groups are present.[21,32−34]

Results of the 2 by 2 calculations of Spearman's correlation coefficients as well as multivariate analyses (PCA) tended to confirm that the in vitro AH activity in terms of EC_{50} was related to CT structural features for both *H. contortus* and *T. colubriformis*. In addition, our results suggest that different mechanisms appear to be involved for each nematode species. For *H. contortus*, AH activity appeared stronger for CTs with higher PD contents and larger sizes (mDP values), although, as described by Williams et al.,[20] there was no effect of mDP or % PD within F2 fractions on the EC_{50} values. For the F1 fractions, lower EC_{50} values were associated with higher % PD and larger tannins (higher mDP values). Novobilský et al.[10] suggested that mDP was a key factor in the LFIA against L3 of *O. ostertagi* and *C. oncophora* after testing *O. viciifolia* extracts and fractions.

However, Naumann et al.[19] found no clear evidence for CT size and inhibition of *H. contortus* motility. However, only a narrow range of CT sizes was investigated. Conversely to the present data, Manoralaki[35] found that lower mDP values were correlated with higher AH activity when extracts from 40 *O. viciifolia* accessions were tested by LEIA against *H. contortus*. Similarly, Barrau et al.[7] found that a fraction that contained CTs (<2000 Da) plus flavonol glycosides had higher AH effects against *H. contortus* larvae than a fraction that contained only CTs (>2000 Da). At this stage, it is important to note that the complexity of plant extract compositions and difficulties in purifying CTs are likely to account for some of these apparent contradictions. Acetone/water extracts from CT-containing plants consist of CTs plus low molecular weight phenolic compounds (flavones, flavonols, flavonol glycosides, etc.). In addition, CTs usually occur as complex mixtures that contain low to high molecular weight tannins, and the mDP value simply describes the average "tannin size" rather than the distribution profile of all CTs. In fact, we recently discovered that mixtures of CTs and flavonoids had higher AH activities than CTs on their own.[36] Kozan et al.[37] also reported that flavonol glycosides (luteolin-7-β-O-glucopyranoside and quercetin-3-O-β-glucopyranoside) from *Vicia pannonica* var. *purpuracens* might also participate in the modulation of bioactivity of the highly AH extract and fractions against trichostrongylid larvae. This emphasizes that the proximity of biochemical structure between flavonol glycosides and CT (which are flavan-3-ols' polymers) could suggest a similar or close mechanism of action for both types of compounds. Taken together, the presence of non-CT compounds (such as flavonoid monomers) could, therefore, explain the apparently contradictory observations by Manoralaki[35]

278

and Barrau et al.[7] The F1 fractions had only half the CT contents of F2 fractions (Table 1). However, the combination of F1+F2 data gave a close to significant correlation of EC_{50} and mDP values (Table 3).

In contrast, for *T. colubriformis*, % PD was consistently (F1, F2, and combined F1+F2) related to AH activity. This agrees with other reports on *T. colubriformis* larvae, which found higher AH in vitro effects of PD-rich compared with PC-rich tannins.[21,22]

Interestingly, there were different susceptibilities between the two parasite species, which suggested that *H. contortus* was more susceptible than *T. colubriformis*. This is indicated by the overall lower EC_{50} values for the abomasal species with both types of CT fractions. Molan et al.[8] also pointed out that the abomasal nematode *T. circumcincta* was more susceptible than *T. colubriformis* to the AH effects of flavan-3-ol monomers and oligomeric CTs in the LMIA. The same conclusion was drawn from in vitro studies that examined extracts from different woody plants (*Rubus fructicosus*, *Quercus robur*, and *Corylus avellana*) against *H. contortus*, *T. circumcincta*, and *T. colubriformis* based on LMIA and LEIA tests.[16] However, other authors found no such differences in the response to quebracho or *O. viciifolia* extracts[11,31] between abomasal or intestinal species. Moreno-Gonzalo et al.[38,39] even found a higher in vitro susceptibility of *T. colubriformis* compared to *H. contortus* and *T. circumcincta* when measuring the AH activity of extracts from different heather species (*Calluna vulgaris*, *Erica cinerea*, and *E. umbellata*). It remains to be seen whether differences in assay conditions could account for some of these contradictory results. Moreover, it will be worth exploring whether there exist species-specific differences in the quality of larval sheath proteins between the abomasal and intestinal species to better understand the mode of actions of polyphenols against the different GIN species.

Although it is difficult to extrapolate from in vitro to in vivo results, our current data provide a screening of CT-containing plants whose AH properties will need to be explored further in controlled in vivo studies to develop their potential for on-farm exploitation. It is also worth noting that the CT fractions from three legumes ranked among the most effective ones (i.e., having the lowest EC_{50} values): *L. cuneata* pellets, *O. viciifolia* plants, and *T. repens* flowers (Figure 1). The past decade has seen an accumulation of in vivo results that confirm the AH effects of *L. cuneata* and *O. viciifolia* against the main GIN species whether offered to small ruminants in the form of freshly grazed pasture[40,41] or as hay,[15,17,42] silages,[42] or pellets.[18]

As far as *T. repens* is concerned, no other data are available because the genus *Trifolium* is usually considered as a tannin-free legume,[43] and consequently the various *Trifolium* species have received little attention for their antiparasitic potential. However, Carlsen and Fomsgaard[44] provided an extensive review of the secondary metabolites in *T. repens* and pointed out the high CT content in flowers. The current study found that CTs from *T. repens* flowers had a strong AH effect and confirmed the dose-dependent inhibition effects of *T. repens* tannins observed for *C. oncophora* in the LFIA.[45]

The CT fractions of *V. paradoxa* were also ranked as highly effective against both nematode species and suggested that some agro-industrial byproducts could be of interest for their antiparasitic properties. It is worth noting that AH effects on *H. contortus* and *T. colubriformis* were recently also described not only for cocoa seed but also for husk extracts using the EHA.[46]

In conclusion, our results showed that structural features of condensed tannins are key factors that affect the anthelmintic effects against gastrointestinal nematodes of ruminants. In addition, there were differences in the susceptibilities of the abomasal as the intestinal nematode species. These differences have been described previously in the literature and could be related to the fact that the nematode sheath proteins differ in these parasite species. This could perhaps affect their interactions with the tannins. It is worth also emphasizing that the current results have been acquired on infective larvae and that other assays that target other parasitic stages might have different outcomes. Further studies will be needed to explore these interactions at the molecular level.

■ **AUTHOR INFORMATION**

Corresponding Author

*(H.H.) Phone: +(33) 05-61-19-38-75. Fax: +(33) 05-61-19-32-43. E-mail: h.hoste@envt.fr.

Notes

The authors declare no competing financial interest.

■ **ACKNOWLEDGMENTS**

■ **ABBREVIATIONS USED**

GINs, gastrointestinal nematodes; CT, condensed tannins; AH, anthelmintic; mDP, mean degree of polymerization; PD, prodelphinidins; PC, procyanidins; PBS, phosphate buffered saline; LEIA, larval exsheathment inhibition assay; L3, infective stage nematode larvae; EC_{50}, effective concentration for 50% inhibition of larvae's exsheathment; LDIA, larval development inhibition assay; LFIA, larval feeding inhibition assay; EHA, egg hatch assay; LMIA, larval migration inhibition assay

■ **REFERENCES**

(1) Jackson, F.; Varady, M.; Bartley, D. J. Managing anthelmintic resistance in goats – can we learn lessons from sheep? *Small Ruminant Res.* **2012**, *103* (1), 3–9.

(2) Hoste, H.; Torres-Acosta, J. F. J. Non chemical control of helminths in ruminants: adapting solutions for changing worms in a changing world. *Vet. Parasitol.* **2011**, *180*, 144–154.

(3) Andlauer, W.; Fürst, P. Nutraceuticals: a piece of history, present status and outlook. *Food Res. Int.* **2002**, *35*, 171–176.

(4) Athanasiadou, S.; Houdijk, J.; Kyriazakis, I. Exploiting synergisms and interactions in the nutritional approaches to parasite control in sheep production systems. *Small Ruminant Res.* **2008**, *76*, 2–11.

(5) Hoste, H.; Martinez-Ortiz-de-Montellano, C.; Manolaraki, F.; Brunet, S.; Ojeda-Robertos, N.; Fourquaux, I.; Torres-Acosta, J. F. J.; Sandoval-Castro, C. A. Direct and indirect effects of bioactive tannin-rich tropical and temperate legumes against nematode infection. *Vet. Parasitol.* **2012**, *186*, 18–27.

(6) Terrill, T. H.; Miller, J. E.; Burke, J. M.; Mosjidis, J. A.; Kaplan, R. M. Experiences with integrated concepts for the control of *Haemonchus contortus* in sheep and goats in the United States. *Vet. Parasitol.* **2012**, *186*, 28–37.

(7) Barrau, E.; Fabre, N.; Fouraste, I.; Hoste, H. Effect of bioactive compounds from Sainfoin (*Onobrychis viciifolia* Scop.) on the *in vitro*

larval migration of *Haemonchus contortus*: role of tannins and flavonol glycosides. *Parasitology* **2005**, *131*, 531–538.

(8) Molan, A. L.; Sivakumaran, S.; Spencer, P. A.; Meagher, L. P. Green tea flavan-3-ols and oligomeric proanthocyanidins inhibit the motility of infective larvae of *Teladorsagia circumcincta* and *Trichostrongylus colubriformis in vitro*. *Res. Vet. Sci.* **2004**, *77*, 239–243.

(9) Novobilský, A.; Mueller-Harvey, I.; Thamsborg, S. M. Condensed tannins act against cattle nematodes. *Vet. Parasitol.* **2011**, *182*, 213–220.

(10) Novobilský, A.; Stringano, E.; Hayot Carbonero, C.; Smith, L. M. J.; Enemark, H. L.; Mueller-Harvey, I.; Thamsborg, S. M. *In vitro* effect of extracts and purified tannins of sainfoin (*Onobrychis viciifolia*) against two cattle nematodes. *Vet. Parasitol.* **2013**, *196*, 532–537.

(11) Athanasiadou, S.; Kyriazakis, I.; Jackson, F.; Coop, R. L. Direct anthelmintic effects of condensed tannins towards different gastro-intestinal nematodes of sheep: *in vitro* and *in vivo* studies. *Vet. Parasitol.* **2001**, *99*, 205–219.

(12) Hoste, H.; Jackson, F.; Athanasiadou, S.; Thamsborg, S. M.; Hoskin, S. The effects of tannin-rich plants on parasitic nematodes in ruminants. *Trends Parasitol.* **2006**, *22*, 253–261.

(13) Joshi, B. R.; Kommuru, D. S.; Terrill, T. H.; Mosjidis, J. A.; Burke, J. M.; Shakya, K. P.; Miller, J. E. Effect of feeding sericea lespedeza leaf meal in goats experimentally infected with *Haemonchus contortus*. *Vet. Parasitol.* **2011**, *178*, 192–197.

(14) Max, R. A. Effect of repeated wattle tannin drenches on worm burdens, faecal egg counts and egg hatchability during naturally acquired nematode infection in sheep and goats. *Vet. Parasitol.* **2010**, *169*, 138–143.

(15) Terrill, T. H.; Dykes, G. S.; Shaik, S. A.; Miller, J. E.; Kouakou, B.; Kannan, G.; Burke, J. M.; Mosjidis, J. A. Efficacy of sericea lespedeza hay as a natural dewormer in goats: dose titration study. *Vet. Parasitol.* **2009**, *163*, 52–56.

(16) Paolini, V.; Fouraste, I.; Hoste, H. *In vitro* effects of three woody plant and sainfoin on third-stage larvae and adult worms of three gastrointestinal nematodes. *Parasitology* **2004**, *129*, 69–77.

(17) Paolini, V.; De La Farge, F.; Prevot, F.; Dorchies, Ph.; Hoste, H. Effects of the repeated distribution of sainfoin hay on the resistant and the resilience of goats naturally infected with gastrointestinal nematodes. *Vet. Parasitol.* **2005**, *127*, 277–283.

(18) Kommuru, D. S.; Barker, T.; Desai, S.; Burke, J. M.; Ramsay, A.; Mueller-Harvey, I.; Miller, J. E.; Mosjidis, J. A.; Kamisetti, N.; Terrill, T. H. Use of pelleted sericea lespedeza (*Lespedeza cuneata*) for natural control of coccidian and gastrointestinal nematodes in weaned goats. *Vet. Parasitol.* **2014**, *204*, 191–198.

(19) Naumann, H. D.; Armstrong, S. A.; Lambert, B. D.; Muir, J. P.; Tedeshi, L. O.; Kothmann, M. M. Effect of molecular weight and concentration of legume condensed tannins on *in vitro* larval migration inhibition of *Haemonchus contortus*. *Vet. Parasitol.* **2014**, *199*, 93–98.

(20) Williams, A. R.; Fryganas, C.; Ramsay, A.; Mueller-Harvey, I.; Thamsborg, S. T. Direct anthelmintic effects of condensed tannins from diverse plant sources against *Ascaris suum*. *PLoS One* **2014**, *9* (5), No. e97053, DOI: 10.1371/journal.pone.0097053.

(21) Brunet, S.; Hoste, H. Monomers of condensed tannins affect the larval exsheathment of parasitic nematodes of ruminants. *J. Agric. Food Chem.* **2006**, *54*, 7481–7487.

(22) Molan, A. L.; Meagher, L. P.; Spencer, P. A.; Sivakumaran, S. Effect of flavan-3-ols *in vitro* hatching, larval development and viability of infective larvae of *Trichostrongylus colubriformis*. *Int. J. Parasitol.* **2003**, *33*, 1691–1698.

(23) Blamey, M.; Grey-Wilson, C. *La Flore d'Europe Occidentale*; Flammarion: Paris, France, 2003.

(24) Stringano, E.; Gea, A.; Salminen, J.-P.; Mueller-Harvey, I. Simple solution for a complex problem: proanthocyanidins, galloyl glucoses and ellagitannins fit on a single calibration curve in high-performance-gel permeation chromatography. *J. Chromatogr. A* **2011**, *1218*, 7804–7812.

(25) Gea, A.; Stringano, E.; Brown, R. H.; Mueller-Harvey, I. *In situ* analysis and structural elucidation of sainfoin (*Onobrychis viciifolia*)

tannins for high-throughput germplasm screening. *J. Agric. Food Chem.* **2011**, *59*, 495–503.

(26) Bahuaud, D.; Martinez-Ortiz De Montellano, C.; Chauveau, S.; Prevot, F.; Torres-Acosta, F.; Fouraste, I.; Hoste, H. Effects of four tanniferous plant extracts on the *in vitro* exsheathment of third-stage larvae of parasitic nematodes. *Parasitology* **2006**, *132*, 545–554.

(27) Molan, A. L.; Alexander, R. A.; Brookes, I. M.; McNabb, W. C. Effect of an extract from sulla (*Hedysarum coronarium*) containing condensed tannins on the migration of three sheep gastrointestinal nematodes *in vitro*. *Proc. N. Z. Soc. Anim. Prod.* **2000**, *60*, 21–25.

(28) Molan, A. L.; Waghorn, G. C.; McNabb, W. C. The impact of condensed tannins on egg hatching and larval development of *Trichostrongylus colubriformis*. *Vet. Rec.* **2002**, *150*, 65–69.

(29) Mueller-Harvey, I. Unravelling the conundrum of tannins in animal nutrition and health. *J. Sci. Food Agric.* **2006**, *86*, 2010–2037.

(30) Jackson, F.; Hoste, H. *In vitro* methods for the primary screening of plant products for direct activity against ruminant gastrointestinal nematodes. In *In Vitro Screening of Plant Resources for Extra Nutritional Attributes in Ruminants: Nuclear and Related Methodologies*; Vercoe, P. E., Makkar, H. P. S., Schlink, A. C., Eds.; FAO/IAEA Springer: Berlin, Germany, 2010; pp 24–45.

(31) Brunet, S.; Aufrere, J.; El Babili, F.; Fouraste, I.; Hoste, H. The kinetics of exsheathment of infective nematode larvae is disturbed in the presence of a tannin-rich plant extract (sainfoin) both *in vitro* and *in vivo*. *Parasitology* **2007**, *134*, 1253–1262.

(32) Brunet, S.; Jackson, F.; Hoste, H. Effects of sainfoin (*Onobrychis viciifolia*) extract and monomer of condensed tannins on the association of abomasal nematode larvae with fundic explants. *Int. J. Parasitol.* **2008**, *38*, 783–790.

(33) Li, C.; Leverence, R.; Trombley, J. D.; Xu, S.; Yang, J.; Tian, Y.; Reed, J. D.; Hagerman, A. E. High molecular weight persimmon (*Diospyros kaki* L.) proanthocyanidin, a highly galloylated, A-linked tannin with an unusual flavonol terminal unit, myricetin. *J. Agric. Food Chem.* **2010**, *58*, 9033–9042.

(34) Okuda, T.; Ito, H. Tannins of constant structure in medicinal and food plants − hydrolysable tannins and polyphenols related to tannins. *Molecules* **2011**, *16*, 2191–2217.

(35) Manolaraki, F. *Propriétés anthelminthiques du sainfoin (Onobrychis viciifolia): analyse des facteurs de variations et du rôle des composés phénoliques impliqués*. Ph.D. Dissertation, INP, Université de Toulouse, Toulouse, France, 2011.

(36) Klongsiriwet, C.; Quijada, J.; Williams, A. R.; Hoste, H.; Williamson, E.; Mueller-Harvey, I. 2014. Synergistic effects between condensed tannins and luteolin on *in vitro* larval exsheathment inhibition of *Haemonchus contortus*. In *Proceedings of XXVIIth International Conference on Polyphenols (ICP2014)*, Nagoya, Japan, Sept 2–6, 2014; ISBN 978-4-9907847-0-6), pp 601–602.

(37) Kozan, E.; Anul, S. A.; Tatli, I. I. *In vitro* anthelmintic effect of *Vicia pannonica* var. *purpurascens* on trichostrongylosis in sheep. *Exp. Parasitol.* **2013**, *134*, 299–303.

(38) Moreno-Gonzalo, J.; Manolaraki, F.; Frutos, P.; Hervas, G.; Celaya, R.; Osoro, K.; Ortega-Mora, L. M.; Hoste, H.; Ferre, I. *In vitro* effect of heather (Ericaceae) extracts on different development stages of *Teladorsagia circumcincta* and *Haemonchus contortus*. *Vet. Parasitol.* **2013**, *197*, 235–243.

(39) Moreno-Gonzalo, J.; Manolaraki, F.; Frutos, P.; Hervas, G.; Celaya, R.; Osoro, K.; Ortega-Mora, L. M.; Hoste, H.; Ferre, I. *In vitro* effect of heather extracts on *Trichostrongylus colubriformis* eggs, larvae and adults. *Vet. Parasitol.* **2013**, *197*, 586–594.

(40) Athanasiadou, S.; Tzamaloukas, O.; Kyriazakis, I.; Jackson, F.; Coop, R. L. Testing for direct anthelmintic effects of bioactive forages against *Trichostrongylus colubriformis* in grazing sheep. *Vet. Parasitol.* **2005**, *28*, 233–243.

(41) Mechineni, A.; Kommuru, D. S.; Gujja, S.; Mosjidis, J. A.; Miller, J. E.; Burke, J. M.; Ramsay, A.; Mueller-Harvey, I.; Kannan, G.; Lee, J. H.; Kouakou, B.; Terrill, T. H. Effect of fall-grazed sericea lespedeza (*Lespedeza cuneata*) on gastrointestinal nematode infections of growing goats. *Vet. Parasitol.* **2014**, *29*, 221–228.

Author's personal copy

(42) Heckendorn, F.; Häring, D. A.; Maurer, V.; Zinsstag, J.; Langhans, W.; Hertzberg, H. Effect of sainfoin (*Onobrychis viciifolia*) silage and hay on established populations of *Haemonchus contortus* and *Cooperia curticei* in lambs. *Vet. Parasitol.* **2006**, *142*, 293–300.

(43) Barry, T. N. The role of condensed tannins in the nutritional value of *Lotus pedunculatus* for sheep. 3. Rates of body and wool growth. *Br. J. Nutr.* **1985**, *54*, 217–221.

(44) Carlsen, S.; Fomsgaard, I. S. Biologically active secondary metabolites in white clover (*Trifolium repens* L.) − a review focusing on contents in the plant, plant−pest interactions and transformation. *Chemoecology* **2008**, *18*, 129–170.

(45) Desrues, O.; Enemark, H. L.; Mueller-Harvey, I.; Fryganas, C.; Thamsborg, S. M. Preliminary analysis of the relationship between structure and anthelmintic activity of condensed tannins in cattle nematodes. In *Proceedings 7th Novel Approaches to the Control of Helminths of Livestock*; Toulouse, France, March 25–28; 2013; p 46.

(46) Vargas-Magaña, J. J.; Torres-Acosta, J. F. J.; Aguilar-Caballero, A. J.; Sandoval-Castro, C. A.; Hoste, H.; Chan-Pérez, J. I. Anthelmintic activity of acetone−water extracts against *Haemonchus contortus* eggs: Interactions between tannins and other plant secondary compounds. *Vet. Parasitol.* **2014**, *206*, 322–327.

281

Appendix E

Original publication:

Impact of chemical structure of flavanol monomers and condensed tannins on *in vitro* anthelmintic activity against bovine nematodes

Olivier Desrues, Christos Fryganas, Honorata Ropiak, Irene Mueller-Harvey, Heidi L. Enemark, Stig M. Thamsborg

Impact of chemical structure of flavanol monomers and condensed tannins on *in vitro* anthelmintic activity against bovine nematodes

OLIVIER DESRUES[1]*, CHRISTOS FRYGANAS[2], HONORATA M. ROPIAK[2], IRENE MUELLER-HARVEY[2], HEIDI L. ENEMARK[3,4] *and* STIG M. THAMSBORG[1]

[1] *Parasitology and Aquatic Diseases, Department of Veterinary Disease Biology, University of Copenhagen, Dyrlægevej 100, DK-1870 Frederiksberg C, Denmark*
[2] *Chemistry and Biochemistry Laboratory, School of Agriculture, Policy and Development, University of Reading, Reading RG6 6AT, UK*
[3] *Section for Bacteriology, Pathology and Parasitology, National Veterinary Institute, Technical University of Denmark, Frederiksberg, Denmark*
[4] *Section for Parasitology, Department of Laboratory Services, Norwegian Veterinary Institute, PO Box 750 Sentrum, N-0106 Oslo, Norway*

SUMMARY

Plants containing condensed tannins (CT) may have potential to control gastrointestinal nematodes (GIN) of cattle. The aim was to investigate the anthelmintic activities of four flavan-3-ols, two galloyl derivatives and 14 purified CT fractions, and to define which structural features of CT determine the anti-parasitic effects against the main cattle nematodes. We used *in vitro* tests targeting L1 larvae (feeding inhibition assay) and adults (motility assay) of *Ostertagia ostertagi* and *Cooperia oncophora*. In the larval feeding inhibition assay, *O. ostertagi* L1 were significantly more susceptible to all CT fractions than *C. oncophora* L1. The mean degree of polymerization of CT (i.e. average size) was the most important structural parameter: large CT reduced larval feeding more than small CT. The flavan-3-ols of prodelphinidin (PD)-type tannins had a stronger negative influence on parasite activity than the stereochemistry, i.e. *cis-* *vs* *trans*-configurations, or the presence of a gallate group. In contrast, for *C. oncophora* high reductions in the motility of larvae and adult worms were strongly related with a higher percentage of PDs within the CT fractions while there was no effect of size. Overall, the size and the percentage of PDs within CT seemed to be the most important parameters that influence anti-parasitic activity.

Key words: proanthocyanidins, ruminant, cattle, *Ostertagia ostertagi*, *Cooperia oncophora*, larval feeding inhibition, motility assay.

INTRODUCTION

The potential of nutraceutical plants for the sustainable control of gastrointestinal nematodes (GIN) in ruminant livestock is still an under-explored area (Hoste *et al.* 2015). Their use could forestall the emergence of GIN resistance to available anthelmintic drugs and reduce the substantial economic losses due to these pathogens. Plants produce a wide range of secondary metabolites mainly to protect themselves from diseases and herbivores. These plant secondary metabolites include condensed tannins (CT; *syn.* proanthocyanidins), which are polyphenols that are able to bind proteins and other molecules such as polysaccharides, lipids, as well as metal ions (Schofield *et al.* 2001; Jakobek, 2015). CT are polymers that consist of various flavan-3-ol units which are defined by their hydroxylation, stereochemistry and substitution patterns. They tend to occur not as single CT molecules but as complex CT mixtures in plants. Therefore, these polymeric mixtures are described in terms of average polymer lengths [or mean degree of polymerization (mDP)] and as molar percentages of their flavan-3-ol subunits; the most common subunits are catechin and epicatechin [which are found in procyanidin (PC)-type tannins] and gallocatechin and epigallocatechin [which are found in prodelphinidin (PD)-type tannins]. Their stereochemistry is defined on the basis of *cis*-flavan-3-ols (epicatechin and epigallocatechin) and *trans*-flavan-3-ols (catechin and gallocatechin) (Williams *et al.* 2014*a*). Moreover, the attachment of substituents such as galloyl groups can also occur in CT (Spencer *et al.* 2007). This structural diversity affects protein-binding affinity as well as the biological activity of CT, as recently shown for *in vitro* ruminal methane production and fermentation (Saminathan *et al.* 2014, 2015; Hatew *et al.* 2015). Therefore it is important to assess how not only the tannin concentration, but also the tannin structure influence anthelmintic properties against different life cycle stages of

* Corresponding author: Parasitology and Aquatic Diseases, Department of Veterinary Disease Biology, University of Copenhagen, Dyrlægevej 100, DK-1870 Frederiksberg C, Denmark. E-mail: olivierd@sund.ku.dk; olivier.desrues@gmail.com

the most important GIN species. A dose-dependency for CT has been demonstrated for small ruminant and cattle nematodes (Brunet *et al.* 2007; Novobilský *et al.* 2013; Molan, 2014). Studies until now have demonstrated that PD subunits were more potent than PC subunits in inhibiting the motility and exsheathment of third-stage larvae (L3) of *Haemonchus contortus* in sheep (Brunet and Hoste, 2006), motility of L3 of *Ascaris suum* of pigs (Williams *et al.* 2014a) or hatching of eggs of *Trichostrongylus colubriformis* of sheep (Molan *et al.* 2003). The galloylation of flavan-3-ols has also been shown to enhance the anthelmintic activity against L3 in ruminants (Molan *et al.* 2003; Brunet and Hoste, 2006). The CT subunits are commercially available as pure flavan-3-ols and CT that differ in subunit composition can be extracted and purified from various plant sources. This approach is much faster than attempting to separate the different CT groups from a single plant source, such as sainfoin or *Lotus* sp., where they occur as complex mixtures. This approach can also be used to overcome constraints in CT structures imposed by biosynthesis, especially for investigating differences in *cis/trans*-stereochemistry, which varies greatly between plant species (Porter, 1988). Such contrasting CT fractions are needed to give an insight into which structural features should be targeted by plant selection or breeding before recommending these bioactive compounds in livestock feeds. It has previously been reported that larger CT polymers in comparison with smaller ones more efficiently inhibit the feeding ability of first-stage larvae (L1) of *Ostertagia ostertagi* and *Cooperia oncophora* in cattle (Novobilský *et al.* 2013), and also the motility of L4 of *A. suum* and *Oesophagostomum dentatum* in pigs (Williams *et al.* 2014a, b). However, CT extracts and fractions tend to vary in terms of tannin contents and composition, which can complicate the interpretation of results compared to using pure compounds, e.g. flavan-3-ols. In fact, the CT contents in the earlier study of bovine nematodes ranged from 3 to 60 g CT/100 g fraction (Novobilský *et al.* 2013), and CT have been sparsely investigated in cattle as compared with small ruminants.

Thus, the aim of our study was to investigate the relation between CT structure and anti-parasitic activity using several commercial flavan-3-ols and galloyl derivatives, and highly purified CT fractions that covered a very wide range of structures. We applied *in vitro* tests to free-living (L1) and adult stages of the most important cattle nematodes, *O. ostertagi* and *C. oncophora*.

MATERIALS AND METHODS

Flavan-3-ol monomers and CT from plants

Four different flavan-3-ols and two galloyl derivatives were purchased from Sigma-Aldrich Ltd.

(Denmark): catechin (C), epicatechin (EC), gallocatechin (GC), epigallocatechin (EGC), gallocatechin gallate (GCg) and epigallocatechin gallate (EGCg). CT previously described and tested *in vitro* against GIN in small ruminants (Quijada *et al.* 2015) from 14 European plants were used. Briefly, they included: bark and phloem from pine tree (*Pinus sylvestris*), above-ground sainfoin plants (*Onobrychis viciifolia*), pericarp from hazelnuts (*Corylus avellana*), leaves from blackcurrant collected from two sites (samples A and B; *Ribes nigrum*), flowers from white clover from two sites (samples A and B; *Trifolium repens*), flowers from *Tilia* spp., bark from willow (*Salix* spp.), leaves from walnut (*Juglans regia*), leaves from birch (*Betula* spp.), leaves and twigs from goat willow (*Salix caprea*) and weeping willow catkins (*Salix babylonica*). The details concerning the collection and drying procedures of plant materials, the extraction of tannins with acetone/water (7:3; v/v) and the purification of CT on Sephadex LH-20 columns yielding fractions F1 and F2 were described in Quijada *et al.* (2015). In the present study, we focused on the F2 fractions whereas only a few F1 fractions were included (goat willow leaves, pine bark and sainfoin). The CT fractions were degraded by thiolysis according to Quijada *et al.* (2015) prior to analysis by high-performance liquid chromatography as described by Williams *et al.* (2014a, b). This provided information on the CT content and composition in terms of mDP, molar percentages of PC- or PD-type subunits (PC/PD ratio) within CT and *cis*- or *trans*-flavan-3-ols within CT.

Nematodes

Young naïve male calves were experimentally infected to propagate the different parasite species. The study was approved by the Animal Experiments Inspectorate, Ministry of Justice, Denmark (Ref. 2013-15-2934-00763). Care and maintenance of the calves were in accordance with applicable Danish and European guidelines. Inocula consisted of infective larvae (L3) of *O. ostertagi* and *C. oncophora* either mixed (assay with flavan-3-ol monomers; L3 recovered were 30% *O. ostertagi* and 70% *C. oncophora*) or separately (assays with CT fractions). Fresh feces was collected rectally during the patency period and L1 were prepared as previously described for cattle nematodes (Novobilský *et al.* 2011) and used for *in vitro* tests. Calves mono-infected with either *C. oncophora* or *O. ostertagi* were euthanized 28 and 38 days post-infection, respectively, and the adult worms were immediately recovered from the contents after embedding in agar and migration in warm saline water (2–3 h at 38 °C), according to Slotved *et al.* (1996).

In vitro *motility and feeding inhibition of first-stage larvae (L1)*

The larval feeding inhibition assay (LFIA) including the preparation of the labelling of *Escherichia coli* with fluorescein isothiocyanate (FITC) as larval food source, was performed as described by Jackson and Hoste (2010). All tested compounds were serially diluted in phosphate buffer saline PBS (milliQ water; pH 6·9) at 3 concentrations, in triplicates, as previously used for LFIA with cattle nematodes (Novobilský *et al.* 2011). Briefly, 1300 μL of either PBS as negative control, flavan-3-ol monomers at concentrations (10, 40 and 160 μg mL^{-1}) or CT fractions (2·5, 10 and 40 μg of CT mL^{-1}) were added to 1·5 mL Eppendorf tubes for each replicate. In the case of CT fractions, dilutions were adjusted for CT content as this parameter varied between 64 and 100%. Then, 100 μL containing approximately 100 newly hatched larvae were added to each tube. After 2 h incubation at 25 °C, 10 μL of FITC labelled *E. coli* was added. Subsequently, the tubes were horizontally incubated for 18 h at 25 °C, then centrifuged (6000 *g*, 2 min) and 850 μL of the supernatant was carefully removed. The remaining solution with larvae was placed in a counting chamber and read under a fluorescent microscope (blue filter 475–490 nм) at ×100 magnification. Fed larvae were differentiated according to Novobilský *et al.* (2011). Additionally, follow-up experiments were performed: (i) in order to ensure that the inhibitory effect of CT on larval feeding was directed against L1 and not due to an alteration of *E. coli* by CT, we modified the procedure by removing CT from two fractions that differed in their mDP values (samples A and B from blackcurrant leaves) and replaced them with control media before adding the bacterial food source. The modified assay was done in triplicate with *O. ostertagi* L1 and CT fractions were adjusted for CT contents; (ii) F1 fractions of sainfoin, goat willow leaves and pine bark were tested against *C. oncophora* L1 at 20 μg of CT mL^{-1}, to verify the lack of anthelmintic activity of sainfoin F1 previously found against pig nematodes (Williams *et al.* 2014*a*); (iii) the putative interference of impurities such as sucrose, which is the major sugar in sainfoin (Marais *et al.* 2000), was assessed in LFIA with *O. ostertagi* by pre-incubating the F2 fraction of sainfoin with or without sucrose (50:50; w/w) at 2·5, 10 and 40 μg of CT mL^{-1}; simultaneously (iv) the inhibition of *O. ostertagi* L1 motility was assessed with 8 CT fractions, where any movement within 5 s was counted as motile larvae.

In vitro *adult motility inhibition assay*

First, adult worms were washed 3 times, following recovery by migration, with a warm solution of PBS (milliQ water; pH 7·2) containing penicillin/streptomycin (P4333, Sigma-Aldrich) at a concentration of 1:100 and amphotericin B (A2942, Sigma-Aldrich) at 1:250. Due to limited number of worms this assay was only performed with CT fractions of willow bark and blackcurrant leaves A and B. The CT fractions were diluted in the same control medium as described for the washing procedure, at 150 and 300 μg mL^{-1} without adjustment for CT content, and transferred to 24-well plates in triplicates (1 mL per well). Then, approximately 5 active worms were selected and added to each well containing control media only (negative control) or diluted CT fractions. The motility of each worm was scored after 10 s observation as: (3) active movements; (2) slow movements; (1) moving only buccal or anterior parts; (0) non-motile; at 4, 6, 8, 20, 24 and 30 h of incubation at 38 °C.

Statistical analyses

Statistical analyses were performed using R (version 3.2.0). In the LFIA with flavan-3-ol monomers, comparison of differences in larval feeding percentages was based on the three replicates including control values and assessed by multiple linear regression depending on the factors: flavan-3-ol monomers and dose, and their interaction. In the LFIA with CT fractions, the mean larval feeding percentage was calculated from the three replicates and was considered as the outcome in the multiple linear regression of explanatory variables: parasite species, dose (categorical), percentage of PD and *cis*-subunits, mDP and their interactions with the dose. Additionally, a model including CT subunit-percentages, i.e. C, EC, GC and EGC instead of percentage of PD and *cis*-subunits was also tested. For these models, the outcomes were square root transformed using the command 'boxcox' and multicollinearity in the model was identified with variance inflation factors (VIF). All final models were checked for normality with the Shapiro–Wilk test. The correlations between structural parameters of CT in fractions, mean percentages of inhibition in LFIA for the two nematode species, and the association of CT composition and larval motility in LFIA, were assessed with Pearson's correlations. The statistical significance was set at $P < 0.05$.

RESULTS

Plant fractions

The CT contents and structural characteristics of the 14 F2 fractions are presented in Table 1. The CT contents varied from 63·6 to 100 g CT/100 g fraction. The mDP ranged from 5·3 to 12·7 and the percentages of different tannin types covered almost the full range: 1–99% of PD and 4·3–95·6%

Table 1. Plant sources and composition of purified condensed tannin (CT) fractions in terms of content (g CT/100 g fraction), mean degree of polymerization (mDP), percentages of procyanidins (PC), prodelphinidins (PD), *cis*- and *trans*-flavan-3-ols and molar percentages of monomeric subunits of CT [PC subunits: catechin (C) and epicatechin (EC); and PD subunits: gallocatechin (GC), epigallocatechin (EGC)]

Plant source	Botanical name	CT	mDP	PC	PD	*cis*	*trans*	GC	EGC	C	EC
Tilia flowers	*Tilia* spp.	91·7	7·9	99·1	0·9	95·6	4·4	0·0	0·9	4·4	94·7
Goat willow leaves	*Salix caprea*	83·8	5·3	95·2	4·8	4·3	95·8	3·0	2·0	92·7	2·3
Willow bark	*Salix* spp.	83·3	9·9	94·0	6·0	78·1	21·9	0·9	5·1	21·0	73·0
Pine bark	*Pinus* spp.	80·0	6·6	88·8	11·2	78·1	21·9	4·9	6·9	17·1	71·1
Hazelnut skin	*Corylus avellana*	67·5	9·1	79·1	20·9	47·8	52·2	12·2	9·6	40·1	38·1
Goat willow twigs	*Salix caprea*	93·2	5·3	78·7	21·3	62·8	37·2	9·5	12·7	27·8	50·0
Walnut leaves	*Juglans regia*	69·0	12·3	69·1	30·9	76·3	23·7	7·0	23·9	16·7	52·4
Weeping willow catkins	*Salix babylonica*	97·4	8·0	67·1	33·0	57·7	42·3	17·4	16·7	25·0	40·8
Birch leaves	*Betula* spp.	63·6	8·3	41·1	58·9	70·7	29·3	15·3	43·6	14·0	27·1
Sainfoin	*Onobrychis viciifolia*	100·0	8·7	35·2	64·9	79·2	20·9	14·8	51·3	6·1	27·8
Blackcurrant leaves A	*Ribes nigrum*	100·0	6·5	5·6	94·5	7·0	93·0	88·8	5·9	4·2	1·0
Blackcurrant leaves B	*Ribes nigrum*	77·1	11·8	4·7	95·3	18·8	81·2	77·9	17·4	3·3	1·4
White clover flowers A	*Trifolium repens*	100·0	8·6	1·3	98·7	58·9	41·1	40·5	58·3	0·7	0·5
White clover flowers B	*Trifolium repens*	82·4	12·7	1·2	98·8	61·8	38·2	37·8	61·0	0·3	0·8

of *cis*-stereochemistry within CT. The analyses of the correlations between these parameters showed non-significant low to moderate correlations: mDP *vs* PD ($r = 0·4$; $P = 0·15$), mDP *vs* *cis* ($r = 0·21$; $P = 0·47$) and PD *vs* *cis* ($r = -0·34$; $P = 0·24$). Additionally, we included the percentages of the different types of monomeric subunits within the CT fractions (C, EC, GC and EGC). The correlations with mDP were: low for EC ($r = -0·12$; $P = 0·68$) and GC ($r = 0·20$; $P = 0·50$) and moderate for C ($r = -0·47$; $P = 0·09$) and EGC ($r = 0·45$; $P = 0·11$). The correlations between subunits were more variable, and significant for EC *vs* GC ($r = -0·68$; $P = 0·007$). The characteristics of F1 fractions tested in the additional LFIA were: sainfoin (CT% = 37·2; mDP = 2·8; PD% = 72; *cis*% = 66·7), goat willow leaves (CT% = 51·5; mDP = 2·1; PD% = 5·8; *cis*% = 6·8) and pine bark (CT% = 54·0; mDP = 2·3; PD% = 15·1; *cis*% = 48·1).

In vitro *assays with first-stage larvae*

Flavan-3-ol monomers. The flavan-3-ols that occur in PD tannins (GC and EGC) and their galloyl derivatives (GCg and EGCg) showed markedly higher reduction of L1 feeding ability as compared with the flavan-3-ols (C and EC) found in PC tannins (Fig. 1); whereas the other structural parameters, i.e. stereochemistry and galloylation, showed less pronounced effects on anthelmintic activity. The interaction between flavan-3-ol monomers and dose was significant ($P < 0·001$), and therefore, the estimates were calculated to compare the larval feeding inhibition for (i) dose effects for each flavan-3-ol monomer (Fig. 1) and (ii) flavan-3-ol monomers at each of the three dose levels. The dose-effect was significant for all flavan-3-ol monomers except for C. It was shown that presence

of gallate in flavan-3-ols (GCg and EGCg) only slightly reduced the larval feeding at 40 μg mL^{-1} in comparison with their respective non-galloylated flavan-3-ols (GC and EGC) ($P < 0·05$), and no difference was seen at other concentrations ($P > 0·25$). Moreover, an effect of *cis*/*trans* configuration was observed only between flavan-3-ols found in PC tannins. In fact, the *cis*-configured monomer (EC) inhibited larval feeding at 160 μg mL^{-1} [$P < 0·001$; and $P < 0·01$ for comparisons with PBS (=negative control) and C at 160 μg mL^{-1}, respectively], while the *trans*-configuration (C) showed no effect at any of the concentrations as compared with the negative control.

Likewise, the motility of L1 was substantially reduced with flavan-3-ols found in PD compared with those found in PC tannins. At 40 and 160 μg mL^{-1} no L1 motility was observed when exposed to GC, EGC, GCg or EGCg while flavan-3-ols C and EC did not affect the larval motility, not even at high concentrations, as compared with the negative control (brief observation without counting).

CT fractions. While significant dose dependent interactions were observed for CT ($P < 0·01$) each parameter was statistically assessed at each concentration. Overall, CT fractions showed a dose-dependent reduction of the larval feeding, which was higher than their respective flavan-3-ol monomers at the same w/v concentrations (Fig. 2). This was substantiated by a statistically significant negative effect of mDP at all concentrations on the larval feeding ($P < 0·01$). Moreover, the feeding of *O. ostertagi* L1 in the modified LFIA was significantly reduced with the CT fraction that had the higher mDP (Fig. 3), in the same manner as LFIA following the standard protocol. The motility of L1 was also strongly reduced with both CT fractions
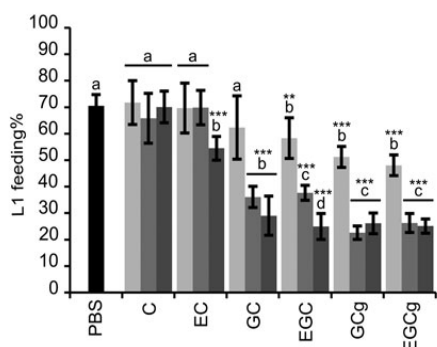
Fig. 1. Results on the LFIA with flavan-3-ol monomers on mixed first-stage larvae (L1) (*Cooperia oncophora* and *Ostertagia ostertagi* 70:30). Bars represent the mean of fed larvae (%) from three replicates incubated in PBS (negative control) or pure flavan-3-ol monomers at 10 (light grey), 40 (grey) and 160 (dark grey) μg mL^{-1} with error bars as S.D. Tested compounds were catechin (C) and epicatechin (EC) (i.e. procyanidin subunits), and gallocatechin (GC) and epigallocatechin (EGC) (i.e. prodelphinidin subunits) and their galloylated derivatives: gallocatechin gallate (GCg) and epigallocatechin gallate (EGCg). Significant differences between the mean in PBS and mean of each monomer at different dose levels are indicated by letters (asterisks **: $P < 0.01$; ***: $P < 0.001$). Thus, for each flavan-3-ol monomer different letters indicate statistical difference between doses ($P < 0.05$). Chemical structures of flavan-3-ol monomers are available from Brunet and Hoste (2006).

as compared with PBS. The higher percentages of *cis* and PD subunits also reduced, but to a lesser extent, the larval feeding ability (Fig. 2). These effects were statistically significant only at 2·5 and 10 μg of CT mL^{-1} for *cis* ($P < 0.01$) and at 10 μg of CT mL^{-1} for PD subunits ($P < 0.05$). Moreover, these variables were kept in the model as they did not show problematic collinearities (VIF < 2). The analysis based on CT subunits was abandoned as it showed strong collinearities and confounding effects (VIF > 1000).

Non-CT compounds (=100% − CT percentage) for each fraction were excluded from the statistical model as they did not show any significant effect (Note: fraction concentrations in the assay were adjusted to account for their varying CT contents). Results of the supplementary LFIA with F1 fractions, adjusted for CT content, showed a poor inhibition for sainfoin and goat willow leaves as compared with pine bark (mean inhibition ± S.D.: 16·1% ± 0·5, 13·2% ± 2·5 and 31·6% ± 3·5, respectively). The pre-incubation of sainfoin F2 with or without sucrose had no effect on the LFIA (similar results as shown in Fig. 2B).

The larval feeding in the control media was lower for *O. ostertagi* compared with *C. oncophora*, although not statistically significant. However, the results with CT indicated that L1 of *O. ostertagi* were more susceptible to CT than *C. oncophora*: at

all three CT concentrations the L1 feeding was much lower for *O. ostertagi* ($P < 0.001$). In addition, the correlations between the mean percentages of larval feeding inhibition for the two nematode species were significant at all concentrations ($P < 0.01$) and overall ($P < 0.001$).

The motility of *O. ostertagi* L1 was reduced in a dose-dependent manner with most of the CT fractions, which could have been more prominent at lower CT concentrations by using a scaled score instead of a dichotomous scale. Furthermore, the motility was clearly inhibited at 40 μg of CT mL^{-1} with PD-rich fractions (white clover A and blackcurrant A) (Fig. 4) and was similar to the effects of flavan-3-ol monomers. In fact, the few remaining motile larvae with these two CT fractions were only moving very slowly. Thus, the percentage of PD was the main factor responsible for the higher inhibition of the larval motility at 40 μg mL^{-1} ($r = -0.92$; $P = 0.001$) and no other structural parameter was statistically correlated with inhibition of larval motility.

In vitro *assay with CT fractions and adult worms*

The three CT fractions inhibited the motility of *C. oncophora* adults, although to different extents, as compared with adult worms in the control media, which were actively moving throughout the observation period (30 h). The two CT fractions from blackcurrant leaves, that contained mainly GC but differed in mDP, showed higher antiparasitic potency when compared with the CT fraction from willow bark which contained mainly (EC) (Fig. 5A). The motility was greatly reduced after 4 h with 150 and 300 μg mL^{-1} of PD-rich CT fractions, and completely inhibited with these two concentrations after 20 and 30 h, respectively. In comparison, CT from willow bark at 150 μg mL^{-1} did not change the nematode motility as compared with the control. Moreover, 300 μg mL^{-1} reduced the motility only after 20 h, and this concentration was not sufficient to kill the worms even after 30 h.

In contrast, adult *O. ostertagi* worms had a reduced motility and died within 30 h in the control media (Fig. 5B), although worms were very active at the time of allocation to the wells. Moreover, at both concentrations no CT fractions showed any difference as compared with the negative control. Although the fitness of adults of *O. ostertagi* was weak during the whole incubation period, the majority of worms were still alive after 20 h with PD-rich CT fractions at 300 μg mL^{-1} (unlike *C. oncophora* adults). Hence, we attempted to verify whether *O. ostertagi* worms were deprived of their ability to feed and subsequently unable to ingest CT. We used a method similar to the LFIA. Briefly, we incubated a few *O. ostertagi* adults in one well with control media only or with CT
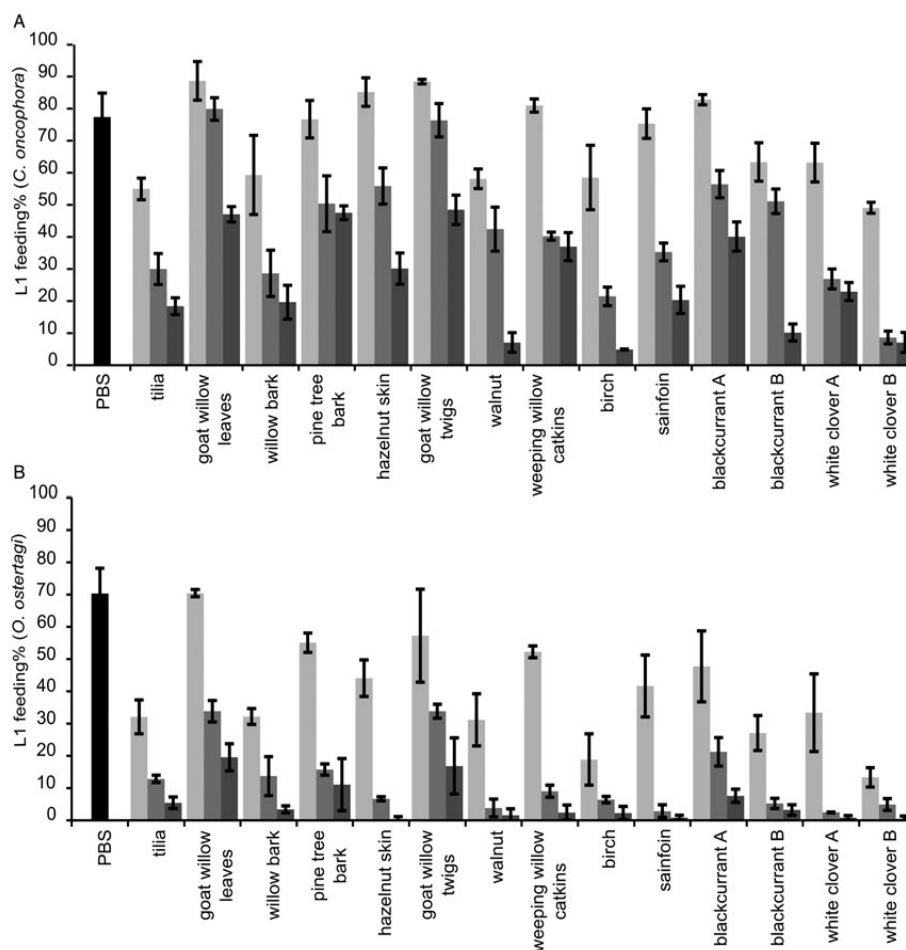
Fig. 2. Results of the LFIA with 14 CT fractions on L1 of *Cooperia oncophora* (A) and *Ostertagia ostertagi* (B). Bars represent the mean percentage of fed larvae (%) from three replicates for each fractions at 2·5 (light grey), 10 (grey) and 40 (dark grey) μg of CT mL^{-1} and the pooled mean for the negative control (PBS) with error bars as s.d. The chemical structure of CT can be found in (Williams *et al.* 2014*a*).

fractions from willow bark and blackcurrant leaves (samples A and B) at 300 μg mL^{-1} for 2 or 30 h at 38 °C. Then, the worms were transferred individually into a well-holding fresh control media containing fluorescent *E. coli*, and incubated for 24 h at 38 °C. The worms were then individually washed in PBS before visualization by microscopy at 400×. We observed traces of fluorescent *E. coli* in the pharyngeal region or the digestive tract of most of the worms pre-incubated for 2 h with or without CT (Fig. 6A and D). Moreover, the pumping activity of the pharyngeal muscles was also observed in a few live worms but the feeding behaviour could not be compared with *C. oncophora* adult worms as the assays with this species were done 1 week earlier. Additionally, we could see the main structures of the external surface of the worms at the highest magnification, even in the presence of

fluorescence. The longitudinal lines of the external cuticle of *O. ostertagi* adults appeared smooth in all groups after 2 and 30 h incubations with or without CT (Fig. 6B and E). However, aggregates around the anterior part were seen only on worms incubated with CT for 2 h and were more pronounced after 30 h (Fig. 6F). Moreover, the cuticle was also covered with aggregates and fluorescent *E. coli* for the worms pre-incubated for 30 h in CT (Fig. 6E), but not the worms incubated in control media (Fig. 6B) or in CT fractions for 2 h. Similar pictures were obtained from dead *C. oncophora* adult worms that had been incubated in the same control media and CT for 5 days (Fig. 7). The surface of the cuticle was not obviously damaged, although aggregates were observed on the cuticle and the anterior part of the worms, similarly to *O. ostertagi*.
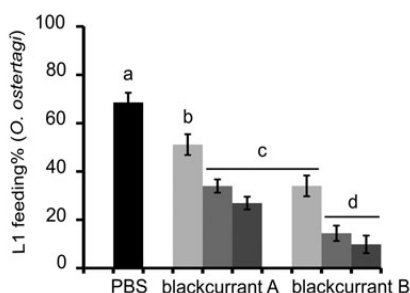
Fig. 3. Results of a LFIA with *O. ostertagi* L1, modified in order to avoid interaction between CT and the bacterial food source. Bars represent the mean percentage of fed larvae incubated in PBS (negative control) or CT fractions at 2·5 (light grey), 10 (grey) or 40 (dark grey) μg of CT mL^{-1} with error bars as s.d.. Different letters indicate a significant difference (one-way ANOVA with Tukey' HSD *post hoc* test; $P < 0.05$).
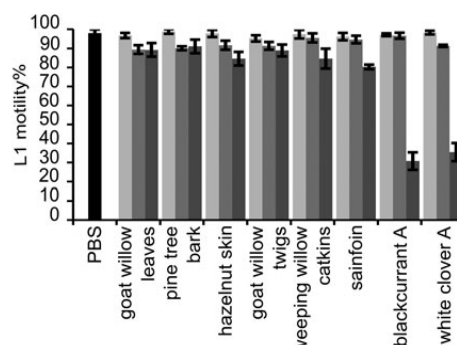

Fig. 4. Motility of the first-stage larvae (L1) of *Ostertagia ostertagi* in the presence of eight different CT fractions. Experiment was performed at the same time as the larval feeding (see Fig. 2B). Any larval movement within 5 s was counted as motile. Bars represent either the pooled mean for the negative control (PBS) or the mean of the percentage of motile L1 incubated at 2·5 (light grey), 10 (grey) and 40 (dark grey) μg of CT mL^{-1} in triplicates with error bars as s.d.

DISCUSSION

It is evident from our findings that the CT levels are decisive for the anti-parasitic activity. This was reflected by a dose-dependent reduction in L1 feeding for all CT fractions in the LFIA, although to different extents. A dose response effect in the LFIA was also found for most flavan-3-ol monomers. Our results also showed that mDP was the main structural CT parameter that influenced the inhibition of feeding without affecting the motility. Motility was instead strongly related with a high percentage of PD for both L1 and adult worms. This is the first report of how these two structural parameters of CT exert different anthelmintic effects. It also clearly shows that the main effect of one parameter may complicate the analysis of effects of other structural parameters. Apparently, the CT stereochemistry (*cis*- or *trans*-configurations) had only a minor effect on the anti-parasitic properties as compared with the two other parameters.

We found that *O. ostertagi* L1 were more susceptible to CT than *C. oncophora* L1, in contrast to previous studies that did not detect any species-specific differences (Novobilský *et al.* 2011, 2013). Moreover, the control values in the LFIAs ranged between 75 and 80%, in the same manner as previously reported (Novobilský *et al.* 2013) or slightly higher (Novobilský *et al.* 2011; Peña-Espinoza *et al.* 2015). One explanation for the different susceptibilities could be that different *O. ostertagi* strains were used. However, several *in vitro* studies with sheep GIN have also reported a greater susceptibility of abomasal nematodes to CT (e.g., *H. contortus, Teladorsagia circumcincta*) as compared with intestinal nematodes (e.g., *T. colubriformis*). This has been demonstrated for different life stages in different assays: egg hatchability, larval development (eggs to L3), migration of L3 (Molan *et al.* 2004;

Molan, 2014) and L3 exsheathment (Quijada *et al.* 2015). Further, the inhibition of larval feeding by the different CT fractions was significantly correlated for both nematode species, indicating that the CT structure influenced the anthelmintic activity similarly for both species, in this assay. In fact, the species differences with regards to the CT structure were minor in studies that targeted the exsheathment of L3 in small ruminants (Brunet and Hoste, 2006; Quijada *et al.* 2015).

The influence of mDP on CT-induced reduction of larval feeding is in agreement with a previous study by Novobilský *et al.* (2013), although the present study explored a substantially smaller range of mDP values, i.e. 5 13 *vs* 2 95. In fact, this effect proved to be the most important for larval feeding, among other CT structure traits. Moreover, we showed that this effect was targeted directly against the larvae and not due to an interference with *E. coli* (Fig. 3). In fact, larger CT have been shown to have a greater binding capacity to bacterial surfaces which could have modified the feed source in the LFIA, perhaps by aggregation (Jones *et al.* 1994; Verhelst *et al.* 2013). This could have rendered the bacteria less accessible thereby indirectly influencing the feeding ability of L1.

Higher PD and *cis*-subunit percentages in CT also reduced the larval feeding but to a lesser extent than mDP, as they were not statistically different at all concentrations. The CT stereochemistry had no significant effect in a previous study (Novobilský *et al.* 2013), most likely because the range was too narrow (60 82% *cis*-subunits in CT). The present set of experiments has now investigated a much wider range (5 96% *cis*-subunits) but was still only able to detect a few significant differences. A more
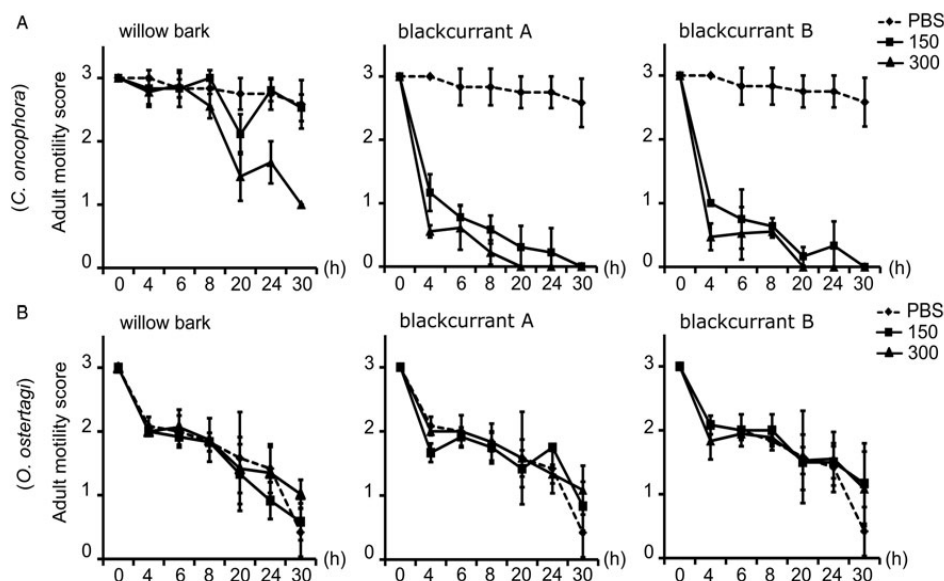
Fig. 5. Results on the motility of adult worms of *Cooperia oncophora* in row (A) and *Ostertagia ostertagi* in row (B), incubated in triplicates either in control media (PBS) or CT fractions of willow bark or blackcurrant leaves at 150 and 300 μg mL^{-1}. The motility was assessed within 10 s by observation using a scaled score 0–3: with 3 (active movement), 2 (slow movement), 1 (only moving one part of the body) and 0 (no movement). At each time point the average motility score of the triplicates was plotted with error bars showing the s.d.

detailed analysis based on the percentages of all CT subunits (C, EC, GC and EGC) was not possible because of strong collinearities and confounding effects. Therefore, it remains easier to interpret results with the commercial flavan-3-ol monomers and to distinguish their anthelmintic properties in relation to their structures. Thus, we have clearly shown that flavan-3-ols giving rise to PD (GC, EGC) were more effective in the LFIA than flavan-3-ols that are found in PC (C, EC); and the *cis*-configuration was of a less importance as EC only had a slightly stronger effect than C (whereas no statistical difference between EGC and GC was observed). Although these results are based on a mixture of nematode species, they are comparable with other studies that tested flavan-3-ols against the exsheathment of *H. contortus* L3 (Brunet and Hoste, 2006) and the motility of *A. suum* L4 (Williams *et al*. 2014*a*). The galloylation of flavan-3-ols also seemed to enhance the anthelmintic activity in the LFIA, as previously reported for L3 in sheep (Molan *et al*. 2003; Brunet and Hoste, 2006). However, we did not test the gallate-derivatives of flavan-3-ols that occur in PC (Cg or ECg) and thus, could not perform a full comparison.

For first stage larvae of both *O. ostertagi* and *C. oncophora* the motility was markedly reduced only with PD-rich CT fractions, GC and EGC, and their galloyl derivatives (GCg, EGCg) at $\geqslant$40 μg mL^{-1}. This was strongly supported by the results of the adult motility assay with *C. oncophora*,

where CT fractions from blackcurrant leaves (PD-rich) were distinctly more potent than those of willow bark (PC-rich) regardless of their mDP values. Although we did not test the influence of mDP with PC-rich fractions in the adult motility assay, this is expected to be minor compared to the overriding effect of the PD percentage. In fact, Spiegler *et al*. (2015) have recently shown that a degree of polymerization (DP) of 3 in PC oligomers represented the lower threshold that significantly reduced the survival of adult *Caenorhabditis elegans*, although to a limited extent (maximum reduction of approximately 55%), and a DP > 4 had no further effect on the anthelmintic activity.

Our findings highlight differences between CT effects on feeding and motility. This can perhaps be explained by various modes and sites of CT action. With the feeding it is expected that larger CT have prevented the ingestion of *E. coli* to a high degree by obstruction of the mouth of the larvae or by precipitation of proteins in the buccal cavity. Precipitates probably confer a pronounced astringency, even at very low CT concentrations, thereby depriving larvae of energy, impairing digestive processes and slowing or blocking development. In fact, ellagitannins do reduce the development of *C. elegans* L1 (Mori *et al*. 2000), and CT have been shown *in vitro* to be detrimental for the moulting of *O. dentatum* L3 to L4 in pigs (Williams *et al*. 2014*b*). Motility was not affected in any of these studies. Likewise, the majority of *O. ostertagi* L1
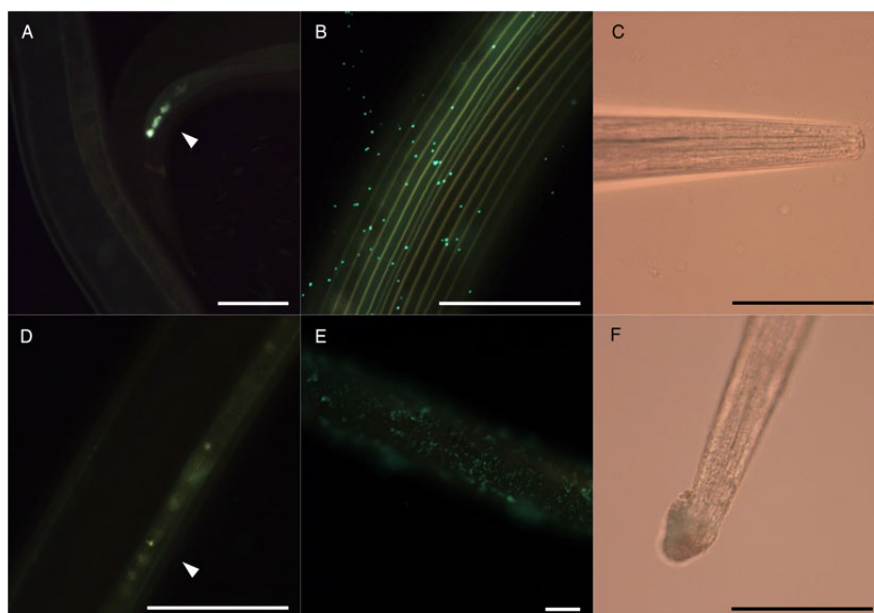
Fig. 6. Micrographs of *Ostertagia ostertagi* adults pre-incubated in control media (A, B, C) or CT fraction from blackcurrant leaves A at $300\,\mu g\,mL^{-1}$ (D, E, F), for 2 h (A, D) or 30 h (B, C, E, F), and then transferred to control media containing fluorescent *E. coli* for 24 h. White arrow heads show presence of fluorescent bacteria in the cloacae (A) or in the digestive tract (B) of the worm. (B, E) show a part of the cuticle and (C, F) the anterior part (scale bars = $100\,\mu M$).

that we exposed to $10\,\mu g$ of CT mL^{-1} of fractions was unfed (Fig. 2B) but remained fully motile (Fig. 4). The lack of feeding is expected to be detrimental to larval development which may be interpreted as an early manifestation of CT toxicity; we did, however, not follow the effect on larval development over time. Then, the reduced motility of L1 incubated with PD-rich fractions at $40\,\mu g$ of CT mL^{-1} relative to PC-rich fractions was not related to starvation but rather to some other mechanism. Williams *et al.* (2014*a*) have shown that *A. suum* L4 incubated with CT fraction from hazelnut skin (PC-rich) were motionless after 12 24 h, which was related with substantial structural damage on external and internal tissues of the larvae. Moreover, the increasing percentage of PD subunits in CT has been often associated with a greater anthelmintic activity (Novobilský *et al.* 2013; Quijada *et al.* 2015) as in our study; yet, it has never been shown whether PC and PD-rich CT induce structural damage of the worms to a different extent.

The low survival of adult *O. ostertagi* as compared with *C. oncophora* in our control medium in the adult motility assay prevented comparison of the two species. A similar observation was made earlier when the motility of adult *H. contortus* was tested against *T. colubriformis* (Paolini *et al.* 2004). In our specific case, this finding could have been influenced by a suboptimal medium and/or use of older worms. In fact, Geldhof *et al.* (2000) used 21-day-old adult *O. ostertagi*, which were kept alive for at least 48 h

in supplemented RPMI medium whereas our worms were 38-day-old and died after 24 h in PBS. Moreover, the motility of these worms was not reduced by CT in contrast to *C. oncophora* where an effect could be observed 4 h post-incubation. Mori *et al.* (2000) concluded that the reduced survival of young *C. elegans* adults exposed to ellagitannins was likely related to the ingestion of compounds as the cuticle of the worms was not visibly damaged. In our study, the changes on the surface of adult worms exposed to CT were mainly characterized by aggregates around the mouth and on the cuticle while pronounced folds on the cuticular ridges, as observed in adult *H. contortus* (Martínez-Ortíz-de-Montellano *et al.* 2013), were not seen. The lesions were comparable between the two cattle nematode species and could evidently not account for the difference in motility observed between the species. We observed that adult *O. ostertagi* were able to ingest *E. coli* to some extent; however, the uptake of CT probably remained too low to observe any effect. This emphasizes the importance of the contact route with CT on their anthelmintic activity.

Although the presence of non-CT compounds in the CT fractions had no statistically significant effect on the LFIA, it may have influenced some of the results. It could perhaps explain the lower larval feeding in the presence of birch leaf CT that had the lowest CT content as compared with sainfoin tannins, despite their close structural
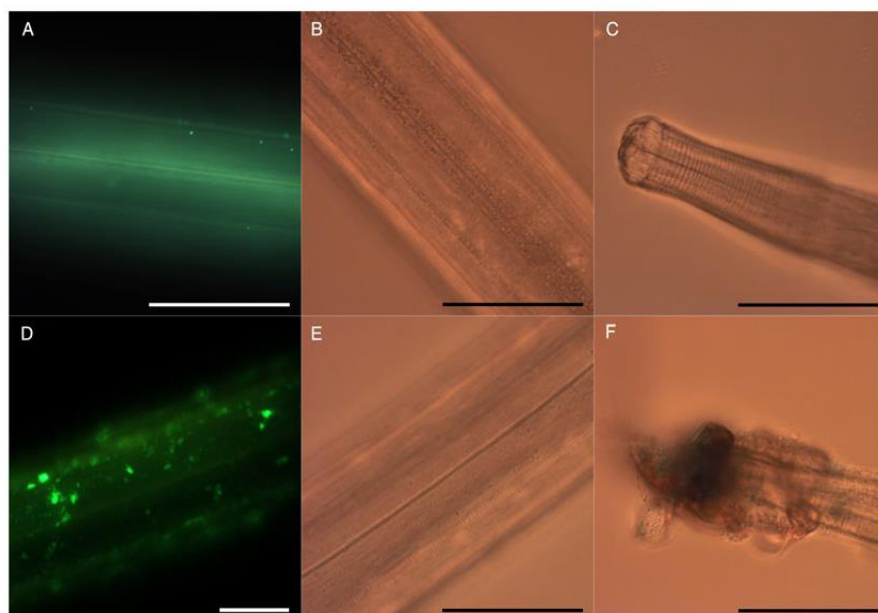
Fig. 7. Micrographs of *Cooperia oncophora* adults pre-incubated for 5 days at 38 °C in control media (A, B, C) or CT fraction from blackcurrant leaves at 300 μg mL^{-1} (D, E, F), and then transferred to control media containing fluorescent *E. coli* for 24 h. The cuticle is shown by fluorescent microscopy (A, D) or light microscopy (B, E) and of the anterior part is illustrated in (C, F) (scale bars = 100 μM).

similarities. Additionally, we obtained a poor inhibition in LFIA with the F1 fraction from sainfoin with lower mDP and CT content values as reported previously for the motility of *A. suum* L3 (Williams *et al.* 2014*a*). This could not be explained by the interference of impurities such as sugars, as the pre-incubation of CT with sucrose had no effect on anthelmintic activity; thus, confirming findings by Williams *et al.* (2014*a*). Nonetheless, it has been shown that the disruptive effect of carbohydrates on the formation of protein tannin complexes depends on the type of carbohydrate and, more importantly, decreases with larger CT (Mateus *et al.* 2004). Therefore, the putative interaction of sugars with CT that is expected to reduce the anthelmintic activity may have been stronger with low mDP tannins (F1 fractions) as compared with higher mDP tannins (F2 fractions) from sainfoin.

In conclusion, CT showed activity against free-living larvae and parasitic adults of *O. ostertagi* and *C. oncophora*, confirming the potential role of these bioactive compounds in control of GIN in cattle. L1 of *O. ostertagi* were more susceptible to CT than *C. oncophora*, but the influence of the CT structure on the anthelmintic activity was similar for both species. Hence, the reduction of nematode motility was highly influenced by the PD percentage in CT, whereas tannin size (in terms of mDP-values) was of importance only when CT interfered with larval feeding ability. Further research is needed to investigate the targets of CT on the cuticle and the

digestive tract of parasitic nematodes and thus their exact mechanisms of action.

REFERENCES

Brunet, S. and Hoste, H. (2006). Monomers of condensed tannins affect the larval exsheathment of parasitic nematodes of ruminants. *Journal of Agricultural and Food Chemistry* **54**, 7481–7487.

Brunet, S., Aufrere, J., El Babili, F., Fouraste, I. and Hoste, H. (2007). The kinetics of exsheathment of infective nematode larvae is disturbed in the presence of a tannin-rich plant extract (sainfoin) both *in vitro* and *in vivo*. *Parasitology* **134**, 1253–1262.

Geldhof, P., Claerebout, E., Knox, D.P., Agneessens, J. and Vercruysse, J. (2000). Proteinases released *in vitro* by the parasitic stages of the bovine abomasal nematode *Ostertagia ostertagi*. *Parasitology* **121**, 639–647.

Hatew, B., Stringano, E., Mueller-Harvey, I., Hendriks, W.H., Carbonero, C.H., Smith, L.M.J. and Pellikaan, W.F. (2015). Impact of variation in structure of condensed tannins from sainfoin (*Onobrychis viciifolia*) on *in vitro* ruminal methane production and fermentation characteristics. *Journal of Animal Physiology and Animal Nutrition*, In press. doi: 10.1111/jpn.12336.

Hoste, H., Torres-Acosta, J. F. J., Sandoval-Castro, C. A., Mueller-Harvey, I., Sotiraki, S., Louvandini, H., Thamsborg, S. M. and Terrill, T. H. (2015). Tannin containing legumes as a model for nutraceuticals against digestive parasites in livestock. *Veterinary Parasitology* 212, 5–17.

Jackson, F. and Hoste, H. (2010). *In vitro* methods for the primary screening of plant products for direct activity against ruminant gastrointestinal nematodes. In *In vitro Screening of Plant Resources for Extra-nutritional Attributes in Ruminants: Nuclear and Related Methodologies* (ed. Vercoe, P. E., Makkar, H. P. S. and Schlink, A. C.), pp. 25–45. Springer, The Netherlands.

Jakobek, L. (2015). Interactions of polyphenols with carbohydrates, lipids and proteins. *Food Chemistry* 175, 556–567.

Jones, G. A., McAllister, T. A., Muir, A. D. and Cheng, K.-J. (1994). Effects of sainfoin (*Onobrychis viciifolia* Scop.) condensed tannins on growth and proteolysis by four strains of ruminal bacteria. *Applied and Environmental Microbiology* 60, 1374–1378.

Marais, J. P. J., Mueller-Harvey, I., Brandt, E. V. and Ferreira, D. (2000). Polyphenols, condensed tannins, and other natural products in *Onobrychis viciifolia* (Sainfoin). *Journal of Agricultural and Food Chemistry* 48, 3440–3447.

Martínez-Ortíz-de-Montellano, C., Arroyo-López, C., Fourquaux, I., Torres-Acosta, J. F. J., Sandoval-Castro, C. A. and Hoste, H. (2013). Scanning electron microscopy of *Haemonchus contortus* exposed to tannin-rich plants under *in vivo* and *in vitro* conditions. *Experimental Parasitology* 133, 281–286.

Mateus, N., Carvalho, E., Luís, C. and de Freitas, V. (2004). Influence of the tannin structure on the disruption effect of carbohydrates on protein-tannin aggregates. *Analytica Chimica Acta* 513, 135–140.

Molan, A. L. (2014). Effect of purified condensed tannins from pine bark on larval motility, egg hatching and larval development of *Teladorsagia circumcincta* and *Trichostrongylus colubriformis* (Nematoda: Trichostrongylidae). *Folia Parasitologica* 61, 371–376.

Molan, A. L., Meagher, L. P., Spencer, P. A. and Sivakumaran, S. (2003). Effect of flavan-3-ols on *in vitro* egg hatching, larval development and viability of infective larvae of *Trichostrongylus colubriformis*. *International Journal for Parasitology* 33, 1691–1698.

Molan, A. L., Sivakumaran, S., Spencer, P. A. and Meagher, L. P. (2004). Green tea flavan-3-ols and oligomeric proanthocyanidins inhibit the motility of infective larvae of *Teladorsagia circumcincta* and *Trichostrongylus colubriformis in vitro*. *Research in Veterinary Science* 77, 239–243.

Mori, T., Mohamed, A. S. A., Sato, M. and Yamasaki, T. (2000). Ellagitannin toxicity in the free-living soil-inhabiting nematode, *Caenorhabditis elegans*. *Journal of Pesticide Science* 25, 405–409.

Novobilský, A., Mueller-Harvey, I. and Thamsborg, S. M. (2011). Condensed tannins act against cattle nematodes. *Veterinary Parasitology* 182, 213–220.

Novobilský, A., Stringano, E., Hayot Carbonero, C., Smith, L. M. J., Enemark, H. L., Mueller-Harvey, I. and Thamsborg, S. M. (2013). *In vitro* effects of extracts and purified tannins of sainfoin (*Onobrychis viciifolia*) against two cattle nematodes. *Veterinary Parasitology* 196, 532–537.

Paolini, V., Fouraste, I. and Hoste, H. (2004). *In vitro* effects of three woody plant and sainfoin extracts on 3rd-stage larvae and adult worms of three gastrointestinal nematodes. *Parasitology* 129, 69–77.

Peña-Espinoza, M., Boas, U., Williams, A. R., Thamsborg, S. M., Simonsen, H. T. and Enemark, H. L. (2015). Sesquiterpene lactone containing extracts from two cultivars of forage chicory (*Cichorium intybus*) show distinctive chemical profiles and *in vitro* activity against *Ostertagia ostertagi*. *International Journal for Parasitology: Drugs and Drug Resistance* 5, 191–200.

Porter, L. J. (1988). Flavans and proanthocyanidins. In *The Flavonoids: Advances in Research Since 1980* (ed. Harbone. J. B.), pp. 21–62. Chapman and Hall, London.

Quijada, J., Fryganas, C., Ropiak, H. M., Ramsay, A., Mueller-Harvey, I. and Hoste, H. (2015). Anthelmintic activities against *Haemonchus contortus* or *Trichostrongylus colubriformis* from small ruminants are influenced by structural features of condensed tannins. *Journal of Agricultural and Food Chemistry* 63, 6346–6354.

Saminathan, M., Tan, H., Sieo, C., Abdullah, N., Wong, C., Abdulmalek, E. and Ho, Y. (2014). Polymerization degrees, molecular weights and protein-binding affinities of condensed tannin fractions from a *Leucaena leucocephala* hybrid. *Molecules* 19, 7990–8010.

Saminathan, M., Sieo, C. C., Abdullah, N., Wong, C. M. V. L. and Ho, Y. W. (2015). Effects of condensed tannin fractions of different molecular weights from a *Leucaena leucocephala* hybrid on *in vitro* methane production and rumen fermentation. *Journal of the Science of Food and Agriculture* 95, 2742–2749.

Schofield, P., Mbugua, D. M. and Pell, A. N. (2001). Analysis of condensed tannins: a review. *Animal Feed Science and Technology* 91, 21–40.

Slotved, H. C., Barnes, E. H., Bjørn, H., Christensen, C. M., Eriksen, L., Roepstorff, A. and Nansen, P. (1996). Recovery of *Oesophagotomum dentatum* from pigs by isolation of parasites migrating from large intestinal contents embedded in agar-gel. *Veterinary Parasitology* 63, 237–245.

Spencer, P., Sivakumaran, S., Fraser, K., Foo, L. Y., Lane, G. A., Edwards, P. J. B. and Meagher, L. P. (2007). Isolation and characterisation of procyanidins from *Rumex obtusifolius*. *Phytochemical Analysis* 18, 193–203.

Spiegler, V., Sendker, J., Petereit, F., Liebau, E. and Hensel, A. (2015). Bioassay-guided fractionation of a leaf extract from *Combretum mucronatum* with anthelmintic activity: pligomeric procyanidins as the active principle. *Molecules* 20, 14810–14832.

Verhelst, R., Schroyen, M., Buys, N. and Niewold, T. A. (2013). *E. coli* heat labile toxin (LT) inactivation by specific polyphenols is aggregation dependent. *Veterinary Microbiology* 163, 319–324.

Williams, A., Fryganas, C., Ramsay, A., Mueller-Harvey, I. and Thamsborg, S. (2014a). Direct anthelmintic effects of condensed tannins from diverse plant sources against *Ascaris suum*. *PLoS ONE* 9, e97053.

Williams, A., Ropiak, H., Fryganas, C., Desrues, O., Mueller-Harvey, I. and Thamsborg, S. (2014b). Assessment of the anthelmintic activity of medicinal plant extracts and purified condensed tannins against free-living and parasitic stages of *Oesophagostomum dentatum*. *Parasites and Vectors* 7, 518.

Appendix F

Original publication:

Direct Anthelmintic Effects of Condensed Tannins from Diverse Plant Sources against *Ascaris suum*.

Andrew R. Williams, Christos Fryganas, Aina Ramsay, Irene Mueller-Harvey, Stig M. Thamsborg

PLoS ONE 9(5): e97053.

DOI:10.1371/journal.pone.0097053.

Author's personal copy

Direct Anthelmintic Effects of Condensed Tannins from Diverse Plant Sources against *Ascaris suum*

Andrew R. Williams[1]*, Christos Fryganas[2], Aina Ramsay[2], Irene Mueller-Harvey[2], Stig M. Thamsborg[1]

1 Department of Veterinary Disease Biology, Faculty of Health and Medical Sciences, University of Copenhagen, Frederiksberg, Denmark, 2 Chemistry and Biochemistry Laboratory, School of Agriculture, Policy and Development, University of Reading, Reading, United Kingdom

Abstract

Ascaris suum is one of the most prevalent nematode parasites in pigs and causes significant economic losses, and also serves as a good model for *A. lumbricoides*, the large roundworm of humans that is ubiquitous in developing countries and causes malnutrition, stunted growth and compromises immunity to other pathogens. New treatment options for *Ascaris* infections are urgently needed, to reduce reliance on the limited number of synthetic anthelmintic drugs. In areas where *Ascaris* infections are common, ethno-pharmacological practices such as treatment with natural plant extracts are still widely employed. However, scientific validation of these practices and identification of the active compounds are lacking, although observed effects are often ascribed to plant secondary metabolites such as tannins. Here, we extracted, purified and characterised a wide range of condensed tannins from diverse plant sources and investigated anthelmintic effects against *A. suum in vitro*. We show that condensed tannins can have potent, direct anthelmintic effects against *A. suum*, as evidenced by reduced migratory ability of newly hatched third-stage larvae and reduced motility and survival of fourth-stage larvae recovered from pigs. Transmission electron microscopy showed that CT caused significant damage to the cuticle and digestive tissues of the larvae. Furthermore, we provide evidence that the strength of the anthelmintic effect is related to the polymer size of the tannin molecule. Moreover, the identity of the monomeric structural units of tannin polymers may also have an influence as gallocatechin and epigallocatechin monomers exerted significant anthelmintic activity whereas catechin and epicatechin monomers did not. Therefore, our results clearly document direct anthelmintic effects of condensed tannins against *Ascaris* and encourage further *in vivo* investigation to determine optimal strategies for the use of these plant compounds for the prevention and/or treatment of ascariosis.

Introduction

The closely related worms *Ascaris suum* and *A. lumbricoides* are among the most prevalent nematode parasites in pigs and humans, respectively. More than 500 million people are estimated to be infected with *A. lumbricoides*, resulting in significant morbidity, stunted development and malnutrition, mainly in children [1]. *Ascaris suum* has a high prevalence in pigs in both developed and developing countries, resulting in significant economic penalties for pig farmers [2,3]. Moreover, *A. suum* is considered a zoonotic parasite and hybridization between *A. suum* and *A. lumbricoides* has been reported [4]. In addition, *Ascaris* infection also predisposes hosts to co-infection with bacteria and/or protozoa and compromises vaccine efficacy against other pathogens [5,6].

At present, *Ascaris* control is based mainly on mass treatment with synthetic anthelmintic drugs. In the long-term this is not sustainable – re-infection after annual or bi-annual drug treatment is more or less unavoidable due to the long-lived and resistant eggs which survive for many years in the environment [7], and the reliance on a limited number of related compounds (mainly albendazole and mebendazole) for mass drug administration against *A. lumbricoides* means that the threat of drug resistance is an on-going concern [1]. Moreover, the use of synthetic drugs is often not feasible for *A. suum* control in many pig production systems. Small holder farmers in many developing countries often do not have access to expensive anthelmintic drugs and, in developed countries, many organic and low-input farms are not able to prophylactically treat animals with synthetic drugs. Therefore, there is an urgent need to investigate alternative and/or complementary options for the control of these parasites.

The use of natural plant extracts as anthelmintics has been practiced in many indigenous cultures for centuries. Indeed, in many developing countries ethno-medicine is still the primary treatment option for many parasitic diseases [8,9]. The use of plant extracts has several obvious advantages that make them attractive for use in developing countries – low cost, access to large amounts of raw material and easy integration into traditional cultural practice [8–10]. However, scientific validation of these traditional treatments is lacking. Most studies that have investigated the anthelmintic potential of traditional medicinal plants have focused on crudely prepared extracts from a limited selection of plants, with only a summary analysis of the chemical constituents, and no further investigation of the active compounds

[11]. Cleary, there is a need for more systematic studies to identify and validate the use of plants as anthelmintics.

Condensed tannins (CT) are a diverse group of plant secondary metabolites commonly found in leaves, roots, nuts and fruits from a wide-range of different plant sources in both tropical and temperate areas [12]. Condensed tannins are formed by the polymerisation of monomeric flavan-3-ols. The structure of CT can vary considerably according to the degree of polymerisation, and the nature of the monomeric flavan-3-ol units; these being either catechin (C) and its *cis* isomer epicatechin (EC) which make up procyanidins, or gallocatechin (GC) and epigallocatechin (EGC), which make up prodelphinidins (Figure 1). Condensed tannins are well-known for their antimicrobial properties [13], with reports of potent effects against, amongst others, *Candida albicans* [14], *Trypanosoma brucei* [15], and *Leishmania donovani* [16]. In addition, a number of studies conducted with nematode parasites of ruminant livestock have demonstrated direct anthelmintic effects of extracts from tannin-containing plants in *in vitro* assays, with *in vivo* verification of these results being reported in some studies [17]. Furthermore, CT have been shown to have *in vitro* and *in vivo* efficacy in rodent models of hookworm and pinworm [18,19], and are speculated to be responsible for the anthelmintic effects of some traditional medicinal plants against *Ascaris* [20,21] although definitive evidence of this has not yet been provided. Therefore, studies to determine whether CT have direct anthelmintic effects against *Ascaris* are clearly warranted. Moreover, it is apparent that the anthelmintic effects of CT that thus far have been reported in other livestock parasites such as *Haemonchus contortus* are influenced by tannin structure [22], and given the diverse nature of CT from different plant sources [23], the relationship between anthelmintic activity and tannin structure also requires investigation.

Here, we extracted and characterised CT with a wide range of structural diversity from a variety of different plant sources, and carried out a detailed analysis of direct anthelmintic effects against *A. suum in vitro*. We show that, similarly to some other nematode species, CT can have potent anthelmintic effects against *A. suum*, and that the strength of the anthelmintic activity is likely related to a complex set of factors including degree of polymerization and the identity of the monomeric flavanol units in the CT molecules. Therefore, our results provide the first clear evidence of the direct anthelmintic effects of CT against *A. suum* and encourage further *in vivo* evaluation of CT-containing plant extracts for the treatment of ascariosis.

Methods

Ethics Statement

All animal experimentation was approved and carried out according to the guidelines of the Danish Animal Experimentation Inspectorate (Licence number 2010/561-1914). Protocols were approved by the Animal Ethics Committee, Department of Experimental Medicine, University of Copenhagen.

Materials

Flavanol monomers (catechin, epicatechin, gallocatechin and epigallocatechin) were purchased from Sigma-Aldrich (Denmark). Plant samples were chosen in order to provide a wide variety of CT structural characteristics and were obtained as follows: cocoa beans were purchased from 'Detox your World' company (Great Yarmouth, UK), hazelnut skins were provided by Dr H. Hoste (INRA Toulouse, France), pine bark (*Pinus sylvestris*) was provided by Dr M. Karonen (University of Turku, Finland), whole sainfoin (*Onobrychis viciifolia*, var. Esparsette) plants were provided by Mr P.
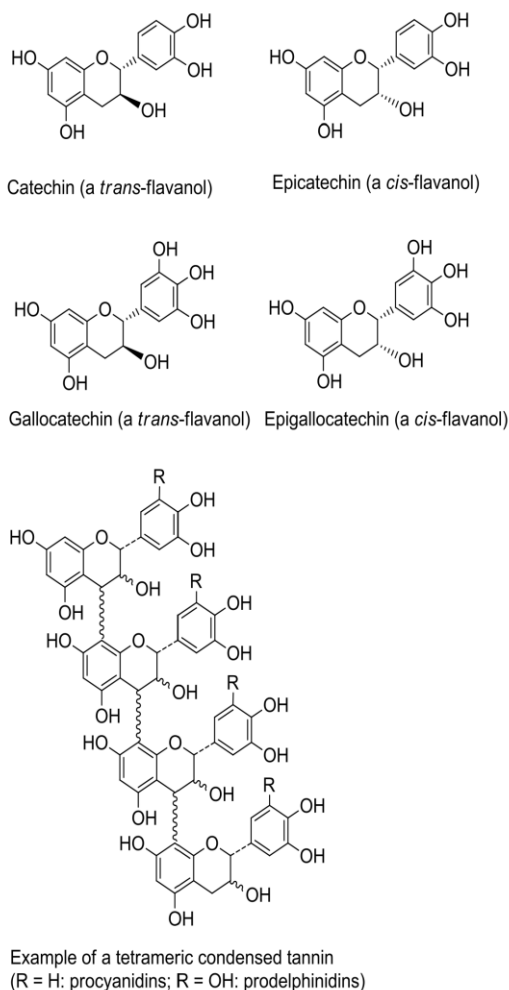

Catechin (a *trans*-flavanol)   Epicatechin (a *cis*-flavanol)

Gallocatechin (a *trans*-flavanol) Epigallocatechin (a *cis*-flavanol)

Example of a tetrameric condensed tannin
(R = H: procyanidins; R = OH: prodelphinidins)

Figure 1. Structures of flavanol monomeric subunits and an example of a tetrameric condensed tannin.
doi:10.1371/journal.pone.0097053.g001

Davy (Barham, Kent, UK), leaves from blackcurrant (*Ribes nigrum*) and redcurrant (*Ribes rubrum*) bushes were collected from Hildred's Pick-Your-Own Farm (Goring-upon-Thames, UK), and white clover (*Trifolium repens*) flowers from NIAB (Cambridge, UK).

Extraction and Fractionation of Tannins from Plants

The freeze-dried, ground cocoa beans (125 g) were defatted three times with hexane (600 mL) at room temperature for 30 min; the extract was filtered and hexane discarded. The defatted powder was air dried for 3 to 4 hours and kept at room temperature. All plant samples (50 g) were treated with acetone/water (7:3; v/v) to extract tannins [24]. Solutions were concentrated and aqueous extracts were freeze-dried. Portions of the freeze-dried extracts were dissolved in water and loaded onto a Sephadex-LH20 column. The column was rinsed with water, low molecular weight tannins were eluted with acetone/water (3:7; v/v; Fraction 1) and higher molecular weight tannins with acetone/water (1:1; v/v; Fraction 2).

Table 1. Chemical analysis of acetone/water extracts.

Sample	CT (g/100 g extract)	PC : PD ratio	mDP	*cis* : *trans* ratio
Sainfoin	12.8	25.3:74.7	5.5	80.2:19.8
Cocoa beans	13.0	100.0:0.0	2.9	96.0:4.0
Pine bark	50.8	64.2:35.8	2.5	79.6: 20.4
Hazelnut skin	73.8	79.5:20.5	9.6	49.8:50.2
Blackcurrant leaves	29.3	5.8: 94.2	5.4	9.1:90.9
Redcurrant leaves	24.5	6.0: 94.0	9.8	77.3:22.7
White clover flowers	33.8	0.8: 99.2	4.4	65.7:34.3

CT = condensed tannins, PC = procyanidin, PD = prodelphinidin, mDP = mean degree of polymerization.
doi:10.1371/journal.pone.0097053.t001

Tannin Analysis by HPLC

Tannins in extracts and fractions (except for cocoa beans – see below) were characterized by thiolytic degradation according to Gea *et al.* [24] with slight modification of the HPLC analysis. Samples (20 μL) were injected into the Gilson HPLC system connected to an ACE C18 column (3 μm; 250×4.6 mm; Hichrom Ltd; Theale; UK) fitted with a corresponding ACE guard column kept at room temperature. The flow rate was 0.75 mL min^{-1} using 1% acetic acid in water (solvent A) and HPLC-grade acetonitrile (solvent B). The following gradient programme was employed: 0–35 min, 36% B; 35–40 min, 36–50% B; 40–45 min, 50–100% B; 45–50 min, 100–0% B; 50–55 min, 0% B. HPLC-analysis provides information on percentage of flavanols (catechin, epicatechin, gallocatechin and epigallocatechin) in terminal and extension units, tannin content, mean degree of polymerization (mDP) or average polymer size, percentage of prodelphinidin and procyanidin tannins and percentage of *cis*- and *trans*-flavanol units in tannins [24] (see also Figure S1).

Cocoa bean tannins were characterised by liquid chromatography-mass spectrometry (LC-MS). Terminal and extension units after thiolysis were identified on a HPLC Agilent 1100 series system consisting of a G1379A degasser, G1312A binary pump, a G1313A ALS autoinjector, a G1314A VWD UV detector and a G1316A column oven and API-ES instrument Hewlett Packard 1100 MSD Series (Agilent Technologies, Waldbronn, Germany) using an ACE C18 column (3 μm; 250×4.6 mm; Hichrom Ltd; Theale; UK) fitted with ACE guard column at room temperature. Data were acquired with ChemStation software (version A 10.01 Rev. B.01.03). The injection volume was set to 20 μL and flow rate to 0.75 mL/min. The sample was eluted using a gradient of 1% acetic acid in MilliQ H$_2$O (solvent A) and HPLC-grade acetonitrile (solvent B) as follows: 0–35 min, 36% B; 35–40 min, 36–50% B; 40–45 min, 50–100% B, which was followed by 45–55 min, 100–0% B; 55–60 min, 0% B. UV-vis spectra were recorded at 280 nm. MS spectra recorded in the negative ionisation scan mode between m/z 100 and 1000 used the following conditions: 3000 V for capillary voltage, nebuliser gas pressure at 35 psig, drying gas at 12 mL/min and dry heater temperature at 350°C. MS spectra recorded in the positive ionization scan were with the same parameters as for negative but the capillary voltage was 3000 V. Terminal and extension units were identified by their retention times and molecular masses.

Parasites

To obtain viable third-stage larvae (L3), gravid *A. suum* female worms were collected from the intestine of pigs at a local slaughterhouse (Danish Crown, Ringsted, Denmark). Eggs were isolated from the uteri of worms and embryonated for at least two months at room temperature as previously described [25]. The eggs were decoated (removing the outer proteinaceous shell) using NaOH and then stored at 4°C in 1 M H$_2$SO$_4$. For hatching, eggs were washed thoroughly with 0.9% NaCl to remove the sulphuric acid, and *in vitro* hatching was then achieved by using a method modified from that of Han *et al.* [26]. 1.25 mL of egg solution (5 eggs/μL) was added to 5 mL of 0.9% NaCl and 300 μL of pig bile in a tissue culture flask. The flasks were then incubated overnight on a plate shaker (120 rpm) in an environment of 37°C and 100% CO$_2$. The next day, hatched L3 were separated from un-hatched eggs and debris by migration through a 20 μm sieve. The larvae were then suspended in RPMI 1640 media (Gibco) containing HEPES, L-glutamine and 100 μg/U/mL of penicillin/streptomycin and used in the L3 migration inhibition assay (see below).

Fourth-stage larvae (L4) were obtained by infecting two eight-week old pigs each with 10,000 embryonated *A. suum* eggs using a stomach tube. Animals were monitored daily – no clinical signs of ascariosis or any other signs of ill-health were observed. 12 after infection, the pigs were killed by captive bolt pistol and exsanguination, and the entire small intestine was removed, opened and the contents collected. The intestine was thoroughly washed with water, and the contents and washings were then combined and added to an equal amount of 2% agar at 50°C as described previously [27]. Larvae were recovered by migration from the agar into warm saline for 2 hours at 37°C. Larvae were then further cleaned by active migration through three layers of gauze into warm saline. The larvae were transferred to 50 mL centrifuge tubes and thoroughly washed by repeated sedimentation, first in warm saline and then in warm, sterile culture media (RPMI 1640 containing HEPES, L-glutamine, 100 μg/U/mL of penicillin/streptomycin and 0.2 μg/mL amphorectin B). After 90 minutes incubation at 37°C, the larvae were washed a further five times in culture media and then used in the L4 motility inhibition assay (see below).

Migration Inhibition Assay with Newly Hatched Larvae

The migration inhibition assay was based on the method described by Han *et al.* [26] with some modifications. Extracts and tannin fractions were dissolved in culture media at appropriate concentrations and then 500 μL added to triplicate wells on a 48-well tissue culture plate. Negative and positive controls consisted of media only and 50 μg/mL ivermectin, respectively. 100 larvae were then added to each well and the plate incubated for 16 hours at 37°C in an atmosphere of 5% CO$_2$. The motility of larvae was then scored by a single observer on a 0–5 scale outlined by Stepek *et al.* [28], where 5 is fully motile (i.e. identical to the motility at the
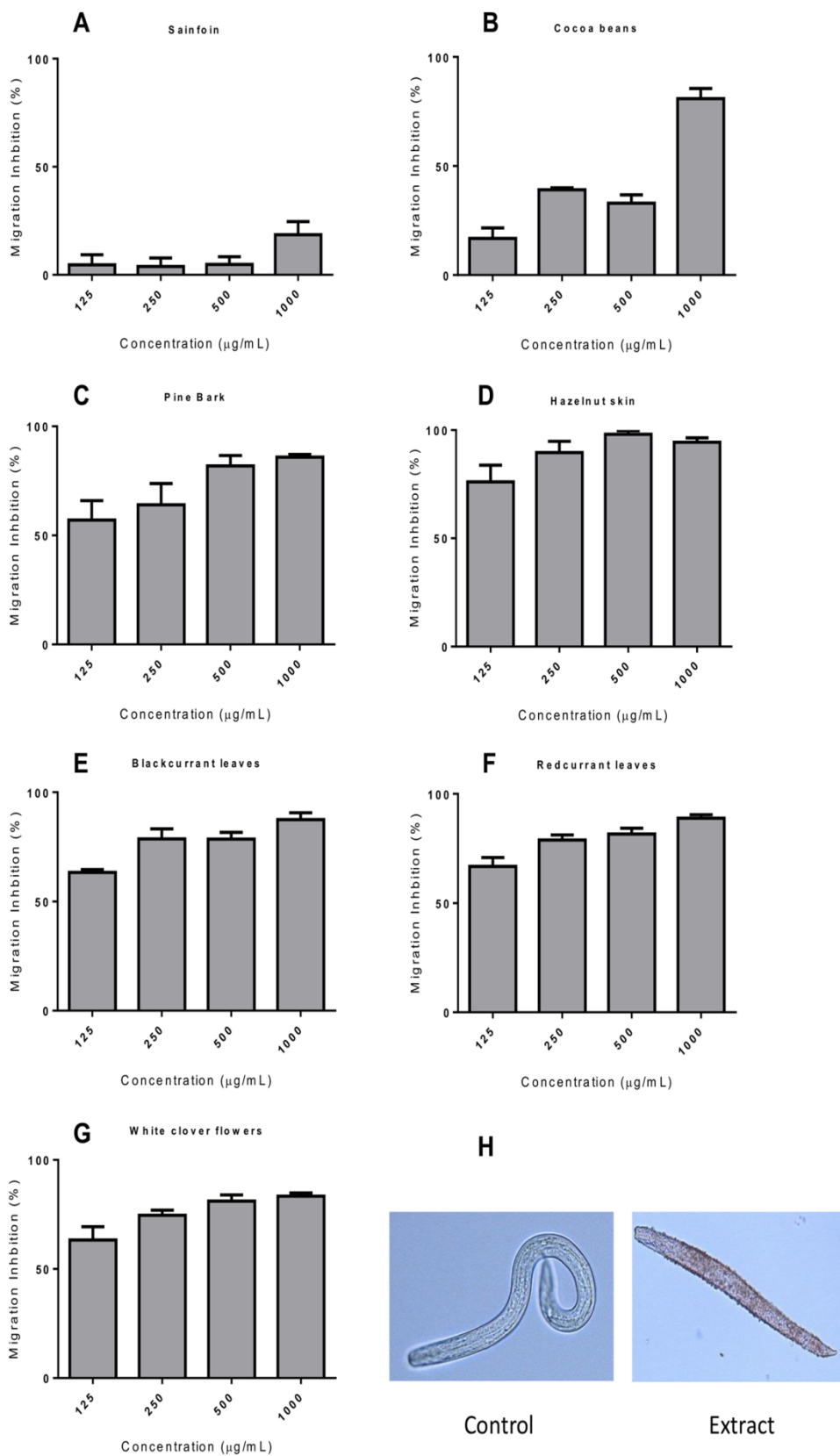
297

A Sainfoin

B Cocoa beans

C Pine Bark

D Hazelnut skin

E Blackcurrant leaves

F Redcurrant leaves

G White clover flowers

H Control   Extract

Figure 2. Inhibition of *Ascaris suum* L3 migration by acetone/water extracts of tannin-containing plants. Panel A–G - Percentage inhibition of migratory activity (MIA) in *Ascaris suum* L3 after 16 hours exposure to tannin-containing acetone/water extracts from **A)** sainfoin, **B)** cocoa beans, **C)** pine bark, **D)** hazelnut skins, **E)** blackcurrant leaves, **F)** redcurrant leaves and, **G)** white clover flowers. MIA is expressed relative to larvae exposed only to culture medium. Data presented are the mean of two independent experiments, each performed in triplicate. Error bars represent SEM of the individual replicates. **Panel H** – Light microscopy of *A. suum* larvae after migration following incubation in media only, or after migration following incubation in 1 mg/mL of tannin-containing acetone/water extract from pine bark (magnification = x200).
doi:10.1371/journal.pone.0097053.g002

start of the incubation period) and 0 is completely motionless. Then, 500 µL of 1.6% agar solution at 45°C was added to each well, immediately mixed, and then 500 µL of this mixture was transferred to the corresponding well on another 48-well plate (i.e. two wells for each original triplicate well, each of final volume of 500 µL, 0.8% agar). The agar was allowed to set, and then culture medium was added on top of the gel and the plates placed back in the incubator overnight. Larvae that migrated to the media on the surface of the gel were counted by light microscopy. Numbers from both wells were summed. Larvae began to migrate out of the gel almost immediately and migration was generally complete after around 4 hours – no further migration was observed during the following 24 hours, and the numbers of larvae in the media did not decrease, indicating that larvae remained in the media on the surface of the gel and did not migrate back into the agar. Therefore, the numbers of larvae migrating from the gel was routinely assessed after 16–18 hours (overnight).

Percentage inhibition of migration was calculated relative to the negative control using the formula:

$$100 - \left(\frac{\text{number of larvae migrated in test well}}{\text{number of larvae migrated in control wells}} \right) * 100$$
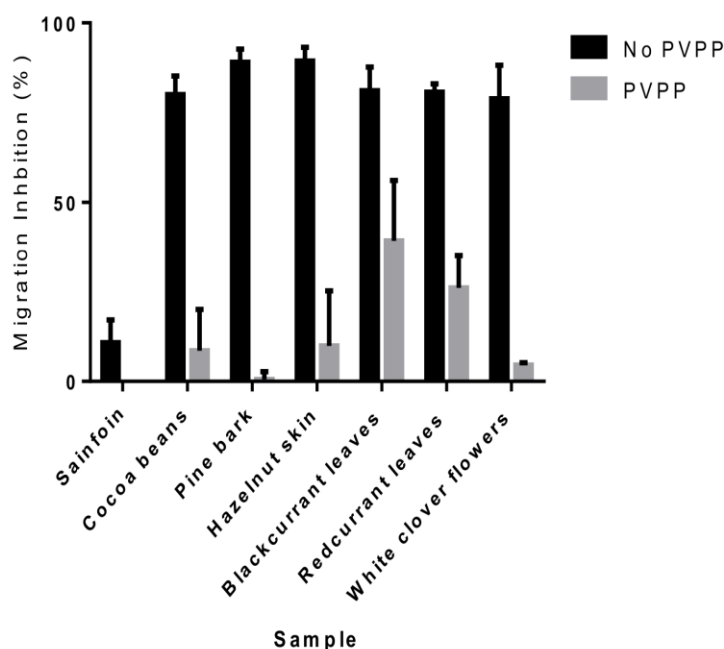
To quantify whether the presence of CT in the media influenced the agar migration assay, in some experiments larvae were washed with RPMI 1640 after the incubation period to remove tannins from the media before the addition of agar – this was done by centrifugation three times for 3 minutes each at 500 g.

Polyvinylpolypyrrolidone (PVPP) Treatment

PVPP was used to selectively remove tannins from the dissolved extracts. Extracts were dissolved at a concentration of 1 mg/mL before the addition of 50 mg/mL PVPP (Sigma-Aldrich) in a plastic tube. Tubes were incubated overnight at 4°C and precipitated tannins removed by centrifugation at 3000 g for ten minutes. The supernatant was used in the assays. Controls consisted of 1) dissolved extract without PVPP and 2) media alone with 50 mg/mL PVPP. These were incubated overnight in an identical fashion and assayed alongside the PVPP-treated extracts.

L4 Motility Inhibition Assay

To assess the anthelmintic effects of the tannins against L4 stage parasites, we used a motility inhibition assay similar to that recently described [29,30]. Five worms were placed into triplicate wells of a 48 well plate with culture media containing either a

Figure 3. Effect of PVPP treatment on anthelmintic activity of tannin-containing plant extracts. Percentage inhibition of migratory activity (MIA) in *Ascaris suum* L3 after 16 hours exposure to tannin-containing acetone/water extracts from sainfoin, cocoa beans, pine bark, hazelnut skins, blackcurrant leaves, redcurrant leaves and white clover flowers, or the same extracts after pre-incubation with PVPP (see materials and methods). MIA is expressed relative to larvae exposed only to culture medium (no PVPP), or culture medium pre-incubated with PVPP (PVPP). Data presented is the mean of two independent experiments, each performed in triplicate. Error bars represent SEM of the individual replicates.
doi:10.1371/journal.pone.0097053.g003

Table 2. Chemical analysis of fractionated tannins.

Sample		CT (g/100 g fraction)	PC : PD ratio	mDP	*cis* : *trans* ratio
Sainfoin	F1	37.8	28.0: 72.0	2.7	66.7:33.3
	F2	100.0	35.2:64.8	8.7	79.2:20.8
Cocoa beans	F1	58.5	100.0:0.0	2.3	91.3: 8.7
	F2	75.5	100.0:0.0	5.4	96.3: 3.7
Pine bark	F1	56.5	84.9:15.1	2.3	48.1: 51.9
	F2	83.8	88.8:11.2	6.6	78.1: 21.9
Hazelnut skin	F1	51.3	81.7: 18.3	4.6	41.0: 59.0
	F2	70.3	79.1:20.9	9.1	47.8: 52.2
Blackcurrant leaves	F1	59.9	6.3: 93.7	2.5	12.8: 87.2
	F2	100.0	5.5:94.5	6.5	7.0:93.0
Redcurrant leaves	F1	58.1	14.2:85.8	4.9	44.4: 55.6
	F2	68.5	9.7:90.3	10.0	64.4:35.6
White clover flowers	F2	100.0	1.3:98.7	8.6	58.9: 41.1

Plant extracts were fractionated on Spehadex-LH20 columns yielding fraction 1 (F1) and fraction 2 (F2). CT = condensed tannins, PC = procyanidin, PD = prodelphinidin, mDP = mean degree of polymerization.
doi:10.1371/journal.pone.0097053.t002

range of tannin concentrations, 100 µg/mL of either ivermectin or levamisole (positive control), or culture media only (negative control). The plates were then incubated at 37°C in an atmosphere of 5% CO_2 in air. At 12-hour intervals the motility of the worms was scored using the above-mentioned 0–5 scale. Larvae that scored 0 on two consecutive time-points were considered dead. Dead larvae were removed and fixed for electron microscopy (see below). Control larvae were fixed at the same time for comparison.

Transmission Electron Microscopy

Worms were washed thoroughly with PBS before fixation in 2% glutaraldehyde in 0.05 M phosphate buffer. The samples were then postfixed, firstly in 1% OsO_4 and 0.05 M K_3FeCN_6 in 0.12 M cacodylate buffer for 2 hours at RT, followed by 1% uranyl acetate for 1 hour at RT. The samples were then dehydrated in an ethanol gradient, infiltrated with epon/propyleneoxide and embedded in 100% expoxy resin and polymerized at 60°C overnight. Samples were then sectioned at 70 nm and stained with uranyl acetate and lead citrate before viewing under a Phillips CM100 transmission electron microscope. Images were obtained with a Olympus Veleta Camera and processed using ITEM software.

Data Analysis and Statistics

The concentration of tannins in the F1 and F2 fractions needed to induce 50% migration inhibition activity (MIA EC_{50}) was estimated by non-linear least squares regression. For each fraction, a variable-slope dose response curve was fitted, with the top of the curve constrained to 100% MIA and the bottom to 0% MIA. Differences between the EC_{50} of the F1 and F2 fractions from the same sample were assessed by extra sum-of-squares F-test, assuming a null hypothesis of equal EC_{50}. The effect of PVPP treatment and individual monomers was assessed on arcsine-transformed MIA data using two-way ANOVA with Bonferroni post-hoc testing. Multiple regression was used to investigate associations between MIA EC_{50} values of the F2 tannin fractions and structural characteristics of the tannin molecules (mDP, % monomeric units and % *cis* isomerism). Graphpad Prism 6 was used for all analyses except for the multiple regression, for which

SPSS 20.0 was used. *P* values of <0.05 were considered significant.

Results

Extracts from Plants Containing Condensed Tannins have Anthelmintic Activity against Ascaris Suum

As a series of contrasting condensed tannins (CT) that differ in polymer size and procyanidin/prodelphinidin proportions cannot be obtained commercially, we extracted tannins from seven common plant sources known to contain different CT types. The extracted tannins were subjected to thiolytic degradation, analysed by HPLC and shown to contain varying amounts of CT of differing flavanol composition (Table S1). From these data, the mean degrees of polymerisation (mDP), PC/PD and *cis/trans* ratios were calculated and are summarised in Table 1. To ascertain whether these extracts had activity against *A. suum*, we hatched fully embryonated eggs *in vitro* to obtain viable, infective L3. Larvae were then incubated either in culture media alone or with one of the seven extracts at each of four concentrations ranging from 1 mg/mL to 125 µg/mL. After 16 hours, the larvae incubated in media alone were still fully motile (Figure S2). Incubation with the extracts at concentrations of ≥500 µg/mL reduced motility compared to the negative control, with the exception of sainfoin, where no obvious differences in motility were observed (Figure S2). Notably, at high concentrations (≥ 500 µg/mL) of all extracts except sainfoin, some dead larvae were observed (up to 15–20% in some extracts at 1 mg/mL). In contrast, dead larvae were never observed in the control group. Thus, it appears that these tannin-containing extracts have anthelmintic activity against *A. suum*.

After ingestion of eggs and hatching *in vivo*, *A. suum* L3 must then undergo a migratory phase which consists of migration through the intestinal wall and through to the liver to the lungs, before they return to the small intestine. Therefore, we also investigated whether the migratory ability of *A. suum* L3 was impaired after incubation with the extracts by using an agar migration inhibition assay. In the negative control wells, a mean of 67% of larvae (SEM ±7.2, range 58–82) of larvae were able to migrate out of the agar gel, and this migration was inhibited by a
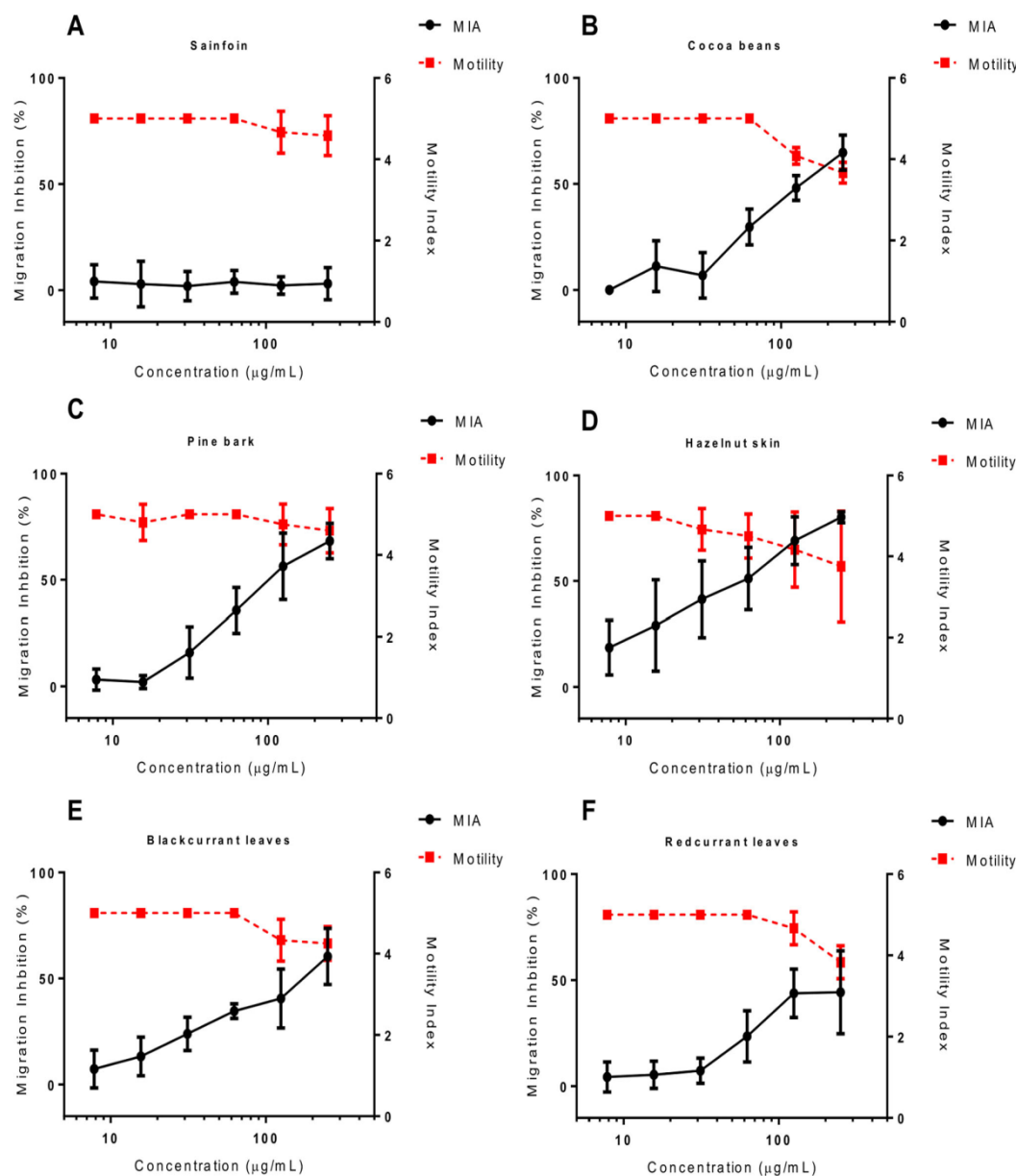
300

Figure 4. Inhibition of *Ascaris suum* L3 motility and migration by condensed tannin fractions (F1). Percentage inhibition of migratory activity (MIA - solid black line, plotted on left Y axis) and motility (dashed red line, plotted on right Y axis) in *Ascaris suum* L3 after 16 hours exposure to tannin fractions (F1) from **A)** sainfoin, **B)** cocoa beans, **C)** pine bark, **D)** hazelnut skins, **E)** blackcurrant leaves and **F)** redcurrant leaves. MIA is expressed relative to larvae exposed only to culture medium. Motility is scored on a 0–5 scale where 5 is completely motile and 0 is completely still (see materials and methods). Data points represent the mean of two independent experiments, each performed in triplicate. Error bars represent SEM of the individual replicates.
doi:10.1371/journal.pone.0097053.g004

mean of 86% (SEM ±4.4, range 73–99) by addition of 50 μg/mL ivermectin to the media at the start of the incubation period. We observed potent, dose-dependent MIA in larvae exposed to six out of seven extracts – in agreement with the motility data, larvae exposed to sainfoin did not have significantly reduced migration (Figure 2). The MIA was similar whether the agar was added directly to the wells containing media and tannin extracts after the overnight incubation, or whether the incubated larvae were first washed and then re-suspended in fresh media without tannins

before the addition of agar (Figure S3), indicating that the MIA was mediated by direct effects of the extracts on the larvae during the incubation period, and not by non-specific inhibition caused by interactions between tannins and agar influencing the composition and penetrability of the agar gel. Moreover, larvae that did migrate from the gel after incubation in tannin-containing extracts appeared sluggish and were often dead at high concentrations of extract (Figure 2H), indicating that they had died after migrating but before subsequent observation by microscopy.
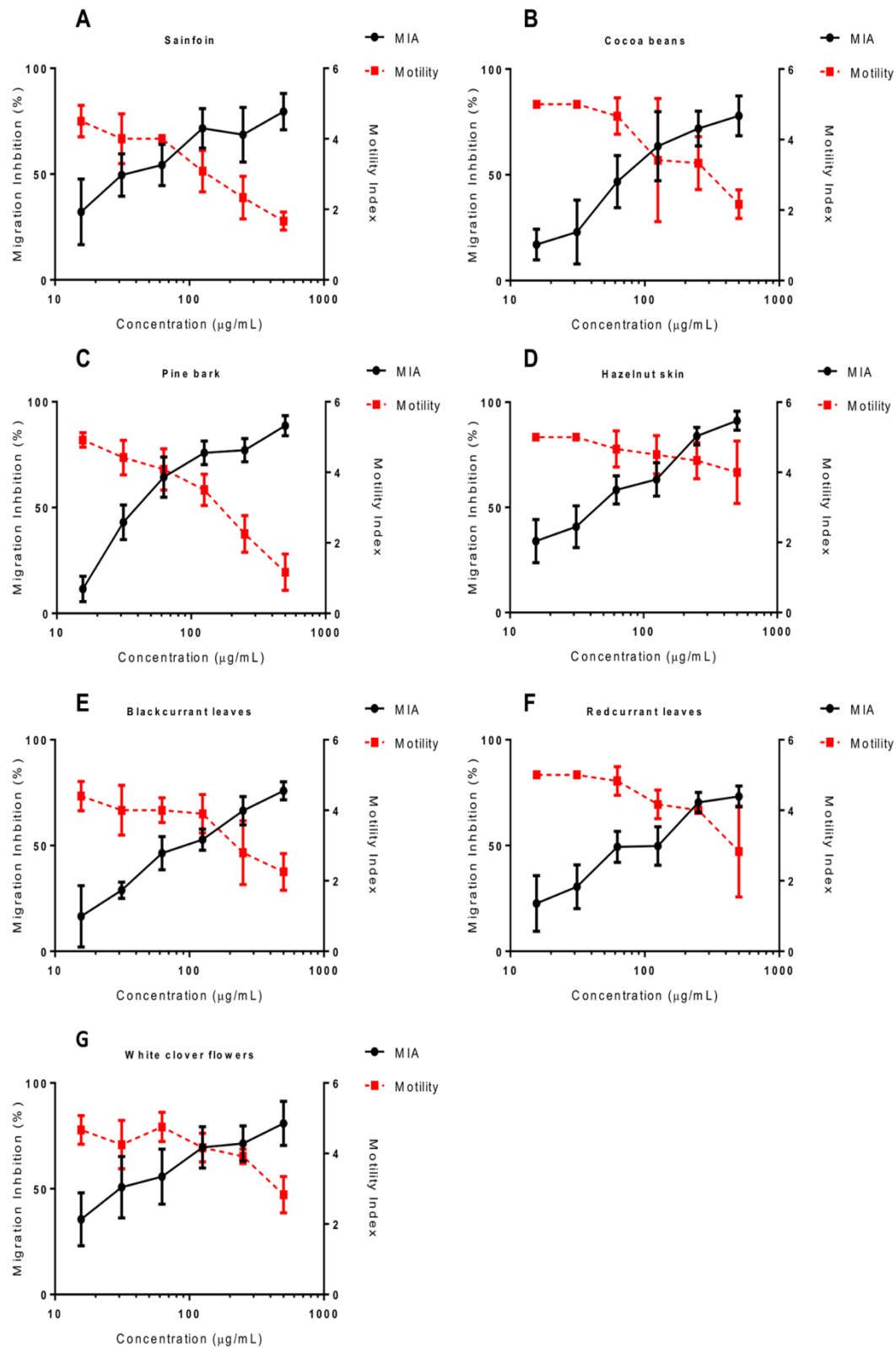
Figure 5. Inhibition of *Ascaris suum* L3 motility and migration by condensed tannin fractions (F2). Percentage inhibition of migratory activity (MIA - solid black line, plotted on left Y axis) and motility (dashed red line, plotted on right Y axis) in *Ascaris suum* L3 after 16 hours exposure to tannin fractions (F2) from **A)** sainfoin, **B)** cocoa beans, **C)** pine bark, **D)** hazelnut skins, **E)** blackcurrant leaves, **F)** redcurrant leaves and **G)** white

Altogether, these data suggest that extracts of plants containing high amounts of CT have direct anthelmintic activity against *A. suum*.

Condensed Tannins are Mainly Responsible for Anthelmintic Activity against *A. suum*

We noted that the extracts that had the most potent activity against *A. suum* were those extracts that had the highest levels of CT. For example, the extract from hazelnut skin contained 70% CT, whereas the extracts that exhibited the least activity (cocoa and sainfoin) had the lowest percentage of CT (Table 1 and Figure 2). This suggests that CT are the active compounds responsible for the observed anthelmintic activity. To confirm this, we pre-treated the extracts with PVPP, which selectively binds and precipitate tannins [31]. With the exception of sainfoin, where only minimal MIA was observed, pre-treatment with PVPP significantly reduced the anthelmintic effect in all of the extracts ($P<0.001$ by two-way ANOVA; Figure 3), although with different levels of entirety. PVPP treatment almost completely abolished the effect in extracts of cocoa beans, pine bark, hazelnut skin and white clover flowers, however this reduction was less apparent in extracts from redcurrant and blackcurrant leaves, indicating that either removal of tannins by PVPP was incomplete in these cases or there are small amounts of other, unidentified bioactive substances in these extracts. Overall, these results strongly suggest that CT are mainly responsible for the observed anthelmintic effects.

Fractionation of Extracts and Further Purification of Condensed Tannins

To further confirm the role of CT in the anthelmintic effects, and to gain insight into the relationship between tannin structure and activity, we fractionated and purified the extracts to yield two tannin fractions. The first fraction (F1) yielded oligomeric tannins (mDP of 2 to 4) with around 50% CT content, whereas the second fraction (F2) contained mainly oligomers and polymers of higher molecular weight tannins (mDP>6) and close to 100% CT content (Table 2).

We then assessed the motility and MIA in larvae exposed to varying concentrations of these fractions. To allow comparison of different tannin samples, the concentrations of the fractions were adjusted in the assay so that all F1 samples contained the same amount of CT (final concentrations ranging from 250 to 7.8 µg/mL), and similarly the F2 samples were adjusted so that all contained CT of concentrations ranging from 500 to 15.6 µg/mL. Similar to the previous results with the crude acetone/water extract, the F1 fraction of sainfoin did not show any anthelmintic activity (Figure 4A). However, F1 fractions from cocoa, hazelnut skin, pine bark and blackcurrant and redcurrant leaves all showed a modest effect on larval motility, and a more pronounced effect on MIA (Figure 4B–F). EC_{50} values were calculated for MIA, with CT from pine bark and hazelnut skin being the most potent (Table 3). The F2 fractions showed more potent anthelmintic activity, with a stronger effect on larval motility and MIA (Figure 5). Interestingly, F2 fractions from sainfoin (which had shown no anthelmintic activity when tested either as a crude acetone/water extract or a low molecular weight F1 fraction), were now highly active with potent effects on both larval motility

and migratory ability (Figure 5A). EC_{50} values for MIA were (with the exception of hazelnut skin, where values were similar between fractions) significantly lower for the F2 samples than for the corresponding F1 fraction (Table 3; $P<0.01$ by extra sum-of-squares F-test), indicating that CT from the second fraction were more effective at inhibiting the migration of *A. suum* than an equivalent concentration of CT from the first fraction. This suggests that the polymer size of the tannin molecules is an important factor in determining their anthelmintic activity, with a higher degree of polymerization increasing the efficacy. However, within F2 fractions from different plant sources there was no effect of mDP on MIA EC_{50}, nor was there any effect of the PC/PD or the *cis/trans* ratios ($P>0.1$ by multiple regression).

Flavanol Monomers of Prodelphinidins have Higher Larval Migratory Inhibitory Activity than Monomers of Procyanidins

Previous studies of the effects of CT on ruminant nematodes have shown that the ratio of prodelphinidins (PD) to procyanidins (PC) in the CT polymer and their corresponding flavanol monomers influence the anthelmintic activity, with a high percentage of PD thought to increase the potency of anthelmintic effects [22,32]. However, multiple regression analysis of our current data with purified F2 fractions showed no correlation between the % of PD units and MIA EC_{50} with L3. The multitude of different tannin molecules, which are present even in purified fractions, may make it difficult to identify structural characteristics that influence activity. Therefore, we also tested commercially available flavanol monomers (catechin (C), epicatechin (EC), gallocatechin (GC) and epigallocatechin (EGC)) to address whether PD/PC ratio and also *cis/trans* ratio may be important in the observed anthelmintic effects. We observed that GC and EGC, which occur in prodelphinidins, both reduced motility of newly hatched L3 (Figure S4), and also markedly inhibited L3 migration at concentrations of 500 and 250 µg/mL (Figure 6). In contrast, larval motility was not significantly reduced by incubation with C or EC, which occur in procyanidins, and the percentage of MIA was lower than for the corresponding GC and EGC flavanols (Figure S4 and Figure 6). Analysis of variance revealed that MIA was significantly different between the GC and C monomers ($P<0.01$ by two-way ANOVA), however the difference between EGC and EC did not reach significance, nor was there any significant effect of *cis/trans* stereochemistry. These data suggest that the presence of an extra hydroxyl group in the B-ring of the flavanols increases the anthelmintic activity, and are in agreement with previous studies that investigated the anthelmintic effects of these flavanols against *H. contortus* [22,32]. However, our results with purified mixtures of CT oligomers and polymers appear to indicate that, in these cases, the PD/PC ratio is less important or is masked by other factors.

Condensed Tannins also have Anthelmintic Activity against Ascaris Suum Fourth-stage Larvae

Whilst the L3 migration assay provides a convenient means by which to screen for anthelmintic activity, it is perhaps more relevant to the *in vivo* situation to examine effects against the L4 stage of the parasite. After the L3 have migrated through the liver to the lungs, they are coughed up and return to the small intestine

Table 3. *Ascaris suum* L3 migratory inhibition activity EC_{50} values.

Sample	Sainfoin	Cocoa beans	Pine bark	Hazelnut skin	Blackcurrant leaves	Redcurrant leaves	White clover flowers
Fraction 1	NC	141.3	114.8	49.6	162.0	247.9	ND
Fraction 2	41.9	86.0	48.2	43.8	98.4	91.8	37.4

Inhibition of migration was assessed in L3 exposed to purified tannins extracted from sainfoin, cocoa beans, pine bark, hazelnut skin, blackcurrant leaves, redcurrant leaves and white clover flowers. ND = not done. NC = not calculated. For all samples except hazelnut skins, the EC_{50} values are significantly lower for the F2 fraction compared to the F1 fraction ($P<0.01$ by extra sum-of-squares F-test).

doi:10.1371/journal.pone.0097053.t003

around 8 days post-infection (p.i.), and at around day 10 p.i. they moult to the L4 stage [33]. The parasite then resides in the small intestine up until adulthood and for the remainder of its lifespan, and is thus exposed for long periods to compounds present in the host digesta. Thus, it may be this post-migration stage of the parasite life-cycle that is most susceptible to anthelmintic dietary compounds. Therefore, we also examined the effects of acetone/water extracts and corresponding F2 CT fractions from sainfoin, cocoa beans, pine bark, hazelnut skin, blackcurrant leaves and white clover flowers on the motility and survival of *A. suum* L4 compared to culture media with no tannins.

Parasites were recovered from pigs 12 days p.i., with >80% of the recovered larvae determined to be L4 by morphological examination [33], with the remainder being late L3. Larvae incubated in media alone remained fully motile over the course of the 60 hours of incubation. In contrast, larvae exposed to either ivermectin or levamisole had a significant reduction in motility within 12 hours, which persisted to the end of the experiment (Figure SF5). Larvae exposed to the sainfoin acetone/water extract did not show significantly reduced motility at any concentration tested, consistent with the poor anthelmintic activity observed in the previous assays (Figure 7A). In contrast, larvae exposed to the acetone/water extracts from the other five plant sources all had lower motility than controls, with an almost total cessation of movement at concentrations of ≥1 mg/mL by the end of the experiment (Figure 7B–F). Results with the F2 fractions confirmed the anthelmintic effects. Larvae exposed to all tested fractions exhibited a rapid reduction in motility (Figure 8), most notably in the prodelphinidin-rich white clover and blackcurrant leaf fractions where larvae exposed to either 1000 or 333 µg/mL of CT exhibited almost a total loss of movement within 12–24 hours (Figure 8E–F). In all tested fractions, all larvae exposed to 1 mg/mL of tannins were dead by the end of the experiment, and reductions in motility were also observed in the lowest concentration of 111 µg/mL (Figure 8). These results indicate that CT have potent anthelmintic effects against the L4 stage as well as the L3 stage of *A. suum*.

Ultrastructural Changes in Larvae Exposed to Condensed Tannins

Transmission electron microscopy (TEM) was performed to investigate possible direct structural damage to L4 exposed to CT. Larvae recovered from pigs and incubated in 1 mg/mL of CT from hazelnut skin were motionless after 12–24 hours; hence worms from this treatment were selected for analysis by TEM. Thin-sections prepared from larvae after 24 hours of incubation revealed significant structural damage (Figure 9). The cuticle was noticeably swollen and irregular, with marked disorganisation of the basal layer and the underlying hypodermis, compared to control larvae which displayed an intact and regular shaped cuticle (Figure 9A–B). Moreover, massive damage was also observed in the intestine with marked destruction of microvilli in the brush-border and the presence of vacuoles in the gut tissue (Figure 9C–D), confirming direct structural damage to both external and internal tissues of worms exposed to CT.

Discussion

The use of plant compounds such as CT as anthelmintics has received renewed interest due to the on-going threat of parasite resistance to the small number of synthetic drug classes currently available, as well as concerns about drug residues arising from prophylactic use of synthetic drugs in food production systems. Whilst the potential of CT to be used as anthelmintics has been
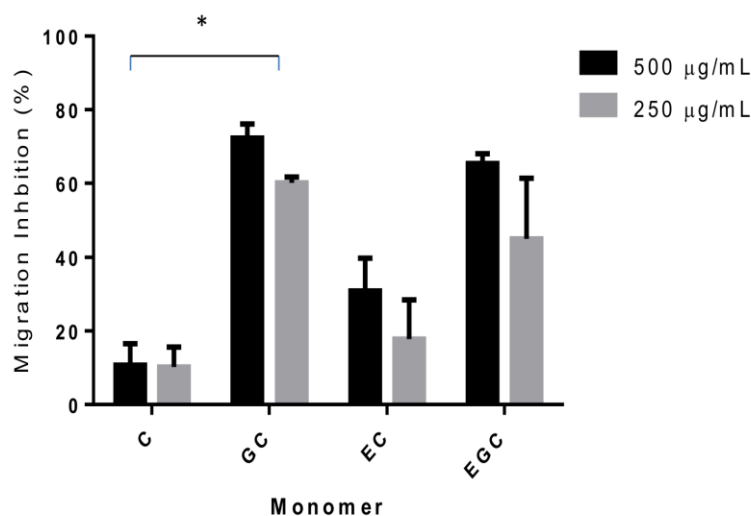
Figure 6. Inhbition of *Ascaris suum* L3 migration by flavanol monomers. Percentage inhibition of migratory activity (MIA) in *Ascaris suum* L3 after 16 hours exposure to flavanol monomers: catechin (C), gallocatechin (GC), epicatechin (EC) and epigallocatechin (EGC). Data points represent the mean of two independent experiments, each performed in triplicate. Error bars represent SEM of the individual replicates. *These values differ significantly (P<0.01, two-way ANOVA with Bonferroni post-hoc testing) at both concentrations (500 and 250 µg/mL).
doi:10.1371/journal.pone.0097053.g006

repeatedly demonstrated in parasites from ruminant livestock, as well as in some rodent models, evidence of direct anthelmintic effects against the pig parasite *A. suum* has been lacking. While some studies have hinted at possible anthelmintic effects [34,35], our results show clearly that multiple larval stages of *A. suum* are susceptible to purified CT derived from a wide variety of plant sources. This provides clear evidence of direct *in vitro* effects against this parasite and encourages further *in vivo* investigation of the use of CT for control of *A. suum* as well as the closely related *A. lumbricoides*.

With the somewhat surprising exception of sainfoin, acetone/water extracts of all the tested plant samples strongly inhibited the migratory ability of newly hatched *A. suum* larvae. Whilst these crude extracts contain other compounds besides CT, pre-treatment with PVPP significantly reduced the anthelmintic effect and abolished it in many cases, strongly implicating CT as the active molecules, a result further confirmed as purified fractions containing near to 100% CT retained potent anthelmintic effects. These results are consistent with studies with other parasitic nematodes such as *H. contortus*, where reduced ability of larvae to migrate has been repeatedly observed after contact with CT. Intestinal-dwelling parasites such as *A. suum* need to retain motility and muscular co-ordination in order to avoid being removed from the gut by peristalsis. Indeed, the mode-of-action of many synthetic drugs such as macrocyclic lactones (e.g. ivermectin) is to remove this motility and co-ordination by activation of glutamate-gated chloride channels [36], resulting in paralysis and removal from the intestine by contractions of normal gut function. Therefore, although the L3 were mostly still alive after overnight incubation with CT, their viability was compromised, as evidenced by their inability to migrate from agar gel. This agar migratory assay is a rather stringent test of the viability of the larvae, as it requires sustained, active migration in a vertical direction and probably resembles the type of environment that larvae may find themselves in *in vivo*, where they have to traverse semi-solid matrices such as mucus and intestinal tissue to begin the hepatic-tracheal migration. Our data suggest that the presence of CT in the digesta will compromise the ability of larvae to undergo

this migration out of the intestine, which takes place in the caecum and upper colon. Moreover, the L4 stage, which is present in the small intestine after this migration and exposed for a lengthy period to the host digesta, was also potently affected by CT with significant larval death occurring in the L4 motility assay. Whilst we did not investigate effects on adult worms in these experiments, other studies with parasitic nematodes have demonstrated a significant reduction in the egg-laying ability of adult females exposed to CT [17]. Overall, these results suggest that CT have anthelmintic activity towards multiple stages of the *Ascaris* life-cycle.

These results should allow rational selection of natural plant extracts that may aid in the treatment and/or prevention of *Ascaris* infections. Whilst the use of plant extracts to treat helminth infections in both pigs and humans is widespread in developing countries, a lack of scientific validation of the active compounds of such plants has hampered the optimisation of these treatment protocols. Condensed tannins are commonly found in plant sources worldwide, and may be administered in several ways. First, livestock may be directly fed whole foodstuffs or forages containing CT. Second, aqueous or alcoholic extracts may be prepared from plant material such as bark or roots and administered as food supplements or in medicinal form. Finally, CT are commonly present in agricultural by-products such as cocoa husks, hazelnut skins or coffee pulp. Such waste products may represent inexpensive sources of CT for many small-holder pig production systems in developing countries. Moreover, the use of CT-containing forages and/or by-products may represent a sustainable method for *A. suum* control in low-input and organic pig farms in developed countries where the routine use of synthetic anthelmintic drugs is not allowed. The use of CT as part of an integrated parasite control program will have the benefit of reducing reliance on the small number of currently available synthetic drugs, slowing the threat of drug-resistant parasites and reducing reliance on expensive drugs, as well as meeting consumer demand for food products produced with minimal input of synthetic antimicrobials.
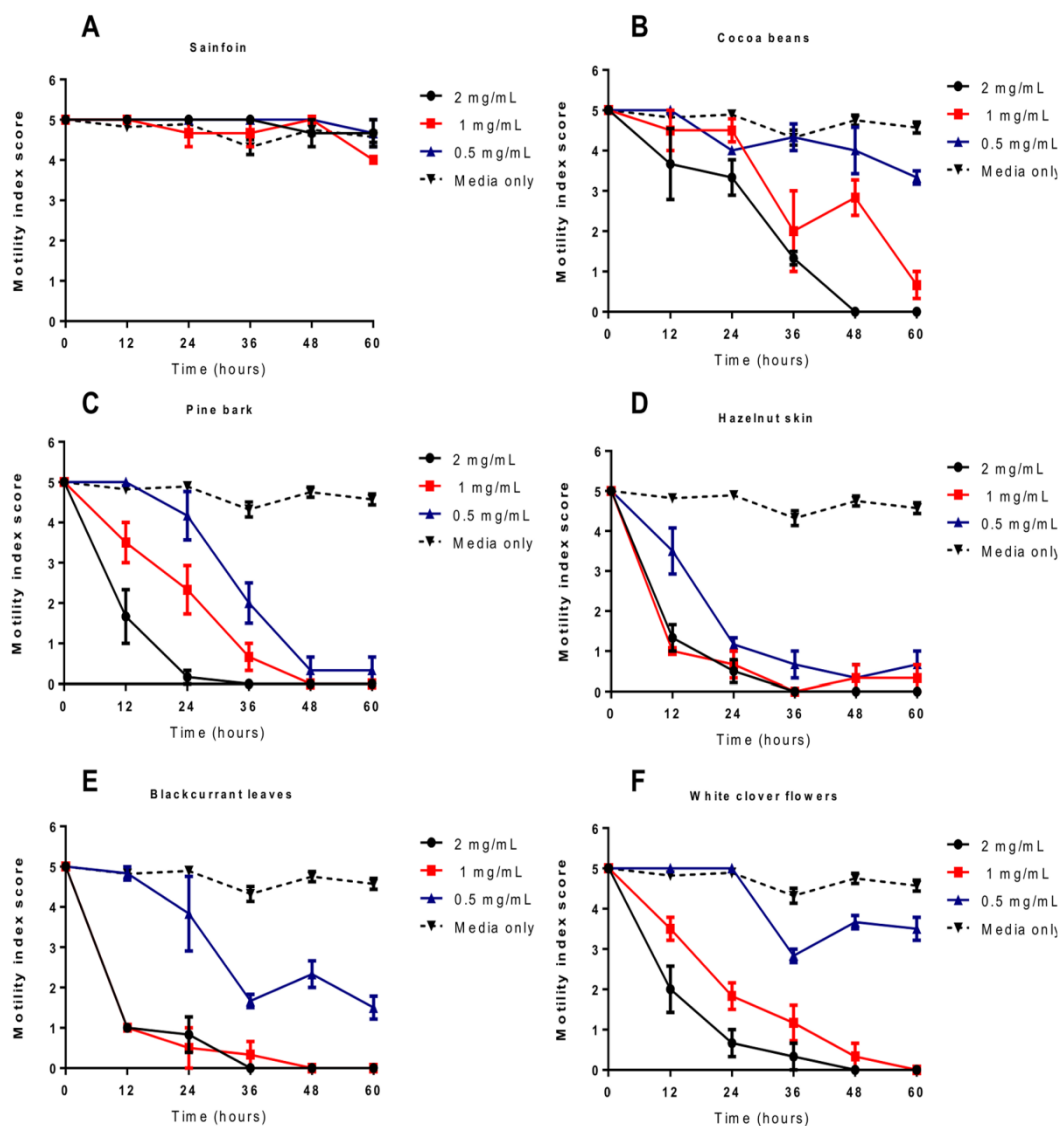
Figure 7. Inhibition of *Ascaris suum* L4 motility by acetone/water extracts of tannin-containing plants. Motility of *Ascaris suum* L4 exposed to tannin-containing acetone/water extracts of **A)** sainfoin, **B)** cocoa beans, **C)** pine bark, **D)** hazelnut skins, **E)** blackcurrant leaves and **F)** white clover flowers. Data points represent the mean of triplicate wells, with the error bars representing the inter-well SEM.
doi:10.1371/journal.pone.0097053.g007

The extrapolation of these *in vitro* results to the *in vivo* situation requires several considerations. Perhaps the most important consideration is what concentration of CT is required to be administered to achieve *in vivo* efficacy. We have, as far as possible, attempted to use concentrations of CT in our *in vitro* assays that represent physiological concentrations that may be expected to be found in the intestine of pigs ingesting CT, although such information in the scientific literature is scant. However, several assumptions can be drawn from studies where humans, pigs and other monogastric animals have consumed diets containing CT. It has been repeatedly shown that the absorption of oligomeric CT from the intestine of monogastrics (including humans and pigs) is poor, with only trace amounts, mainly of monomers or dimers and their metabolites, being detected in the plasma or urine after ingestion. Indeed, much of the orally administered CT can be

recovered from digesta at the terminal ileum, suggesting that there is minimal absorption of CT along the small intestine [12,37–40]. This stability of oligomeric CT through the stomach and proximal part of the small intestine implies that parasites such as *A. suum*, whose L4 and adult stages reside in the small intestine should come into contact with CT at sufficiently high concentrations to exert biological activity, such as has been recently reported for pigs infected with *Escherichia coli*, whereby feeding CT-enriched extracts significantly reduced *E. coli* colonisation of the intestine [41]. Moreover, this poor absorption of CT has generally led them to being considered to have low toxicity; however detrimental effects may be observed in the form of reduced nutrient absorption due to formation of insoluble complexes with CT, as well as the possibility of irritation of the gastrointestinal mucosa at high concentrations [12]. Therefore, it would appear that there is an upper limit to the
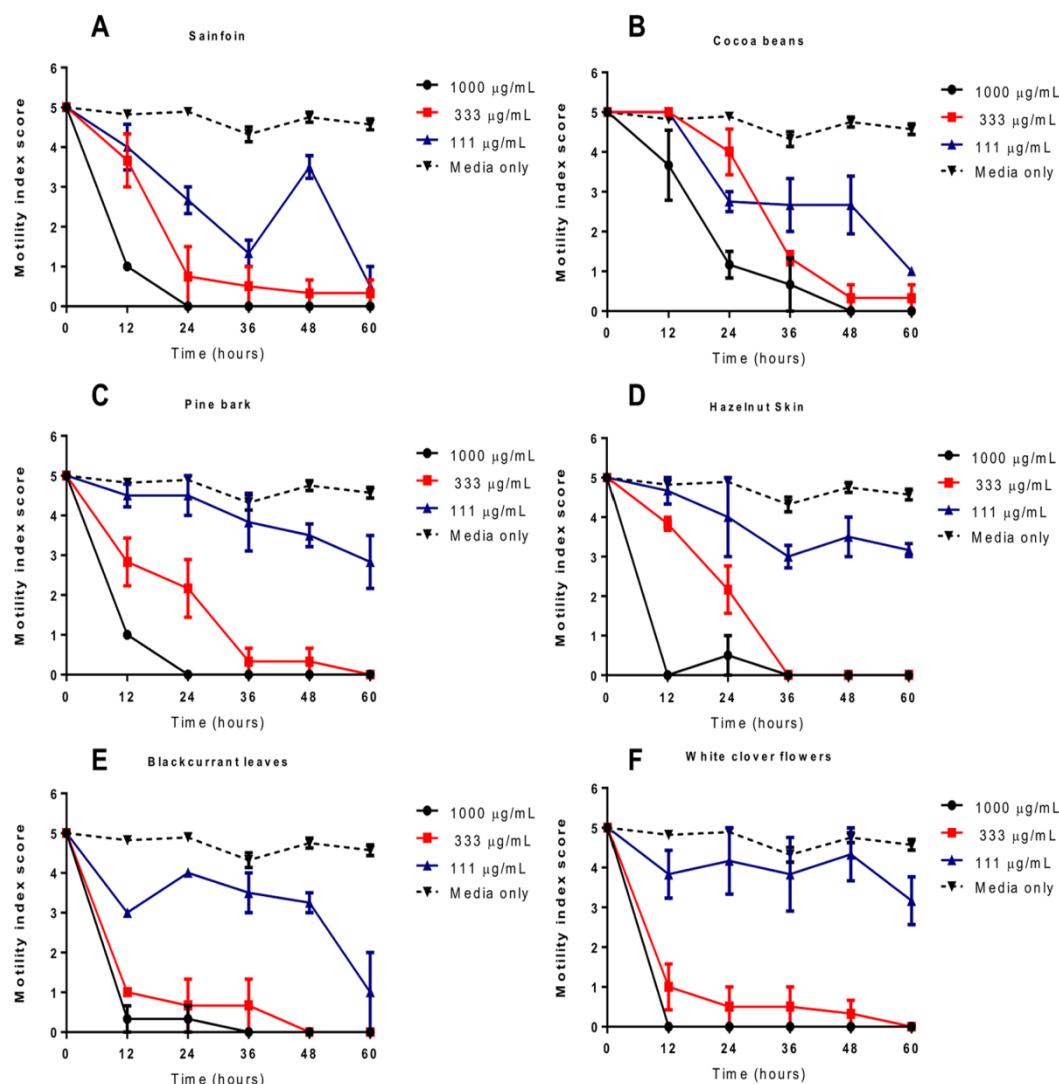
Figure 8. Inhibition of *Ascaris suum* L4 motility by condensed tannin fractions (F2). Motility of *Ascaris suum* L4 exposed to varying concentrations of tannins (F2 fractions) from **A)** sainfoin, **B)** cocoa beans, **C)** pine bark, **D)** hazelnut skins, **E)** blackcurrant leaves and **F)** white clover flowers. Data points represent the mean of triplicate wells, with the error bars representing the inter-well SEM.
doi:10.1371/journal.pone.0097053.g008

amount of CT that can be ingested without side-effects; however it is likely that anthelmintic effects will be manifested at concentrations well below this threshold. In pigs, the volume of the digesta in the small intestine of a growing animal (40–60 kg) is around 5L, depending on age [42]. Thus, to achieve a concentration of 1 mg/mL of CT in the small intestine it will require the animal to ingest around 5 g of CT. As a growing pig most likely eats around 2 kg of food a day, this level of CT represents less than 0.25% of the daily dietary intake. In practice, the ingested amount will need to be higher, in order to compensate for some break-down and decreased bioavailability due to binding to dietary or endogenous proteins and fibres, however it should be still well within the limits of what can be feasibly incorporated into the diet with no adverse effects. Indeed, some *in vivo* verification is already in existence in a monogastric model; burdens of the rodent parasite *Nippostronglyus brasilleinas*, another parasitic nematode which resides in the small intestine, were significantly reduced in rats fed a diet of 4% CT

[18]. Moreover, given that *A. suum* infection may impose a significant penalty on the nutrient economy of the animal [2], the benefits of CT intake may outweigh any possible anti-nutritional effects. Therefore, ingestion of dietary supplements or extracts containing CT should feasibly exert *in vivo* anthelmintic activity, although further experiments are required to substantiate this, which forms part of on-going work in our laboratory.

The lack of effect with the acetone/water extract or F1 fraction of sainfoin, despite potent anthelmintic activity with the F2 fraction is not easily explained. The most logical postulate is that impurities in the extract and F1 fraction interfere with the CT, and that these impurities are removed in the pure F2 fraction. However, it is not clear what such impurities may be. Sainfoin contains a large amount of sucrose [43], however pre-treatment of the F2 fraction with sucrose did not remove its anthelmintic activity (data not shown). Moreover, previous studies have demonstrated marked *in vitro* anthelmintic effects of both aqueous
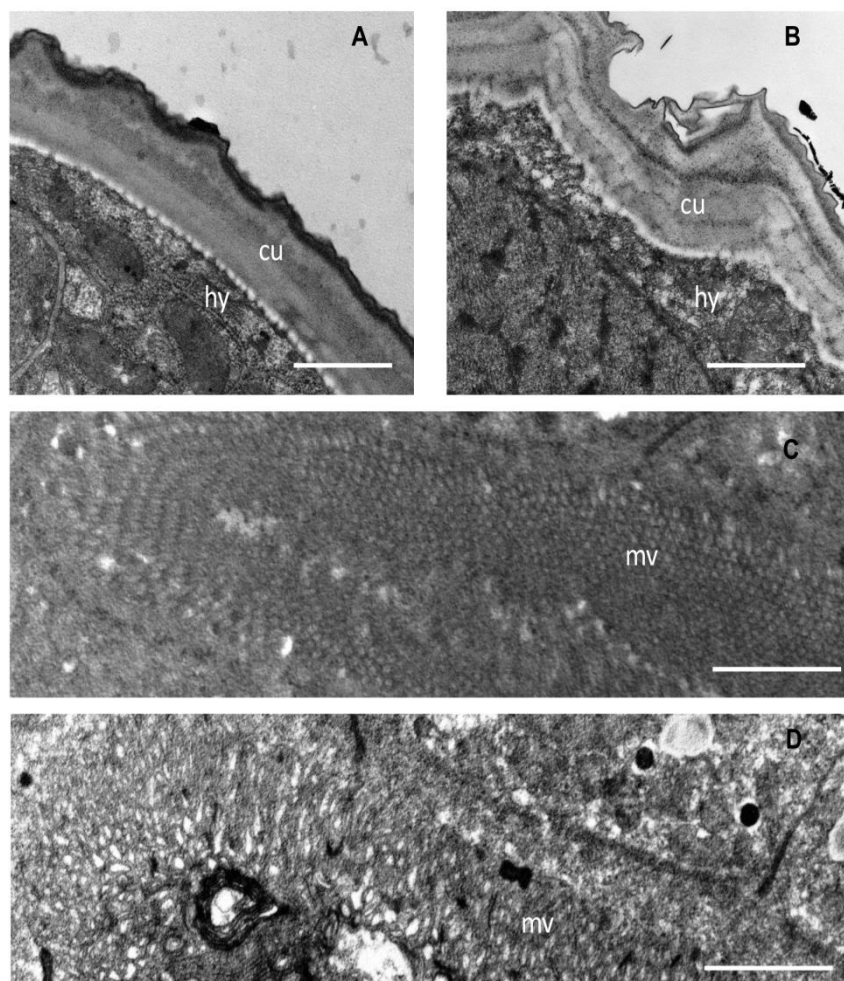
Figure 9. Ultrastructural changes in *Ascaris suum* L4 exposed to condensed tannins. Transmission electron microscopy of thin sections through *Ascaris suum* larvae recovered from pigs 12 days post-infection and then incubated for 24 hours in either culture media alone (**A,C**) or with 1 mg/mL condensed tannins (fraction 2 from hazelnut skin – **B,D**). **Panel A, B** – 'cu' indicates cuticle, 'hy' indicates hypodermis; scale bar represents 1 μm. **Panel C,D** – 'mv' indicates microvilli in brush-border of intestine; scale bar represents 2 μm.
doi:10.1371/journal.pone.0097053.g009

extracts and associated CT fractions of sainfoin towards other parasitic nematodes [22,44,45], although it cannot be ruled out that this phenomenon is specific to *A. suum*, or else to the particular accession of sainfoin used in our current study. Further studies will be necessary to elucidate this; for now, our results highlight the importance of considering the effects of complex extracts from plants, as well as pure compounds, when the whole plant or crude extract is to be used as a potential anthelmintic agent.

We observed significantly lower EC_{50} values in the L3 migration assay for the F2 tannin fractions than for the corresponding F1 fraction for each sample, with the exception of hazelnut skin. Of note, the F1 fraction from hazelnut skin had the highest mDP (4.1) of all the F1 fractions (Table 2) – perhaps explaining the lack of significant difference in MIA between the F1 and F2 fractions for this sample, as the size of the F1 fraction was still sufficient to exert significant anthelmintic activity. We have also previously noted a correlation between the mDP of CT extracted from sainfoin and the degree of anthelmintic activity against the cattle parasitic nematodes *Cooperioa oncophra* and *Ostertagia ostertagi* [45]. The reasons for this relationship are not

yet clear. It is thought that CT may exert anthelmintic activity by binding to proline-rich proteins on the cuticle or in the digestive system [32], and indeed we observed evidence of significant damage to these tissue in thin sections of larvae exposed to CT. It may be that the binding of larger CT polymers exerts a steric hindering effect on neighbouring parasite molecules. Protein-CT binding experiments have shown that CT coat the surface of proteins such as bovine serum albumin (M. Dobreva and IMH, manuscript in preparation), and it is conceivable that such a coating effect will interfere with the function of key parasite proteins and free movement of larvae, similar to the role proposed for host antibodies in growth inhibition of *A. suum* larvae [46]. Further experiments are necessary to elucidate these mechanisms. However, it is apparent that while CT size may contribute to the activity, anthelmintic effects can still be mediated by smaller CT molecules; indeed, significant activity was observed with the GC/EGC monomers (but not the C/EC monomers). The increased activity of GC/EGC monomers has previously been noted with experiments with *H. contortus* and *Trichostrongylus colubriformis* [32,47], as well as with other microbes such as *Streptococcus* [48].

The increased hydroxylation in the B-ring of PD monomers is thought to favour increased hydrogen-bonding with proteins and thus increase biological activity. However, despite this clear effect with monomers, we were unable to detect a strong influence of PD/PC ratio in the activity of the purified tannins – whilst CT purified from white clover flowers (made up>98% of PD units) appeared to have the most potent anthelmintic activity (Table 3 and Figure 8) – CT purified from blackcurrant and redcurrant leaves, which are also comprised almost exclusively of PD had similar activity in the MIA assay to cocoa and pine bark, both of which are comprised of 85–100% PC units.

In conclusion, we have provided clear evidence of the direct anthelmintic effects of CT against *Ascaris suum*. We have also highlighted several structural features of CT which may influence the anthelmintic activity. These studies pave the way for further, *in vivo* studies to determine the optimal use of CT as a sustainable and complementary means of control of *Ascaris suum* in pigs and *Ascaris lumbricoides* in humans.

Supporting Information

Figure S1 Explanation of thiolytic degradation scheme for determining chemical composition of condensed tannin molecules.
(TIF)

Figure S2 Motility of *Ascaris suum* L3 after exposure to extracts from tannin-containing plants. Motility of *Ascaris suum* L3 after 16 hours exposure to tannin-containing acetone/water extracts from hazelnut skins (HN), cocoa (COC), pine tree bark (PTB), sainfoin (SF), blackcurrant leaves (BC), redcurrant (RC) leaves and white clover flowers (WC). Motility is scored on a 0–5 scale where 5 is completely motile and 0 is completely still (see materials and methods). Dashed black line indicates the motility of larvae exposed to only culture medium (negative control). IVM = ivermectin at 50 μg/mL (positive control). Data points represent the mean of two independent experiments, each performed in triplicate. Error bars represent SEM of the individual replicates.
(TIF)

Figure S3 Effect of washing on inhibition of migratory activity (MIA). *Ascaris suum* L3 were incubated for 16 hours in tannin-containing acetone/water extracts from hazelnut skins, redcurrant leaves or pine bark. Larvae were then washed to remove tannins and resuspend in fresh media before addition of agar ('washing'), or agar was added directly to the larvae in the tannin-containing media ('no washing').
(TIF)

Figure S4 Motility of *Ascaris suum* L3 after exposure to flavanol monomers. Larvae were incubated for 16 hours with either catechin (C), gallocatechin (GC), epicatechin (EC) or epigallocatechin (EGC). Motility is scored on a 0–5 scale where 5 is completely motile and 0 is completely still (see materials and methods). Data points represent the mean of two independent experiments, each performed in triplicate. Error bars represent SEM of the individual replicates.
(TIF)

Figure S5 Motility of *Ascaris suum* L4 exposed to synthetic anthelmintic drugs. Motility of *Ascaris suum* L4 exposed to either 100 μg/mL ivermectin (IVM) or levamisole (LVM), or culture media only. Data points represent the mean of triplicate wells, with the error bars representing the inter-well SEM.
(TIF)

Checklist S1 ARRIVE Checklist.
(DOC)

Table S1 Proportions of monomeric flavanol subunits in extracts and fractions. Proportions of gallocatechin (GC), epigallocatechin (EGC), catechin (C) and epicatechin (EC)
(DOCX)

Acknowledgments

Author Contributions

Conceived and designed the experiments: ARW IMH SMT. Performed the experiments: ARW CF AR. Analyzed the data: ARW CF AR. Contributed reagents/materials/analysis tools: CF AR IMH. Wrote the paper: ARW IMH SMT.

References

1. Keiser J, Utzinger J (2008) Efficacy of current drugs against soil-transmitted helminth infections: Systematic review and meta-analysis. JAMA 299: 1937 1948.
2. Hale OM, Stewart TB, Marti OG (1985) Influence of an Experimental Infection of Ascaris suum on Performance of Pigs. Journal of Animal Science 60: 220 225.
3. Thamsborg SM, Nejsum P, Mejer H (2013) Chapter 14 - Impact of Ascaris suum in Livestock. In: Holland C, editor. Ascaris: the Neglected Parasite. Amsterdam: Elsevier. 363 381. Available: http://www.sciencedirect.com/science/article/pii/B9780123969781000148.
4. Nejsum P, Betson M, Bendall RP, Thamsborg SM, Stothard JR (2012) Assessing the zoonotic potential of Ascaris suum and Trichuris suis: looking to the future from an analysis of the past. Journal of Helminthology 86: 148 155.
5. Cooper PJ, Chico ME, Sandoval C, Espinel I, Guevara A, et al. (2000) Human Infection with Ascaris lumbricoides Is Associated with a Polarized Cytokine Response. Journal of Infectious Diseases 182: 1207 1213.
6. Steenhard NR, Jungersen G, Kokotovic B, Beshah E, Dawson HD, et al. (2009) Ascaris suum infection negatively affects the response to a Mycoplasma hyopneumoniae vaccination and subsequent challenge infection in pigs. Vaccine 27: 5161 5169.
7. Jia T W, Melville S, Utzinger J, King CH, Zhou X-N (2012) Soil-Transmitted Helminth Reinfection after Drug Treatment: A Systematic Review and Meta-Analysis. PLoS Negl Trop Dis 6: e1621.
8. Tanner S, Chuquimia-Choque ME, Huanca T, McDade TW, Leonard WR, et al. (2011) The effects of local medicinal knowledge and hygiene on helminth infections in an Amazonian society. Social Science & Medicine 72: 701 709.
9. Stangeland T, Dhillion SS, Reksten H (2008) Recognition and development of traditional medicine in Tanzania. Journal of Ethnopharmacology 117: 290 299.
10. Gazzinelli A, Correa-Oliveira R, Yang G-J, Boatin BA, Kloos H (2012) A Research Agenda for Helminth Diseases of Humans: Social Ecology, Environmental Determinants, and Health Systems. PLoS Negl Trop Dis 6: e1603.
11. Githiori JB, Höglund J, Waller PJ (2005) Ethnoveterinary plant preparations as livestock dewormers: practices, popular beliefs, pitfalls and prospects for the future. Animal Health Research Reviews 6: 91 103.
12. Jansman AJM (1993) Tannins in Feedstuffs for Simple-Stomached Animals. Nutrition Research Reviews 6: 209 236.
13. Cowan MM (1999) Plant Products as Antimicrobial Agents. Clinical Microbiology Reviews 12: 564 582.
14. Ishida K, de Mello JCP, Cortez DAG, Filho BPD, Ueda-Nakamura T, et al. (2006) Influence of tannins from Stryphnodendron adstringens on growth and virulence factors of Candida albicans. Journal of Antimicrobial Chemotherapy 58: 942 949.
15. Kubata BK, Nagamune K, Murakami N, Merkel P, Kabututu Z, et al. (2005) Kola acuminata proanthocyanidins: a class of anti-trypanosomal compounds

effective against Trypanosoma brucei. International Journal for Parasitology 35: 91 103.

16. Kolodziej H, Kiderlen AF (2005) Antileishmanial activity and immune modulatory effects of tannins and related compounds on Leishmania parasitised RAW 264.7 cells. Phytochemistry 66: 2056 2071.

17. Hoste H, Martinez-Ortiz-De-Montellano C, Manolaraki F, Brunet S, Ojeda-Robertos N, et al. (2012) Direct and indirect effects of bioactive tannin-rich tropical and temperate legumes against nematode infections. Veterinary Parasitology 186: 18 27.

18. Butter NL, Dawson JM, Wakelin D, Buttery PJ (2001) Effect of dietary condensed tannins on gastrointestinal nematodes. The Journal of Agricultural Science 137: 461 469.

19. Costa CTC, Bevilaqua CML, Morais SM, Camurca-Vasconcelos ALF, Maciel MV, et al. (2010) Anthelmintic activity of *Cocos nucifera* L. on intestinal nematodes of mice. Research in Veterinary Science 88: 101 103.

20. Fakae BB, Campbell AM, Barrett J, Scott IM, Teesdale-Spittle PH, et al. (2000) Inhibition of glutathione S-transferases (GSTs) from parasitic nematodes by extracts from traditional Nigerian medicinal plants. Phytotherapy Research 14: 630 634.

21. Nalule AS, Mbaria JM, Kimenju JW (2013) In vitro anthelmintic potential and phytochemical composition of ethanolic and water crude extracts of Euphorbia heterophylla Linn. Journal of Medicinal Plants Research 7: 3202 3210.

22. Brunet S, Jackson F, Hoste H (2008) Effects of sainfoin (Onobrychis viciifolia) extract and monomers of condensed tannins on the association of abomasal nematode larvae with fundic explants. International Journal for Parasitology 38: 783 790.

23. Mueller-Harvey I (2006) Unravelling the conundrum of tannins in animal nutrition and health. Journal of the Science of Food and Agriculture 86: 2010 2037.

24. Gea A, Stringano E, Brown RH, Mueller-Harvey I (2011) In Situ Analysis and Structural Elucidation of Sainfoin (Onobrychis viciifolia) Tannins for High-Throughput Germplasm Screening. Journal of Agricultural and Food Chemistry 59: 495 503.

25. Oksanen A, Eriksen L, Roepstorff A, Ilsøe B, Nansen P, et al. (1990) Embryonation and infectivity of Ascaris suum eggs. A comparison of eggs collected from worm uteri with eggs isolated from pig faeces. Acta veterinaria Scandinavica 31: 393 398.

26. Han Q, Eriksen L, Boes J, Nansen P (2000) Effects of bile on the in vitro hatching, exsheathment, and migration of Ascaris suum larvae. Parasitology Research 86: 630 633.

27. Slotved HC, Barnes EH, Eriksen L, Roepstorff A, Nansen P, et al. (1997) Use of an agar-gel technique for large scale application to recover Ascaris suum larvae from intestinal contents of pigs. Acta veterinaria Scandinavica 38: 207 212.

28. Stepek G, Buttle DJ, Duce IR, Lowe A, Behnke JM (2005) Assessment of the anthelmintic effect of natural plant cysteine proteinases against the gastrointestinal nematode, Heligmosomoides polygyrus, in vitro. Parasitology 130: 203 211.

29. Urban JF, Jr., Hu Y, Miller MM, Scheib U, Yiu YY, et al. (2013) *Bacillus thuringiensis*-derived Cry5B Has Potent Anthelmintic Activity against *Ascaris suum*. PLoS Negl Trop Dis 7: e2263.

30. Hu Y, Ellis BL, Yiu YY, Miller MM, Urban JF, et al. (2013) An Extensive Comparison of the Effect of Anthelmintic Classes on Diverse Nematodes. PLoS ONE 8: e70702.

31. Makkar HPS, Blummel M, Becker K (1995) Formation of complexes between polyvinyl pyrrolidones or polyethylene glycols and tannins, and their implications in gas production and true digestiblity in *in vitro* techniques. British Journal of Nutrition 73: 897 913.

32. Brunet S, Hoste H (2006) Monomers of Condensed Tannins Affect the Larval Exsheathment of Parasitic Nematodes of Ruminants. Journal of Agricultural and Food Chemistry 54: 7481 7487.

33. Douvres F, Tromba FG, Malakatis GM (1969) Morphogenesis and migration of *Ascaris suum* larvae developing to fourth stage in swine. The Journal of Parasitology 55: 689 712.

34. Urban J, Kokoska L, Langrova I, Matejkova J (2008) In Vitro Anthelmintic Effects of Medicinal Plants Used in Czech Republic. Pharmaceutical Biology 46: 808 813.

35. Salajpal K, Karolyi D, Beck R, Kis G, Vickovic I, et al. (2004) Effect of acorn (*Quercus robur*) intake on faecal egg count in outdoor reared black Slavonian pig. Acta Agriculture Slovenica 84, Supplement 1: 173 178.

36. Arena JP, Liu KK, Paress PS, Frazier EG, Cully DF, et al. (1995) The Mechanism of Action of Avermectins in Caenorhabditis Elegans: Correlation between Activation of Glutamate-Sensitive Chloride Current, Membrane Binding, and Biological Activity. The Journal of Parasitology 81: 286 294.

37. Rios LY, Bennett RN, Lazarus SA, Rémésy C, Scalbert A, et al. (2002) Cocoa procyanidins are stable during gastric transit in humans. The American Journal of Clinical Nutrition 76: 1106 1110.

38. Reed JD (1995) Nutritional toxicology of tannins and related polyphenols in forage legumes. Journal of Animal Science 73: 1516 1528.

39. Gonthier M-P, Donovan JL, Texier O, Felgines C, Remesy C, et al. (2003) Metabolism of dietary procyanidins in rats. Free Radical Biology and Medicine 35: 837 844.

40. Manach C, Williamson G, Morand C, Scalbert A, Rémésy C (2005) Bioavailability and bioefficacy of polyphenols in humans. I. Review of 97 bioavailability studies. The American Journal of Clinical Nutrition 81: 230S 242S.

41. Verhelst R, Schroyen M, Buys N, Niewold T (2014) Dietary polyphenols reduce diarrhoea in enterotoxigenic *Escherichia coli* (ETEC) infected post-weaning piglets. Livestock Science 160: 138 140.

42. Lærke HN, Hedemann MS (2012) Chapter 5: The digestive system of the pig. In: Knudsen KEB, editor. Nutritional Physiology of Pigs. Copenhagen: Danish Pig Research Centre.http://vsp.lf.dk/Viden/Laerebog_fysiologi/.

43. Marais JPJ, Mueller-Harvey I, Brandt EV, Ferreira D (2000) Polyphenols, Condensed Tannins, and Other Natural Products in Onobrychis viciifolia (Sainfoin). Journal of Agricultural and Food Chemistry 48: 3440 3447.

44. Novobilský A, Mueller-Harvey I, Thamsborg SM (2011) Condensed tannins act against cattle nematodes. Veterinary Parasitology 182: 213 220.

45. Novobilský A, Stringano E, Hayot Carbonero C, Smith LMJ, Enemark HL, et al. (2013) In vitro effects of extracts and purified tannins of sainfoin (Onobrychis viciifolia) against two cattle nematodes. Veterinary Parasitology 196: 532 537.

46. Tsuji N, Miyoshi T, Islam MK, Isobe T, Yoshihara S, et al. (2004) Recombinant *Ascaris* 16-Kilodalton Protein-Induced Protection against *Ascaris suum* Larval Migration after Intranasal Vaccination in Pigs. Journal of Infectious Diseases 190: 1812 1820.

47. Molan AL, Meagher LP, Spencer PA, Sivakumaran S (2003) Effect of flavan-3-ols on in vitro egg hatching, larval development and viability of infective larvae of Trichostrongylus colubriformis. International Journal for Parasitology 33: 1691 1698.

48. Scalbert A (1991) Antimicrobial properties of tannins. Phytochemistry 30: 3875 3883.

310

Appendix G

Original publication:

Assessment of the anthelmintic activity of medicinal plant extracts and purified condensed tannins against free-living and parasitic stages of *Oesophagostomum dentatum*

Andrew R Williams, Honorata M Ropiak, Christos Fryganas, Olivier Desrues, Irene Mueller-Harvey and Stig M Thamsborg

RESEARCH

Assessment of the anthelmintic activity of medicinal plant extracts and purified condensed tannins against free-living and parasitic stages of *Oesophagostomum dentatum*

Andrew R Williams[1]*, Honorata M Ropiak[2], Christos Fryganas[2], Olivier Desrues[1], Irene Mueller-Harvey[2] and Stig M Thamsborg[1]

Abstract

Background: Plant-derived condensed tannins (CT) show promise as a complementary option to treat gastrointestinal helminth infections, thus reducing reliance on synthetic anthelmintic drugs. Most studies on the anthelmintic effects of CT have been conducted on parasites of ruminant livestock. *Oesophagostomum dentatum* is an economically important parasite of pigs, as well as serving as a useful laboratory model of helminth parasites due to the ability to culture it *in vitro* for long periods through several life-cycle stages. Here, we investigated the anthelmintic effects of CT on multiple life cycle stages of *O. dentatum*.

Methods: Extracts and purified fractions were prepared from five plants containing CT and analysed by HPLC-MS. Anthelmintic activity was assessed at five different stages of the *O. dentatum* life cycle; the development of eggs to infective third-stage larvae (L3), the parasitic L3 stage, the moult from L3 to fourth-stage larvae (L4), the L4 stage and the adult stage.

Results: Free-living larvae of *O. dentatum* were highly susceptible to all five plant extracts. In contrast, only two of the five extracts had activity against L3, as evidenced by migration inhibition assays, whilst three of the five extracts inhibited the moulting of L3 to L4. All five extracts reduced the motility of L4, and the motility of adult worms exposed to a CT-rich extract derived from hazelnut skins was strongly inhibited, with electron microscopy demonstrating direct damage to the worm cuticle and hypodermis. Purified CT fractions retained anthelmintic activity, and depletion of CT from extracts by pre-incubation in polyvinylpolypyrrolidone removed anthelmintic effects, strongly suggesting CT as the active molecules.

Conclusions: These results suggest that CT may have promise as an alternative parasite control option for *O. dentatum* in pigs, particularly against adult stages. Moreover, our results demonstrate a varied susceptibility of different life-cycle stages of the same parasite to CT, which may offer an insight into the anthelmintic mechanisms of these commonly found plant compounds.

Keywords: *Oesophagostomum dentatum*, Plant extracts, Condensed tannins, Anthelmintic

* Correspondence: arw@sund.ku.dk
[1]Department of Veterinary Disease Biology, Faculty of Health and Medical Sciences, University of Copenhagen, Frederiksberg, Denmark
Full list of author information is available at the end of the article

Background

Parasitic worms (helminths) of the gastrointestinal (GI) tract are pathogens of major global importance. Over a billion people, mainly in developing countries, are estimated to be infected with soil-transmitted helminths, whilst helminth infection is also a serious problem in livestock production worldwide, causing significant economic losses and threatening food security [1-3]. Control of helminths relies almost exclusively on a limited number of synthetic anthelmintic drugs. The limitations of this reliance on chemotherapy are the threat of parasites developing resistance to drug treatment (already widespread in some livestock production systems) [4,5] , the cost of drugs for small-scale farmers in developing countries and for some helminths, lack of efficacy of current available drugs [1]. Therefore, novel and complementary helminth control options are urgently needed.

The use of natural plant extracts as de-wormers for humans and livestock has long been practiced, however scientific validation of these practices and identification of active compounds has been lacking [6-8]. Anthelmintic effects of plants are normally ascribed to secondary metabolites such as alkaloids, terpenoids or polyphenols such as proanthocyanidins [9], also known as condensed tannins (CT). Proanthocyanidins are a diverse and widely-occurring group of compounds, and consist of polymers of either catechin and/or epicatechin (termed procyanidins - PC), or of gallocatechin and/or epigallocatechin (termed prodelphinidins - PD), with hetero-polymers being common [10]. They are found in plant material from both tropical and temperate areas, and have been widely investigated for their antioxidant and anti-inflammatory properties [11,12]. It is also apparent that CT can have anthelmintic effects; reduced worm burdens have been reported in rats administered CT in the diet, or in livestock grazing forages containing CT [13,14]. Moreover, direct anthelmintic effects of purified CT have been confirmed in in vitro assays against, amongst others, Haemonchus contortus [15], Ostertagia ostertagi [16] and Ascaris suum [17]. However, much work remains to be done to establish the spectra of activity of CT, i.e. the range of helminth species that are susceptible, and what stages of the life cycle are targeted by these molecules.

Oesophagostomum dentatum is a common helminth parasite that resides in the large intestine of pigs, and is of economic importance as it causes significant production losses for farmers [18-20]. Resistance of O. dentatum to levamisole, pyrantel and possibly ivermectin has been reported in Europe [21,22]. Moreover, O. dentatum also serves as a good model parasite due to its amenability to culture in the laboratory – several different life-cycle stages can be easily maintained and manipulated, and hence this worm is being increasingly used as a model parasite for biological investigations [23]. In the present study we investigated 1) whether CT have direct anthelmintic activity against O. dentatum in vitro, and 2) which stages of the life cycle of this parasite were specifically targeted by CT.

Methods

Extraction of plant material and analysis of proanthocyanidins

Five sources of plant material were selected, on the basis of known high concentrations of CT and/or use as traditional medicinal plants. Three traditional medicinal plants were obtained from Flos (Mokrsko, Poland) – these were leaves from blackcurrant (Ribes nigrum), flowers from Tilia (Tilia L., a mixture of T. cordata, T. platyphyllos and T. vulgaris) and bark from willow (Salix spp.). Flowers from white clover (Trifolium repens) were obtained from Ziola Kurpi (Jednorozec, Poland). Extraction and analysis were as previously described [17]. Briefly, plant material was extracted with acetone/water (excluding addition of ascorbic acid). To purify CT, extracts were applied to Sephadex LH-20 columns, and eluted with acetone/water (3:7 and 1:1, v/v). Condensed tannin content was quantified by thiolytic degradation [16] and HPLC [17] with the use of dihydroquercetin as external standard. The identification of compounds was confirmed by LC-MS [17]. In addition, skins from hazelnut (Corylus avellana), which had previously been shown to contain CT with potent in vitro anthelmintic effects against A. suum [17], were prepared as previously described.

Larval development assay with free-living stages

All animal experimentation was conducted under the guidelines and with approval of the Danish Animal Experimentation Inspectorate (Licence number 2010/561-1914). Two 8-week-old pigs were each infected with two doses of 5,000 third-stage larvae (L3) O. dentatum by stomach tube, three weeks apart. Upon patency, eggs were isolated from freshly collected faeces by sieving and saturated salt flotation [24].

For the development assay, plant extracts were dissolved in distilled water at appropriate concentrations and added to 96-well plates together with 15% (v/v) of a larval feeding solution (1% yeast extract (Sigma-Aldrich) in Earle's balanced salt solution), antibiotics (300 U/mL penicillin, 300 µg mL/streptomycin) and antimycotic (10 µg/mL amphotericin B). Negative and positive controls consisted of water and 50 µg/mL levamisole, respectively. One hundred eggs were then added per well and the plates incubated at 25°C in a humidified environment for 7 days. Larvae were then killed by the addition of iodine and the numbers of L3 per well were determined.

Larval migration assay

Third-stage larvae were produced from the faeces of mono-infected donor pigs by standard copro-culture,

collected by Baermann apparatus and stored in water at 10°C. On the day of the assay, L3 were rapidly exsheathed by the addition of 2% sodium hypochlorite (10-15% available chloride, Sigma-Aldrich). L3 were then washed five times in sterile water. To assess the migratory ability of the L3, we performed a migration inhibition assay essentially as described previously [17]. Briefly, larvae were suspended in RPMI 1640 media with HEPES (Gibco) containing L-glutamine (2 mM), 100 U/mL penicillin and 100 µg/mL streptomycin. One hundred larvae were then added in triplicate to each well of a 48-well plate containing medium with either plant extracts or purified CT fractions, 50 µg/mL ivermectin (positive control) or medium alone (negative control). The larvae were then incubated overnight at 37°C in an atmosphere of 5% CO_2, before addition of agar to a final concentration of 0.8%. After a four hour migration period, the numbers of larvae able to migrate out of the setting agar were counted by light microscopy. In some experiments, plant extracts were pre-incubated with polyvinylpolypyrrolidone (PVPP) to selectively deplete CT – this was done by overnight incubation as described previously [17].

Larval development assay with parasitic stages

Third-stage larvae were exsheathed as above, washed and then 100 larvae per well were seeded in 2 mL of culture medium (LB broth containing 10% heat-inactivated porcine serum, 200 U/mL penicillin, 200 µg/mL streptomycin and 1 µg/mL amphotericin B) in 24-well plates. Acetone/water plant extracts were added at a concentration of 1 mg/mL. Positive control wells received 25 mM of diethylcarbamazine (Sigma-Aldrich) in order to block the development from third-stage to fourth-stage larvae, whilst negative control wells received only culture medium. The larvae were then incubated at 37°C in an atmosphere of 5% CO_2 for 14 days, with the medium being replenished on days 5 and 10. On day 14 the percentage of L4 in each well was determined.

Motility assay with fourth-stage larvae

Third-stage larvae were exsheathed as above, washed and then seeded at a concentration of 1000 larvae/mL in tissue culture flasks containing complete LB broth culture medium. Larvae were then incubated at 37°C in an atmosphere of 5% CO_2 with medium changes every five days. Larvae were cultured for 21–24 days to allow development of large numbers of L4. The L4 were then separated from L3 by repeated sedimentation, washed five times in warm sterile saline, and then suspended in the same medium as used for the L3 migration assay above. Approximately 10 larvae were then added to each well of a 48-well plate containing either acetone/water plant extracts or purified CT fractions, medium

only or ivermectin (50 µg/mL). The motility of the larvae was then scored daily for four days. Motility was scored on a 0–5 scale where 0 is no movement and 5 is vigorous movement, as described in more detail by Stepek *et al.* [25].

Motility assay with adult worms

Donor pigs were infected with *O. dentatum* larvae as described above. Approximately five weeks after the second infective dose, the pigs were killed by captive bolt pistol and exsanguination, and the large intestine was removed. Adult worms were manually plucked from the gut contents with forceps and washed well with warm saline. The worms were then taken to the laboratory and washed repeatedly in the same sterile culture medium as used for the L3 migration assay. Four worms were then seeded in each well of a 24-well plate containing either medium only, ivermectin (50 µg/mL) or hazelnut skin extract. The worms were incubated at 37°C in an atmosphere of 5% CO_2 for three days, with motility assessed twice daily as described above. After 24 hours, a subset of worms from the negative control wells and from the wells containing the highest concentration of CT were washed, fixed and examined by transmission electron microscopy as previously described [17].

Statistical analysis

The effect of plant extracts and CT fractions on larval migration and moulting was assessed by two-way ANOVA with Bonferonni post-hoc testing. Graphpad Prism 6 was used for the analyses.

Results

Analysis of plant extracts

Acetone/water extraction of the five plant materials yielded extracts with varying yields of CT ranging from 13.1 g CT/100 g extract (white clover flowers) to 73.8 g CT/100 g extract for hazelnut skins (Table 1). Fractionation on Sephadex LH-20 with acetone/water yielded a first fraction (F1) containing from 13.3 to 55.4 g CT/100 g fraction, whilst the second fraction (F2) contained more CT (ranging from 70.3-96.7 g CT/100 g fraction - Table 1).

Tannin-containing extracts inhibit the development of free-living larvae

Acetone/water extracts were first tested in the widely-used assay of free-living larval development, which measures the ability of newly-hatched larvae from eggs to develop to infective L3 in the presence of a putative anthelmintic agent. In negative control wells, 80% of larvae developed to L3 after 7 days. The addition of 50 µg/mL levamisole resulted in 100% inhibition of egg hatching and therefore subsequent larval development. Egg hatching was not inhibited by the plant extracts, but all five plant extracts

Table 1 Chemical analysis of plant extracts and derived fractions

Sample	PAC (g/100 g extract or fraction)
Hazelnut skin extract	73.8
F1	51.3
F2	70.3
White clover flower extract	13.1
F1	13.3
F2	81.9
Blackcurrant leaves extract	20.2
F1	55.4
F2	76.8
Willow bark extract	16.2
F1	24.2
F2	87.0
Tilia flowers extract	21.0
F1	49.7
F2	96.1

'PAC' – proanthocyanidins, 'F1' – fraction 1, 'F2' – fraction 2. Results from the hazelnut skin extract and fractions were also reported previously in [17].
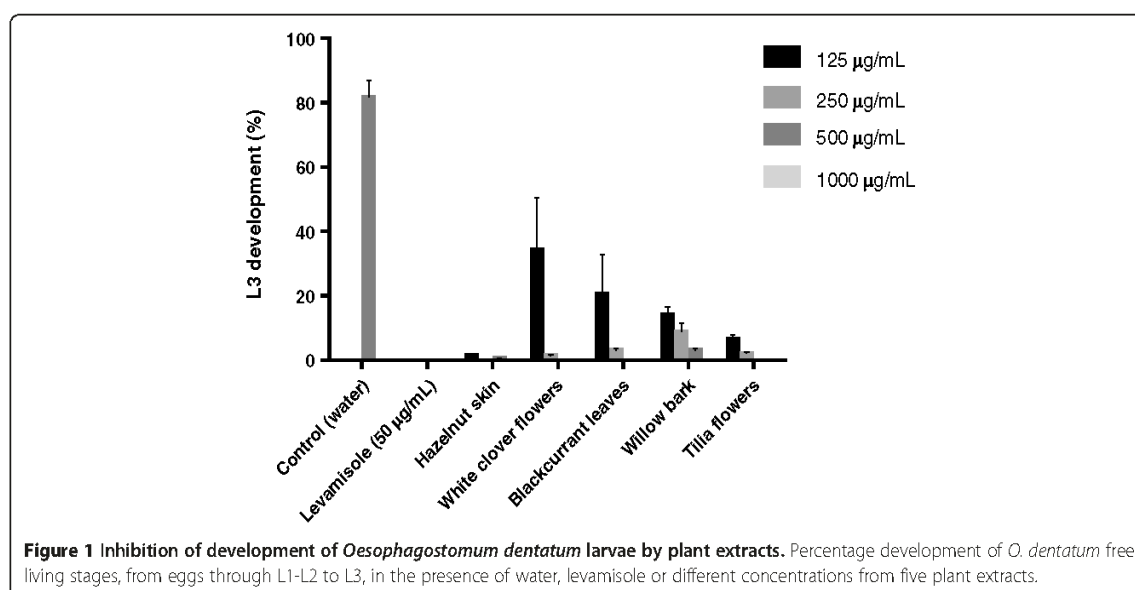
strongly inhibited the development of L1 to infective L3, with most larvae dying at the L1 or L2 stage (Figure 1). A dose-dependent relationship was evident for all extracts except for hazelnut skin, where all four tested concentrations (125 – 1000 µg/mL) inhibited development by more than 90% (Figure 1). Overall, these results clearly show that CT-containing plant extracts have anthelmintic activity against the free-living stages of *O. dentatum*.
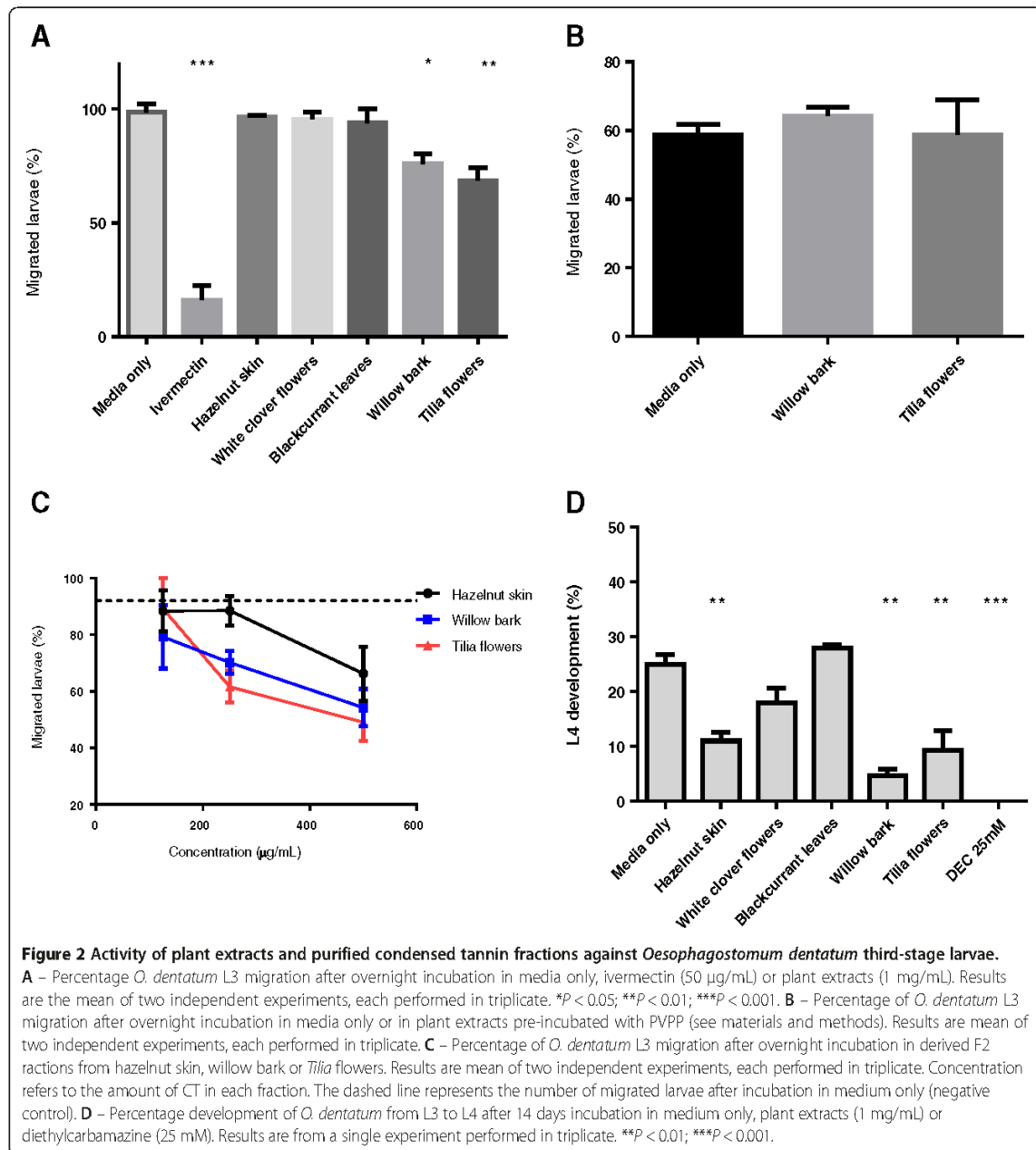
Activity of extracts and tannin fractions against parasitic third-stage larvae

Having established that all five extracts had activity against free-living larvae, anthelmintic effects were next assessed against the L3 larval stage that is infective to pigs and develops within the GI tract. First, the migratory ability of exsheathed L3 was quantified after incubation in the extracts. Migration of L3 was reduced ($P < 0.01$) after overnight incubation with extracts of willow bark and *Tilia* flowers at a concentration of 1 mg/mL; in contrast, migration was not significantly reduced after incubation in the other three extracts (Figure 2A). To assess whether CT were the active molecules responsible for the inhibitory activity of willow bark and *Tilia* extracts, the samples were pre-incubated with PVPP, which selectively binds and precipitates CT [10]. Incubation of larvae in these CT-depleted extracts did not affect migratory ability, strongly suggesting CT as the active compounds (Figure 2B).

To further confirm the role of CT in the observed effects, F1 and F2 fractions were isolated from the acetone/water extracts of willow bark and *Tilia* and used in migration inhibition assays. The activity of hazelnut skin fractions, which had previously demonstrated potent anthelmintic effects against *A. suum* [17], were also examined. No anthelmintic activity was evident with the F1 fractions at concentrations up to 500 µg/mL of CT (data not shown). However, F2 fractions inhibited migration in a dose-dependent manner (Figure 2C).

We next investigated whether long-term incubation of L3 in the extracts would reduce subsequent moulting to the L4 larval stage. After 14 days incubation in medium

Figure 1 Inhibition of development of *Oesophagostomum dentatum* larvae by plant extracts. Percentage development of *O. dentatum* free living stages, from eggs through L1-L2 to L3, in the presence of water, levamisole or different concentrations from five plant extracts.

Figure 2 Activity of plant extracts and purified condensed tannin fractions against *Oesophagostomum dentatum* **third-stage larvae.**
A – Percentage *O. dentatum* L3 migration after overnight incubation in media only, ivermectin (50 µg/mL) or plant extracts (1 mg/mL). Results are the mean of two independent experiments, each performed in triplicate. *$P < 0.05$; **$P < 0.01$; ***$P < 0.001$. **B** – Percentage of *O. dentatum* L3 migration after overnight incubation in media only or in plant extracts pre-incubated with PVPP (see materials and methods). Results are mean of two independent experiments, each performed in triplicate. **C** – Percentage of *O. dentatum* L3 migration after overnight incubation in derived F2 ractions from hazelnut skin, willow bark or *Tilia* flowers. Results are mean of two independent experiments, each performed in triplicate. Concentration refers to the amount of CT in each fraction. The dashed line represents the number of migrated larvae after incubation in medium only (negative control). **D** – Percentage development of *O. dentatum* from L3 to L4 after 14 days incubation in medium only, plant extracts (1 mg/mL) or diethylcarbamazine (25 mM). Results are from a single experiment performed in triplicate. **$P < 0.01$; ***$P < 0.001$.
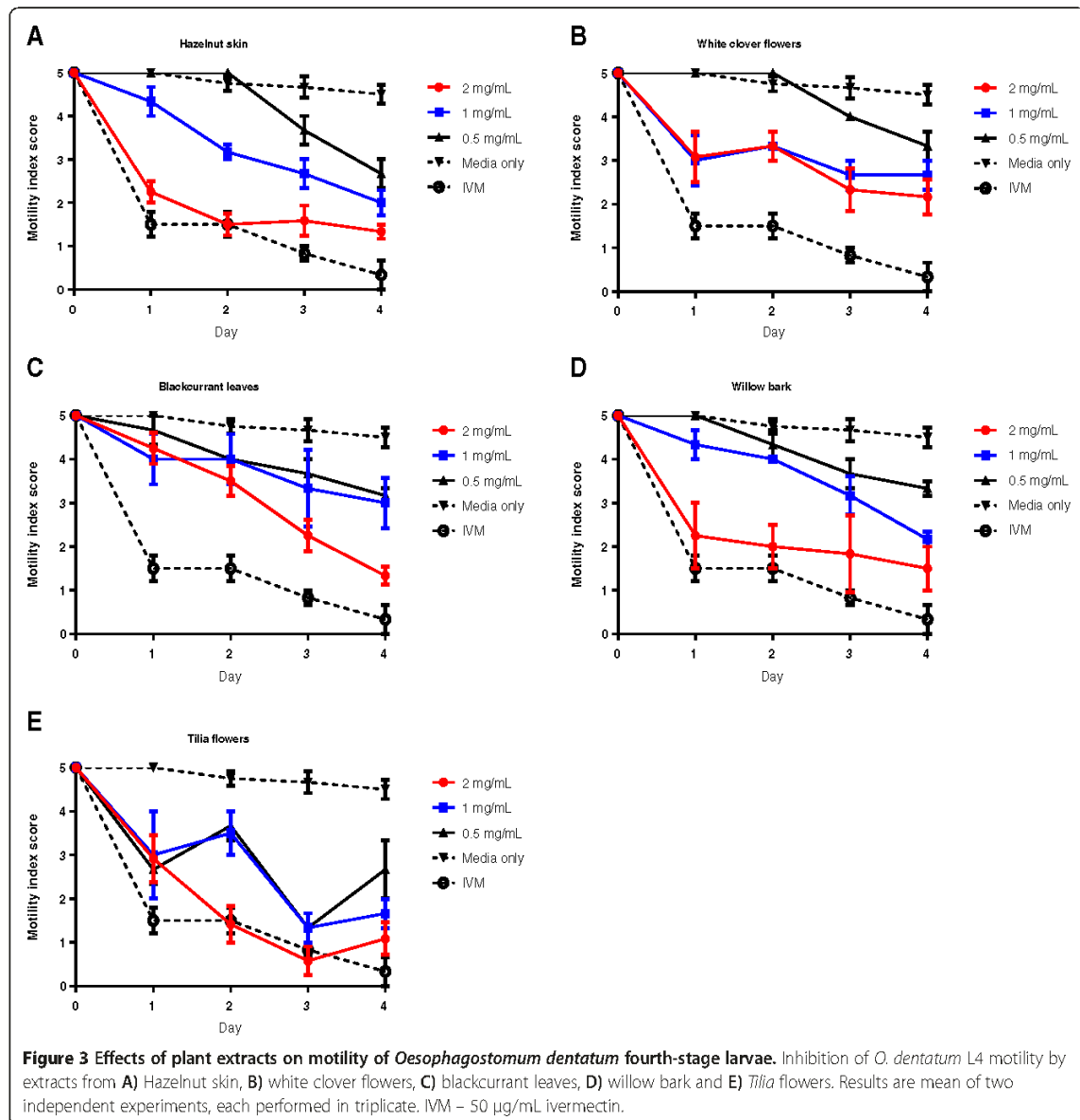
alone, 25% of L3 had moulted to the L4 stage. In contrast, the number of L3 that successfully moulted to L4 was significantly reduced after incubation in extract from hazelnut skins, willow bark or *Tilia* flowers (Figure 2D). No inhibition of moulting was observed after incubation with extracts from white clover flowers or blackcurrant. These data indicate that some CTs are able to interfere with the moulting process of *O. dentatum*.

Effects of extracts and tannin fractions on motility of fourth-stage larvae

Anthelmintic effects of the plant extracts and purified CT fractions were further assessed against *in vitro* cultured L4 parasites. After incubation in each of the five plant extracts at concentrations of 2 or 1 mg/mL, a reduction in motility was noted in all parasites after 24 hours (Figure 3). In parasites exposed to extracts from white clover flowers, no further reductions in motility were observed over the
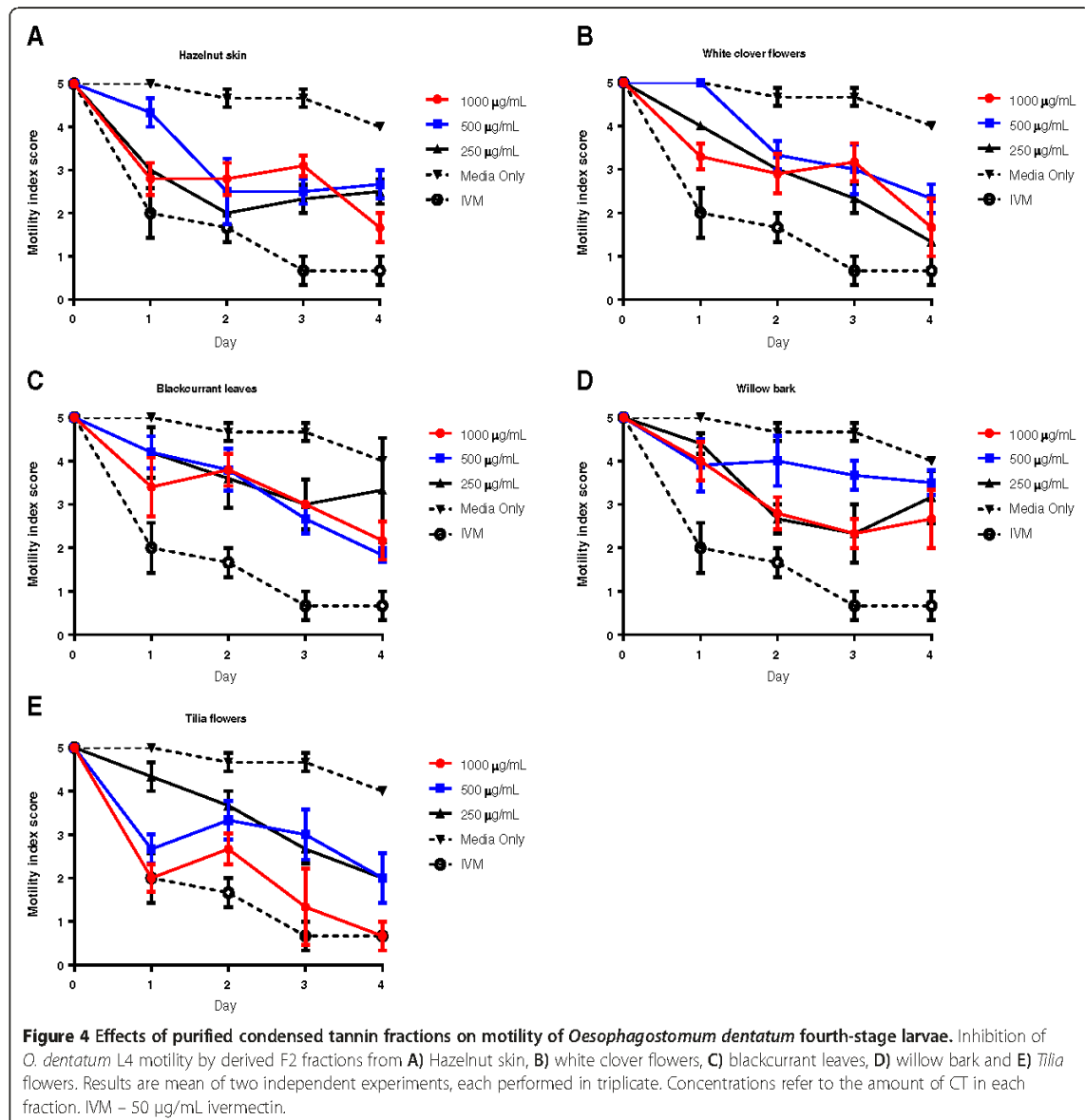
Figure 3 Effects of plant extracts on motility of *Oesophagostomum dentatum* fourth-stage larvae. Inhibition of *O. dentatum* L4 motility by extracts from **A)** Hazelnut skin, **B)** white clover flowers, **C)** blackcurrant leaves, **D)** willow bark and **E)** *Tilia* flowers. Results are mean of two independent experiments, each performed in triplicate. IVM – 50 µg/mL ivermectin.

next 3 days (Figure 3B), whereas motility continued to decline in worms exposed to the other four extracts, resulting in a near-cessation of movement at the high concentrations of extract by the end of the experiment (Figure 3A, C-E).

To explore the relative contribution of the different CT molecules to the observed effects, isolated F2 fractions from all five extracts were then tested in the motility assay, as anthelmintic activity had been associated with this fraction in the L3 migration assay. The concentrations of CT were normalised between fractions to allow direct comparison between samples. Similar to the results with the acetone/water extracts, incubation in the F2 fractions

resulted in reductions of motility after 24 hours of incubation (Figure 4). Motility continued to decline substantially in L4 exposed to fractions of *Tilia* flowers, resulting in near-paralysis by the end of the experiment (Figure 4E). In worms exposed to the other four fractions, further reductions in motility were less apparent, even after four days of incubation; however, motility did not return to pre-incubation levels (Figure 4A-D).

Effects of hazelnut skin-extract on motility and morphology of adult worms

We also assessed the ability of hazelnut extract to reduce the motility of adult worms recovered directly from pigs –
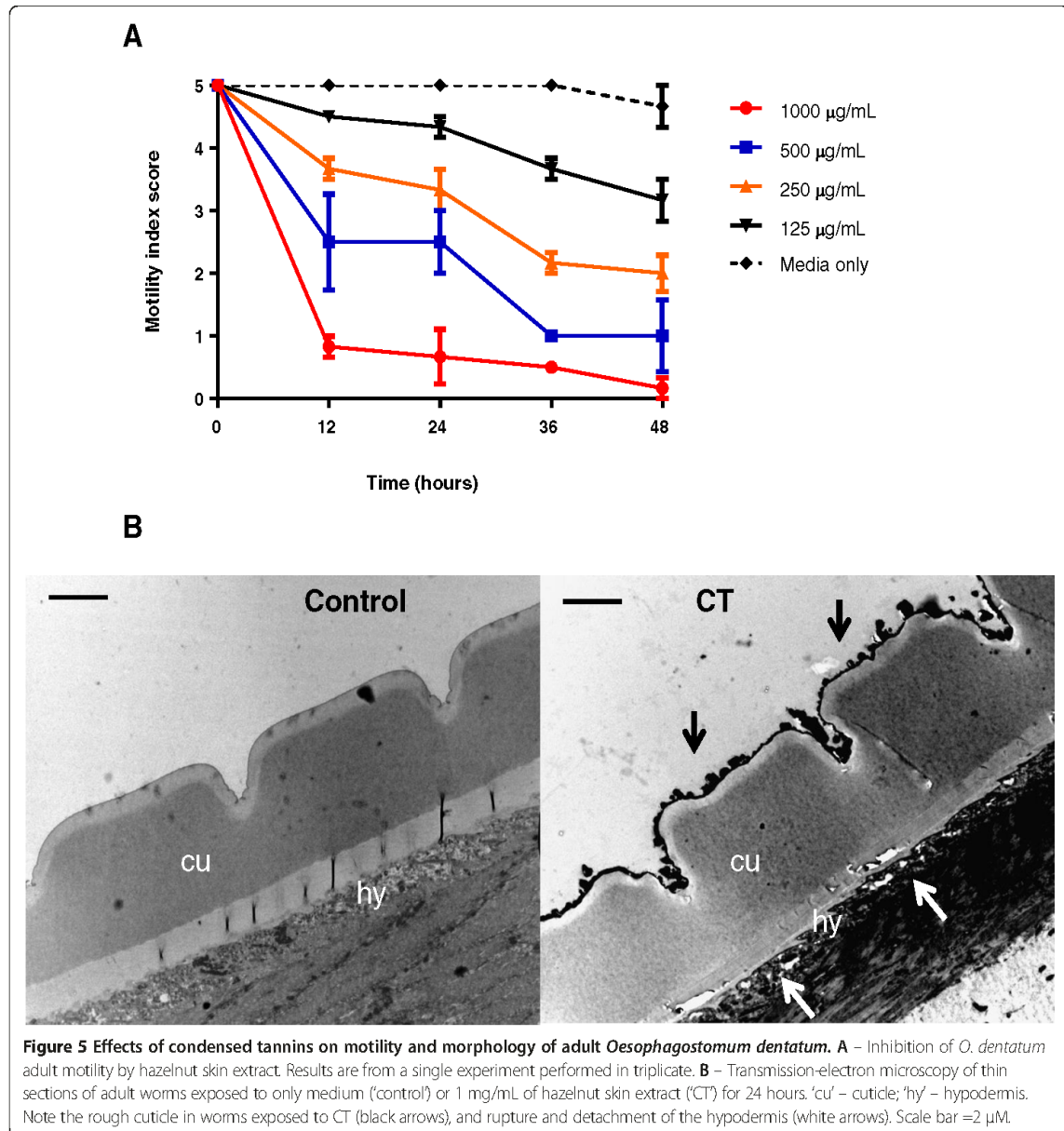
Figure 4 Effects of purified condensed tannin fractions on motility of *Oesophagostomum dentatum* fourth-stage larvae. Inhibition of *O. dentatum* L4 motility by derived F2 fractions from **A)** Hazelnut skin, **B)** white clover flowers, **C)** blackcurrant leaves, **D)** willow bark and **E)** *Tilia* flowers. Results are mean of two independent experiments, each performed in triplicate. Concentrations refer to the amount of CT in each fraction. IVM – 50 μg/mL ivermectin.

only a single extract was used here due to limited numbers of adult parasites. There was a clear dose-dependent reduction in motility, with worms exposed to 1 mg/mL of extract displaying little or no movement after 12 hours of incubation (Figure 5), and after 48 hours worms exposed to concentrations of ≥250 μg/mL showed clear signs of paralysis and structural damage including blebbing and a 'rough' cuticle. To explore further the structural damage caused by exposure to CT, the cuticle of worms exposed to the highest concentration of CT (1 mg/mL) was examined by transmission electron microscopy, which revealed clear damage with marked irregularity of the cuticular surface, in contrast to the smooth surface observed in control

worms (Figure 5). In addition, the underlying hypodermis appeared to be torn and detached from the basal layer of the cuticle, with rupturing and lesions also observed within the hypodermis itself (Figure 5).

Discussion

Continued reliance on mass drug administration with a limited number of synthetic anthelmintics has the potential to place heavy selection pressure on drug-resistant parasites, and widespread anthelmintic drug resistance is already a serious problem in many livestock production systems. The use of natural dietary compounds has the potential to be a complementary control option which

Figure 5 Effects of condensed tannins on motility and morphology of adult *Oesophagostomum dentatum*. A – Inhibition of *O. dentatum* adult motility by hazelnut skin extract. Results are from a single experiment performed in triplicate. **B** – Transmission-electron microscopy of thin sections of adult worms exposed to only medium ('control') or 1 mg/mL of hazelnut skin extract ('CT') for 24 hours. 'cu' – cuticle; 'hy' – hypodermis. Note the rough cuticle in worms exposed to CT (black arrows), and rupture and detachment of the hypodermis (white arrows). Scale bar =2 μM.

may reduce this reliance on drug treatment, and slow the development of resistance. Here we have carried out a comprehensive *in vitro* assessment of the effects of CT from five different plant sources on one of the most prevalent parasites of pigs, *O. dentatum*.

We found that the development of free-living larvae was potently inhibited by all five extracts from CT-containing plants. This larval development assay is commonly used to screen potential anthelmintic compounds [26], however it has the drawback of focusing on stages of the parasite life cycle which are not exposed to the compound *in vivo*. Therefore, it cannot be automatically assumed that results observed with these free-living stages can be extrapolated to the parasitic stages found within the GI tract. Indeed, we found that a concentration (1 mg/mL) that completely inhibited larval development with all five extracts had only modest inhibitory effects against migration of exsheathed L3 parasites. Hazelnut skin, blackcurrant leaf and white clover flower extracts had no significant effects on larval migration, whilst extracts from willow bark and *Tilia* flowers did significantly inhibit migration but only by 20-30% - an

319

effect considerably less than the 95% inhibition observed after incubation in ivermectin. Therefore, it is apparent that whilst some CT-containing extracts can inhibit migration of infective larvae, overall the anthelmintic effect is less pronounced against this early parasitic stage than against free-living larvae. Therefore, our results highlight the importance of assessing putative anthelmintic compounds against not only free-living parasites but also parasitic stages. The active compounds within *Tilia* flowers and willow bark were confirmed as CT by both PVPP-incubation and fractionation experiments, which demonstrated that anthelmintic activity was retained in CT fractions of 80-90% purity. It is interesting to contrast the results obtained here with our previous work with another pig nematode, *A. suum*, where incubation of L3 in comparable concentrations of CT led to a substantially higher inhibition of larval migration [17]. This suggests that not all helminth species are equally susceptible to the anthelmintic effects of CT, and careful assessment of activity is necessary before the suitability of these natural anti-parasitic compounds can be considered as viable control options in varying host-parasite systems.

Moulting of L3 to L4 parasites was significantly reduced after incubation in hazelnut skin, willow bark or *Tilia* flower extracts. Moreover, it was apparent that the motility of L4 was also reduced after incubation in extracts and fractions from the five plant sources. In the L3/L4 moulting assay, the motility and survival of the larvae was not affected by CT (data not shown), indicating that the reduction of development to L4 may be related to inhibition of specific metabolic processes involved in the moulting process [27]. To our knowledge, this is the first report that plant extracts can specifically inhibit the moulting process of a parasitic nematode, and further experiments are warranted to determine the mechanisms behind this inhibitory effect. It is also notable that adult worms appeared to be quite susceptible to the anthelmintic properties of CT. Further experiments with adult worms were not possible due to lack of parasite material, however the clear and rapid reductions in motility in adults exposed to the hazelnut skin extract indicate a potent effect. This suggests that dietary CT could potentially be used as a therapeutic option to specifically target adult worms and potentially prevent egg excretion and environmental contamination; however, further experiments will be necessary to explore this possibility. Overall, these experiments highlighted that while all stages of the parasite life cycle appeared to have some susceptibility to the plant extracts, clear differences between stages were observed. Interestingly, a recent study has also reported that a selection of medicinal plant extracts have increased activity towards *Caenorhabditis elegans* adults as compared to L3 or L4 stages, perhaps consistent with our results [28]. This

has clear implications for the potential use of these plants for parasite control measures, as well as raising mechanistic questions about the observed anthelmintic activities.

Besides the quantity of CT, the structural characteristics of the polymers such as molecular weight and the ratio of different flavanol monomer units are known to affect anthelmintic activity [29,30]. In the current experiments, anthelmintic activity appeared to be associated with the higher molecular weight F2 fractions, suggesting that the anthelmintic activity in the extracts derives from CT with a high degree of polymerisation, consistent with previous studies with *A. suum* and *O. ostertagi* [17,29]. Moreover, extracts from *Tilia* flowers and willow bark were more potent in the L3 migration assays than hazelnut skin, white clover flower and blackcurrant extracts. Furthermore, *Tilia* flower, willow bark and hazelnut skin extracts significantly inhibited larval moulting, whereas white clover flower and blackcurrant extracts had no effect. Extracts and fractions derived from *Tilia* flowers also appeared to be most potent in the L4 motility assays, even when purified fractions were used with normalised concentrations of CT. Therefore, the observed differences in potency between the different acetone/water extracts do not appear to be related to the quantity of CT. Tannins in *Tilia* flowers, hazelnut skin and willow bark are comprised mainly of PC, whilst white clover flowers and blackcurrant leaves contain PD [17,31,32]. This suggests that PC-rich extracts/fractions may have higher activity towards *O. dentatum*, which is somewhat surprising given that PD are generally considered to have higher biological activity than PC (and the same applies to their corresponding, monomeric flavanol constituents) due to an extra hydroxyl group in the B-ring favouring increased hydrogen bonding with proteins [33]. Indeed, the monomeric constituents of PD (gallocatechin and epigallocatechin) have been shown to have higher anthelmintic activity than catechin and epicatechin against the ruminant nematodes *Trichostrongylus colubriformis and Haemonchus contortus* [30,34], and a correlation has also been noted between the proportion of PD in polymeric CT and anthelmintic activity against *O. ostertagi* [29]. Further studies with larger panels of well-characterised CT fractions will be necessary to determine if the PC:PD ratio plays a role in the anthelmintic effects observed here.

Given the overall lower efficacy of the isolated molecules against *O. dentatum* than comparable studies with *A. suum* [17], it may be that the mechanism of action of CT against *O. dentatum* is subtly different than to other helminths. At present, the anthelmintic mode-of-action of CT is not known, but is proposed to involve biochemical interactions between CT and proline-rich proteins on the nematode sheath or cuticle that interfere with both worm motility and feeding, and also key metabolic

processes such as exsheathment (and perhaps also moulting, as suggested by our current data). This is supported by electron microscopy studies of worms exposed to CT that demonstrate direct structural damage to the cuticle [17,35], consistent with the ultrastructural changes we observed in the present study with adult *O. dentatum*. Such a mechanism would appear to be fairly non-specific and broad-spectrum in nature, hence it is interesting to note the differences in susceptibility between different nematodes. *O. dentatum* falls within the Strongyloididea superfamily of nematodes, a distinct family from the Ascaraidoidea (e.g. *A. suum*) and Trichostrongylidae (e.g. *T. colubriformis* and *O. ostertagi*) superfamilies [36], and this divergence may represent biological differences that determine susceptibility to CT. Comparative studies of these two nematodes, including transcriptomic and proteomic analyses of worms exposed to equivalent amounts of CT, may shed some light on the more precise mechanisms of the anthelmintic effect, and such studies are on-going in our laboratory. The marked differences in the response of *O. dentatum* during free-living development and adults to CT, compared to L3 stages, is also deserving of further studies to determine the mechanisms responsible.

An important consideration is how these *in vitro* results may be translated to *in vivo* studies in pigs. Experimental use of CT as an alternative anthelmintic in livestock has been characterised by two (somewhat overlapping) approaches, these being either short term consumption with the aim of either reducing establishment of incoming larvae or targeted therapeutic administration to remove adult worms [37,38], or long-term incorporation into the diet with the aim of disturbing key processes throughout the parasite life cycle, resulting in cumulative anthelmintic effects [39,40]. The fact that multiple processes in the life cycle of *O. dentatum* are affected by CT raises the possibility of a cumulative anthelmintic effect *in vivo*, whereby if a diet is consumed which contains CT, the additive sub-lethal effects against the different life cycle stages may reduce the viability and perhaps fecundity of worms as they mature within the host. In addition, the apparent susceptibility of adult worms to relatively low concentrations of CT raises the possibility of short-term feeding of CT as a complementary or alternative option to therapeutic drug treatment. Further *in vivo* studies to explore these options are necessary.

Moreover, the location of *O. dentatum* within the GI tract needs to be considered. Whilst there are a plethora of *in vivo* studies on the effects of CT-containing plants on worm infections in sheep and goats, as well as several rodent studies, most of these have focused on worms that reside in the stomach or small intestine, and thus there is only limited information on the effects of dietary CT upon large intestinal parasites. There is some evidence that pigs

fed tannin-containing acorns (albeit hydrolysable tannins, quite different in structure to the CT tested here) have marked reductions in *O. dentatum* egg excretion [41]. However, sheep grazing the PC-rich forage *Lotus corniculatus* did not have reductions in burdens of *Oesophagostomum* spp., despite significant reductions in numbers of the abomasal parasite *H. contortus* and the small intestinal worm *Cooperia curticei* [42]. These authors speculated that changes to the structure of CT molecules in distal parts of the GI tract could affect anthelmintic activity. Whilst polymeric CT molecules are poorly absorbed from the GI tract [43], some fermentation and/or bacterial degradation of CT can occur in the monogastric large intestine [44-46]. This implies that dietary CT that are efficacious against parasites residing in the upper regions of the GI tract may not have comparable activity against parasites in distal regions, due to increased breakdown and a decrease in polymerization which may reduce potency. Therefore, further studies should focus on elucidating concentrations of CT in the local gut environments and whether polymeric CT retain their structure and anthelmintic activity through the entirety of the GI system.

Conclusion

We have for the first time shown anthelmintic effects of CT-containing plant extracts and purified CT fractions against *O. dentatum*, and demonstrated that free-living/non-infective stages and adults appear to be highly susceptible to the effects of CT, whereas L4 are less susceptible and L3 are only modestly affected. Moreover, the moulting of L3 to L4 can be inhibited by CT, suggesting that specific, key processes in the parasite life cycle can be disrupted by CT. These data encourage further investigations to determine *in vivo* efficacy in pigs. In addition, further mechanistic studies, such as the relationship between the fine structure of CT molecules and anthelmintic activity, are also a high priority.

Author details
[1]Department of Veterinary Disease Biology, Faculty of Health and Medical Sciences, University of Copenhagen, Frederiksberg, Denmark. [2]Chemistry and Biochemistry Laboratory, School of Agriculture, Policy and Development, University of Reading, Reading, UK.

References
1. Keiser J, Utzinger J: Efficacy of current drugs against soil-transmitted helminth infections: Systematic review and meta-analysis. *JAMA* 2008, 299(16):1937–1948.
2. Charlier J, van der Voort M, Kenyon F, Skuce P, Vercruysse J: Chasing helminths and their economic impact on farmed ruminants. *Trends Parasitol* 2014, 30(7):361–367.
3. Fitzpatrick JL: Global food security: The impact of veterinary parasites and parasitologists. *Vet Parasitol* 2013, 195(3–4):233–248.
4. Sutherland IA, Leathwick DM: Anthelmintic resistance in nematode parasites of cattle: a global issue? *Trends Parasitol* 2011, 27(4):176–181.
5. Sargison ND: Pharmaceutical treatments of gastrointestinal nematode infections of sheep—Future of anthelmintic drugs. *Vet Parasitol* 2012, 189(1):79–84.
6. Githioñ JB, Höglund J, Waller PJ: Ethnoveterinary plant preparations as livestock dewormers: practices, popular beliefs, pitfalls and prospects for the future. *Anim Health Res Rev* 2005, 6(01):91–103.
7. Athanasiadou S, Githiori J, Kyriazakis I: Medicinal plants for helminth parasite control: facts and fiction. *Animal* 2007, 1(09):1392–1400.
8. Tolossa K, Debela E, Athanasiadou S, Tolera A, Ganga G, Houdijk J: Ethnomedicinal study of plants used for treatment of human and livestock ailments by traditional healers in South Omo, Southern Ethiopia. *J Ethnobiol Ethnomed* 2013, 9(1):32.
9. Cowan MM: Plant Products as Antimicrobial Agents. *Clin Microbiol Rev* 1999, 12(4):564–582.
10. Mueller-Harvey I: Unravelling the conundrum of tannins in animal nutrition and health. *J Sci Food Agric* 2006, 86(13):2010–2037.
11. Martinez-Micaelo N, González-Abuin N, Ardèvol A, Pinent M, Blay MT: Procyanidins and inflammation: Molecular targets and health implications. *Biofactors* 2012, 38(4):257–265.
12. González R, Ballester I, López-Posadas R, Suárez MD, Zarzuelo A, Martínez-Augustin O, Medina FSD: Effects of flavonoids and other polyphenols on inflammation. *Crit Rev Food Sci Nutr* 2011, 51(4):331–362.
13. Butter NL, Dawson JM, Wakelin D, Buttery PJ: Effect of dietary condensed tannins on gastrointestinal nematodes. *J Agric Sci* 2001, 137(04):461–469.
14. Heckendorn F, Häring DA, Maurer V, Zinsstag J, Langhans W, Hertzberg H: Effect of sainfoin (*Onobrychis viciifolia*) silage and hay on established populations of *Haemonchus contortus* and *Cooperia curticei* in lambs. *Vet Parasitol* 2006, 142(3–4):293–300.
15. Brunet S, Jackson F, Hoste H: Effects of sainfoin (*Onobrychis viciifolia*) extract and monomers of condensed tannins on the association of abomasal nematode larvae with fundic explants. *Int J Parasitol* 2008, 38(7):783–790.
16. Novobilský A, Mueller-Harvey I, Thamsborg SM: Condensed tannins act against cattle nematodes. *Vet Parasitol* 2011, 182(2–4):213–220.
17. Williams AR, Fryganas C, Ramsay A, Mueller-Harvey I, Thamsborg SM: Direct anthelmintic effects of condensed tannins from diverse plant sources against *Ascaris suum*. *PLoS One* 2014, 9(5):e97053.
18. Roepstorff A, Mejer H, Nejsum P, Thamsborg SM: Helminth parasites in pigs: New challenges in pig production and current research highlights. *Vet Parasitol* 2011, 180(1–2):72–81.
19. Hale OM, Stewart TB, Marti OG, Wheat BE, McCormick WC: Influence of an experimental infection of nodular worms (*Oesophagostomum* spp.) on performance of pigs. *J Anim Sci* 1981, 52(2):316–322.
20. Stewart TB, Hale OM: Losses to internal parasites in swine production. *J Anim Sci* 1988, 66(6):1548–1554.
21. Gerwert S, Failing K, Bauer C: Prevalence of levamisole and benzimidazole resistance in *Oesophagostomum* populations of pig-breeding farms in North Rhine-Westphalia, Germany. *Parasitol Res* 2002, 88(1):63–68.
22. Dangolla A, Bjørn H, Willeberg P, Barnes EH: Faecal egg count reduction percentage calculations to detect anthelmintic resistance in *Oesophagostomum* spp. in pigs. *Vet Parasitol* 1997, 68(1–2):127–142.
23. Gasser RB, Cottee P, Nisbet AJ, Ruttkowski B, Ranganathan S, Joachim A: *Oesophagostomum dentatum* — Potential as a model for genomic studies of strongylid nematodes, with biotechnological prospects. *Biotechnol Adv* 2007, 25(3):281–293.
24. Várady M, Bjørn H, Craven J, Nansen P: In vitro characterization of lines of *Oesophagostomum dentatum* selected or not selected for resistance to pyrantel, levamisole and ivermectin. *Int J Parasitol* 1997, 27(1):77–81.
25. Stepek G, Buttle DJ, Duce IR, Lowe A, Behnke JM: Assessment of the anthelmintic effect of natural plant cysteine proteinases against the gastrointestinal nematode, *Heligmosomoides polygyrus*, in vitro. *Parasitology* 2005, 130(02):203–211.
26. Kotze AC: Target-based and whole-worm screening approaches to anthelmintic discovery. *Vet Parasitol* 2012, 186(1–2):118–123.
27. Ondrovics M, Silbermayr K, Mitreva M, Young ND, Razzazi-Fazeli E, Gasser RB, Joachim A: Proteomic Analysis of *Oesophagostomum dentatum* (Nematoda) during Larval Transition, and the Effects of Hydrolase Inhibitors on Development. *PLoS One* 2013, 8(5):e63955.
28. Kumarasingha R, Palombo EA, Bhave M, Yeo TC, Lim DSL, Tu CL, Shaw JM, Boag PR: Enhancing a search for traditional medicinal plants with anthelmintic action by using wild type and stress reporter *Caenorhabditis elegans* strains as screening tools. *Int J Parasitol* 2014, 44(5):291–298.
29. Novobilský A, Stringano E, Hayot Carbonero C, Smith LMJ, Enemark HL, Mueller-Harvey I, Thamsborg SM: In vitro effects of extracts and purified tannins of sainfoin (*Onobrychis viciifolia*) against two cattle nematodes. *Vet Parasitol* 2013, 196(3–4):532–537.
30. Brunet S, Hoste H: Monomers of Condensed Tannins Affect the Larval Exsheathment of Parasitic Nematodes of Ruminants. *J Agric Food Chem* 2006, 54(20):7481–7487.
31. Esatbeyoglu T, Wray V, Winterhalter P: Dimeric procyanidins: screening for B1 to B8 and semisynthetic preparation of B3, B4, B6, and B8 from a polymeric procyanidin fraction of White Willow bark (*Salix alba*). *J Agric Food Chem* 2010, 58(13):7820–7830.
32. Ropiak HM, Ramsay A, Mueller-Harvey I: Condensed tannins from European medicinal plants. In *Polyphenol Communications (Proceedings of the XXVIIth International Conference on Polyphenols & 8th tannin conference)*. Nagoya, Japan: Groupe Polyphenols; 2014:609–610.
33. Scalbert A: Antimicrobial properties of tannins. *Phytochemistry* 1991, 30(12):3875–3883.
34. Molan AL, Meagher LP, Spencer PA, Sivakumaran S: Effect of flavan-3-ols on in vitro egg hatching, larval development and viability of infective larvae of *Trichostrongylus colubriformis*. *Int J Parasitol* 2003, 33(14):1691–1698.
35. Brunet S, Fourquaux I, Hoste H: Ultrastructural changes in the third-stage, infective larvae of ruminant nematodes treated with sainfoin (*Onobrychis viciifolia*) extract. *Parasitol Int* 2011, 60(4):419–424.
36. Roberts LS, Janovy J: *Foundations of Parasitology.* 6th edition. Singapore: McGraw-Hill; 2000.
37. Athanasiadou S, Kyriazakis I, Jackson F, Coop RL: Direct anthelmintic effects of condensed tannins towards different gastrointestinal nematodes of sheep: in vitro and in vivo studies. *Vet Parasitol* 2001, 99(3):205–219.
38. Brunet S, Montellano CM-O, Torres-Acosta JFJ, Sandoval-Castro CA, Aguilar-Caballero AJ, Capetillo-Leal C, Hoste H: Effect of the consumption of *Lysiloma latisiliquum* on the larval establishment of gastrointestinal nematodes in goats. *Vet Parasitol* 2008, 157(1–2):81–88.
39. Hoste H, Martinez-Ortiz-De-Montellano C, Manolaraki F, Brunet S, Ojeda-Robertos N, Fourquaux I, Torres-Acosta JFJ, Sandoval-Castro CA: Direct and indirect effects of bioactive tannin-rich tropical and temperate legumes against nematode infections. *Vet Parasitol* 2012, 186(1–2):18–27.
40. Niezen JH, Robertson HA, Waghorn GC, Charleston WAG: Production, faecal egg counts and worm burdens of ewe lambs which grazed six contrasting forages. *Vet Parasitol* 1998, 80(1):15–27.
41. Salajpal K, Karolyi D, Beck R, Kis G, Vickovic I, Dikic M, Kovacic D: Effect of acorn (*Quercus robur*) intake on faecal egg count in outdoor reared black Slavonian pig. *Acta Agric Slovenica* 2004, 84(Supplement 1):173–178.
42. Ramírez-Restrepo CA, Barry TN, Pomroy WE, López-Villalobos N, McNabb WC, Kemp PD: Use of *Lotus corniculatus* containing condensed tannins to increase summer lamb growth under commercial dryland farming conditions with minimal anthelmintic drench input. *Anim Feed Sci Tech* 2005, 122(3–4):197–217.
43. Reed JD: Nutritional toxicology of tannins and related polyphenols in forage legumes. *J Anim Sci* 1995, 73(5):1516–1528.

44. Déprez S, Brezillon C, Rabot S, Philippe C, Mila I, Lapierre C, Scalbert A: Polymeric proanthocyanidins are catabolized by human colonic microflora into low-molecular-weight phenolic acids. *J Nutr* 2000, **130**(11):2733–2738.
45. Gu L, House SE, Rooney L, Prior RL: Sorghum bran in the diet dose dependently increased the excretion of catechins and microbial-derived phenolic acids in female rats. *J Agric Food Chem* 2007, **55**(13):5326–5334.
46. Touriño S, Pérez-Jiménez J, Mateos-Martín ML, Fuguet E, Vinardell MP, Cascante M, Torres JL: Metabolites in contact with the rat digestive tract after ingestion of a phenolic-rich dietary fiber matrix. *J Agric Food Chem* 2011, **59**(11):5955–5963.

Appendix H

Original publication:

Efficacy of condensed tannins against larval *Hymenolepis diminuta* (Cestoda) *in vitro* and in the intermediate host *Tenebrio molitor* (Coleoptera) *in vivo*

Suraj Dhakal, Nicolai V. Meyling, Andrew R. Williams, Irene Mueller-Harvey, Christos Fryganas, Christian M.O. Kapel, Brian L. Fredensborg

Efficacy of condensed tannins against larval *Hymenolepis diminuta* (Cestoda) *in vitro* and in the intermediate host *Tenebrio molitor* (Coleoptera) *in vivo*

Suraj Dhakal[a], Nicolai V. Meyling[a], Andrew R. Williams[b],
Irene Mueller-Harvey[c], Christos Fryganas[c], Christian M.O. Kapel[a],
Brian L. Fredensborg[a,*]

[a] *Department of Plant and Environmental Sciences, Faculty of Science, University of Copenhagen, Frederiksberg C, Denmark*
[b] *Department of Veterinary Disease Biology, Faculty of Health and Medical Sciences, University of Copenhagen, Frederiksberg C, Denmark*
[c] *Chemistry and Biochemistry Laboratory, School of Agriculture, Policy and Development, University of Reading, Reading, United Kingdom*

ARTICLE INFO

ABSTRACT

Natural anti-parasitic compounds in plants such as condensed tannins (CT) have anthelmintic properties against a range of gastrointestinal nematodes, but for other helminths such effects are unexplored. The aim of this study was to assess the effects of CT from three different plant extracts in a model system employing the rat tapeworm, *Hymenolepis diminuta*, in its intermediate host, *Tenebrio molitor*. An *in vitro* study examined infectivity of *H. diminuta* cysticercoids (excystation success) isolated from infected beetles exposed to different concentrations of CT extracts from pine bark (PB) (*Pinus sps*), hazelnut pericarp (HN) (*Corylus avellana*) or white clover flowers (WC) (*Trifolium repens*), in comparison with the anthelmintic drug praziquantel (positive control). In the *in vitro* study, praziquantel and CT from all three plant extracts had dose-dependent inhibitory effects on cysticercoid excystation. The HN extract was most effective at inhibiting excystation, followed by PB and WC. An *in vivo* study was carried out on infected beetles (measured as cysticercoid establishment) fed different doses of PB, HN and praziquantel. There was a highly significant inhibitory effect of HN on cysticercoid development ($p = 0.0002$). Overall, CT showed a promising anti-cestodal effect against the metacestode stage of *H. diminuta*.

© 2014 Elsevier B.V. All rights reserved.

1. Introduction

For decades, parasite control in livestock has relied intensively on prophylactic treatment with synthetic anthelmintics, but increasing resistance to such drugs and consumer requests for organic animal products increases the need for alternative control strategies. Bioactive plants may offer potential alternatives for parasite control in vertebrates (Waller and Thamsborg, 2004). Condensed tannins (CT) are a group of secondary metabolites commonly found in tropical and temperate plants (Jansman, 1993). They vary widely in their molecular weights and the identity of the monomeric flavan-3-ol units, which make up the tannin polymers. Procyanidins (PC) consist of catechin or epicatechin, whereas prodelphinidins (PD) are comprised of gallocatechin or epigallocatechin flavan-3-ols (Williams et al., 2014). More complex CT

* Corresponding author at: Department of Plant and Environmental Sciences, Faculty of Science, University of Copenhagen, Thorvaldsensvej 40, Room 70-3-B324, Frederiksberg C, Copenhagen, Denmark. Tel.: +45 35 33 26 76.
E-mail address: blf@plen.ku.dk (B.L. Fredensborg).

structures may occur as heteropolymers (Mueller-Harvey and McAllan, 1992; Molan et al., 2003). Several laboratory and field experiments have shown that plant CT may control gastro-intestinal nematodes (Hoste et al., 2006; Novobilský et al., 2011, 2013). Besides anthelminthic properties, these bioactive plant products can also have beneficial effects on animal health and production (Hoskin et al., 2000; Ramírez-Restrepo et al., 2004; Hoste et al., 2005, 2006), and reduce the level of host infection (Hoste et al., 2012). Although, *in vitro* anthelmintic efficacy of natural plant cysteine proteinases has also been reported against excysted scolices and adult worms of the rodent cestodes *Hymenolepis diminuta* and *Hymenolepis microstoma* (Mansur et al., 2014), the effect of CT against helminth taxa other than nematodes has not yet been investigated.

Due to close resemblance of drug effects between animals and humans (Lin, 1995), mammals are often used in pre-clinical pharmacological and toxicological assessment of new compounds (Baumans, 2004). International awareness on animal experimentation has enforced the focus on the "3Rs" to Reduce, Replace and Refine (nc3rs, 2014). An insect model could present an alternative to a range of experimental studies, *e.g.* as a model for human microbiology (Tan, 2002; Kavanagh and Reeves, 2004) and immunology (Pursall and Rolff, 2011). Further, invertebrate models may simplify and reduce costs of laboratory maintenance (Scully and Bidochka, 2006; Vokřál et al., 2012) and ease concerns associated with animal experimentation (Kemp and Massey, 2007).

In the present study, a host–parasite model employing the flour beetle *Tenebrio molitor* (Coleoptera) and the rat tapeworm *H. diminuta* (Cestoda) was used to investigate the anti-cestodal effects of CT in three different plant extracts. *T. molitor–H. diminuta* is a well-known host–parasite model for studies on ecological and evolutionary host–parasite relationships (Shostak, 2014), and Woolsey (2012) studied its potential for pre-clinical screening of anthelmintics (praziquantel, levamisole hydrochloride and mebendazole).

In the natural lifecycle, rats excrete infective *H. diminuta* eggs which are ingested by the flour beetles where they encyst as larvae (cysticercoid) in the hemocoel (Burt, 1980). The life cycle completes when an infected beetle is eaten by a rat, in which the cysticercoid excysts, attaches to the intestinal wall and develops into an egg producing tapeworm (Chappell et al., 1970). Since the development of egg into cysticercoid and its excystation plays a crucial role in maintaining the life-cycle of *H. diminuta*, interruption of these processes with CT would indicate that CT contains anti-cestodal properties.

The objective of the present study was to assess the anti-cestodal effects of three different CT types against cysticercoids of *H. diminuta* both freely exposed (*in vitro*) and within their intermediate host (*in vivo*), at a range of concentrations.

2. Materials and methods

The *in vitro* experiments were performed with cysticercoids dissected from experimentally infected beetles. The effect of CT was measured as a reduction of excystation

of cysticercoids, which serves as an important measure (proxy) for infectivity to rats. The *in vivo* study was conducted in live beetles in order to measure the establishment of cysticercoids in the presence of CT.

2.1. Condensed tannins and praziquantel

Condensed tannins were extracted and purified from three different plant sources. These were pine bark (PB) (*Pinus sp*), hazelnut pericarp (HN) (*Corylus avellana*) and white clover flowers (WC) (*Trifolium repens*). Most tannin-rich plants contain complex mixtures of procyanidins (PC) and prodelphinidins (PD), however our previous work has demonstrated that these three plants contain narrower tannin profiles, *i.e.* mainly PC or PD (Williams et al., 2014). Therefore, we used these plants as a source of well-defined model tannins that would allow us to investigate whether the molecular structure of the tannins influenced possible anti-parasitic activity. Tannins were extracted and analyzed as previously described (Williams et al., 2014). Briefly, 50 g of plant material was extracted with acetone/water (7:3; v/v) at room temperature, concentrated and freeze-dried. Tannin analysis was carried out by thiolytic degradation of the polymers and subsequent HPLC analysis of the reaction products, providing information on CT content in the extract, the mean degree of polymerization (mDP, *i.e.* average CT polymer size) and the PC/PD ratio (Williams et al., 2014). Pine bark contained 50.8 g CT/100 g extract, with an mDP value of 2.5 and a PC/PD ratio of 64.2. Hazelnut pericarp contained 73.8 g CT/100 g extract with an mDP value of 9.6 and a PC/PD ratio of 79.5. White clover contained 33.8 g CT/100 g extract with an mDP value of 4.4 and, in contrast to the other extracts, its tannins were almost exclusively comprised of PD, *i.e.* the PC/PD ratio was 0.8/99.2 (Williams et al., 2014). The well-known anti-cestodal drug praziquantel (99.7%, VETRANAL^{TM}) was used as a positive control for both *in vitro* and *in vivo* studies.

2.2. Management of the beetles

T. molitor larvae (obtained from Avifauna ApS, Denmark) were propagated in plastic containers ($30 \times 21 \times 20$ cm), placed in a dark incubator (26 °C), and provided with fresh oatmeal and fresh slices of potato. The potato slices were changed twice a week. After 2 weeks of incubation, pupae started to develop and these were then transferred into another plastic container ($30 \times 21 \times 20$ cm) and kept in a dark incubator (26 °C) until emergence of adults. Newly emerged adults were transferred to new plastic containers ($30 \times 21 \times 20$ cm) twice a week and held under the conditions described above.

2.3. Infection of beetles

Feces was collected from *H. diminuta* infected rats (*Rattus norvigecus* – Wistar strain) stabled at the Veterinary Institute, Technical University of Denmark (Animal permission no. 2010/561-1914 – section C10) and stored at 10 °C until use (two weeks maximum). Ten grams of fecal pellets were soaked 1 h in 25 ml of tap water and then stirred with a wooden stick to make a uniform paste. The fecal

paste was poured through a double layer of cotton gauze (1×1 mm pore size) into a 200 ml plastic cup, and the gauze was rinsed thoroughly with approximately 75 ml of tap water to increase egg recovery. The resulting suspension was equally transferred into two 50 ml centrifuge tubes. The tubes were centrifuged (Universal 16R) at 1148 g for 7 min. The supernatant was removed and the sediment was again stirred with a wooden stick. This fecal paste containing the *H. diminuta* eggs was used to infect the beetles.

Before administration of the paste, a group of 50 beetles were left without feed for 72 h in plastic containers ($30 \times 21 \times 20$ cm) with filter paper at the base, and stored in a dark incubator (26 °C). For infection, a 10 µl fecal suspension was deposited on a coverslip (1.5×1.5 cm) placed on filter paper in a series of petri dishes (5.5 cm diameter, 1.42 cm depth). A starved beetle was placed inside each Petri dish covered by a lid, and placed in a dark room for an hour. For assessment of eventual evaporation of the fecal suspension, one petri dish setup (without a beetle) was left an hour. Only beetles that had consumed the entire 10 µl of fecal suspension after 1 h were considered successfully inoculated and were included in the experiments.

2.4. In vitro study with praziquantel and pine bark extract

At 15 days post inoculation, beetles were dissected and cysticercoids were recovered using a Pasteur pipette under a dissection microscope ($40\times$). A maximum of 10 cysticercoids (first observed) from each beetle were transferred to a watch-glass (33 mm diameter, 7 mm deep) containing phosphate buffered saline (PBS) and a total of 80 cysticercoids were collected. From these, 10 cysticercoids (first observed) were placed in each of 8 wells (2 wells from 4 different 48 multi-well plastic plates). Then each well was treated with 150 µl of either praziquantel dissolved in 2% dimethyl sulfoxide (DMSO) with a final concentration of 10^{-2} (high concentration), 10^{-3} (medium concentration) or 10^{-4} mg/ml (low concentration), or CT extracts from PB dissolved in Milli-Q™ water at a final concentration of 0.1, 0.5 or 2.5 mg CT/ml. Control consisted of 2% DMSO or Milli-Q™ water. All plates were subsequently kept in an incubator at 37 °C for 1 h.

After 1 h of incubation, the 10 cysticercoids along with the respective treatment solution from each well were transferred separately to a watch glass and the treatment solution was then removed with a Pasture pipette under a dissection microscope. One ml of HCl-pepsin solution [2 ml 37% HCl, 20 ml warm 0.9% saline, 0.8 g pepsin powder from porcine gastric mucosa (1:2500, Sigma Life Science)] was added and placed in an incubator (37 °C). After 10 min of incubation, all the HCl-pepsin solution was removed. The cysticercoids were washed three times with 1 ml warm (37 °C) PBS and 1 ml of trypsin-taurocholate solution [0.1 g sodium taurocholate hydrate powder, 0.1 g trypsin powder from porcine pancreas, (97%, Sigma Life Science), 10 ml warm PBS] was added to the watch glass and placed in the incubator at 37 °C for 2.5 h. The cysticercoids were then observed under the dissection microscope ($40\times$) and recorded as excystated (complete evagination and emergence of scolex and body part from the cyst) or

non excystated (absence of the above) (Roberts and Janovy, 2008). This experiment was repeated five times.

2.5. In vitro study with pine bark, hazelnut and white clover extracts

Concentrations of PB, HN, and WC extracts were adjusted such that each extract contained equal final concentrations of CT in the assay. Three different concentrations: 2.5 (high concentration), 0.25 (medium concentration) and 0.025 mg CT/ml (low concentration) in Milli-Q™ water from each were prepared. Pure Milli-Q™ water was used as a control. The procedure was as described above (see: Section 2.4) and was repeated five times.

2.6. In vitro condensed tannin depletion assay

As the CT extracts used in this experiment were not 100% pure, CT depletion experiments were performed, to investigate whether inhibition of cysticercoid excystation was exclusively due to the effect of CT. A total volume of 250 µl solution with concentration 2.5 mg CT/ml of Milli-Q™ water was prepared separately from three types of CT extracts (PB, HN, and WC). For each solution, 12.5 mg of polyvinylpolypyrrolidone (PVPP) (at a dose rate of 50 mg PVPP/ml of solution) was added to precipitate CT, and was incubated (4 °C) overnight. After centrifugation at 3000 g for 5 min, supernatant (CT depleted extract) was removed and used in the test assay (Novobilský et al., 2011). As a control, each CT solution was also incubated (4 °C) overnight. The above procedure (see: Section 2.4) was then followed and was repeated three times.

2.7. In vivo study with praziquantel, pine bark and hazelnut extracts

Eighty uninfected beetles (7–14 days after eclosion) were randomly selected and depleted feed for 72 h as described above. Starved beetles were then randomly allocated into 8 groups, each with 10 beetles. The beetles of each group were presented individually to a droplet of 5 µl containing one of the following treatments: praziquantel (25, 50 and 100 mg/kg body weight of beetle), or PB (125, 250 and 500 mg CT/kg body weight of beetle), or 2% DMSO, or Milli-Q™ water for 15 min. Doses were formulated by measuring the average weight (+SE) of the beetles (103 ± 4.4 mg), which was calculated by weighing randomly allocated 25 beetles in 6 different groups. After 15 min, beetles that consumed the entire treatment solution were infected and maintained individually as described earlier (see: In vitro study).

After 15 days of incubation, 4 beetles were selected randomly from each treatment group for quantification of the establishment of cysticercoids. All cysticercoids in the haemocoel of the beetle were counted and recorded. The experiment for praziquantel and PB was repeated five and three times, respectively.

A separate study tested the effects of HN on cysticercoid establishment. A single dose of HN (500 mg CT/kg body weight) or a control (Milli-Q™ water) were fed to infected
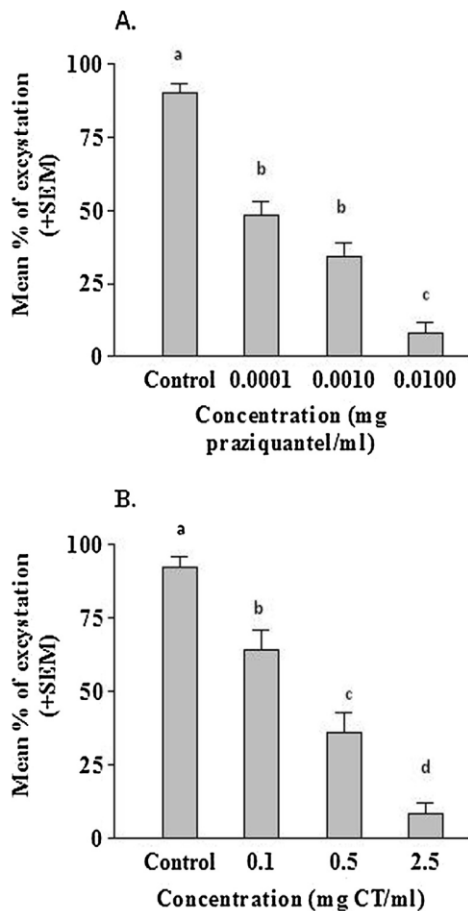
Fig. 1. *In vitro* mean percentage ($n = 5$, ±SEM) of cysticercoids excystation treated with praziquantel (A) and condensed tannin (CT) extract from pine bark (B) at different concentrations. Ten cysticercoids were used for each concentration. Control refers to 2% DMSO for (A) and to Milli-Q™ water for (B). Different letters within each figure represent statistical significance ($\alpha = 0.05$).

Fig. 2. *In vitro* mean percentage ($n = 5$, ±SEM) of cysticercoids excystation treated with three different condensed tannin (CT) extracts [white clover flower (WC), pine bark (PB), and hazelnut skin (HN)] at different concentrations. Ten cysticercoids were used for each concentration. Control refers to Milli-Q™ water. Different letters within each figure represent statistical significance ($\alpha = 0.05$).

beetles and all the procedures were done as described above, and was repeated three times.

2.8. Data analysis

All statistical analyses were performed using SAS® version 9.3 (SAS Institute Inc, Cary, North Carolina). Data from the *in vitro* study (except the CT depletion assay) fulfilled all three assumptions of ANOVA. So, the proportions of cysticercoid excystation in treatment groups were analyzed using PROC GLM fitting repetitions of experiments as a random variable. When an overall significant effect was seen, pair-wise comparisons were done using a *post hoc* Tukey test. The data from the CT depletion assay were analyzed by using a non-parametric Wilcoxon rank sum test. In the *in vivo* study, the numbers of cysticercoids established in the treatment groups were analyzed using PROC GENMOD, fitting negative binomial distributions. When overall differences were observed individual comparisons were done using least square means.

3. Results

3.1. In vitro study with praziquantel and pine bark extract

All concentrations of praziquantel and PB significantly reduced the mean percentage of cysticercoid excystation compared to their respective controls (Fig. 1A and B) and a significant concentration dependent effect was observed for both treatments with the highest concentrations having the strongest inhibitory effect on excystation ($F_{2,4} = 26.87$, $p = 0.0003$ for praziquantel and $F_{2,4} = 25.57$, $p = 0.0003$ for PB). The cysticercoid excystation inhibitory effect was the same for the praziquantel and PB treatments ($F_{1,4} = 0.49$, $p = 0.4887$).

3.2. In vitro study with pine bark, hazelnut and white clover extracts

The mean percentages of excystation of cysticercoids after exposure to the three CT were significantly different among the treatment groups ($F_{3,4} = 28.37$, $p < 0.0001$) and concentrations ($F_{2,4} = 110.58$, $p < 0.0001$; Fig. 2) and there was an interaction between treatment groups and concentrations ($F_{4,4} = 5.48$, $p = 0.0015$). Concentration was found to be a significant parameter for all three CT with the highest concentrations having the strongest negative effect on excystation ($F_{2,4} = 66.48$, $p < 0.0001$ for PB, $F_{2,4} = 9.97$, $p = 0.0067$ for HN and WC).

The mean percentage of cysticercoid excystation with all three CT depleted solutions showed significantly more cysticercoid excystation compared to their respective controls ($\chi^2 = 4.09$, $df = 1$, $p = 0.043$ for PB and WC, $\chi^2 = 3.97$, $df = 1$, $p = 0.043$ for HN; Fig. 3).

3.3. In vivo study with praziquantel, pine bark and hazelnut extracts

There was a significant effect of treatment (praziquantel and PB) on cysticercoid establishment ($\chi^2 = 133.1$, $df = 3$, $p < 0.0001$) but the effect was not dose dependent ($\chi^2 = 1.92$, $df = 2$, $p = 0.382$). All three doses of praziquantel reduced cysticercoid establishment to almost zero while each beetle in the control treatment had +SE 27.1 ± 6.65
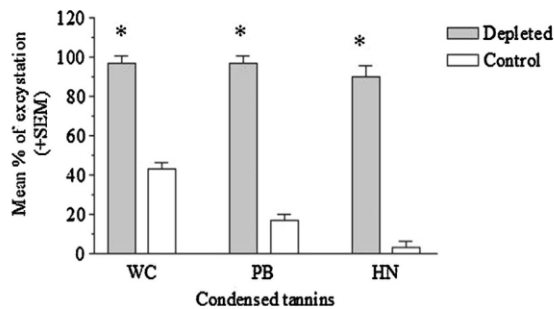
Fig. 3. *In vitro* mean percentage (*n* = 3, ±SEM) of cysticercoid excystation treated with three different condensed tannin (CT) depleted solutions (depleted) and condensed tannin extract solutions (control) at 2.5 mg CT/ml concentration. Ten cysticercoids were used for each solution of white clover flower (WC), pine bark (PB) and hazelnut pericarp (HN). *Refers to a significant difference relative to the respective controls.

cysticercoids (Fig. 4A), whereas the effect of CT from PB at all doses did not differ from the control, although there was a trend of reduced establishment (*p* = 0.841, 0.374 and 0.098 for low, medium and high doses respectively; Fig. 4B).

The separate experiment with HN at 500 mg CT/kg beetle body weight revealed significantly lower cysticercoid establishment (mean cysticercoids per beetle +SE: 25.5 ± 2.54) in comparison to the control group (mean cysticercoids per beetle +SE: 36.3 ± 2.33) (χ^2 = 10.48, d*f* = 1, *p* = 0.0012).

4. Discussion

The results from the *in vitro* study suggest that treatment with CT from three different plants (PB, HN and WC) and praziquantel can substantially reduce the excystation of *H. diminuta* cysticercoids in a concentration-dependent manner. A similar concentration-dependent inhibitory effect of praziquantel has been previously shown using the same model (Woolsey, 2012). Our *in vivo* results showed that PB did not significantly inhibit cysticercoid establishment, but praziquantel and HN were associated with a

reduction in the number of established cysticercoids. The cysticercoid excystation inhibitory effect of CT from the three plant extracts disappeared in the presence of tannin-inhibitor polyvinylpolypyrrolidone (PVPP) (Hagerman and Butler, 1981), confirming that CT are the major active compounds for the observed inhibition. The observed effects of CT in this model are most likely due to their direct anti-parasitic activity, although additional, indirect effects by increasing host resistance may occur in mammals (Hoste et al., 2006).

The cysticercoid capsule, scolex and other cellular structures contain protein with polysaccharides and lipids (Burt, 1980). As CT are able to bind to proteins (Hoste et al., 2006), they might interact with the protein portion of the cystic capsule and alter its physical and chemical properties, as reported previously for *Trichostrongylus colubriformis*, where direct damage to the cuticle was observed after incubation with CT (Hoste et al., 2006). Condensed tannins might also interfere with enzyme activities, which are involved in metabolic pathways responsible for the development and functioning of parasites (Athanasiadou et al., 2001). Furthermore, due to the presence of pores and vesicles in the cystic capsule (Burt, 1980), bioactive compounds may reach the internal structures of the scolex and other cellular proteins. Taken together, all of these changes might interfere with the cysticercoid structures and metabolic pathways, which are essential in cysticercoid functioning and excystation. However, the exact mode of action of CT and the active compounds responsible for the anthelmintic activity are still unknown (Novobilský et al., 2013) and could differ depending on the species of parasite, its developmental stage, and possibly the biochemical characters and structures of the forage species (Min and Hart, 2003).

The different potency of CT from these plant extracts may be associated with the percentage of procyanidin monomer units or the mDP of the CT polymer, as the CT content in all three applied samples was standardized in the assays. However, HN also contains a small percentage of galloylated CTs (Irene Mueller-Harvey and Christos Fryganas, unpublished results), which may also
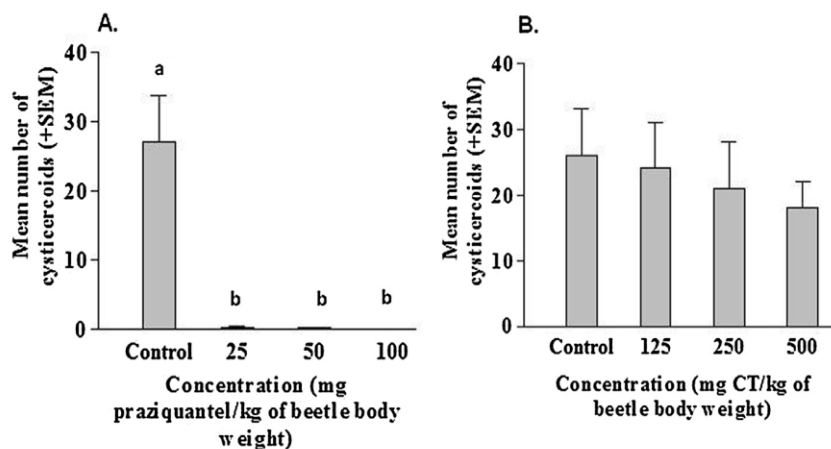

Fig. 4. *In vivo* mean number of cysticercoids (*n* = 5 for A and *n* = 3 for B, ±SEM) treated with praziquantel (A), and a condensed tannin (CT) extract from pine tree bark (B) at different concentrations. Average numbers of cysticercoids from four beetles were used for each treatment. Control refers to 2% DMSO in (A) and to Milli-Q™ water in (B).

influence anti-parasitic activity (Brunet and Hoste, 2006). The preliminary conclusion from this CT series is that the procyanidin tannins were more effective than prodelphinidin tannins in the *in vitro* and *in vivo* experiments. This is an unexpected finding as most other studies ascribed higher anthelmintic activities to the prodelphinidins (Brunet and Hoste, 2006). There may be two possible reasons: (1) the presence of galloylated CT in HN or (2) the fact that the pH values of insect guts tend to be alkaline (Gullan and Cranston, 2010) and are therefore quite different from the rumen or abomasum of ruminants. Relatively little is known about the reactivity of PC and PD tannins under alkaline conditions with constituents of the insect gut. Anthelminthic activities of CT from different plants or plant extracts are known to have markedly different effects on parasites. For example, grazing of sheep on *Lotus pedunculatus* reduced nematode fecal egg counts more effectively than grazing on *L. corniculatus* (Niezen et al., 1998), as *L. pedunculatus* has a higher PD/PC ratio than *L. corniculatus* (Foo et al., 1997). Thus, the multitude of different CT structures (Mueller-Harvey and McAllan, 1992) may influence their biological activities (Athanasiadou et al., 2001). Further experiments are needed to determine the relative contributions of mDP and PD/PC ratio on cysticercoid excystation.

Availability of free CT in the intestine may be important factor for CT to be effective. Formation and dissociation of the protein–CT complex is highly pH dependent. Stable protein–CT complexes are formed at pH 5–7, but the complexes easily dissociate and release proteins at higher and lower pH (Mueller-Harvey and McAllan, 1992). Optimum complex formation occurs at the isoelectric point of the protein, but little is known about the isoelectric point of proteins in the beetle gut. There is thus a possibility of lack of formation of protein–CT complex in the intestine of beetles or CT being subjected to oxidative changes.

In summary, our *in vitro* results indicate concentration dependent inhibitory effect of all tested CT in plant extracts on cysticercoid excystation, the HN extract being most potent, followed by PB and WC. Anti-excystation activity appeared to be positively linked to the presence of procyanidin tannins. The *in vivo* treatment with HN reduced cysticercoid establishment, and is the first observation on anti-cestodal properties of CT from plant extracts. Although the invertebrate–parasite model is not fully representative of the biological action of CT in the mammalian system, this model could be useful for a first screening of potentially interesting compounds. This invertebrate model has several advantages over vertebrate models as far as, ethical clearance, legislation, time and cost are concerned. Future studies will need to address the mechanism of CT action and include comparative studies with vertebrate animals in order to explore their effects against the different lifecycle stages and species of tapeworms.

Acknowledgements

References

Athanasiadou, S., Kyriazakis, I., Jackson, F., Coop, R.L., 2001. Direct anthelmintic effects of condensed tannins towards different gastrointestinal nematodes of sheep: *in vitro* and *in vivo* studies. Vet. Parasitol. 99, 205–219.

Baumans, V., 2004. Use of animals in experimental research: an ethical dilemma? Gene Ther. 11, S64–S66.

Brunet, S., Hoste, H., 2006. Monomers of condensed tannins affect the larval exsheathment of parasitic nematodes of ruminants. J. Agric. Food Chem. 54, 7481–7487.

Burt, M.D.B., 1980. Aspects of the life history and systematics of *Hymenolepis diminuta*. In: Arai, H.P. (Ed.), Biology of the Tapeworm *Hymenolepis diminuta*. Academic Press, New York, pp. 1–57.

Chappell, L.H., Arai, H.P., Dike, S.C., Read, C.P., 1970. Circadian migration of *Hymenolepis* (Cestoda) in the intestine – I observations on *H. diminuta* in the rat. Comp. Biochem. Physiol. 34, 31–46.

Foo, L.Y., Lu, Y., McNabb, W.C., Waghorn, G., Ulyatt, M.J., 1997. Proanthocyanidins from *Lotus pedunculatus*. Phytochemistry 45, 1689–1696.

Gullan, P.J., Cranston, P.S., 2010. The Insects: An Outline of Entomology. Wiley-Blackwell, UK, pp. 79.

Hagerman, A.E., Butler, L.G., 1981. The specificity of proanthocyanidin-protein interactions. J. Biol. Chem. 266, 4494–4497.

Hoskin, S.O., Wilson, P.R., Barry, T.N., Charleston, W.A.G., Waghorn, G.C., 2000. Effect of forage legumes containing condensed tannins on lungworm (*Dictyocaulus sp.*) and gastrointestinal parasitism in young red deer (*Cervus elaphus*). Res. Vet. Sci. 68, 223–230.

Hoste, H., Gaillard, L., Le Frileux, Y., 2005. Consequences of the regular distribution of *sainfoin* hay on gastrointestinal parasitism with nematodes and milk production in dairy goats. Small Rumin. Res. 59, 265–271.

Hoste, H., Jackson, F., Athanasiadou, S., Thamsborg, S.M., Hoskin, S.O., 2006. The effects of tannin-rich plants on parasitic nematodes in ruminants. Trends Parasitol. 22, 253–261.

Hoste, H., Martinez-Ortiz-De-Montellano, C., Manolaraki, F., Brunet, S., Ojeda-Robertos, N., Fourquaux, I., Torres-Acosta, J.F.J., Sandoval-Castro, C.A., 2012. Direct and indirect effects of bioactive tannin-rich tropical and temperate legumes against nematode infections. Vet. Parasitol. 186, 18–27.

Jansman, A.J.M., 1993. Tannins in feedstuffs for simple-stomached animals. Nutr. Res. Rev. 6, 209–236.

Kavanagh, K., Reeves, E.P., 2004. Exploiting the potential of insects for *in vivo* pathogenicity testing of microbial pathogens. FEMS Microbiol. Rev. 28, 101–112.

Kemp, M.W., Massey, R.C., 2007. The use of insect models to study human pathogens. Drug. Discov. Today Dis. Models 4, 105–110.

Lin, J.H., 1995. Species similarities and differences in pharmacokinetics. Drug Metab. Dispos. 23, 1008–1021.

Mansur, F., Luoga, W., Buttle, D.J., Duce, I.R., Lowe, A., Behnke, J.M., 2014. The anthelmintic efficacy of natural plant cysteine proteinases against two rodent cestodes *Hymenolepis diminuta* and *Hymenolepis microstoma in vitro*. Vet. Parasitol. 201, 48–58.

Min, B.R., Hart, S.P., 2003. Tannins for suppression of internal parasites. J. Anim. Sci. 81, E102–E109.

Molan, A.L., Meagher, L.P., Spencer, P.A., Sivakumaran, S., 2003. Effect of flavan-3-ols on *in vitro* egg hatching, larval development and viability of infective larvae of *Trichostrongylus colubriformis*. Int. J. Parasitol. 33, 1691–1698.

Mueller-Harvey, I., McAllan, A.B., 1992. Tannins: their biochemistry and nutritional properties. Adv. Plant Cell Biochem. Biotechnol. 1, 151–217.

nc3rs, 2014. http://www.nc3rs.org.uk/page.asp?id=7 (accessed 7.07.14).

Niezen, J.H., Robertson, H.A., Waghorn, G.C., Charleston, W.A.G., 1998. Production, faecal egg counts and worm burdens of ewe lambs which grazed six contrasting forages. Vet. Parasitol. 80, 15–27.

Novobilský, A., Mueller-Harvey, I., Thamsborg, S.M., 2011. Condensed tannins act against cattle nematodes. Vet. Parasitol. 182, 213–220.

Novobilský, A., Stringano, E., Hayot Carbonero, C., Smith, L.M.J., Enemark, H.L., Mueller-Harvey, I., Thamsborg, S.M., 2013. In vitro effects of

extracts and purified tannins of sainfoin (*Onobrychis viciifolia*) against two cattle nematodes. Vet. Parasitol. 196, 532–537.

Pursall, E.R., Rolff, J., 2011. Immune responses accelerate ageing: proof-of-principle in an insect model. PLoS ONE 6, 1–7.

Ramírez-Restrepo, C.A., Barry, T.N., López-Villalobos, N., Kemp, P.D., McNabb, W.C., 2004. Use of *Lotus corniculatus* containing condensed tannins to increase lamb and wool production under commercial dryland farming conditions without the use of anthelmintics. Anim. Feed Sci. Technol. 117, 85–105.

Roberts, L.S., Janovy, J., 2008. Gerald D. Schmidt and Larry S. Roberts' Foundations of Parasitology. McGraw-Hill, New York, pp. 313–363.

Scully, L.R., Bidochka, M.J., 2006. Developing insect models for the study of current and emerging human pathogens. FEMS Microbiol. Lett. 263, 1–9.

Shostak, A.W., 2014. *Hymenolepis diminuta* infections in *Tenebrionid* beetles as a model system for ecological interactions between helminth parasites and terrestrial intermediate hosts: a review and meta-analysis. J. Parasitol. 100, 46–58.

Tan, M.-W., 2002. Cross-species infections and their analysis. Annu. Rev. Microbiol. 56, 539.

Vokřál, I., Jirásko, R., Jedličková, V., Bártíková, H., Skálová, L., Lamka, J., Holčapek, M., Szotáková, B., 2012. The inability of tapeworm *Hymenolepis diminuta* and fluke *Dicrocoelium dendriticum* to metabolize praziquantel. Vet. Parasitol. 185, 168–174.

Waller, P.J., Thamsborg, S.M., 2004. Nematode control in 'green' ruminant production systems. Trends Parasitol. 20, 493–497.

Williams, A.R., Fryganas, C., Ramsay, A., Mueller-Harvey, I., Thamsborg, S.M., 2014. Direct anthelmintic effects of condensed tannins from diverse plant sources against *Ascaris suum*. PLOS ONE 9, e97053.

Woolsey, I., (MSc Thesis) 2012. Assessment of Pharmaceutical Efficacy in the *Tenebrio molitor* (Coleoptera)–*Hymenolepis diminuta* (Cestoda) Invertebrate–Parasite Model. University of Copenhagen.

Appendix I

Original publication:

Proanthocyanidins inhibit *Ascaris suum* glutathione-S-transferase activity and increase susceptibility of larvae to levamisole *in vitro*

Tina V.A. Hansen, Christos Fryganas, Nathalie Acevedo, Luis Caraballo, Stig M. Thamsborg, Irene Mueller-Harvey, Andrew R. Williams

Short communication

Proanthocyanidins inhibit *Ascaris suum* glutathione-S-transferase activity and increase susceptibility of larvae to levamisole *in vitro*

Tina V.A. Hansen [a], Christos Fryganas [b], Nathalie Acevedo [c], Luis Caraballo [c], Stig M. Thamsborg [a], Irene Mueller-Harvey [b], Andrew R. Williams [a,*]

[a] Department of Veterinary Disease Biology, Faculty of Health and Medical Sciences, University of Copenhagen, Frederiksberg, Denmark
[b] Chemistry and Biochemistry Laboratory, School of Agriculture, Policy and Development, University of Reading, Reading, United Kingdom
[c] Institute for Immunological Research, University of Cartagena, Cartagena, Colombia

ARTICLE INFO

ABSTRACT

Proanthocyanidins (PAC) are a class of plant secondary metabolites commonly found in the diet that have shown potential to control gastrointestinal nematode infections. The anti-parasitic mechanism(s) of PAC remain obscure, however the protein-binding properties of PAC suggest that disturbance of key enzyme functions may be a potential mode of action. Glutathione-S-transferases (GSTs) are essential for parasite detoxification and have been investigated as drug and vaccine targets. Here, we show that purified PAC strongly inhibit the activity of both recombinant and native GSTs from the parasitic nematode *Ascaris suum*. As GSTs are involved in detoxifying xenobiotic substances within the parasite, we hypothesised that this inhibition may render parasites hypersusceptible to anthelmintic drugs. Migration inhibition assays with *A. suum* larvae demonstrated that the potency of levamisole (LEV) and ivermectin (IVM) were significantly increased in the presence of PAC purified from pine bark (4.6-fold and 3.2-fold reduction in IC$_{50}$ value for LEV and IVM, respectively). Synergy analysis revealed that the relationship between PAC and LEV appeared to be synergistic in nature, suggesting a specific enhancement of LEV activity, whilst the relationship between PAC and IVM was additive rather than synergistic, suggesting independent actions. Our results demonstrate that these common dietary compounds may increase the efficacy of synthetic anthelmintic drugs *in vitro*, and also suggest one possible mechanism for their well-known antiparasitic activity.

© 2016 Elsevier Ireland Ltd. All rights reserved.

Gastrointestinal nematodes represent a major threat to sustainable and profitable livestock production worldwide. The current reliance on a small arsenal of synthetic anthelmintic drugs has serious limitations due to the threat of drug resistance, which has already reached crisis levels in small ruminant production [1], and has also been detected in nematodes of pigs and cattle [2,3]. A complementary approach is the identification of bioactive diets that contain natural plant compounds with anti-parasitic activity, and which can be used as nutriceuticals [4]. Such an approach may slow the threat of drug resistance by reducing the frequency of drug interventions, as well as potentially boosting the host's natural immunity [5].

Diets that are rich in proanthocyanidins (PAC-syn. condensed tannins) have been demonstrated to be effective in reducing nematode fecundity and/or burdens in a variety of livestock species [4]. Moreover, *in vitro* assays have confirmed that PAC have direct effects on parasite survival, with electron microscopy studies demonstrating direct physical damage to both external and internal parasite structures [6,7].

However, the mechanisms that lead to parasite death have not yet been elucidated. As PAC have a strong protein-binding affinity, interference with key enzymes is an attractive hypothesis. Consistent with this, Fakae et al. [8]) have shown that extracts from some traditional Nigerian medicinal plants inhibit the function of glutathione-S-transferases from the swine nematode *Ascaris suum*. This inhibition was speculated to be due to, at least in some cases, the presence of PAC. Glutathione-S-transferases play a key role in detoxification of reactive oxygen species as well as xenobiotics, and have been proposed as helminth vaccine targets [9]. Thus, interference with GST function may result in endogenous toxicity to the parasite and also potentially increase the susceptibility of parasites to xenobiotics such as synthetic drugs. Indeed, Whitney et al. [10]) recently reported that ivermectin (IVM) treatment of *Haemonchus contortus* in lambs was more effective when the lambs consumed PAC-containing red juniper berries.

We have previously shown that *A. suum* third-stage larvae (L3) are susceptible to the anti-parasitic activity of PAC [7]. In the present study, we derived highly purified PAC from two plant sources to investigate 1) whether *A. suum* GST function was inhibited by PAC, and 2) whether exposure of *A. suum* larvae to PAC *in vitro* would result in synergistic increases in the efficacy of IVM and levamisole (LEV).

* Corresponding author.
E-mail address: arw@sund.ku.dk (A.R. Williams).

We first purified native *A. suum* GST (nGST) from adult worms collected from the small intestine of pigs at a local slaughterhouse (Danish Crown, Ringsted, Denmark). Worms were pulverised mechanically using liquid nitrogen and the powder was then dissolved in 15 mL cold Binding Buffer (140 mM NaCl, 2.7 mM KCl, 10 mM Na_2HPO_4, 1.8 mM KH_2PO_4) and centrifuged for 10 min at 3134g. The supernatant was filtrated through a 0.20 μm syringe filter (Corning) and nGST isolated on glutathione columns (GSTrap HP®, GE Healthcare) following the protocol of the manufacturer. The eluate was concentrated to 500 μL and subsequently exchanged with PBS using Amicon Ultra-4 centrifugal filter units (MWCO 10 kDa). Protein concentration was determined by the BCA assay using BSA as a standard. In addition, recombinant GST1 (rGST1) from *A. suum* was produced as described elsewhere [11]. Isolation of nGST was confirmed by coomassie stain using rGST1 as a reference. SDS-PAGE was performed in a 10% polyacrylamide (NuPAGE® Novex® 10% Bis-Tris Midi Gels, Life Technologies) according to the manufacturer's recommendations except that 0.5 μL DL-Dithiolthreitol (Sigma-Aldrich) was used as the reducing agent. An amount of 1.4 μg nGST and 1.05 μg rGST1 was applied. After electrophoresis, proteins were stained with SimplyBlue™ SafeStain (Life Technologies) for 1 h, and visualised using Odyssey FC Imager (Li-Cor Biotechnologies). As shown if Fig. 1A, nGST was successfully isolated as indicated by two bands (23 and 24 kDa) corresponding to the GST1 and GST2 isoforms previously described by Liebau et al. [12]), and consistent with the 25 kDa single band obtained with rGST1 [11].

In order to test whether PAC inhibited GST function, PAC were extracted from white clover flowers (WCF; *Trifolium repens*) and pine bark (PB; *Pinus sylvestris*), purified on Sephadex-LH20 columns, and analysed by HPLC-MS as previously described [7,13]. These plant samples were chosen as they represented the two most common classes of PAC, these being procyanidins (found in PB) and prodelphinidins (found in WCF). The second fraction to elute from the column, containing high molecular weight PAC of high purity (84% for PB, 100% for WCF), was used in these experiments. GST activity was assayed at 26 °C using the GST Detection Module (GE Healthcare Life Sciences) with a final concentration of 5 μg/mL protein. The assay was conducted in 96 well plates and read at 340 nm (Spectra Max Plus 384, Molecular Devices) using 1-chloro-2,4-dinitrobenzene (CDNB, 1 mM) as GST

substrate and reduced glutathione as the reducing agent (0.308 μg/mL). Enzyme activity (nGST) was significantly reduced in the presence of PAC (Fig. 1B). Similar vales were obtained with rGST1 (data not shown). The IC_{50} values were 0.96 and 0.20 μg/mL for PB and WCF, respectively. Thus, both procyanidin and prodelphinidin type-PAC efficiently inhibit GST activity from *A. suum*.

We next investigated whether exposure of *A. suum* third-stage larvae (L3) to PAC purified from PB would improve the *in vitro* efficacy of LEV and IVM. Pine bark PAC were chosen for these experiments as procyanidins are more commonly found in the diet than prodelphinidins. Third-stage larvae were obtained by mechanically hatching embryonated eggs as described [7]. The larvae were then pre-treated for 60 min with either 20 or 10 μg/mL of purified PAC, or PBS as a control. Then, concentration gradients of either LEV or IVM (both obtained from Sigma-Aldrich, Stellenbosch, Germany) were added to the PAC- or PBS-treated larvae and incubated overnight. Additional groups of larvae were incubated overnight with either PAC or PBS alone. The pre-treatment time for PAC of 60 min was chosen as this time-frame allows irreversible binding of PAC to *A. suum* larvae (A.R. Williams, unpublished data), whilst the concentrations of PAC were chosen as preliminary experiments demonstrated that they achieved approximately 15% inhibition of larval migration, thus allowing the possibility to test for synergistic effects between PAC and the synthetic drugs. Migratory ability was assessed by an agar-based assay as previously described [7]. Inhibition of migration was expressed relative to L3 incubated in media only.

Incubation of larvae in LEV or IVM alone resulted in a dose dependent inhibition of migration (Fig. 2A). For both drugs, the addition of PAC increased the efficacy, resulting in a 4.6-fold and 3.2-fold reduction in IC_{50} value for LEV and IVM, respectively, when combined with 20 μg/mL PAC. To assess whether these increase in efficacy represented a synergistic or additive interaction, predicted additive values for the percentage of migration inhibition were calculated from the observed inhibitory effects of the individual treatments (each concentration of drug or PAC) according to Bliss' definition of independent action [14]. The observed effect of the combined PAC/drug treatments was then compared to these calculated vales, with efficacy greater than the predicted additive effect defined as synergy. This approach demonstrated
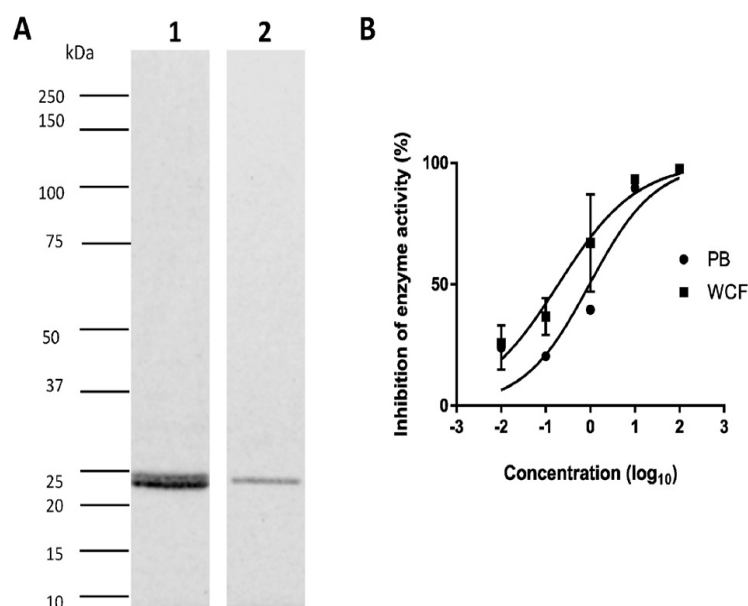

Fig. 1. Isolation of *Ascaris suum* glutathione-S-transferase (GST) and inhibition by proanthocyanidins (PAC). A) *A. suum* GST was isolated from adult worms and visualised by SDS-PAGE. Lane 1 — isolated native GST, Lane 2 — recombinant GST1. B) Inhibition of native GST activity by PAC purified from pine bark (PB) and white clover flowers (WCF). Results are the mean (± S.E.M) of two independent experiments, each performed in duplicate.

A
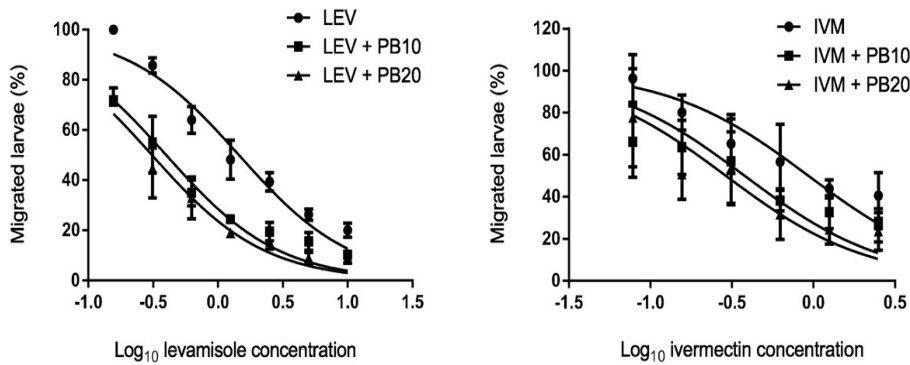
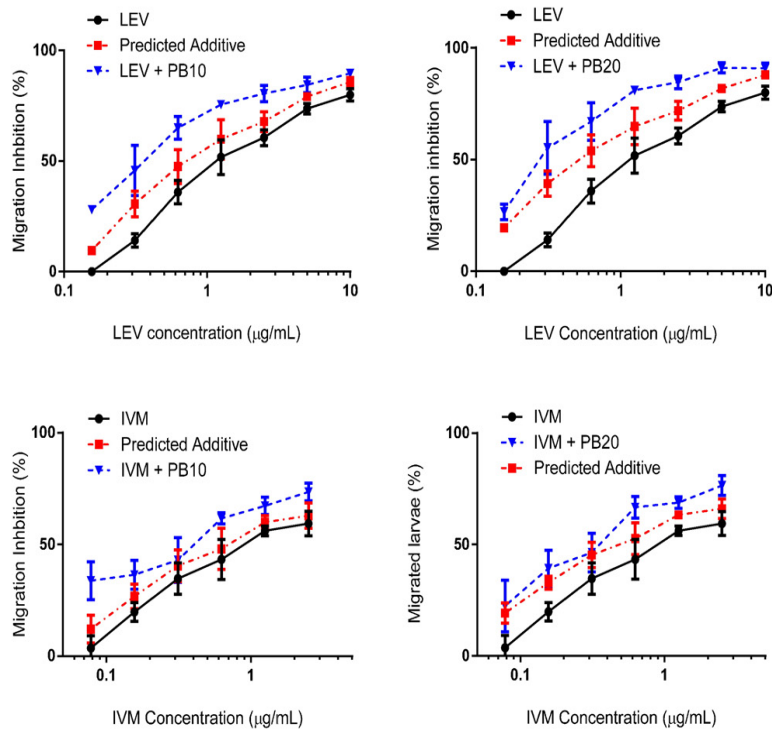|	IC$_{50}$ values (µg/mL)		
	Drug alone	Drug + 10 µg/mL PAC	Drug + 20 µg/mL PAC
Levamisole	1.45[a]	0.39[b]	0.31[b]
Ivermectin	0.93[a]	0.37[b]	0.29[b]

B

Fig. 2. Proanthocyanidins (PAC) increase the efficacy of levamisole and ivermectin *in vitro*. A) Percentage migration of *Ascaris suum* larvae in the presence of levamisole (LEV) and ivermectin (IVM) with or without 10 (PB10) or 20 (PB20) µg/mL of PAC isolated from pine bark. Results are the mean (±S.E.M) of two independent experiments, each performed in duplicate. Also shown are IC$_{50}$ values calculated by non-linear regression. For each drug, values followed by different subscripts indicate significantly ($P < 0.0001$) different IC$_{50}$ values. B) Synergy analysis of levamisole (LEV) or ivermectin (IVM) combined with 10 or 20 µg/mL PAC from pine bark (PB). Shown is the percentage inhibition of larval migration achieved by the drug alone and in combination with PAC, and the additive values predicted by the assumption of independent action of the drug and PAC (see text). Combined data from two independent experiments is presented.

that the relationship between PAC and LEV tended to be synergistic, with consistently higher observed values for the combination than the additive values predicted by independent action (Fig. 2B). The effect

was particular noticeable at low concentrations of LEV and 10 µg/mL PAC. For IVM, the relationship was better described as additive (Fig. 2B), indicating that PAC tend to enhance the activity of LEV, but

in the case of IVM the two agents seem to act independently of each other to inhibit larval migration. This differential interaction of PAC with LEV and IVM is perhaps consistent with the distinct anthelmintic mechanisms of these two drugs, whereby LEV acts on nicotinic acetylcholine receptors [15] and IVM acts by binding to glutamate-gated chloride channels [16].

We have thus demonstrated that *A. suum* GST function is efficiently inhibited by PAC, which may offer a mechanistic explanation to their well-documented anthelmintic activity. However, the high affinity that PAC have for proteins means it is highly unlikely that any one parasite metabolic pathway is specifically targeted. Instead, it is more plausible that a range of enzymatic functions are inhibited by PAC. In addition, previous studies using electron microscopy to observe nematodes exposed to PAC have noted aggregates of material forming around the buccal cavities [17], and have proposed that a 'coating' effect whereby PAC form complexes with external parasite proteins leads to an inhibition of parasite feeding and subsequent mortality. Furthermore, PAC are likely to interact *in vivo* with both host proteins as well as the parasite, adding further complexity to the situation.

Whilst it is clear that no one single mechanism may be responsible for the anthelmintic activity of PAC, inhibition of GST function raises the possibility that the parasite's detoxification mechanisms may be impaired, which may result in increased susceptibility to drugs, or, *in vivo*, reactive oxygen species produced by host phagocytes. Our data suggest that the efficacy of drugs (particular LEV) may be increased when larvae are co-incubated with PAC, which is in agreement with some previous *in vitro* and *in vivo* studies involving *H. contortus* [10,18]. Further studies will be necessary to determine the mechanisms behind these combinatorial effects. Given the rapid binding of PAC to proteins [19], we speculate that in our experiments key parasite proteins were neutralised and/or destroyed during the pre-incubation with PAC, leaving the larvae more susceptible to the subsequent addition of levamisole. In addition to inhibition of GST function, other plausible mechanisms include decreased cuticle integrity due to PAC-binding, which may result in increased diffusion of drugs, and inhibition of other detoxification mechanisms such as xenobiotic efflux pumping by p-glycoproteins, or activity of gluconyl transferases. Thus, we cannot conclude that the synergistic effects of PAC and levamisole are due only to the GST inhibition, and the effect of PAC on the activity of these other parasite pathways is worthy of further investigation.

In conclusion, we have confirmed that PAC strongly inhibit GST function from an important parasitic nematode, and we also have demonstrated that PAC can synergistically improve the efficacy of LEV and also act additively with IVM *in vitro*. Further studies will focus on the mechanisms involved and whether PAC-rich diets can improve drug efficacy *in vivo*.

Acknowledgements

References

[1] N.D. Sargison, Pharmaceutical treatments of gastrointestinal nematode infections of sheep—future of anthelmintic drugs, Vet. Parasitol. 189 (2012) 79–84.
[2] J.L. Cotter, A. Van Burgel, R.B. Besier, Anthelmintic resistance in nematodes of beef cattle in south-west Western Australia, Vet. Parasitol. 207 (2015) 276–284.
[3] S. Gerwert, K. Failing, C. Bauer, Prevalence of levamisole and benzimidazole resistance in Oesophagostomum populations of pig-breeding farms in North Rhine-Westphalia, Germany, Parasitol. Res. 88 (2002) 63–68.
[4] H. Hoste, J.F.J. Torres-Acosta, C.A. Sandoval-Castro, I. Mueller-Harvey, S. Sotiraki, H. Louvandini, S.M. Thamsborg, T.H. Terrill, Tannin containing legumes as a model for nutraceuticals against digestive parasites in livestock, Vet. Parasitol. 212 (2015) 5–17.
[5] C.A. Ramírez-Restrepo, A. Pernthaner, T.N. Barry, N. López-Villalobos, R.J. Shaw, W.E. Pomroy, W.R. Hein, Characterization of immune responses against gastrointestinal nematodes in weaned lambs grazing willow fodder blocks, Anim. Feed Sci. Technol. 155 (2010) 99–110.
[6] S. Brunet, I. Fourquaux, H. Hoste, Ultrastructural changes in the third-stage, infective larvae of ruminant nematodes treated with sainfoin (Onobrychis viciifolia) extract, Parasitol. Int. 60 (2011) 419–424.
[7] A.R. Williams, C. Fryganas, A. Ramsay, I. Mueller-Harvey, S.M. Thamsborg, Direct anthelmintic effects of condensed tannins from diverse plant sources against Ascaris suum, PLoS One 9 (2014), e97053.
[8] B.B. Fakae, A.M. Campbell, J. Barrett, I.M. Scott, P.H. Teesdale-Spittle, E. Liebau, P.M. Brophy, Inhibition of glutathione S-transferases (GSTs) from parasitic nematodes by extracts from traditional Nigerian medicinal plants, Phytother. Res. 14 (2000) 630–634.
[9] G.N. Goud, V. Deumic, R. Gupta, J. Brelsford, B. Zhan, P. Gillespie, J.L. Plieskatt, E.I. Tsao, P.J. Hotez, M.E. Bottazzi, Expression, purification, and molecular analysis of the Necator americanus glutathione S-transferase 1 (Na-GST-1): a production process developed for a lead candidate recombinant hookworm vaccine antigen, Protein Expr. Purif. 83 (2012) 145–151.
[10] T.R. Whitney, S. Wildeus, A.M. Zajac, The use of redberry juniper (Juniperus pinchoti) to reduce Haemonchus contortus fecal egg counts and increase ivermectin efficacy, Vet. Parasitol. 197 (2013) 182–188.
[11] N. Acevedo, J. Mohr, J. Zakzuk, M. Samonig, P. Briza, A. Erler, A. Pomés, C.G. Huber, F. Ferreira, L. Caraballo, Proteomic and immunochemical characterization of glutathione transferase as a new allergen of the nematode Ascaris lumbricoides, PLoS One 8 (2013), e78353.
[12] E. Liebau, Ö.L. Schönberger, R.D. Walter, K.J. Henkle-Dührsen, Molecular cloning and expression of a cDNA encoding glutathione S-transferase from Ascaris suum, Mol. Biochem. Parasitol. 63 (1994) 167–170.
[13] A. Gea, E. Stringano, R.H. Brown, I. Mueller-Harvey, In situ analysis and structural elucidation of sainfoin (Onobrychis viciifolia) tannins for high-throughput germplasm screening, J. Agric. Food Chem. 59 (2011) 495–503.
[14] C. Klongsiriwet, J. Quijada, A.R. Williams, I. Mueller-Harvey, E.M. Williamson, H. Hoste, Synergistic inhibition of Haemonchus contortus exsheathment by flavonoid monomers and condensed tannins, Int. J. Parasitol. Drugs Drug Resist. 5 (2015) 127–134.
[15] R.S. Sarai, S.R. Kopp, M.R. Knox, G.T. Coleman, A.C. Kotze, In vitro levamisole selection pressure on larval stages of Haemonchus contortus over nine generations gives rise to drug resistance and target site gene expression changes specific to the early larval stages only, Vet. Parasitol. 211 (2015) 45–53.
[16] R.E. Hibbs, E. Gouaux, Principles of activation and permeation in an anion-selective Cys-loop receptor, Nature 474 (2011) 54–60.
[17] C. Martínez-Ortíz-de-Montellano, C. Arroyo-López, I. Fourquaux, J.F.J. Torres-Acosta, C.A. Sandoval-Castro, H. Hoste, Scanning electron microscopy of Haemonchus contortus exposed to tannin-rich plants under in vivo and in vitro conditions, Exp. Parasitol. 133 (2013) 281–286.
[18] S.A. Armstrong, D.R. Klein, T.R. Whitney, C.B. Scott, J.P. Muir, B.D. Lambert, T.M. Craig, Effect of using redberry juniper (Juniperus pinchotii) to reduce Haemonchus contortus in vitro motility and increase ivermectin efficacy, Vet. Parasitol. 197 (2013) 271–276.
[19] I. Mueller-Harvey, Unravelling the conundrum of tannins in animal nutrition and health, J. Sci. Food Agric. 86 (2006) 2010–2037.

Appendix J

Original publication:

Polymerization-dependent activation of porcine γδ T-cells by proanthocyanidins

Andrew R. Williams, Christos Fryganas, Kirsten Reichwald, Søren Skov, Irene Mueller-Harvey, Stig M. Thamsborg

Polymerization-dependent activation of porcine γδ T-cells by proanthocyanidins

Andrew R. Williams [a,*], Christos Fryganas [b], Kirsten Reichwald [a], Søren Skov [a], Irene Mueller-Harvey [b], Stig M. Thamsborg [a]

[a] Department of Veterinary Disease Biology, Faculty of Health and Medical Sciences, University of Copenhagen, Frederiksberg, Denmark
[b] Chemistry and Biochemistry Laboratory, School of Agriculture, Policy and Development, University of Reading, Reading, United Kingdom

ARTICLE INFO

ABSTRACT

Plant-derived proanthocyanidins (PAC) have been promoted as a natural method of improving health and immune function in livestock. It has previously been shown that PAC are effective agonists for activating ruminant γδ T-cells *in vitro*, however effects on other livestock species are not yet clear. Moreover, the fine structural characteristics of the PAC which contribute to this stimulatory effect have not been elucidated. Here, we demonstrate activation of porcine γδ T-cells by PAC via up-regulation of CD25 (IL-2Rα) and show that 1) activation is dependent on degree of polymerization (DP), with PAC fractions containing polymers with mean DP > 6 significantly more effective than fractions with mean DP < 6, whilst flavan-3-ol monomers (the constituent monomeric units of PAC) did not induce CD25 expression and 2) both procyanidin and prodelphinidin-type PAC are effective agonists. Furthermore, we show that this effect of PAC is restricted to the γδ T-cell population within porcine peripheral mononuclear cells as significant CD25 up-regulation was not observed in non γδ T-cells, and no activation (via CD80/86 up-regulation) was evident in monocytes. Our results show that dietary PAC may contribute to enhancement of innate immunity in swine via activation of γδ T-cells.

© 2016 Elsevier Ltd. All rights reserved.

1. Introduction

There is currently intense interest in increasing the efficiency and output of modern livestock production, in order to ensure food security for a rapidly growing population (Wu et al., 2014). At the same time, consumer demand for healthy animal produce and rising antibiotic resistance due to prophylactic inclusion in animal feed, means that routine use of antimicrobial drugs to control pathogens and ensure high quality end products is unsustainable (Marshall and Levy, 2011; Thornton, 2010). An alternative approach is to identify natural dietary compounds that promote healthy and robust animal performance, through modulatory and/or stimulatory effects on the animal's immune system.

The gastrointestinal (GI) tract is one of the most immunologically active tissues in the body, and is exposed to a variety of bacterial and parasitic pathogens that can result in acute and chronic inflammation, diarrhoea and weight loss (Hale et al., 1985; Nagy and Fekete, 2005). Therefore, maintenance of healthy gut function is essential for robust performance. The GI mucosa is home to a variety of innate immune system effectors including defensins, natural killer cells and γδ T-cells (Bevins et al., 1999; Smith and Garrett, 2011). γδ T-cells are increasingly recognised as crucial players in responses to GI pathogens. A key

distinguishing feature from αβ T-cells is that γδ T-cells are not clonal for a specific antigen, and do not require antigens to be presented in the context of major histocompatibility complex (MHC) molecules, but rather have the ability to recognise conserved pathogen pattern receptors such as phosphoantigens (Gu et al., 2015). In contrast to humans and mice, where γδ T-cells make up only a small proportion of the peripheral lymphocyte population (Kalyan and Kabelitz, 2013), mammalian livestock (particularly young animals) have large numbers of circulating γδ T-cells – in some cases up to 50% of the lymphocyte pool, depending on age – and this is true of both ruminants (Holderness et al., 2007; Tibe et al., 2012) and swine (Gerner et al., 2009). Despite this large population of γδ T-cells in livestock, how these cells function during GI infections is not fully understood (Gerner et al., 2009). Therefore, much of our knowledge on the role of γδ T-cells in GI infections derives from studies in mice, where it is known that they are able to secrete both pro- and anti-inflammatory cytokines, help to recruit neutrophils and B-cells, and maintain homeostasis and repair of mucosal barriers (Witherden and Havran, 2013). Moreover, their importance has been demonstrated in a number of host-pathogen systems. Mice deficient in γδ T-cell receptor expression have impaired immunity to the GI helminth *Nippostrongylus brasiliensis*, resulting in higher parasite burdens as well as increased lesions and pathology in the intestine compared to wild-type mice (Inagaki-Ohara et al., 2011), and are also more susceptible to infection with the mucosal bacterium *Salmonella typhimurium* (Ismail et al., 2011). Furthermore, γδ T-cells have been shown to play important roles

* Corresponding author.
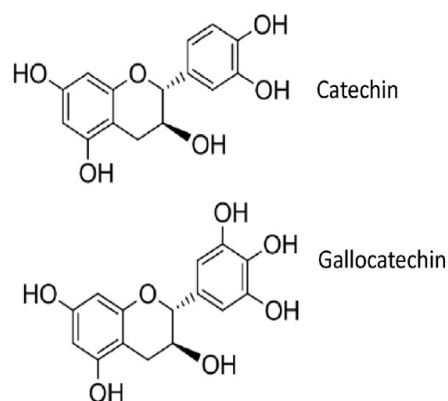 *E-mail address:* arw@sund.ku.dk (A.R. Williams).

Fig. 1. Structure of the *trans* flavan-3-ols catechin (gives rise to procyanidin-type PAC) and gallocatechin (gives rise to prodelphinidin-type PAC). Note the extra hydroxyl group in the B-ring of gallocatechin.

Table 1
Chemical analysis of fractionated proanthocyanidins from two different plant sources. PC – procyanidin, PD – prodelphinidin, mDP – mean degree of polymerization. % purity – g PAC/100 g fraction.

Sample	Fraction	PC:PD ratio	mDP	% purity
Hazelnut skin	F1	81.7:18.3	4.6	51.3
	F2	79.1:20.9	9.1	70.3
Blackcurrant leaves	F1	6.3:93.7	2.5	59.9
	F2	5.5:94.5	6.5	100

Also reported by Williams et al. (2014).

in control of viral (MCMV) and fungal (*Candida albicans*) infections (Conti et al., 2014; Khairallah et al., 2015), indicating key functions against a variety of pathogens.

It has become apparent that in addition to activation by pathogen ligands, γδ T-cells may also be activated by non-pathogen related molecules such as bioactive dietary compounds. For example, proanthocyanidins (PAC) are a group of plant secondary metabolites that are widely found in common plant sources such as berries, grapes and nuts. They consist of polymers of flavan-3-ol monomers, and their structure can vary widely depending on the degree of polymerization and the nature of the monomeric sub-units, most of which are either catechin and its *cis* isomer epicatechin (which give rise to procyanidin-type PAC–PC) or gallocatechin and its *cis*-isomer epigallocatechin (which give rise to prodelphinidin-type PAC–PD). The major difference between these groups is an extra hydroxyl group in the B-ring of PD-type PAC (Fig. 1).

PAC have been widely investigated for both their anti-oxidant activities and their putative positive effects on gut health due to both anti-microbial and immuno-stimulatory properties (Martinez-Micaelo et al., 2012). It has been shown that PAC can effectively activate both human and ruminant γδ T cells *in vitro* by inducing cell proliferation and expression of CD25 and CD69 (Holderness et al., 2007; Tibe et al., 2012). In addition, increased numbers of peripheral γδ T-cells have been observed in sheep fed PAC-containing willow fodder (Ramírez-Restrepo et al., 2010) and peripheral γδ T-cell proliferation is increased in humans ingesting PAC-rich cranberry juice (Nantz et al., 2013). However, the structural characteristics of PAC that contribute to these

stimulatory effects on γδ T-cells have not been fully elucidated. Moreover, there is no information on whether porcine γδ T-cells can be activated by PAC in a similar fashion to ruminants. PAC-containing feedstuffs have recently been investigated as a cost-effective feed supplement for pigs to promote gut health without reliance on antimicrobials (Feisel et al., 2014; Sehm et al., 2007) and thus an exploration of the effects of PAC on porcine γδ T-cell function is warranted.

Here, we used well characterised PAC fractions containing distinct PC and PD profiles and mean degree of polymerization (mDP) to determine whether porcine γδ T cells could be effectively activated by PAC via increased CD25 expression, and the contribution of PC/PD profile and mDP to this effect.

2. Methods

2.1. Materials

Skins from hazelnut (*Corella avellana*; hereafter referred to as HN) were provided by Dr Hervé Hoste (INRA, Toulouse, France). Leaves from blackcurrant (*Ribes nigrum*; hereafter referred to as BC) were sourced from Goring-upon-Thames, UK. Catechin, epicatechin, concavalin A (con A) and lipopolysaccharide (LPS) were obtained from Sigma-Aldrich (Schnelldorf, Germany).

2.2. Extraction, fractionation and analysis of proanthocyanidins

Detailed procedures for the extraction and purification of PAC are described elsewhere (Williams et al., 2014). Briefly, plant material was extracted with acetone/water, and the resulting extract was freeze-dried, suspended in water and then loaded onto Sephadex LH-20 columns. Low-molecular weight PAC were eluted with acetone water (3:7) to yield fraction 1 (F1), and high-molecular weight PAC eluted with acetone/water (1:1) to yield fraction 2 (F2). Fractions were analysed using thiolytic degradation and HPLC-MS (Gea et al., 2011) which yielded information on the purity of PAC, mDP and PC/PD ratio.

2.3. Blood samples and isolation of PBMC

The use of animals was approved by the Experimental Animal Unit, University of Copenhagen, and procedures carried out according to the guidelines of the Danish Animal Experimentation Inspectorate (licence number 2010/561-1914). Blood samples were drawn by jugular venipuncture from 9–12 week old healthy female pigs (Danish Landrace/Yorkshire/Duroc) into vacutainers containing sodium heparin. PBMCs were isolated on histopaque 1.077, washed in PBS and then suspended in complete culture media (RPMI 1640 supplemented with 10% inactivated foetal bovine serum, 2 mM L-glutamine, 100 U/mL of penicillin and 100 μg/mL of streptomycin). Viability of PBMC was assessed by trypan blue staining and was routinely >98%.

2.4. Cell culture

For whole PBMC culture, cells were seeded in duplicate at 10^6/mL in 48-well plates. Purified PAC fractions were dissolved in PBS and added at concentrations of 20 or 10 μg/mL – preliminary experiments showed that higher concentrations significantly reduced cell viability (data not shown). Con A (5 μg/mL) and PBS-stimulated cells were included in all experiments as positive and negative controls, respectively. Cells were incubated for 48 h at 37 °C and 5% CO_2 before being harvested for analysis. For monocyte culture, monocytes were purified (>90%

Fig. 2. Proanthocyanidins (PAC) from hazelnut skin (HN) induce CD25 expression in porcine γδ T-cells. A) Gating strategy and staining controls. Lymphocytes were gated based on forward/side scatter. Staining controls consisted of APC and FITC isotype controls. B) Representative plots from one experiment of CD25 expression in γδ T-cells. The percentage of CD25 positive cells in the γδ T-cell population was quantified after exposure to 20 μg/mL HN PAC (fraction 1 or 2) or 5 μg/mL con A (positive control). C) Mean results of 4 independent experiments using cells from different pigs. Results are presented as mean ± SEM. 'F2' refers to fraction 2 and 'F1' refers to fraction 1 (see Methods). 'C' – catechin. 'EC' – epicatechin. **$P < 0.01$, *$P < 0.05$, ns – non-significant. D) PAC from fraction 2 of HN do not significantly increase percentage of CD25+ cells in the γδ- lymphocyte population from porcine PBMC. 'ns' – non-significant. Results are mean ± SEM from four experiments with cells from different pigs.
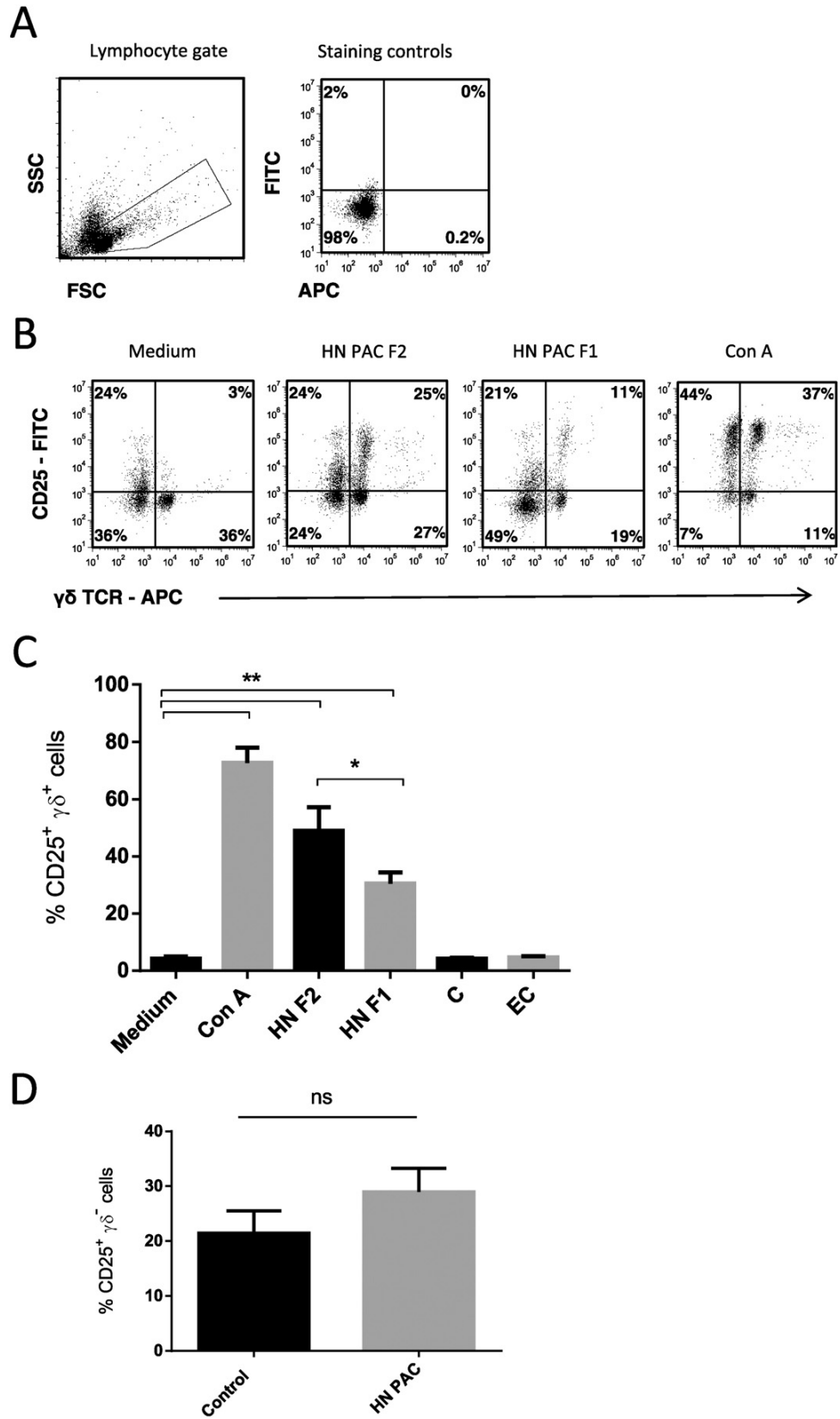
purity) from PBMC with anti-human CD14 microbeads (Auray et al., 2013) and magnetic separation (MACS, Miltenyl Biotech). Purified monocytes were suspended in RPMI 1640 media supplemented with 10% inactivated foetal bovine serum, 1% MEM non-essential amino acids, 10 mM HEPES, 50 μM β-mercaptoethanol, 100 U/mL of penicillin and 100 μg/mL of streptomycin. The cells were rested for 24 h, and then stimulated in duplicate for a further 24 h with either LPS (500 ng/mL) or PAC fractions at 20 or 10 μg/mL. For PBMC, four separate experiments were performed with cells from different pigs and for monocytes, three separate experiments were performed with cells from different pigs.

2.5. Flow cytometry

For PBMC, cells were harvested and stained with anti-porcine γδ TCR (Clone PGBL22A; Monoclonal Antibody Centre, Washington State University, Pullman, USA) and anti-porcine CD25 (Clone K231.3B2; AbD serotec, Kidlington, UK). CD25 (IL-2Rα) was used as a common and well-studied marker of peripheral T-cell activation (Caruso et al., 1997; Jouen-Beades et al., 1997). The mAbs were conjugated to either FITC or APC fluorophores using Zenon antibody labelling kits (Invitrogen), according to the manufacturer's instructions. For monocytes, cells were stained for CD80/86 expression using human CTLA-4/mouse IgG-FITC fusion protein (Ancell, Bayport, USA). Appropriate isotype controls (BD biosciences) were included in every experiment. Cells were acquired on an Accuri C6 flow cytometer. Gating for lymphocytes or monocytes was carried out based on forward/side scatter and at least 10,000 events were acquired. Data were analysed using FCS express version 5 (De Novo Software, Glendale, CA).

2.6. ELISA

TNF-α in monocyte culture supernatants was quantified using the swine TNF-α ELISA kit (Life Technologies) according to the manufacturer's instructions.

2.7. Statistical analysis

Differences in CD25 or CD80/86 expression were determined by ANOVA with Bonferroni post-hoc testing (Graphpad Prism v6.00, GraphPad Software, La Jolla, California, USA, www.graphpad.com).

3. Results and discussion

Extraction and purification of two fractions each from two different plant sources (HN and BC) yielded PAC with contrasting PC/PD profiles. Full details of the chemical analysis have been presented previously (Williams et al., 2014), and are summarised briefly in Table 1. Proanthocyanidins purified from HN consisted of around 80% PC units, whereas those from BC were PD-rich, with more than 90% of the PAC consisting of PD units. For both plant sources, F1 contained lower molecular weight polymers with mDP <6, and F2 contained high-molecular weight PAC with mDP >6.

We first tested the PC-rich PAC fractions from HN for their ability to induce CD25 (IL-2Rα) expression in γδ T-cells. The F2 fraction (20 μg/mL) induced significant up-regulation of CD25, with around 50% of γδ TCR⁺ cells positive for CD25 expression compared to <5% in unstimulated cells ($P < 0.01$) although the effect was not as strong as that induced by the positive control con A (Fig. 2B,C). This effect was dose-dependent, as a concentration of 10 μg/mL induced lower, but still statistically significant up-regulation (data not shown). When the F1 fraction was tested at an equivalent concentration of PAC, activation was still observed but significantly less CD25 positive cells were present compared to the F2 fraction ($P < 0.05$; Fig. 2B,C), showing clearly that this effect is dependent on degree of polymerization. Consistent with this, we observed that the flavan-3-ol monomers catechin and

epicatechin, which are the dominant monomeric units of HN PAC polymers, did not induce CD25 expression (Fig. 2C). In addition, this effect appeared to be largely confined to the γδ T-cell population; whilst there was an increase in the number of CD25⁺ cells in the non-γδ lymphocyte population after exposure to the F2 fraction, this was not statistically significant (Fig. 2D).

We next tested whether the predominantly PD polymers purified from BC could also induce CD25 expression. Similar to the results with the HN PAC, we found that incubation of γδ T-cells with the F2 BC fraction induced marked up-regulation of CD25 ($P < 0.05$; Fig. 3A), although the effect tended to be less strong than that observed with HN PAC. This effect was still present, but not significantly ($P > 0.05$), with an equivalent concentration of the F1 fraction (Fig. 3B). Thus, both PC and PD type PAC are able to induce CD25 up-regulation on porcine γδ T-cells, and the degree of polymerization of the molecule appears to play a major role in the degree of activation.

As the activity of PAC seemed to be confined to γδ T-cells within the lymphocyte population, we investigated whether other mononuclear cells such as monocytes could be activated by PAC or whether γδ T-cells were particularly amenable to this effect. Monocytes were purified from PBMC and exposed to either the TLR agonist LPS, or the F2 fractions from HN and BC, and up-regulation of CD80/86 and TNF-α secretion was quantified. We detected a small, but statistically significant up-regulation of CD80/86 in monocytes exposed to LPS. Moreover, LPS induced a marked secretion of TNF-α, indicating a significant activation of the monocytes ($P < 0.01$; Fig. 4A,B). In contrast, no increased expression of CD80/86 or TNF-α secretion was induced by either of the PAC fractions (Fig. 4A, B). Thus, within the porcine mononuclear population, γδ T-cells appear to be specifically responsive to PAC.

The present work has demonstrated that PAC are effective agonists for porcine γδ T-cells *in vitro*. This is consistent with previous work showing this effect in human, bovine and caprine γδ T-cells (Holderness et al., 2007; Tibe et al., 2012). Thus, this appears to be a highly conserved process across different animal species. Whilst for practical reasons our experiments were performed from PBMC-derived γδ T-cells, rather than GI-resident cells, this apparently widely conserved process suggests that all γδ⁺ cells may respond in a similar fashion to PAC - as evidenced by Holderness et al. (2007) who reported similar responses to PAC from the two major primary subsets (CD8⁺ or CD8⁻) of bovine γδ T-cells (with the CD8⁺ cells being primarily a tissue-associated subset), as well as observing similar responses between Vδ1 and Vδ2 human T-cells.

The ability of PAC to effectively activate these cells may be reflected in functional activity in animals fed a PAC-rich diet, such as enhanced innate immunity to GI pathogens such as helminths, protozoa and bacteria, if γδ T-cells primed by dietary PAC respond faster and more robustly to the presence of pathogens. The role of γδ T-cells in immunity to porcine pathogens has yet to be fully elucidated, however they are known to produce IL-17 and IFN-γ after stimulation with mitogens or bacterial antigens (Lee et al., 2004; Stepanova et al., 2012), and increased numbers of γδ T-cells are present shortly after infection with parasites such as *Cystoisospora suis* (Gabner et al., 2014), suggesting that these cells likely play a functional role in immunity to GI pathogens, as has been reported in mice (Smith and Hayday, 2000).

Interestingly, Nantz et al. (2013) noted that, unlike γδ T-cells, αβ T-cell and B-cell proliferation was not enhanced by dietary PAC in humans. Similarly, Holderness et al. (2007) reported that whereas bovine γδ T-cells were activated by PAC, αβ T-cells were not, however in this study a proportion of human αβ T-cells were also responsive to PAC. Our current results with porcine cells demonstrated that whilst some activation of αβ T-cells was evident, this was non-significant and clearly not as pronounced as the robust response of the γδ T-cell population. Thus, it appears whilst there may be some conserved lymphocyte responses to PAC, the invariant nature of the γδ TCR seems to be uniquely suited to ligation by PAC.

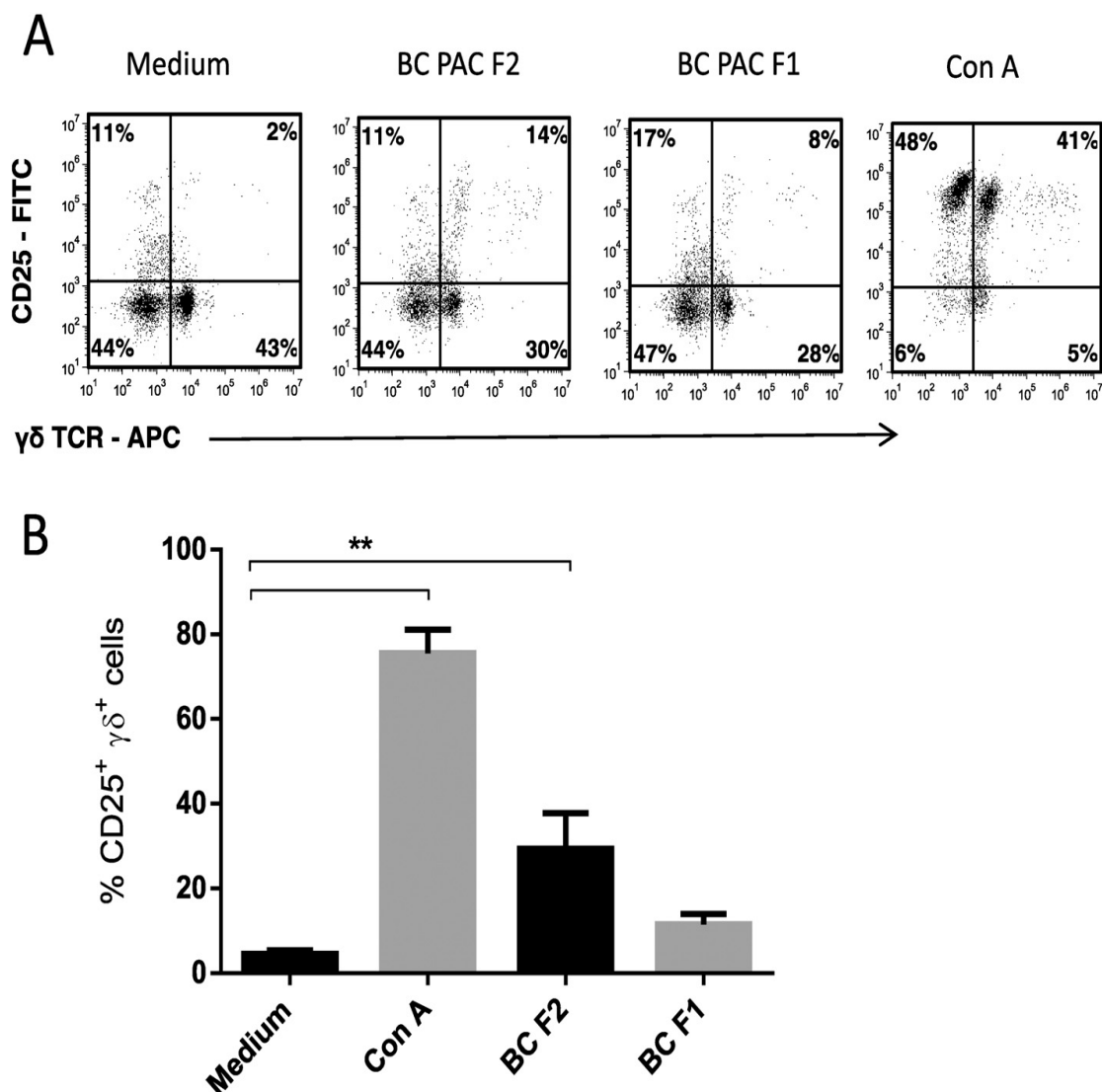**Fig. 3.** Proanthocyanidins (PAC) from blackcurrant leaves (BC) induce CD25 expression in porcine γδ T-cells. A) Representative plots from one experiment of CD25 expression in γδ T-cells. The percentage of CD25 positive cells in the γδ T-cell population was quantified after exposure to 20 µg/mL BC PAC (fraction 1 or 2) or 5 µg/mL con A (positive control). B) Mean results of 4 independent experiments using cells from different pigs. Results are presented as mean ± SEM. 'F2' refers to fraction 2 and 'F1' refers to fraction 1 (see Methods). **P < 0.01, *P < 0.05.

We also observed that the ability of PAC to induce CD25 expression was clearly dependent on the degree of polymerization, whilst monomeric flavan-3-ols had no effect. This is consistent with a number of studies demonstrating that the biological effects of PAC are related to polymer size. Our group and others have shown that *in vitro* anti-parasitic effects are also enhanced by increasing degree of polymerization (Quijada et al., 2015; Williams et al., 2014). In addition, other immune-modulating effects of PAC, such as the phosphorylation of STAT1 in human CD11b+ cells, are instigated only by oligomeric PAC and not by monomeric sub-units such as catechin (Snyder et al., 2014). It is also apparent that differences in biological activity of PAC can be related to the ratio of PC to PD within PAC (Novobilský et al., 2013; Scalbert, 1991). Increased biological activity is often associated with PAC molecules that have a high percentage of PD, perhaps due to the increased possibility of hydrogen-bonding with proteins resulting from the extra hydroxyl group in the B-rings. Our current data demonstrated that both PC and PD rich-PAC were able to induce CD25 expression, though the PC-type PAC from HN appeared to be more potent. However, this difference between HN and BC cannot be ascribed

only to PC/PD ratio as mDP values were higher in the HN fractions (Table 1), which makes direct comparisons problematic. Further studies using larger panels of well-defined PAC will be necessary to determine the exact contribution of these monomeric subunits to the observed activity. For now, our data indicate that both PC and PD-type PAC are capable of priming porcine γδ T-cells, and that the size of the PAC molecule appears to be a critical factor in determining the potency of the effect.

In conclusion, we have shown for the first time that PAC from two different plants are able to activate porcine γδ T-cells through CD25 up-regulation. The degree of polymerization of the PAC polymers appeared to be the most critical structural characteristic for effective activation. Further *in vivo* experiments will aim to determine the functional importance of this relationship.
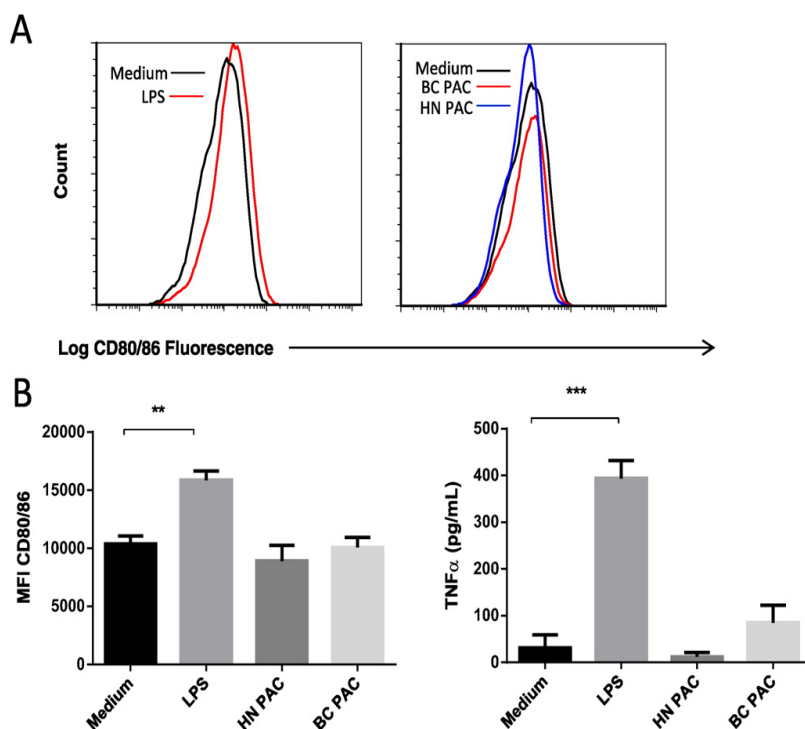
Fig. 4. LPS, but not proanthocyanidins (PAC), induce CD80/86 expression and TNF-α secretion in porcine monocytes. A) Representative histograms showing CD80/86 expression in porcine monocytes exposed to LPS, or 20 μg/mL PAC from fraction 2 of hazelnut skins (HN) or blackcurrant leaves (BC). B) Mean fluorescence intensity (MFI) of CD80/86 and TNF-α secretion from monocytes. Mean results of 3 independent experiments using cells from different pigs. Results are presented as mean ± SEM. ***$P < 0.001$, **$P < 0.01$.

References

Auray, G., Facci, M.R., van Kessel, J., Buchanan, R., Babiuk, L.A., Gerdts, V., 2013. Porcine neonatal blood dendritic cells, but not monocytes, are more responsive to TLRs stimulation than their adult counterparts. PLoS ONE 8, e59629.

Bevins, C.L., Martin-Porter, E., Ganz, T., 1999. Defensins and innate host defence of the gastrointestinal tract. Gut 45, 911–915.

Caruso, A., Licenziati, S., Corulli, M., Canaris, A.D., De Francesco, M.A., Fiorentini, S., Peroni, L., Fallacara, F., Dima, F., Balsari, A., Turano, A., 1997. Flow cytometric analysis of activation markers on stimulated T cells and their correlation with cell proliferation. Cytometry 27, 71–76.

Conti, H.R., Peterson, A.C., Brane, L., Huppler, A.R., Hernández-Santos, N., Whibley, N., Garg, A.V., Simpson-Abelson, M.R., Gibson, G.A., Mamo, A.J., Osborne, L.C., Bishu, S., Ghilardi, N., Siebenlist, U., Watkins, S.C., Artis, D., McGeachy, M.J., Gaffen, S.L., 2014. Oral-resident natural Th17 cells and γδ T cells control opportunistic Candida albicans infections. J. Exp. Med. 211, 2075–2084.

Feisel, A., Gessner, D., Most, E., Eder, K., 2014. Effects of dietary polyphenol-rich plant products from grape or hop on pro-inflammatory gene expression in the intestine, nutrient digestibility and faecal microbiota of weaned pigs. BMC Vet. Res. 10, 196.

Gabner, S., Worliczek, H.L., Witter, K., Meyer, F.R.L., Gerner, W., Joachim, A., 2014. Immune response to Cystoisospora suis in piglets: local and systemic changes in T-cell subsets and selected mRNA transcripts in the small intestine. Parasite Immunol. 36, 277–291.

Gea, A., Stringano, E., Brown, R.H., Mueller-Harvey, I., 2011. In situ analysis and structural elucidation of sainfoin (Onobrychis viciifolia) tannins for high-throughput germplasm screening. J. Agric. Food Chem. 59, 495–503.

Gerner, W., Käser, T., Saalmüller, A., 2009. Porcine T lymphocytes and NK cells – an update. Dev. Comp. Immunol. 33, 310–320.

Gu, S., Nawrocka, W., Adams, E.J., 2015. Sensing of pyrophosphate metabolites by Vγ9Vδ2 T cells. Front. Immunol. 5, 688.

Hale, O.M., Stewart, T.B., Marti, O.G., 1985. Influence of an experimental infection of Ascaris suum on performance of pigs. J. Anim. Sci. 60, 220–225.

Holderness, J., Jackiw, L., Kimmel, E., Kerns, H., Radke, M., Hedges, J.F., Petrie, C., McCurley, P., Glee, P.M., Palecanda, A., Jutila, M.A., 2007. Select plant tannins induce IL-2Rα up-regulation and augment cell division in γδ T cells. J. Immunol. 179, 6468–6478.

Inagaki-Ohara, K., Sakamoto, Y., Dohi, T., Smith, A.L., 2011. γδ T cells play a protective role during infection with Nippostrongylus brasiliensis by promoting goblet cell function in the small intestine. Immunology 134, 448–458.

Ismail, A.S., Severson, K.M., Vaishnava, S., Behrendt, C.L., Yu, X., Benjamin, J.L., Ruhn, K.A., Hou, B., DeFranco, A.L., Yarovinsky, F., Hooper, L.V., 2011. γδ intraepithelial lympho-cytes are essential mediators of host–microbial homeostasis at the intestinal mucosal surface. Proc. Natl. Acad. Sci. 108, 8743–8748.

Jouen-Beades, F., Paris, E., Dieulois, C., Lemeland, J.F., Barre-Dezelus, V., Marret, S., Humbert, G., Leroy, J., Tron, F., 1997. In vivo and in vitro activation and expansion of gammadelta T cells during Listeria monocytogenes infection in humans. Infect. Immun. 65, 4267–4272.

Kalyan, S., Kabelitz, D., 2013. Defining the nature of human γδ T cells: a biographical sketch of the highly empathetic. Cell. Mol. Immunol. 10, 21–29.

Khairallah, C., Netzer, S., Villacreces, A., Juzan, M., Rousseau, B., Dulanto, S., Giese, A., Costet, P., Praloran, V., Moreau, J.-F., Dubus, P., Vermijlen, D., Déchanet-Merville, J., Capone, M., 2015. γδ T cells confer protection against murine Cytomegalovirus (MCMV). PLoS Pathog. 11, e1004702.

Lee, J., Choi, K., Olin, M.R., Cho, S.-N., Molitor, T.W., 2004. γδ T cells in immunity induced by Mycobacterium bovis Bacillus Calmette-Guérin vaccination. Infect. Immun. 72, 1504–1511.

Marshall, B.M., Levy, S.B., 2011. Food animals and antimicrobials: impacts on human health. Clin. Microbiol. Rev. 24, 718–733.

Martinez-Micaelo, N., González-Abuín, N., Ardèvol, A., Pinent, M., Blay, M.T., 2012. Procyanidins and inflammation: molecular targets and health implications. Biofactors 38, 257–265.

Nagy, B., Fekete, P.Z., 2005. Enterotoxigenic Escherichia coli in veterinary medicine. Int. J. Med. Microbiol. 295, 443–454.

Nantz, M., Rowe, C., Muller, C., Creasy, R., Colee, J., Khoo, C., Percival, S., 2013. Consump-tion of cranberry polyphenols enhances human gammadelta-T cell proliferation and reduces the number of symptoms associated with colds and influenza: a randomized, placebo-controlled intervention study. Nutr. J. 12, 161.

Novobilský, A., Stringano, E., Hayot Carbonero, C., Smith, L.M.J., Enemark, H.L., Mueller-Harvey, I., Thamsborg, S.M., 2013. In vitro effects of extracts and purified tannins of sainfoin (Onobrychis viciifolia) against two cattle nematodes. Vet. Parasitol. 196, 532–537.

Quijada, J., Fryganas, C., Ropiak, H.M., Ramsay, A., Mueller-Harvey, I., Hoste, H., 2015. Anthelmintic activities against Haemonchus contortus or Trichostrongylus colubriformis from small ruminants are influenced by structural features of condensed tannins. J. Agric. Food Chem. 63, 6346–6354.

Ramírez-Restrepo, C.A., Pernthaner, A., Barry, T.N., López-Villalobos, N., Shaw, R.J., Pomroy, W.E., Hein, W.R., 2010. Characterization of immune responses against gastrointestinal nematodes in weaned lambs grazing willow fodder blocks. Anim. Feed Sci. Technol. 155, 99–110.

Scalbert, A., 1991. Antimicrobial properties of tannins. Phytochemistry 30, 3875–3883.

Sehm, J., Lindermayer, H., Dummer, C., Treutter, D., Pfaffl, M.W., 2007. The influence of polyphenol rich apple pomace or red-wine pomace diet on the gut morphology in weaning piglets. J. Anim. Physiol. Anim. Nutr. 91, 289–296.

Smith, P., Garrett, W., 2011. The gut microbiota and mucosal T cells. Front. Microbiol. 2, 111.

Smith, A.L., Hayday, A.C., 2000. An αβ T-cell-independent immunoprotective response towards gut coccidia is supported by γδ cells. Immunology 101, 325–332.

Snyder, D.T., Robison, A., Kemoli, S., Kimmel, E., Holderness, J., Jutila, M.A., Hedges, J.F., 2014. Oral delivery of oligomeric procyanidins in Apple Poly® enhances type I IFN responses in vivo. J. Leukoc. Biol. 95, 841–847.

Stepanova, H., Mensikova, M., Chlebova, K., Faldyna, M., 2012. CD4+ and γδTCR+ T lymphocytes are sources of interleukin-17 in swine. Cytokine 58, 152–157.

Thornton, P.K., 2010. Livestock production: recent trends, future prospects. Philos. Trans. R. Soc. Lond. B Biol. Sci. 365, 2853–2867.

Tibe, O., Pernthaner, A., Sutherland, I., Lesperance, L., Harding, D.R.K., 2012. Condensed tannins from Botswanan forage plants are effective priming agents of γδ T cells in ruminants. Vet. Immunol. Immunopathol. 146, 237–244.

Williams, A.R., Fryganas, C., Ramsay, A., Mueller-Harvey, I., Thamsborg, S.M., 2014. Direct anthelmintic effects of condensed tannins from diverse plant sources against Ascaris suum. PLoS ONE 9, e97053.

Witherden, D.A., Havran, W.L., 2013. Cross-talk between intraepithelial γδ T cells and epithelial cells. J. Leukoc. Biol. 94, 69–76.

Wu, G., Fanzo, J., Miller, D.D., Pingali, P., Post, M., Steiner, J.L., Thalacker-Mercer, A.E., 2014. Production and supply of high-quality food protein for human consumption: sustainability, challenges, and innovations. Ann. N. Y. Acad. Sci. 1321, 1–19.